THE EVOLUTION OF ENDOTHERMY - FROM PATTERNS TO MECHANISMS

EDITED BY: Elias T. Polymeropoulos, Rebecca Oelkrug and Martin Jastroch
PUBLISHED IN: Frontiers in Physiology

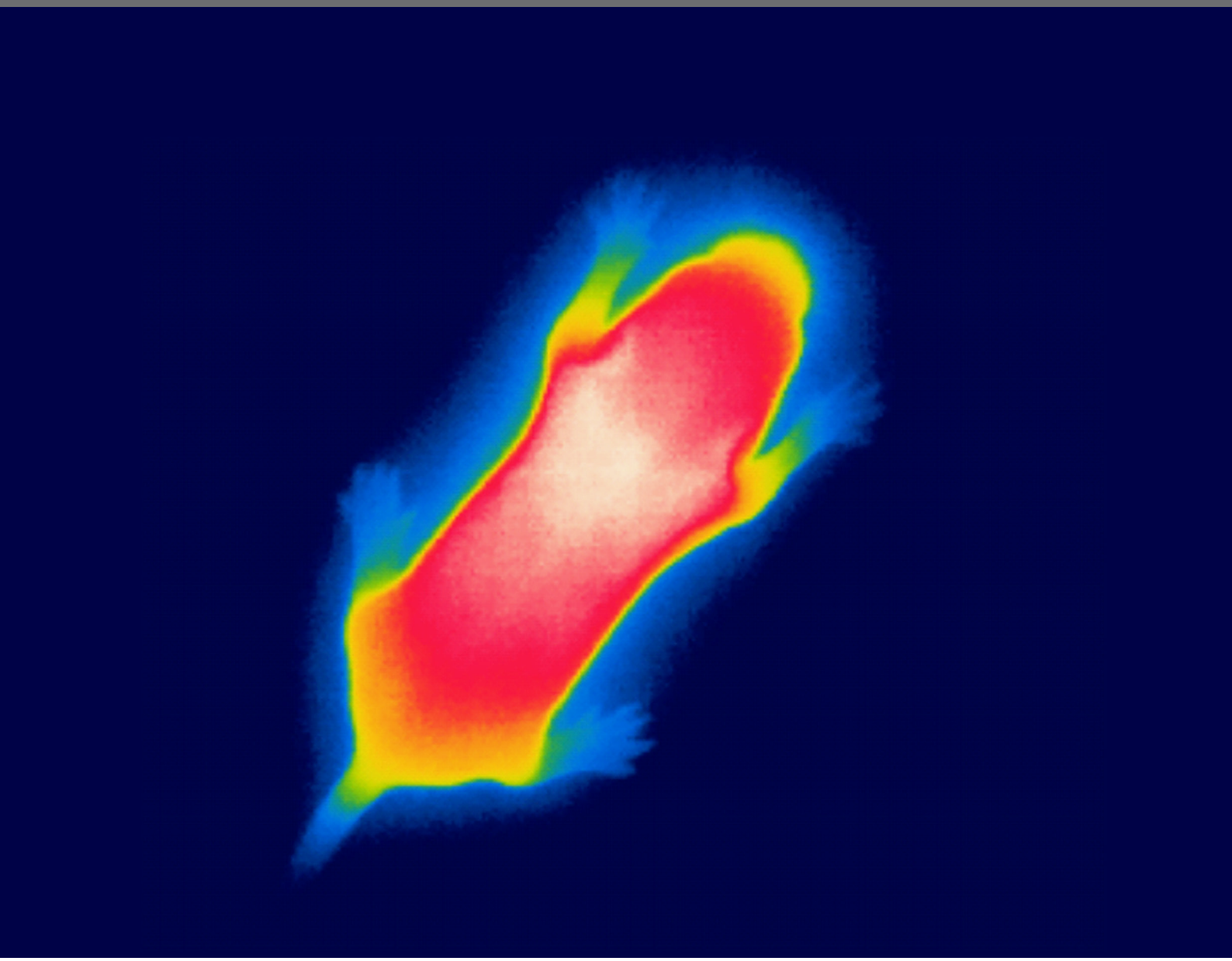

frontiers Research Topics

ISSN 1664-8714
ISBN 978-2-88945-569-0
DOI 10.3389/978-2-88945-569-0

About Frontiers

Frontiers is more than just an open-access publisher of scholarly articles: it is a pioneering approach to the world of academia, radically improving the way scholarly research is managed. The grand vision of Frontiers is a world where all people have an equal opportunity to seek, share and generate knowledge. Frontiers provides immediate and permanent online open access to all its publications, but this alone is not enough to realize our grand goals.

Frontiers Journal Series

The Frontiers Journal Series is a multi-tier and interdisciplinary set of open-access, online journals, promising a paradigm shift from the current review, selection and dissemination processes in academic publishing. All Frontiers journals are driven by researchers for researchers; therefore, they constitute a service to the scholarly community. At the same time, the Frontiers Journal Series operates on a revolutionary invention, the tiered publishing system, initially addressing specific communities of scholars, and gradually climbing up to broader public understanding, thus serving the interests of the lay society, too.

Dedication to Quality

Each Frontiers article is a landmark of the highest quality, thanks to genuinely collaborative interactions between authors and review editors, who include some of the world's best academicians. Research must be certified by peers before entering a stream of knowledge that may eventually reach the public - and shape society; therefore, Frontiers only applies the most rigorous and unbiased reviews.
Frontiers revolutionizes research publishing by freely delivering the most outstanding research, evaluated with no bias from both the academic and social point of view. By applying the most advanced information technologies, Frontiers is catapulting scholarly publishing into a new generation.

What are Frontiers Research Topics?

Frontiers Research Topics are very popular trademarks of the Frontiers Journals Series: they are collections of at least ten articles, all centered on a particular subject. With their unique mix of varied contributions from Original Research to Review Articles, Frontiers Research Topics unify the most influential researchers, the latest key findings and historical advances in a hot research area! Find out more on how to host your own Frontiers Research Topic or contribute to one as an author by contacting the Frontiers Editorial Office: researchtopics@frontiersin.org

THE EVOLUTION OF ENDOTHERMY - FROM PATTERNS TO MECHANISMS

Topic Editors:
Elias T. Polymeropoulos, University of Tasmania, Australia
Rebecca Oelkrug, University of Luebeck, Germany
Martin Jastroch, Stockholm University, Sweden, and Helmholtz Zentrum, Germany

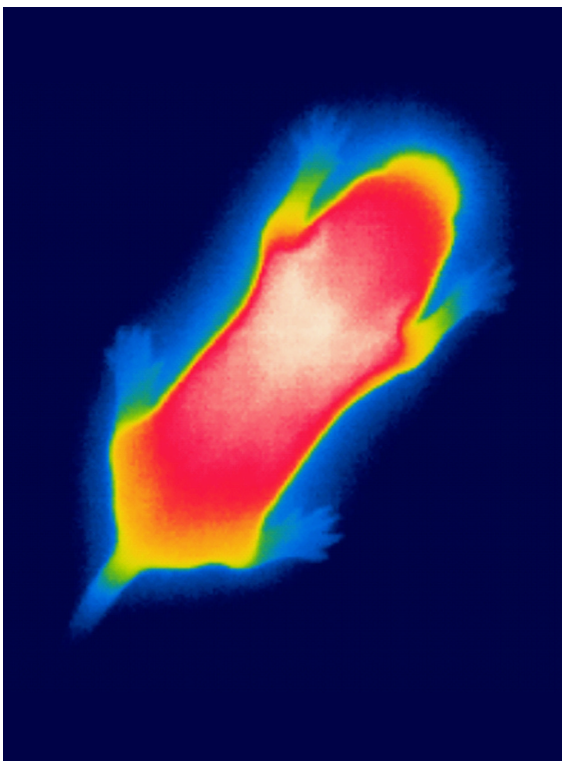

Thermal image of a newborn mouse five days after birth.
Image: Rebecca Oelkrug

Metabolic rate is a key ecophysiological factor determining fitness, distribution, survival and reproductive strategies of organisms. The ability to endogenously produce heat and elevate body temperature beyond ambient, has far reaching ecological implications. The diversity of thermogenic mechanisms and strategies employed throughout the animal kingdom is truly phenomenal and one of the greatest biological mysteries. Interestingly, even heat producing plants have been characterised.

Over the last several decades, the oversimplified distinction between warm- and cold blooded animals has well and truly been put to rest and the terms "endo- and ectotherm" have been established. Birds and mammals are regarded as endotherms, capable of maintaining high body temperatures within highly precise boundaries. On contrary, in ectothermic organisms ambient temperature governs body temperature and metabolism, encompassing the majority of present day species. However, it has recently become very clear that this distinction is still not accurate enough to

describe the vastness of heat generating mechanisms within endo- but also ectotherms. Indeed, a plethora of ectothermic animals display endogenous as well as behavioural means of temperature control and mechanisms for heat generation. There is large diversity in regards to thermoregulatory ability and strategy within endotherms as well, with some groups being classified by separate categories such as basoendotherms and mesotherms.

Considerable interest and efforts has been put into the quest to understand the underlying physiological mechanisms leading and facilitating high metabolic rates and body temperatures of endotherms. These mechanisms are far from being exhaustively studied and the evolutionary trajectory leading to high metabolic rates and stable body temperatures is equally, vividly debated. This discussion includes an array of questions and theories surrounding the presence of endothermy in extinct dinosaurs. In addition, a lively debate surrounds the evolutionary drivers promoting the establishment of endothermy with clear support of direct or indirect selective benefits.

Within this Research Topic we plan to compile the latest ideas, knowledge and experimental work to elucidate the patterns of the evolution of endothermy and its transition/distinction from ectothermy. The focus is on key physiological mechanisms supporting this transition and contributing to the maintenance of high metabolic rates and body temperature in endotherms, as well as mechanisms for local heterothermy and heat dissipation in ectotherms. These mechanisms and conclusions may be derived from different levels of organisation such as population, taxon, species as well as tissue, cellular or molecular levels. It may also encompass novel experimental or theoretical models testing evolutionary theories of endothermy. A comparative approach is encouraged but not fundamental.

Citation: Polymeropoulos, E. T., Oelkrug, R., Jastroch, M., eds (2018). The Evolution of Endothermy - From Patterns to Mechanisms. Lausanne: Frontiers Media.
doi: 10.3389/978-2-88945-569-0

Table of Contents

frontiers in Physiology

EDITORIAL
published: 12 July 2018
doi: 10.3389/fphys.2018.00891

Editorial: The Evolution of Endothermy–From Patterns to Mechanisms

Elias T. Polymeropoulos[1]*, *Rebecca Oelkrug*[2] and *Martin Jastroch*[3,4]

[1] Institute for Marine and Antarctic Studies, University of Tasmania, Hobart, TAS, Australia, [2] Department of Internal Medicine I, Group of Molecular Endocrinology, University of Lübeck, Lübeck, Germany, [3] Institute for Diabetes and Obesity, Helmholtz Zentrum, Munich, Germany, [4] The Arrhenius Laboratories F3, Department of Molecular Biosciences, The Wenner-Gren Institute, Stockholm University, Stockholm, Sweden

Keywords: endotherms, ectotherms, heterothermy, evolution, thermoregulation, comparative physiology

Editorial on the Research Topic

The Evolution of Endothermy–From Patterns to Mechanisms

What makes endothermy one of the most fascinating traits in evolution? Metabolic heat production required a complex degree of coordination from the organism to the molecule to achieve a high, stable body temperature (T_b), or homeothermic endothermy, which has convergently evolved as key trait of birds and mammals (Crompton et al., 1978). The resulting expansion of endotherms into thermal niches that were not accessible to ectotherms, whose T_b is dictated by ambient temperature (T_a), proved to be the crucial evolutionary advantage. Yet, the evolutionary framework and events leading to endothermy are still unclear.

Generally, three streams of hypotheses have been proposed aiming to explain this extraordinary transition from ecto- to endothermy during vertebrate evolution. The first school of thought promotes that the thermoregulatory advantages of high T_bs *per se*, resulting in higher metabolic rates (MR), suffice to explain the evolutionary advantage (Heinrich, 1977; Crompton et al., 1978). Others have put forward that the selection for higher MRs is a consequence of increased exercise, consequently raising T_b (Bennett and Ruben, 1979; Hayes and Garland, 1995). More recently, the parental care hypothesis has gained more traction (Farmer, 2000; Koteja, 2000), which stipulates an increase in T_b being beneficial for growth while reducing mortality, thus increasing species' fitness.

While this research topic aims at furthering and challenging these concepts through different methodological and theoretical approaches, it also provides novel experimental insights into physiological mechanisms on various levels of organization that may have underlay the transition to endothermy. The current issue also focuses on mechanisms that have enabled the maintenance of high, as well as fluctuations in T_b or MR in species that display local heterothermy or are facultative, homeothermic endotherms, thus filling missing links in our knowledge on why, how and when endothermy arose.

How is endothermy measured? Technically, measuring T_b or MR *per se*, despite being a common procedure, is not always a straight forward task. Detecting regional heterothermy and monitoring transitory states (e.g., hibernation) can be challenging, depending on the animal's body size, anatomy, and geographical distribution under free ranging conditions. However, characterizing metabolic phenotypes through thermometry is crucial to understand the evolution of different

OPEN ACCESS

Edited and reviewed by:
Geoffrey A. Head,
Baker Heart and Diabetes Institute, Australia

***Correspondence:**
Elias T. Polymeropoulos
eliasp@utas.edu.au

Specialty section:
This article was submitted to Integrative Physiology, a section of the journal Frontiers in Physiology

Received: *07 June 2018*
Accepted: *20 June 2018*
Published: *12 July 2018*

Citation:
Polymeropoulos ET, Oelkrug R and Jastroch M (2018) Editorial: The Evolution of Endothermy–From Patterns to Mechanisms. Front. Physiol. 9:891. doi: 10.3389/fphys.2018.00891

thermoregulatory strategies as well as linking genetic alterations to energy metabolism. The most commonly studied endotherms are small rodents and numerous thermometric techniques have been applied for metabolic phenotyping, whose accuracy and pitfalls are summarized by Meyer et al.

How did endothermy/ heterothermy impact mammalian evolution and survival? Previous hypotheses ascribe the survival of mammals during the mass extinction event at the K-Pg boundary to their heterothermic capacity (Lovegrove, 2016). Geiser et al. propose that this was achieved thanks to the ability of mammals to enter periods of reduced T_b and MR (torpor) induced by the wildfires of the asteroid impact and enabled some species to survive periods without food. In addition, such heterothermic states are considered beneficial during the transition to endothermy.

Tracing back the heterothermic ancestor giving rise to strict homeothermy has been a matter of a vivid debate. Not surprisingly, the holy grail in this quest has been the identification of heterothermic primates, whose presence appears restricted to the order of Strepsirrhini (Lovegrove, 2012). So far, no heterothermic relatives in the sister clades of Haplorrhini have been identified, including tarsiers (Welman et al.), the closest extant relative to Strepsirrhini.

Fluctuations in T_b is very common among facultative endotherms, who display regional heterothermy, torpor or hibernation (Angilletta et al., 2010; Ruf and Geiser, 2015). The question thus arises whether reaction rates of biochemical processes in endotherms are plastic and thus adaptable to T_a fluctuations. Seebacher and Little consider reaction rates of endotherms as thermally plastic, a trait that may be conserved from ectothermic ancestors. Amongst others, this notion is based on cellular pathways responding to thermal cues in tissues, like the transient potential receptor ion channels (TRPV and TRPM) and the AMP-activated protein kinase (AMPK) that affect energy expenditure.

The lesser hedgehog tenrec (*Echinops telfairi*) displays highly pronounced, reptile like thermoregulatory flexibility, which may be indicative of its phylogeny, representing a transitory state between ecto- and endotherms called basoendotherms. Polymeropoulos et al. show that this thermoregulatory flexibility is supported by the maintenance of the efficiency of mitochondrial ATP production (coupling efficiency). In particular the reduction of the basal mitochondrial proton leak compensates the reduction in substrate oxidation capacity at low temperatures.

How do mammals adapt heat production? Brown adipose tissue (BAT) mediated, nonshivering thermogenesis (NST) has long been recognized as a key thermogenic mechanism of small placental mammals and neonates that has proven as an evolutionary and thermoregulatory advantage in cold climates (Cannon and Nedergaard, 2004). The high concentration of mitochondria and expression of uncoupling protein 1 (UCP1) in BAT is crucial to the generation of heat. Therefore, understanding the molecular control of UCP1 expression and its evolution by identifying transcriptional regulatory elements across the mammalian phylogeny beyond murid rodents is essential to understand how UCP1 and BAT have been integrated allowing cellular heat production. The recent, most comprehensive analysis of UCP1 regulatory elements in mammals so far (Gaudry and Campbell), identifies various regulatory genomic elements and regions which appear less crucial than suggested previously, while highlighting others like the proximal TATA box and the distal enhancer region which are universally in control of intact UCP1 orthologs. This ground work allows targeted, comparative studies into UCP1 regulation that may shed new light into the evolution of adaptive thermogenesis in the vertebrate lineage (Fromme).

While numerous studies consider the evolution of BAT as a critical mechanism during the evolution toward endothermy, a separate BAT-independent mechanism of NST in skeletal muscle has been proposed (Bal et al., 2012). Here heat dissipation relies on Ca^{2+}-slippage by a sarcoplasmatic reticulum Ca^{2+}-ATPase (SERCA) that is controlled by sarcolipin (SLN). Nowack et al. summarize support to the hypothesis that muscle based NST is the earliest form of NST giving rise to endothermy, rather than BAT-mediated NST, which in addition to muscle-based NST, supported heterothermic endotherms during their early evolution. In stark contrast, Campbell and Dicke argue that evidence for an adaptive, thermogenic role (especially in larger bodied mammals) of the interaction between SLN and SERCA, regulating Ca^{2+}-slippage, is inconclusive so far and that more comparative analyses on SLN expression across multiple taxa are required to uncover its physiological role during mammalian evolution.

The large amounts of energy expended by endotherms in order to maintain high T_bs, especially in cold climates, not only appears energetically wasteful (Koteja, 2004) but also demands an efficient machinery minimizing the production of potentially harmful byproducts. Tissues of high aerobic capacity may produce reactive oxygen species (ROS) in excess when e.g., muscular work is performed in order to maintain a higher T_b such as in endothermic fish. These ROS may cause macromolecular damage and are shown to increase with increasing T_a (Banh et al., 2016). However, ROS production in red muscle of endothermic tuna is similar to ectothermic fish when measured at the physiological temperature, indicating the lack of compensatory mechanisms for increased ROS production, that may have coevolved with endothermy (Wiens et al.).

The advent of modern molecular tools allowing the formulation of comparative and functional genomic and quantitative genetic models (Nespolo et al., 2011) adds support for the parental care hypothesis (Bacigalupe et al.). Here a quantitative genetic model of maternal effects suggests that an increase in basal metabolic rate (BMR) and T_b (based on increased size/ activity of visceral organs to maintain elevated assimilation rates) may have been the result of their natural selection since there is a positive covariance between growth rate and the daily energy expenditure.

In support of the aerobic capacity model, previous work by Sadowska et al. (2015) in bank voles has shown that selection for high aerobic metabolism leads to an increase in BMR and thermogenic capacity. Following this work, Stawski et al. now demonstrate that this adaptation also affects the thermoregulatory curve through an increase in RMR as well as T_b

but also increases maximum thermogenesis yielding the selected lines more cold tolerant.

Endothermic T_bs reach their peak within birds, exceeding those of mammals by up to 2.5°C (Prinzinger et al., 1991). These extraordinarily high T_bs pose a significant problem for migrating birds because of the large amount of work performed and concomitant muscular heat produced during flight, increasing the risk of hyperthermia. Consequently large eider ducks (*Somateria mollissima*) adapt their migration strategy to prevent hyperthermia by decreasing in flight duration (Guillemette et al., 2016) and prolonged periods of cooling during breaks, resulting in a behavioral stop-and-go, thermoregulatory strategy that poses a significant migratory time cost (Guillemette et al.).

Neural control of mammalian thermoregulation has been well defined, including pathways eliciting shivering as well as non-shivering thermogenic responses (Morrison and Nakamura, 2011). Strikingly however, thermoregulation appears to be impaired during mammalian REM sleep (Parmeggiani, 2003) a phenomenon which is less well understood. Cerri et al. conclude that REM sleep is a transient heterothermic state that coevolved with endothermy, which benefits regeneration of brain activity rather than energy conservation.

The outstanding contributions to this research topic will refine our understanding of when, how and why the evolution of endothermy emerged. The diversity of approaches, fusing technological advances, ecological, physiological and molecular insights, complement the picture on the evolution of endothermy–that still remains one of the patchiest mysteries of nature. The use of modern molecular and comparative techniques will allow an acceleration in the understanding of the evolution of endothermy that will, however, likely raise just as many questions as it will answer in the future.

AUTHOR CONTRIBUTIONS

EP, RO, and MJ contributed to manuscript writing, provided important interpretations, critically revised the work, and provided final approval of the opinion content.

REFERENCES

Angilletta, M. J., Cooper, B. S., Schuler, M. S., and Boyles, J. G. (2010). The evolution of thermal physiology in endotherms. *Front. Biosci. (Elite Ed)*. 2, 861–881. doi: 10.2741/E148

Bal, N. C., Maurya, S. K., Sopariwala, D. H., Sahoo, S. K., Gupta, S. C., Shaikh, S. A., et al. (2012). Sarcolipin is a newly identified regulator of muscle-based thermogenesis in mammals. *Nat. Med*. 18, 1575–1579. doi: 10.1038/nm.2897

Banh, S., Wiens, L., Sotiri, E., and Treberg, J. R. (2016). Mitochondrial reactive oxygen species production by fish muscle mitochondria: potential role in acute heat-induced oxidative stress. *Comp. Biochem. Physiol. B Biochem. Mol. Biol.* 191, 99–107. doi: 10.1016/j.cbpb.2015.10.001

Bennett, A. F., and Ruben, J. A. (1979). Endothermy and activity in vertebrates. *Science* 206, 649–654. doi: 10.1126/science.493968

Cannon, B., and Nedergaard, J. (2004). Brown adipose tissue: function and physiological significance. *Physiol. Rev*. 84, 277–359. doi: 10.1152/physrev.00015.2003

Crompton, A. W., Taylor, C. R., and Jagger, J. A. (1978). Evolution of homeothermy in mammals. *Nature* 272, 333–336. doi: 10.1038/272333a0

Farmer, C. G. (2000). Parental care: the key to understanding endothermy and other convergent features in birds and mammals. *Am. Nat*. 155, 326–334. doi: 10.1086/303323

Guillemette, M., Woakes, A. J., Larochelle, J., Polymeropoulos, E. T., Granbois, J., Butler, P. J., et al. (2016). Does hyperthermia constrain flight duration in a short-distance migrant? *Phil. Trans. R. Soc. B*. 371:20150386. doi: 10.1098/rstb.2015.0386

Hayes, J. P., and Garland, T. (1995). The evolution of endothermy: testing the aerobic capacity model. *Evolution*. 49, 836–847.

Heinrich, B. (1977). Why have some animals evolved to regulate a high body temperature? *Am. Nat*. 111, 623–640. doi: 10.1086/283196

Koteja, P. (2000). Energy assimilation, parental care and the evolution of endothermy. *Proc. Biol. Sci*. 267, 479–484. doi: 10.1098/rspb.2000.1025

Koteja, P. (2004). The evolution of concepts on the evolution of endothermy in birds and mammals. *Physiol. Biochem. Zool*. 77, 1043–1050. doi: 10.1086/423741

Lovegrove, B. G. (2012). The evolution of endothermy in Cenozoic mammals: a plesiomorphic-apomorphic continuum. *Biol. Rev. Camb. Philos. Soc*. 87, 128–162. doi: 10.1111/j.1469-185X.2011.00188.x

Lovegrove, B. G. (2016). A phenology of the evolution of endothermy in birds and mammals. *Biol. Rev*. 1220, 1213–1240. doi: 10.1111/brv.12280

Morrison, S. F., and Nakamura, K. (2011). Central neural pathways for thermoregulation. *Front. Biosci. (Landmark Ed)*. 16, 74–104.

Nespolo, R. F., Bacigalupe, L. D., Figueroa, C. C., Koteja, P., and Opazo, J. C. (2011). Using new tools to solve an old problem: the evolution of endothermy in vertebrates. *Trends Ecol. Evol*. 26, 414–423. doi: 10.1016/j.tree.2011.04.004

Parmeggiani, P. L. (2003). Thermoregulation and sleep. *Front. Biosci*. 8, s557–s567. doi: 10.2741/1054

Prinzinger, R., Preßmar, A., and Schleucher, E. (1991). Body temperature in birds. *Comp. Biochem. Physiol. A Physiol*. 99, 499–506. doi: 10.1016/0300-9629(91)90122-S

Ruf, T., and Geiser, F. (2015). Daily torpor and hibernation in birds and mammals. *Biol. Rev*. 90, 891–926. doi: 10.1111/brv.12137

Sadowska, E. T., Stawski, C., Rudolf, A., Dheyongera, G., Chrześcik, K. M., Baliga-Klimczyk, K., et al. (2015). Evolution of basal metabolic rate in bank voles from a multidirectional selection experiment. *Proc. R. Soc. B Biol. Sci*. 282, 20150025–20150025. doi: 10.1098/rspb.2015.0025

Conflict of Interest Statement: The authors declare that the research was conducted in the absence of any commercial or financial relationships that could be construed as a potential conflict of interest.

frontiers in Physiology

METHODS
published: 31 July 2017
doi: 10.3389/fphys.2017.00520

Body Temperature Measurements for Metabolic Phenotyping in Mice

Carola W. Meyer[1], Youichirou Ootsuka[2] and Andrej A. Romanovsky[3]*

[1] Department of Pharmacology, Max-Planck Institute for Heart and Lung Research, Bad Nauheim, Germany, [2] Centre for Neuroscience, School of Medicine, Flinders University of South Australia, Adelaide, SA, Australia, [3] FeverLab, St. Joseph's Hospital and Medical Center, Phoenix, AZ, United States

Endothermic organisms rely on tightly balanced energy budgets to maintain a regulated body temperature and body mass. Metabolic phenotyping of mice, therefore, often includes the recording of body temperature. Thermometry in mice is conducted at various sites, using various devices and measurement practices, ranging from single-time probing to continuous temperature imaging. Whilst there is broad agreement that body temperature data is of value, procedural considerations of body temperature measurements in the context of metabolic phenotyping are missing. Here, we provide an overview of the various methods currently available for gathering body temperature data from mice. We explore the scope and limitations of thermometry in mice, with the hope of assisting researchers in the selection of appropriate approaches, and conditions, for comprehensive mouse phenotypic analyses.

Keywords: mouse, phenotyping, body temperature, thermography, metabolism, telemetric recordings, mouse models

OPEN ACCESS

Edited by:
Martin Jastroch, Helmholtz Zentrum München, Germany

Reviewed by:
Jens Mittag, University of Lübeck, Germany
Dmitry Zaretsky, Intarcia Therapeutics, Inc., United States
Miklós Székely, Medical School, University of Pécs, Hungary

****Correspondence:***
Carola W. Meyer
carola.meyer@mpi-bn.mpg.de

Specialty section:
This article was submitted to Integrative Physiology, a section of the journal Frontiers in Physiology

Received: *20 May 2017*
Accepted: *06 July 2017*
Published: *31 July 2017*

Citation:
Meyer CW, Ootsuka Y and Romanovsky AA (2017) Body Temperature Measurements for Metabolic Phenotyping in Mice. Front. Physiol. 8:520. doi: 10.3389/fphys.2017.00520

KEY POINTS

- Rectal probing is subject to procedural bias. This method is suitable for first-line phenotyping, provided probe depth and measurement duration are standardized. It is also useful for detecting individuals with out-of-range body temperatures (during hypothermia, torpor).
- The colonic temperature attained by inserting the probe >2 cm deep is a measure of deep (core) body temperature.
- IR imaging of the skin is useful for detecting heat leaks and autonomous thermoregulatory alterations, but it does not measure body temperature.
- Temperature of the hairy or shaved skin covering the inter-scapular brown adipose tissue can be used as a measure of BAT thermogenesis. However, obtaining such measurements of sufficient quality is very difficult, and interpreting them can be tricky. Temperature differences between the inter-scapular and lumbar areas can be a better measure of the thermogenic activity of inter-scapular brown adipose tissue.
- Implanted probes for precise determination of BAT temperature (changes) should be fixed close to the Sulzer's vein. For measurement of BAT thermogenesis, core body temperature and BAT temperature should be recorded simultaneously.
- Tail temperature is suitable to compare the presence or absence of vasoconstriction or vasodilation.
- Continuous, longitudinal monitoring of core body temperature is preferred over single probing, as the readings are taken in a non-invasive, physiological context.
- Combining core body temperature measurements with metabolic rate measurements yields insights into the interplay between heat production and heat loss (thermal conductance), potentially revealing novel thermoregulatory phenotypes.

INTRODUCTION

Precise phenotyping of mice strains and genetically modified mice has become increasingly important for revealing correlations and inferring causality amongst specific physiological pathways. Important targets in mouse phenotyping include changes in energy balance, which can result in altered body composition (Tschöp et al., 2012; Rozman et al., 2014). The majority of studies targeting energy balance involve measurements of body mass, fat mass, and food (energy) intake (Moir et al., 2016). Many authors also report energy expenditure by using indirect calorimetry (Speakman, 2013; Meyer et al., 2015). In addition, body temperature is often measured.

At present, mouse body temperature data for metabolic phenotyping is mainly obtained by one of three methods: (1) inserting a probe into the rectum (or, less typically, into the sigmoid colon); (2) measuring temperature in the abdominal cavity or in the subcutaneous compartment with a pre-implanted probe; or (3) measuring surface temperature with infrared (IR) thermography (e.g., from the tail, trunk areas, external auditory meatus, or eyes). In many cases, thermometry data obtained by any of these methods is presented as a single (often the mean) value labeled "body temperature." Unfortunately, this simplistic approach ignores the fact that the body of a mouse is thermally heterogeneous - and that all sites produce different output values. For example, IR thermography of a mouse tail provides information about the vasomotor tone of the tail vasculature, whereas colonic thermometry produces a value of deep body temperature. This creates a need for the appropriate labeling of temperature data. Condensing complex data into a single mean value also dismisses the pronounced circadian rhythms of body temperature in mice and, in general, ignores the fact that body temperature is constantly affected by changes in both the external and internal environments (Gordon, 1993).

We think that the method of thermometry (i.e., where and how body temperature is measured) and the experimental conditions (e.g., ambient temperature, whether or not the animals are restrained, and whether or not they are acclimated to the experimental setups and procedures) are of enormous importance for the interpretation of any body temperature data obtained during metabolic phenotyping of genetically modified mice. Below, we overview the main methods used for thermometry at different sites of the body in the mouse (with occasional reference to the rat) and address the utility of these methods in the context of mouse metabolic phenotyping.

Rectal (or Colonic) Thermometry

Rectal thermometry is a common method of measuring body temperature in rodents. It involves inserting a small-diameter temperature probe through the anus. The temperature-sensitive element of the probe is either a thermistor, a resistance temperature detector (RTD), or the "hot" (active) junction of a thermocouple (**Box 1**). As the core of the body is warmer than the shell, the body temperature value obtained with a rectal probe critically depends on the insertion depth. In adult mice, an insertion depth of >2 cm will yield colonic temperatures. In fact, the temperature measured by this method is one of highest temperatures in the body of endotherms, corresponding to deep (core) body temperature (Donhoffer, 1980).

Less-deep insertion of the probe results in somewhat lower and more variable readings, corresponding to rectal temperatures. Despite the fact that rectal temperature is somewhat inferior to colonic temperature; it is still a valid measure. Rectal thermometry is the simplest, and sometimes lowest-cost, method for obtaining body temperature data in conscious mice. It is also the lowest-impact method, as the procedure is fast and painless for mice, and no surgery is required. To obtain a rectal temperature, the mouse is usually hand-restrained and placed on a horizontal surface, e.g., a cage lid. The tail is then lifted, and a probe (covered with Vaseline) is gently inserted into the rectum to a fixed depth (typically, up to 2 cm). Although different laboratories and manufacturers recommend different insertion depths, it is critical that the depth be exactly the same for each measurement to reduce within-group variability. For comparative purposes, insertion depth should be routinely reported in publications involving rectal thermometry.

The time of rectal readings depends on the time constant of the probe and is often specified by the manufacturer. If the reading is taken too fast, the value obtained underestimates the real temperature. However, waiting too long may also create a problem as body temperature increases rapidly (i.e., within seconds) as part of the stress response of the mouse to being

BOX 1 | Thermocouples, thermistors, and RTDs.

A thermocouple is formed by two dissimilar metals. The voltage produced by such a junction is temperature-dependent. Different types of thermocouples use different metal combinations and, therefore, have different characteristics. By convention, the color of the thermocouple connector identifies the type. For most physiological purposes, including rectal thermometry, copper-constantan (T-type) thermocouples are used; their plugs are usually made of blue plastic. The response time of these temperature probes is often around 0.5 s, but it can vary widely based on the probe size and insulating materials used. The accuracy of thermocouple probes can be rather high (<0.1°C), but in most commercially available devices for rectal thermometry, it is somewhere between 0.1 and 0.5°C.

Thermistors and the so-called RTDs (resistance temperature detectors) are used to measure temperature because their electrical resistance depends on temperature. Thermistors are generally made from certain metal oxides, often incased in ceramic, and their resistance decreases with increasing temperatures. RTDs are made of metals, such as platinum and nickel, and their resistance increases with temperature. In general, RTDs have technical characteristics that are superior to those of thermistors and thermocouples, but these minor technical differences are of little relevance to the typical tasks of rectal thermometry in mice. RTDs are also more expensive.

The material of the probe shaft is relevant when environmental parameters are significantly deviating from physiological, i.e., during cold exposure. If the metal holder of the probe is short, it is able to transfer energy to the sensor, hence pushing the readings toward cooler values in cold. In this case, non-metal shafts are preferred in order to reduce bias.

handled and fixated (Clement et al., 1989). Hence, rectal body temperature readings obtained at longer time periods are more likely to be "contaminated" by stress hyperthermia. Acute stress-induced increases in body temperature can be greatly alleviated if the mice are trained to the measurement procedure and to restraint (Garami et al., 2011). Rodents are readily adaptable to confinement, and-when habituated-incur neither a stress fever (Romanovsky et al., 1998) nor show any other signs of stress (Hashimoto et al., 1988; Melia et al., 1994; Stamp and Herbert, 1999).

Rectal probing is particularly useful in diagnosing body temperatures outside the normal range, e.g., during conditions of torpor and hypothermia (Haemmerle et al., 2006). Provided that variations in probe depth, mouse age and sex, as well as other factors impacting body temperature are controlled for, rectal thermometry can also be used for first-line phenotyping of cohorts of genetically modified mice (Willershäuser et al., 2012). Because the method is prone to environmental and procedural variations (Zethof et al., 1994), it is more useful for screening for large effects on body temperature rather than for studying mechanisms of effects on body temperature - especially if the effects are moderate or small. Assuming an insertion depth of 2 cm and a standard deviation of 0.4°C for inbred C57BL/6J mice (Willershäuser et al., 2012), detecting a moderate difference of 0.5°C in rectal temperature at $p < 0.05$ and a power of 80% (two-sided *t*-test) would require the use of at least 12 animals per group.

Wireless Measurements of Body Temperature Using Implanted Probes

Wireless monitoring of temperature can be achieved using probes that are firmly anchored to the inside of the body to obtain temperature data from freely-moving, conscious animals. **Table 1** gives an overview of the current products available for measuring internal temperatures in unrestrained mice and other small mammals. Some of the probes not only provide temperature readings, but also enable the measurement of gross motor activity. The devices listed are transmitters, transponders and data loggers (**Boxes 2–4**). In addition, novel implantable transponder-logger hybrids have been made available to enable the identification and monitoring of multiple animals in one cage (see **Table 1**). This relieves the constraint to house animals individually for measuring body temperature, thus allowing for no-contact thermometry in a social context.

Owing to their size, miniature transponders, e.g., IPTT-300, are typically implanted subcutaneously. They represent advanced versions of animal identification chips and, as such, provide subcutaneous temperature measurements as an "added bonus." At most locations (e.g., on the back of the animal), the subcutaneous temperature determined by a transponder will be close to the temperatures of the adjacent hairy (non-glabrous) skin (Romanovsky, 2014). Subcutaneous temperatures can vary widely and are strongly affected by the ambient temperature. They cannot serve as a measure of deep body temperature.

In some mouse studies, miniature transponders are implanted in proximity to the inter-scapular brown adipose tissue (BAT) depots (e.g., Bal et al., 2012; Gerhart-Hines et al., 2013; Muller et al., 2013; Lateef et al., 2014). Although some of these studies claim successful use of such implants for assessing the (change in) temperature of BAT (as a measure of thermogenic activity), we are skeptical about such applications and do not recommend them - considering the rather large size of the transponder in relation to the BAT tissue. There are also some technical concerns: when thermogenesis in BAT is activated, the generated heat is collected throughout the brown fat pads by venous blood and leaves the tissue through Sulzer's vein (Smith and Horwitz, 1969). The amount of heat generated is so high that it is sufficient to rapidly warm the entire body of an animal by a few degrees Celsius. Hence, in active BAT, a proper measurement of brown fat temperature is substantially (sometimes by more than 1°C)

TABLE 1 | Temperature probes for measuring body temperatures in unrestrained mice.

Product name	Type	Mass (g)	Volume (cm^3)	Simultaneous acquisition in multiple animals	Average battery life[d] (months)	Manufacturer URL
DSI PhysioTel TA-F10[c]	Transmitter	1.6	1.1	No	6	www.datasci.com
Anipill	Transmitter	1.7	1.2	Yes	7	www.datasci.com
E-Mitter Series 3000 XM-FH[c]	Transponder	1.6	1.1	No	Battery-free	http://www.minimitter.com/ www.respironics.com[a]
G2 E- Mitter[c]	Transponder	1.1	0.6	No	Battery-free	www.starrlifesciences.com[b]
IPTT-300	Transponder	0.1	0.1	No	Battery-free	www.bmds.com
SubCue Mini	Logger	2.5	1.5	Yes	30	www.subcue.com
DST nano-T	Logger	1.0	0.5	Yes	14	www.star-oddi.com
DST nano RF-T	Transponder-logger	1.3	0.6	Yes	12	www.star-oddi.com
XS Stellar telemetry[c]	Transponder-logger	2.5	1.5	Yes	5	www.tse-systems.com
Mouse Monitor™ C19BTA[c]	Transponder-logger	2.7	1.9	Yes	0.5 rechargeable	www.indusinstruments.com

[a] *This product is no longer commercially available, but is still used in some laboratories.*

[b] *In 2013, STARR Life Sciences (international distributor: Harvard Apparatus Ltd) acquired the VitalView/E-Mitter product line from Philips Respironics.*

[c] *This product also collects information on gross motor activity.*

[d] *Battery life depends on sampling frequency. Battery-free devices require no refurbishment. Their maximal lifetime is variable (usually >2 years).*

BOX 2 | Transponders.

A transponder is an electronic device that can receive radiofrequency signals in response to predetermined signals. Hence, it can function as both a transmitter and a responder. If used for animal identification purpose, its function is to send out an identifier signal when an outside signal requests identification. A transponder consists of a coil antenna coupled to an integrated circuit chip, both covered by biocompatible glass or plastic. For temperature-measuring transponders, the chip includes a thermistor to measure temperature and a memory unit to store temperature data. An example of a transponder, IPTT-300, is listed in **Table 1**. This is a low-accuracy (0.5°C) device used mostly in large-scale animal husbandry operations, where some rough estimate of body temperature is obtained "for free" along with the animal's identifier. A main advantage of transponders is the ease of their implantation (using a syringe-like injector) and their battery-free operation. Once implanted, a transponder can provide temperature data for the entire life of the animal.

BOX 3 | Telemetry transmitters.

A transmitter is an electronic device that generates and amplifies a carrier wave, modulates it according to its temperature, and broadcasts the resulting signal from an antenna. Signal modulation by temperature is typically achieved through changes in either the frequency (frequency modulated, FM) or the amplitude (amplitude modulated, AM). For implantable transmitters used to measure body temperature, all the electronics involved in sensing temperature, modulating and transmitting the signal are hidden inside a miniature biocompatible capsule. Several examples of transmitters are listed in **Table 1**. Their accuracy is generally greater than 0.2°C. For those experimental conditions where a radio signal from a transmitter implanted in an animal can be easily detected by a receiver, transmitter-based telemetry is often a method of choice for real-time thermometry.

BOX 4 | Data loggers.

A temperature data logger is an electronic device that stores temperature signals in digital form on silicon or wax-coated memory chips integrated with a temperature probe. The device is programmed and implanted into an animal. The temperature information can be read only after the logger is removed from the animal, which usually happens at the end of the experiment when the animal is euthanized. The sampling frequency is set during programming, and the amount of data that can be stored and retrieved depends on the memory size. For example, if the memory size is 2,000 data points, the logger can store the data for ∼1.4 days of recordings at 1-min sampling, or for about 85 days of recordings at 1-h sampling. The major advantage of data loggers is that they can be used under those conditions that do not permit communication between a transmitter and receiver, e.g., in a field experiment, or when an animal is placed in an environment impermeable to radio waves, such as in some designs of a thermogradient apparatus (Almeida et al., 2006; Garami et al., 2011).

higher than core body temperature, as was shown in rats with thermocouples acutely implanted in the inter-scapular depots of brown fat immediately before an experiment (Szekely et al., 1973; Szekely and Szelenyi, 1979), and in some experiments using chronic implantation techniques (Romanovsky et al., 1997; Ootsuka et al., 2007; Almeida et al., 2012). In chronic experiments, it is difficult to achieve the quality of measurements that would allow one to accurately quantify this phenomenon. To achieve a high-quality BAT temperature measurement, a probe must be fixed in the immediate proximity of Sulzer's vein with special techniques (e.g., Almeida et al., 2012; and **Figure 1**).

Even when a probe is properly positioned near Sulzer's vein, BAT temperature can be influenced by temperature changes in the muscles underneath the BAT depots, and in the skin above. To control for these influences, at least partially, it is important to measure core body temperature at the same time. The difference between BAT and core body temperature, sometimes referred to as "BAT themogenic index," can be used to assess BAT heat production (Almeida et al., 2012). Comparing the slope of an increase in BAT temperature during the initial phase of BAT thermogenesis with the slope of core body temperature is a way to assess the validity of BAT temperature measurements (Mohammed et al., 2014).

Most often, the probes listed in **Table 1** are implanted into the peritoneal cavity to measure what is commonly referred to as "abdominal temperature." Abdominal temperature is a valid measure of deep (core) body temperature. The associated surgical intervention involves a small midline incision through the skin, followed by an opening of the peritoneal cavity through the *linea alba*. In order to prevent probe migration in the peritoneal cavity, some devices have small loops for suture-anchoring to the abdominal wall. Alternatively, the probe is sometimes left free-floating in the peritoneal cavity, which increases the intra- and inter-animal variation in recorded temperature, and is not recommended.

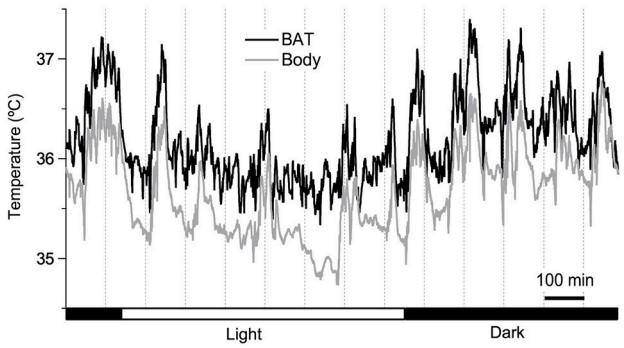

FIGURE 1 | Twenty four-hour brown adipose tissue (BAT) thermometry and abdominal body temperature readings in a freely-moving C57BL/6 mouse maintained at 26°C. Abdominal temperature was measured using an implanted telemetry transmitter (DSI, ETA-F10). BAT temperature was measured using a thermistor (NTH5G10P, muRata, Kyoto, Japan) implanted between the BAT and the underlying muscle layer in the inter-scapular region near Sulzer's vein, and was connected to a swivel. The resolution of readings was set to 1 Hz. Y. Ootsuka, unpublished data.

Un-tethered, continuous monitoring of body temperature is more informative compared to single-point probing, e.g., by rectal thermometry, as periodic temperature changes are

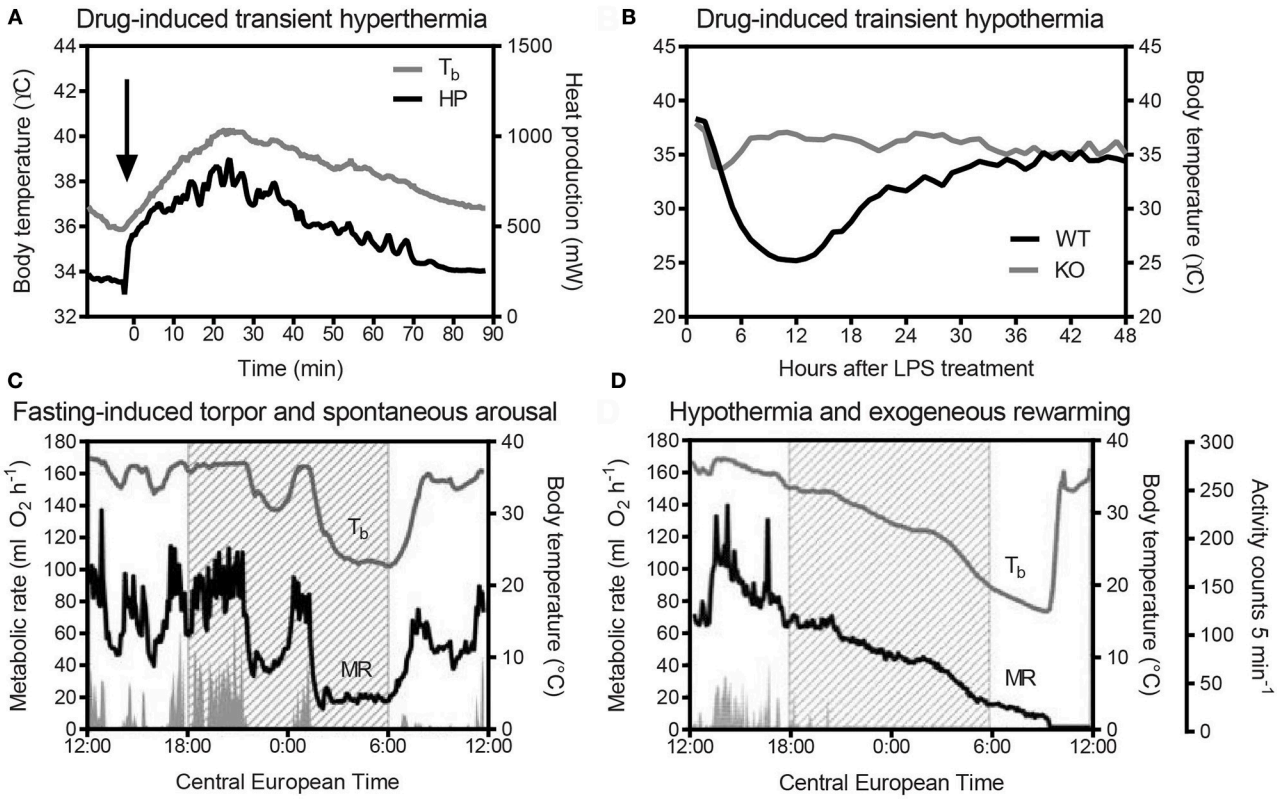

FIGURE 2 | (A) Adrenergically-stimulated thermogenesis [heat production (HP)] following 1 mg/kg norepinephrine, s.c. (Arterenol, Merck; the arrow indicates the time-point of injection), and transient hyperthermia in a male AKR/J mouse kept at 30°C (N. Rink and C. W. Meyer; unpublished data). Body temperature (T_b) of the individual was recorded with an intraperitoneally-implanted probe (MiniMitter, Sunriver, OR, USA) at a frequency of 2 min. HP was determined in parallel using indirect calorimetry (Meyer et al., 2015). **(B)** Genotype-dependent variation in lipopolysaccharide (LPS)-induced (15 μg/g, i.p.) transient hypothermia in mice, as determined by an intra-abdominal temperature sensor (DSI TA-F10). KO: knockout mouse, WT: wild-type control (B. Strilic, unpublished data). **(C)** Simultaneous metabolic rate (MR) and abdominal body temperature (T_b) recordings (E-Mitter Series 3000 XM-FH, 4-min resolution) of a physiological torpor event in a female C57BL/6 mouse, compared to a hypothermic individual. **(D)** MR was measured using an indirect calorimetry set-up (Heldmaier and Ruf, 1992). In **(C,D)**, shaded areas indicate the duration of "lights off." Note in **(C)**, the steep decrease in MR and T_b during the middle of the dark phase, and the spontaneous arousal shortly after "lights-on," in contrast to the slowly-decreasing MR and T_b in **(D)**. The hypothermic mouse in example **(D)** was removed from the calorimetry cage (arrow) and externally rewarmed without experiencing consequential damage from hypothermia. Activity counts in **(C,D)** were measured via integrated gross motor detection of the E-Mitter in the receiver field. Data are taken from Oelkrug et al. (2011).

revealed, and data can be obtained in a more physiological-longitudinal framework. Some examples of valuable readouts derived from metabolic studies involving continuous body temperature measurements in unrestrained mice include circadian temperature patterns (Garami et al., 2011; Gerhart-Hines et al., 2013), ultradian-episodic ("jaggy") events (Blessing and Ootsuka, 2016; Miyata et al., 2016), genotype- or sex-specific heterothermy (Wither et al., 2012), hyper- or hypothermic responses to pharmacological treatments (Rudaya et al., 2005; Steiner et al., 2007; Garami et al., 2011; Wanner et al., 2012; and **Figure 2A**), experimental fevers (Rudaya et al., 2005; Steiner et al., 2006), thermoregulatory manifestations of sepsis (Wanner et al., 2012; and **Figure 2B**), and body temperature patterns of the entrance into, and exit from, torpor (Oelkrug et al., 2011; Solymar et al., 2015; and **Figure 2C**). An example of an added value of continuous body temperature measurements in the context of cold tolerance is given in **Figure 3**, which depicts the data from a typical 5-h cold test performed at 4–5°C (Meyer et al., 2010). Hourly probing would have correctly identified the cold-tolerant phenotype of the uncoupling protein-1 (UCP1)-KO mouse after pre-acclimation to moderate cold, but this experimental setup would have failed to uncover the absence of periodic fluctuations in abdominal temperature, compared to wild-type. The translational value of continuous data acquisition, as compared to single probing, is also highlighted from studies in female methyl-CpG-binding protein 2 (MeCP2)-deficient mice, which initially demonstrated lower neck temperature determined by transponder. Using telemetry probes, this observation could be extended to reflect disrupted daily rhythmic patterning that mirrors impaired autonomic nervous system function and cardinal phenotypes of clinical Rett syndrome (Ward et al., 2011; Wither et al., 2012).

Some researchers also measure brain temperature in mice and other small rodents by using thermocouples, wired thermistors, or telemetry probes (Deboer et al., 1994; Romanovsky and

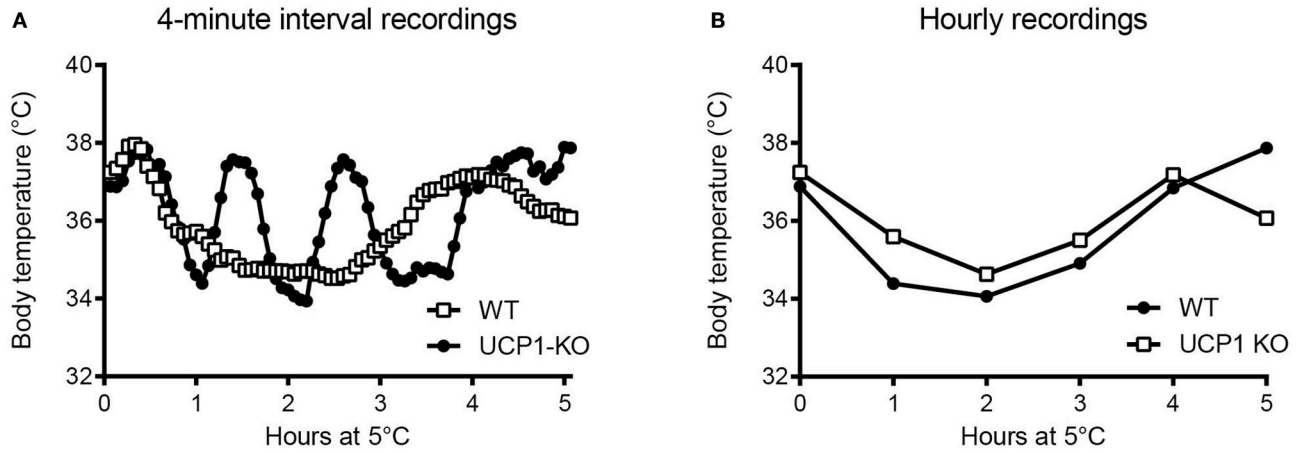

FIGURE 3 | (A) Intra-abdominal body temperature (E-Mitter Series 3000 XM-FH) recorded every 4 min in a wild-type (WT) and an uncoupling protein-1 (UCP1)-knockout (KO) mouse previously acclimated to 18°C and acutely exposed to 5°C. Note the pronounced episodic fluctuations in body temperature of the WT mouse that are absent in the UCP1-KO mouse. Using the same data sets, we simulated hourly probing **(B)**, demonstrating resolution legacy and the information potentially missed from less-frequent sampling. Data are taken from Meyer et al. (2010).

BOX 5 | IR thermography.

At temperatures >0 K (−273°C), all object surfaces emit electromagnetic radiation in the infrared range of the electromagnetic spectrum (~5–15 μm). The efficacy by which energy is emitted from surfaces is called emissivity, and the emissivity coefficient (i.e., the radiation of an object in relation to that of a black body) has been determined to be 0.95–0.98 for biological materials (Cossins and Bowler, 1987). Using this information, infrared energy can be captured by infrared-sensitive cameras and processed into a thermogram, a color-coded image of the surface temperature (Speakman and Ward, 1998).

In order to retrieve reproducible data with IR thermography, important technical aspects need to be considered. For example, the intensity of emitted radiation received from an object is not just affected by its temperature, but also by the angle at which the object is viewed and the distance between the object and the camera. For assessment of living mice, most IR cameras need to be placed vertically above the mouse and within less than 1 m distance from the animal. Hence, although claiming to be non-invasive, IR measurements of live animals may require a confined space or immobilization (fixation) in order to standardize measurement conditions and the exposed surface area.

Blatteis, 1996; Romanovsky et al., 1996; DeBow and Colbourne, 2003; Conti et al., 2006; Baracchi and Opp, 2008; Steiner et al., 2008; Ootsuka et al., 2009; Baud et al., 2013). In a telemetry probe typically used for this purpose, the XM-FH transmitter, which used to be sold by MiniMitter, the temperature sensor is located at the tip of a stainless steel cannula, which is implanted into the brain, whereas the body of the probe (which contains all the electronics) is affixed to the skull (Steiner et al., 2008).

Brain temperature is measured for different purposes and, therefore, at different locations. In the sleep field, brain temperature is often measured as a cortex temperature and used, for among other purposes, to determine the rapid-eye-movement (REM, or paradoxical) phase of sleep. In REM sleep, the activity of the cortex (and, therefore, the cortex temperature) increases. Hence, in most sleep studies, a brain probe is implanted very superficially—in the cortex, over (just above) the cortex, or even at the *dura mater* (Deboer et al., 1994; Baracchi and Opp, 2008; Baud et al., 2013). In the thermoregulation field, brain temperature is usually used as an index of deep body temperature or measured in an attempt to determine the temperature at which thermosensitive neurons, that drive autonomic thermoeffector responses, are exposed. For either purpose, the probe is implanted deeper—often into the medial anterior hypothalamus, which in most species is located close to the geometric center of the head (Romanovsky and Blatteis, 1996; Conti et al., 2006; Baracchi and Opp, 2008; Steiner et al., 2008; Baud et al., 2013). Not surprisingly, therefore, brain temperatures reported in sleep studies (cortex temperature) are often a degree or two lower than brain temperatures reported in thermoregulation studies (hypothalamic temperature).

Infrared (IR) Thermography

IR thermography, or thermal imaging, decodes the IR radiation emitted from the surface (of an animal) into a color-coded image that can be analyzed in real time or post-recording (**Box 5**). Of all the methods described in this paper, IR thermography is the least invasive.

In typical applications, IR thermography does not yield deep body temperature, but measures surface (skin) temperature. As evident from individual IR thermograms (**Figure 4A**), surface heat radiation and, hence, surface temperature are not uniform across the body of the animal, which consists of both non-glabrous (hairy) and glabrous (non-hairy) skin (Romanovsky, 2014). Because of this heterogeneity, radiative temperature data in adult mice are often retrieved not from the entire body surface, but rather from predefined fields of view (FOVs) of a standardized size. Local surface temperature is then calculated as the average temperature across a selected FOV. Alternatively, a series of images is taken and the

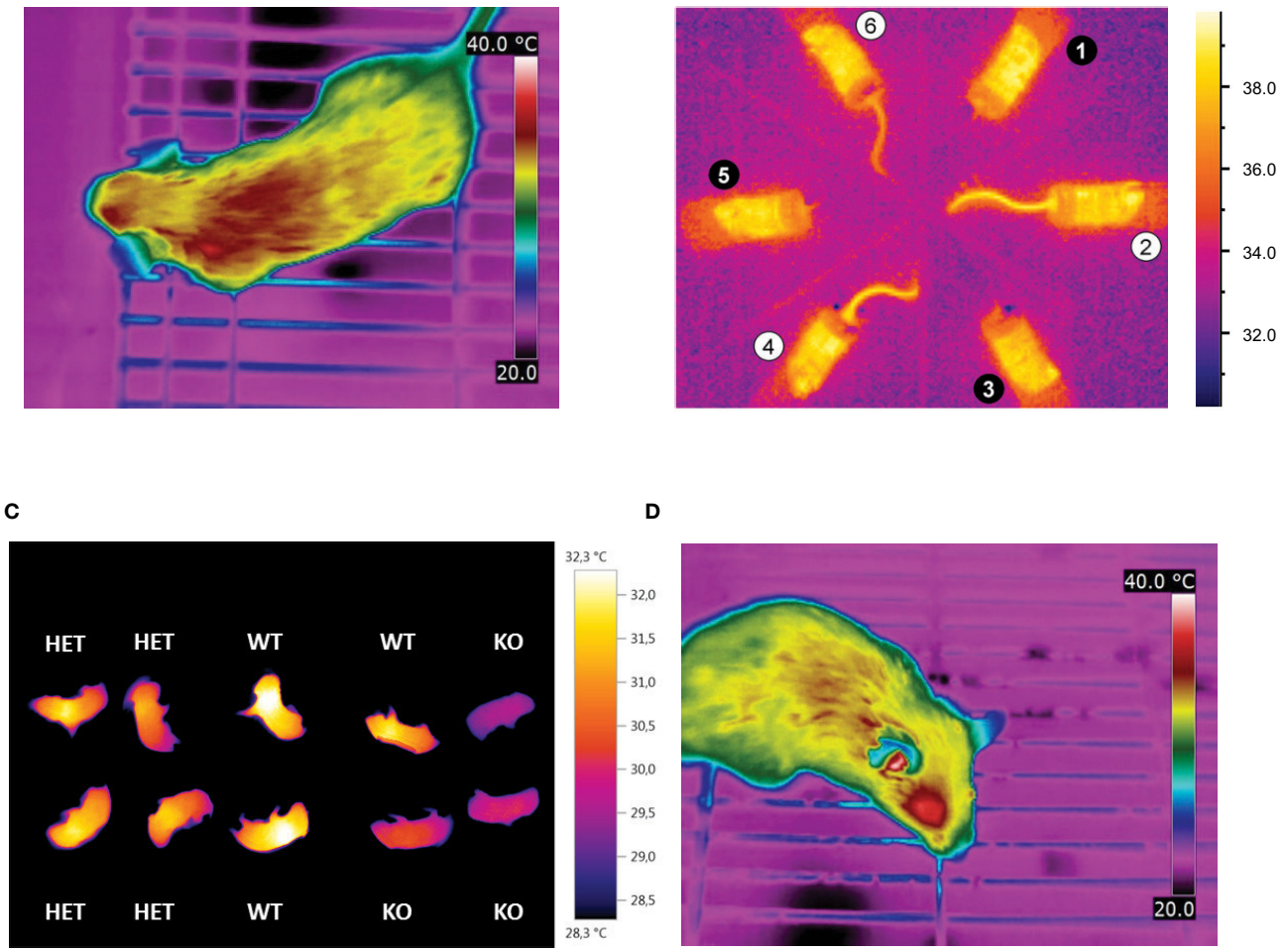

FIGURE 4 | Infrared (IR) thermography in mouse metabolic studies and phenotyping. In each panel, specific color coding of radiant heat is indicated to the right. **(A)** Dorsal view from an unrestrained, conscious wild-type mouse, captured by IR thermography (T335, FLIR Systems), demonstrating heterogeneity in surface temperatures by color coding. The ambient temperature was set to 22–23°C. Image kindly provided by R. Oelkrug and J. Mittag, unpublished. **(B)** Radiant temperature from mouse tails reveals enhanced skin vasoconstriction and altered autonomous vasomotor control in transient receptor potential vanilloid-1 (Trpv1)-knockout (KO) mice compared to wild-type controls (Garami et al., 2011). The IR camera (ThermoVision A20M, FLIR Systems) was positioned above a group of confined, conscious mice inside a climatic chamber at 32°C. The mice had been previously habituated to the experimental setup by extensive handling. **(C)** Whole-body thermography in neonates (p1–p3), highlighting reduced inter-scapular skin-surface temperature in association with genetic knockout of uncoupling protein-1 (UCP-1) and impaired non-shivering thermogenesis. For the measurement, pups were placed in 6-well cell culture plates at 22–23°C ambient temperature (Maurer et al., 2015). **(D)** Lateral view from an unrestrained, conscious wild-type mouse, captured by IR thermography (T335, FLIR Systems) for specific measurement of external acoustic meatus temperature. Ambient temperature was set to 22–23°C. Image kindly provided by R. Oelkrug and J. Mittag, unpublished.

maximum temperature is determined from the back surface area of the animal (Gachkar et al., 2017). For rather complex technical reasons, some researchers prefer to assess the surface temperature from the frequency distribution of temperature readings across the FOV, e.g., from the warmest 10% portion (Crane et al., 2014). In general, temperature determined by IR thermography can never overestimate but only underestimate skin temperature.

One of the most robust uses of IR thermography is to assess the thermoeffector role of the glabrous skin of specialized heat-loss organs, such as the tail in mice or rats, the ear in guinea pigs and rabbits, or the hand in humans. Specifically, IR thermography is used as a measure of vasomotor tone in these organs in order to confirm the presence or absence of vasoconstriction or vasodilation (Rudaya et al., 2005; Wang et al., 2006; Garami et al., 2011; Fischer et al., 2016; **Figure 4B**). It should be noted, however, that in most circumstances several skin temperature-based indices (e.g., the heat loss index Romanovsky et al., 2002) are better suited for this purpose than the tail-skin temperature *per se*. As an interesting modification suitable for some specific tasks, a semi-quantitative evaluation of the vasomotor tone of the skin covering heat-loss organs can be obtained by painting it with temperature-sensitive paint (Romanovsky et al., 2002).

Another application of IR thermometry is to use the information from vasomotor tone of heat-loss organs to determine the thermoneutral zone (TNZ; see Romanovsky et al., 2002). The authoritative sources (IUPS Thermal Commission, see Bligh and Johnson, 1973; Mercer and Werner, 2001) define the TNZ as the range of ambient temperatures at which body temperature regulation is achieved only by control of sensible heat loss, i.e., without changes in metabolic heat production or evaporative heat loss. "Sensible," or "Newtonian," heat loss is the total heat loss due to all heat exchange mechanisms, except for evaporation. In practice, the major physiological mechanism of sensible heat loss is cutaneous vasodilation, especially in body parts that serve as heat exchangers with the environment, such as the tail of a mouse. Hence, in a subneutral (cold) environment, the tails of mice exhibit constant maximal vasoconstriction (and are difficult to see in an IR thermogram as they have nearly the same temperature as the environment). In a supraneutral (hot) environment, the tails exhibit constant maximal vasodilation (and may or may not be well-seen on thermograms, depending on the ambient temperature). In a neutral environment (i.e., within the TNZ), the tails constantly change their vasomotor tone from mild vasoconstriction to mild vasodilation, thus become intermittently from almost invisible to highly visible (see Romanovsky et al., 2002, for more detailed information; see Garami et al., 2011, and **Figure 4B** for examples in mice). For studying thermogenic responses by IR thermography, tight control of the ambient temperature is essential. In such studies, mice should be conscious, as most anesthetics decrease the threshold body temperature for activation of cold defenses - thus, effectively inhibiting thermogenesis (Garami et al., in press).

The utility of IR thermography in assessing the vasomotor control in mice tails is exemplified by the metabolic phenotype of mice expressing a mutant thyroid hormone receptor alpha 1 (TRa1+m). In these mice, impaired vasoconstriction of the tail arteries leads to increased heat loss in cold environments and promotes hypothermia, despite elevated brown fat activity and energy expenditure. At first sight, the hypermetabolic phenotype was "paradoxical" (Warner and Mittag, 2014), since the mutation was expected to reduce the affinity of TRa1 to thyroid hormones and, hence, was predicted to lower thermogenesis. Subsequent studies of the thermoregulatory effector organs revealed that TRa1+m mice had a greater need for adaptive thermogenesis, as their vasomotor responses were ineffective at maintaining euthermia. These studies revealed an unexpected role of thyroid hormones in thermoregulation (Sjogren et al., 2007; Warner et al., 2013). Furthermore, these findings demonstrate that hypermetabolism is not necessarily associated with high body temperature.

IR thermography is also used to assess BAT thermogenesis in rodents. For this purpose, most researchers use the difference between radiative temperatures of the inter-scapular back-skin (covers the inter-scapular BAT depots) and the lumbar back-skin (reference point) as an index of thermogenesis in the inter-scapular BAT (e.g., Marks et al., 2009; Pazos et al., 2015). We find this approach to be well-grounded. Other researchers capture the absolute values of, or the changes (from basal value) in, the inter-scapular skin temperature for the same purpose (Gerhart-Hines et al., 2013; Crane et al., 2015). This latter approach is more prone to error, but still seems to work in some cases. For example, the increase in inter-scapular skin temperature observed in wild-type mice (1.7°C) in response to the selective beta-3 adrenergic agonist CL-316,243 was absent in UCP1-KO mice, corroborating compromised BAT-function (Crane et al., 2014). In contrast, this approach did not allow for the successful quantification of BAT thermogenic capacity following beta-adrenergic stimulation or cold acclimation in a study in voles (*Microtus agrestis*; Jackson et al., 2001).

Some researchers prefer shaving the skin in trunk FOVs, whilst others do not. Under most conditions, the shaved patches give higher surface temperature readings, as any insulative effect of the pelage is eliminated. In addition, shaving lessens the confounding diffusion and reflection effects of the pelage. Of course, this is not an issue in experiments with nude pups (**Figure 4C**) or genetically hairless animals (Chen et al., 2013; Schulz et al., 2013; Romanovsky, 2014; Maurer et al., 2015). Whether or not shaving is required depends on the IR signal intensity and the specific goal of measurements. However, we feel that shaving should be avoided whenever possible, as it creates "thermal windows," which may substantially increase heat loss, and thus, potentially change deep body temperature and affects the recruitment of thermoeffectors. Removing the hair also irritates the skin and can lead to inflammation, which can affect local temperatures. If repeated measurements, over a longer period of time, are required - shaving needs to be repeated frequently, as the trunk hair re-grows relatively fast (∼3 weeks in adult mice Muller-Rover et al., 2001). This alters conductivity and may subsequently change the cold-stress responsiveness.

IR thermometry also has the potential of assessing deep body temperature, but not by measuring trunk-skin temperature. The recent study by Vogel et al. (2016) proposes measuring radiative temperature of the eyes in mice, as an index of their brain temperature. The external acoustic meatus is another "window to the brain" that can possibly be used for assessing brain temperature of rodents by IR thermography or thermometry (Romanovsky, 2014; Hoefig et al., 2015, 2016, and **Figure 4D**).

CONCLUDING REMARKS

Metabolic phenotypes of genetically modified mice can help to establish causality between a specific gene or pathway and energy metabolism *in vivo*. In this context, animal temperature is often measured to uncover thermoregulatory alterations. Here, we have summarized the main thermometry methods used for the purposes of metabolic phenotyping in mice, and have investigated their utility. It is not only the type of sensor, but also the experimental conditions, probe location and sampling frequency, that determine the biological value of the results, driving successful phenotyping.

For comprehensive phenotyping involving thermometry, the thermal environment of the animals measured must be tightly controlled. Mice are small-sized endotherms with relatively high basal metabolic costs, owing to their unfavorable surface area to volume ratio (Kleiber, 1961). Mouse pelage has relatively poor insulative capacities, making this species sensitive

to cold and specifically reliant on creating and exploiting thermally advantageous microenvironments for cost-efficient body temperature regulation (Hart, 1971). Any metabolic study in mice, therefore, not only requires considerations of room temperature (gradients and variation) in the animal facility/experimental location, but also of the "operative ambient temperature" created by the animals inside the cage (Gordon et al., 1998). Factors known to affect individual metabolic costs, at otherwise constant room air temperature, are the type and amount of bedding material, nest material, and the opportunity to huddle with cagemates (Himms-Hagen and Villemure, 1992; Gordon et al., 1998; Gordon, 2004; David et al., 2013; Maher et al., 2015). Hence, control of any of these parameters potentially reduces variance in output values. Following the same reasoning, researchers should also keep in mind that any intervention or incident that disrupts the integrity of the skin/fur (e.g., shaving, surgery, alopecia) may cause specific thermoregulatory adjustments potentially contributing to extra variation in metabolic costs.

In order to provide a more complete thermoregulatory portrait of a certain genotype, it is essential that thermometry not be limited to measurements of body temperature under standard housing conditions. Rather, temperature readings should be obtained and compared at thermoneutral vs. sub-thermoneutral (cold) and supra-neutral (warm) conditions - aiming to reveal specific deficiencies in cold and heat defenses. For the same purpose, we advocate combining measurements of core body temperature with tail thermography and back thermography (Gachkar et al., 2017). In order to reveal thermoregulatory phenotypes associated with behavioral thermoregulation, temperature readings could be combined with, for example, food restriction challenges (Haemmerle et al., 2006; Meyer et al., 2010), behavioral tasks, e.g., temperature preference chambers, thermal gradients (Gordon et al., 1998; Bautista et al., 2007), or operant conditioning for thermal reward (Baldwin, 1968; Carlisle and Dubuc, 1982).

It is advantageous to conduct high-resolution core body temperature measurements in conjunction with measurements of metabolic rate, for the assessment for heat production rates at tightly controlled ambient temperatures. This experimental scheme not only determines the energy expenditure and associated body temperature variations, but also allows for the assessment of thermal conductance of the animals (**Box 6**)-a quantitative measure of the rate of heat exchange between the animal's body and the environment (McNab, 1980). In the example shown in **Figure 5**, thermal conductance is compared in the context of cold tolerance in UCP1-KO mice. Conductance is consistently lower in cold-acclimated UCP1-KO mice, which supports the conclusion that cold acclimation in the absence of functional BAT involves specific heat-conserving mechanisms, including improved tail vasoconstriction (Wang et al., 2006).

In terms of animal welfare, hyper- or hypothermic thresholds are to be established and applied carefully, as periodic deviations from "normal" temperature ranges are context-, time- and strain-dependent, and may not unequivocally indicate an acute life-threatening condition. For example, during torpor, a physiological state of metabolic depression (Jastroch et al., 2016), the abdominal body temperature of a mouse may transiently reach values that are only half a degree higher than the ambient temperature. Murine torpor commonly occurs during the early morning hours and can, in principle, be diagnosed by rectal probing. Following handling, acoustic, haptic or mechanical stimulation, a healthy mouse "alarm-arouses" and regains what is often referred to as normal metabolism and normothermy within 1–2 h, depending on the degree of metabolic depression and the ambient temperature. Of note, the classification of normothermy vs. torpor is often based on metrics of heterothermy, e.g., the amplitude of daily body temperature fluctuations (see Levesque

BOX 6 | Thermal conductance.

Metabolic phenotypes involving alterations in body temperature often depend on changes in thermogenesis (heat production), but they also reflect altered heat loss characteristics. Thermal conductance [*C*] describes the rate of heat production necessary to compensate for heat loss, i.e., the difference in temperature between the body and its surroundings (ambient temperature, T_a). Mathematically, *C* is obtained from the slope of the linear increase in (dry) heat loss (excluding evaporation) with decreasing ambient temperature (T_a) at temperatures cooler than thermoneutrality (Equation 1). For comparative purposes, thermal conductance should be indicated as a positive number, indicating that heat exchange is directed from the warmer to the cooler environment and not vice versa (McNab, 1980).

$$\text{Equation 1: } C = HP^{*}(T_b - T_a)^{-1}$$

$$C = \text{thermal conductance } (\text{Watts}^{\circ}\text{C}^{-1})$$

$$HP = \text{heat production (Watts, W)}$$

$$T_b = \text{body temperature } (^{\circ}\text{C})$$

$$T_a = \text{ambient (air) temperature } (^{\circ}\text{C})$$

Figure 5A depicts an example of this type of analysis for cold-acclimated uncoupling-protein 1 (UCP1)-knockout (KO) mice. HP was determined using indirect calorimetry. When only HP associated with resting conditions is considered, the HP-T_a regression extrapolates to predicted resting body temperature ("theoretical body temperature") at zero HP, and the slope of the T_a-HP regression elucidates minimal conductance (i.e., the minimal rate of heat production required to maintain the largest possible normothermic T_b-T_a gradient; McNab, 1980). In the example shown in **Figure 5A**, the predicted thermal conductance (slope) is lower in UCP1-KO mice (at $p < 0.08$), and the expected core T_b is similar between genotypes, with a trend toward higher values in KO mice. Biologically, this indicates that UCP1-KO mice are more efficient at conserving heat.

Alternatively, HP, T_a, and core T_b are measured jointly and *C* is obtained using Equation (1). Re-analysing the data and including the corresponding abdominal T_bs measured in the same individuals confirmed that average thermal conductance in moderate cold was lower in UCP1-KO mice, (**Figure 5B**).

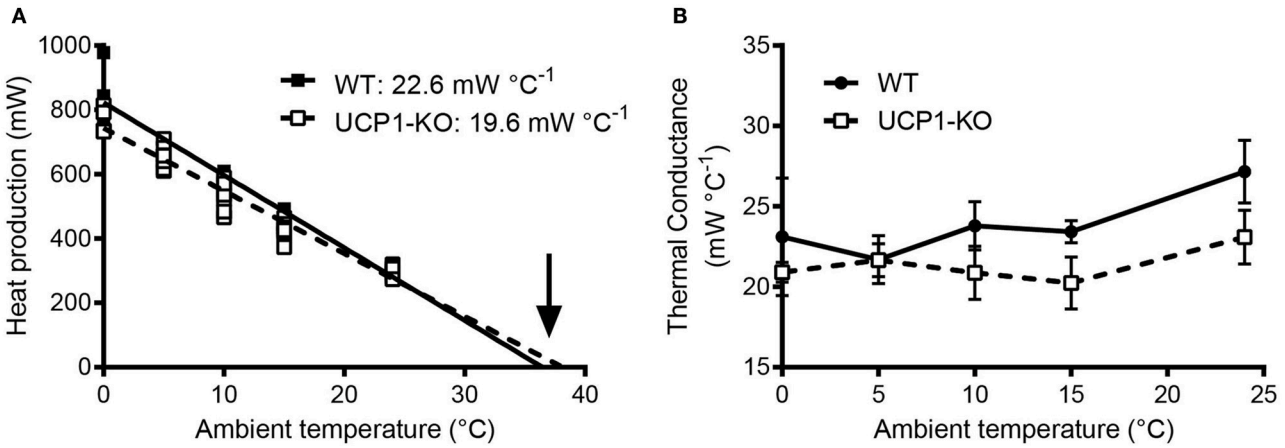

FIGURE 5 | (A) Assessment of thermal conductance using resting heat production rates collected in wild-type and uncoupling-protein-1 (UCP1-KO)-deficient littermates at different ambient temperatures ("Scholander-Irving plot"; Scholander et al., 1950). Average slopes corresponding to predicted minimal thermal conductance (expressed as positive values) are indicated for each genotype ($p = 0.08$, t-test). The arrow highlights the x-axis intersection points corresponding to the predicted average body temperature during resting conditions (not different between genotypes; $p = 0.44$, t-test). **(B)** Calculated thermal conductance (see **Box 6**) involving core body temperature readings (E-Mitter Series 3000 XM-FH) in the animals shown in **(A)**. Each point indicates mean ± SD ($n = 4$–7). Both analyses, **(A,B)**, are supporting lower thermal conductance and thus an altered thermoregulatory strategy involving improved heat conservation in UCP1-KO mice. Data are taken from Meyer et al. (2010).

et al., 2016, for further reading and current discussion). If a torpid mouse is left undisturbed, spontaneous arousal usually takes place by late morning to midday, but the specific onset of this process and the duration of torpor can be highly variable among strains and individuals (Dikic et al., 2008). In contrast, animals with severe energetic depletion or some metabolic deficiencies are often unable to rewarm themselves endogenously (Haemmerle et al., 2006; Oelkrug et al., 2011). In this case, 1–2 h of passive rewarming (e.g., through infrared heaters) and food and water provision are warranted (**Figure 2D**). Torpor frequency and associated temperature changes can be considered a metabolic phenotype and, as such, merit exploration (Jethwa et al., 2008; Swoap, 2008; Willershäuser et al., 2012).

In naive mice, a stress-induced body temperature rise can be initiated by opening the cage or even by entering the animal room. In addition, when mice are picked one-by-one from a cage, the level of distress builds up in the remaining mice kept in this cage, and the measured body temperature increases drastically from the first to the last mouse taken from the cage (Zethof et al., 1994). In this case, and in many other cases, part of the increase in body temperature can be explained by motor activity, which is directly thermogenic. Indeed, changes in the body temperature of mice follow, with some delay, changes in their motor activity (Lateef et al., 2014). In contrast, data in rats and humans suggest that rises in core temperature precede the onset of activity (Refinetti and Menaker, 1992; Decoursey et al., 1998; Ootsuka et al., 2009), as is noted to occur during ultradian cycles. While the discussion of the presence and significance of ultradian rhythms in thermogenesis is beyond the scope of this review, the technical sensitivity assessing ultradian fluctuations and temporal associations in body temperature with other physiological parameters is critically dependent on the sampling interval. In this context, we and others (Blessing and Ootsuka, 2016) recommend examination of the individual records be routinely performed before any results are averaged.

Taken together, thermometry significantly expands the metabolic phenotyping toolbox, because the interplay between heat loss and heat production can be addressed (e.g., Kaiyala et al., 2015; Abreu-Vieira et al., 2015; Fischer et al., 2016, 2017). Multi-parametric measurements involving thermometry increase the probability of revealing distinct metabolic and thermoregulatory phenotypes.

ETHICS STATEMENT

This work does not contain any animal data that was specifically collected for the purpose of publication in this manuscript. Animal data presented refer to approved experiments published elsewhere.

AUTHOR CONTRIBUTIONS

All authors have made substantial contributions to the conception or design of the work, which includes drafting the work, and revising it critically for important intellectual content.

ACKNOWLEDGMENTS

CWM would like to thank Iain Patten for support with the initial drafting of this work. All authors thank Anna Antipov for language editing.

REFERENCES

Abreu-Vieira, G., Xiao, C., Gavrilova, O., and Reitman, M. L. (2015). Integration of body temperature into the analysis of energy expenditure in the mouse. *Mol. Metab.* 4, 461–470. doi: 10.1016/j.molmet.2015.03.001

Almeida, M. C., Hew-Butler, T., Soriano, R. N., Rao, S., Wang, W., Wang, J., et al. (2012). Pharmacological blockade of the cold receptor TRPM8 attenuates autonomic and behavioral cold defenses and decreases deep body temperature. *J. Neurosci.* 32, 2086–2099. doi: 10.1523/JNEUROSCI.5606-11.2012

Almeida, M. C., Steiner, A. A., Branco, L. G., and Romanovsky, A. A. (2006). Cold-seeking behavior as a thermoregulatory strategy in systemic inflammation. *Eur. J. Neurosci.* 23, 3359–3367. doi: 10.1111/j.1460-9568.2006.04854.x

Bal, N. C., Maurya, S. K., Sopariwala, D. H., Sahoo, S. K., Gupta, S. C., Shaikh, S. A., et al. (2012). Sarcolipin is a newly identified regulator of muscle-based thermogenesis in mammals. *Nat. Med.* 18, 1575–1579. doi: 10.1038/nm.2897

Baldwin, B. A. (1968). Behavioural thermoregulation in mice. *Physiol. Behav.* 3, 401–407. doi: 10.1016/0031-9384(68)90069-3

Baracchi, F., and Opp, M. R. (2008). Sleep-wake behavior and responses to sleep deprivation of mice lacking both interleukin-1 beta receptor 1 and tumor necrosis factor-alpha receptor 1. *Brain Behav. Immun.* 22, 982–993. doi: 10.1016/j.bbi.2008.02.001

Baud, M. O., Magistretti, P. J., and Petit, J. M. (2013). Sustained sleep fragmentation affects brain temperature, food intake and glucose tolerance in mice. *J. Sleep Res.* 22, 3–12. doi: 10.1111/j.1365-2869.2012.01029.x

Bautista, D. M., Siemens, J., Glazer, J. M., Tsuruda, P. R., Basbaum, A. I., Stucky, C. L., et al. (2007). The menthol receptor TRPM8 is the principal detector of environmental cold. *Nature* 448, 204–208. doi: 10.1038/nature05910

Blessing, W., and Ootsuka, Y. (2016). Timing of activities of daily life is jaggy: how episodic ultradian changes in body and brain temperature are integrated into this process. *Temperature (Austin)* 3, 371–383. doi: 10.1080/23328940.2016.1177159

Bligh, J., and Johnson, K. G. (1973). Glossary of terms for thermal physiology. *J. Appl. Physiol.* 36, 941–961.

Carlisle, H. J., and Dubuc, P. U. (1982). Unchanged thermoregulatory set-point in the obese mouse. *Nature* 297, 678–679. doi: 10.1038/297678a0

Chen, Y., Siegel, F., Kipschull, S., Haas, B., Frohlich, H., Meister, G., et al. (2013). miR-155 regulates differentiation of brown and beige adipocytes via a bistable circuit. *Nat. Commun.* 4:1769. doi: 10.1038/ncomms2742

Clement, J. G., Mills, P., and Brockway, B. (1989). "Use of telemetry to record body temperature and activity in mice." *J. Pharmacol. Methods* 21, 129–140. doi: 10.1016/0160-5402(89)90031-4

Conti, B., Sanchez-Alavez, M., Winsky-Sommerer, R., Morale, M. C., Lucero, J., Brownell, S., et al. (2006). Transgenic mice with a reduced core body temperature have an increased life span. *Science* 314, 825–828. doi: 10.1126/science.1132191

Cossins, A. R., and Bowler, K. (1987). *Temperature Biology of Animals*. London; New York, NY: Chapman and Hall.

Crane, J. D., Mottillo, E. P., Farncombe, T. H., Morrison, K. M., and Steinberg, G. R. (2014). A standardized infrared imaging technique that specifically detects UCP1-mediated thermogenesis *in vivo*. *Mol. Metab.* 3, 490–494. doi: 10.1016/j.molmet.2014.04.007

Crane, J. D., Palanivel, R., Mottillo, E. P., Bujak, A. L., Wang, H., Ford, R. J., et al. (2015). Inhibiting peripheral serotonin synthesis reduces obesity and metabolic dysfunction by promoting brown adipose tissue thermogenesis. *Nat. Med.* 21, 166–172. doi: 10.1038/nm.3766

David, J. M., Knowles, S., Lamkin, D. M., and Stout, D. B. (2013). Individually ventilated cages impose cold stress on laboratory mice: a source of systemic experimental variability. *J. Am. Assoc. Lab. Anim. Sci.* 52, 738–744.

Deboer, T., Franken, P., and Tobler, I. (1994). Sleep and cortical temperature in the Djungarian hamster under baseline conditions and after sleep deprivation. *J. Com. Physiol. A* 174, 145–155. doi: 10.1007/bf00193782

DeBow, S., and Colbourne, F. (2003). Brain temperature measurement and regulation in awake and freely moving rodents. *Methods* 30, 167–171. doi: 10.1016/s1046-2023(03)00080-x

Decoursey, P. J., Pius, S., Sandlin, C., Wethey, D., and Schull, J. (1998). Relationship of circadian temperature and activity rhythms in two rodent species. *Physiol. Behav.* 65, 457–463. doi: 10.1016/S0031-9384(98)00187-5

Dikic, D., Heldmaier, G., and Meyer, C. W. (2008). "Induced torpor in different strains of laboratory mice," in *Hypometabolism in Animals: Torpor, Hibernation and Cryobiology*, eds B. G. Lovegrove and A. E. McKechnie (Pietermaritzburg: University of KwaZulu-Natal), 223–230.

Donhoffer, S. (1980). *Homeothermia of the Brain: Cerebral Blood Flow, Metabolic Rate, and Brain Temperature in the Cold: the Possible Role of Neuroglia*. Budapest, Akadémiai Kiadó.

Fischer, A. W., Hoefig, C. S., Abreu-Vieira, G., de Jong, J. M., Petrovic, N., Mittag, J., et al. (2016). Leptin raises defended body temperature without activating thermogenesis. *Cell Rep.* 14, 621–1631. doi: 10.1016/j.celrep.2016.01.041

Fischer, K., Ruiz, H. H., Jhun, K., Finan, B., Oberlin, D. J., van der Heide, V., et al. (2017). Alternatively activated macrophages do not synthesize catecholamines or contribute to adipose tissue adaptive thermogenesis. *Nat. Med.* 23, 623–630. doi: 10.1038/nm.4316

Gachkar, S., Oelkrug, R., Martinez-Sanchez, N., Rial-Pensado, E., Warner, A., Hoefig, C. S., et al. (2017). 3-Iodothyronamine induces tail vasodilation through central action in male mice. *Endocrinology* 158, 1977–1984. doi: 10.1210/en.2016-1951

Garami, A., Ibrahim, M., Gilbrait, K., Khanna, R., Pakai, E., Miko, A., et al. (in press). TRPV1 antagonists prevent anesthesia-induced hypothermia and decrease post-incisional opioid dose requirements in rodents. *Anesthesiology*.

Garami, A., Pakai, E., Oliveira, D. L., Steiner, A. A., Wanner, S. P., Almeida, M. C., et al. (2011). Thermoregulatory phenotype of the Trpv1 knockout mouse: thermoeffector dysbalance with hyperkinesis. *J. Neurosci.* 31, 1721–1733. doi: 10.1523/JNEUROSCI.4671-10.2011

Gerhart-Hines, Z., Feng, D., Emmett, M. J., Everett, L. J., Loro, E., Briggs, E. R., et al. (2013). The nuclear receptor Rev-erbalpha controls circadian thermogenic plasticity. *Nature* 503, 410–413. doi: 10.1038/nature12642

Gordon, C. J. (1993). *Temperature Regulation in Laboratory Rodents*. Cambridge: Cambridge University Press.

Gordon, C. J. (2004). Effect of cage bedding on temperature regulation and metabolism of group-housed female mice. *Comp. Med.* 54, 63–68.

Gordon, C. J., Becker, P., and Ali, J. S. (1998). Behavioral thermoregulatory responses of single- and group-housed mice. *Physiol. Behav.* 65, 255–262. doi: 10.1016/S0031-9384(98)00148-6

Haemmerle, G., Lass, A., Zimmermann, R., Gorkiewicz, G., Meyer, C., Rozman, J., et al. (2006). Defective lipolysis and altered energy metabolism in mice lacking adipose triglyceride lipase. *Science* 312, 734–737. doi: 10.1126/science.1123965

Hart, J. S. (1971). "Rodents," in *Comparative Physiology of Thermoregulation*, Vol. 2, eds G. C. Whittow (New York, NY; London: Academic Press), 1–149.

Hashimoto, K., Suemaru, S., Takao, T., Sugawara, M., Makino, S., and Ota, Z. (1988). Corticotropin-releasing hormone and pituitary-adrenocortical responses in chronically stressed rats. *Regul. Pept.* 23, 17–126. doi: 10.1016/0167-0115(88)90019-5

Heldmaier, G., and Ruf, T. (1992). Body temperature and metabolic rate during natural hypothermia in endotherms. *J. Comp. Physiol. B. Biochem. Syst. Environ. Physiol.* 162, 696–706. doi: 10.1007/BF00301619

Himms-Hagen, J., and Villemure, C. (1992). Number of mice per cage influences uncoupling protein content of brown adipose tissue. *Proc. Soc. Exp. Biol. Med.* 200, 502–506. doi: 10.3181/00379727-200-43461

Hoefig, C. S., Harder, L., Oelkrug, R., Meusel, M., Vennstrom, B., Brabant, G., et al. (2016). Thermoregulatory and cardiovascular consequences of a transient Thyrotoxicosis and recovery in male mice. *Endocrinology* 157, 2957–2967. doi: 10.1210/en.2016-1095

Hoefig, C. S., Jacobi, S. F., Warner, A., Harder, L., Schanze, N., Vennstrom, B., et al. (2015). 3-Iodothyroacetic acid lacks thermoregulatory and cardiovascular effects *in vivo*. *Br. J. Pharmacol.* 172, 3426–3433. doi: 10.1111/bph.13131

Jackson, D. M., Hambly, C., Trayhurn, P., and Speakman, J. R. (2001). Can non-shivering thermogenesis in brown adipose tissue following NA injection be quantified by changes in overlying surface temperatures using infrared thermography? *J. Therm. Biol.* 26, 85–93. doi: 10.1016/S0306-4565(00)00023-1

Jastroch, M., Giroud, S., Barrett, P., Geiser, F., Heldmaier, G., and Herwig, A. (2016). Seasonal control of mammalian energy balance: recent advances in the understanding of daily torpor and hibernation. *J. Neuroendocrinol.* 28. doi: 10.1111/jne.12437

Jethwa, P. H., I'Anson, H., Warner, A., Prosser, H. M., Hastings, M. H., Maywood, E. S., et al. (2008). Loss of prokineticin receptor 2 signaling predisposes mice

to torpor. *Am. J. Physiol. Regul. Integr. Comp. Physiol.* 294, R1968–R1979. doi: 10.1152/ajpregu.00778.2007

Kaiyala, K. J., Ogimoto, K., Nelson, J. T., Schwartz, M. W., and Morton, G. J. (2015). Leptin signaling is required for adaptive changes in food intake, but not energy expenditure, in response to different thermal conditions. *PLoS ONE* 10:e0119391. doi: 10.1371/journal.pone.0119391

Kleiber, M. (1961). *The Fire of Life*. New York, NY; London: John Wiley and Sons Inc.

Lateef, D. M., Abreu-Vieira, G., Xiao, C., and Reitman, M. L. (2014). Regulation of body temperature and brown adipose tissue thermogenesis by bombesin receptor subtype-3. *Am. J. Physiol. Endocrinol. Metab.* 306, E681–E687. doi: 10.1152/ajpendo.00615.2013

Levesque, D., Nowack, J., and Stawski, C. (2016). Modelling mammalian energetics: the heterothermy problem. *Clim. Change Respon.* 3:7. doi: 10.1186/s40665-016-0022-3

Maher, R. L., Barbash, S. M., Lynch, D. V., and Swoap, S. J. (2015). Group housing and nest building only slightly ameliorate the cold stress of typical housing in in female C57BL/6J mice. *Am. J. Physiol. Regul. Integr. Comp. Physiol.* 308, R1070–R1079. doi: 10.1152/ajpregu.00407.2014

Marks, A., Vianna, D. M., and Carrive, P. (2009). Nonshivering thermogenesis without interscapular brown adipose tissue involvement during conditioned fear in the rat. *Am. J. Physiol. Regul. Integr. Comp. Physiol.* 296, R1239–R1247. doi: 10.1152/ajpregu.90723.2008

Maurer, S. F., Fromme, T., Grossman, L. I., Huttemann, M., and Klingenspor, M. (2015). The brown and brite adipocyte marker Cox7a1 is not required for non-shivering thermogenesis in mice. *Sci. Rep.* 5:17704. doi: 10.1038/srep17704

McNab, B. K. (1980). On estimating thermal conductance in endotherms. *Physiol. Zool.* 53, 145–156. doi: 10.1086/physzool.53.2.30152577

Melia, K. R., Ryabinin, A. E., Schroeder, R., Bloom, F. E., and Wilson, M. C. (1994). Induction and habituation of immediate early gene expression in rat brain by acute and repeated restraint stress. *J. Neurosci.* 14, 5929–5938.

Mercer, J. G., and Werner, J. (2001). Glossary of terms for thermal physiology. *Jpn. J. Physiol.* 51, 245–280.

Meyer, C. W., Reitmeir, P., and Tschop, M. H. (2015). Exploration of Energy Metabolism in the Mouse Using Indirect Calorimetry: measurement of daily energy expenditure (DEE) and basal metabolic rate (BMR). *Curr. Protoc. Mouse Biol.* 5, 205–222. doi: 10.1002/9780470942390.mo140216

Meyer, C. W., Willershauser, M., Jastroch, M., Rourke, B. C., Fromme, T., Oelkrug, R., et al. (2010). Adaptive thermogenesis and thermal conductance in wild-type and UCP1-KO mice. *Am. J. Physiol. Regul. Integr. Comp. Physiol.* 299, R1396–R1406. doi: 10.1152/ajpregu.00021.2009

Miyata, K., Kuwaki, T., and Ootsuka, Y. (2016). The integrated ultradian organization of behavior and physiology in mice and the contribution of orexin to the ultradian patterning. *Neuroscience* 334, 119–133. doi: 10.1016/j.neuroscience.2016.07.041

Mohammed, M., Ootsuka, Y., Yanagisawa, M., and Blessing, W. (2014). Reduced brown adipose tissue thermogenesis during environmental interactions in transgenic rats with ataxin-3-mediated ablation of hypothalamic orexin neurons. *Am. J. Physiol. Regul. Integr. Comp. Physiol.* 307, R978–R989. doi: 10.1152/ajpregu.00260.2014

Moir, L., Bentley, L., and Cox, R. D. (2016). Comprehensive energy balance measurements in mice. *Curr. Protoc. Mouse Biol.* 6, 211–222. doi: 10.1002/cpmo.13

Muller, T. D., Lee, S. J., Jastroch, M., Kabra, D., Stemmer, K., Aichler, M., et al. (2013). p62 links beta-adrenergic input to mitochondrial function and thermogenesis. *J. Clin. Invest.* 123, 469–478. doi: 10.1172/JCI64209

Muller-Rover, S., Handjiski, B., van der Veen, C., Eichmuller, S., Foitzik, K., McKay, I. A., et al. (2001). A comprehensive guide for the accurate classification of murine hair follicles in distinct hair cycle stages. *J. Invest. Dermatol.* 117, 3–15. doi: 10.1046/j.0022-202x.2001.01377.x

Oelkrug, R., Heldmaier, G., and Meyer, C. W. (2011). Torpor patterns, arousal rates, and temporal organization of torpor entry in wildtype and UCP1-ablated mice. *J. Comp. Physiol. B. Biochem. Syst. Environ. Physiol.* 181, 137–145. doi: 10.1007/s00360-010-0503-9

Ootsuka, Y., de Menezes, R. C., Zaretsky, D. V., Alimoradian, A., Hunt, J., Stefanidis, A., et al. (2009). Brown adipose tissue thermogenesis heats brain and body as part of the brain-coordinated ultradian basic rest-activity cycle. *Neuroscience* 164, 849–861. doi: 10.1016/j.neuroscience.2009.08.013

Ootsuka, Y., Heidbreder, C. A., Hagan, J. J., and Blessing, W. W. (2007). Dopamine D2 receptor stimulation inhibits cold-initiated thermogenesis in brown adipose tissue in conscious rats. *Neuroscience* 147, 127–135. doi: 10.1016/j.neuroscience.2007.04.015

Pazos, P., Lima, L., Tovar, S., Gonzalez-Touceda, D., Dieguez, C., and Garcia, M. C. (2015). Divergent responses to thermogenic stimuli in BAT and subcutaneous adipose tissue from interleukin 18 and interleukin 18 receptor 1-deficient mice. *Sci. Rep.* 5:17977. doi: 10.1038/srep17977

Refinetti, R., and Menaker, M. (1992). The circadian rhythm of body temperature. *Physiol. Behav.* 51, 613–637. doi: 10.1016/0031-9384(92)90188-8

Romanovsky, A. (2014). Skin temperature: its role in thermoregulation. *Acta Physiol.* 210, 498–507. doi: 10.1111/apha.12231

Romanovsky, A. A., and Blatteis, C. M. (1996). Heat stroke: opioid-mediated mechanisms. *J. Appl. Physiol.* 81, 2565–2570.

Romanovsky, A. A., Ivanov, A. I., and Shimansky, Y. P. (2002). Selected contribution: ambient temperature for experiments in rats: a new method for determining the zone of thermal neutrality. *J. Appl. Physiol.* 92, 2667–2679. doi: 10.1152/japplphysiol.01173.2001

Romanovsky, A. A., Kulchitsky, V. A., Akulich, N. V., Koulchitsky, S. V., Simons, C. T., Sessler, D. I., et al. (1996). First and second phases of biphasic fever: two sequential stages of the sickness syndrome? *Am. J. Physiol.* 271(1 Pt 2), R244–R253.

Romanovsky, A. A., Simons, C. T., and Kulchitsky, V. A. (1998). Biphasic fevers often consist of more than two phases. *Am. J. Physiol.* 275(1 Pt 2), R323–R331.

Romanovsky, A. A., Simons, C. T., Szekely, M., and Kulchitsky, V. A. (1997). The vagus nerve in the thermoregulatory response to systemic inflammation. *Am. J. Physiol.* 273(1 Pt 2), R407–R413.

Rozman, J., Klingenspor, M., and Hrabe de Angelis, M. (2014). A review of standardized metabolic phenotyping of animal models. *Mamm. Genome* 25, 497–507. doi: 10.1007/s00335-014-9532-0

Rudaya, A. Y., Steiner, A. A., Robbins, J. R., Dragic, A. S., and Romanovsky, A. A. (2005). Thermoregulatory responses to lipopolysaccharide in the mouse: dependence on the dose and ambient temperature. *Am. J. Physiol. Regul. Integr. Comp. Physiol.* 289, R1244–R1252. doi: 10.1152/ajpregu.00370.2005

Scholander, P. F., Hock, R., Walters, V., and Irving, L. (1950). Adaptation to cold in arctic and tropical mammals and birds in relation to body temperature insulation, and basal metabolic rate. *Biol. Bull.* 99, 259–271. doi: 10.2307/1538742

Schulz, T. J., Huang, P., Huang, T. L., Xue, R., McDougall, L. E., Townsend, K. L., et al. (2013). Brown-fat paucity due to impaired BMP signalling induces compensatory browning of white fat. *Nature* 495, 379–383. doi: 10.1038/nature11943

Sjogren, M., Alkemade, A., Mittag, J., Nordstrom, K., Katz, A., Rozell, B., et al. (2007). Hypermetabolism in mice caused by the central action of an unliganded thyroid hormone receptor alpha1. *EMBO J.* 26, 4535–4545. doi: 10.1038/sj.emboj.7601882

Smith, R. E., and Horwitz, B. A. (1969). Brown fat and thermogenesis. *Physiol. Rev.* 49, 330–425.

Solymar, M., Petervari, E., Balasko, M., and Szelenyi, Z. (2015). The onset of daily torpor is regulated by the same low body mass in lean mice and in mice with diet-induced obesity. *Temperature (Austin)* 2, 129–134. doi: 10.1080/23328940.2015.1014250

Speakman, J. R. (2013). Measuring energy metabolism in the mouse - theoretical, practical, and analytical considerations. *Front. Physiol.* 4:34. doi: 10.3389/fphys.2013.00034

Speakman, J. R., and Ward, S. (1998). Infrared thermography: principles and applications. *Zool. Anal. Complex Systems* 101, 224–232.

Stamp, J. A., and Herbert, J. (1999). Multiple immediate-early gene expression during physiological and endocrine adaptation to repeated stress. *Neuroscience* 94, 1313–1322. doi: 10.1016/S0306-4522(99)00368-1

Steiner, A. A., Chakravarty, S., Rudaya, A. Y., Herkenham, M., and Romanovsky, A. A. (2006). Bacterial lipopolysaccharide fever is initiated via Toll-like receptor 4 on hematopoietic cells. *Blood* 107, 4000–4002. doi: 10.1182/blood-2005-11-4743

Steiner, A. A., Oliveira, D. L., Roberts, J. L., Petersen, S. R., and Romanovsky, A. A. (2008). Nicotine administration and withdrawal affect survival in systemic inflammation models. *J. Appl. Physiol.* 105, 1028–1034. doi: 10.1152/japplphysiol.90619.2008

Steiner, A. A., Turek, V. F., Almeida, M. C., Burmeister, J. J., Oliveira, D. L., Roberts, J. L., et al. (2007). Nonthermal activation of transient receptor potential vanilloid-1 channels in abdominal viscera tonically inhibits autonomic cold-defense effectors. *J. Neurosci.* 27, 7459–7468. doi: 10.1523/JNEUROSCI.1483-07.2007

Swoap, S. J. (2008). The pharmacology and molecular mechanisms underlying temperature regulation and torpor. *Biochem. Pharmacol.* 76, 817–824. doi: 10.1016/j.bcp.2008.06.017

Szekely, M., and Szelenyi, Z. (1979). Endotoxin fever in the rat. *Acta Physiol. Acad. Sci. Hung.* 53, 265–277.

Szekely, M., Szelenyi, Z., and Sumegi, I. (1973). Brown adipose tissue as a source of heat during pyrogen-induced fever. *Acta Physiol. Acad. Sci. Hung.* 43, 85–88.

Tschöp, M. H., Speakman, J. R., Arch, J. R., Auwerx, J., Bruning, J. C., Chan, L., et al. (2012). A guide to analysis of mouse energy metabolism. *Nat. Methods* 9, 57–63. doi: 10.1038/nmeth.1806

Vogel, B., Wagner, H., Gmoser, J., Worner, A., Loschberger, A., Peters, L., et al. (2016). Touch-free measurement of body temperature using close-up thermography of the ocular surface. *MethodsX* 3, 407–416. doi: 10.1016/j.mex.2016.05.002

Wang, Y., Kimura, K., Inokuma, K., Saito, M., Kontani, Y., Kobayashi, Y., et al. (2006). Potential contribution of vasoconstriction to suppression of heat loss and homeothermic regulation in UCP1-deficient mice. *Pflugers Arch.* 452, 363–369. doi: 10.1007/s00424-005-0036-3

Wanner, S. P., Garami, A., Pakai, E., Oliveira, D. L., Gavva, N. R., Coimbra, C. C., et al. (2012). Aging reverses the role of the transient receptor potential vanilloid-1 channel in systemic inflammation from anti-inflammatory to proinflammatory. *Cell Cycle* 11, 343–349. doi: 10.4161/cc.11.2.18772

Ward, C. S., Arvide, E. M., Huang, T. W., Yoo, J., Noebels, J. L., and Neul, J. L. (2011). MeCP2 is critical within HoxB1-derived tissues of mice for normal lifespan. *J. Neurosci.* 31, 10359–10370. doi: 10.1523/JNEUROSCI.0057-11.2011

Warner, A., and Mittag, J. (2014). Brown fat and vascular heat dissipation: the new cautionary tail. *Adipocyte* 3, 221–223. doi: 10.4161/adip.28815

Warner, A., Rahman, A., Solsjo, P., Gottschling, K., Davis, B., Vennstrom, B., et al. (2013). Inappropriate heat dissipation ignites brown fat thermogenesis in mice with a mutant thyroid hormone receptor alpha1. *Proc. Natl. Acad. Sci. U.S.A.* 110, 16241–16246. doi: 10.1073/pnas.1310300110

Willershäuser, M., Ehrhardt, N., Elvert, R., Wirth, E. K., Schweizer, U., Gailus-Durner, V., et al. (2012). "Systematic screening for mutant mouse lines with defects in body temperature regulation," in *Living in a Seasonal World: Thermoregulatory and Metabolic Adaptations*, eds T. Ruf, C. Bieber, W. Arnold, and E. Millesi (Berlin, Heidelberg: Springer-Verlag), 459–469.

Wither, R. G., Colic, S., Wu, C., Bardakjian, B. L., Zhang, L., and Eubanks, J. H. (2012). Daily rhythmic behaviors and thermoregulatory patterns are disrupted in adult female MeCP2-deficient mice. *PLoS ONE* 7:e35396. doi: 10.1371/journal.pone.0035396

Zethof, T. J., Van der Heyden, J. A., Tolboom, J. T., and Olivier, B. (1994). Stress-induced hyperthermia in mice: a methodological study. *Physiol. Behav.* 55, 109–115. doi: 10.1016/0031-9384(94)90017-5

Conflict of Interest Statement: The authors declare that the research was conducted in the absence of any commercial or financial relationships that could be construed as a potential conflict of interest.

frontiers in Physiology

OPINION
published: 02 November 2017
doi: 10.3389/fphys.2017.00842

Phoenix from the Ashes: Fire, Torpor, and the Evolution of Mammalian Endothermy

Fritz Geiser[1]*, *Clare Stawski*[1], *Chris B. Wacker*[1] and *Julia Nowack*[1,2]

[1] Centre for Behavioural and Physiological Ecology, Zoology, University of New England, Armidale, NSW, Australia,
[2] Department of Integrative Biology and Evolution, Research Institute of Wildlife Ecology, University of Veterinary Medicine Vienna, Vienna, Austria

Keywords: torpor, evolution of endothermy, K-Pg boundary, fire, development of thermoregulation

OPEN ACCESS

Edited by:
Martin Jastroch, Helmholtz Zentrum München (HZ), Germany

Reviewed by:
Gerhard Heldmaier, Philipps University of Marburg, Germany
Carola Waltraud Meyer, Max Planck Institute for Heart and Lung Research (MPG), Germany

***Correspondence:**
Fritz Geiser
fgeiser@une.edu.au

Specialty section:
This article was submitted to Integrative Physiology, a section of the journal Frontiers in Physiology

Received: *30 June 2017*
Accepted: *09 October 2017*
Published: *02 November 2017*

Citation:
Geiser F, Stawski C, Wacker CB and Nowack J (2017) Phoenix from the Ashes: Fire, Torpor, and the Evolution of Mammalian Endothermy. Front. Physiol. 8:842. doi: 10.3389/fphys.2017.00842

INTRODUCTION

The evolution of endothermy in mammals and birds has been widely debated. Endothermy is characterized by high endogenous heat production via combustion of metabolic fuels. This differs from ectothermy in most living organisms, which generally do not produce substantial amounts of internal heat for thermoregulation (Tattersall et al., 2012; Withers et al., 2016). Endogenous heat production is energetically very costly. In comparison to ectothermic terrestrial vertebrates, namely the amphibians and reptiles, the minimum metabolic rate (MR) of normothermic or homeothermic (high constant body temperature, T_b) animals at rest is about 4–8-fold higher in the endotherms. This difference is even more pronounced at low ambient temperatures (T_a) at which the T_b of ectotherms follows T_a, and the MR decreases to even lower levels. In contrast, the T_b of homeothermic endotherms remains high and constant over a wide range of T_a. Therefore, to compensate for increased heat loss at low T_a, MR of especially small mammals and birds must increase substantially and can be 100-fold or more of that in ectotherms (Bartholomew, 1982). Of course this high MR requires a substantial uptake of food and in endotherms much of this chemical energy is simply converted into heat for thermoregulation rather than growth or reproduction as in ectotherms.

Endothermy, however, brings a number of advantages. Most often discussed are higher stamina and peak performance of muscle due to a better oxygen and fuel delivery system (Bennett and Ruben, 1979; Nespolo et al., 2017), fast assimilation and growth rates due to better processing of food and improved metabolic machinery or production of larger litters via increased parental care (Koteja, 2000; Farmer, 2003). While all of these hypotheses have merit, they also have some limitations. The argument that the "aim" of endothermy was primarily not for maintenance of high T_b, but rather an increase in aerobic performance, seems a chicken and egg question to some extent, because obviously improvements of thermogenesis and aerobic performance go hand in hand, and both would have increased together over time (Farmer, 2003). Similarly, the hypothesis regarding the function of endothermy in facilitating improved reproductive output via increased metabolism and homeothermy, although correct for many species, also has several potential shortcomings with regard to its generality. A number of mammalian species have been observed that show little or no increase in metabolism during reproduction as, for example, a monotreme and some marsupials (Nagy and Suckling, 1985; Holloway and Geiser, 2000; Nicol, 2017). To some extent this is because in endothermic monotremes and marsupials, conception to weaning times are about twice of those in placental mammals (Lee and Cockburn, 1985) and therefore energetic demands of reproduction are extended over prolonged periods. In contrast, in gravid ectothermic lizards MR increases significantly (Angilletta and Sears, 2000), and reproductive tegu lizards can maintain an increased T_b-T_a differential via increased heat production (Tattersall et al., 2016). Therefore, although the

argument makes sense and is correct for some endotherms with very high reproductive outputs and therefore energy and nutrient requirements, the relative cost for reproduction does not always differ between ectotherms and endotherms. Further, more and more species from all mammalian subclasses and also some birds even during reproduction are "heterothermic endotherms" (Greek *hetero* = other or different; *therme* = heat). Heterothermy in endotherms can be seen as a large temporal fluctuation of T_b above and below the homeothermic mean in large mammals (Hetem et al., 2016). However, in the context of our review heterothermy refers to torpor, which is a reduction of T_b by >5°C below the resting T_b (Ruf and Geiser, 2015) and/or a reduction of the metabolic rate (MR) below the basal MR (Geiser and Ruf, 1995), occurring predominantly in small endotherms. Importantly, even during the state of torpor these mammals and birds do not abandon endothermy as they can defend their T_b against a large T_b-T_a differential and can rewarm from torpor using endogenously produced heat (Ruf and Geiser, 2015). These heterothermic endotherms may express torpor during pregnancy and/or lactation and even then show pronounced reductions of MR and T_b (McAllan and Geiser, 2014; Stawski and Rojas, 2016). When torpor is used in pregnant mammals, the period of pregnancy is usually extended by the time the animal spends in torpor, which can be by days or even weeks (Racey, 1973; Willis et al., 2006). Nevertheless, torpor expression during reproduction can have positive aspects. For example it can enable reproduction on limited resources, permits survival of adverse conditions during reproduction and can delay parturition until thermal conditions are more benign for mother and offspring (Geiser and Masters, 1994; Willis et al., 2006; Morrow and Nicol, 2009; Stawski, 2010). Clearly, some endotherms are willing to trade a fast development and growth rate for an increased chance for survival of offspring and mother, thereby also increasing their fitness.

Interestingly, the assumption of most discussions about the evolution of endothermy seems to be that reptilian ectothermy evolved into mammalian and avian endothermy by some stepwise increase in metabolism permitting an intermediate homeothermic T_b of around 20–30°C that went hand in hand with the growth in size and/or fur (Crompton et al., 1978; Ruben, 1995). The problem with this interpretation is, however, that homeothermy with a low MR even at low T_b is highly unlikely under most thermal conditions including the slightly warmer conditions in the Cretaceous (Royer et al., 2004) in small endotherms like the ancestral mammals for a number of reasons: (1) Even when the earth was warmer, it still will have experienced daily and yearly fluctuations in T_a; now tropical areas can get rather cold in winter and many animals use torpor under these conditions (McKechnie and Mzilikazi, 2011; Dausmann, 2014). (2) A slight increase in MR, no matter what its purpose was, is insufficient for maintenance of a constant high or even slightly elevated T_b when the T_b-T_a differential is large as for example at night (many small mammals can maintain a T_b-T_a differential of >40°C requiring a manyfold increase in MR). (3) The lower critical temperature of the thermo-neutral zone below which MR must increase substantially if T_b is to be maintained in most small mammals is ∼30°C or more, i.e., even when it is warm they must defend T_b against a substantial loss of heat (Riek and Geiser, 2013). (4) An intermediate T_b would have in fact interfered with high maximum heat production (Currie et al., 2015) and hindered a contribution of MR to thermoregulation. (5) Extant terrestrial ectotherms show large daily fluctuations in T_b and it is highly probable that the partially endothermic ancestors did exactly the same.

With regard to the asteroid strike causing the K-Pg extinctions 65 mya, a severe challenge for endotherms, the cost for thermoregulation in a small terrestrial homeothermic mammal would have been too high to survive the post-asteroid fires and the ensuing impact winter *in situ*. Consequently, the few species that did survive must have had physiological as well as behavioral adaptations to do so.

In this paper we discuss how, from a functional point of view, endothermy could have been attained. We use data both from extant developing as well as adult mammals to support our arguments. Data for developing animals are especially useful in the context of examining the transition from ectothermy to endothermy because altricial mammals and birds, the vast majority of all species, actually do show how an increase in metabolism from a largely ectothermic to an entirely endothermic organism is functionally and morphologically possible (Dawson and Evans, 1960). Thus, our arguments are founded on biologically relevant facts from thermal energetics data unlike many others that had to be largely speculative because the basic physiological mechanisms for thermoregulation like shivering and non-shivering thermogenesis are not preserved in the fossil record, although evidence for insulation can be (Withers et al., 2016). Developmental data may not reveal exactly the same pathways and sequences as those during evolution, but rather show biologically likely and possible scenarios. This is a far more promising approach than relying exclusively data on adults that do not show the transient states seen during development of altricial endotherms. Finally, we discuss how mammals could have managed to survive the post-impact winter following the asteroid strike. New data on post-fire behavior and physiology of terrestrial mammals provide examples for possible survival avenues on that topic. With regard to the latter we mainly discuss mammals in our paper because birds can fly and thus avoid or select areas that were more or less affected by the asteroid strike.

WERE ANCESTRAL ENDOTHERMS HOMEOTHERMIC OR HETEROTHERMIC?

Imagine a reptile with a MR that was increased by 10% above that of its ancestor. How would this have affected its biology? It may have allowed some increased stamina to obtain food because an improved delivery system for oxygen and fuels would have enhanced both locomotion and the capacity for shivering. However, the most obvious advantage would have been an increase in the time the animal was able to be active with an elevated T_b when T_a was falling in the evening and perhaps at the beginning of warm nights. This temporal pattern has been observed in several small extant nocturnal mammals that show extremely brief activity and foraging periods of an

hour or two early in the evening when they maintain a high T_b (Warnecke et al., 2008; Körtner and Geiser, 2009; Stawski and Geiser, 2010). Later at night, as for its fully ectothermic ancestors and extant reptiles, the mammalian ancestor, as do its extant relatives, would have become cold, because a small increase in metabolism would not have been high enough for a sustained elevated T_b throughout the night. Although the rather large (∼2,000 g) reproductive tegu lizards could maintain a raised T_b by using increased heat production and peripheral vasoconstriction (Tattersall et al., 2016), T_b still fluctuated during the day and the average T_b-T_a differential of 6–7°C was well below that of the often >30°C T_b-T_a differential observed in modern normothermic mammals and birds even at body mass of <5 g.

On the next morning, the metabolism of the ancestral endotherm would not have been high enough to raise T_b endogenously because that requires a manyfold increase of MR, or high metabolic scope, which would have been further hindered by the low T_b (Currie et al., 2015). However, it could rewarm in the sun or with an increasing T_a, as do many extant torpid mammals with a very low MR that remains below BMR (i.e., near the values of reptiles) for much of the rewarming process (Lovegrove et al., 1999; Geiser et al., 2002, 2004; Dausmann et al., 2004). With time an even higher metabolism would have been selected in ancestral endotherms via increased shivering and non-shivering thermogenesis (Oelkrug et al., 2015) together with an external cover of fur or feathers resulting in a prolongation of periods with a high and constant T_b. Importantly, and in contrast to what was believed in the past (Cowles, 1958), fur cover in living animals does not necessarily make basking energetically ineffective (Geiser et al., 2004), because unlike dead fur coats used to cloak ectothermic lizards (Cowles, 1958), mammals can adjust the angle of hair to maximize heat gain (Wacker et al., 2016). Basking mammals during normothermia can maintain resting MR near basal MR values over a wide range of T_a well below the thermo-neutral zone and can reduce rewarming cost by up to 75% in comparison to endothermic rewarming from torpor (Geiser and Drury, 2003). Moreover, and also in contrast to what was believed in the past (IUPS Thermal Commission, 2003), torpid animals can travel at low T_b of ∼15°C or less to move to basking sites and their ability to do so also aids in predator avoidance (Rojas et al., 2012).

Fortunately, we do have examples of extant mammals supporting these evolutionary arguments on the use of heterothermy during the evolution of endothermy. Marsupial dunnarts (*Sminthopsis* spp.), small insectivorous mammals, are born naked at a small body mass/size with low endogenous heat production (Wacker et al., 2017). They do not need a high heat production because initially they are kept warm within their mother's pouch and in birds and placental mammals brooding and nests serve a similar purpose. At the time of pouch exit young dunnarts are partially furred, but like other small marsupials are still only partially endothermic as they cool rapidly when exposed to low T_a (Morrison and Petajan, 1962; Geiser et al., 2006; Wacker et al., 2017). Interestingly, almost competent endothermic thermoregulation develops soon after pouch exit and the young can maintain a high T_b for some of the night, but in the second part of the night they enter an apparent bout of torpor (Wacker et al., 2017). They do so despite the fact that they lack high enough endogenous heat production to rewarm from low T_b. Instead these juveniles seem to "know" that they can rely on behavioral thermoregulation and bask under a radiant heat source to raise T_b to high level as their ectothermic ancestors must have done, and extant reptiles continue to do, on sunny days. So here we have a highly plausible and functionally possible model as to how endothermy could have evolved via a transient partially endothermic heterothermic phase requiring behavioral thermoregulation, but permitting some crepuscular and nocturnal activity and foraging to avoid dinosaur predators (McNab, 2002). The ability of using a combination of behavioral and physiological thermoregulation to reach high T_b would have maximized biological functions during a somewhat prolonged activity phase. This in turn would have increased stamina and, if nutrition was sufficient, would have allowed production and fast growth of many young.

Importantly, torpor during reproduction and development is not restricted to marsupials. Data on torpor during incubation, brooding, pregnancy, and lactation are now available for nightjars, hummingbirds, echidnas, several marsupials, tenrecs, hedgehogs, bats, carnivores, primates, and rodents (McAllan and Geiser, 2014; Stawski and Rojas, 2016). During development, although published work is scant, torpor has been observed in several birds, marsupials, rodents, and shrews and there is some evidence that it also occurs in bats (Geiser, 2008; Giroud et al., 2014). This use of torpor during reproduction and development in so many diverse vertebrates lends further support to our arguments.

The proposal that homeothermy in mammals must have evolved via heterothermy makes functional sense, because this avenue provides a plausible explanation as to how metabolism could have increased gradually over time (Lovegrove, 2017). While torpor patterns may have not been the same as those expressed in modern mammals with the ability to inhibit MR and defend T_b during torpor (Geiser, 2008) it still would have been advantageous during the transition to endothermy. Heterothermy would have permitted a low T_b and energy conservation during cold exposure, and passive rewarming from low T_b before the activity phase would have been possible with a relatively low MR (Geiser and Drury, 2003; Grigg et al., 2004). Consequently, prolonged activity and foraging during the first part of the night to avoid predation appears to be the initial selective advantage of an increased MR in ancestral endotherms. Over time, activity would have been extended and perhaps in some species homeothermy evolved whereas others continued to be heterothermic, which is consequential for our next chapter addressing mammalian survival of a calamity that caused the extinction of many terrestrial animals.

THE FUNCTION OF MAMMALIAN HETEROTHERMY AT THE K-PG BOUNDARY

The asteroid impact at the Cretaceous-Palaeogene (K-Pg) boundary, about 65 million years ago, ended the era of dinosaurs, but was the beginning of the diversification of extant mammals.

Geological evidence suggests that the asteroid caused global wildfires that killed all terrestrial life unable to seek safe refuge mainly underground (Morgan et al., 2013). The disappearance of the dinosaurs opened new niches and permitted a rapid radiation of mammalian lineages (O'Leary et al., 2013). However, before mammals could diversify they had to (i) survive the fires caused by the asteroid impacts and (ii) survive the post-impact winter that lasted for many months. As for the evolution of endothermy *per se*, heterothermy and torpor expression were likely crucial for both (Lovegrove et al., 2014; Nowack et al., 2016).

A homeothermic small mammal may have had the ability to survive the immediate effect of the fires if hidden underground, however, it would not have been able to survive without food for months during the post-impact winter. The only way for small sedentary endotherms to achieve this without enormous food caches is the ability to enter torpor, which would have permitted these mammals to stay inactive and hidden for long periods without the need to forage (Turbill et al., 2011). During multiday torpor in hibernators, the metabolic rate can be reduced to <5% of the basal MR and T_b often falls to near 0°C, but substantial energy saving can also be achieved at relative high T_b (Tøien et al., 2011; Ruf and Geiser, 2015). Huddling in groups could have further enhanced energy savings (Arnold, 1993; Gilbert et al., 2010; Eto et al., 2014; Nowack and Geiser, 2016). Although it is widely accepted that hibernating mammals can survive without food for about 6 months, recent data have shown that some can do even better than that. For example, captive fattened eastern pygmy-possums (*Cercartetus nanus*) a small marsupial, can survive when hibernating at low T_a for up to an entire year on stored fat despite periodic arousals (Geiser, 2007). Similarly, dormice (*Glis glis*) during non-reproductive years can hibernate for up to 11 months per year in the wild and in captivity (Bieber and Ruf, 2009; Hoelzl et al., 2015). Tenrecs (*Tenrec ecaudatus*) and lemurs (*Cheirogaleus* spp.) can hibernate for prolonged periods even in the tropics (Dausmann et al., 2004; Blanco et al., 2013; Lovegrove et al., 2014). Such periods would have been sufficient for some individuals to survive the post-impact winter.

New evidence also suggests that torpor is used extensively to deal with fires or the scorched post-fire environment in extant terrestrial mammals. Echidnas, *Tachyglossus aculeatus*, egg-laying mammals that have many ancestral functional and morphological traits (Nicol, 2017), hide and enter torpor during forest fires (Nowack et al., 2016). Before the fire echidnas expressed brief and shallow bouts of torpor whereas after the fire animals entered prolonged periods of torpor although T_a was rather mild. Interestingly animals also reduced activity but remained within their original home range. Similarly, antechinus

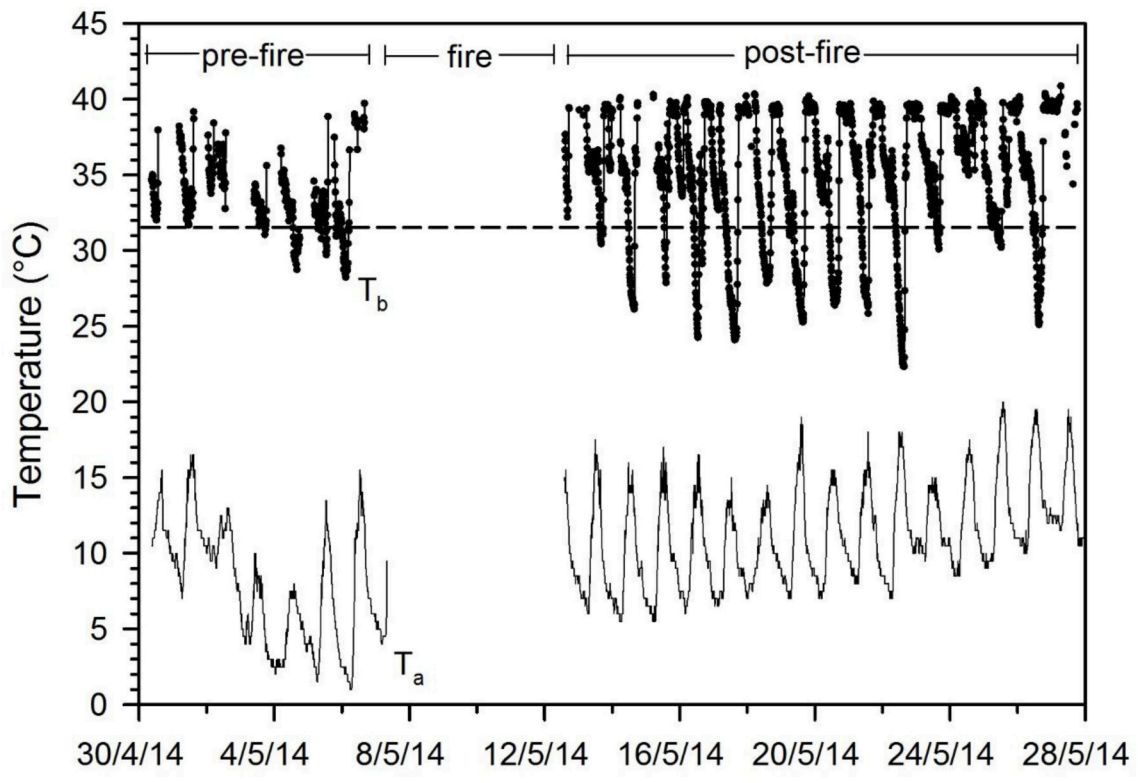

FIGURE 1 | Body temperature (T_b) and ambient temperature (T_a) fluctuations in the free-ranging marsupial *Antechinus stuartii* in the late Austral fall before and after a controlled forest fire. Access during the fire for data collection was not permitted. Note the substantial increase of the T_b fluctuations and prolonged duration of torpor bouts after the fire although T_a increased somewhat during that time in comparison to before the fire (data from Stawski et al., 2015). The horizontal dashed line is the torpor threshold.

(*Antechinus stuartii* and *A. flavipes*), small insectivorous marsupials, increased torpor expression and duration, both after a controlled forest fire for fuel reduction (**Figure 1**) as well as a wildfire, and at the same time decreased daily activity (Stawski et al., 2015; Matthews et al., 2017). The reduction in activity was mainly achieved by reducing daytime activity, likely to avoid exposure to predators in a habitat with little vegetation cover, as would have been the case during the post-impact winter caused by the asteroid. The post-fire increase in torpor use in extant mammals was initially assumed to be to a large extent related to a decrease in food availability that typically follows a fire. However, recent data show that the presence of charcoal-ash substrate and smoke enhances mammalian torpor use beyond that simply induced by food restriction, suggesting that these post-fire cues signal a period of imminent food shortage to the animals (Stawski et al., 2017). This is further evidence that during the post-impact winter, when mammals would have been exposed to food shortage, a habitat with limited cover, ash/charcoal substrate and perhaps smoke, torpor expression would have increased to minimize energy expenditure and foraging requirements, providing an avenue for survival to mammals. Birds also suffered extinctions during the K-Pg calamity, but the survivors likely relied on mobility rather than prolonged torpor because only one extant avian species is known to hibernate (Brigham, 1992) in contrast to the many mammalian hibernators (Ruf and Geiser, 2015). However, it cannot be excluded that birds also employed torpor to some extent when faced with energetic and thermal challenges as is known for many diverse extant species (Brigham, 1992; McKechnie and Lovegrove, 2002).

More and more evidence is accumulating on the adaptive advantages of heterotherms over homeothermic species. Heterothermic species do not only use torpor to survive seasonal energetic and thermal challenges, but can also endure the consequences of unpredictable energy bottlenecks or natural disasters (Nowack et al., 2015, 2016, 2017) and consequently have a lower risk of becoming extinct (Geiser and Turbill, 2009; Turbill et al., 2011; Hanna and Cardillo, 2014). Ancestral mammals were small and nocturnal and presumably had a relaxed endothermic thermoregulation, expressing torpor during the colder periods of the day and possibly also were able to use multiday hibernation for highly effective energy conservation (Grigg et al., 2004). Many of today's heterotherms hibernate in underground burrows (Arnold et al., 1991) that would allow survival largely independent of the conditions on the Earth's surface, as would have been the case during the K-Pg boundary. Thus both during the initial evolution of endothermy in birds and mammals and the survival of mammals during the K-Pg boundary, heterothermy likely played a key role because it permitted an intermediate metabolism during the evolution of endothermy as well as prolonged survival without food at the K-Pg boundary.

AUTHOR CONTRIBUTIONS

All authors listed, have made substantial, direct and intellectual contribution to the work, and approved it for publication.

ACKNOWLEDGMENTS

This work was supported by a University of New England Postdoctoral Research Fellowship and by a Discovery Early Career Researcher Award from the Australian Research Council to CS, an Australian Postgraduate Award to CW, a German Academic Exchange Service, a Endeavour Research Fellowship and a Alexander von Humboldt Feodor Lynen Fellowship to JN, and grants from the Australian Research Council and the University of New England to FG.

REFERENCES

Angilletta, M. J., and Sears, M. W. (2000). The metabolic cost of reproduction in an oviparous lizard. *Funct. Ecol.* 14, 39–45. doi: 10.1046/j.1365-2435.2000.00387.x

Arnold, W. (1993). "Energetics of social hibernation," in *Life in the Cold*: *Ecological, Physiological and Molecular Mechanisms*, eds C. Carey, G. L. Florant, B. A. Wunder, and B. Horwitz (Boulder, CO: Westview), 65–80.

Arnold, W., Heldmaier, G., Ortmann, S., Pohl, H., Ruf, T., and Steinlechner, S. (1991). Ambient temperatures in hibernacula and their energetic consequences for alpine marmots (*Marmota marmota*). *J. Therm. Biol.* 16, 223–226. doi: 10.1016/0306-4565(91)90029-2

Bartholomew, G. A. (1982). "Energy metabolism," in *Animal Physiology*: *Principles* and *Adaptations*, ed M. S. Gordon (New York, NY: MacMillian Publishing Co., Inc.), 46–93.

Bennett, A. F., and Ruben, J. A. (1979). Endothermy and activity in vertebrates. *Science* 206, 649–654. doi: 10.1126/science.493968

Bieber, C., and Ruf, T. (2009). Summer dormancy in edible dormice (*Glis glis*) without energetic constraints. *Naturwissenschaften* 96, 165–171. doi: 10.1007/s00114-008-0471-z

Blanco, M. B., Dausmann, K. H., Ranaivoarisoa, J. F., and Yoder, A. D. (2013). Underground hibernation in a primate. *Sci. Rep.* 3:1768. doi: 10.1038/srep01768.

Brigham, R. M. (1992). Daily torpor in a free-ranging goatsucker, the common poorwill (*Phalaenoptilus nuttallii*). *Physiol. Zool.* 65, 457–472. doi: 10.1086/physzool.65.2.30158263

Cowles, R. B. (1958). Possible origin of dermal temperature regulation. *Evolution* 12, 347–357. doi: 10.1111/j.1558-5646.1958.tb02964.x

Crompton, A. W., Taylor, C. R., and Jagger, J. A. (1978). Evolution of homeothermy in mammals. *Nature* 272, 333–336. doi: 10.1038/272333a0

Currie, S. E., Noy, K., and Geiser, F. (2015). Passive rewarming from torpor in hibernating bats: minimizing metabolic costs and cardiac demands. *Am. J. Physiol.* 308, R34–R41. doi: 10.1152/ajpregu.00341.2014

Dausmann, K. H. (2014). Flexible patterns in energy savings: heterothermy in primates. *J. Zool.* 292, 101–111. doi: 10.1111/jzo.12104

Dausmann, K. H., Glos, J., Ganzhorn, J. U., and Heldmaier, G. (2004). Hibernation in a tropical primate. *Nature* 429, 825–826. doi: 10.1038/429825a

Dawson, W. R., and Evans, F. C. (1960). Relation of growth and development to temperature regulation in nestling vesper sparrows. *Condor* 62, 329–340. doi: 10.2307/1365163

Eto, T., Sakamoto, S. H., Okubo, Y., Koshimoto, C., Kashimura, A., and Morita, T. (2014). Huddling facilitates expression of daily torpor in the large Japanese field mouse *Apodemus speciosus*. *Physiol. Behav.* 133, 22–29. doi: 10.1016/j.physbeh.2014.04.051

Farmer, C. G. (2003). Reproduction: the adaptive significance of endothermy. *Am. Nat.* 162, 826–840. doi: 10.1086/380922

Geiser, F. (2007). Yearlong hibernation in a marsupial mammal. *Naturwissenschaften* 94, 941–944. doi: 10.1007/s00114-007-0274-7

Geiser, F. (2008). Ontogeny and phylogeny of endothermy and torpor in mammals and birds. *Comp. Biochem. Physiol.* 150, 176–180. doi: 10.1016/j.cbpa.2007.02.041

Geiser, F., Drury, R .L., Körtner, G., Turbill, C., Pavey, C. R. and Brigham, R. M. (2004). "Passive rewarming from torpor in mammals and birds: energetic, ecological and evolutionary implications," in *Life in the Cold: Evolution, Mechanisms, Adaptation, and Application. 12th International Hibernation Symposium. Biological Papers of the University of Alaska #27*, eds B. M. Barnes and H. V. Carey (Fairbanks, AK: Institute of Arctic Biology, University of Alaska), 51–62.

Geiser, F., and Drury, R. L. (2003). Radiant heat affects thermoregulation and energy expenditure during rewarming from torpor. *J. Comp. Physiol. B* 173, 55–60. doi: 10.1007/s00360-002-0311-y

Geiser, F., Goodship, N., and Pavey, C. R. (2002). Was basking important in the evolution of mammalian endothermy? *Naturwissenschaften* 89, 412–414. doi: 10.1007/s00114-002-0349-4

Geiser, F., and Masters, P. (1994). Torpor in relation to reproduction in the mulgara, *Dasycercus cristicauda* (Dasyuridae: Marsupialia). *J. Therm. Biol.* 19, 33–40. doi: 10.1016/0306-4565(94)90007-8

Geiser, F., and Ruf, T. (1995). Hibernation versus daily torpor in mammals and birds: physiological variables and classification of torpor patterns. *Physiol. Zool.* 68, 935–966. doi: 10.1086/physzool.68.6.30163788

Geiser, F., and Turbill, C. (2009). Hibernation and daily torpor minimize mammalian extinctions. *Naturwissenschaften* 96, 1235–1240. doi: 10.1007/s00114-009-0583-0

Geiser, F., Westman, W., McAllan, B. M., and Brigham, R. M. (2006). Development of thermoregulation and torpor in a marsupial: energetic and evolutionary implications. *J. Comp. Physiol. B* 176, 107–116. doi: 10.1007/s00360-005-0026-y

Gilbert, C., McCafferty, D., LeMaho, Y., Martrette, J. M., Giroud, S., Blanc, S., et al. (2010). One for all and all for one: the energetics benefits of huddling in endotherms. *Biol. Rev.* 85, 545–569. doi: 10.1111/j.1469-185X.2009.00115.x

Giroud, S., Zahn, S., Criscuolo, F., Chery, I., Blanc, S., Turbill, C., et al. (2014). Late-born intermittently fasted juvenile garden dormice use torpor to grow and fatten prior to hibernation: consequences for ageing patterns. *Proc. R. Soc. B* 281:20141131. doi: 10.1098/rspb.2014.1131

Grigg, G. C., Beard, L. A., and Augee, M. L. (2004). The evolution of endothermy and its diversity in mammals and birds. *Physiol. Biochem. Zool.* 88, 982–997. doi: 10.1086/425188

Hanna, E., and Cardillo, M.,(2014). Clarifying the relationship between torpor and anthropogenic extinction risk in mammals. *J. Zool.* 293, 211–217. doi: 10.1111/jzo.12136

Hetem, R. S., Maloney, S. K., Fuller, A., and Mitchell, D. (2016). Heterothermy in large mammals: inevitable or implemented? *Biol. Rev.* 91, 187–205. doi: 10.1111/brv.12166

Hoelzl, F., Bieber, C., Cornils, J. S., Gerritsmann, H., Stalder, G. L., Walzer, C., et al. (2015). How to spend the summer? Free-living dormice (*Glis glis*) can hibernate for 11 months in non-reproductive years. *J. Comp. Physiol. B* 185, 931–939. doi: 10.1007/s00360-015-0929-1

Holloway, J. C., and Geiser, F. (2000). Development of thermoregulation in the sugar glider *Petaurus breviceps* (Marsupialia: Petauridae). *J. Zool.* 252, 389–397. doi: 10.1111/j.1469-7998.2000.tb00634.x

IUPS Thermal Commission (2003). Glossary and terms in thermal physiology. *J. Therm. Biol.* 28, 75–106. doi: 10.1016/S0306-4565(02)00055-4

Körtner, G., and Geiser, F. (2009). The key to winter survival: daily torpor in a small arid-zone marsupial. *Naturwissenschaften* 96, 525–530. doi: 10.1007/s00114-008-0492-7

Koteja, P. (2000). Energy assimilation, parental care and the evolution of endothermy. *Proc. R. Soc.B* 267, 479–484. doi: 10.1098/rspb.2000.1025

Lee, A. K., and Cockburn, A. (1985). *Evolutionary Ecology of Marsupials*. London: Cambridge University Press.

Lovegrove, B. G. (2017). A phenology of the evolution of endothermy in birds and mammals. *Biol. Rev.* 92, 1213–1240. doi: 10.1111/brv.12280

Lovegrove, B. G., Körtner, G., and Geiser, F. (1999). The energetic cost of arousal from torpor in the marsupial *Sminthopsis macroura*: benefits of summer ambient temperature cycles. *J. Comp. Physiol. B* 169, 11–18. doi: 10.1007/s003600050188

Lovegrove, B. G., Lobban, K. D., and Levesque, D. L. (2014). Mammal survival at the Cretaceous-paleogene boundary: metabolic homeostasis in prolonged tropical hibernation in tenrecs. *Proc. R. Soc. B* 281:20141303. doi: 10.1098/rspb.2014.1304

Matthews, J. K., Stawski, C., Körtner, G., and Geiser, F. (2017). Torpor and basking after a severe wildfire: mammalian survival strategies in a scorched landscape. *J. Comp. Physiol. B* 187, 385–393. doi: 10.1007/s00360-016-1039-4

McAllan, B. M., and Geiser, F. (2014). Torpor during reproduction in mammals and birds: dealing with an energetic conundrum. *Integr. Comp. Biol.* 56, 516–532. doi: 10.1093/icb/icu093

McKechnie, A. E., and Lovegrove, B. G. (2002). Avian facultative hypothermic responses: a review. *Condor* 104, 705–724. doi: 10.1650/0010-5422(2002)104[0705:AFHRAR2.0.CO;2]

McKechnie, A. E., and Mzilikazi, N. (2011). Heterothermy in Afrotropical mammals and birds: a review. *Int. Comp. Biol.* 51, 349–363. doi: 10.1093/icb/icr035

McNab, B. K. (2002). *The Physiological Ecology of Vertebrates: A View from Energetics*. Comstock, MI: Cornell University Press.

Morgan, J., Artemieva, N., and Goldin, T. (2013). Revisiting wildfires at the K–Pg boundary. *J. Geophys. Res.* 118, 1508–1520. doi: 10.1002/2013JG002428

Morrison, P., and Petajan, J. H. (1962). The development of temperature regulation in the opossum, *Didelphis marsupialis virginiana*. *Physiol. Zool.* 35, 52–65. doi: 10.1086/physzool.35.1.30152713

Morrow, G., and Nicol, S. C. (2009). Cool sex? Hibernation and reproduction overlap in the echidna. *PLoS ONE* 4:e6070. doi: 10.1371/journal.pone.0006070

Nagy, K. A., and Suckling, G. C. (1985). Field energetics and water balance of sugar gliders, *Petaurus breviceps* (Marsupialia: Petauridae). *Aust. J. Zool.* 33, 683–691. doi: 10.1071/ZO9850683

Nespolo, R. F., Solano-Iguaran, J. J., and Bozinovic, F. (2017). Phylogenetic analysis supports the aerobic-capacity model for the evolution of endothermy. *Am. Nat.* 189, 13–27. doi: 10.1086/689598

Nicol, S. C. (2017). Energy homeostasis in monotremes. *Front. Neurosci.* 11:195. doi: 10.3389/fnins.2017.00195

Nowack, J., Cooper, C. E., and Geiser, F. (2016). Cool echidnas survive the fire. *Proc. R. Soc. B* 283:20160382. doi: 10.1098/rspb.2016.0382

Nowack, J., and Geiser, F. (2016). Friends with benefits: the role of huddling in mixed groups of torpid and normothermic animals. *J. Exp. Biol.* 219, 590–596. doi: 10.1242/jeb.128926

Nowack, J., Rojas, A. D., Körtner, G., and Geiser, F. (2015). Snoozing through the storm: torpor use during a natural disaster. *Sci. Rep.* 5:11243. doi: 10.1038/srep11243

Nowack, J., Stawski, C., and Geiser, F. (2017). More functions of torpor and their roles in a changing world. *J. Comp. Physiol. B* 187, 889–897. doi: 10.1007/s00360-017-1100-y

Oelkrug, R., Polymeropoulos, E. T., and Jastroch, M. (2015). Brown adipose tissue: physiological function and evolutionary significance. *J. Comp. Physiol. B* 185, 587–606. doi: 10.1007/s00360-015-0907-7

O'Leary, M. A., Bloch, J. I., Flynn, J. J., Gaudin, T. J., Giallombardo, A., Giannini, N. P., et al. (2013). The placental mammal ancestor and the post-K–Pg radiation of placentals. *Science* 339, 662–667. doi: 10.1126/science.1229237

Racey, P. A. (1973). Environmental factors affecting the length of gestation in heterothermic bats. *J. Reprod. Fert. Suppl.* 19, 175–189.

Riek, A., and Geiser, F. (2013). Allometry of thermal variables in mammals: consequences of body size and phylogeny. *Biol. Rev.* 88, 564–572. doi: 10.1111/brv.12016

Rojas, A. D., Körtner, G., and Geiser, F. (2012). Cool running: locomotor performance at low body temperature in mammals. *Biol. Lett.* 8, 868–870. doi: 10.1098/rsbl.2012.0269

Royer, D. L., Berner, R. A., Montañez, I. P., Tabor, N. J., and Beerling, D. J. (2004). CO_2 as a primary driver of Phanerozoic climate change. *GSA Today* 14, 4–10.

Ruben, J. (1995). The evolution of endothermy in mammals and birds: from physiology to fossils. *Annu. Rev. Physiol.* 57, 69–95. doi: 10.1146/annurev.ph.57.030195.000441

Ruf, T., and Geiser, F. (2015). Daily torpor and hibernation in birds and mammals. *Biol. Rev.* 90, 891–926. doi: 10.1111/brv.12137

Stawski, C. (2010). Torpor during the reproductive season in a free-ranging subtropical bat, *Nyctophilus bifax*. *J. Therm. Biol.* 35, 245–249. doi: 10.1016/j.jtherbio.2010.05.009

Stawski, C., and Geiser, F. (2010). Fat and fed: frequent use of summer torpor in a subtropical bat. *Naturwissenschaften* 97, 29–35. doi: 10.1007/s00114-009-0606-x

Stawski, C., Körtner, G., Nowack, J., and Geiser, F. (2015). The importance of mammalian torpor for survival in a post-fire landscape. *Biol. Lett.* 11:20150134. doi: 10.1098/rsbl.2015.0134

Stawski, C., Nowack, J., Körtner, G., and Geiser, F. (2017). A new cue for torpor induction: charcoal, ash and smoke. *J. Exp. Biol.* 220, 220–226. doi: 10.1242/jeb.146548

Stawski, C., and Rojas, A. D. (2016). Thermal physiology of a reproductive female marsupial, *Antechinus flavipes*. *Mamm. Res.* 61, 417–421. doi: 10.1007/s13364-016-0287-8

Tattersall, G. J., Leite, C. A. C., Sanders, C. E., Cadena, V., Andrade, D. V., Abe, A. S., et al. (2016). Seasonal reproductive endothermy in tegu lizards. *Sci. Adv.* 201:e1500951. doi: 10.1126/sciadv.1500951

Tattersall, G. J., Sinclair, B. J., Withers, P. C., Field, P. A., Seebacher, F., Cooper, C. E., et al. (2012). Coping with thermal challenges: physiological adaptations to environmental temperature. *Compr. Physiol.* 2, 2151–2202. doi: 10.1002/cphy.c110055

Tøien, Ø., Blake, J., Edgar, D. M., Grahn, D. A., Heller, H. C., and Barnes, B. M. (2011). Hibernation in black bears: independence of metabolic suppression from body temperature. *Science* 331, 906–909. doi: 10.1126/science.1199435

Turbill, C., Bieber, C., and Ruf, T. (2011). Hibernation is associated with increased survival and the evolution of slow life histories among mammals. *Proc. R. Soc. B* 278, 3355–3363. doi: 10.1098/rspb.2011.0190

Wacker, C. B., McAllan, B. M., Körtner, G., and Geiser, F. (2016). The functional requirements of mammalian hair: a compromise between crypsis and thermoregulation? *Sci. Nat.* 103:53. doi: 10.1007/s00114-016-1376-x

Wacker, C. B., McAllan, B. M., Körtner, G., and Geiser, F. (2017). The role of basking in the development of endothermy and torpor in a marsupial. *J. Comp. Physiol. B.* 187, 1029–1238. doi: 10.1007/s00360-017-1060-2

Warnecke, L., Turner, J. M., and Geiser, F. (2008). Torpor and basking in a small arid zone marsupial. *Naturwissenschaften* 95, 73–78. doi: 10.1007/s00114-007-0293-4

Willis, C. K., Brigham, R. M., and Geiser, F. (2006). Deep, prolonged torpor by pregnant, free-ranging bats. *Naturwissenschaften* 93, 80–83. doi: 10.1007/s00114-005-0063-0

Withers, P. C., Cooper, C. E., Maloney, S. K., Bozinovic, F., and Cruz-Neto, A. P. (2016). *Ecological and Environmental Physiology of Mammals*. Oxford: Oxford University Press.

Conflict of Interest Statement: The authors declare that the research was conducted in the absence of any commercial or financial relationships that could be construed as a potential conflict of interest.

frontiers in Physiology

ORIGINAL RESEARCH
published: 26 September 2017
doi: 10.3389/fphys.2017.00745

Searching for the Haplorrhine Heterotherm: Field and Laboratory Data of Free-Ranging Tarsiers

Shaun Welman[1]*, *Andrew A. Tuen*[2] and *Barry G. Lovegrove*[1]

[1] School of Life Sciences, University of KwaZulu-Natal, Pietermaritzburg, South Africa, [2] Institute of Biodiversity and Environmental Conservation, Universiti Malaysia Sarawak, Kota Samarahan, Malaysia

The observation of heterothermy in a single suborder (Strepsirrhini) only within the primates is puzzling. Given that the placental-mammal ancestor was likely a heterotherm, we explored the potential for heterothermy in a primate closely related to the Strepsirrhini. Based upon phylogeny, body size and habitat stability since the Late Eocene, we selected western tarsiers (*Cephalopachus bancanus*) from the island of Borneo. Being the sister clade to Strepsirrhini and basal in Haplorrhini (monkeys and apes), we hypothesized that *C. bancanus* might have retained the heterothermic capacity observed in several small strepsirrhines. We measured resting metabolic rate, subcutaneous temperature, evaporative water loss and the percentage of heat dissipated through evaporation, at ambient temperatures between 22 and 35°C in fresh-caught wild animals (126.1 ± 2.4 g). We also measured core body temperatures in free-ranging animals. The thermoneutral zone was 25–30°C and the basal metabolic rate was 3.52 ± 0.06 W.kg^{-1} (0.65 ± 0.01 ml O_2.g^{-1}.h^{-1}). There was no evidence of adaptive heterothermy in either the laboratory data or the free-ranging data. Instead, animals appeared to be cold sensitive ($T_b \sim 31$°C) at the lowest temperatures. We discuss possible reasons for the apparent lack of heterothermy in tarsiers, and identify putative heterotherms within Platyrrhini. We also document our concern for the vulnerability of *C. bancanus* to future temperature increases associated with global warming.

Keywords: metabolism, primate thermoregulation, tropics, evolution, tarsiers

OPEN ACCESS

Edited by:
Martin Jastroch, Helmholtz Zentrum München (HZ), Germany

Reviewed by:
Kathrin Dausmann, University of Hamburg, Germany
Gordon Clifford Grigg, The University of Queensland, Australia

***Correspondence:**
Shaun Welman
shaun.welman@gmail.com

Specialty section:
This article was submitted to Integrative Physiology, a section of the journal Frontiers in Physiology

Received: *30 April 2017*
Accepted: *12 September 2017*
Published: *26 September 2017*

Citation:
Welman S, Tuen AA and Lovegrove BG (2017) Searching for the Haplorrhine Heterotherm: Field and Laboratory Data of Free-Ranging Tarsiers. Front. Physiol. 8:745. doi: 10.3389/fphys.2017.00745

INTRODUCTION

The capacity to become heterothermic conveys significant fitness benefits and promotes survivability (Geiser and Turbill, 2009; Geiser and Brigham, 2012; Lovegrove et al., 2014b; Nowack et al., 2015, 2016; Stawski et al., 2015; Lovegrove, 2017). These benefits may be derived either as a direct consequence of the reduction in energy expenditure and, in the case of hibernators specifically, the preservation of fat reserves during low resource availability (Lovegrove, 2000; Dausmann, 2014), or, indirectly by reducing the risk of predation due to decreased foraging effort (Bieber and Ruf, 2009; Stawski and Geiser, 2010; Bieber et al., 2014) as well as aiding in reproduction by manipulating foetal growth rate or by enhancing sperm storage (reviewed in Geiser and Brigham, 2012). However, whereas the benefits of heterothermy may be well documented, its origin remains hotly debated (Crompton et al., 1978; McNab, 1978; Bennett and Ruben, 1979; Hayes and Garland, 1995; Farmer, 2000; Koteja, 2000; Grigg et al., 2004; Kemp, 2006; Clarke and Pörtner, 2010; Lovegrove, 2012a,b, 2017).

With the aid of maximum likelihood character state reconstruction, Lovegrove (2012a) attempted to consolidate the literature and resolve the debate surrounding the antiquity of heterothermy relative to strict homeothermy in mammals. The study confirmed earlier work (see Grigg and Beard, 2000; Grigg et al., 2004) and showed that contrary to a long-standing paradigm, strict homeothermy is, as argued by Augee and Gooden (1992), the more derived state. This conclusion, in combination with recent work on brown antechinus (*Antechinus stuartii*; Stawski et al., 2015), sugar gliders (*Petaurus breviceps*; Nowack et al., 2015), and short-beaked echidnas (*Tachyglossus aculeatus*; Nowack et al., 2016), provided support for the argument that the ancestors of the three crown mammalian clades namely, the Monotremata, Marsupialia and Placentalia, likely survived the mass extinction event marking the Cretaceous-Paleogene (K-Pg) boundary because of their heterothermic capacity (Lovegrove et al., 2014b; Lovegrove, 2017).

For many decades, it appeared that heterothermy within the primates was geographically restricted to a single family—the Cheirogaleidae of Madagascar (see Dausmann, 2008). Now, in addition to observations of torpor and hibernation in Malagasy mouse lemurs (Ortmann et al., 1997; Aujard et al., 1998; Schmid and Kappeler, 1998; Schmid, 2000; Kobbe and Dausmann, 2009; Schmid and Ganzhorn, 2009) and hibernation in dwarf lemurs (Dausmann et al., 2000, 2005), heterothermy has been observed in two non-Malagasy primates. Torpor, despite the initial lack of evidence for it (Knox and Wright, 1989; Mzilikazi et al., 2006), occurs in the African lesser bushbaby (*Galago maholi*; Nowack et al., 2010), albeit under extreme conditions only. Hibernation has now also been observed in the pygmy slow loris in Vietnam (*Nycticebus pygmaeus*; Ruf et al., 2015). Even with the additional observations of heterothermy in the Galagidae and Lorisidae, all observations within Primates remain within the Strepsirrhini clade prompting the question why it has not also been observed in the haplorrhines? Has heterothermy potentially been "lost" in more derived primate clades or does its absence reflect an artefact of sampling bias?

In this paper, we sought to explore the potential for heterothermy in a non-strepsirrhine primate in an attempt to gain further insight into the primate heterothermy phenotype. Our choice of study animal was determined by three principal factors; (a) close phylogenetic relatedness to the strepsirrhines, (b) an insular tropical existence, and (c) small body size. Choosing a close relative provides the best opportunity to confirm a potential retention of the ancestral heterothermy condition. The island existence and small body size criteria stem from observations of extensive employment of heterothermy by small-bodied Malagasy lemurs and because most heterothermic mammals are small (<1 kg) (Geiser, 1998; Lovegrove, 2012a; Ruf and Geiser, 2015). It has been proposed that, in general, mammals that colonised tropical islands during the Early Cenozoic, that is, prior to the onset of global cooling during the Late Eocene, retained plesiomorphic climate-adaptation traits through stabilising selection (Hansen, 1997; Lovegrove, 2012a; Lobban et al., 2014).

Based on the aforementioned criteria, the most *apropos* model to search for the evidence of adaptive heterothermy in non-strepsirrhine primates is the tarsier (Tarsiidae). Tarsiers are small (80–150 g; but see Clarke, 1943), tropical, nocturnal and arboreal primates which inhabit the forests of South-east Asia (MacKinnon and MacKinnon, 1980; Crompton and Andau, 1986, 1987; Neri-Arboleda et al., 2002; Groves and Shekelle, 2010). The reported body temperatures (T_b) of 33.3°C (Lovegrove et al., 2014a) and 33.8°C (McNab and Wright, 1987) for the Philippine tarsier (*Tarsius syrichta*) show that they are "basoendotherms" i.e., $T_b < 35$°C and thus similar to the predicted ancestral condition (*sensu* Lovegrove, 2012a); ca. 3°C lower than the average T_b of the primate clade (see Clarke et al., 2010). Since their evolution during the Eocene, tarsiers have persisted within a continuously tropical environment in habitats that are argued to be very similar to those that their ancestors inhabited; despite some changes in floristic composition (Jablonski, 2003; Simons, 2003). They are also the only strictly carnivorous primate and, as a rule, take live prey (Jablonski and Crompton, 1994; Gursky, 2000). With regards to their phylogeny, their position has been hotly debated and shuffled around the primate tree (Schwartz, 1984; Schmitz et al., 2001; Meireles et al., 2003; Simons, 2003; Yoder, 2003; Matsui et al., 2009; Perelman et al., 2011). However, the most recent study by Hartig et al. (2013) supports the Haplorrhini hypothesis i.e., that tarsiers are the sister taxa to the Anthropoids, as originally proposed by Pocock (1918). Tarsiers are thus the closest extant relatives to the strepsirrhines.

Given the close phylogenetic relationship of tarsiers to the Strepsirrhini, as well as the varied observations of torpor in the Strepsirrhini (Dausmann, 2014; Dausmann and Warnecke, 2016), we predicted that stabilizing selection may have favoured the retention of the plesiomorphic capacity for heterothermy within tarsiers (Lovegrove, 2012a). Currently, there is no physiological evidence in tarsiers that supports our prediction. Most of our understanding of tarsier thermoregulation does however stem from three studies on *T. syrichta* (Clarke, 1943; McNab and Wright, 1987; Lovegrove et al., 2014a), but it has been speculated that western tarsiers (*Cephalopachus bancanus*, previously *T. bancanus*) may be capable of torpor (Niemitz, 1984; Niemitz et al., 1984).

Our study had two main objectives. The first was to determine the thermoregulatory response of wild-caught *C. bancanus* to varying ambient temperatures (T_a), noting any potential indication of hypometabolism or the associated reduction in T_b. The second was to document free-ranging core temperatures (T_{core}) continuously over several months to determine whether torpor occurs in their natural setting.

MATERIALS AND METHODS

Animal Capture and Husbandry

Nine male and four non-pregnant female adult tarsiers were used in the study. Animals were captured in mist nets during two sampling periods between August–October 2014 and March–August 2015, at Sama Jaya Nature Reserve (1°31′16″ N;

110°23′15″ E) in Kuching City, Sarawak, on the island of Borneo. The vegetation type of the study area was secondary forest and the reserve encompassed an area of approximately 38 hectares. The number of daylight hours remained fairly constant, with sunrise typically occurring shortly after 06:00 and sunset occurring shortly before 19:00. Nets were set in areas with a dense concentration of narrow-stemmed trees, as well as in areas with notable olfactory cues from scent markings of resident tarsiers. All nets were opened at dusk (ca. 18:00) and checked at regular intervals throughout the night during the tarsier's active phase (α-phase). Captured individuals were sexed and weighed using an electronic scale. Temperature-sensitive passive integrated transponder (PIT) tags (Biomark HDX12, Boise, Idaho, USA) were injected into their flanks. The PIT tags enabled us to measure the animals' subcutaneous body temperatures (T_{sub}) and also provided a unique identification code. The PIT tag's location was chosen in order to avoid any potential harm to their vital organs, while still being situated in close proximity to their core region during normal posture. After the injection, the animals were rehydrated and housed in a covered wire mesh cage fitted with branches. During captivity, animals were fed live lizards or crickets and provided with water *ad libitum*. However, to ensure a post-absorptive status during measurements, all animals received their last meal 6 h prior to respirometry measurements. Tarsiers are notoriously difficult to maintain in captivity so all animals were held captive for a maximum of 36 h only.

All experimental procedures were reported to and approved by the University of Kwazulu-Natal Animal Ethics Committee (116/13/Animal), which adopts the guidelines described by the Canadian Council on Animal Care. All experimental protocols were also approved by the Sarawak Forestry Department [permit number: NCCD.907.4.4(9)-223, NCCD.907.4.4(13)-277].

Gas Exchange Measurements

We used the incurrent flow measurement flow-through respirometry design described in Lighton (2008) to measure the rate of oxygen consumption ($\dot{V}O_2$), carbon dioxide production ($\dot{V}CO_2$), and evaporative water loss (EWL) of tarsiers exposed to varying T_as. Animals were housed in sealed 4l respirometers that were constructed from clear plexiglass acrylic. Respirometers were fitted with a grid platform elevated above a 1 cm deep layer of mineral oil used to trap urine and faeces. Dried and CO_2-free air was flowed through the chamber at constant rates between 400 and 500 ml.min^{-1}, sufficient to maintain O_2 concentrations of 20.8–20.0% within the respirometer. Incurrent air was dried and scrubbed of CO_2 by drawing it through a PC-4 Condensing Dryer (Sable Systems, Las Vegas, USA), followed by a column of silica gel and a column of indicating soda lime, and finally a column of indicating Drierite before reaching the pump and flow meter unit (SS-4 sub-sampler, Sable Systems). With the aid of a RM-8 Flow Multiplexer (Sable Systems), the excurrent air from the animal chamber and a stream of reference air were sequentially subsampled and passed through a series of gas analysers. The water vapour content of the air was measured using a RH-300 water vapour analyser (Sable Systems), whereafter it was dried again and flowed through a field gas analysis system (Foxbox-C, Sable Systems) to measure the fractional concentrations of CO_2 and O_2. CO_2 was scrubbed from the air stream prior to the O_2 analyser. Sable System's data acquisition software, Expedata (v 1.7.22), was used to interpret and record the digital outputs from the equipment using a laptop at 1-s intervals. The respective rates of EWL, $\dot{V}CO_2$, and $\dot{V}O_2$ were calculated using the equations presented in Withers (2001).

The O_2 analyser was spanned prior to every measurement and the water vapour and CO_2 gas analysers were calibrated monthly. Compressed pure nitrogen gas was used to set the zero point during all calibrations. A bubbler flask and waterbath were used to generate humid air of a known dew point in order to set the water vapour span values. The CO_2 span value was set using certified commercially available compressed CO_2 gas.

Experimental Protocol for Gaseous Exchange Measurements

We determined the animals' thermoregulatory response by concurrently measuring resting metabolic rate (RMR) and T_{sub} adjustments while exposed to temperatures between 22 and 35°C. The air temperature within the respirometers was measured using commercially available temperature sensitive data-loggers (iButton DS1922L, Thermochron, Dallas, TX, USA; resolution: 0.0625°C), hereafter temperature loggers. The experimental temperatures were controlled by partially submerging the respirometers into a body of water within a modified coolerbox, wherein the temperature of the water was regulated using a waterbath via a closed loop, such that the water flowed from the waterbath into the coolerbox and back into the waterbath. A Biomark HPR plus reader and antennae were used to read and record T_{sub} every 30 s; providing a real-time visualization of the animals' thermal profile during measurements. Temperature loggers and PIT tags were calibrated following the method of Cory Toussaint and McKechnie (2012).

All measurements were performed on solitary individuals during their rest phase (ρ-phase; 06:00–18:00). Each tarsier was exposed to a maximum of three temperatures per measurement, in a random order, for 3–6 h to allow adequate time for thermal adjustment. There were two instances where measurements were terminated prematurely because the individuals remained restless and their T_{sub}s increased rapidly to 38°C; both occurred at T_a = 35°C. Data from these two individuals were excluded from analyses.

Surgical Procedure and Free-Ranging Body Temperature Measurements

After the completion of respirometery measurements, five of the 13 animals (three males and two females) used in the respirometry study, were surgically implanted with the same custom designed temperature sensitive data-loggers (MCP 9800, Microchip Technology, Chandler, AZ; resolution: 0.0625°C) described in Lovegrove et al. (2014a) to measure T_{core} in free-ranging animals. The loggers were assembled on site at our research station at the Universiti Malaysia Sarawak. A 3-volt CR 1632 coin battery was soldered to the terminals of the logger circuit board and the units were then coated with an

acrylic protective lacquer (Electrolube, HK Wentworth Ltd., Leicestershire, UK) and encapsulated in surgical wax; yielding a final weight of ca. 4g. In compliance with the conditions stipulated for the approval of permits, all surgical procedures were performed by a local veterinarian (Dr. Samuel Kiyui, Malaysian Veterinary Council registration number: 049) under sterile conditions at his surgery. Anaesthesia was induced by a 1ml intramuscular injection of a cocktail containing Tiletamine and Zolazepam as active ingredients (Zoletil 100, Virbac Veterinary Pharmaceutics), whereafter the data loggers were inserted into the peritoneal cavity via an incision along the *linea alba*. The incision was sutured using 3/0 absorbable Dexon polyglycolic acid suture and a topical antiseptic [Chlorhexidine gluconate 5% (w/v) and Isopropyl alcohol 3.15% (w/v)] was liberally applied to the area. While anaesthetized, animals were also fitted with external VHF radio-telemetry transmitters (PD-2C, Holohil Systems Ltd., Ottawa, Canada; weight = 4 g) to allow us to track and monitor the animals. Tarsiers were released at their site of capture as soon as possible once they had regained their mental acuity and monitored for the first hour following release. Thereafter, daily observations were made for the first week and then monitoring became periodical to minimize disturbance.

The T_{core} data loggers were calibrated in a similar manner to that previously mentioned. They were programmed to record readings every 30 min for a period of 6 months. Of the five implants, we recovered 3 and 5 weeks of data from a male and female, respectively. The unsuccessful attempts were due to premature battery failure caused by the soldering process.

The T_a within the forest was recorded throughout the study period using the same type of temperature loggers that were used during metabolic measurements. The loggers were housed in black and white solar radiation shields that were attached as a pair (1 black and 1 white) at a height of 1.5m above the ground to three trees located in different sections of the reserve. All three trees were observed tarsier rest sites.

Data Analyses

Laboratory Measurements

A lag correction was performed in Expedata in order to synchronize the respective gas-exchange traces before any calculations were made. RMR and EWL were calculated from steady-state traces corresponding to the most level continuous 10-min section of the $\dot{V}O_2$ trace identified using Expedata functions. The accompanying body mass (M_b) was calculated using a regression of the animals' M_b at the start and end of metabolic measurements. Metabolic rate (in Watts) was calculated by converting the respiratory exchange ratio ($\dot{V}CO_2/\dot{V}O_2$) using the thermal equivalence data in Table 4.2 in Withers (1992). Evaporative heat loss (in Watts) was calculated assuming 2.26 J. mg H_2O^{-1}, and then used to calculate the amount of metabolic heat dissipated through evaporation as the ratio of evaporative heat loss to metabolic heat production (EHL/MHP).

In order to objectively identify inflection points along the profiles of RMR, T_{sub}, EWL and EHL/MHP as a function of T_a, we performed a piecewise regression analysis in R 3.0.2 (R Core Team, 2017) using the package "segmented" (Muggeo, 2008). Each section of data identified through the analysis was treated as independent and we adopted the approach of implementing mixed-effect models using the R package "nlme" (Pinheiro et al., 2016) to evaluate the effect of T_a while accounting for other variables. We developed models using various permutations of M_b and sex as fixed factors. To account for repeated measurements in laboratory measurements ($n = 13$) we included individual ID as a random factor in all of the models. We then compared their Akaike Information Criterion values that were corrected for small sample size (AICc and AICcWt; Burnham and Anderson, 2003) to determine the model of best fit using the R package "AICcmodavg" (Mazerolle, 2015). We tested for a gender difference in M_b at the time of first capture using a Student's *t*-test. All values are reported as mean ± standard error unless stated otherwise. The assumptions of the models were verified in a similar manner to Levesque et al. (2014).

Free-Ranging Measurements

We used Rayleigh's tests to assess whether there was any uniformity in the times at which maximum and minimum T_{core} in free-ranging animals ($n = 2$) and forest temperatures were observed. We also tested whether T_{core} followed a normally distributed pattern, using a Shapiro-Wilk's test.

RESULTS

Thermoregulatory Measurements

All thermoregulatory measurements represent complete sets of physiological variables obtained concurrently during laboratory experiments using 13 wild-caught animals. The mean M_b at first capture was 126.1 ± 2.4 g. Males ($n = 9$, $M_b = 126.9 \pm 2.7$ g) were significantly heavier than females [$n = 4$, $M_b = 117.1 \pm 2.7$ g; one-tailed $t_{(11)} = 2.76$, $p = 0.009$].

Mass-specific RMR displayed inflection points at $T_a = 25.0 \pm 1.3$°C (±95% confidence interval; CI) and $T_a = 30.0 \pm 2.5$°C (±95% CI), and displayed a significant and linear relationship with T_as < 25°C [$F_{(1, 7)} = 9.44$, $p < 0.018$, $r^2 = 0.57$] and T_as > 30°C [$F_{(1, 13)} = 9.99$, $p = 0.007$, $r^2 = 0.43$], but not with T_as between these values (**Figure 1A**, **Table 1**). Thus, the species' thermoneutral zone (TNZ) was ca. 25–30°C. We calculated a basal metabolic rate (BMR) of 3.52 ± 0.06 W.kg^{-1} (0.65 ± 0.01 ml O_2.g^{-1}.h^{-1}) by averaging all RMR values between and excluding those at the inflection points; including the values from both inflection points made no difference. The accuracy of the thermal limits proposed by the piecewise regression analysis was confirmed by substituting BMR into the respective regression equation of each line, in order to calculate the T_a at which they intersected BMR. The intersection corresponding to the lower limit of thermoneutrality (T_{lc}) was at $T_a = 25.2$°C and the upper limit (T_{uc}) was at $T_a = 30.6$°C. The models which best predicted whole-animal RMR above (Akaike weight = 0.74) and below (Akaike weight = 0.70) TNZ included T_a as the only fixed factor (**Table 2**). In both cases, the next best models contained M_b as an additional factor, and explained all of the remaining Akaike weight for metabolism below TNZ. The

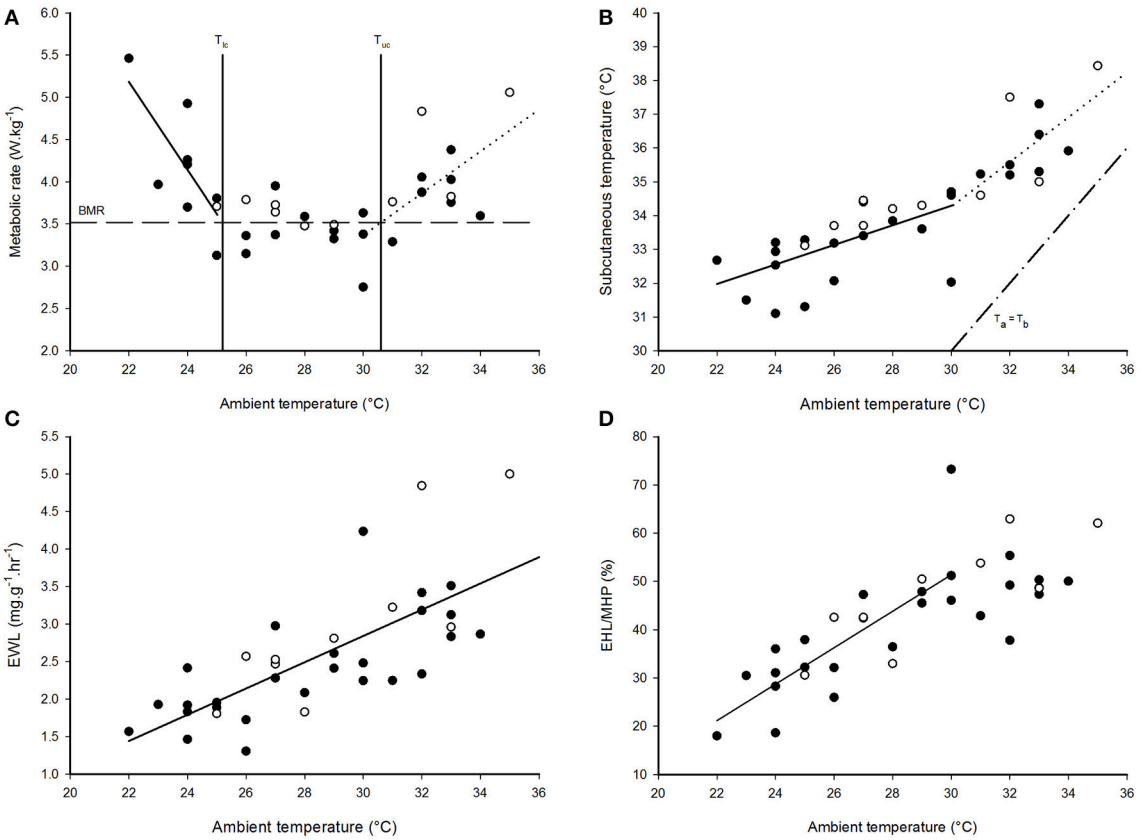

FIGURE 1 | The thermoregulatory profile of *Cephalopachus bancanus*. **(A)** Effect of ambient temperature on resting metabolic rate. **(B)** Effect of ambient temperature on subcutaneous temperature. **(C)** Effect of ambient temperature on the rate of evaporative water loss. **(D)** Effect of ambient temperature on the amount of metabolic heat dissipated through evaporative cooling. Plotted regression lines indicate the best fit for the data based on piecewise regression analysis and the equations are presented in **Table 1**. Closed circles = males, open circles = females.

remaining Akaike weight for metabolism above TNZ included gender as a factor.

T_{sub} displayed a single inflection point during the thermoregulatory measurements coincident with T_{uc} (**Figure 1B**). Both sections of the T_{sub} profile had a significant and linear relationship with T_a [$T_a < 30°C$: $F_{(1, 19)} = 19.58$, $p < 0.001$; $T_a > 30°C$: $F_{(1, 13)} = 15.68$, $p = 0.002$], but the slope of the relationship for $T_a < 30°C$ was lower (**Table 1**). The model which best predicted T_{sub} above T_{uc} included T_a as the only fixed factor (Akaike weight = 0.82), whereas the model best suited to predict T_{sub} below T_{uc} included all of the variables (Akaike weight = 0.73). The mean minimum T_{sub} was 32.4 ± 0.5°C observed at $T_a = 24°C$, whereas at higher T_as there was no difference in the mean maximum T_{sub} observed at $T_a = 32°C$ ($T_{sub} = 35.9 \pm 0.5°C$) and $T_a = 33°C$ ($T_{sub} = 36.0 \pm 0.5°C$).

EWL had a significant, positive linear relationship with T_a [$F_{(1, 34)} = 37.9$, $p < 0.001$, $r^2 = 0.53$, **Figure 1C**, **Table 1**] and was best predicted by a model containing T_a as the only fixed factor (Akaike weight = 0.58, **Table 2**). EWL ranged from a mean minimum of 1.86 ± 0.37 $mg^{-1}.g^{-1}.h^{-1}$ at $T_a = 26°C$, to a mean maximum of 3.44 ± 0.52 $mg^{-1}.g^{-1}.h^{-1}$ at $T_a = 32°C$. Barring the elevated rate at $T_a = 27°C$, EWL remained <2 $mg^{-1}.g^{-1}.h^{-1}$ and was stable at T_as ≥ 28°C. In addition, EWL displayed a strong correlation with T_{sub} ($r = 0.81$), and T_{sub} was correlated to the amount of EHL/MHP ($r = 0.67$).

The percentage of EHL/MHP scaled linearly with T_a below T_{uc} [$F_{(1, 19)} = 29.7$, $p < 0.001$, **Figure 1D**, **Table 1**]. At T_as > 30°C, EHL/MHP remained relatively constant and no longer displayed any relationship with T_a. The mean maximum percentage of EHL/MHP was 57 ± 6% and was achieved at $T_a = 30°C$. The model which best predicted EHL/MHP below T_{uc} was again the one which included T_a as the only fixed factor (Akaike weight = 0.65).

Free-Ranging Body Temperature Profile

Both tarsiers were implanted on the 19th June 2015, but we excluded all values prior to the 24th of June to minimize any potentially misleading data recorded during the period of recuperation.

The frequency distribution (0.5°C incremental bin category) of T_{core} did not conform to a Gaussian distribution pattern (♂: $W = 0.98$, $p < 0.001$; ♀: $W = 0.96$, $p < 0.001$), but displayed a slightly left-skewed unimodal pattern. For both individuals, the

TABLE 1 | Linear regression models describing the relationship between ambient temperature (T_a) and various physiological parameters in *Cephalopachus bancanus*.

Parameter	Temperature range	Regression equation
RMR	$T_a < 25°C$:	$RMR = 16.65 - 0.5212 \times T_a$*
	$T_a > 30°C$:	$RMR = 0.2479 \times T_a - 4.069$**
T_{sub}	$T_a < 30°C$:	$T_{sub} = 25.64 + 0.2879 \times T_a$*
	$T_a > 30°C$:	$T_{sub} = 14.64 + 0.6547 \times T_a$*
EWL	All	$EWL = 0.17512 \times T_a - 2.41254$*
EHL/MHP	$T_a < 30°C$:	$EHL/MHP = 3.761 \times T_a - 61.52$*

*Mass-specific resting metabolic rate = RMR, subcutaneous temperature = T_{sub}, the rate of evaporative water loss = EWL, the amount of metabolic heat dissipated through evaporative cooling = EHL/MHP, * $p < 0.05$, ** $p < 0.01$.*

TABLE 2 | Linear mixed-effect models which best describe the significant relationships between ambient temperature (T_a) and resting metabolic rate (RMR), subcutaneous temperature (T_{sub}), the rate of evaporative water loss (EWL) and the amount of metabolic heat dissipated through evaporative cooling (EHL/MHP) in *Cephalopachus bancanus*.

Fixed factors	Random factor	*k*	AICc	Akaike weights
RMR ($T_a > 30°C$)				
T_a	~1|ID	4	−37.92	0.74
$T_a + M_b$	~1|ID	5	−34.89	0.16
T_a + Sex	~1|ID	5	−33.34	0.07
$T_a + M_b$ + Sex	~1|ID	6	−31.08	0.02
RMR ($T_a < 25°C$)				
T_a	~1|ID	4	−0.69	0.7
$T_a + M_b$	~1|ID	5	1.01	0.3
T_{sub} ($T_a > 30°C$)				
T_a	~1|ID	4	51.57	0.82
T_a + Sex	~1|ID	5	56.01	0.09
$T_a + M_b$	~1|ID	5	56.15	0.08
$T_a + M_b$ + Sex	~1|ID	6	61.34	0.01
T_{sub} ($T_a < 30°C$)				
$T_a + M_b$ + Sex	~1|ID	6	43.15	0.73
$T_a + M_b$	~1|ID	5	45.81	0.19
T_a	~1|ID	4	48.06	0.06
T_a + Sex	~1|ID	5	50.88	0.02
EWL				
T_a	~1|ID	4	117.26	0.58
T_a + Sex	~1|ID	5	119.66	0.17
$T_a + M_b$	~1|ID	5	119.67	0.17
$T_a + M_b$ + Sex	~1|ID	6	121.47	0.07
EHL/MHP ($T_a < 30°C$)				
T_a	~1|ID	4	−52.66	0.65
$T_a + M_b$	~1|ID	5	−50.19	0.19
T_a + Sex	~1|ID	5	−49.62	0.14
$T_a + M_b$ + Sex	~1|ID	6	−46.19	0.03

Only models with Akaike weights ≥ 0.01 are presented.

modal T_{core} was 35.0 ± 0.5°C (**Figures 2C,D**) and only once, in the male, did T_{core} exceed 37°C. Quantile 1 of the free-ranging T_{core}s were similar between individuals (Q1: ♂ = 34.5°C vs. Q1: ♀ = 34.3°C) but the female displayed a higher propensity for T_{core} to decrease below Q1 (♀: 16% of all T_{core}s vs. ♂: 8% of all T_{core}s). The mean daily range in T_{core} was 2.4°C for both individuals and the times at which the maximum and minimum T_as and T_{core}s (excluding the maximum T_{core} of the male) were observed were not uniformly distributed throughout a 24-h period (Rayleigh's test, $p < 0.001$; **Table 3**). Peak T_{core}s during the α-phase occurred consistently at 19:00 or 06:00 which coincided with the highest and lowest scotophase T_as, respectively. The lowest T_{core}s were consistently observed at or before 10:00, preceding the onset of the rapid increase in T_a to the daily maximum (range: 27.9–35.2°C, **Table 3**) at ca. 14:30. The frequency distribution of T_as during the scotophase were slightly right skewed and unimodal, with a peak in frequency at T_a = 25°C (**Figure 3**). The frequency distribution of T_as during the photophase were left skewed and had a flat-shaped distribution; the highest frequencies were observed between T_a = 30.0–32.5°C (**Figure 3**). The T_{core}-T_a gradient was lowest during the ρ-phase and was ≤3°C on 75 and 70% of the observation days for the male and female, respectively; of those, 42 and 61% were ≤2°C (**Figures 2A,B**).

DISCUSSION

Our study provides no clear indication of metabolic suppression or the characteristic concomitant decrease in body temperature associated with heterothermy in either wild-caught animals measured in the laboratory or in free-ranging individuals. For the field data, having a single individual per sex limits our deductions regarding the finer details and interpretation of the species' free-ranging T_{core} pattern. Nonetheless, we are able to provide a few key observations and relate them to data from the laboratory.

The lowest temperatures to which tarsiers were exposed, both in the laboratory and in the field, was approximately 20°C, that is, about 5°C lower than the T_{lc}. Typically, it is at temperatures <T_{lc} that heterotherms enter daily torpor or hibernation. Instead, tarsiers appeared to show cold sensitivity. During laboratory measurements, it became increasingly difficult for the animals to maintain T_bs > 33°C at T_as < 30°C despite their best thermoregulatory attempts at metabolic upregulation. The decreasing trend in T_b at low temperatures suggests that the animals may have been heading towards mild pathological hypothermia at the lowest ambient temperatures. One observation in the free-ranging data provides a margin of support for our argument. T_{core} in the female decreased to 31.5°C during the afternoon on the 29th of June (**Figure 2A**) following a cold snap and only rebounded after T_a started to increase later during the day. However, the male did not display the same response during the cold snap. That tarsiers may be acutely cold sensitive does not seem far-fetched considering that they evolved in a warm tropical climate and have never left those conditions (Jablonski, 2003; Simons, 2003).

In contrast to the body temperature profile observed in free-ranging *T. syrichta* individuals on Bohol Island in the Phillipines (Lovegrove et al., 2014a), free-ranging *C. bancanus* maintained

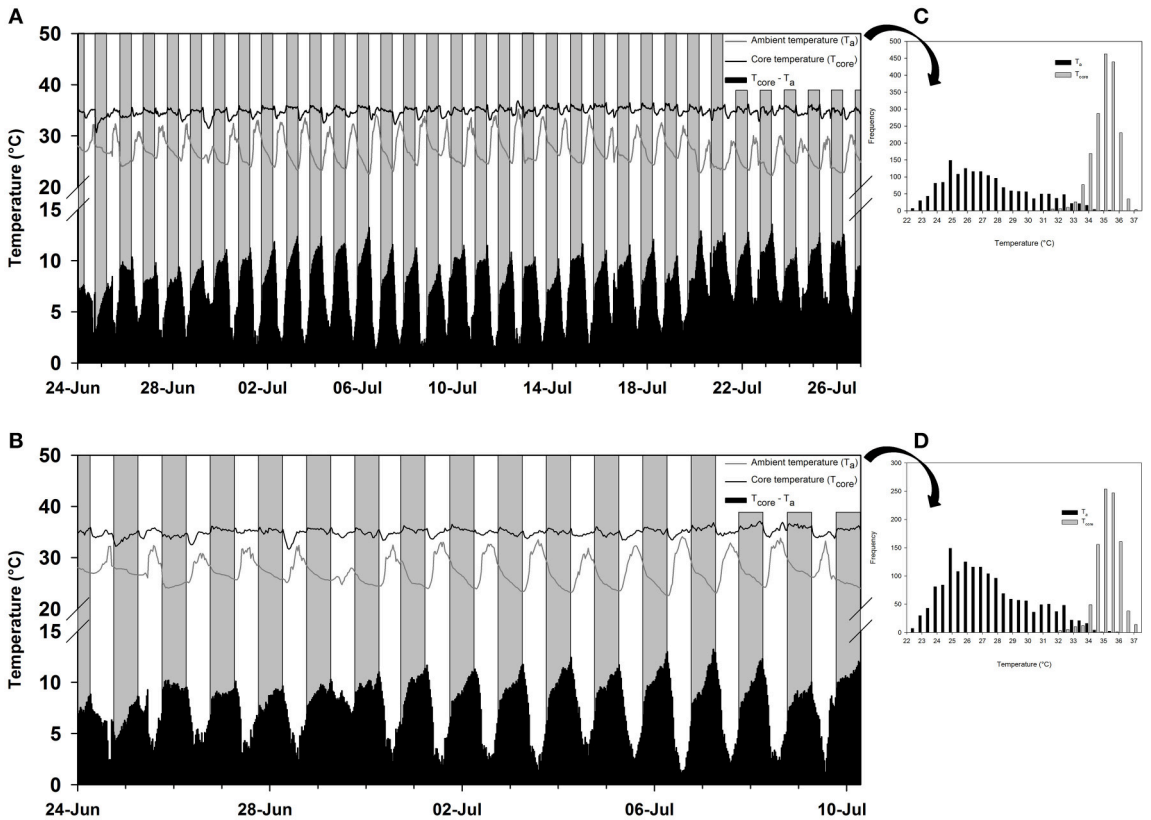

FIGURE 2 | The free-ranging temperature profile in western tarsiers (*Cephalopachus bancanus*). **(A)** The ambient temperatures (T_a; gray line) and core temperatures (T_{core}; black line) recorded in a female from 00:00 24th June 2015 to 00:00 27th July 2015. **(B)** The ambient temperatures (T_a; gray line) and core temperatures (T_{core}; black line) recorded in a male from 00:00 24th June 2015 to 06:30 10th July 2015. The grey and white bars represent night and day, respectively, and the black bars at the base of each plot represent the temperature differential between the T_a and T_{core}. **(C,D)** The frequency distribution of the respective T_as and T_{core}s observed in the female and male tarsier's temperature profile.

higher T_{core}s during their active phase. In that study, *T. syrichta* displayed an extremely unusual pattern for a nocturnal mammal (Aschoff, 1983; Refinetti and Menaker, 1992) with consistent and considerable heat storage occurring during the photophase. Heat storage, barring one exceptionally hot day where T_{core} was elevated to $T_{core} = 36.8°C$ (see July 13, **Figure 2B**), did not occur routinely during the photophase in this study. Furthermore, *C. bancanus* maintained a range of T_{core}s that bordered the boundary between basoendothermy and "mesoendothermy" ($35°C \leq T_b \leq 37.9°C$) (*sensu* Lovegrove, 2012a), but were more frequently representative of mesoendothermic values. Thus, whereas *T. syrichta* appeared to be a strict basoendotherm (Lovegrove et al., 2014a), *C. bancanus* maintained normothermic T_{core}s which were closer to the average T_b of the primate clade (see Clarke et al., 2010). The free-ranging T_{core} in our study suggests that tarsiers are intermediate between the ancestral low T_b condition and the derived higher T_b condition (Lovegrove, 2012a), which supports the phylogenetic position of tarsiers as the link between the older and derived primates (Hartig et al., 2013). Notably, the data from *T. syrichta* were skin temperatures (T_{skin}) measured as a proxy for core temperatures; a technique which is susceptible to unreliable measures (Dausmann, 2012; Lovegrove et al., 2014a) especially, as we suspect is the case in the Bohol study, by loose-fitting collars. For now, heat storage may not be as prominent in tarsiers as the Bohol data suggested, but this may change within the near future.

It has been argued that the temperature increase associated with global warming will have a mild effect on *T. syrichta*, in spite of their T_{skin} pattern, because their TNZ was above the maximum T_as observed in their habitat (McNab and Wright, 1987; Lovegrove et al., 2014a). The same notion does not apply here. The TNZ range of *C. bancanus* (**Figure 1A**), is approximately 5°C lower than that of *T. syrichta*. A conservative prediction of a 3°C increase in T_as, relative to the modal T_as observed in our study, would result in a large proportion of the photophase T_as shifting above the TNZ of *C. bancanus* (see **Figure 3**). Offloading excess body heat as T_a approaches T_{core} is effective through evaporative cooling only (Sherwood and Huber, 2010). The laboratory data show that heat dissipation through evaporation, in a dry atmosphere, was effective up to $T_a = 30°C$ only (**Figures 1C,D**). Above that, heat storage culminated in dangerously high T_{sub}s (**Figure 1B**). Worrisomely, wild tarsiers are faced with constantly high relative humidity conditions which retard heat dissipation. A further concern is

TABLE 3 | The daily mean, maximum and minimum ambient (T_a) and tarsier core (T_{core}) temperatures observed throughout the period of free-ranging data collection (values in parenthesis represent the range in daily means), as well as the times at which these parameters where most frequently observed.

	Photophase (ρ-phase)			Scotophase (α-phase)		
	T_a ($n = 33$)	♀ T_{core} ($n = 33$)	♂ T_{core}($n = 16$)	T_a ($n = 33$)	♀ T_{core} ($n = 33$)	♂ T_{core} ($n = 17$)
Mean	28.6°C (25.75–31.0°C)	34.4°C (32.9–35.2°C)	34.7°C (33.9–35.6°C)	25.8°C (23.8–27.7°C)	35.1°C (33.5–35.7°C)	35.3°C (34.1–36.4°C)
Maximum	32.1°C (28.0–35.2°C)	35.8 (34.9–36.8°C)	35.7°C (35.0–36.9°C)	28.2°C (24.3–29.9°C)	35.8°C (34.0–36.4°C)	36.1°C (37.1–35.3°C)
Minimum	24.3°C (22.3–27.0°C)	33.4°C (31.5–34.4°C)	33.7°C (31.6–35.3°C)	24.30°C (22.2–27.1°C)	34.4°C (30.6–35.3°C)	34.4°C (32.2–35.8°C)
The time of the day at which maximum and minimum temperatures occurred and the relative percentage of observations						
	T_a max	T_a min	♀ T_{core} max	♀ T_{core} min	♂ T_{core} max	♂ T_{core} min
Photophase (ρ-phase)	†13:00 (12%); 13:30 (15%); 14:00 (24%); 14:30 (18 %)	†06:30 (15%); 07:00 (61%)	†06:30 (76%)	†08:30 (15%); 09:00 (21%); 09:30 (30%)	06:30 (53%); 14:30 (12%); 16:00 (18%)	†08:30 (12%); 09:00 (24%); 09:30 (24%); 10:00 (12%); 18:00 (12%)
Scotophase (α-phase)	†00:30 (12%); 18:30 (82%)	†05:30 (24%); 06:00 (45%)	†06:00 (18%); 19:00 (42%)	†02:00 (12%); 04:00 (12%); 04:30 (15%); 18:30 (27%)	06:00 (18%); 19:00 (59%)	†00:00 (18%); 00:30 (12%); 01:00 (12%); 03:30 (18%);

Photophase corresponds to the animals rest phase, whereas scotophase corresponds to their active phase. ♂, male; ♀, female; max, highest temperature; min, lowest temperature; n, periods of observations and † indicates a significant ($p < 0.05$) Rayleigh's test.

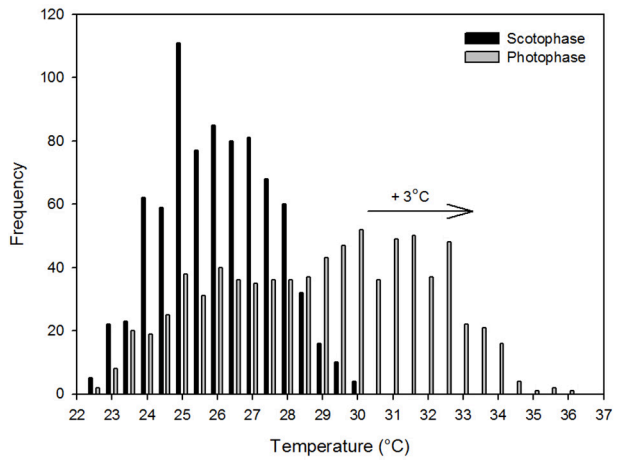

FIGURE 3 | The frequency distribution of the scotophase and photophase ambient temperatures recorded within the forest at Sama Jaya Nature Reserve from 00:00 24th June 2015 to 00:00 27th July 2015. The arrow indicates the commonly predicted shift of three degree Celsius in the modal temperature associated with global warming.

the argument that the rate of global warming has been greatly underestimated by the IPCC (IPCC, 2007; Rahmstorf et al., 2007; van Oldenborgh et al., 2009), and might be much higher than the feasible adaptive response of the species (Hughes, 2000; Root et al., 2003; Quintero and Wiens, 2013). Increases in the severity and frequency of extreme weather events, which are known to have devastating consequences (Boyles et al., 2011), have also been predicted (Meehl and Tebaldi, 2004; Jentsch et al., 2007; Luber and McGeehin, 2008). The future survival of wild *C. bancanus* is therefore highly questionable and supports the concerns expressed by Lovegrove et al. (2014a).

South East Asia is highly susceptible to the effects of El Niño-Southern Oscillation (ENSO). Thus, even though temperatures within the tropical belt may remain relatively stable, the region as a whole is highly unpredictable due to the effects of ENSO (Allan et al., 1996). As such, from an evolutionary perspective, the capacity for heterothermy, should tarsiers possess the ability, is likely to have been retained. Coincidently, there was a switch from El Niño to La Niña during the study, which would have resulted in a degree of climatic unpredictability. Given the shift in climate, the early morning cold snap on the 29th of June would have been an opportune time for them to enter torpor and they could have maximized the benefits by exploiting the daily increase in temperature to rewarm passively. Thus, based on the results of our study and those of previous work on tarsiers (Clarke, 1943; McNab and Wright, 1987; Lovegrove et al., 2014a), we conclude that heterothermy has yet to be observed in tarsiers. However, given the low sample size of free-ranging T_b data here and by Lovegrove et al. (2014a), we cannot rule out the potential for heterothermy within *C. bancanus* or *T. syrichta*, and certainly not for the rest of the Tarsiidae for which there are no data. That said, the apparent loss of heterothermy in tarsiers, as well as the lack of evidence for heterothermy in other haplorrhines, if true, suggests that adaptive heterothermy may have been lost either in the ancestor of the tarsiers or in the tarsier clade. We muse on our rationale below and identify also several potential haplorrhine primate species in which a search

for heterothermy might fruitfully aid in resolving the primate adaptive-heterothermy phenotype.

Barring a few notable exceptions within the carnivores, monotremes and rodents, heterothermy is mostly observed in mammals smaller than 1 kg; mean weight of approximately 340 g (Geiser, 1998; Lovegrove, 2012a; Ruf and Geiser, 2015). Body size is an important consideration because thermal inertia in large-bodied animals hampers the reduction in T_b and thus the energetic benefits of heterothermy (Geiser, 1998; Ruf and Geiser, 2015). Observations of heterothermy in large and small sized animals suggests that they may even represent different conditions but more work on this topic is required (Geiser, 2001). Specifically within primates, heterothermic species range in M_b from the 30 g Madame Berthe's mouse lemur (*Microcebus berthae*; Dausmann and Warnecke, 2016) to the 350 g furry-eared dwarf lemur (*Cheirogaleus crossleyi*; Blanco and Rahalinarivo, 2010; Blanco et al., 2013), but the heaviest known primate heterotherm is the 400 g pygmy slow loris (*Nycticebus pygmaeus*; Ruf et al., 2015). No heterothermy was observed in the large 600 g sportive lemur (*Lepilemur ruficaudatus*; Schmid and Ganzhorn, 1996). Thus, even though body size may not be the only determining factor, it is an important consideration so we analysed the database of Isler et al. (2008) to identify other potential primate candidates that, based on body mass, could be heterotherms. The database contained the body mass values for 239 primates, 177 of which were haplorrhines. Excluding the tarsiers (Tarsiidae), there are 11 other haplorrhines that weigh 500 g or less and all belong to the family Cebidae namely *Callithrix pygmaea*, *C. jacchus*, *C. penicillate*, *C. argentata*, *C. humeralifera*, *C. aurita*, *Saguinus fuscicollis*, *S. niger*, *S. oedipus*, *S. nigricollis*, and *Callimico goeldii*. To the best of our knowledge, no evidence of torpor has been observed in these primates. However, although metabolic studies do exist for some (Boere et al., 2005; Kuehnel et al., 2012; Go et al., 2015; Ross et al., 2015; Lelegren et al., 2016), thermoregulatory studies with the potential to observe heterothermy have only been conducted for *C. jacchus* (Petry et al., 1986), *C. pygmaea* (Genoud et al., 1997), *S. oedipus* (Stonerook et al., 1994), and *C. goeldii* (Kälin et al., 2003; Power et al., 2003). While we cannot, at this point, discount the possibility of torpor in all Platyrrhini, the lack of torpor by *C. pygmaea,* the smallest and most eligible platyrrhine heterotherm, is congruent with our reasoning. We urge further investigation and suggest that future studies focus on the species listed here as they are the most likely to disprove our idea of the loss of heterothermy in non-Shrepsirrhini.

The reason(s) why adaptive heterothermy appears to have been lost in tarsiers at the Strepsirrhini-Haplorrhini split is unclear. However, it is worth exploring the similarities and dissimilarities between heterothermic members of the Strespirrhini and members of the Tarsiidae which might also explain the apparent loss of heterothermy in other haplorrhines. We share thoughts on factors directly related to energy expenditure namely, body size including the size of the brain, nocturnal habits, the effect of diet, reproduction and locomotion.

As discussed earlier, based on their M_b, tarsiers should be eligible to express heterothermy. Thus, there may be another size-related factor that accounts for the lack of torpor use, such as brain size. Brain tissue is a metabolically expensive tissue. The increase in brain size of the haplorrhines and the consequent increase in metabolic demands reflected in higher BMRs (Isler and van Schaik, 2006) may have prohibited the use of heterothermy (Lovegrove, 2017). Tarsiers are nocturnal hunters that leap from tree to tree. The ability to successfully navigate, let alone hunt, in low light environments requires tremendous visual acuity, depth perception and neuronal accompaniment (Collins et al., 2005). Indeed, tarsiers display numerous specialized adaptations such as an enlarged lens, cornea and retina, as well as a high density of rods in the retina (>300,000 per mm^2) in addition to neuronal adjustments, most notably enlarged primary and secondary visual cortex regions (Castenholz, 1984; Collins et al., 2005). However, these adaptations appear subject to a trade-off. Tarsier brains, relative to other primates, do not show an increase in mass, endocranial volume or encephalization quotient (Stephan, 1984; Grabowski et al., 2016). Instead, tarsiers compensate through a morphological readjustment of the brain by having enlarged occipital and temporal lobes and a diminished frontal lobe (Schwartz, 2003).

The Expensive-Tissue Hypothesis predicts that the metabolic costs associated with large brains in primates are off-set by reductions in the equally costly splanchnic tissue (Aiello and Wheeler, 1995). Thus, in addition to the morphological readjustment in tarsier brains, a further trade-off may be their dietary simplification and specialization. As previously mentioned, tarsiers are the only strict carnivorous primates, and it has been suggested that their dietary constriction may preclude the ability to employ heterothermy (Dausmann, 2008). However, the restricting factor may not be their diet *per se*, but rather the trade-off which their diet represents. An expansion of The Expensive-Tissue Hypothesis, the Expensive Brain Framework Hypothesis (Isler and van Schaik, 2009), proposed that the costs associated with relatively large brains must either accompany an increase in energy turnover or a reduction in energy expenditure; not limited to digestion. Within this framework, a portion of the energetic costs associated with a large primate brain and visual adaptations needed for their carnivorous nocturnal lifestyle (Crompton and Andau, 1986, 1987; Jablonski and Crompton, 1994) may be shared by a reduction in foetal growth rate, reproductive output and the cost of locomotion.

Tarsiers typically produce a single offspring and have gestation periods ranging between 157 and 180 days, longer than the gestation period of *Microcebus* spp. and *Cheirogaleus* spp., but comparable to those of *Galago* spp. and *Loris* spp. (Izard et al., 1985; Roberts, 1994). However, the M_b of tarsier neonates relative to their adult M_b as well as their neonate brain size is significantly larger than other primates (Roberts, 1994). The large neonatal brain size explains why, despite similar or even slower postnatal growth rates and weaning periods relative to other primates, tarsier infants have extremely rapid behavioural development, particularly in foraging behaviour (Roberts, 1994). As such, development factors, in combination with dietary constraints may preclude heterothermy. Furthermore, in *C. bancanus* at least, homeothermy may be related to the fact that they remain reproductively active throughout the year (MacKinnon and MacKinnon, 1980; Wright et al., 1986). Males thus continuously produce sperm and a greater variation in body temperature may compromise sperm viability as spermatogenesis, sperm storage

and sperm maturation processes are optimized at 34–36°C (Lovegrove, 2014).

With regards to the cost of locomotion, irrespective of the mode of locomotion the energetic investment is proportional to M_b (Schmidt-Nielsen, 1997; Withers et al., 2016). Of the various modes of locomotion, saltation, while at low speed, is known to be energetically more costly than typical walking. However, it becomes energetically more efficient as the speed increases (Withers et al., 2016). Tarsiers do not typically hop around on the ground at low speed, but leap fleetly around in trees. In comparison to other saltatorial primates, tarsiers seemingly have the lowest energetic investment (Warren and Crompton, 1998). Warren and Crompton (1998) considered the kinetic cost of leaping, M_b, distant travelled, home range size and metabolism, and showed that even though tarsiers travelled the farthest and had the largest home range of all their study species, they had the lowest absolute and relative cost of locomotion. This reduction in energetic expense presumably stems from the tarsiers' musculoskeletal anatomical adaptations (Jouffroy et al., 1984; Peters and Preuschoft, 1984; Schultz, 1984; Anemone and Nachman, 2003); the most obvious of which is the eponymous elongated tarsal bones.

AUTHOR CONTRIBUTIONS

SW and BL conceived and designed the study. SW performed the data collection, analyses and drafted the manuscript. BL contributed to and approved the manuscript. AT secured capture permits, provided logistical support, as well as approved the manuscript.

FUNDING

The research was support by the National Research Foundation (South Africa), GreenMatter fellowship (South Africa) and their partners, as well as the Ministry of Higher education of Malaysia (FRGS/1/2013/ST03/UNIMAS/01/2).

ACKNOWLEDGMENTS

We thank the friendly staff at Sama Jaya Nature Reserve, as well as Dr. Samuel Kiyui and his staff at Country Veterinary Clinic. We also thank Danielle Levesque, Tunmise Otitoju, Miyn Naharuddin, Anthony Pine, Sally Soo, and Frances Hii for their help in the field.

REFERENCES

Aiello, L. C., and Wheeler, P. (1995). The expensive-tissue hypothesis: the brain and the digestive system in human and primate evolution. *Curr. Anthropol.* 36, 199–221. doi: 10.1086/204350

Allan, R. J., Lindesay, J., and Parker, D. E. (1996). *El Niño, Southern Oscillation, and Climatic Variability*. Collingwood, VIC: CSIRO Publishing.

Anemone, R. L., and Nachman, B. A. (2003). "Morphometrics, functional anatomy, and the biomechanics of locomotion among tarsiers," in *Tarsiers: Past, Present, and Future*, eds P. C. Wright, E. L. Simons, and S. Gursky (New Brunswick, NJ: Rutgers University Press), 97–120.

Aschoff, J. (1983). Circadian control of body temperature. *J. Therm. Biol.* 8, 143–147. doi: 10.1016/0306-4565(83)90094-3

Augee, M. L., and Gooden, B. A. (1992). "Monotreme hibernation—some afterthoughts," in *Platypus and Echidnas*, ed M. L. Augee (Sydney, NSW: Royal Zoological Society of New South Wales), 174–176.

Aujard, F., Perret, M., and Vannier, G. (1998). Thermoregulatory responses to variations of photoperiod and ambient temperature in the male lesser mouse lemur: a primitive or an advanced adaptive character? *J. Comp. Physiol. B* 168, 540–548. doi: 10.1007/s003600050175

Bennett, A. F., and Ruben, J. A. (1979). Endothermy and activity in vertebrates. *Science* 206, 649–654. doi: 10.1126/science.493968

Bieber, C., Lebl, K., Stalder, G., Geiser, F., and Ruf, T. (2014). Body mass dependent use of hibernation: why not prolong the active season, if they can? *Funct. Ecol.* 28, 167–177. doi: 10.1111/1365-2435.12173

Bieber, C., and Ruf, T. (2009). Summer dormancy in edible dormice (*Glis glis*) without energetic constraints. *Naturwissenschaften* 96, 165–171. doi: 10.1007/s00114-008-0471-z

Blanco, M. B., Dausmann, K. H., Ranaivoarisoa, J. F., and Yoder, A. D. (2013). Underground hibernation in a primate. *Sci. Rep.* 3:1768. doi: 10.1038/srep01768

Blanco, M. B., and Rahalinarivo, V. (2010). First direct evidence of hibernation in an eastern dwarf lemur species (*Cheirogaleus crossleyi*) from the high-altitude forest of Tsinjoarivo, central-eastern Madagascar. *Naturwissenschaften* 97, 945–950. doi: 10.1007/s00114-010-0707-6

Boere, V., Pinheiro, E. C., de Oliveira e Silva, I., Paludo, G. R., Canale, G., Pianta, T., et al. (2005). Comparison between sex and age class on some physiological, thermal, and hematological indices of the cerrado's marmoset (*Callithrix penicillata*). *J. Med. Primatol.* 34, 156–162. doi: 10.1111/j.1600-0684.2005.00101.x

Boyles, J. G., Seebacher, F., Smit, B., and McKechnie, A. E. (2011). Adaptive thermoregulation in endotherms may alter responses to climate change. *Integr. Comp. Biol.* 51, 676–690. doi: 10.1093/icb/icr053

Burnham, K. P., and Anderson, D. R. (2003). *Model Selection and Multimodel Inference: A Practical Information-Theoretic Approach*. New York, NY: Springer.

Castenholz, A. (1984). "The eye of Tarsius," in *Biology of Tarsiers*, ed C. Niemitz (Stuggart: Gustav Fischer Verlag), 303–318.

Clarke, A., and Pörtner, H. O. (2010). Temperature, metabolic power and the evolution of endothermy. *Biol. Rev.* 85, 703–727. doi: 10.1111/j.1469-185X.2010.00122.x

Clarke, A., Rothery, P., and Isaac, N. J. (2010). Scaling of basal metabolic rate with body mass and temperature in mammals. *J. Anim. Ecol.* 79, 610–619. doi: 10.1111/j.1365-2656.2010.01672.x

Clarke, R. W. (1943). The respiratory exchange of *Tarsius spectrum*. *J. Mammal.* 24, 94–96. doi: 10.2307/1374785

Collins, C. E., Hendrickson, A., and Kaas, J. H. (2005). Overview of the visual system of tarsius. *Anat. Rec. A. Discov. Mol. Cell. Evol. Biol.* 287A, 1013–1025. doi: 10.1002/ar.a.20263

Cory Toussaint, D., and McKechnie, A. E. (2012). Interspecific variation in thermoregulation among three sympatric bats inhabiting a hot, semi-arid environment. *J. Comp. Physiol. B.* 182, 1129–1140. doi: 10.1007/s00360-012-0683-6

Crompton, A. W., Taylor, C. R., and Jagger, J. A. (1978). Evolution of homeothermy in mammals. *Nature* 272, 333–336. doi: 10.1038/272333a0

Crompton, R. H., and Andau, P. M. (1986). Locomotion and habitat utilization in free-ranging *Tarsius bancanus*: a preliminary report. *Primates* 27, 337–355. doi: 10.1007/BF02382075

Crompton, R. H., and Andau, P. M. (1987). Ranging, activity rhythms, and sociality in free-ranging *Tarsius bancanus*: a preliminary report. *Int. J. Primatol.* 8, 43–71. doi: 10.1007/BF02737113

Dausmann, K. H. (2008). "Hypometabolism in primates: torpor and hibernation," in *Hypometabolism in Animals: Hibernation, Torpor and Cryobiology*, eds B. G. Lovegrove and A. E. McKechnie (Pietermaritzburg: University of KwaZulu-Natal), 327–336.

Dausmann, K. H. (2012). The pitfalls of body temperature measurements. *Naturwissenschaften* 99, 511–513. doi: 10.1007/s00114-012-0924-2

Dausmann, K. H. (2014). Flexible patterns in energy savings: heterothermy in primates. *J. Zool.* 292, 101–111. doi: 10.1111/jzo.12104

Dausmann, K. H., Ganzhorn, J. U., and Heldmaier, G. (2000). "Body temperature and metabolic rate of a hibernating primate in Madagascar: preliminary results from a field study," in *Life in the Cold: Eleventh International Hibernation Symposium*, eds G. Heldmaier and M. Klingenspor (Berlin; Heidelberg: Springer Berlin Heidelberg), 41–47.

Dausmann, K. H., Glos, J., Ganzhorn, J. U., and Heldmaier, G. (2005). Hibernation in the tropics: lessons from a primate. *J. Comp. Physiol. B* 175, 147–155. doi: 10.1007/s00360-004-0470-0

Dausmann, K. H., and Warnecke, L. (2016). Primate torpor expression: ghost of the climatic past. *Physiology* 31, 398–408. doi: 10.1152/physiol.00050.2015

Farmer, C. G. (2000). Parental care: the key to understanding endothermy and other convergent features in birds and mammals. *Am. Nat.* 155, 326–334. doi: 10.1086/303323

Geiser, F. (1998). Evolution of daily torpor and hibernation in birds and mammals: importance of body size. *Clin. Exp. Pharmacol. Physiol.* 25, 736–740. doi: 10.1111/j.1440-1681.1998.tb02287.x

Geiser, F. (2001). "Hibernation: endotherms," in *eLS* (Chichester: John Wiley & Sons, Ltd.). doi: 10.1002/9780470015902.a0003215.pub2

Geiser, F., and Brigham, R. M. (2012). "The other functions of torpor," in *Living in a Seasonal World: Thermoregulatory and Metabolic Adaptations*, eds T. Ruf, C. Bieber, W. Arnold, and E. Millesi (Berlin; Heidelberg: Springer), 109–121.

Geiser, F., and Turbill, C. (2009). Hibernation and daily torpor minimize mammalian extinctions. *Naturwissenschaften* 96, 1235–1240. doi: 10.1007/s00114-009-0583-0

Genoud, M., Martin, R. D., and Glaser, D. (1997). Rate of metabolism in the smallest simian primate, the pygmy marmoset (*Cebuella pygmaea*). *Am. J. Primatol.* 41, 229–245.

Go, Y. M., Liang, Y., Uppal, K., Soltow, Q. A., Promislow, D. E., Wachtman, L. M., et al. (2015). Metabolic characterization of the common marmoset (*Callithrix jacchus*). *PLoS ONE* 10:e0142916. doi: 10.1371/journal.pone.0142916

Grabowski, M., Voje, K. L., and Hansen, T. F. (2016). Evolutionary modeling and correcting for observation error support a 3/5 brain-body allometry for primates. *J. Hum. Evol.* 94, 106–116. doi: 10.1016/j.jhevol.2016.03.001

Grigg, G., and Beard, L. (2000). "Hibernation by echidnas in mild climates: Hints about the evolution of endothermy?" in *Life in the Cold: Eleventh International Hibernation Symposium*, eds G. Heldmaier and M. Klingenspor (Berlin; Heidelberg: Springer Berlin Heidelberg), 5–19.

Grigg, G. C., Beard, L. A., and Augee, M. L. (2004). The evolution of endothermy and its diversity in mammals and birds. *Physiol. Biochem. Zool.* 77, 982–997. doi: 10.1086/425188

Groves, C., and Shekelle, M. (2010). The genera and species of Tarsiidae. *Int. J. Primatol.* 31, 1071–1082. doi: 10.1007/s10764-010-9443-1

Gursky, S. (2000). Effect of seasonality on the behavior of an insectivorous primate, *Tarsius spectrum*. *Int. J. Primatol.* 21, 477–495. doi: 10.1023/A:1005444020059

Hansen, T. F. (1997). Stabilizing selection and the comparative analysis of adaptation. *Evolution* 51, 1341–1351. doi: 10.1111/j.1558-5646.1997.tb01457.x

Hartig, G., Churakov, G., Warren, W. C., Brosius, J., Makalowski, W., and Schmitz, J. (2013). Retrophylogenomics place tarsiers on the evolutionary branch of anthropoids. *Sci. Rep.* 3:1756. doi: 10.1038/srep01756

Hayes, J. P., and Garland, T. (1995). The evolution of endothermy: testing the aerobic capacity model. *Evolution* 49, 836–847. doi: 10.1111/j.1558-5646.1995.tb02320.x

Hughes, I. (2000). Biological consequences of global warming: is the signal already apparent? *Trends Ecol. Evol.* 15, 56–61. doi: 10.1016/S0169-5347(99)01764-4

IPCC (2007). *Climate Change 2007: Synthesis Report. Contribution of Working Groups I, II and III to the Fourth Assessment Report of the Intergovernmental Panel on Climate Change*. Geneva.

Isler, K., Christopher Kirk, E., Miller, J. M., Albrecht, G. A., Gelvin, B. R., and Martin, R. D. (2008). Endocranial volumes of primate species: scaling analyses using a comprehensive and reliable data set. *J. Hum. Evol.* 55, 967–978. doi: 10.1016/j.jhevol.2008.08.004

Isler, K., and van Schaik, C. P. (2006). Metabolic costs of brain size evolution. *Biol. Lett.* 2, 557–560. doi: 10.1098/rsbl.2006.0538

Isler, K., and van Schaik, C. P. (2009). The Expensive Brain: a framework for explaining evolutionary changes in brain size. *J. Hum. Evol.* 57, 392–400. doi: 10.1016/j.jhevol.2009.04.009

Izard, M. K., Wright, P. C., and Simons, E. L. (1985). Gestation length in *Tarsius bancanus*. *Am. J. Primatol.* 9, 327–331. doi: 10.1002/ajp.1350090408

Jablonski, N. G. (2003). "The evolution of the Tarsiid niche," in *Tarsiers: Past, Present, and Future*, eds P. C. Wright, E. L. Simons, and S. Gursky (New Brunswick, NJ: Rutgers University Press), 35–49.

Jablonski, N. G., and Crompton, R. H. (1994). Feeding-behavior, mastication, and tooth wear in the Western tarsier (*Tarsius bancanus*). *Int. J. Primatol.* 15, 29–59. doi: 10.1007/BF02735233

Jentsch, A., Kreyling, J., and Beierkuhnlein, C. (2007). A new generation of climate-change experiments: events, not trends. *Front. Ecol. Environ.* 5, 365–374. doi: 10.1890/1540-9295(2007)5[365:ANGOCE]2.0.CO;2

Jouffroy, F. K., Berge, C., and Niemitz, C. (1984). "Comparative study of the lower extremity in the genus Tarsius," in *Biology of Tarsiers*, ed C. Niemitz (Stuttgart: Gustav Fischer Verlag), 167–190.

Kälin, N., Martin, R. D., and Genoud, M. (2003). Basal rate of metabolism and temperature regulation in Goeldi's monkey (*Callimico goeldii*). *Comp. Biochem. Phys. A* 135, 279–290. doi: 10.1016/S1095-6433(03)00077-1

Kemp, T. S. (2006). The origin of mammalian endothermy: a paradigm for the evolution of complex biological structure. *Zool. J. Linnean. Soc.* 147, 473–488. doi: 10.1111/j.1096-3642.2006.00226.x

Knox, C. M., and Wright, P. G. (1989). Thermoregulation and energy metabolism in the lesser bushbaby, *Galago senegalensis moholi*. *S. Afr. J. Zool.* 24, 89–94. doi: 10.1080/02541858.1989.11448138

Kobbe, S., and Dausmann, K. H. (2009). Hibernation in Malagasy mouse lemurs as a strategy to counter environmental challenge. *Naturwissenschaften* 96, 1221–1227. doi: 10.1007/s00114-009-0580-3

Koteja, P. (2000). Energy assimilation, parental care and the evolution of endothermy. *Proc. R. Soc. B* 267, 479–484. doi: 10.1098/rspb.2000.1025

Kuehnel, F., Grohmann, J., Buchwald, U., Koeller, G., Teupser, D., and Einspanier, A. (2012). Parameters of haematology, clinical chemistry and lipid metabolism in the common marmoset and alterations under stress conditions. *J. Med. Primatol.* 41, 241–250. doi: 10.1111/j.1600-0684.2012.00550.x

Lelegren, M., Liu, Y., Ross, C., Tardif, S., and Salmon, A. B. (2016). Pharmaceutical inhibition of mTOR in the common marmoset: effect of rapamycin on regulators of proteostasis in a non-human primate. *Pathobiol. Aging Age Relat. Dis.* 6, 31793. doi: 10.3402/pba.v6.31793

Levesque, D. L., Lobban, K. D., and Lovegrove, B. G. (2014). Effects of reproductive status and high ambient temperatures on the body temperature of a free-ranging basoendotherm. *J. Comp. Physiol. B* 184, 1041–1053. doi: 10.1007/s00360-014-0858-4

Lighton, J. R. B. (2008). *Measuring Metabolic Rates: A Manual for Scientists*. New York, NY: Oxford University Press.

Lobban, K. D., Lovegrove, B. G., and Rakotondravony, D. (2014). The energetics of a Malagasy rodent, Macrotarsomys ingens (Nesomyinae): a test of island and zoogeographical effects on metabolism. *J. Comp. Physiol. B* 184, 1077–1089. doi: 10.1007/s00360-014-0853-9

Lovegrove, B. G. (2000). "Daily heterothermy in mammals: coping with unpredictable environments," in *Life in the Cold: Eleventh International Hibernation Symposium*, eds G. Heldmaier and M. Klingenspor (Heidelberg; Berlin: Springer), 29–40.

Lovegrove, B. G. (2012a). The evolution of endothermy in Cenozoic mammals: a plesiomorphic-apomorphic continuum. *Biol. Rev.* 87, 128–162. doi: 10.1111/j.1469-185X.2011.00188.x

Lovegrove, B. G. (2012b). The evolution of mammalian body temperature: the Cenozoic supraendothermic pulses. *J. Comp. Physiol. B* 182, 579–589. doi: 10.1007/s00360-011-0642-7

Lovegrove, B. G. (2014). Cool sperm: why some placental mammals have a scrotum. *J. Evol. Biol.* 27, 801–814. doi: 10.1111/jeb.12373

Lovegrove, B. G. (2017). A phenology of the evolution of endothermy in birds and mammals. *Biol. Rev. Camb. Philos. Soc.* 92, 1213–1240. doi: 10.1111/brv.12280

Lovegrove, B. G., Canale, C., Levesque, D., Fluch, G., Rehakova-Petru, M., and Ruf, T. (2014a). Are tropical small mammals physiologically vulnerable to arrhenius effects and climate change? *Physiol. Biochem. Zool.* 87, 30–45. doi: 10.1086/673313

Lovegrove, B. G., Lobban, K. D., and Levesque, D. L. (2014b). Mammal survival at the Cretaceous–Palaeogene boundary: metabolic homeostasis in prolonged tropical hibernation in tenrecs. *Proc. R. Soc. B* 281:20141304. doi: 10.1098/rspb.2014.1304

Luber, G., and McGeehin, M. (2008). Climate change and extreme heat events. *Am. J. Prev. Med.* 35, 429–435. doi: 10.1016/j.amepre.2008.08.021

MacKinnon, J., and MacKinnon, K. (1980). The behavior of wild spectral tarsiers. *Int. J. Primatol.* 1, 361–379. doi: 10.1007/BF02692280

Matsui, A., Rakotondraparany, F., Munechika, I., Hasegawa, M., and Horai, S. (2009). Molecular phylogeny and evolution of prosimians based on complete sequences of mitochondrial DNAs. *Gene* 441, 53–66. doi: 10.1016/j.gene.2008.08.024

Mazerolle, M. J. (2015). AICcmodavg: model selection and multimodel inference based on (Q)AIC(c). R package version 2.0-3 ed. Available online at: http://CRAN.R-project.org

McNab, B. K. (1978). The evolution of endothermy in the phylogeny of mammals. *Am. Nat.* 112, 1–21. doi: 10.1086/283249

McNab, B. K., and Wright, P. C. (1987). Temperature regulation and oxygen consumption in the Philippine tarsier *Tarsius syrichta*. *Physiol. Zool.* 60, 596–600. doi: 10.1086/physzool.60.5.30156133

Meehl, G. A., and Tebaldi, C. (2004). More intense, more frequent, and longer lasting heat waves in the 21st century. *Science* 305, 994–997. doi: 10.1126/science.1098704

Meireles, C. M., Czelusniak, J., Page, S. L., Wildman, D. E., and Goodman, M. (2003). "Phylogenetic position of tarsiers within the order primates: evidence from gamma-globin DNA sequences," in *Tarsiers: Past, Present, and Future*, eds P. C. Wright, E. L. Simons, and S. Gursky (New Brunswick, NJ: Rutgers University Press), 145–160.

Muggeo, V. M. R. (2008). Segmented: an R package to fit regression models with broken-line relationships. *R News* 8, 20–25. Available online at: https://cran.r-project.org/doc/Rnews/

Mzilikazi, N., Masters, J. C., and Lovegrove, B. G. (2006). Lack of torpor in free-ranging southern lesser galagos, *Galago moholi*: ecological and physiological considerations. *Folia Primatol.* 77, 465–476. doi: 10.1159/000095392

Neri-Arboleda, I., Stott, P., and Arboleda, N. P. (2002). Home ranges, spatial movements and habitat associations of the Philippine tarsier (*Tarsius syrichta*) in Corella, Bohol. *J. Zool.* 257, 387–402. doi: 10.1017/S0952836902000997

Niemitz, C. (1984). "Synecological relationships and feeding behaviour of the genus *Tarsius*," in *Biology of Tarsiers*, ed C. Niemitz (Stuttgart: Gustav Fischer Verlag), 59–75.

Niemitz, C., Klauer, G., and Eins, S. (1984). "The interscapular brown fat body in *Tarsius bancanus*, with comparisons to *Tupaia* and man," in *Biology of Tarsiers*, ed C. Niemitz (Stuttgart: Gustav Fischer Verlag), 257–273.

Nowack, J., Cooper, C. E., and Geiser, F. (2016). Cool echidnas survive the fire. *Proc. R. Soc. B* 283:20160382. doi: 10.1098/rspb.2016.0382

Nowack, J., Mzilikazi, N., and Dausmann, K. H. (2010). Torpor on demand: heterothermy in the non-lemur primate *Galago moholi*. *PLoS ONE* 5:e10797. doi: 10.1371/journal.pone.0010797

Nowack, J., Rojas, A. D., Körtner, G., and Geiser, F. (2015). Snoozing through the storm: torpor use during a natural disaster. *Sci. Rep.* 5:11243. doi: 10.1038/srep11243

Ortmann, S., Heldmaier, G., Schmid, J., and Ganzhorn, J. U. (1997). Spontaneous daily torpor in Malagasy mouse lemurs. *Naturwissenschaften* 84, 28–32. doi: 10.1007/s001140050344

Perelman, P., Johnson, W. E., Roos, C., Seuánez, H. N., Horvath, J. E., Moreira, M. A., et al. (2011). A molecular phylogeny of living primates. *PLoS Genet.* 7:e1001342. doi: 10.1371/journal.pgen.1001342

Peters, A., and Preuschoft, H. (1984). "External biomechanics of leaping in *Tarsius* and its morphological and kinematic consequences," in *Biology of Tarsiers*, ed C. Niemitz (Stuttgart: Gustav Fischer Verlag), 227–255.

Petry, H., Riehl, I., and Zucker, H. (1986). Energieumsatzmessungen an Weißbüscheläffchen (*Callithrix jacchus*). *J. Anim. Physiol. Anim. Nutr.* 55, 214–224. doi: 10.1111/j.1439-0396.1986.tb00722.x

Pinheiro, J., Bates, D., DebRoy, S., Deepayan, S., and Team, R. C. (2016). Nlme: linear and nonlinear mixed effects models. R package version 3.1–128.

Pocock, R. I. (1918). On the external characters of the lemurs and of *Tarsius*. *Proc. Zool. Soc. Lond.* 88, 19–53. doi: 10.1111/j.1096-3642.1918.tb02076.x

Power, M. L., Tardif, S. D., Power, R. A., and Layne, D. G. (2003). Resting energy metabolism of Goeldi's monkey (*Callimico goeldii*) is similar to that of other callitrichids. *Am. J. Primatol.* 60, 57–67. doi: 10.1002/ajp.10078

Quintero, I., and Wiens, J. J. (2013). Rates of projected climate change dramatically exceed past rates of climatic niche evolution among vertebrate species. *Ecol. Lett.* 16, 1095–1103. doi: 10.1111/ele.12144

Rahmstorf, S., Cazenave, A., Church, J. A., Hansen, J. E., Keeling, R. F., Parker, D. E., et al. (2007). Recent climate observations compared to projections. *Science* 316:709. doi: 10.1126/science.1136843

Refinetti, R., and Menaker, M. (1992). The circadian rhythm of body temperature. *Physiol. Behav.* 51, 613–637. doi: 10.1016/0031-9384(92)90188-8

R Core Team (2017). *R: A Language and Enviroment for Statistical Computing*. Vienna: R Foundation for Statistical Computing.

Roberts, M. (1994). Growth, development, and parental care in the western tarsier (*Tarsius bancanus*) in captivity: evidence for a "slow" life-history and nonmonogamous mating system. *Int. J. Primatol.* 15, 1–28. doi: 10.1007/BF02735232

Root, T. L., Price, J. T., Hall, K. R., Schneider, S. H., Rosenzweig, C., and Pounds, J. A. (2003). Fingerprints of global warming on wild animals and plants. *Nature* 421, 57–60. doi: 10.1038/nature01333

Ross, C., Salmon, A., Strong, R., Fernandez, E., Javors, M., Richardson, A., et al. (2015). Metabolic consequences of long-term rapamycin exposure on common marmoset monkeys (*Callithrix jacchus*). *Aging* 7, 964–973. doi: 10.18632/aging.100843

Ruf, T., and Geiser, F. (2015). Daily torpor and hibernation in birds and mammals. *Biol. Rev.* 90, 891–926. doi: 10.1111/brv.12137

Ruf, T., Streicher, U., Stalder, G. L., Nadler, T., and Walzer, C. (2015). Hibernation in the pygmy slow loris (*Nycticebus pygmaeus*): multiday torpor in primates is not restricted to Madagascar. *Sci. Rep.* 5:17392. doi: 10.1038/srep17392

Schmid, J. (2000). Daily torpor in the gray mouse lemur (*Microcebus murinus*) in Madagascar: energetic consequences and biological significance. *Oecologia* 123, 175–183. doi: 10.1007/s004420051003

Schmid, J., and Ganzhorn, J. U. (1996). Resting metabolic rates of *Lepilemur ruficaudatus*. *Am. J. Primatol.* 38, 169–174.

Schmid, J., and Ganzhorn, J. U. (2009). Optional strategies for reduced metabolism in gray mouse lemurs. *Naturwissenschaften* 96, 737–741. doi: 10.1007/s00114-009-0523-z

Schmid, J., and Kappeler, P. M. (1998). Fluctuating sexual dimorphism and differential hibernation by sex in a primate, the Gray mouse lemur (*Microcebus murinus*). *Behav. Ecol. Sociobiol.* 43, 125–132. doi: 10.1007/s002650050474

Schmidt-Nielsen, K. (1997). *Animal Physiology: Adaptation and Environment*. Cambridge: Cambridge University Press.

Schmitz, J., Ohme, M., and Zischler, H. (2001). SINE insertions in cladistic analyses and the phylogenetic affiliations of *Tarsius bancanus* to other primates. *Genetics* 157, 777–784.

Schultz, M. (1984). "Osteology and myology of the upper extremity of *Tarsius*," in *Biology of Tarsier*, ed C. Niemitz (Stuttgart: Gustav Fischer Verlag), 143–165.

Schwartz, J. H. (1984). "What is a Tarsier?" in *Living Fossils*, eds N. Eldredge and S. M. Stanley (New York, NY: Springer New York), 38–49.

Schwartz, J. H. (2003). "How close are the similarities between Tarsius and other primates," in *Tarsiers: Past, Present, and Future*, eds P. C. Wright, E. L. Simons, and S. Gursky (New Brunswick, NJ: Rutgers University Press), 50–96.

Sherwood, S. C., and Huber, M. (2010). An adaptability limit to climate change due to heat stress. *Proc. Natl. Acad. Sci. U.S.A.* 107, 9552–9555. doi: 10.1073/pnas.0913352107

Simons, E. L. (2003). "The fossil record of Tarsier evolution," in *Tarsiers: Past, Present, and Future*, eds P. C. Wright, E. L. Simons, and S. Gursky (New Brunswick, NJ: Rutgers University Press), 9–34.

Stawski, C., and Geiser, F. (2010). Fat and fed: frequent use of summer torpor in a subtropical bat. *Naturwissenschaften* 97, 29–35. doi: 10.1007/s00114-009-0606-x

Stawski, C., Körtner, G., Nowack, J., and Geiser, F. (2015). The importance of mammalian torpor for survival in a post-fire landscape. *Biol. Lett.* 11:20150134. doi: 10.1098/rsbl.2015.0134

Stephan, A. (1984). "Morphology of the brain in *Tarsius*," in *Biology of Tarsiers*, ed C. Niemitz (Stuttgart: Gustav Fischer Verlag), 317–344.

Stonerook, M. J., Weiss, H. S., Rodriguez, M. A., Rodríguez, J. V., Hernández, J. I., Peck, O. C., et al. (1994). Temperature-metabolism relations in the cotton-top tamarin (*Saguinus oedipus*) model for ulcerative colitis. *J. Med. Primatol.* 23, 16–22. doi: 10.1111/j.1600-0684.1994.tb00090.x

van Oldenborgh, G. J., Drijfhout, S., van Ulden, A., Haarsma, R., Sterl, A., Severijns, C., et al. (2009). Western Europe is warming much faster than expected. *Clim. Past* 5, 1–12. doi: 10.5194/cp-5-1-2009

Warren, R. D., and Crompton, R. H. (1998). Diet, body size and the energy costs of locomotion in saltatory primates. *Folia Primatol.* 69, 86–100. doi: 10.1159/000052701

Withers, P. C. (1992). *Comparative Animal Physiology*. Orlando, FL: Saunder College.

Withers, P. C. (2001). Design, calibration and calculation for flow-through respirometry systems. *Aus. J. Zool.* 49, 445–461. doi: 10.1071/ZO00057

Withers, P. C., Cooper, C. E., Maloney, S. K., Bozinovic, F., and Cruz-Neto, A. P. (2016). *Ecological and Environmental Physiology of Mammals*. New York, NY: Oxford University Press.

Wright, P. C., Izard, M. K., and Simons, E. L. (1986). Reproductive cycles in *Tarsius bancanus*. *Am. J. Primatol.* 11, 207–215. doi: 10.1002/ajp.1350110302

Yoder, A. D. (2003). "The phylogenetic position of genus Tarsius: whose side are you on?" in *Tarsiers: Past, Present, and Future*, eds P. C. Wright, E. L. Simons, and S. Gursky (New Brunswick, NJ: Rutgers University Press), 161–175.

Conflict of Interest Statement: The authors declare that the research was conducted in the absence of any commercial or financial relationships that could be construed as a potential conflict of interest.

frontiers in Physiology

PERSPECTIVE
published: 04 August 2017
doi: 10.3389/fphys.2017.00575

Plasticity of Performance Curves Can Buffer Reaction Rates from Body Temperature Variation in Active Endotherms

Frank Seebacher[1]* *and Alexander G. Little*[2]

[1] School of Life and Environmental Sciences, University of Sydney, Sydney, NSW, Australia, [2] Rosenstiel School of Marine and Atmospheric Science, The University of Miami, Miami, FL, United States

Endotherms regulate their core body temperature by adjusting metabolic heat production and insulation. Endothermic body temperatures are therefore relatively stable compared to external temperatures. The thermal sensitivity of biochemical reaction rates is thought to have co-evolved with body temperature regulation so that optimal reaction rates occur at the regulated body temperature. However, recent data show that core body temperatures even of non-torpid endotherms fluctuate considerably. Additionally, peripheral temperatures can be considerably lower and more variable than core body temperatures. Here we discuss whether published data support the hypothesis that thermal performance curves of physiological reaction rates are plastic so that performance is maintained despite variable body temperatures within active (non-torpid) endotherms, and we explore mechanisms that confer plasticity. There is evidence that thermal performance curves in tissues that experience thermal fluctuations can be plastic, although this question remains relatively unexplored for endotherms. Mechanisms that alter thermal responses locally at the tissue level include transient potential receptor ion channels (TRPV and TRPM) and the AMP-activated protein kinase (AMPK) both of which can influence metabolism and energy expenditure. Additionally, the thermal sensitivity of processes that cause post-transcriptional RNA degradation can promote the relative expression of cold-responsive genes. Endotherms can respond to environmental fluctuations similarly to ectotherms, and thermal plasticity complements core body temperature regulation to increase whole-organism performance. Thermal plasticity is ancestral to endothermic thermoregulation, but it has not lost its selective advantage so that modern endotherms are a physiological composite of ancestral ectothermic and derived endothermic traits.

Keywords: thermoregulation, body temperature, climate, metabolism, mitochondria, AMPK, thyroid hormone, transient receptor potential ion channel

OPEN ACCESS

Edited by:
Elias T. Polymeropoulos, Menzies Research Institute Tasmania, Australia

Reviewed by:
Danielle L. Levesque, University of Maine, France
Frank Van Breukelen, University of Nevada, Las Vegas, United States

***Correspondence:**
Frank Seebacher
frank.seebacher@sydney.edu.au

Specialty section:
This article was submitted to Integrative Physiology, a section of the journal Frontiers in Physiology

Received: *28 April 2017*
Accepted: *25 July 2017*
Published: *04 August 2017*

Citation:
Seebacher F and Little AG (2017) Plasticity of Performance Curves Can Buffer Reaction Rates from Body Temperature Variation in Active Endotherms. Front. Physiol. 8:575. doi: 10.3389/fphys.2017.00575

INTRODUCTION

The basic principles of thermodynamics dictate that the rates of physiological functions in both endotherms and ectotherms are sensitive to changes in temperature (Landeira-Fernandez et al., 2012; Tattersall et al., 2012; Arcus et al., 2016; Else, 2016). However, the relationship between temperature and reaction rates is not constant (Huey and Kingsolver, 1989; Kingsolver, 2003).

Thermal performance curves represent the change in a physiological reaction rate across a range of acute temperatures (**Figure 1A**). Thermal plasticity in response to a (non-acute) chronic change in body temperature may manifest as a horizontal shift in the performance curve, so that maximal performance (mode) occurs at the new temperature. Additionally, the range of values around the mode within which performance remains high (e.g., >80% of maximal) can increase or decrease, leading to generalist and specialist phenotypes, respectively (**Figure 1**; Huey and Kingsolver, 1989; Sinclair et al., 2016). The resultant plasticity of reaction rates is advantageous because it permits animals to maintain relatively constant physiological rates in variable environments (Guderley, 1990; St-Pierre et al., 1998; Piersma and Drent, 2003; Forsman, 2014). Ectothermic animals, in particular, benefit from such phenotypic plasticity, because body temperatures are largely determined by environmental conditions (Porter and Gates, 1969).

In endotherms, the gradient between body temperature and environmental temperature impacts metabolic rates and heat production, which typically increase under cold conditions (Rezende et al., 2004; Lovegrove, 2005; McKechnie et al., 2015). Importantly, body temperatures of non-torpid endotherms are not constant (Boyles et al., 2013; Hetem et al., 2016; Levesque et al., 2016). By lowering body temperatures in cooler environments, for example, even active (non-torpid and non-hibernating) endotherms reduce the differential between internal and external temperatures and can thereby reduce the energy needed for thermoregulation (Crompton et al., 1978; Glanville et al., 2012; Tattersall et al., 2016), resulting in increased survival and fitness (Dammhahn et al., 2017). Any changes in body temperature, however, will negatively affect cellular reaction rates unless these are buffered by plastic responses similar to those described above, which are common among ectotherms (Huey and Kingsolver, 1989).

Similarly, body temperatures are not homogenous within organisms, and even in non-dormant endotherms temperatures in peripheral muscle are often several degrees lower than core body temperature (Mutungi and Ranatunga, 1998; Yaicharoen et al., 2012). Again, reduced peripheral body temperatures lower the energetic costs of thermoregulation, but need to be accompanied by shifts in thermal performance curves of peripheral tissues to avoid a trade-off between thermoregulatory cost and physiological function.

Here we suggest that plasticity of thermal performance curves is an ancestral trait that has been maintained in endotherms to buffer physiological reaction rates from variation in core body or tissue temperatures. Note that there is an important distinction between acclimation of metabolic rates to increase heat production in response to cold environmental temperatures (e.g., Boratyński et al., 2017; Noakes et al., 2017), and the plasticity of performance curves we are suggesting (**Figure 1A**). The former serves to maintain body temperatures in variable

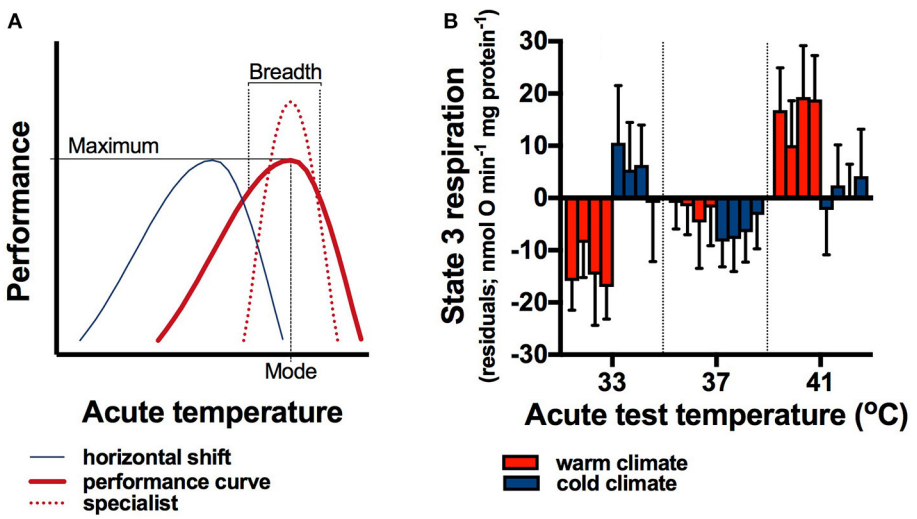

FIGURE 1 | Responses of animals to variable environments. Thermal performance curves (**A**; thick red line) have a maximum at the optimal temperature (mode), and decreasing performance at either side of the maximum. The performance breadth, typically defined as the temperature range over which performance is greater than 80–90%, can change in response to temperature variation, producing specialist phenotypes (broken red line) with a narrower performance breadth but greater maximum. Plastic responses to temperature variation as a result of developmental processes or reversible acclimation can shift the performance curve so that the mode coincides with a different mean temperature (blue line), which may be advantageous for endotherms that experience lower body temperatures in colder climates. Thermal performance curves of maximal mitochondrial respiration rates (state 3 rates) shifted between populations of bush rats (*Rattus fuscipes*) living in different climates **(B)**. Rats from cold climate populations had significantly lower body temperatures than those from warm climate populations (Glanville et al., 2012). Concomitantly to body temperature differences, state 3 respiration rate was highest at low temperatures in cold climate rats, but it increased with increasing temperature in warm climate rats (climate*test temperature interaction), indicating that thermal performance curves shifted to compensate for the lower body temperatures in cold climates. Residuals are shown here, and within each group of four bars within acute test temperatures the first (left) bar shows data from vastus lateralis muscle, the second from heart ventricle, the third from liver, and the forth (right) bar shows data from brown adipose tissue. Means ± s.e.m. are shown, n = 10 rats from each population (averaged within climates), and data measured at different temperatures are separated by a thin dotted line to aid in visual clarity.

climates, and the latter optimizes reaction rates when tissue temperatures change despite adjustments of metabolic heat production. Here we review plasticity in performance curves in response to core body temperature variation, and in response to peripheral tissue temperature variation in non-torpid and non-hibernating endotherms. Additionally, we review mechanisms that can confer plasticity in thermal performance curves at the tissue level, which are promising candidates for future research aimed at understanding the consequences of heterothermy in endotherms.

PLASTICITY OF PERFORMANCE CURVES IN RESPONSE TO CORE BODY TEMPERATURE VARIATION

Physiological rates in endotherms tend to be optimized around the regulated core body temperature with relatively narrow performance breadth (Shinoda et al., 1997; James, 2013). However, there are exceptions to this pattern. Round-tailed ground squirrels (*Spermophilus terreticaudus*), for example, let their body temperature vary considerably with environmental temperature (Wooden, 2004). At the same time, their muscle force production and sprint speed was maintained over body temperatures ranging from 30 to 41°C. These data exemplify an extreme generalist phenotype, where the benefits of variation in body temperature are not traded off for a decrease in performance.

In addition to generalist responses, the mode of thermal performance curves may shift in response to body temperature changes. Heart rate represents a physiological rate that is closely related to performance (Eliason et al., 2011; Hillman and Hedrick, 2015), and thermal performance curves of heart rate can shift in response to chronic changes in body temperature. For example, mean rectal temperature of humans significantly decreased following cool acclimation, but was elevated to 39°C following acclimation to hot conditions (Racinais et al., 2017). Initially, heart rates were higher in hot conditions but decreased following acclimation to hot temperatures, indicating a shift in thermal sensitivity of heart rates (Racinais et al., 2017). On the other hand, red deer (*Cervus elaphus*) and Przewalski's horse (*Equus ferus przewalskii*) lowered peripheral temperatures in winter, with concomitant decreases in heart rates during activity and rest (Arnold et al., 2004, 2006). However, there was no indication that heart rates were compensated for the lower winter temperatures.

In a rodent (the Australian bush rat, *Rattus fuscipes*), physiological reaction rates shifted with seasonal and altitudinal changes in climate. *R. fuscipes* from two populations living in cold high altitude climates had significantly lower body temperatures compared to those from two warm coastal populations (Glanville et al., 2012). Paralleling differences in body temperatures, the thermal sensitivity of mitochondrial respiration rates differed significantly between populations from different climates. We published mitochondrial substrate oxidation rates (state 3 rates) and uncoupled (state 4) oxygen consumption rates measured at 37°C test temperatures previously (Glanville et al., 2012). However, at the same time (and using the same techniques as in Glanville et al., 2012) we also measured mitochondrial respiration at 33° and 41°C, and these previously unpublished data provide an opportunity to compare thermal sensitivities between populations experiencing different body temperatures naturally. Hence, here we used a permutational analysis (Wheeler and Torchiano, 2016) to analyse state 3 mitochondrial substrate oxidation rates (data for state 4 rates available from the corresponding author) with climate and test temperature as independent factors, and population nested within climate. We calculated residuals for each population to analyse thermal sensitivity without the effects of differences in absolute rates between populations (see Glanville et al., 2012).

In rats from warm climates, residuals of state 3 rates were lowest at 33°C and increased with temperature. In contrast, state 3 rates of cold-climate rats were highest at 33°C and decreased with increasing temperature (**Figure 1B**; climate*test temperature interaction, $p < 0.0001$ for muscle, $p = 0.04$ for heart, $p = 0.008$ for liver, and $p < 0.0001$ for brown adipose tissue; there was no effect of population on any residuals, all $p > 0.12$). These data indicate that adaptation or developmental processes lower the mode of thermal performance curves in cold climates, which would be beneficial for rats experiencing lower body temperatures.

Similarly, rats had significantly lower body temperatures in winter compared to summer (Glanville and Seebacher, 2010a,b). There were interactions between season and test temperature in determining metabolic enzyme activities, which indicate that the mode of performance curves shifted in response to seasonally changing temperatures as well (Glanville and Seebacher, 2010b).

PLASTICITY OF PERFORMANCE CURVES IN RESPONSE TO TISSUE TEMPERATURE VARIATION

Even when core body temperature remains stable within organisms, there can be considerable temperature variation in peripheral tissues (Ponganis et al., 2003). Muscle temperatures in humans may be several degrees Celsius below rectal or core body temperatures at rest, even in large muscle groups (Sargeant, 1987; Ducharme et al., 1991; Bishop, 2003). These decreases in temperature constrain muscle performance (James, 2013), leading to increased sporting performance following warm-ups (Bishop, 2003; Yaicharoen et al., 2012; Cunniffe et al., 2017).

It would be advantageous therefore if the thermal sensitivity of performance curves differed between core and peripheral tissues. Muscle at the core should show greater thermal sensitivity with a narrow performance breadth around core body temperature, while peripheral muscle should be less sensitive to temperature changes and perform better than core muscle at low temperatures. Such a division between generalist and specialist phenotypes was found in isolated mouse muscle (James et al., 2015). Core diaphragm muscle had greater power output at core body temperature and was more sensitive to

changes in temperature than peripheral soleus muscle, which would experience much greater temperature fluctuations *in vivo* (James et al., 2015).These patterns of regional specialization were similar in an endothermic shark that maintains elevated core body temperatures (Bernal et al., 2005). Endotherms can therefore show regional specialization correlated with temperature variation.

In mouse muscle, the capacity to shift performance curves in response to temperature is independent from central neuroendocrine input and can occur in isolated cells (Little and Seebacher, 2016). Cool (32°C) growth temperature of muscle precursor cells (myoblasts) lowered the mode of the thermal performance curve for metabolic rate compared to control (37°C) conditions, where increased metabolic rate at 32°C compensated for the negative thermodynamic effects. Similarly, decreased differentiation temperature (32°C) of myoblasts into functional myotubes lowered the mode of the thermal performance curve for metabolic rate, again compensating for cool temperatures. Interestingly, myoblast growth temperature influenced myotube thermal performance independently from differentiation temperature (Little and Seebacher, 2016). These thermal responses of mouse myocytes are comparable to the interaction between developmental and reversible plasticity in ectotherms (Scott and Johnston, 2012; Little et al., 2013; Beaman et al., 2016).

MECHANISMS MEDIATING PLASTICITY

Plasticity of thermal performance curves may be regulated centrally via sympathetic output from the hypothalamus (Nakamura and Morrison, 2007; Seebacher, 2009), and peripherally by circulating levels of thyroid hormone (Little and Seebacher, 2013, 2014; Little et al., 2013). However, the capacity to adjust thermal sensitivity in response to local changes in temperature can also occur independently from neuroendocrine input (Al-Fageeh et al., 2006; Underhill and Smales, 2007; Ye et al., 2013; Little and Seebacher, 2016). For example, changes in membrane fluidity resulting from temperature-sensitive shifts in fatty acid profiles can maintain cellular, organelle, and protein function in variable thermal environments (Cossins and Prosser, 1978). Changes in membrane composition occur at the cellular level in ectotherms and endotherms (Dymond, 2016; Ballweg and Ernst, 2017).

There has been considerable medical interest in cell-autonomous pathways regulating thermal responses in mammalian tissues (Ye et al., 2013; Borowiec et al., 2016; Quesada-López et al., 2016; Bastide et al., 2017). Additionally, thermal responses have been used as a biotechnology strategy to enhance recombinant protein production in mammalian cell lines (Al-Fageeh et al., 2006). Together these studies point toward a local "thermal switch" in peripheral tissues, where thermosensory information is integrated with compensatory response(s) entirely at the level of the cell. The "thermal switch" may comprise pathways that sense temperature changes directly, and those that sense subsequent imbalances in important cellular metabolites following thermal change (**Figure 2**).

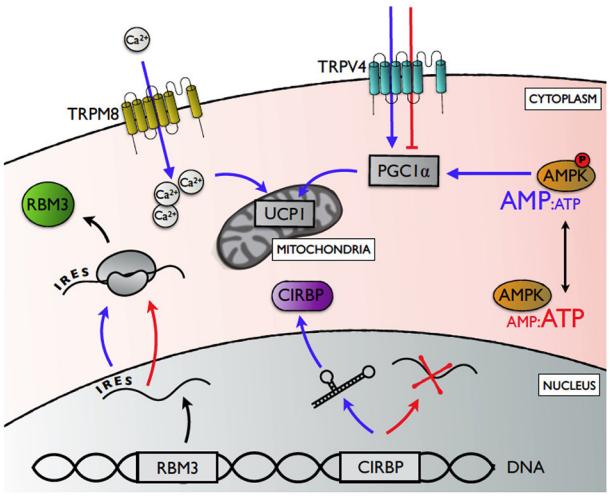

FIGURE 2 | A summary of the potential mechanisms underlying cell-autonomous thermal plasticity. Transient receptor potential channels vanilloid 4 (TRPV4) and melastatin 8 (TRPM8) upregulate expression of peroxisome proliferator-activated receptor γ coactivator 1α (PGC1α) and uncoupling protein 1 (UCP1), respectively, in response to local hypothermia (blue arrows; normothermic conditions depicted by red arrows). Cold-inducible RNA binding protein (CIRBP) expression is enhanced in response to cold exposure through a temperature-sensitive change in RNA splicing that determines the proportion pre-mRNA processed into mature mRNA. Relative translation rates for RNA binding motif protein 3 (RBM3) is enhanced during cold exposure via a 5' internal ribosome entry site (IRES), while global protein synthesis declines. AMP-activated protein kinase (AMPK) is activated by increasing ratio of AMP:ATP with cold exposure, thereby enhancing PGC1α activity.

Transient receptor potential ion channels (TRPs) represent the best studied mechanism that allows cells to detect changes in their environment directly (Nilius and Voets, 2005; Ahern, 2013). Many of these receptors are temperature-gated, and different receptors are activated at specific temperature ranges (Baez et al., 2014). TRPs are expressed ubiquitously, and are best known for their afferent role in thermoregulation (Caterina, 2006), where peripheral changes in temperature are relayed to the preoptic area of the hypothalamus for central regulation (Morrison et al., 2014). Interestingly, certain TRPs can also regulate local responses in a cell-autonomous manner (Ahern, 2013; Ye et al., 2013). In mammals, TRP vanilloid 4 (TRPV4) is activated at physiological temperatures (Shibasaki et al., 2015). TRPV4 knockout mice showed increased energy expenditure in white adipocytes (Ye et al., 2012), mediated by the cell-autonomous release of TRPV4-induced repression of the metabolic co-regulator PGC1α, and uncoupling protein 1 (UCP1) (Ye et al., 2012). TRP melastatin 8 (TRPM8), which detects cool temperatures (<26°C) (Bautista et al., 2007), can regulate cell-autonomous responses to hypothermia in brown adipose tissue (BAT) and germ cells of mice (Ma et al., 2012; Borowiec et al., 2016). In cold-exposed BAT, for instance, TRPM8 enhanced Ca^{2+}-influx and increased the expression of UCP1 independently from the canonical β-adrenergic pathway (Ma et al., 2012). Our results, showing

that mild hypothermia (32°C) altered metabolic phenotypes of myoblasts and subsequent myotubes (Little and Seebacher, 2016), are especially interesting because brown adipocytes and skeletal myocytes both share a myf-5 positive mesenchymal stem cell origin (Seale et al., 2008), which means that TRPM8 activation may also underlie metabolic programming to compensate for mild hypothermia in skeletal muscle development, repair, and maintenance.

Temperature can also have direct effects on post-transcriptional processes, such as mRNA degradation, splicing, and translation efficiency. For example, temperature-dependent expression patterns of cold-inducible proteins are determined by the thermal sensitivity of post-transcriptional mechanisms (Sonna et al., 2002; Potla et al., 2015; Gotic et al., 2016; Bastide et al., 2017). The expression of the cold-inducible cold shock RNA-binding protein (CIRBP) increased in response to mild hypothermia (Sonna et al., 2002), UV irradiation (Yang and Carrier, 2001), and hypoxia (Wellmann, 2004) in mammals. CIRBP was also upregulated during cold exposure in ectothermic vertebrates, including common carp (*Cyprinus carpio*; Gracey et al., 2004) and Japanese treefrogs (*Hyla japonica*; Sugimoto and Jiang, 2008). CIRBP regulated cell growth at low temperature by protecting target mRNA from degradation in mammalian cell culture (Phadtare et al., 1999). Increases in cellular CIRBP content in response to body temperature variation occurred through a temperature-sensitive change in RNA splicing efficiency that determined the proportion of CIRBP pre-mRNA processed into mature mRNAs (Gotic et al., 2016). Pre-mRNA contain secondary structures that regulate splice site recognition and splicesome binding. These secondary structures are dynamic and highly sensitive to changes in temperature, so that they can destabilize and unfold in ways that determine ultimate levels of CIRBP mRNA expression (Gotic et al., 2016).

The cold-shock RNA-binding protein RBM3 binds mRNAs to maintain translational efficiency (Peretti et al., 2015; Zhu et al., 2016; Bastide et al., 2017). Cooling reduces protein synthesis globally, except for specific proteins such as RBM3 (Bastide et al., 2017). The translation of RBM3 is enhanced during cold exposure by internal ribosome entry site (IRES) regions in its mRNA 5′ untranslated regions (5-UTR) (Bastide et al., 2017). Under cold exposure, the typical cap-dependent initiation of translation is impaired (Jackson et al., 2015; Bastide et al., 2017). However, IRES regions recruit the translational machinery, thereby facilitating initiation of translation in a cap-independent manner (Chappell et al., 2001; Pan and van Breukelen, 2011). As a result, RBM3 expression is maintained, or even enhanced with cold exposure. In addition to facilitating translational efficiency of mRNA in the cold, RBM3 can also regulate microRNAs by facilitating their processing by Dicer (Zhu et al., 2016). Cold exposure increased transcript levels for five microRNAs involved in cell cycle progression in primary cultured human small airway epithelial cells (Potla et al., 2015). These microRNAs are regulated post-transcriptionally, but it is not known whether their changes in expression rely on stabilization by RBM3, or temperature-sensitive splicing mechanisms similar to CIRBP (Potla et al., 2015).

Peripheral cells and tissues may also mount autonomous responses to local changes in temperature by indirect thermosensory pathways, where temperature-induced imbalances in cellular metabolites trigger compensatory responses. In skeletal muscle, decreasing temperatures cause an energy deficit, resulting in an increase in the AMP:ATP ratio (Towler and Hardie, 2007). Increased concentrations of AMP activate the cellular energy-sensor AMP-stimulated protein kinase (AMPK) to increase mitochondrial density and ATP production (Jäger et al., 2007; Lira et al., 2010; Hardie et al., 2016). Increases in AMPK activity shifted mouse muscle to a more oxidative metabolic phenotype (Ljubicic et al., 2011), and altered the expression of thyroid receptors in adipose tissue (Wang et al., 2014). The AMPK-mediated response can thereby alter how cells and tissues respond to central inputs via changes in receptor profiles, as well as acting on the metabolic machinery at the cellular level directly. As a result, metabolic capacity is increased in response to cold. AMPK may thereby represent a thermal switch by integrating temperature-induced energy deficit with compensatory cellular responses.

CONCLUSIONS

The concept that endotherms have high and stable body temperatures despite environmental temperature fluctuations (Scholander et al., 1950; Rezende and Bacigalupe, 2015) has been challenged by the increasing evidence that body and tissue temperatures of non-torpid and non-hibernating endotherms can fluctuate substantially (e.g., Hetem et al., 2016; Levesque et al., 2016). Consequently, the notion that optimal physiological reaction rates of endotherms have evolved to be fixed within a narrow range of regulated body temperatures is also questionable. Instead, body and tissue temperature fluctuations in endotherms would favor selection for thermal plasticity. Endothermic thermoregulation is distinct from that of ectotherms, but thermal plasticity of physiological reaction rates can be as advantageous in endotherms as in ectotherms.

The mechanisms that mediate thermal plasticity are highly conserved among animals, and their broad range of functions is likely to preclude negative selection. For example, thyroid hormone action is essential for a broad range of physiological responses in animals, and is highly conserved across taxa (Heyland and Moroz, 2005; Darras and Van Herck, 2012). It is likely that thyroid hormone has retained its early functions as well as assuming additional roles in endotherms (Cannon and Nedergaard, 2010; Little, 2016). Similarly, AMPK-mediated signaling evolved in early eukaryotes as an energy sensing mechanism (Towler and Hardie, 2007; Hardie et al., 2016; Ross et al., 2016). Hence, the role of AMPK in conferring thermal plasticity evolved in ectothermic organisms and has been retained by endotherms. In a final example, transient receptor potential ion channels (TRP) act in thermoregulation in both ectotherms and endotherms (Caterina, 2006; Seebacher and Murray, 2007; Laursen et al., 2016). Like thyroid hormone and AMKP, TRPs are highly conserved among animals (Peng et al., 2015). These three mechanisms, and possibly others, such

as micro RNAs and post-transcriptional modifications, therefore represent evolutionarily conserved regulatory systems that adjust cellular responses to the environment.

AUTHOR CONTRIBUTIONS

FS and AL conceived the ideas, prepared the manuscript and figures, and approved the manuscript.

FUNDING

This work was funded by an Australian Research Council Discovery Grant to FS (DP160102260).

ACKNOWLEDGMENTS

We thank E. Glanville for permission to use unpublished data.

REFERENCES

Ahern, G. P. (2013). Transient receptor potential channels and energy homeostasis. *Trends Endocrin. Metabol.* 24, 554–560. doi: 10.1016/j.tem.2013.06.005

Al-Fageeh, M. B., Marchant, R. J., Carden, M. J., and Smales, C. M. (2006). The cold-shock response in cultured mammalian cells: harnessing the response for the improvement of recombinant protein production. *Biotechnol. Bioeng.* 93, 829–835. doi: 10.1002/bit.20789

Arcus, V. L., Prentice, E. J., Hobbs, J. K., Mulholland, A. J., Van der Kamp, M. W., Pudney, C. R., et al. (2016). On the temperature dependence of enzyme-catalyzed rates. *Biochemistry* 55, 1681–1688. doi: 10.1021/acs.biochem.5b01094

Arnold, W., Ruf, T., and Kuntz, R. (2006). Seasonal adjustment of energy budget in a large wild mammal, the Przewalski horse (*Equus ferus przewalskii)* II. Energy expenditure. *J. Exp. Biol.* 209, 4566–4573. doi: 10.1242/jeb.02536

Arnold, W., Ruf, T., Reimoser, S., Tataruch, F., Onderscheka, K., and Schober, F. (2004). Nocturnal hypometabolism as an overwintering strategy of red deer (*Cervus elaphus*). *Am. J. Physiol. Regul. Integr. Comp. Physiol.* 286, R174–R181. doi: 10.1152/ajpregu.00593.2002

Baez, D., Raddatz, N., Ferreira, G., Gonzalez, C., and Latorre, R. (2014). Gating of thermally activated channels. *Therm. Sens. Curr. Top. Membr.* 74, 51–87. doi: 10.1016/B978-0-12-800181-3.00003-8

Ballweg, S., and Ernst, R. (2017). Control of membrane fluidity: the OLE pathway in focus. *Biol. Chem.* 398, 1–14. doi: 10.1515/hsz-2016-0277

Bastide, A., Peretti, D., Knight, J. R. P., Grosso, S., Spriggs, R. V., Pichon, X., et al. (2017). RTN3 is a novel cold-induced protein and mediates neuroprotective effects of RBM3. *Curr. Biol.* 27, 638–650. doi: 10.1016/j.cub.2017.01.047

Bautista, D. M., Siemens, J., Glazer, J. M., Tsuruda, P. R., Basbaum, A. I., Stucky, C. L., et al. (2007). The menthol receptor TRPM8 is the principal detector of environmental cold. *Nature* 448, 204–208. doi: 10.1038/nature05910

Beaman, J. E., White, C. R., and Seebacher, F. (2016). Evolution of plasticity: mechanistic link between development and reversible acclimation. *Trends Ecol. Evol.* 31, 237–249. doi: 10.1016/j.tree.2016.01.004

Bernal, D., Donley, J. M., Shadwick, R. E., and Syme, D. A. (2005). Mammal-like muscles power swimming in a cold-water shark. *Nature* 437, 1349–1352. doi: 10.1038/nature04007

Bishop, D. (2003). Warm up I: potential mechanisms and the effects of passive warm up on exercise performance. *Sports Med.* 33, 439–454. doi: 10.2165/00007256-200333060-00005

Boratyński, J. S., Jefimow, M., and Wojciechowski, M. S. (2017). Individual differences in the phenotypic flexibility of basal metabolic rate in siberian hamsters are consistent on short- and long-term timescales. *Physiol. Biochem. Zool.* 90, 139–152. doi: 10.1086/689870

Borowiec, A. S., Sion, B., Chalmel, F. D., Rolland, A., Lemonnier, L., De Clerck, T., et al. (2016). Cold/menthol TRPM8 receptors initiate the cold-shock response and protect germ cells from cold-shock-induced oxidation. *FASEB J.* 30, 3155–3170. doi: 10.1096/fj.201600257R

Boyles, J. G., Thompson, A. B., McKechnie, A. E., Malan, E., Humphries, M. M., and Careau, V. (2013). A global heterothermic continuum in mammals. *Global Ecol. Biogeogr.* 22, 1029–1039. doi: 10.1111/geb.12077

Cannon, B., and Nedergaard, J. (2010). Thyroid hormones: igniting brown fat via the brain. *Nat. Med.* 16, 965–967. doi: 10.1038/nm0910-965

Caterina, M. J. (2006). Transient receptor potential ion channels as participants in thermosensation and thermoregulation. *Am. J. Physiol. Regul. Integr. Comp. Physiol.* 292, R64–R76. doi: 10.1152/ajpregu.00446.2006

Chappell, S. A., Owens, G. C., and Mauro, V. P. (2001). A 5' Leader of Rbm3, a cold stress-induced mrna, mediates internal initiation of translation with increased efficiency under conditions of mild hypothermia. *J. Biol. Chem.* 276, 36917–36922. doi: 10.1074/jbc.M106008200

Cossins, A., and Prosser, C. L. (1978). Evolutionary adaptation of membranes to temperature. *Proc. Natl. Acad. Sci. U.S.A.* 75, 2040–2043.

Crompton, A. W., Taylor, C. R., and Jagger, J. A. (1978). Evolution of homeothermy in mammals. *Nature* 272, 333–336.

Cunniffe, B., Ellison, M., Loosemore, M., and Cardinale, M. (2017). Warm-up practices in elite boxing athletes: impact on power output. *J. Strength Cond. Res.* 31, 95–105. doi: 10.1519/JSC.0000000000001484

Dammhahn, M., Landry-Cuerrier, M., Réale, D., Garant, D., and Humphries, M. M. (2017). Individual variation in energy-saving heterothermy affects survival and reproductive success. *Funct. Ecol.* 31, 866–875. doi: 10.1111/1365-2435.12797

Darras, V. M., and Van Herck, S. L. J. (2012). Iodothyronine deiodinase structure and function: from ascidians to humans. *J. Endocrinol.* 215, 189–206. doi: 10.1530/JOE-12-0204

Ducharme, M. B., VanHelder, W. P., and Radomsky, M. W. (1991). Tissue temperature profile in the human forearm during thermal stress at thermal stability. *J. Appl. Physiol.* 71, 1973–1978.

Dymond, M. K. (2016). Mammalian phospholipid homeostasis: evidence that membrane curvature elastic stress drives homeoviscous adaptation *in vivo*. *J. R. Soc. Interf.* 13, 20160228–20160212. doi: 10.1098/rsif.2016.0228

Eliason, E. J., Clark, T. D., Hague, M. J., Hanson, L. M., Gallagher, Z. S., Jeffries, K. M., et al. (2011). Differences in thermal tolerance among sockeye salmon populations. *Science* 332, 109–112. doi: 10.1126/science.1199158

Else, P. L. (2016). The thermal dependence of Na^+ flux in isolated liver cells from ectotherms and endotherms. *J. Exp. Biol.* 219, 2098–2102. doi: 10.1242/jeb.136747

Forsman, A. (2014). Rethinking phenotypic plasticity and its consequences for individuals, populations and species. *Heredity* 115, 276–284. doi: 10.1038/hdy.2014.92

Glanville, E. J., and Seebacher, F. (2010a). Advantage to lower body temperatures for a small mammal (*Rattus fuscipes*) experiencing chronic cold. *J. Mammal.* 91, 1197–1204. doi: 10.1644/10-MAMM-A-003.1

Glanville, E. J., and Seebacher, F. (2010b). Plasticity in body temperature and metabolic capacity sustains winter activity in a small endotherm (*Rattus fuscipes*). *Comp. Biochem. Physiol. A* 155, 383–391. doi: 10.1016/j.cbpa.2009.12.008

Glanville, E. J., Murray, S. A., and Seebacher, F. (2012). Thermal adaptation in endotherms: climate and phylogeny interact to determine population-level responses in a wild rat. *Funct. Ecol.* 26, 390–398. doi: 10.1111/j.1365-2435.2011.01933.x

Gotic, I., Omidi, S., Fleury-Olela, F., Molina, N., Naef, F., and Schibler, U. (2016). Temperature regulates splicing efficiency of the cold-inducible RNA-binding protein gene CIRBP. *Genes Dev.* 30, 2005–2017. doi: 10.1101/gad.287094.116

Gracey, A. Y., Fraser, E. J., Li, W. Z., Fang, Y. X., Taylor, R. R., Rogers, J., et al. (2004). Coping with cold: an integrative, multitissue analysis of the transcriptome of a poikilothermic vertebrate. *Proc. Natl. Acad. Sci. U.S.A.* 101, 16970–16975. doi: 10.1073/pnas.0403627101

Guderley, H. (1990). Functional significance of metabolic responses to thermal acclimation in fish muscle. *Am. J. Physiol.* 259, R245–R252.

Hardie, D. G., Schaffer, B. E., and Brunet, A. (2016). AMPK: an energy-sensing pathway with multiple inputs and outputs. *Trends Cell Biol.* 26, 190–201. doi: 10.1016/j.tcb.2015.10.013

Hetem, R. S., Maloney, S. K., Fuller, A., and Mitchell, D. (2016). Heterothermy in large mammals: inevitable or implemented? *Biol. Rev.* 91, 187–205. doi: 10.1111/brv.12166

Heyland, A., and Moroz, L. (2005). Cross-kingdom hormonal signaling: an insight from thyroid hormone functions in marine larvae. *J. Exp. Biol.* 208, 4355–4361. doi: 10.1242/jeb.01877

Hillman, S. S., and Hedrick, M. S. (2015). A meta-analysis of *in vivo* vertebrate cardiac performance: implications for cardiovascular support in the evolution of endothermy. *J. Exp. Biol.* 218, 1143–1150. doi: 10.1242/jeb.118372

Huey, R. B., and Kingsolver, J. (1989). Evolution of thermal sensitivity of ectotherm performance. *Trends Ecol. Evol.* 4, 131–135.

Jackson, T. C., Manole, M. D., Kotermanski, S. E., Jackson, E. K., Clark, R. S. B., and Kochanek, P. M. (2015). Cold stress protein RBM3 responds to temperature change in an ultra-sensitive manner in young neurons. *Neuroscience* 305, 268–278. doi: 10.1016/j.neuroscience.2015.08.012

Jäger, S., Handschin, C., St-Pierre, J., and Spiegelman, B. M. (2007). AMP-activated protein kinase (AMPK) action in skeletal muscle via direct phosphorylation of PGC-1alpha. *Proc. Natl. Acad. Sci. U.S.A.* 104, 12017–12022. doi: 10.1073/pnas.0705070104

James, R. S. (2013). A review of the thermal sensitivity of the mechanics of vertebrate skeletal muscle. *J. Comp. Physiol. B* 183, 723–733. doi: 10.1007/s00360-013-0748-1

James, R. S., Tallis, J., and Angilletta, M. J. (2015). Regional thermal specialisation in a mammal: temperature affects power output of core muscle more than that of peripheral muscle in adult mice (*Mus musculus*). *J. Comp. Physiol. B* 185, 135–142. doi: 10.1007/s00360-014-0872-6

Kingsolver, J. G. (2003). Environmental variation and selection on performance curves. *Am. Zool.* 43, 470–477. doi: 10.1093/icb/43.3.470

Landeira-Fernandez, A. M., Castilho, P. C., and Block, B. A. (2012). Thermal dependence of cardiac SR Ca^{2+}-ATPase from fish and mammals. *J. Therm. Biol.* 37, 217–223. doi: 10.1016/j.jtherbio.2012.01.003

Laursen, W. J., Schneider, E. R., Merriman, D. K., Bagriantsev, S. N., and Gracheva, E. O. (2016). Low-cost functional plasticity of TRPV1 supports heat tolerance in squirrels and camels. *Proc. Natl. Acad. Sci. U.S.A.* 113, 11342–11347. doi: 10.1073/pnas.1604269113

Levesque, D. L., Nowack, J., and Stawski, C. (2016). Modelling mammalian energetics: the heterothermy problem. *Clim. Change Resp.* 3, 7. doi: 10.1186/s40665-016-0022-3

Lira, V. A., Brown, D. L., Lira, A. K., Kavazis, A. N., Soltow, Q. A., Zeanah, E. H., et al. (2010). Nitric oxide and AMPK cooperatively regulate PGC-1 in skeletal muscle cells. *J. Physiol.* 588, 3551–3566. doi: 10.1113/jphysiol.2010.194035

Little, A. G. (2016). A review of the peripheral levels of regulation by thyroid hormone. *J. Comp. Physiol. B* 186, 677–688. doi: 10.1007/s00360-016-0984-2

Little, A. G., and Seebacher, F. (2013). Thyroid hormone regulates muscle function during cold acclimation in zebrafish (*Danio rerio*). *J. Exp. Biol.* 216, 3514–3521. doi: 10.1242/jeb.089136

Little, A. G., and Seebacher, F. (2014). Thyroid hormone regulates cardiac performance during cold acclimation in zebrafish (*Danio rerio*). *J. Exp. Biol.* 217, 718–725. doi: 10.1242/jeb.096602

Little, A. G., and Seebacher, F. (2016). Thermal conditions experienced during differentiation affect metabolic and contractile phenotypes of mouse myotubes. *Am. J. Physiol Regul. Integr. Comp. Physiol.* 311, R457–R465. doi: 10.1152/ajpregu.00148.2016

Little, A. G., Kunisue, T., Kannan, K., and Seebacher, F. (2013). Thyroid hormone actions are temperature-specific and regulate thermal acclimation in zebrafish (*Danio rerio*). *BMC Biol.* 11:26. doi: 10.1186/1741-7007-11-26

Ljubicic, V., Miura, P., Burt, M., Boudreault, L., Khogali, S., Lunde, J. A., et al. (2011). Chronic AMPK activation evokes the slow, oxidative myogenic program and triggers beneficial adaptations in mdx mouse skeletal muscle. *Hum. Mol. Gen.* 20, 3478–3493. doi: 10.1093/hmg/ddr265

Lovegrove, B. G. (2005). Seasonal thermoregulatory responses in mammals. *J. Comp. Physiol. B* 175, 231–247. doi: 10.1007/s00360-005-0477-1

Ma, S., Yu, H., Zhao, Z., Luo, Z., Chen, J., Ni, Y., et al. (2012). Activation of the cold-sensing TRPM8 channel triggers UCP1-dependent thermogenesis and prevents obesity. *J. Mol. Cell Biol.* 4, 88–96. doi: 10.1093/jmcb/mjs001

McKechnie, A. E., Noakes, M. J., and Smit, B. (2015). Global patterns of seasonal acclimatization in avian resting metabolic rates. *J. Ornithol.* 156, 367–376. doi: 10.1007/s10336-015-1186-5

Morrison, S. F., Madden, C. J., and Tupone, D. (2014). Central neural regulation of brown adipose tissue thermogenesis and energy expenditure. *Cell Metab.* 19, 741–756. doi: 10.1016/j.cmet.2014.02.007

Mutungi, G., and Ranatunga, K. W. (1998). Temperature-dependent changes in the viscoelasticiy of intact resting mammalian (rat) fast- and slow-twitch muscle fibres. *J. Physiol.* 508, 253–265.

Nakamura, K., and Morrison, S. F. (2007). A thermosensory pathway that controls body temperature. *Nat. Neurosci.* 11, 62–71. doi: 10.1038/nn2027

Nilius, B., and Voets, T. (2005). TRP channels: a TR(I)P through a world of multifunctional cation channels. *Pflug. Arch. Eur. J. Physiol.* 451, 1–10. doi: 10.1007/s00424-005-1462-y

Noakes, M. J., Wolf, B. O., and McKechnie, A. E. (2017). Seasonal metabolic acclimatization varies in direction and magnitude among populations of an afrotropical passerine bird. *Physiol. Biochem. Zool.* 90, 178–189. doi: 10.1086/689030

Pan, P., and van Breukelen, F. (2011). Preference of IRES-mediated initiation of translation during hibernation in golden-mantled ground squirrels, *Spermophilus lateralis*. *Am. J. Physiol. Regul. Integr. Comp. Physiol.* 301, R370–R377. doi: 10.1152/ajpregu.00748.2010

Peng, G., Shi, X., and Kadowaki, T. (2015). Evolution of TRP channels inferred by their classification in diverse animal species. *Mol. Phylogen. Evol.* 84, 145–157. doi: 10.1016/j.ympev.2014.06.016

Peretti, D., Bastide, A., Radford, H., Verity, N., Molloy, C., Martin, M. G., et al. (2015). RBM3 mediates structural plasticity and protective effects of cooling in neurodegeneration. *Nature* 518, 236–239. doi: 10.1038/nature14142

Phadtare, S., Alsina, J., and Inouye, M. (1999). Cold shock response and cold-shock proteins. *Curr. Opin. Microbiol.* 2, 175–180. doi: 10.1016/S1369-5274(99)80031-9

Piersma, T., and Drent, J. (2003). Phenotypic flexibility and the evolution of organismal design. *Trends Ecol. Evol.* 18, 228–233. doi: 10.1016/S0169-5347(03)00036-3

Ponganis, P. J., Van Dam, R. P., Levenson, D. H., Knower, T., Ponganis, K. V., and Marshall, G. (2003). Regional heterothermy and conservation of core temperature in emperor penguins diving under sea ice. *Comp. Biochem. Physiol. A* 135, 477–487. doi: 10.1016/S1095-6433(03)00133-8

Porter, W. P., and Gates, D. M. (1969). Thermodynamic equilibria of animals with environment. *Ecol. Monogr.* 39, 227–244.

Potla, R., Singh, I. S., Atamas, S. P., and Hasday, J. D. (2015). Shifts in temperature within the physiologic range modify strand-specific expression of select human microRNAs. *RNA* 21, 1261–1273. doi: 10.1261/rna.049122.114

Quesada-López, T., Cereijo, R., Turatsinze, J.-V., Planavila, A., Cairó, M., Gavaldà-Navarro, A., et al. (2016). The lipid sensor GPR120 promotes brown fat activation and FGF21 release from adipocytes. *Nat. Commun.* 7, 13479–13417. doi: 10.1038/ncomms13479

Racinais, S., Wilson, M. G., and Périard, J. D. (2017). Passive heat acclimation improves skeletal muscle contractility in humans. *Am. J. Physiol. Regul. Integr. Comp. Physiol.* 312, R101–R107. doi: 10.1152/ajpregu.00431.2016

Rezende, E. L., and Bacigalupe, L. D. (2015). Thermoregulation in endotherms: physiological principles and ecological consequences. *J. Comp. Physiol. B* 185, 709–727. doi: 10.1007/s00360-015-0909-5

Rezende, E. L., Bozinovic, F., and Garland, T. Jr (2004). Climatic adaptation and the evolution of basal and maximum rates of metabolism in rodents. *Evolution* 58, 1361–1374. doi: 10.1554/03-499.1.s1

Ross, F. A., MacKintosh, C., and Hardie, D. G. (2016). AMP-activated protein kinase: a cellular energy sensor that comes in 12 flavours. *FEBS J.* 283, 2987–3001. doi: 10.1111/febs.13698

Sargeant, A. J. (1987). Effect of muscle temperature on leg extension force and short-term power output in humans. *Eur. J. Appl. Physiol.* 56, 693–698.

Scholander, P. F., Hock, R., Walters, V., Johnson, F., and Irving, L. (1950). Heat regulation in some arctic and tropical mammals and birds. *Biol. Bull.* 99, 237–258.

Scott, G. R., and Johnston, I. (2012). Temperature during embryonic development has persistent effects on thermal acclimation capacity in zebrafish. *Proc. Natl. Acad. Sci. U.S.A.* 109, 14247–14252. doi: 10.1073/pnas.1205012109

Seale, P., Bjork, B., Yang, W., Kajimura, S., Chin, S., Kuang, S., et al. (2008). PRDM16 controls a brown fat/skeletal muscle switch. *Nature* 454, 961–967. doi: 10.1038/nature07182

Seebacher, F. (2009). Responses to temperature variation: integration of thermoregulation and metabolism in vertebrates. *J. Exp. Biol.* 212, 2885–2891. doi: 10.1242/jeb.024430

Seebacher, F., and Murray, S. A. (2007). Transient receptor potential ion channels control thermoregulatory behaviour in reptiles. *PLoS ONE* 2:e281. doi: 10.1371/journal.pone.0000281

Shibasaki, K., Sugio, S., Takao, K., Yamanaka, A., Miyakawa, T., Tominaga, M., et al. (2015). TRPV4 activation at the physiological temperature is a critical determinant of neuronal excitability and behavior. *Pflug. Arch. Eur. J. Physiol.* 467, 2495–2507. doi: 10.1007/s00424-015-1726-0

Shinoda, K., Morishita, Y., Matsuda, Y., Takahashi, I., and Nishi, T. (1997). Enzymatic characterization of human 1,3-fucosyltransferase fuc-tvii synthesized in a b cell lymphoma cell line. *J. Biol. Chem.* 272, 31992–31997.

Sinclair, B. J., Marshall, K. E., Sewell, M. A., Levesque, D. L., Willett, C. S., Slotsbo, S., et al. (2016). Can we predict ectotherm responses to climate change using thermal performance curves and body temperatures? *Ecol. Lett.* 19, 1372–1385. doi: 10.1111/ele.12686

Sonna, L. A., Fujita, J., Gaffin, S. L., and Lilly, C. M. (2002). Invited review: effects of heat and cold stress on mammalian gene expression. *J. Appl. Physiol.* 92, 1725–1742. doi: 10.1152/japplphysiol.01143.2001

St-Pierre, J., Charest, P.-M., and Guderley, H. (1998). Relative contribution of quantitative and qualitative changes in mitochondria to metabolic compensation during seasonal acclimatisation of rainbow trout *Oncorhynchus mykiss*. *J. Exp. Biol.* 201, 2961–2970.

Sugimoto, K., and Jiang, H. (2008). Cold stress and light signals induce the expression of cold-inducible RNA binding protein (cirp) in the brain and eye of the Japanese treefrog (*Hyla japonica*). *Comp. Biochem. Physiol. A* 151, 628–636. doi: 10.1016/j.cbpa.2008.07.027

Tattersall, G. J., Roussel, D., Voituron, Y., and Teulier, L. (2016). Novel energy-saving strategies to multiple stressors in birds: the ultradian regulation of body temperature. *Proc. R. Soc. B* 283, 20161551–20161557. doi: 10.1098/rspb.2016.1551

Tattersall, G. J., Sinclair, B. J., Withers, P. C., FIields, P. A., Seebacher, F., Cooper, C. E., et al. (2012). Coping with thermal challenges: physiological adaptations to environmental temperatures. *Compr. Physiol.* 2, 2151–2202. doi: 10.1002/cphy.c110055

Towler, M. C., and Hardie, D. G. (2007). AMP-activated protein kinase in metabolic control and insulin signaling. *Circ. Res.* 100, 328–341. doi: 10.1161/01.RES.0000256090.42690.05

Underhill, M. F., and Smales, C. M. (2007). The cold-shock response in mammalian cells: investigating the HeLa cell cold-shock proteome. *Cytotechnology* 53, 47–53. doi: 10.1007/s10616-007-9048-5

Wang, C.-Z., Wei, D., Guan, M.-P., and Xue, Y.-M. (2014). Triiodothyronine regulates distribution of thyroid hormone receptors by activating AMP-activated protein kinase in 3T3-L1 adipocytes and induces uncoupling protein-1 expression. *Mol. Cell Biochem.* 393, 247–254. doi: 10.1007/s11010-014-2067-6

Wellmann, S. (2004). Oxygen-regulated expression of the RNA-binding proteins RBM3 and CIRP by a HIF-1-independent mechanism. *J. Cell Sci.* 117, 1785–1794. doi: 10.1242/jcs.01026

Wheeler, R. E., and Torchiano, M. (2016). *Permutation Tests for Linear Models in R*. R Package Version 2.1.0. Available online at: https://github.com/mtorchiano/lmPerm

Wooden, K. M. (2004). Body temperature and locomotor capacity in a heterothermic rodent. *J. Exp. Biol.* 207, 41–46. doi: 10.1242/jeb.00717

Yaicharoen, P., Wallman, K., Morton, A., and Bishop, D. (2012). The effect of warm-up on intermittent sprint performance and selected thermoregulatory parameters. *J. Sci. Med. Sport* 15, 451–456. doi: 10.1016/j.jsams.2012.02.003

Yang, C., and Carrier, F. (2001). The UV-inducible RNA-binding protein A18 (A18 hnRNP) plays a protective role in the genotoxic stress response. *J. Biol. Chem.* 276, 47277–47284. doi: 10.1074/jbc.M105396200

Ye, L., Kleiner, S., Wu, J., Sah, R., Gupta, R. K., Banks, A. S., et al. (2012). TRPV4 is a regulator of adipose oxidative metabolism, inflammation, and energy homeostasis. *Cell* 151, 96–110. doi: 10.1016/j.cell.2012.08.034

Ye, L., Wu, J., Cohen, P., Kazak, L., Khandekar, M. J., Jedrychowski, M. P., et al. (2013). Fat cells directly sense temperature to activate thermogenesis. *Proc. Natl. Acad. Sci. U.S.A.* 110, 12480–12485. doi: 10.1073/pnas.1310261110

Zhu, X., Bührer, C., and Wellmann, S. (2016). Cold-inducible proteins CIRP and RBM3, a unique couple with activities far beyond the cold. *Cell. Mol. Life Sci.* 73, 3839–3859. doi: 10.1007/s00018-016-2253-7

Conflict of Interest Statement: The authors declare that the research was conducted in the absence of any commercial or financial relationships that could be construed as a potential conflict of interest.

frontiers in Physiology

ORIGINAL RESEARCH
published: 10 November 2017
doi: 10.3389/fphys.2017.00909

Mitochondrial Proton Leak Compensates for Reduced Oxidative Power during Frequent Hypothermic Events in a Protoendothermic Mammal, *Echinops telfairi*

Elias T. Polymeropoulos[1*†], *R. Oelkrug*[2†] *and M. Jastroch*[3,4]

[1] *Institute for Marine and Antarctic Studies, University of Tasmania, Hobart, TAS, Australia,* [2] *Center of Brain, Behavior and Metabolism, University of Lübeck, Lübeck, Germany,* [3] *Institute for Diabetes and Obesity, Helmholtz Zentrum München, Munich, Germany,* [4] *Helmholtz Diabetes Center, German Center for Diabetes Research (DZD), Neuherberg, Germany*

The lesser hedgehog tenrec (*Echinops telfairi*) displays reptile-like thermoregulatory behavior with markedly high variability in body temperature and metabolic rate. To understand how energy metabolism copes with this flexibility, we studied the bioenergetics of isolated liver mitochondria from cold (20°C) and warm (27°C) acclimated tenrecs. Different acclimation temperatures had no impact on mitochondrial respiration using succinate as the substrate. Mimicking the variation of body temperature by changing assay temperatures from 22 to 32°C highlighted temperature-sensitivity of respiration. The 40% reduction of respiratory control ratio (RCR) at 22°C compared to 32°C, a common estimate for mitochondrial efficiency, was caused by reduced substrate oxidation capacity. The simultaneous measurement of mitochondrial membrane potential enabled the precise assessment of efficiency with corrected respiration rates. Using this method, we show that proton leak respiration at the highest common membrane potential was not affected by acclimation temperature but was markedly decreased by assay temperature. Using membrane potential corrected respiration values, we show that the fraction of ATP-linked respiration (coupling efficiency) was maintained (70–85%) at lower temperatures. Collectively, we demonstrate that compromised substrate oxidation was temperature-compensated by the reduction of proton leak, thus maintaining the efficiency of mitochondrial energy conversion. Therefore, membrane potential data suggest that adjustments of mitochondrial proton leak contribute to energy homeostasis during thermoregulatory flexibility of tenrecs.

Keywords: mitochondria, proton leak, lesser hedgehog tenrec, endothermy, protoendotherm, cold acclimatization

OPEN ACCESS

Edited by:
Brian G. Drew,
Baker Heart and Diabetes Institute, Australia

Reviewed by:
Michael B. Morris,
University of Sydney, Australia
Steven Paul Gieseg,
University of Canterbury, New Zealand

****Correspondence:***
Elias T. Polymeropoulos
eliasp@utas.edu.au

† These authors have contributed equally to this work.

Specialty section:
This article was submitted to Integrative Physiology, a section of the journal Frontiers in Physiology

Received: *29 May 2017*
Accepted: *26 October 2017*
Published: *10 November 2017*

Citation:
Polymeropoulos ET, Oelkrug R and Jastroch M (2017) Mitochondrial Proton Leak Compensates for Reduced Oxidative Power during Frequent Hypothermic Events in a Protoendothermic Mammal, Echinops telfairi. Front. Physiol. 8:909. doi: 10.3389/fphys.2017.00909

INTRODUCTION

Endotherms like mammals and birds display the unique ability to maintain a high body temperature (T_b) over a wide ambient temperature (T_a) range (Crompton et al., 1978). Unlike in ectotherms, where T_b is generally dependent on T_a, this evolutionary strategy has enabled endotherms to expand into highly specialized niches and a wide geographical distribution. Despite

the establishment of the gross classification into endo- and ectothermic animals, the distinction is often not clear cut, with several endothermic taxa displaying distinct ectothermic physiological traits and vice versa.

The lesser hedgehog tenrec (*Echinops telfairi*) as a prime example, displays reptile-like thermoregulatory behavior with markedly high variability in T_b and metabolic rate (Scholl, 1974; Lovegrove and Génin, 2008; Oelkrug et al., 2013). The tenrec displays one of the lowest normothermic T_b (∼32°C) compared to all other placental mammals in winter conditions and exhibits regular daily torpor behavior with substantial reductions in T_b (following reductions in T_a) and metabolic rate. Extraordinarily, *E. telfairi* females only display constantly high T_b during reproduction and parental care (Poppitt et al., 1994). Hence, this afrotherian species is referred to as protoendothermic, representing an intermediate state of thermoregulatory rigor compared to more "modern" homeothermic eutherian species. This thermoregulatory setup of protoendotherms is therefore often considered a representative characteristic of the evolutionary transition from ecto- to endothermy (Lovegrove and Génin, 2008; Mckechnie and Mzilikazi, 2011).

Interestingly, the basal metabolic rate (BMR) of the tenrec is similar to ectothermic metabolic rates of the same body mass, while the basal mitochondrial proton leak in the liver, a significant contributor of metabolic heat production (Brand et al., 1994; Rolfe and Brown, 1997), is at an intermediate level between endo- and ectotherms (Polymeropoulos et al., 2017).

Prolonged cold exposure triggers complex physiological adjustments to ensure cellular homeostasis at a constant T_b in many mammals. There is evidence that *E. telfairi* is capable of non-shivering thermogenesis mediated by functional brown adipose tissue (BAT) and hence of a mechanism that is unique to "modern" eutherian mammals (Oelkrug et al., 2013, 2015). The bioenergetic setup of tenrec mitochondria in other tissues may also be highly advanced and equipped to adjust energy metabolism in response to environmental stressors such as low ambient temperatures.

While UCP1-mediated non-shivering thermogenesis in BAT is the most prominent mechanism to enable survival in the cold and arousal from torpid or hibernating states of small eutherian mammals (Cannon and Nedergaard, 2004; Oelkrug et al., 2011), mitochondrial adjustments in other tissues of high oxygen uptake have also been described. It appears that another important thermogenic tissue is skeletal muscle which contributes with shivering and possibly other alternative mechanisms of non-shivering thermogenesis using SERCA pathways (Rowland et al., 2015). The liver is commonly studied to assess the relationship between metabolism and mitochondrial bioenergetics as the liver contributes significantly (10–20%) to the metabolic rate of mammals (Field et al., 1939) and mitochondria are easy to isolate as compared to e.g., skeletal muscle.

In general, mitochondria convert nutritional energy into cellular energy by oxidative phosphorylation, a process that consumes about 90% of the cellular oxygen uptake in mammals (Rolfe and Brown, 1997). Mitochondrial substrates are oxidized and their electrons are transported along the respiratory complexes before reducing oxygen to water. The potential energy of the electrons is used to pump protons out of the matrix, generating a proton motive force that drives the ATP synthesis. The energy transduction to ATP is, however, not fully efficient as the proton motive force is also consumed by the mitochondrial proton leak (Jastroch et al., 2010). The management of the energy budget of an animal can be adjusted by alterations in mitochondrial efficiency when exposed to environmental stress, either by a decrease of substrate oxidation or by changes in proton permeability as shown for many ectotherms (Gnaiger et al., 2000; St-Pierre et al., 2000; Trzcionka et al., 2008).

During episodes of energy shortage such as cold seasons or food scarcity, small mammals use energy conserving mechanisms such as torpor or hibernation to decrease energy demand by dramatic reduction of T_b and metabolic rate. During torpor and hibernation, state 3 (phosphorylating) respiration and maximal substrate oxidation are reversibly suppressed in isolated liver mitochondria (Staples and Brown, 2008; Kutschke et al., 2013). The degree of suppression is, not surprisingly, highly dependent on experimental assay temperature. Interestingly, it appears that the suppression of state 3 respiration in hypothermic states is only detectable above a critical assay temperature of 30°C. Above 30°C assay temperature, passive thermal effects rather than active suppression may become more important for metabolic rate (Staples and Brown, 2008). This is further supported by the lack of active suppression in isolated liver mitochondria of the Golden spiny mouse (*Acomys russatus*), a desert species that displays significant reduction of energy metabolism without pronounced reduction of T_b (Grimpo et al., 2014). The findings at lower assay temperatures may well be related to changes of the biophysical properties of mitochondrial membranes.

In isolated liver mitochondria of the homeothermic rat (*Rattus norvegicus*), lowering the assay temperature from 37 to 25°C reduces state 3 (phosphorylating) and state 4 (non-phosphorylating) respiration by 50%, (Dufour et al., 1996). In the heterothermic Djungarian hamster (*Phodopus sungorus*), substrate oxidation of isolated liver mitochondria is suppressed in torpid animals ($T_b < 31$°C). The suppression of substrate oxidation affects respiration rates the most at normothermic assay temperatures (37°C) but not at torpor-like assay temperatures (15°C). At 15°C, mitochondrial proton leak is increased in mitochondria of torpid but not normothermic animals (Brown et al., 2007). The respiration of liver mitochondria correlates with body temperature but there is no suppression found for kidney, skeletal muscle, and heart mitochondria, suggesting tissue-specificity of mitochondrial suppression (Kutschke et al., 2013).

Given these findings in rodents, it may be expected that frequent body temperature changes of the tenrec affect mitochondrial respiration through passive Q_{10} driven changes but it is unknown whether mechanistic alterations in response to cold exposure, such as active suppression, contribute as well.

While the general thermoregulatory patterns of the lesser hedgehog tenrec, a representative protoendothermic species, have become more transparent through recent research, underlying function or mechanisms that have co-evolved with thermoregulatory flexibility, remain unclear. Here, we studied

the bioenergetics of isolated liver mitochondria of cold vs. warm acclimated, non-torpid tenrecs at different assay temperatures to understand functional adjustments that may assist the animals to manage energy homeostasis during the transition to various body temperatures.

MATERIALS AND METHODS

Animal Husbandry

Laboratory bred male ($n = 4$) and female ($n = 8$) lesser hedgehog tenrecs (*E. telfairi*) were measured during their annual activity period. Throughout the experiment, animals were housed individually in Typ IV makrolon cages (1,800 cm^2) with sawdust bedding and plastic nest boxes and were kept on a 12:12 h light-dark cycle at an ambient temperature of 23 ± 1°C. They had free access to water and were fed with canned cat food (KiteKat), cockroaches, seeds and fruits every second day at 2–5 p.m. All experimental procedures were approved by the German Animal Welfare Authorities (Regierungspräsidium Gießen, Hessen, MR 17/1-Nr.116/2010).

Body Temperature Recordings

For continuous body temperature recordings on freely moving animals, implantable radio transmitters and receiver plates (Model X; Mini Mitter, Sunriver, OR, USA; accuracy 0.1°C) were used as described in detail previously (Oelkrug et al., 2013). After implantation animals were allowed to recover for at least 3 weeks before one group of animals was sequentially acclimated to 20°C (4 days at 24°C, 3 days at 21–22°C; cold acclimated group = CA group; $n = 6$) while the other group remained at 27°C (warm acclimated group = WA group; $n = 6$) (Oelkrug et al., 2013). After an acclimation period of 2 weeks, core body temperature (±1°C) was recorded every 6 min for 7–12 days at 27°C and 3–6 days at 20°C (only CA group).

Minimum and Resting Metabolic Rate

To assess the impact of ambient temperature on energy turnover in the tenrecs, the minimum (MR_{min}) and resting metabolic rate (RMR) were determined over a temperature range of 14°C (20–34°C) in tenrecs acclimatized to 20°C (CA) or 27°C (WA) using a two-channel respiratory system as described previously (Oelkrug et al., 2013). Briefly, tenrecs were exposed for 4–5 h per day to one randomly selected ambient temperature and readings of MR (O_2 consumption) and T_b were taken every 3–5 min. At ambient temperatures below 30°C animals immediately decreased their metabolism to minimum values (MR_{min}), resembling a torpor-like state, and had to be disturbed by the introduction of food to their cage (RMR, non-post absorptive) to obtain resting, non-torpid metabolic rate.

Mitochondrial Isolation

Before sacrifice animals were disturbed and allowed to reach normothermic T_b (>30°C). The rewarming took less than 30 min and after additional 30 min at normothermia the animals were sacrificed and their livers were harvested. Liver mitochondria were isolated by homogenization in STE buffer (250 mM sucrose, 5 mM Tris, 2 mM EGTA, pH 7.4 at 4°C) using a glass-glass-homogenizer, followed by differential centrifugation (see Trzcionka et al., 2008 for further details). All steps of mitochondrial isolation were performed on ice or at 4°C. After isolation, mitochondrial protein content was determined photometrically using the Biuret method (Gornall et al., 1949) and fatty acid free bovine serum albumin as standard. Measurements were started 45 min after mitochondria preparation.

Mitochondrial Respiration Rates

Mitochondrial oxygen consumption was measured with a Clark-type electrode connected to a temperature controlled water bath and calibrated with air-saturated medium [KHE buffer: 120 mM KCl, 5 mM KH_2PO_4, 3 mM HEPES, 1 mM EGTA, 0.3% bovine serum albumin (BSA; w/v), pH 7.2 at RT] which was assumed to contain 432 nmol O/ml at 32°C (Reynafarje et al., 1985). Mitochondria were diluted to 1.5 mg/ml mitochondrial protein in 500 µl KHE buffer and rotenone (4.8 µM) was added to inhibit complex I of the respiratory chain. Afterwards mitochondrial respiration was started by adding 4 mM succinate (state 2), followed by 600 µM ADP (state 3), and 1 µg/ml oligomycin (state 4). At the end of each measurement FCCP (carbonyl cyanide-p-triuoromethoxyphenylhydrazone) was added to induce maximum substrate oxidation.

The respiratory control ratio (RCR), determined by calculating the quotient of state 3 and state 4 respiration, was measured to ascertain the integrity of isolated mitochondria.

Temperature-dependency of mitochondrial respiration rates was calculated by performing measurements at different assay temperatures (22, 27, and 32°C).

Mitochondrial Proton Leak Kinetics and Coupling Efficiency

The kinetics of mitochondrial proton leak were measured by sequentially inhibiting respiration that drives the proton leak and plotting respiration rates against their corresponding membrane potentials. Measurements were performed with 1.5 mg/ml of liver mitochondria in KHE buffer. Mitochondrial membrane potential was measured simultaneously to mitochondrial respiration by using a $TPMP^+$ (triphenylmethylphosphonium)—sensitive probe. State 4 potentials were assessed in the presence of 100 nM nigericin (Cadenas and Brand, 2000), 4.8 µM rotenone, and 1 µg/ml oligomycin. At the beginning of each measurement, sequential additions of $TPMP^+$ up to 2.5 mM served to calibrate the $TPMP^+$ -sensitive electrode. Mitochondrial oxidation was initiated afterwards by the addition of 4 mM succinate and progressively inhibited with malonate up to 11.3 mM to establish decreasing steady state membrane potentials. Finally, FCCP was added to dissipate the membrane potential and release $TPMP^+$ from the mitochondria, allowing for correction of baseline drift.

State 3 potential was measured using the same experimental setup. First, 4.8 µM rotenone was added to inhibit complex I, followed by 4 mM succinate (state 2), 600 µM ADP (state 3), 50 nM nigericin (state 3), and finally FCCP for correction.

The simultaneous measurement of mitochondrial membrane potential enabled to compare mitochondrial electron flux of state 3 and proton leak at the same steady state potential. Thus,

we determined the oxygen consumption that either drives the ATP synthase or drives the mitochondrial proton leak. What proportion of the total electron flux is dedicated to the synthesis of ATP, while the rest is lost as heat through the proton leak, that is defined as coupling efficiency (efficiency of respiration "coupled" to ATP synthesis)(Affourtit and Brand, 2009). In our measurements, this is calculated as ATP-linked respiration (state 3 minus proton leak) divided by total respiration (state 3).

This determination was performed at assay temperatures of 22, 27, and 37°C.

Statistical Analysis

Body mass between WA and CA groups was tested for differences using the *t*-test. The Mann-Whitney test for two independent samples was used to test for differences of T_b frequencies between $T_a = 20°C$ and $T_a = 27°C$. RMR or MR_{min} values, and corresponding T_b values were tested for differences at various T_a using a two-way repeated measures analysis of variance (ANOVA) approach, considering acclimation (20 vs. 27°C) and T_a as factors. Similar analysis was performed considering T_a and metabolic rate (RMR vs. MR_{min}) as factors. Changes in RMR, $MR_{min,}$ and T_b with changes in T_a were further analyzed by standard least squares linear regression. The slopes of the linear regressions (m) were tested for significance using ANOVA. Mitochondrial respiration rates and RCR between acclimation groups or between assay temperature changes were tested for differences using two-way repeated measures ANOVA and least squares regression for changes with T_a in addition. HCP is defined as Highest Common mitochondrial membrane Potential of all proton leak curves that are compared. The oxygen consumption driving proton leak at HCP is estimated based on the leak kinetics, assuming linearity between two adjacent proton leak measurements of the curve. Coupling efficiency at different assay temperatures was analyzed using least squares linear regression. All pairwise multiple comparisons procedures were performed using adjusted Bonferroni *post-hoc* modified *t*-tests.

RESULTS

Body Mass, Metabolic Rate, and T_b

Liver mitochondria were isolated from *E. telfairi* individuals for which post- experimental body mass, metabolic rate, and T_b have been assessed previously (Oelkrug et al., 2013). Briefly, acclimation did not impact body mass which was 159 ± (*SD*) 17 g for 20°C and 132 ± (*SD*) 23 g for 27°C acclimated animals.

For the purpose of this study we re-analyzed core body temperature data (T_b, °C). T_b in tenrecs kept at 20°C was different to T_b in animals at 27°C (**Figure 1A**). The frequency distribution for T_b at $T_a = 20°C$ peaked at 21°C while the distribution at 27°C peaked at 29°C, which also equals the median values at each T_a. The mean value for T_b at $T_a = 20°C$ was 22.5 ± 3.4 and 29.6 ± 1.3°C at $T_a = 27°C$ and was significantly different.

RMR data from Oelkrug et al. (2013) revealed significant increase of metabolism at T_a below 30°C (Two-way ANOVA, $P \leq 0.01$, **Figure 1B**). The RMR between 30 and 34°C was

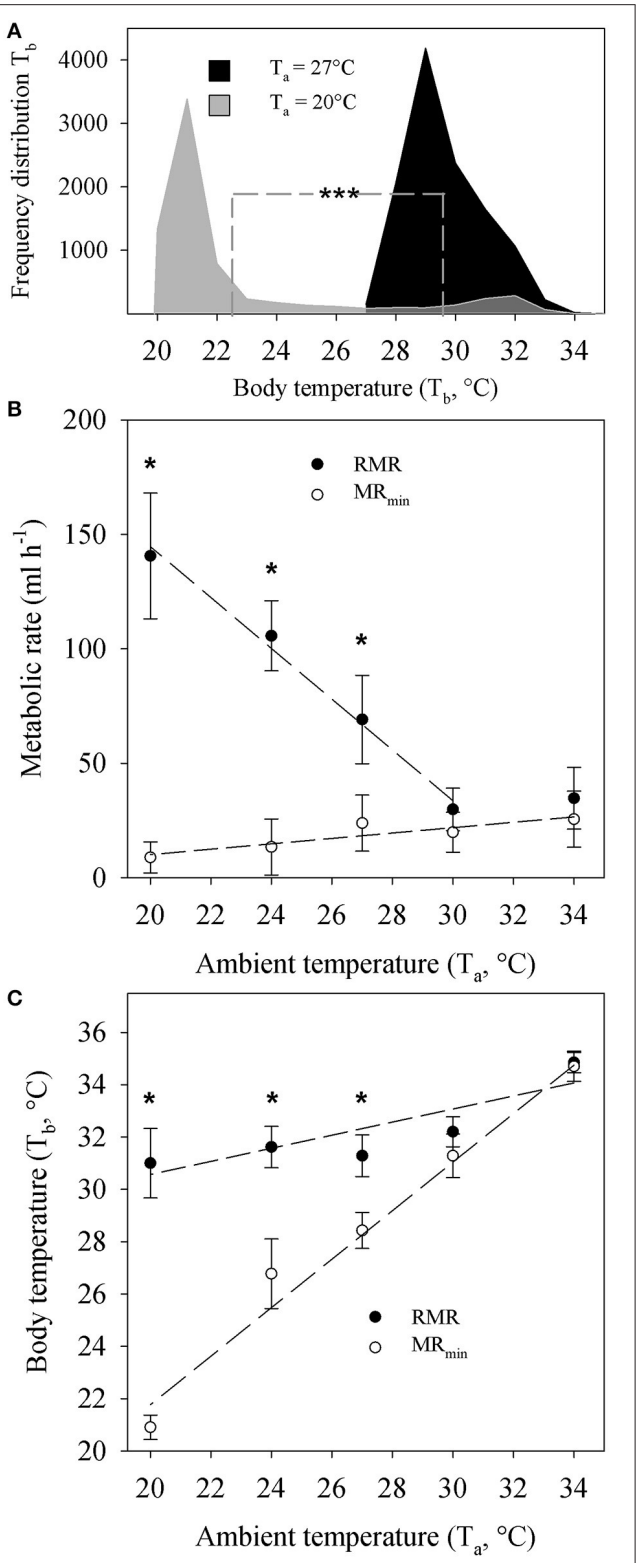

FIGURE 1 | (A) Frequency distribution of repeatedly measured core body temperature recordings (T_b) of *Echinops telfairi* exposed to 20°C (light gray, 3–6 days, $n = 6$) and 27°C (black, 7–12 days, $n = 6$) ambient temperatures (T_a). Dashed line indicates mean values for each temperature, which were

(Continued)

FIGURE 1 | Continued
significantly different from each other (Mann-Whitney, $^{***}P < 0.001$).
(B) Temperature dependent resting metabolic rate (RMR) and minimum metabolic rate (MR_{min}) of *Echinops telfairi* at different T_a. There was no significant difference in RMR or MR_{min} between animals acclimated to 20 or 27°C. Hence the data presented here is the average ± SE of both groups.
(C) Temperature dependent T_b changes during measurements of RMR and MR_{min} above. Values are means ± SE. * indicates significant differences between measurements of MR and MRmin and T_b at different T_a (two-way repeated measures ANOVA, $P < 0.05$). Dashed lines for **(B,C)** denote linear regressions fits to the data of the form $y = mx + b$ and the P values indicate where the slope of the regression (m) was significantly different from zero (ANOVA, $P < 0.05$). RMR: $y = -11.098x + 366.52$, m: $P = 0.005$; MR_{min}: $y = 1.18x - 13.4$, m: $P = 0.039$; T_b at RMR: $y = 0.2474x + 25.571$, m: $P = 0.049$; T_b at MR_{min}: $y = 0.9277x + 3.204$, m: $P = 0.002$. Note, the value for RMR at 34°C was not included in the linear regression analysis for RMR as it did not significantly differ from the value at 30°C. Hence, these two data points are within the TNZ for this species. The content of this figure was adapted from Oelkrug et al. (2013).

similar, indicating that both values are within the thermoneutral zone (TNZ) of the tenrec. Here, we re-analyzed the data by applying a linear regression analysis and confirmed a significantly negative correlation coefficient for RMR with increasing T_a (**Figure 1B**). MR_{min} showed a small but significant positive regression coefficient with increasing T_a from 20 to 34°C but MR_{min} values were significantly lower (Two-way ANOVA, $P \leq 0.01$) compared to RMR below a T_a of 30°C, and below the TNZ. There were no significant differences between acclimation groups at each T_a for RMR or MR_{min}, hence the data were pooled for the analyses and figures.

T_b during measurements of RMR significantly decreased with decreasing T_a by overall 2.8°C (**Figure 1C**). During measurements of MR_{min} on the contrary, the absolute decrease in T_b was 13.8°C. Here, T_b tracked T_a closely as T_a decreased with a scaling coefficient of 0.93 that was statistically, significantly different from zero ($P = 0.039$). There also was a statistically significant difference in T_b between RMR and MR_{min} measurements below a T_a of 30°C, corresponding to changes in MR_{min} (**Figure 1C**).

Mitochondrial Respiration

We investigated the bioenergetics of isolated liver mitochondria from cold and warm acclimated animals that were normothermic when sacrificed. We mimicked the variation of T_b by changing experimental assay temperatures from 22 to 32°C (**Figures 2A–D**). Between acclimation groups, we found no differences in any of the respiration states. As expected, mitochondrial respiration decreased significantly with decreased assay temperature by about 40% (two-way repeated measures ANOVA, $P < 0.01$). The reduction of respiration without respiratory control (state 3 and FCCP) suggests an average Q10 of 2.84 ± 0.65 (SE) of substrate oxidation. However, respiratory control (state3/4), as a rough estimate for mitochondrial coupling and efficiency, was compromised only at 22°C (**Figure 2E**, two-way repeated measures ANOVA, $P < 0.01$).

Mitochondrial Proton Leak Kinetics

To test whether the differences in state 4 (proton leak respiration) are caused by differences in proton conductance, or whether they are just a consequence of altered substrate oxidation (Keipert and Jastroch, 2014), we determined the proton leak kinetics of isolated tenrec liver mitochondria by simultaneous measurement of oxygen consumption and mitochondrial membrane potential. Plotting oxygen consumption driving the proton leak vs. membrane potential (**Figures 3A–C**), we found no statistical differences of proton leak at the highest common membrane potential between acclimation groups irrespective of assay temperature (**Figures 3D–F**). The proton leak at the HCP across the different T_a, decreases significantly with decreasing assay temperature (data for acclimation groups combined, **Figure 3G**), demonstrating reduced proton conductance at colder temperatures by passive thermal effects.

Mitochondrial Coupling Efficiency

Next, we precisely determined coupling efficiency, which represents the proportion of oxygen consumption driving the ATP synthase of total respiration (i.e., corrected for proton leak respiration). The proportion of proton leak was determined from proton leak kinetic curves at the state 3 membrane potential (see **Figure 4A**). The proportion of respiration to drive ATP synthesis at 32°C is about 70% and although statistically not significantly different, trends to increase up to 85% at lower temperatures (**Figure 4B**).

DISCUSSION

In this study, we report on adjustments of mitochondrial bioenergetics allowing energy homeostasis in the lesser hedgehog tenrec, a protoendothermic eutherian, during its T_b cycles. We find that the mitochondrial system maintains mitochondrial efficiency at lower assay temperatures, partially by decreases in proton leak, counteracting decreases in temperature-dependent substrate oxidation rates.

While these passive thermal effects appear to control mitochondrial energy turnover, cold acclimation of the tenrec had neither effect on the *in vivo* physiology such as body mass, T_b and metabolic rate, nor on bioenergetics parameters of isolated liver mitochondria.

The patterns of T_b to acute changes in T_a (**Figure 1**) as described previously (Oelkrug et al., 2013) clearly support the observations of a distinct ectotherm-like nature where T_b closely matches changes in T_a (Scholl, 1974; Lovegrove and Génin, 2008). This was particularly true for cases where animals entered torpid-like minimal metabolic states during the experiments (**Figure 1C**). Here, the correlation between T_b and T_a was very close to 1. Although the familiar Scholander-Irving model of thermoregulation is typically only applied to euthermic endotherms (McNab, 2002), metabolic heat production was adjusted similarly to euthermic endotherms below the TNZ when measuring RMR in the tenrecs (**Figure 1B**), clearly demonstrating the ability of classical euthermic, eutherian thermoregulation. Nevertheless, T_b in the tenrecs is amongst

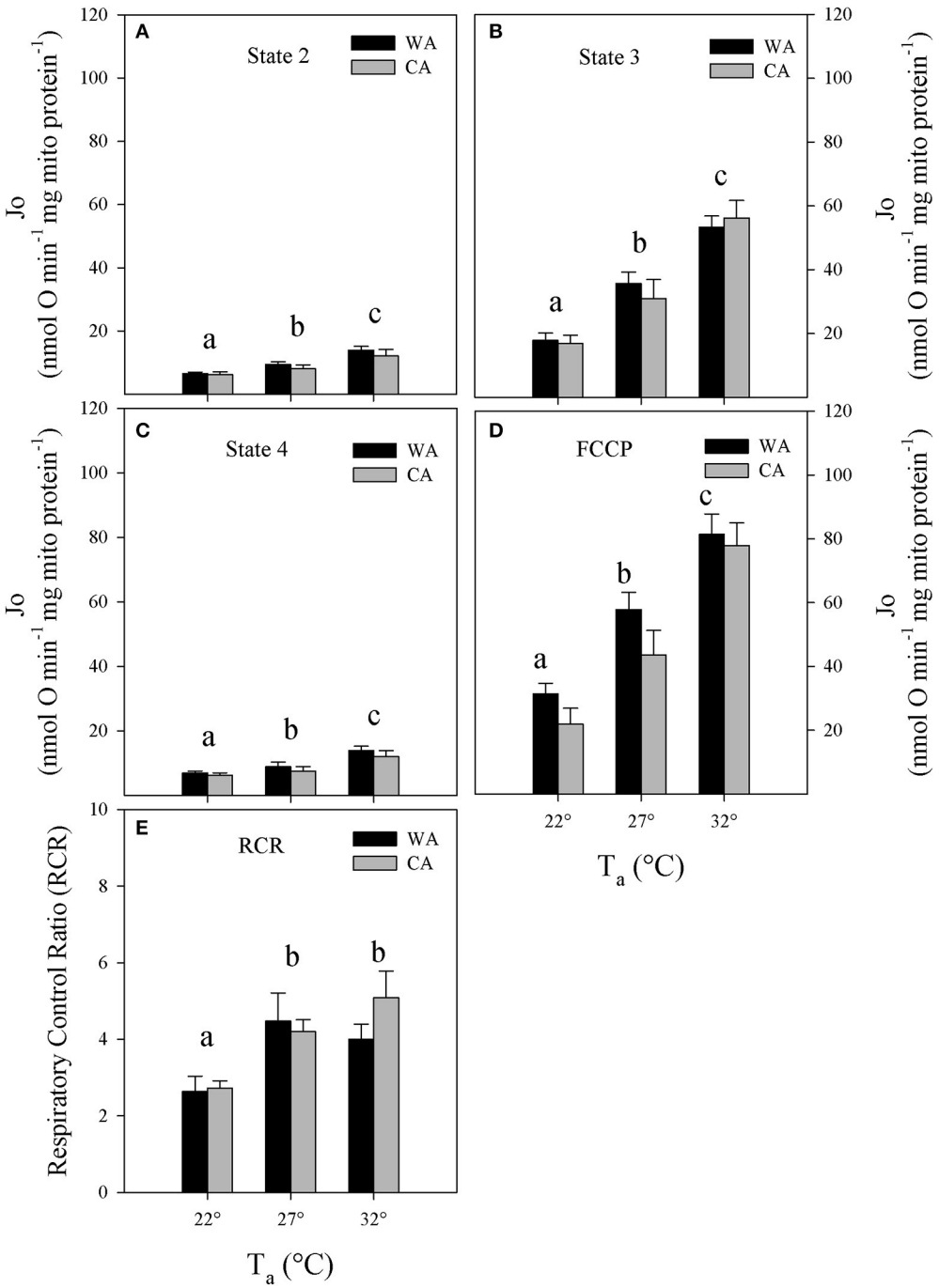

FIGURE 2 | Mitochondrial respiration rates (Jo) at **(A)** state 2, **(B)** 3, and **(C)** state 4; **(D)** upon chemical uncoupling with FCCP as well as **(E)** corresponding respiratory control ratios (RCR) of liver mitochondria, isolated from *Echinops telfairi* acclimated to 20°C cold acclimated (CA, gray bars, $n = 6$) or 27°C warm acclimated (WA, black bars, $n = 6$) at assay temperatures of 32, 27, and 22°C. Values are means ± SE. Differing letters denote statistically significant differences between assay temperatures for each state, as determined by 2-way repeated measures ANOVA, $P < 0.05$. There were no significant differences between acclimation groups for any of the parameters.

the lowest within mammals and similar to monotremes (Nicol, 2017). Interestingly, when undisturbed, tenrecs will drop their metabolic rates to a minimum, while adjusting their T_b to T_a. Even though the reduction in MR_{min} with changes in T_a that we observed here (**Figure 1B**) was only marginal in comparison to changes in RMR, the continuous reduction in MR_{min} appears relevant given the continuous reduction in T_b. It remains to be investigated whether passive heat loss is the major driver in the

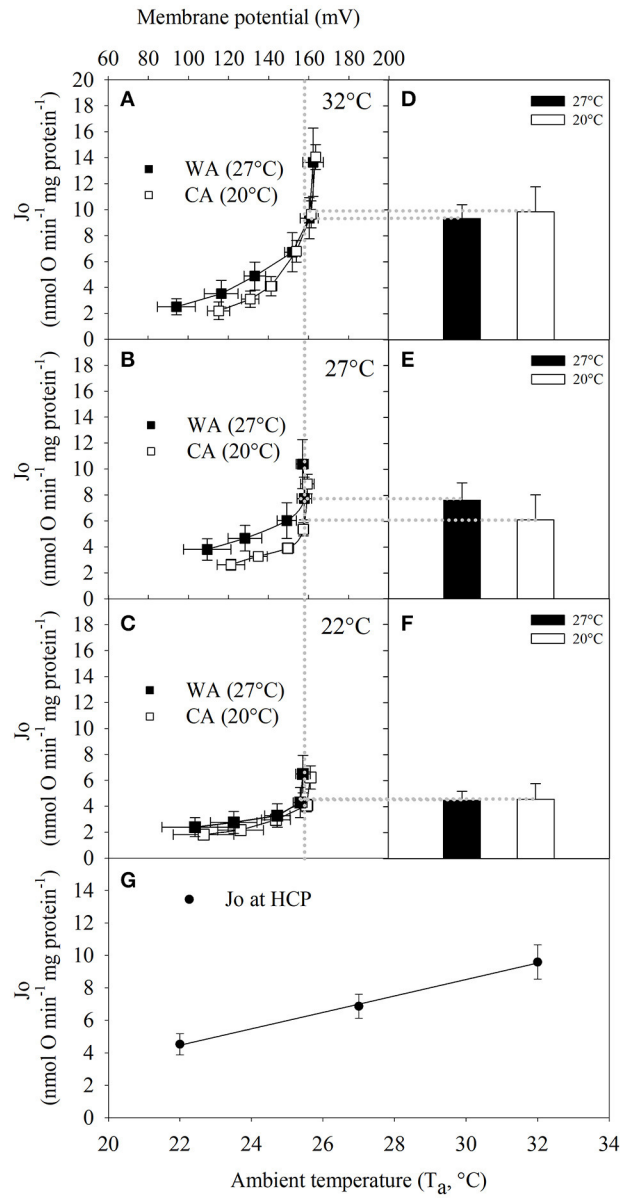

FIGURE 3 | The full kinetic response of proton leak rate to changes in membrane potential of liver mitochondria from *Echinops telfairi* acclimated to 20°C (CA, white squares, $n = 6$) or 27°C (WA, black squares, $n = 5$) at assay temperatures of **(A)** 32, **(B)** 27, and **(C)** 22°C in the presence of 1 μg/ml oligomycin. **(D–F)** Mean ± SE of proton leak respiration (Jo) at the highest common membrane potential across all T_a (HCP = 157 mV, vertical dotted line). **(G)** Proton leak respiration of HCP at different assay temperatures (acclimation groups combined). Values are means ± SE. Least squares regression: $y = -0.5059x + 20.659$, where the slope of the regression was significantly different from zero (ANOVA, $P = <0.001$).

reduction of T_b as is the case in many species entering torpor (Nicol and Andersen, 2007; Oelkrug et al., 2011), rather than the controlled reduction in MR and hence T_b.

While our understanding of the overarching thermoregulatory patterns of tenrecs has become clearer, the cellular basis supporting this unique pattern is not well-understood. The bioenergetics of liver mitochondria are well-established nominators of (basal) metabolic rates (Porter and Brand, 1995; Polymeropoulos et al., 2012) and actively adjust in response to hypothermic states in some rodent species (Staples and Brown, 2008; Kutschke et al., 2013). Thus, investigating temperature-dependent bioenergetics in the frequently heterothermic tenrec may yield relevant insights into concepts and mechanisms that occurred during early evolution of eutherian metabolism. Therefore, we investigated the flexibility of mitochondrial function in response to acute and chronic temperature changes in isolated liver mitochondria of tenrecs. In contrast to some ectothermic vertebrates such as fish and amphibians, where mitochondrial state 4 respiration and proton leak rate is suppressed in chronic cold (Jastroch et al., 2007; Trzcionka et al., 2008), acclimation temperature had no such impact on liver mitochondrial proton leak in the tenrec (**Figure 3**). This finding may indicate that there are no functional, long-term changes accompanied by cold acclimatization. In our experiments, we sacrificed the animals at normothermic temperatures for experimental consistency. Under these experimental conditions, putative, rapid molecular changes in response to hypothermic or hypometabolic states in torpor may be missed.

The capacity of ATP production is cold-sensitive with a 50% reduction of respiration rates in state 4 (**Figure 2C**) and 70% reduction in state 3 over a 10°C temperature decrease (32 vs. 22°C, **Figure 3B**). Similar findings, but with lesser physiological significance, have been reported for rat liver mitochondria, where a 12°C decrease in assay temperature resulted in a 50% decrease of state 3 and 4 respiration rates (Dufour et al., 1996).

For tenrec mitochondria, the respiratory control ratio at 22°C was 40% lower than that at 27 and 32°C (**Figure 2E**). However, the correction of ATP-linked state 3 for proton leak respiration at the state 3 mitochondrial membrane potential reveals maintenance of mitochondrial efficiency of about 70–85%, strongly trending to increase at lower temperatures (**Figure 4B**). This is a striking finding demonstrating an inherent thermal plasticity of tenrec mitochondria that favors a thermoregulatory strategy allowing optimal mitochondrial function in heterothermic states that are naturally experienced by tenrecs. If this may be a trait unique to tenrecs or protoendotherms remains to be elucidated. Clearly, more data are required to phylogenetically generalize this suggestion.

Within vertebrates, the level of the basal mitochondrial proton leak of *E. telfairi* is at an intermediate level between endo- and ectotherms (Polymeropoulos et al., 2017). However, on a phylogenetically informed basis, the tenrec mitochondrial proton leak scales within other eutherian mammals but not reptiles, corroborating that the molecular, mitochondrial setup is "mammalian" while the behavioral pattern could be classified as "reptilian." It would therefore be interesting to study whether mitochondrial efficiency at colder temperatures in ectothermic vertebrate species exhibits a similar pattern, thus being a plesiomorphic trait, or whether these mechanistic

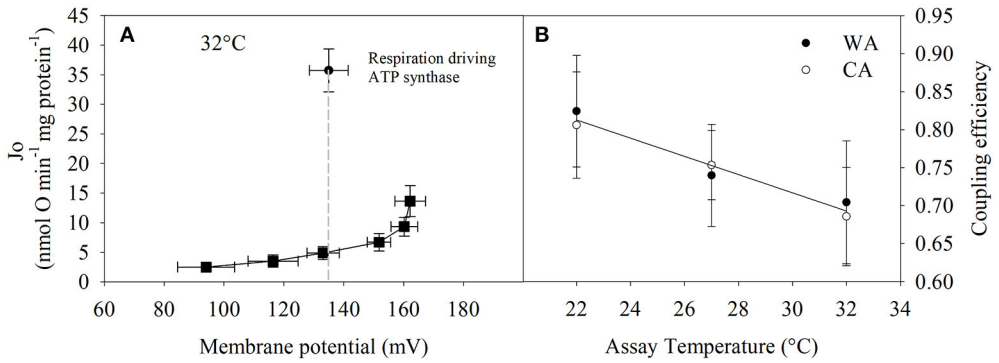

FIGURE 4 | Calculation of coupling efficiency that is defined as the respiratory fraction that drives the ATP synthase. **(A)** Single example how coupling efficiency is assessed per individual. State 3 and proton leak respiration at the state 3 membrane potential (indicated by the dashed line) are required. **(B)** Coupling efficiency = (state 3—proton leak respiration)/ (state 3 respiration at state 3 membrane potential). 20°C acclimated (CA, white circles, $n = 3$) vs. 27°C acclimated (WA, black circles, $n = 4$) groups were not significantly different (two-way repeated measures ANOVA). Therefore, the linear regression analysis was performed on the combined data from both acclimation groups; $y = -0.012x + 1.077$ (ANOVA, $P = 0.064$). Values are means ± SE.

adjustments were derived in the need to adjust to endothermic metabolism.

In conclusion, the bioenergetic setup of tenrec liver mitochondria resembles mammalian and ectothermic features. Mammalian features are reflected in the amplitude of tenrec liver proton leak within the eutherian range, while increased mitochondrial efficiency may have enabled to cope with energy conversion at low T_b. The latter possibly enables the unique thermoregulation of the tenrec with exceptionally long ectothermic episodes—an assumed prerogative of eutherian survival at the Cretaceous-Paleogene boundary.

AUTHOR CONTRIBUTIONS

EP and RO equally contributed to this manuscript. RO and MJ conceived the ideas, RO conducted the experiments, EP, RO, and MJ prepared the manuscript and figures and analyzed the data, and approved the manuscript.

FUNDING

This work was funded by the German Center for Diabetes Research (DZD).

REFERENCES

Affourtit, C., and Brand, M. D. (2009). Measuring mitochondrial bioenergetics in INS-1E insulinoma cells. *Methods Enzymol.* 457, 405–424. doi: 10.1016/S0076-6879(09)05023-X

Brand, M. D., Couture, P., and Hulbert, A. J. (1994). Liposomes from mammalian liver mitochondria are more polyunsaturated and leakier to protons than those from reptiles. *Comp. Biochem. Physiol. Part B Comp. Biochem.* 108, 181–188. doi: 10.1016/0305-0491(94)90064-7

Brown, J. C. L., Gerson, A. R., and Staples, J. F. (2007). Mitochondrial metabolism during daily torpor in the dwarf Siberian hamster: role of active regulated changes and passive thermal effects. *Am. J. Physiol. Regul. Integr. Comp. Physiol.* 293, R1833–R1845. doi: 10.1152/ajpregu.00310.2007

Cadenas, S., and Brand, M. D. (2000). Effects of magnesium and nucleotides on the proton conductance of rat skeletal-muscle mitochondria. *Biochem. J.* 348(Pt 1), 209–213.

Cannon, B., and Nedergaard, J. A. N. (2004). Brown adipose tissue: function and physiological significance. *Physiol. Rev.* 84, 277–359. doi: 10.1152/physrev.00015.2003

Crompton, A. W., Taylor, C. R., and Jagger, J. A. (1978). Evolution of homeothermy in mammals. *Nature* 272, 333–336.

Dufour, S., Rousse, N., Canioni, P., and Diolez, P. (1996). Top-down control analysis of temperature effect on oxidative phosphorylation. *Biochem. J.* 314, 743–751.

Field, J., Belding, H. S., and Martin, A. W. (1939). An analysis of the relation between basal metabolism and summated tissue respiration in the rat. I. The post-pubertal albino rat. *J. Cell. Comp. Physiol.* 14, 143–157. doi: 10.1002/jcp.1030140202

Gnaiger, E., Méndez, G., and Hand, S. C. (2000). High phosphorylation efficiency and depression of uncoupled respiration in mitochondria under hypoxia. *Proc. Natl. Acad. Sci. U.S.A.* 97, 11080–11085.

Gornall, A. G., Bardawill, C. J., and David, M. M. (1949). Determination of serum proteins by means of the biuret reaction. *J. Biol. Chem.* 177, 751–766.

Grimpo, K., Kutschke, M., Kastl, A., Meyer, C. W., Heldmaier, G., Exner, C., et al. (2014). Metabolic depression during warm torpor in the Golden spiny mouse (*Acomys russatus*) does not affect mitochondrial respiration and hydrogen peroxide release. *Comp. Biochem. Physiol. Part A Mol. Integr. Physiol.* 167, 7–14. doi: 10.1016/j.cbpa.2013.09.002

Jastroch, M., Buckingham, J. A., Helwig, M., Klingenspor, M., and Brand, M. D. (2007). Functional characterisation of UCP1 in the common carp: uncoupling activity in liver mitochondria and cold-induced expression in the brain. *J. Comp. Physiol. B* 177, 743–752. doi: 10.1007/s00360-007-0171-6

Jastroch, M., Divakaruni, A. S., Mookerjee, S., Treberg, J. R., and Brand, M. D. (2010). Mitochondrial proton and electron leaks. *Essays Biochem.* 47, 53–67. doi: 10.1042/bse0470053

Keipert, S., and Jastroch, M. (2014). Brite/beige fat and UCP1 — is it thermogenesis? *Biochim. Biophys. Acta Bioenerg.* 1837, 1075–1082. doi: 10.1016/j.bbabio.2014.02.008

Kutschke, M., Grimpo, K., Kastl, A., Schneider, S., Heldmaier, G., Exner, C., et al. (2013). Depression of mitochondrial respiration during daily torpor of the Djungarian hamster, *Phodopus sungorus*, is specific for liver and correlates with body temperature. *Comp. Biochem. Physiol. Part A Mol. Integr. Physiol.* 164, 584–589. doi: 10.1016/j.cbpa.2013.01.008

Lovegrove, B. G., and Génin, F. (2008). Torpor and hibernation in a basal placental mammal, the Lesser Hedgehog Tenrec *Echinops telfairi*. *J. Comp. Physiol. B* 178, 691–698. doi: 10.1007/s00360-008-0257-9

Mckechnie, A. E., and Mzilikazi, N. (2011). Heterothermy in afrotropical mammals and birds : a review. *Integr. Comp. Biol.* 51, 349–363. doi: 10.1093/icb/icr035

McNab, B. K. (2002). *The Physiolgical Ecology of Vertebrates.* Ithaca, NY; London: Cornell University Press.

Nicol, S. C. (2017). Energy homeostasis in monotremes. *Front. Neurosci.* 11:195. doi: 10.3389/fnins.2017.00195

Nicol, S. C., and Andersen, N. A. (2007). Cooling rates and body temperature regulation of hibernating echidnas (*Tachyglossus aculeatus*). *J. Exp. Biol.* 210, 586–592. doi: 10.1242/jeb.02701

Oelkrug, R., Goetze, N., Exner, C., Lee, Y., Ganjam, G. K., Kutschke, M., et al. (2013). Brown fat in a protoendothermic mammal fuels eutherian evolution. *Nat. Commun.* 4:2140. doi: 10.1038/ncomms3140

Oelkrug, R., Heldmaier, G., and Meyer, C. W. (2011). Torpor patterns, arousal rates, and temporal organization of torpor entry in wildtype and UCP1-ablated mice. *J. Comp. Physiol. B* 181, 137–145. doi: 10.1007/s00360-010-0503-9

Oelkrug, R., Polymeropoulos, E. T., and Jastroch, M. (2015). Brown adipose tissue: physiological function and evolutionary significance. *J. Comp. Physiol. B Biochem. Syst. Environ. Physiol.* 185, 587–606. doi: 10.1007/s00360-015-0907-7

Polymeropoulos, E. T., Heldmaier, G., Frappell, P. B., Mcallan, B. M., Withers, K. W., Klingenspor, M., et al. (2012). Phylogenetic differences of mammalian basal metabolic rate are not explained by mitochondrial basal proton leak. *Proc. R. Soc. B Biol. Sci.* 279, 185–193. doi: 10.1098/rspb.2011.0881

Polymeropoulos, E. T., Oelkrug, R., White, C. R., and Jastroch, M. (2017). Phylogenetic analysis of the allometry of metabolic rate and mitochondrial basal proton leak. *J. Therm. Biol.* 68, 83–88. doi: 10.1016/j.jtherbio.2017.01.013

Poppitt, S. D., Speakman, J. R., and Racey, P. A. (1994). Energetics of reproduction in the lesser hedgehog tenrec, *Echinops telfairi* (Martin). *Physiol. Zool.* 67, 976–994.

Porter, R. K., and Brand, M. D. (1995). Causes of differences in respiration rate of hepatocytes from mammals of different body mass. *Am. J. Physiol. Regul. Integr. Comp. Physiol.* 269, R1213–R1224.

Reynafarje, B., Costa, L. E., and Lehninger, A. L. (1985). O2 solubility in aqueous media determined by a kinetic method. *Anal. Biochem.* 145, 406–418.

Rolfe, D. F., and Brown, G. C. C. (1997). Cellular energy utilization and molecular origin of standard metabolic rate in mammals. *Physiol. Rev.* 77:731.

Rowland, L. A., Bal, N. C., and Periasamy, M. (2015). The role of skeletal-muscle-based thermogenic mechanisms in vertebrate endothermy. *Biol. Rev.* 90, 1279–1297. doi: 10.1111/brv.12157

Scholl, P. (1974). Temperaturregulation beim madegassischen Igeltanrek *Echinops telfairi* (Martin, 1838). *J. Comp. Physiol.* 89, 175–195. doi: 10.1007/BF00694790

Staples, J. F., and Brown, J. C. L. (2008). Mitochondrial metabolism in hibernation and daily torpor: a review. *J. Comp. Physiol. B* 178, 811–827. doi: 10.1007/s00360-008-0282-8

St-Pierre, J., Brand, M. D., and Boutilier, R. G. (2000). The effect of metabolic depression on proton leak rate in mitochondria from hibernating frogs. *J. Exp. Biol.* 203, 1469–1476.

Trzcionka, M., Withers, K. W., Klingenspor, M., and Jastroch, M. (2008). The effects of fasting and cold exposure on metabolic rate and mitochondrial proton leak in liver and skeletal muscle of an amphibian, the cane toad *Bufo marinus*. *J. Exp. Biol.* 211, 1911–1918. doi: 10.1242/jeb.016519

Conflict of Interest Statement: The authors declare that the research was conducted in the absence of any commercial or financial relationships that could be construed as a potential conflict of interest.

frontiers in Physiology

ORIGINAL RESEARCH
published: 20 September 2017
doi: 10.3389/fphys.2017.00670

Evolution of *UCP1* Transcriptional Regulatory Elements Across the Mammalian Phylogeny

*Michael J. Gaudry and Kevin L. Campbell**

Department of Biological Sciences, University of Manitoba, Winnipeg, MB, Canada

Uncoupling protein 1 (UCP1) permits non-shivering thermogenesis (NST) when highly expressed in brown adipose tissue (BAT) mitochondria. Exclusive to placental mammals, BAT has commonly been regarded to be advantageous for thermoregulation in hibernators, small-bodied species, and the neonates of larger species. While numerous regulatory control motifs associated with *UCP1* transcription have been proposed for murid rodents, it remains unclear whether these are conserved across the eutherian mammal phylogeny and hence essential for UCP1 expression. To address this shortcoming, we conducted a broad comparative survey of putative *UCP1* transcriptional regulatory elements in 139 mammals (135 eutherians). We find no evidence for presence of a *UCP1* enhancer in monotremes and marsupials, supporting the hypothesis that this control region evolved in a stem eutherian ancestor. We additionally reveal that several putative promoter elements (e.g., CRE-4, CCAAT) identified in murid rodents are not conserved among BAT-expressing eutherians, and together with the putative regulatory region (PRR) and CpG island do not appear to be crucial for UCP1 expression. The specificity and importance of the upTRE, dnTRE, URE1, CRE-2, RARE-2, NBRE, BRE-1, and BRE-2 enhancer elements first described from rats and mice are moreover uncertain as these motifs differ substantially—but generally remain highly conserved—in other BAT-expressing eutherians. Other *UCP1* enhancer motifs (CRE-3, PPRE, and RARE-3) as well as the TATA box are also highly conserved in nearly all eutherian lineages with an intact *UCP1*. While these transcriptional regulatory motifs are generally also maintained in species where this gene is pseudogenized, the loss or degeneration of key basal promoter (e.g., TATA box) and enhancer elements in other *UCP1*-lacking lineages make it unlikely that the enhancer region is pleiotropic (i.e., co-regulates additional genes). Importantly, differential losses of (or mutations within) putative regulatory elements among the eutherian lineages with an intact *UCP1* suggests that the transcriptional control of gene expression is not highly conserved in this mammalian clade.

Keywords: uncoupling protein 1, evolution, transcriptional regulation, enhancer, comparative analysis

OPEN ACCESS

Edited by:
Elias T. Polymeropoulos, Institute for Marine and Antarctic Studies (IMAS), Australia

Reviewed by:
François Criscuolo, Centre National de la Recherche Scientifique (CNRS), France
Tobias Fromme, Technische Universität München, Germany

****Correspondence:***
Kevin L. Campbell
kevin.campbell@umanitoba.ca

Specialty section:
This article was submitted to Integrative Physiology, a section of the journal Frontiers in Physiology

Received: *21 June 2017*
Accepted: *23 August 2017*
Published: *20 September 2017*

Citation:
Gaudry MJ and Campbell KL (2017) Evolution of UCP1 Transcriptional Regulatory Elements Across the Mammalian Phylogeny. Front. Physiol. 8:670. doi: 10.3389/fphys.2017.00670

INTRODUCTION

Uncoupling protein 1 (UCP1) expression is a defining characteristic of brown adipose tissue (BAT), allowing this specialized eutherian heater organ to function in non-shivering thermogenesis (NST). UCP1 spans the mitochondrial inner-membrane of brown adipocytes, acting to promote mitochondrial proton leak, which dissipates the electrochemical gradient that typically drives ATP

synthase. In an effort to defend the mitochondrial proton motive force, the electron transport chain thus pumps protons into the inter-membrane space at an elevated rate via an increased level of substrate combustion, thereby resulting in substantial heat production in the form of NST (Cannon and Nedergaard, 2004; Klingenspor and Fromme, 2012).

Vital to its function, BAT is highly vascularized and localized primarily to the thoracic region, lying adjacent to major blood vessels of the heart (e.g., the Sulzer's vein) permitting effective transfer of NST heat to the rest of the body via the circulatory system (Klingenspor and Fromme, 2012; Oelkrug et al., 2015). This provides a more efficient means of heat production than shivering thermogenesis, which has major drawbacks as it impedes locomotion and produces heat in large muscle groups of the limbs that are prone to heat loss due to their high surface area to volume ratios (Oelkrug et al., 2015). For these reasons, UCP1 is widely considered to have provided a key thermoregulatory and evolutionary advantage to the eutherian lineage, particularly for small-bodied and hibernating species, and, while BAT in larger-bodied species (e.g., humans) is typically lost with the onset of adulthood, it has been generally understood to play vital role in their neonates (Cannon and Nedergaard, 2004).

The *UCP1* gene predates the divergence of ray- and lobe-finned fishes (420 million years ago [MYA]) and can be distinguished from *UCP2* and *UCP3* paralogs by its conserved synteny among vertebrates, as *UCP1* is flanked by the upstream *TBC1D9* and downstream *ELMOD2* loci (Jastroch et al., 2008; Klingenspor et al., 2008). UCP2 and UCP3 have been long-believed to play non-thermogenic roles, and are instead hypothesized to perform a multitude of functions including the reduction of reactive oxygen species by promoting a low level of mitochondrial proton leak when activated by fatty acids (Brand and Esteves, 2005; Echtay, 2007; Mailloux and Harper, 2011). However, a recent study by Lin et al. (2017) suggests that proton uncoupling by UCP3 permits heat production in beige adipose tissue of pigs, compensating for the loss of UCP1 in this lineage (Berg et al., 2006). Nevertheless, the functional roles of both UCP2 and UCP3 remain hotly debated. Similarly, the ancestral function of UCP1 in non-eutherians is currently unclear (Klingenspor et al., 2008). UCP1 expression has been shown to increase with cold exposure in common carp (*Cyprinus carpio*) brain tissue, suggesting a possible role in local thermogenesis (Jastroch et al., 2007). However, to date, this protein has not been definitively linked to heat production in ectothermic vertebrates (Jastroch et al., 2007). While the fat-tailed dunnart (*Sminthopsis crassicaudata*), a marsupial, displays a primitive "brownish" interscapular adipose depot that up-regulates UCP1 expression in response to cold exposure (Jastroch et al., 2008), this tissue is incapable of adaptive NST (Polymeropoulos et al., 2012) with no study demonstrating that UCP1 contributes to NST in marsupials. Although *UCP1* appears to have been inactivated early in the evolution of the eutherian superorder Xenarthra (Gaudry et al., 2017), BAT-mediated adaptive thermogenesis is widely known to occur in small-bodied members of the superorders Laurasiatheria and Euarchontoglires (Oelkrug et al., 2015), and has been documented in the rock elephant shrew (*Elephantulus myurus*; Mzilikazi et al., 2007) and the lesser hedgehog tenrec (*Echinops telfairi*; Oelkrug et al., 2013), both members of the eutherian superorder Afrotheria. These observations strongly suggest that UCP1 was recruited for BAT-mediated NST in a common eutherian ancestor by gain of function mutations in the amino acid sequence of the protein and/or greater control over gene transcription that allowed highly concentrated UCP1 expression within BAT mitochondria (Klingenspor et al., 2008).

Consistent with the gain of function hypothesis, comparative phylogenetic analyses reveal that the stem eutherian branch is highly elongated in *UCP1* gene trees relative to that of *UCP2* and *UCP3* paralogs (Saito et al., 2008; Hughes et al., 2009; Gaudry et al., 2017; **Figure 1**). It is thus likely that an elevated rate of non-synonymous *UCP1* nucleotide substitutions in the stem eutherian branch conferred this protein with the ability to facilitate proton leak at physiologically significant levels (Jastroch et al., 2008; Klingenspor et al., 2008). While Saito et al. (2008) first proposed *UCP1* evolved under positive selection in basal eutherians, more recent selection pressure analyses reveal non-synonymous to synonymous substitution ratios (dN/dS or ω) of ∼0.5–0.6 that are more consistent with relaxed purifying selection (Hughes et al., 2009; Gaudry et al., 2017). However, given that UCP1 of placental mammals possess several unique amino acids relative to non-eutherians, it is possible that directional selection was limited to certain codons along the stem eutherian branch, though, so far this hypothesis remains statistically unsupported (Hughes et al., 2009; Gaudry et al., 2017).

Along with the increased rate of UCP1 evolution in stem eutherians, expression of this protein also became highly tissue-specific during the rise of BAT (Cannon and Nedergaard, 2004). In contrast to the seemingly constitutive presence of UCP1 in common carp brain, liver, and kidney tissues (Jastroch et al., 2007), eutherian UCP1 expression is tightly regulated, occurring predominantly in BAT (Cannon and Nedergaard, 2004). One notable exception, however, is the recently discovered "beige or brite (brown in white)" adipocytes in rodents (mice and rats) and humans. These are derived from white adipose cells that, upon cold exposure, become BAT-like by expressing UCP1 and by having multilocular lipid droplets and an elevated mitochondrial concentration (Harms and Seale, 2013). An important distinction in BAT (and *UCP1*) evolution is that BAT-dependent NST relies upon exceptionally high levels of UCP1 expression, constituting up to 10% of the mitochondrial membrane proteins, whereas UCP2 and UCP3 expression is several orders of magnitude lower (0.01–0.1%) in other tissues (Brand and Esteves, 2005). Interestingly, an enhancer box has been well documented to play a major role in eutherian *UCP1* gene transcription, but is absent in the gray short-tailed opossum (*Monodelphis domestica*; Jastroch et al., 2008), suggesting that it originated with the advent of eutherian UCP1-mediated NST, thus highlighting the importance that gene regulation likely played in the rise of eutherian BAT-mediated thermogenesis.

Given the thermoregulatory advantages conferred by BAT, it is believed that this tissue was fundamental to the evolutionary success of eutherian mammals, and it has even been hypothesized to underlie their colonization of cold ecological

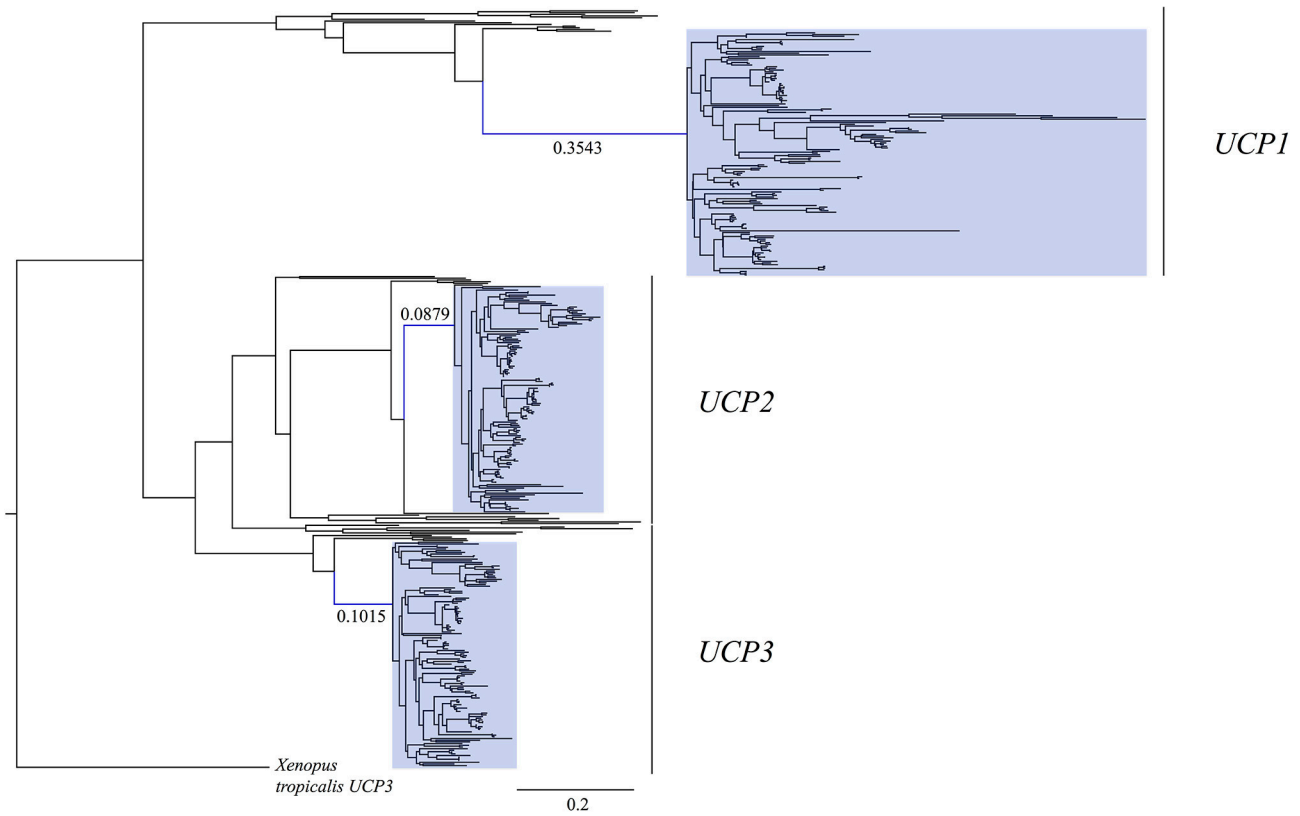

FIGURE 1 | Maximum likelihood gene tree of *UCP1*, *UCP2*, and *UCP3* coding sequences ($N = 448$) modified from Gaudry et al. (2017) to include the 16 additional species with recently available genome projects (see **Table 1**). The stem placental mammal branches are indicated in blue. Note that the *UCP1* stem placental branch is much longer than those of *UCP2* and *UCP3*, demonstrating a greater number of nucleotide substitutions per site. Placental mammal genes are highlighted with blue boxes. The tree was rooted with the western clawed frog (*Xenopus tropicalis*) *UCP3*.

niches (Cannon and Nedergaard, 2004). The documented inactivation of the *UCP1* gene in suids (pigs) (Berg et al., 2006) initially emphasized the importance of BAT-mediated thermogenesis, as this inactivation appears to have had detrimental consequences as newborn piglets are widely known to have meager thermoregulatory abilities, suffering from high infant mortality when cold-stressed and relying upon shivering thermogenesis and maternal nest-building in order to maintain homeothermy (Herpin et al., 2002; Berg et al., 2006). By contrast, two recent studies (Gaudry et al., 2017; McGaugh and Schwartz, 2017) contested the conventional belief regarding the importance of BAT-mediated NST throughout the course of placental evolution. Indeed, Gaudry et al. (2017) not only detailed ancient pseudogenization events of *UCP1* in eight additional eutherian lineages: Equidae (horses), Cetacea (whales and dolphins), Proboscidea (elephants and mammoths), Sirenia (sea cows), Hyracoidea (hyraxes), Pholidota (pangolins), Pilosa (sloths and anteaters), and Cingulata (armadillos), but concluded that extreme cold tolerance evolved in many of these groups in the absence of UCP1-mediated thermogenesis.

With the exception of xenarthrans and pangolins, who have adopted a strategy of reduced energy expenditure (i.e., low metabolic rates and body temperatures) associated with their low energy diets, and pigs, for which no credible explanation for *UCP1* inactivation has yet been put forward, Gaudry et al. (2017) proposed that *UCP1* inactivations date back to a period of substantial planetary cooling ∼55 to 22 MYA that triggered pronounced increases in body size in other UCP1-lacking lineages (Gaudry et al., 2017). The inverse relationship between the surface-area-to-volume ratio and size imparts greater retention of heat in larger bodied mammals, thus larger mammals have proportionally lower rates of heat production per gram of body mass (McNab, 1983). This linkage is reflected in the diminishing fraction of eutherian body mass constituted by BAT, as well as a reduced NST capacity, with increasing body size (Heldmaier, 1971; Oelkrug et al., 2015). Heldmaier (1971) further suggested that BAT-mediated NST is negligible for mammals >10 kg. Nonetheless, several large-bodied taxa retain an intact *UCP1* gene (e.g., rhinoceroses, pinnipeds, hippopotamus, and camel; Gaudry et al., 2017). Despite this finding, it remains conceivable that members of these groups do not express *UCP1* in BAT, even as neonates. For example, Rowlatt et al. (1971) noted the absence of BAT upon examination of a single newborn hippopotamus (*Hippopotamus amphibious*), while both UCP1 expression and discernable BAT was not detected in either Weddell seal (*Leptonychotes weddellii*) or hooded seal neonates

TABLE 1 | Presence and absence of the *UCP1* enhancer, putative regulatory region (PPR), and CpG island in 139 mammalian species.

Species name	Enhancer	PPR	CPG island	Accession number
MONTREMATA				
Ornithorhynchus anatinus	X	X	X	NW_001794248.1
MARSUPIALIA				
Monodelphis domestica	X	X	X	AAFR03015618.1
Macropus eugenii	/	/	X	ABQO020217652.1
Sarcophilus harrisii	/	/	X	AEFK01228715.1
XENARTHRA				
Choloepus hoffmanni	X	/	/	
Dasypus novemcinctus	X	X	Yes	AAGV03181320.1
Mylodon darwinii	Yes	/	/	SRX327588
AFROTHERIA				
Chrysochloris asiatica	Yes	Yes	X	AMDV01244955.1
Dugong dugon	Yes	Yes	/	MF871621
Echinops telfairi	Yes	Yes	Yes	AAIY02209271.1
Elephantulus edwardii	Yes	Yes	X	AMGZ01097263.1
Elephas maximus	Yes	Yes	Yes	SRX1015608; SRX1015606; SRX1015604; SRX1015603
Hydrodamalis gigas	Yes	/	/	MF871622
Loxodonta africana	Yes	Yes	Yes	AAGU03034821.1
Mammuthus primigenius	Yes	Yes	/	SRX1015727; SRX1015732; SRX1015743; SRX1015748; SRX001906; ERP008929
Orycteropus afer	Yes	Yes	X	ALYB01104541.1
Procavia capensis	X	Yes	Yes	ABRQ02143236.1
Trichechus manatus latirostris	Yes	Yes	Yes	AHIN01109623.1
LAURASIATHERIA				
Acinonyx jubatus	Yes	Yes	Yes	LLWD01000416.1
Ailuropoda melanoleuca	Yes	Yes	Yes	LNAT01000144.1
Balaena mysticetus	Yes	Yes	Yes	SRX790318, SRX790317, SRX790316, SRX790303, SRX790319
Balaenoptera acutorostrata	Yes	Yes	Yes	ATDI01065547.1
Balaenoptera bonaerensis	Yes	Yes	Yes	BAUQ01197845.1
Balaenoptera physalus	Yes	Yes	Yes	SRX1571086, SRX323050
Bison bison	Yes	Yes	Yes	JPYT01100523.1
Bos grunniens	Yes	Yes	Yes	AGSK01075302.1
Bos indicus	/	Yes	/	AGFL01142554.1
Bos taurus	Yes	Yes	Yes	DAAA02044420.1
Bubalus bubalis	Yes	Yes	Yes	AWWX01630119.1
Camelus dromedarius *	Yes	Yes	Yes	LSZX01012659.1
Camelus ferus	Yes	Yes	Yes	AGVR01051296.1; AGVR01051297.1
Canis lupus familiaris	Yes	X	/	AAEX03011713.1
Capra aegagrus	Yes	Yes	Yes	CBYH010071014.1
Capra hircus	Yes	Yes	/	AJPT01162992.1; AJPT01162993.1
Capreolus capreolus	Yes	Yes	Yes	CCMK010092645.1; CCMK010104759.1
Ceratotherium simum	Yes	Yes	Yes	AKZM01017598.1
Coelodonta antiquitatis	Yes	Yes	Yes	MF871623
Condylura cristata	Yes	X	X	AJFV01047153.1
Dicerorhinus sumatrensis	Yes	Yes	Yes	MF871625
Diceros bicornis	Yes	Yes	Yes	MF871624
Eidolon helvum	Yes	Yes	/	AWHC01286101.1; AWHC01029981.1
Eptesicus fuscus	Yes	X	Yes	ALEH01005956.1
Equus asinus	Yes	Yes	Yes	JREZ01000001.1
Equus caballus	Yes	Yes	/	AAWR02018850.1; AAWR02018851.1
Equus przewalskii	Yes	Yes	Yes	ATBW01036321.1; ATBW01036322.1
Erinaceus europaeus	/	/	X	AMDU01193160.1; AMDU01193161.1; AMDU01193162.1
Felis catus	Yes	Yes	Yes	AANG02062919.1
Giraffa camelopardalis *	Yes	Yes	X	LVKQ01071482.1
Hipposideros armiger *	Yes	Yes	Yes	NW_017731683.1
Leptonychotes weddellii	Yes	Yes	Yes	APMU01115165.1; APMU01141180.1
Lipotes vexillifer	Yes	Yes	Yes	AUPI01000024.1
Lycaon pictus *	Yes	X	/	LPRB01000019.1
Manis javanica *	X	X	X	NW_016530114.1
Manis pentadactyla	X	X	X	JPTV01131901.1
Megaderma lyra	Yes	/	/	AWHB01167753.1; AWHB01348443.1; AWHB01348444.1
Miniopterus natalensis *	Yes	X	Yes	NW_015504404.1
Mustela putorius furo	Yes	Yes	Yes	AGTQ01041845.1
Myotis brandtii	Yes	X	Yes	ANKR01273867.1; ANKR01273868.1
Myotis davidii	Yes	X	Yes	ALWT01125743.1
Myotis lucifugus	Yes	X	Yes	AAPE02001462.1
Odobenus rosmarus	Yes	Yes	Yes	ANOP01028105.1
Okapia johnstoni *	Yes	Yes	Yes	LVCL010093660.1; LVCL010093662.1
Orcinus orca	X	X	X	ANOL02004931.1
Ovis aries	Yes	Yes	Yes	AMGL01037664.1; JN604985.1
Panthera pardus *	Yes	Yes	Yes	NW_017619848.1
Panthera tigris altaica	Yes	Yes	Yes	ATCQ01112915.1
Panthera uncia	Yes	Yes	/	SRX273036
Pantholops hodgsonii	Yes	Yes	Yes	AGTT01188813.1

(Continued)

TABLE 1 | Continued

Species name	Enhancer	PPR	CPG island	Accession number
Physeter macrocephalus	X	Yes	Yes	AWZP01062081.1
Pteropus alecto	Yes	Yes	Yes	ALWS01011689.1
Pteropus vampyrus	Yes	Yes	Yes	ABRP02126915.1
Rhinoceros unicornis	Yes	Yes	Yes	MF871626
Rhinolophus ferrumequinum	Yes	Yes	Yes	AWHA01040305.1
Rhinolophus sinicus *	Yes	Yes	Yes	NW_017738992.1
Rousettus aegyptiacus *	Yes	Yes	Yes	NW_015494583.1
Sorex araneus	Yes	X	Yes	AALT02056093.1
Sus cebrifrons	Yes	/	/	ERX953604-ERX953626; ERX149172
Sus scrofa	Yes	X	X	LUXQ01106311.1
Sus verrucosus	Yes	/	/	ERX1054048-ERX1054067; ERX149174
Tapirus indicus	Yes	/	Yes	MF871627
Tursiops truncatus	X	X	X	ABRN02199412.1
Ursus maritimus	Yes	Yes	/	AVOR01014285.1; AVOR01014286.1
Vicugna pacos	Yes	Yes	Yes	ABRR02134987.1; ABRR02134989.1
EUARCHONTOGLIRES				
Aotus nancymaae	Yes	Yes	Yes	JYKP01215429.1
Apodemus sylvaticus	Yes	/	X	LIPJ01452544.1; LIPJ01184746.1; LIPJ01447868.1; LIPJ01014497.1
Callithrix jacchus	Yes	Yes	Yes	ACFV01002817.1
Cavia aperea	/	/	/	AVPZ01000778.1
Cavia porcellus	Yes	Yes	Yes	AAKN02011801.1
Cebus capuchinis *	Yes	Yes	Yes	NW_016107319.1
Cercocebus atys	Yes	Yes	Yes	JZLG01060688.1
Chinchilla lanigera	Yes	Yes	Yes	AGCD01027651.1
Chlorocebus sabaeus	Yes	Yes	Yes	AQIB01017419.1
Colobus angolensis	Yes	Yes	Yes	JYKR01122839.1
Cricetulus griseus	Yes	Yes	X	AFTD01128393.1; AFTD01128394.1
Daubentonia madagascariensis	Yes	Yes	/	AGTM011584638.1; AGTM011584996.1; AGTM011708528.1; AGTM012010142.1; AGTM011594144.1
Dipodomys ordii	Yes	X	Yes	ABRO02057411.1
Ellobius lutescens *	Yes	X	Yes	LOEQ01000193.1
Ellobius talpinus *	Yes	X	Yes	LOJH01032235.1
Eulemur flavifrons	Yes	Yes	Yes	LGHW01000184.1
Eulemur macaco	Yes	Yes	Yes	LGHX01000184.1
Fukomys damarensis	Yes	Yes	Yes	AYUG01151056.1
Galeopterus variegatus	Yes	Yes	/	JMZW01045215.1; JMZW01045216.1
Gorilla gorilla gorilla	Yes	Yes	Yes	NW_004002547.1
Heterocephalus glaber	Yes	Yes	Yes	AFSB01162372.1; AFSB01162373.1
Homo sapiens	Yes	Yes	Yes	NG_012139.1
Jaculus jaculus	Yes	Yes	Yes	AKZC01091543.1
Macaca fascicularis	Yes	Yes	Yes	CAEC01514737.1
Macaca mulatta	Yes	Yes	Yes	AANU01271750.1
Macaca nemestrina	Yes	Yes	Yes	JZLF01028562.1
Mandrillus leucophaeus	Yes	Yes	Yes	JYKQ01107154.1; JYKQ01107155.1
Marmota marmota	Yes	Yes	Yes	CZRN01000015.1
Mesocricetus auratus	Yes	X	Yes	APMT01116524.1; NM_001281332.1
Microcebus murinus	Yes	Yes	Yes	ABDC01082367.1
Microtus agrestis	Yes	X	Yes	LIQJ01004042.1
Microtus ochrogaster	Yes	X	X	AHZW01157105.1; AHZW01157106.1
Mus musculus	Yes	X	X	CAAA01024310.1
Mus spretus *	Yes	X	X	LVXV01001867.1
Myodes glareolus	Yes	/	/	LIPI01003929.1
Nannospalax galili	Yes	Yes	X	AXCS01128925.1
Nasalis larvatus	Yes	Yes	Yes	JMHX01319533.1
Neotoma lepida *	/	/	X	LZPO01075894.1
Nomascus leucogenys	Yes	Yes	Yes	ADFV01177960.1
Ochotona princeps	Yes	X	X	ALIT01060999.1
Octodon degus	Yes	Yes	Yes	AJSA01193669.1; AJSA01193670.1; AJSA01193671.1
Oryctolagus cuniculus	Yes	Yes	Yes	AAGW02045633.1
Otolemur garnettii	Yes	Yes	X	AAQR03074138.1
Pan paniscus	Yes	Yes	Yes	AJFE01070904.1
Pan troglodytes	Yes	Yes	/	AACZ03032212.1; AACZ03032213.1
Papio anubis	Yes	Yes	Yes	AHZZ01043343.1
Peromyscus maniculatus	Yes	X	X	AYHN01134223.1
Pongo abelii	Yes	Yes	Yes	ABGA01062109.1
Propithecus coquereli	Yes	Yes	Yes	JZKE01017273.1
Rattus norvegicus	Yes	X	X	AAHX01097782.1
Rhinopithecus bieti *	Yes	Yes	Yes	NW_016805762.1
Rhinopithecus roxellana	Yes	Yes	Yes	JABR01098768.1
Saimiri boliviensis	Yes	Yes	Yes	AGCE01051213.1
Spermophilus tridecemlineatus	Yes	Yes	Yes	AGTP01049378.1
Tarsius syrichta	Yes	Yes	/	ABRT02355486.1
Tupaia belangeri chinensis	Yes	Yes	Yes	ALAR01031045.1

*Xs = absent, / = inconclusive due to insufficient data, * = 16 species with recently published genome projects since the Gaudry et al. (2017) publication. Accession numbers are also provided for contigs and SRA projects.*

(*Cystophora cristata*) (Pearson et al., 2014). Additionally, the Bactrian camel (*Camelus ferus*) *UCP1* gene displays a 12 base pair nucleotide deletion in exon 5 that would impart the loss of

4 amino acids in close proximity to a site that putatively binds GDP to act as a regulator (inhibitor) of protein activity (Gaudry et al., 2017). Consequently, disruptions to *UCP1* regulatory regions may preclude expression of this protein in BAT of these lineages.

Evolution of Eutherian *UCP1* Regulatory Elements

In eutherian mammals, the neuro-hormonal modulation and tissue-specific expression of *UCP1* is under the control of two regulatory regions in the 5′ non-coding region of the gene—a complex distal enhancer region and a proximal promoter—through their interactions with a broad assemblage of transcription factors (Villarroya et al., 2017). Based primarily on murid rodent studies, several putative transcription factor binding motifs (see **Figure 2**) have been proposed within a conserved ∼200 bp *UCP1* enhancer box located ∼2–5 kb upstream of the transcriptional start site in eutherians (Cannon and Nedergaard, 2004; Jastroch et al., 2008; Shore et al., 2012). For instance, two cAMP response elements (CREs) were discovered in mice and termed "CRE-3" and "CRE-2" (Kozak et al., 1994). CRE sites typically have a palindromic consensus sequence of 5′-T(G/T)ACGTCA-3′ (Bokar et al., 1988; Kozak et al., 1994). While the first three nucleotides of the two mouse CREs deviate from the typical consensus sequence (**Figure 2**), the 5′-CGTCA-3′ nucleotides remain conserved and are believed to be key for *UCP1* expression. Indeed, site-directed mutagenesis of these nucleotides within the enhancer CRE of glycoprotein hormone and phosphoenolpyruvate carboxykinase genes has been shown to drastically reduce transcription factor (i.e., cAMP response element binding protein [CREB]) binding and expression in human and rat cells (Bokar et al., 1988). Two "brown adipocyte regulatory element" (BRE) protein-binding motifs (Kozak et al., 1994) also occur in the mouse *UCP1* enhancer box (**Figure 2**). Again, site directed mutagenesis of the "TTCC" nucleotides within the BREs to a "GTAC" sequence drastically reduces *UCP1* enhancer activity measured using transient expression assays (Kozak et al., 1994). In addition, Sears et al. (1996) found a stretch of nucleotides they termed "UCP regulatory element 1" (URE1), though this is referred to as the peroxisome proliferator response element (PPRE) by Jastroch et al. (2008); Jastroch also predicted a second possible PPRE motif downstream of the URE1 (PPRE) site. The URE1 motif displays high similarity to DR-1 elements (Sears et al., 1996), which are known to comprise of two direct repeats of the "AGGTCA" half-site consensus sequence separated by a single nucleotide (hence the term DR-1; i.e., direct repeats separated by 1 spacer nucleotide). In mice this sequence occurs in the reverse and complement orientation of the first DNA strand (5′- TCACCCTTGACCA-3′), and although it is not an exact match to the consensus sequence, it has been shown to bind the peroxisome proliferator-activated receptor γ and retinoid X receptor α (PPARγ-RXRα) heterodimer transcription factor (Sears et al., 1996). Conversely, mutant variants of the URE1 sequence (i.e., 5′-TCACAATTGACCA-3′ or 5′-TCACCCTAGACCA-3′) failed to bind the PPARγ-RXRα transcription factor, suggesting a key role in the functionality of the *UCP1* enhancer (Sears et al., 1996). Additionally, in light of the requirement of triiodothyronine (T3) for proper BAT expression (Bianco and Silva, 1987), Rabelo et al. (1995) described two putative thyroid hormone response elements (TREs) in the rat *UCP1* enhancer termed "upTRE" and "dnTRE" (**Figure 2**). TREs typically include two or more variations of the "AGGT(C/A)A" half-site consensus sequence separated by four nucleotides (Brent et al., 1991; Umesono et al., 1991). This same half-site sequence was mentioned above for URE1 and is indeed recognized by multiple transcription factors (Brent et al., 1991). Mutations of the 3′ portion of the upTRE (5′-AGGCAA-3′) and the dnTRE (5′-AGGTCA-3′) to "5′-ATTTAA-3′" and "5′-ATATTA-3′", respectively, eliminate T3 receptor interactions with the rat *UCP1* enhancer (Rabelo et al., 1995). Three putative retinoic acid response elements (RAREs) within the rat *UCP1* enhancer have also been described by Rabelo et al. (1996), though both RARE-1 and RARE-2 overlap with other binding motifs (see **Figure 2**). Nonetheless, mutations increasing the AT-richness of these former regulatory elements were shown to significantly disrupt retinoic acid receptor (RAR) and retinoid X receptor (RXR) transcription factor binding (Rabelo et al., 1996). Finally, Kumar et al. (2008) noted a putative nerve growth factor response element (NBRE) within the *UCP1* enhancer of mice (**Figure 2**) that binds nuclear receptors 4A (NR4A), which acts to promote gene transcription. In addition to the enhancer box, Shore et al. (2012) described a 678 bp putative regulatory region (PRR) located 2,095 bp upstream of the transcriptional start site in humans that was conserved in 14 of 25 of the eutherian species they examined. While Shore et al. (2012) found no evidence that this conserved region plays a role in *UCP1* expression, they did note that it encompassed several possible transcription factor binding motifs, including DR1, DR3, DR4, CEBP (CCAAT-enhancer-binding proteins), CREB, and PPAR.

Transcriptional control of the *UCP1* gene has also been hypothesized to be regulated by a basal promoter occurring within ∼250 bp upstream of the transcription start site (Shore et al., 2010). Within this region, Bouillaud et al. (1988) identified a putative TATA box and a CCAAT binding site located ∼20 and ∼30 bp upstream of the transcriptional start site of the rat *UCP1* gene, respectively. Generally, the TATA box consists of an A/T-rich consensus sequence (5′-TATAAAA-3′; Xu et al., 1991) that interacts with the TATA binding protein (TBP), one of the components of the transcription factor IID (TFIID) that initiates transcription via RNA polymerase II (Nakajima et al., 1988; Patikoglou et al., 1999). The promoters of some mammalian genes (e.g., globins) also contain a CCAAT box typically situated –60 to –100 bp upstream of the transcription start site that binds nuclear transcription factor Y (NF-Y) subunit or CCAAT/enhancer binding protein (C/EBP), which then aids in the initiation of transcription via RNA polymerase II (Mantovani, 1999). Additionally, a putative CRE site (termed CRE-4) occurs ∼130 bp upstream of the mouse *UCP1* transcriptional start site in a reverse and compliment orientation (5′-TGACGCGC-3′), with mutations to this sequence eliminating 90–95% of reporter gene expression (Kozak et al., 1994). Yubero et al. (1994) further noted three GCCCCT sequences occurring within ∼210 bp of the transcriptional start site of the rat, which DNAse 1 footprinting

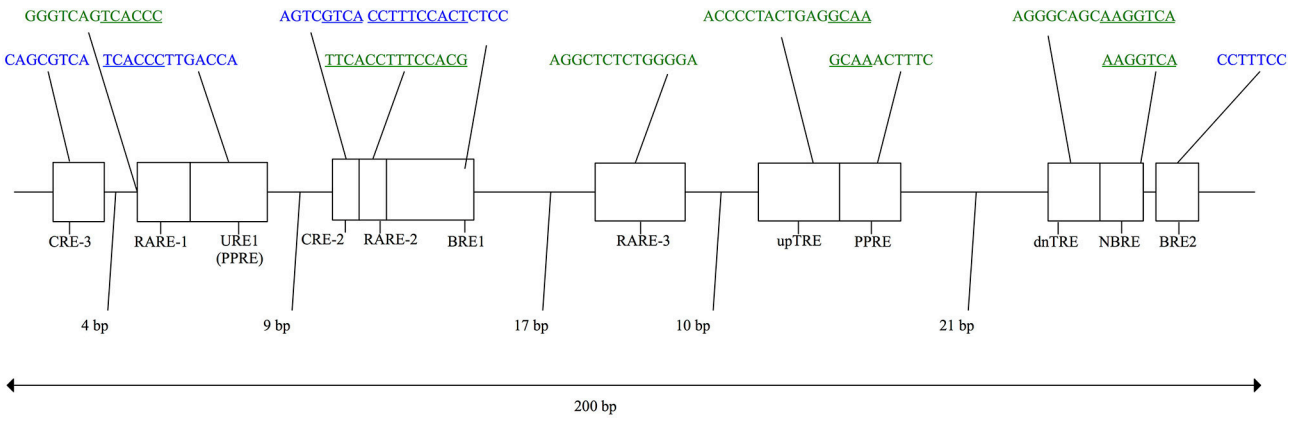

FIGURE 2 | Schematic of the murid *UCP1* enhancer with putative transcription factor binding motifs shown for the rat (green) and mouse (blue) based on a combination of previous studies (see text for details). Regions of overlap between adjacent transcription factor motifs are underlined.

analyses suggest interact with nuclear proteins found within BAT cells, but these have not been defined as protein binding motifs.

Finally, a CpG island surrounding the *UCP1* proximal promoter and extending into exon 1 has been described in several eutherian species (Kiskinis et al., 2007; Shore et al., 2010, 2012). CpG islands contain high densities of cytosine (C) and guanine (G) nucleotide pairs occurring in the 5′ to 3′ direction and linked by a phosphate (i.e., 5′–C–phosphate–G–3′). These CpG dinucleotides are uncommon in vertebrate genomes, typically occurring at only 20–25% of the frequency anticipated by random chance and act as DNA methylation sites that can modulate gene transcription (Gardiner-Garden and Frommer, 1987). Located immediately upstream of many housekeeping genes, CpG islands are believed to play a major role in their transcriptional control (Gardiner-Garden and Frommer, 1987). Indeed, methylation of CpG dinucleotides immediately upstream of the *UCP1* gene have been shown to modulate gene activity by blocking transcription, whereas demethylation promotes transcription (Shore et al., 2010). Thus, this CpG island has been postulated to be important for *UCP1* gene regulation and, potentially, tissue specific expression within BAT (Kiskinis et al., 2007; Shore et al., 2010).

Because the majority of studies investigating the transcriptional control of *UCP1* have focused on rodents, the status of these transcription factor binding motifs in other eutherian species remain largely unexplored. Here we use genome mining and hybridization-capture techniques coupled with next-generation sequencing to identify and examine *UCP1* transcriptional regulatory elements in 139 mammals (135 eutherians). Briefly, putative transcription factor binding motifs and CpG islands were evaluated using a comparative approach to first determine if they are universally conserved among eutherian superorders with functional BAT, and second to test if they are mutated or lost in large-bodied species that presumably have little or no need for NST. We further anticipated that crucial DNA motifs involved in *UCP1* transcription would have deteriorated via millions of years of neutral evolution in the nine lineages for which *UCP1* has been inactivated.

MATERIALS AND METHODS

UCP1 Regulatory Sequences

In total, *UCP1* upstream regions of 139 mammals (1 monotreme, 3 marsupials, 3 xenarthrans, 11 afrotherians, 65 laursiatherians, and 56 euarchontoglires) were examined for transcriptional regulatory elements (see **Table 1** for species list). This data set employed 116 species whose *UCP1* loci were previously annotated by Gaudry et al. (2017) together with 16 additional species whose genomes have recently been sequenced (denoted by asterisks in **Table 1**). Regulatory elements of seven additional eutherians were also retrieved by hybridization capture and next-generation sequencing techniques. Briefly, *UCP1* enhancers, PRRs, and basal promoters of four rhinoceroses (black rhinoceros: *Diceros bicornis*, Indian rhinoceros: *Rhinoceros unicornis,* Sumatran rhinoceros; *Dicerorhinus sumatrensis,* and woolly rhinoceros; *Coelodonta antiquitatis*), one tapir (Malayan tapir; *Tapirus indicus*), and two sirenians (dugong; *Dugong dugon*, and Steller's sea cow; *Hydrodamalis gigas*), were targeted using hybridization capture and next-generation sequencing techniques (Springer et al., 2015; Gaudry et al., 2017). Barcoded rhinoceros DNA libraries were constructed using NEBNext Fast DNA Library Prep Set for Ion Torrent and NEBNext DNA Library Prep Master Mix Set for 454 kits (New England Biolabs; Ipswich, Massachusetts, USA) and target-enriched using MyBaits (Mycroarray; Ann Arbor, Michigan, USA) 120mer RNA probes designed to capture *UCP1* exons and regulatory elements based on the orthologous sequences of the white rhinoceros (*Ceratotherium simum*) genome. The captured rhinoceros reads were sequenced on an Ion Torrent PGM platform using Ion 314 v2 and Ion 318 v2 barcoded chips and an Ion PGM Hi-Q sequencing kit (Applied Biosystems; Foster City, California, USA). Sirenian DNA libraries prepared following the methods of Meyer and Kircher (2010) were enriched using an Agilent SureSelect Capture array with probes designed from African elephant (*Loxodonta africana*) *UCP1* upstream sequences. Sirenian DNA reads were sequenced on Illumina GAIIx and HiSeq2500 (Illumina Inc.; San Diego, California,

USA) platforms. Sequenced reads were assembled to reference sequences of the white rhinoceros or manatee (*Trichechus manatus*) using the "map to reference" feature in Geneious R9.1 (Biomatters Ltd.; Auckland, New Zealand) at 20% maximum mismatch per read and consensus sequences were generated.

For publically available genomes, *UCP1* regulatory sequences were acquired using genome-mining techniques of sequences available on the National Center for Biotechnology Information web server. *UCP1*-containing contigs were first acquired by performing nucleotide BLAST searches employing the "discontinuous megablast" option against whole genome shotgun (WGS) contigs of mammalian genome projects using human *UCP1* CDS (NM_021833.4) as a query. If the contigs did not extend ∼5 kb upstream of the *UCP1* transcriptional start site to include the enhancer box, an additional nucleotide BLAST was performed using the human *UCP1* enhancer sequence as a query. For several species with genome projects that have not yet been fully assembled (e.g., *Sus cebifrons*, *Sus verrucosus*, *Elephas maximus*, *Mammuthus primigenius, Balaena mysticetus, Balaenoptera physalus, Mylodon darwinii, Panthera unica*), short read archive (SRA) BLASTs were performed in order to obtain the *UCP1* regulatory elements. Contigs from top BLAST hits were then imported into Sequencher v5.1 (Gene Codes Corporation; Ann Arbor, Michigan, USA) and the exons and regulatory regions annotated by aligning orthologous human *UCP1* sequences (exons 1–6 and enhancer), initially at a 85% minimum match percentage. If the sequences were too divergent to assemble at that stringency, the minimum match percentage was progressively decreased to 60% or until the sequences successfully assembled. *UCP1* coding regions for the 16 species not included in the Gaudry et al. (2017) study were also examined for the presence of inactivating (e.g., splice site, frameshift, and non-sense) mutations.

The PRR proposed by Shore et al. (2012) was generally less conserved than the enhancer, often with large insertions or deletions, therefore the same annotation methods described above could not be effectively applied to this region. Instead, dot plots were performed in Geneious R9.1 (Biomatters Ltd.) which uses the EMBOSS 6.5.7 dotmatcher tool to compare sequence identities of the human PRR vs. the upstream sequence of other mammalian species using a window size of 25, a threshold of 45, and the high sensitivity setting with a probabilistic scoring matrix. The PRR was determined to be present if a conserved region >100 bp relative to the human sequence was discernible from the dot plots. The boundaries of the PRRs were estimated using the dot plot and annotated. The PRRs of species listed in **Table 2** were then screened in rVista 2.0 (Loots and Ovcharenko, 2004) for the presence of putative transcription factor binding motifs [DR1, DR3, DR4, CEBP (CCAAT-enhancer-binding proteins), CREB, and PPAR] shared with humans, as performed by Shore et al. (2012). Insertions larger than 100 bp relative to the human PRR were removed prior to screening in rVista using the vertebrate TRANSFAC professional V10.2 library with the "matrix similarity optimized for function" setting.

Basal promoter regions were identified by performing alignments of 600 bp upstream of the ATG start codon for each

TABLE 2 | Possible transcription factor binding motifs within the PRR of selected species screened using rVista 2.0.

Species	Motif	Position	Sequence
Homo sapiens	CREB	24+	catggCATCAgttc
	DR3	227−	cagaGGTTCACTAGAGTCaac
	DR4	230−	agGTTCACTAGAGTCAa
Marmota marmota	PPAR_DR1	50−	tGGTCAAAGGACt
	DR4	326−	tgGGTCCCTTAAGGTCa
	DR1	393−	TGACACTTATCCc
Oryctolagus cuniculus	CREB	373−	ccTAACATCAcc
	CEBP	519−	gcTCCATTGCCTAACTCt
	PPAR_DR1	592+	tGGCCCTTGGCCc
	PPAR_DR1	601+	gCCCCTTTGTCCc
Camelus ferus	CEBP	271−	taTACATTTGGGCATACt
	CEBP	503−	tgTTCCTTTCCTAATTGt
	CREB	636−	tgtCATCAcct
Bos taurus	CREB	149+	CGTCAg
	CEBP	240−	taTGCATTATAACAAACa
	CEBP	471−	tgTTTCTTTCCTAATTTg
	PPAR_DR1	487+	tGACCTTTGATAa
	PPAR_DR1	542+	tGACCCTTGACCc
Giraffa camelopardalis	CREB	150+	CGTCAg
	CREB	476−	tgTTTCTTTCCTAATTTg
	PPAR_DR1	492+	tGACCTTTGATAa
	PPAR_DR1	547+	tGACCCTTGACCc
Balaenoptera acutorostrata	DR1	96+	aGGGGAAGGGACA
	CEBP	518−	taTTTCTTTCCTAACTTt
	PPAR_DR1	587+	tGGCCCTTGACCc
	DR1	587−	TGGCCCTTGACCc
	DR1	594−	TGACCCCTTTCCc
Lipotes vexillifer	DR3	291+	accGAACATTCTCAATCtgct
	CEBP	509−	taTTTCTTTCCTAACTTt
	PPAR_DR1	580+	tGGCCCTTGACCc
	DR1	587−	TGACCCCTTTCCc
Ceratotherium simum	DR1	108+	aGGGGAAGGGACA
	DR4	246−	agGATCACTAGAGTTAg
	CEBP	284−	taTACATTTAGTCATACt
	DR3	304+	accGAACATTCTCAATCtctg
	DR4	425+	tGTCCTCTTTTGACAtt
	PPAR_DR1	453+	tCACACTTGACCc
Equus przewalskii	CEBP	9+	cTTTCACAAtcc
	CREB	36−	caTAGCGTCAgt
	CREB	41+	CGTCAg
	DR4	234−	agGTTCACTAGAGTTAg
	PPAR_DR1	537+	tTACCTTTGACCa
	DR1	592−	TGGTCCTTGACCc
	CREB	667+	ttGCTGACTccc
Equus caballus	DR4	224−	agGTTCACTAGAGTTAg
	PPAR_DR1	524+	tTACCTTTGACCa
	DR1	579−	TGGTCCTTGACCc

(Continued)

TABLE 2 | Continued

Species	Motif	Position	Sequence
	CREB	654+	ttGCTGACTccc
Pteropus vampyrus	CREB	37+	catagCATCAgctc
	DR4	408+	tGTCCTCTTTTGACAtt
	PPAR_DR1	575+	tGGCCCTTGACCc
	DR1	582−	TGACCCCTTTCCt
Ailuropoda melanoleuca	DR1	85+	aGGGGAAGGGACA
	CREB	505+	ttGATGAGGccc
	DR1	554−	TGGCCCATGACCc
	PPAR_DR1	561+	tGACCCTTTGCCt
	CREB	628+	ttGCTGACTccc
Odobenus rosmarus	DR1	92+	aGGGGAAGGGACA
	DR4	406+	tGTCCTCTTTTGACAtt
	DR1	567−	TGGCCCATGACCc
	PPAR_DR1	574+	tGACCCTTTTCCt
	CREB	670+	ttGCTGACTccc
Panthera pardus	DR4	240+	tGTCCTCTTTTGACACa
Leptonychotes weddellii	DR1	90+	aGGGGAAGGGACA
	DR4	403+	tGTCCTCTTTTGACAtt
	DR1	564−	TGGCCCATGACCc
	PPAR_DR1	571+	tGACCCTTTTCCt
	CREB	671+	ttGCTGACTccc
Procavia capensis	CREB	59−	ccTAACATCAcc
	DR1	273−	TGGTCCTTGACCt
	CREB	278+	cttgaCCTCAttgc
	CREB	280+	TGACCTca
Loxodonta africana	CREB	32+	acataCATCAgctc
	CREB	347−	caTAACATCAcc
	CREB	424−	tTGACG
	PPAR_DR1	566+	tGGCCCTTGACCc
Trichechus manatus	CREB	140−	tgAGGTCA
	CREB	369−	taaCATCACCaa
	PPAR_DR1	587+	tGGCCCTTGACCc
Echinops telfairi	PPAR_DR1	189−	gGGTCAAGGATCa
	CREB	326−	ccTGACATCAct

Duplicates sites were removed. Position is indicated relative to the start of the PRR sequence and the strand is indicated with + or − symbols.

species with available sequence data. The rat and mouse upstream sequences contain several putative promoter motifs (e.g., TATA box, CCAAT site, CRE-4, and GCCCCT sites) and thus were used as reference sequences. CpG islands within the 5′ region of *UCP1* were identified using the EMBOSS CpGplot tool (http://www.ebi.ac.uk/Tools/seqstats/emboss_cpgplot/). Kiskinis et al. (2007) noted that the *UCP1* CpG island occurs immediately upstream of the *UCP1* open reading frame but may also extend into exon 1, therefore, 1 kb upstream of exon 2 was screened for the presence of CpG islands. EMBOSS CpGplot positively identifies CpG islands if a sequence >200 bp contains an observed/expected ratio of CpGs exceeding 0.6, with a GC content >50%, meeting the criteria proposed by Gardiner-Garden and Frommer (1987). The default window size of 100 bp was used for these runs.

The *UCP1* genes of non-eutherian mammals were also examined for the presence or absence of regulatory elements. Contigs of the Tasmanian devil (*Sarcophilus harrisii*) and Tammar wallaby (*Macropus eugenii*) were too short to encompass a potential enhancer occurring ∼5 kb upstream of the transcriptional start site. However, contigs of the platypus (*Ornithorhynchus anatinus*) and gray short-tailed opossum were sufficiently long to create dot plots of the upstream sequence in order to screen for homologous regulatory elements occurring in the human. Some eutherian species displayed inactivated *UCP1* genes with deletions of whole exons (e.g., Chinese pangolin; *Manis pentacatyla*, Javan pangolin; *Manis javanica*, nine-banded armadillo; *Dasypus novemcinctus*), or deletion of the entire gene (killer whale and bottlenose dolphin). The annotation techniques described above did not reveal the presence of a *UCP1* enhancer in these species; thus, sequence identity comparisons against human *UCP1* were performed using Easyfig 2.1 (Sullivan et al., 2011). This analysis was also performed for the rat and cow (*Bos taurus*) since these were species are known to display *UCP1* enhancers while the cow also contains a PRR region (Shore et al., 2012).

Finally, regions containing enhancer and basal promoter sequences for each species were imported into Geneious 9.1 and multispecies nucleotide alignments were generated using the MUSCLE alignment tool (Edgar, 2004) with default settings. A consensus eutherian sequence representing the simple majority (>50%) was generated from this dataset based only on species for which the *UCP1* gene is intact (i.e., species with documented *UCP1* pseudogenes (Gaudry et al., 2017) were not included in the consensus calculations). For some eutherian species, pairwise alignments were also created against the human enhancer to obtain the percent sequence identity values. Conserved motifs and putative transcription factor binding sites were annotated. Recognized transcription factor binding motifs within the *UCP1* enhancer (illustrated in **Figure 2**) were examined by eye in each eutherian species and scrutinized for mutations that potentially affect DNA-protein interactions based on previous site directed mutagenesis studies. Additionally, the consensus enhancer region sequence (see above), together of those of seven species spanning the three mammalian superorders for which *UCP1* is intact, were screened for the presence of all vertebrate transcription factors in the TRANSFAC professional V10.2 library using rVista with the "matrix similarity optimized for function" setting.

Phylogenetic Trees

To generate a combined *UCP1*, *UCP2*, and *UCP3* coding sequence phylogenetic tree, the data set of Gaudry et al. (2017) was updated to include coding sequences of the 16 additional species with recently published genomes (**Table 1**). The resulting 448 *UCP* genes were aligned using MUSCLE (Edgar, 2004), and a maximum likelihood tree constructed using RAxML

(Randomized Axelerated Maximum likelihood) version 7.2.8 (Stamatakis, 2006) with the "GTR Gamma" nucleotide model and "rapid bootstrapping and search for best scoring tree" setting. The program was performed for 500 bootstrap replicates.

In order to trace the evolutionary gain and loss of *UCP1* transcriptional regulatory elements, we also constructed a 41-gene species tree for the 139 mammals included in this study following the methods of Gaudry et al. (2017). Briefly, this data set included coding and non-coding sequences from 30 nuclear (*A2AB, ADRB2, APP, ATP7A, ADORA3, APOB, BCHE, BDNF, BMI1, BRCA1, BRCA2, CHRNA1, CMYC, CNR1, CREM, DMP1, ENAM, EDG1, FBN1, GHR, IRBP, MC1R, PLCB4, PNOC, RAG1, RAG2, SWS1, TTN, TYR1, VWF*) and 11 mitochondrial loci (*12S rRNA, 16S rRNA, CYTB, COI, COII, COIII, ND1, ND2, ND3, ND4, ND5*). A 50,911 bp concatenated supermatrix was aligned in MUSCLE. The supermatrix was divided into 32 partitions (see Supplementary Materials). Each nuclear gene was assigned an individual partition, while *12S rRNA* and *16S rRNA* were combined to create one partition, and the nine remaining mitochondrial genes were also combined into a single partition. An independent GTR Gamma model was estimated for of these partitions and a maximum likelihood tree was generated in RAxML 7.2.8 using the same settings described above with 100 bootstrap replicates.

RESULTS

UCP1 Coding Sequences

All of the 16 newly acquired *UCP1* CDSs were intact with the exception of the Javan pangolin, which displays the same mutations as the Chinese pangolin pseudogene (i.e., frameshift, splice site and non-sense mutations, deletion of exons 1 and 2) documented by Gaudry et al. (2017). Similarly, the 12 bp deletion that calls into question the functionality of the Bactrian camel *UCP1* gene (Gaudry et al., 2017) is also present in the dromedary camel (*Camelus dromedarius*). Conversely, the *UCP1* CDS of the giraffe (*Giraffa camelopardalis*) is intact, despite its large body size.

The predicted platypus *UCP1* CDS available on GenBank (accession number: XM_001512650) is unique in that it creates a hypothetical open reading frame composed of seven exons; the usual 126 bp exon 1 is divided into two separate exons of 30 and 120 bp in length. The placement of these putative exons are displayed in a dot plot comparison with the 5′ region of the gray short-tailed opossum *UCP1* locus (**Figure 3**). Notably, two separate regions within the platypus read display homology to the opossum *UCP1* exon 1 sequence, revealing what appears to be a 186 bp insertion in the platypus exon 1 sequence. The original platypus start codon also appears to be mutated to "AAG" thus translocating the predicted 30 bp 'exon 1′ of the platypus 176 bp upstream of the gray short-tailed opossum start codon (**Figure 3**). By contrast, BLAST searches of platypus RNA sequencing projects (SRX182802, SRX17144, SRX17145, SRX081892, SRX081881, SRX081882, SRX328084, SRX328085, SRX081887-SRX081890) reveal an intact *UCP1* mRNA sequence (Supplemental File 5) that differs from the predicted coding sequence. Briefly, the platypus mRNA coding sequence indicates that the predicted 30 bp "exon 1" coding sequence is not translated, that there is no insertion in exon 1 of the platypus, and that the ATG start codon found in other mammals is indeed

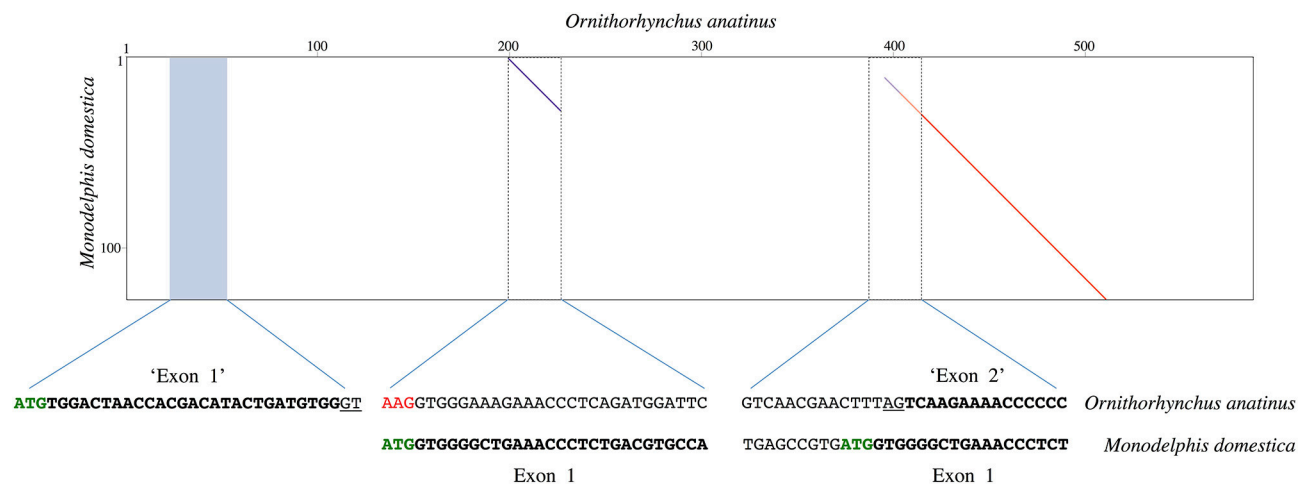

FIGURE 3 | Dot plot comparison of the gray short-tailed opossum *UCP1* exon 1 vs. a section of the platypus *UCP1* gene occurring between *TBC1D9* and *ELMOD2* (accession number: NW_001794248.1). Sequence alignments of the platypus (**top**) and gray-short tailed opossum (**bottom**) are provided with the potential coding sequences indicated in bold; putative splice sites are underlined. Note that two regions within the platypus clearly display homology to the opossum exon 1 (199–226 and 400–520), suggesting the presence of a 186 bp insertion in the platypus exon 1 sequence. The blue shaded area represents the region where an automated predictor program, which created a seven exon *UCP1* gene for the platypus, placed a 30 bp "exon 1" in order to obtain an open reading frame free from premature stop codons (accession number: XM_001512650), though this region shares no homology with exon 1 of the opossum. The original platypus start codon also appears to be mutated to AAG (red font), with the predicted platypus "exon 2" occurring 6 bp downstream of the "ATG" start site in the opossum. Note that these differences between the two species likely arise from a misassembly error in the platypus (see text for details).

intact at the expected position (i.e., there is a misassembly error in the predicted GenBank sequence).

UCP1 Basal Promoter

An alignment of the basal *UCP1* promoter for representative species is displayed in **Figure 4**. Notably, the most upstream GCCCCT motif (nucleotides 1–6 of the promoter alignment; **Figure 4**) described in the rat by Yubero et al. (1994) is not present in any non-murid species. While the CRE-4 consensus sequence (5′-TGAAGGGC-3′) is similar to that described by Kozak et al. (1994) in mice (5′-TGACGCGC-3′), this site does differ substantially in many species (e.g., common shrew [*Sorex araneus*], human, etc.) and is absent in the gray short-tailed opossum, walrus, cow, and giraffe (**Figure 4**). The second and third GCCCCT sites, respectively occurring at 242–248 and 308–315 of the alignment, are relatively well conserved (**Figure 4**). By contrast, the putative CCAAT site in the rat (Bouillaud et al., 1988) is highly variable in other mammals. The TATA box described by Bouillaud et al. (1988) is intact in the majority of species including all marsupials where it occurs as a 5′-TATAARR-3′ sequence 260–280 upstream of the ATG start codon of exon 1. While a 5′-TATAAGG-3′ sequence is found ∼200 bp upstream of the platypus *UCP1* coding sequence, the validity of this site is uncertain due to a misassembly in this region of the GenBank sequence (see above). Interestingly, the walrus motif contains a T→A mutation causing a 5′-TAAATAA-3′ sequence, while the panda, white rhinoceros, horse, and bats share a 5′-TACAWAA-3′ sequence. Among species that possess pseudogenized *UCP1* genes, an intact TATA box still remains ∼290 bp upstream of the African elephant (*L. africana*) and manatee (*T. manatus*) coding sequence while the closely related Cape rock hyrax (*Procavia capensis*) deviates from the consensus (5′-TACGTGA-3′). Similarly, the pig retains a TATA box identical to that of the cow, camel, and giraffe (5′-GATATAA-3′), though a number of mutations in cetaceans have resulted in a sequence (5′-GACGTCAA-3′) that is virtually unrecognizable as a TATA box (**Figure 4**).

CpG Island

CpG islands meeting the criteria of Gardiner-Garden and Frommer (1987) were not detected in the monotreme or marsupial assemblies. Conversely, a CpG island within or immediately upstream of exon 1 was identified in 91 of 113 eutherian species with available sequence coverage for this region (**Table 1**). The presence of the CpG island was found to vary extensively among small-bodied species as it was detected in the common shrew, but is absent from the European hedgehog (*Erinaceus europaeus*) and star-nosed mole (*Condylura cristata*; **Table 1**). Many rodent species (e.g., mouse, rat), known to express functional BAT, also lack a CpG island (**Table 1**). Similarly, among the four afroinsectiphilians examined, a CpG island was only identified in the lesser hedgehog tenrec (containing 39 CpG dinucleotides), despite a relatively high number of CpG sites (37–41) located between 600 bp upstream and 200 bp downstream of the start codon in the other three species. Conversely, CpG islands were identified in closely related paenungulates (elephants, sirenians, and hyraxes), which have >50 CpG dinucleotides in the same region, and armadillos—despite both of these groups having a non-functional *UCP1*. Among artiodactyls, CpG islands were detected in camels, the okapi (*Okapia johnstoni*), and all whale *UCP1* pseudogenes (except for the killer whale and bottlenose dolphin for which the entire gene is deleted; **Figure 5**), but not the giraffe or the pig (*Sus scrofa*). This element is also missing in the pangolin pseudogenes, which is likely due to deletion of a portion of the gene upstream of exon 3 (**Figure 5**).

Putative Regulatory Region (PRR)

A distinct PRR was found to be present in 97 of the 125 eutherian mammals examined for which sequence is available (**Table 1**), though this element was not observed in the platypus or gray short-tailed opossum (**Figure 6**). PRRs were observed from all afrotherians, but not the armadillo, a xenarthran (**Table 1**), though insertions within this region are prevalent in the elephant shrew, lesser hedgehog tenrec, and aardvark (**Figure 6**). By contrast, the dot plots of the elephant and manatee—for which *UCP1* is pseudogenized—reveal a high conservation of the PRR with virtually no indels, though only the 3′ half of the PRR is present in the hyrax (**Figure 6**). As seen for the cow (**Figure 5**), giraffe, camel, and several whales (**Figure 6**), the PRR is conserved among most artiodactyls, but is missing in the pig *UCP1* pseudogene (**Figure 6**) and deleted in the bottlenose dolphin, killer whale, and Javan pangolin (**Figure 5**). A PRR is also absent in several species known to express functional BAT, including the shrew and star-nosed mole, several bats (*Myotis* spp. and *Eptesicus fuscus,* etc.), and many rodents (**Table 1**), including the mouse and rat (**Figures 5**, **6**). Similarly, both *Canis familiaris* and *Lycaon pictus* lack a PRR, despite this feature being present in all other carnivores (**Table 1**). The transcription factor binding sites identified within PRRs of selected species using rVista 2.0 are listed in **Table 2**. PPAR, DR1, DR3, DR4, CREB, and CEBP sites are relatively common within this region in species with and without a functional *UCP1* locus.

UCP1 Enhancer

UCP1 enhancer sequences were retrieved for 121 eutherian species (**Table 1**). Enhancer boxes were typically found within 5 kb upstream of exon 1, however, for some members of the afroinsectiphilia (i.e., aardvark and elephant shrew), the enhancer occurs at ∼ –7.5 kb (**Figure 6**). Dot plots of the upstream regions of the platypus and the gray short-tailed opossum reveal no evidence for a *UCP1* enhancer (**Figure 6**), suggesting it is absent within both monotremes and marsupials.

Contrary to the findings of Shore et al. (2012), who noted the absence of an enhancer in the upstream region of the common marmoset (*Callithrix jacchus*), American pika (*Ochotona princeps*), thirteen-lined ground squirrel (*Spermophilus tridecemlineatus*), common shrew, and European hedgehog, we identified this element in each of these species except the hedgehog. The contig encompassing hedgehog *UCP1* CDS (accession number: AMUD01193160.1), however, only extends 1126 bp upstream of exon 1 and BLAST searches failed to provide hits of a *UCP1* enhancer located on other contigs, thus its presence or absence from the genome remains inconclusive.

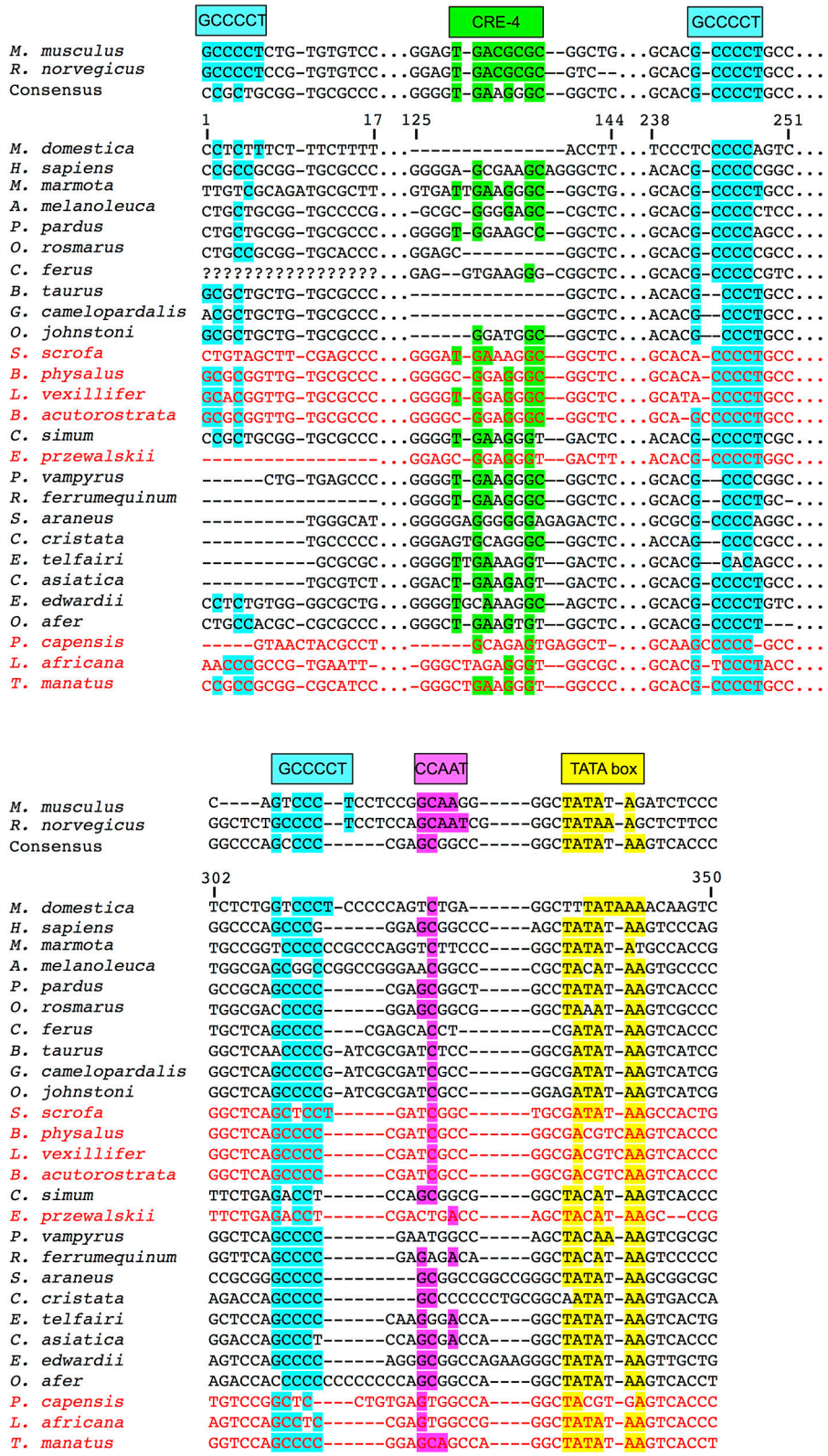

FIGURE 4 | *UCP1* basal promoter elements alignment for select mammalian species with putative protein binding motifs indicated. Highlighted sites indicate shared nucleotides to the species in which the motif was first described (mouse or rat) and the typical TATA box (5′-TATAAAA-3′) sequence (Xu et al., 1991). The consensus sequence represents the simple majority based on species for which the *UCP1* gene is intact. Species with documented *UCP1* pseudogenes (Gaudry et al., 2017) are denoted in red font and were not included in the consensus calculations.

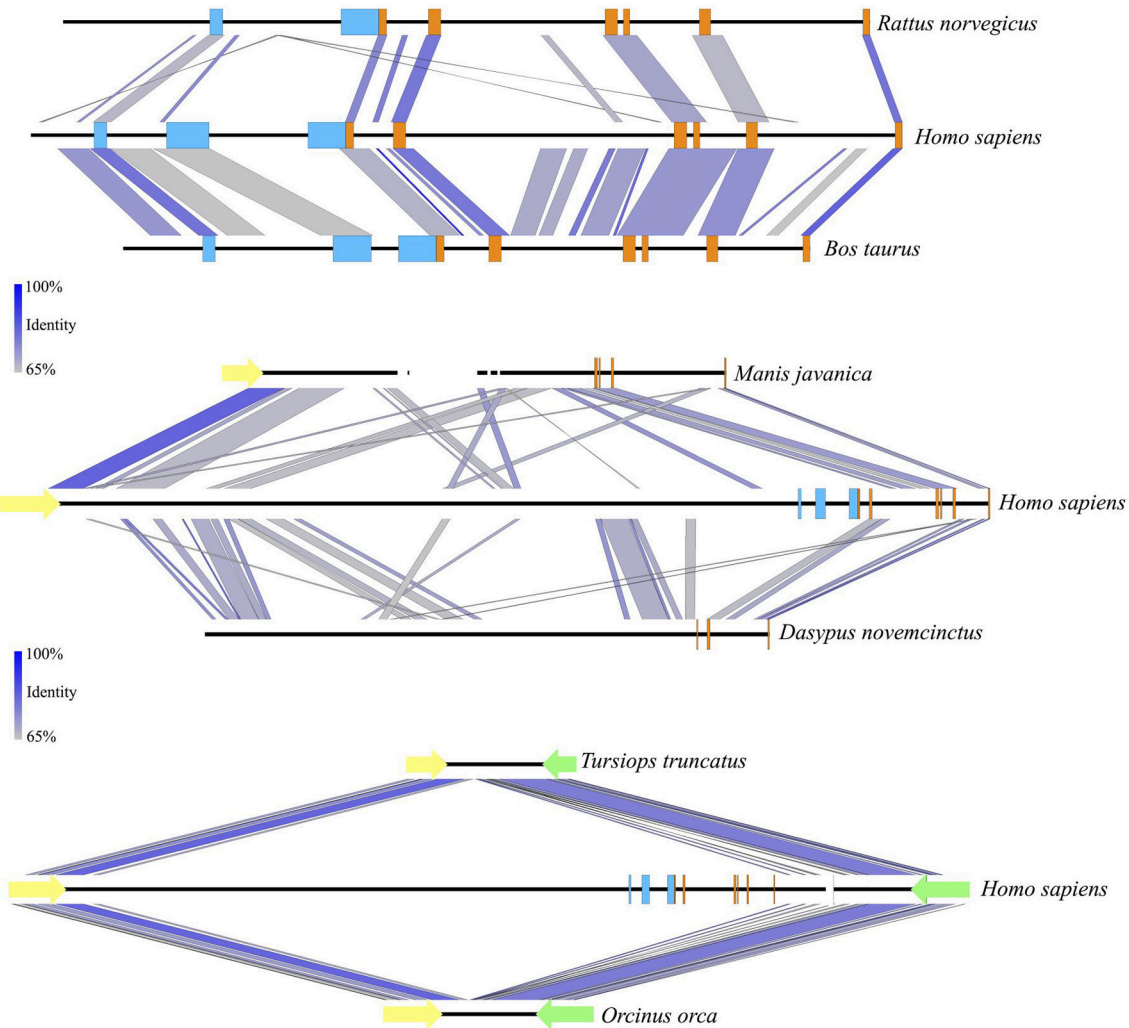

FIGURE 5 | Sequence identity comparisons of the *UCP1* genes of the rat, cow, pangolin, armadillo, bottlenose dolphin, and killer whale vs. the human. All DNA sequences are shown 5′ (**left**) to 3′ (**right**). *UCP1* exons 1–6 are denoted with orange rectangles while *UCP1* upstream transcriptional regulatory elements are denoted in light blue (enhancer box, putative regulatory region, CpG island; from left to right). Gaps in sequence coverage are represented by white rectangles. Notably, the putative regulatory region is absent in the rat, but conserved in the cow. Upstream regulatory elements also appear to have been deleted in the Javan pangolin and armadillo, which have deletions of *UCP1* exons 1–2, and 3–5, respectively. Deletion of the entire *UCP1* gene between *TBC1D9* (yellow arrows) and *ELMOD2* (green arrows) has occurred in bottlenose dolphin and killer whale ∼8–15 MYA (Gaudry et al., 2017) and included the upstream regulatory elements. Sequence identity percentage is represented with a color scale.

Similarly, low sequencing coverage likely explains the apparent lack of a *UCP1* enhancer in the zebu (*Bos indicus*), Brazilian guinea pig (*Cavia apera*), and desert woodrat (*Neotoma lepida*), as enhancers have been recovered from their close phylogenetic relatives (**Table 1**).

The enhancer is highly conserved in large-bodied species with intact *UCP1* loci (i.e., rhinoceroses, camels, giraffe, and pinnipeds) as well as several species with *UCP1* pseudogenes (e.g., elephantids, sirenians, suids, equids, and some cetaceans; **Table 1**). However, seven species lack both a *UCP1* enhancer and an intact *UCP1*. For instance, the entire *UCP1* gene including the enhancer has been deleted in the killer whale and bottlenose dolphin (**Figure 5**). The enhancer has also been deleted in the sperm whale (*Physeter macrocephalus*; **Figure 6**), yet it remains present in the baiji (*Lipotes vexillifer*) and all baleen whales, indicating an independent loss in both the sperm whale and delphinids. The dot plots also fail to provide evidence for an *UCP1* enhancer in the Cape rock hyrax, though this element is present in other paenungulates for which this gene is also pseudogenized (**Figure 6**). Sequence identity comparisons also suggest the enhancer is lost in pangolins and the nine-banded armadillo (**Figure 5** and **Table 1**). Interestingly, BLAST searches failed to identify this regulator in the WGS contigs or SRA of the two-toed sloth (*Choleopus hoffmanni*), although partial coverage was recovered for the extinct giant ground sloth (*M. darwinii*) from a pair of SRA reads (**Figure 7**).

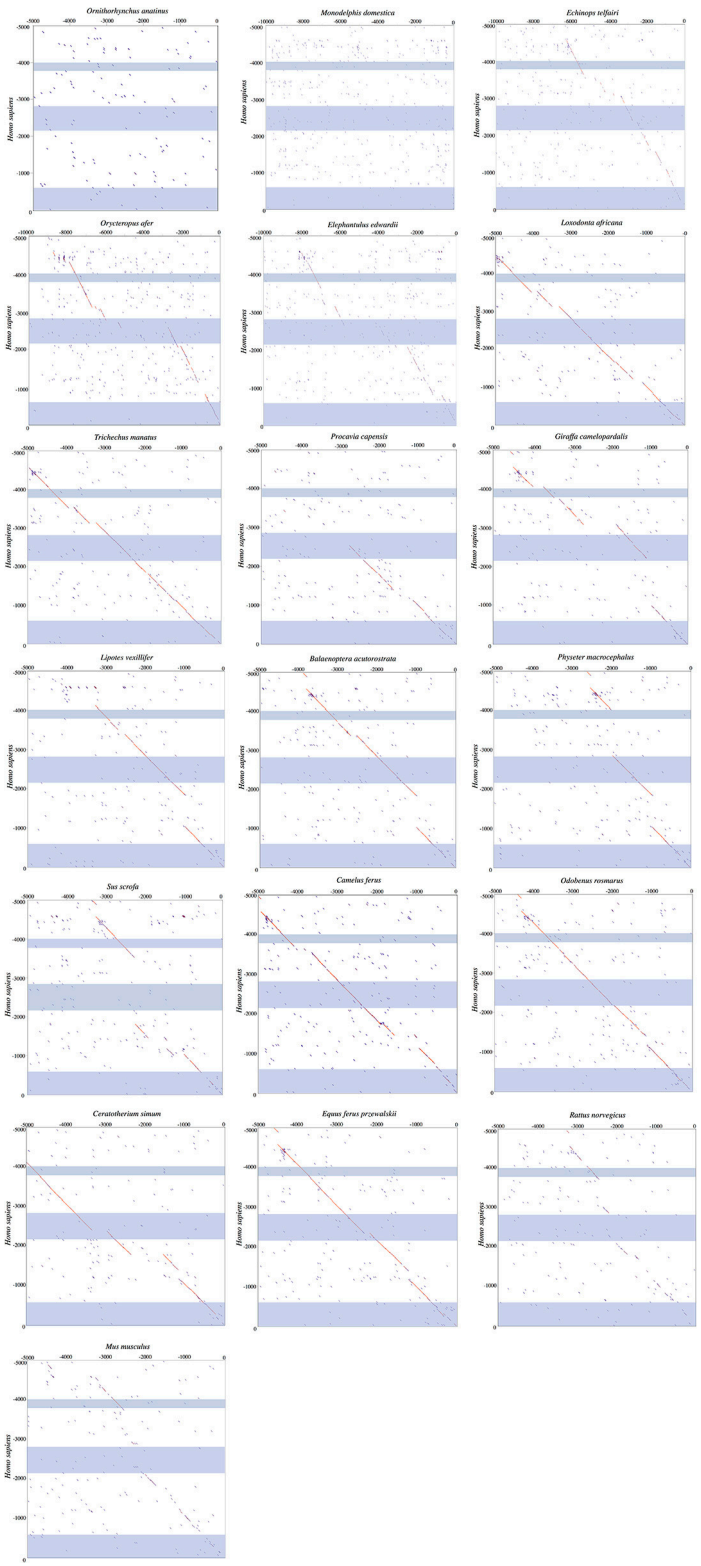

FIGURE 6 | Dot plots of the 5,000 or 10,000 bp upstream of *UCP1* exon 1 of select mammalian species compared to the upstream sequence of humans. Blue shading represents the *UCP1* enhancer (∼ −4,000 to −3,800 in human), putative regulatory region (∼ −2,700 to −2,500 in human), and promoter/CpG island (−600 to 0 in human), in that order, from top to bottom.

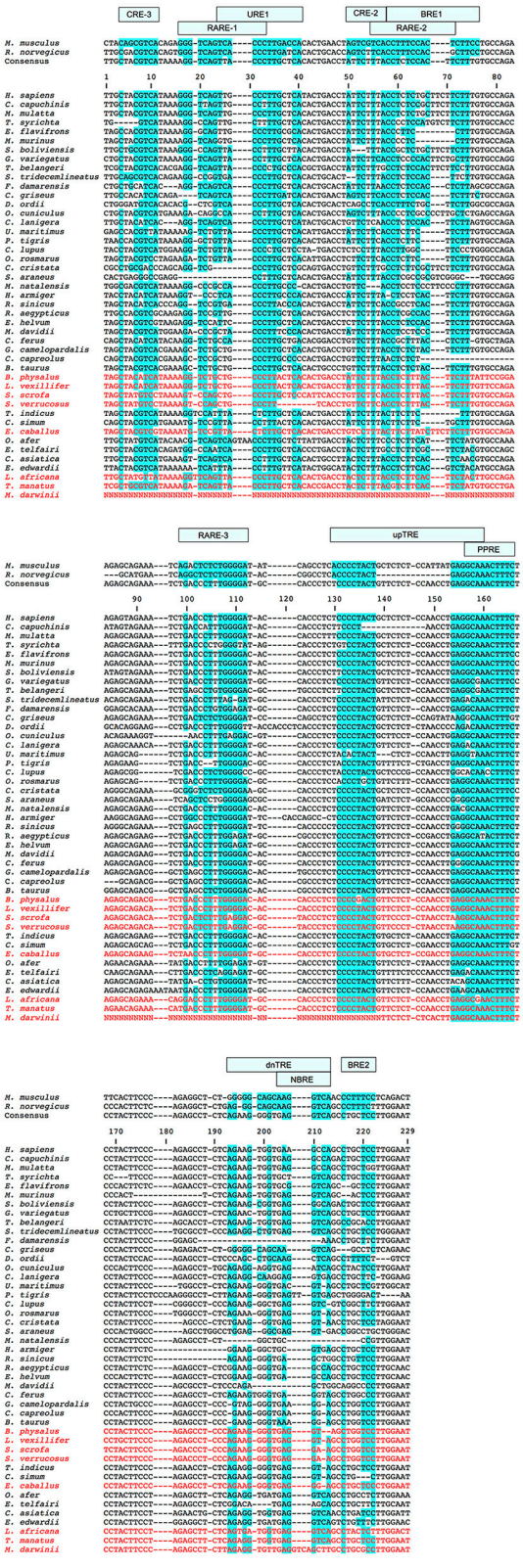

FIGURE 7 | *UCP1* enhancer alignment for select eutherian species. Sequences highlighted in blue denote the degree of conservation relative to *(Continued)*

FIGURE 7 | Continued
transcription factor binding sites first described in mice or rats (see also **Figure 2**). The consensus sequence represents the simple majority based on species for which the *UCP1* gene is intact. Species with documented *UCP1* pseudogenes (Gaudry et al., 2017) are denoted in red font and were not included in the consensus calculations.

Dot plots of the murid (rat and mouse) upstream sequence (**Figure 6**) illustrate marked divergence from humans with the exception of a small region encompassing the *UCP1* enhancer. By contrast, the upstream sequence of many laurasiatherians, and even paenungulates lacking an intact *UCP1* (e.g., elephants and manatees) is surprisingly similar to that of humans (**Figure 6**). In fact, pairwise sequence comparisons of these enhancers vs. that of the human reveal that this region is more highly conserved (>80%) in large-bodied species that both possess and lack an intact *UCP1* than the mouse (74%) and rat (69%) *UCP1* (data not show), despite the latter sharing a more recent common ancestor with humans. This pattern is mirrored in the *UCP1* gene tree (**Figure 8**) as many small-bodied lineages (i.e., afroinsectiphlians, myomorph rodents, vesper bats, and most notably, eulipotyphlans) display long branch lengths indicative of high rates of molecular evolution that are comparable to those of many species with *UCP1* pseudogenes (e.g., pangolins, pigs, armadillo, and hyrax). Canines are also worth noting, as their branch is highly elongated compared to other carnivores. By contrast, short branches found for most large-bodied species, even among those with non-functional *UCP1* (e.g., paenungulates, cetaceans, and equids), reflect low nucleotide substitution rates.

Enhancer region alignments revealed a number of marked differences within transcription factor binding motifs among species (**Figure 7**). For instance, while the CRE-3 site contains a set of core nucleotides (5′-CGTCA-3′) that are highly conserved in most eutherians, mutations to one or two nucleotides within this region are observed in a number of species (e.g., *C. cristata*, *Dipodomys ordi*, *Cricetulus griseus*), while the 5′ portion of this site appears to be deleted in the Philippine tarsier (*Tarsius syrichta*). Notably, the CRE-3 motif was detected in each species for which the enhancer was screened in rVista except for *C. cristata* (Table S1). Various mutations to this motif are also found in species with a pseudogenized *UCP1* (e.g., elephants, pigs, whales, and horses; **Figure 7**). The RARE-1 site is especially conserved in the section that overlaps with the URE1 motif, where the consensus sequence (5′-TTACCCTTGCTCA-3′) closely resembles the mouse URE1 site proposed by Sears et al. (1996). However, mutations at sites (e.g., nucleotide positions 32–33 of the alignment in **Figure 7**) shown to block transcription binding in mice (Sears et al., 1996) are observed in several species with intact *UCP1* (e.g., rabbit; *Oryctolagus cunculus,* Philippine tarsier; *T. syrichta*, white rhino; *C. simum*, and tapir; *T. indicus*). The aardvark displays a 4 bp insertion occurring within the URE1 that results in a single nucleotide (C→A) substitution to this motif. Notably, among species lacking a functional *UCP1*, the Javan warty pig (*S. verrucosus*) exhibits a marked disruption to the URE1 site.

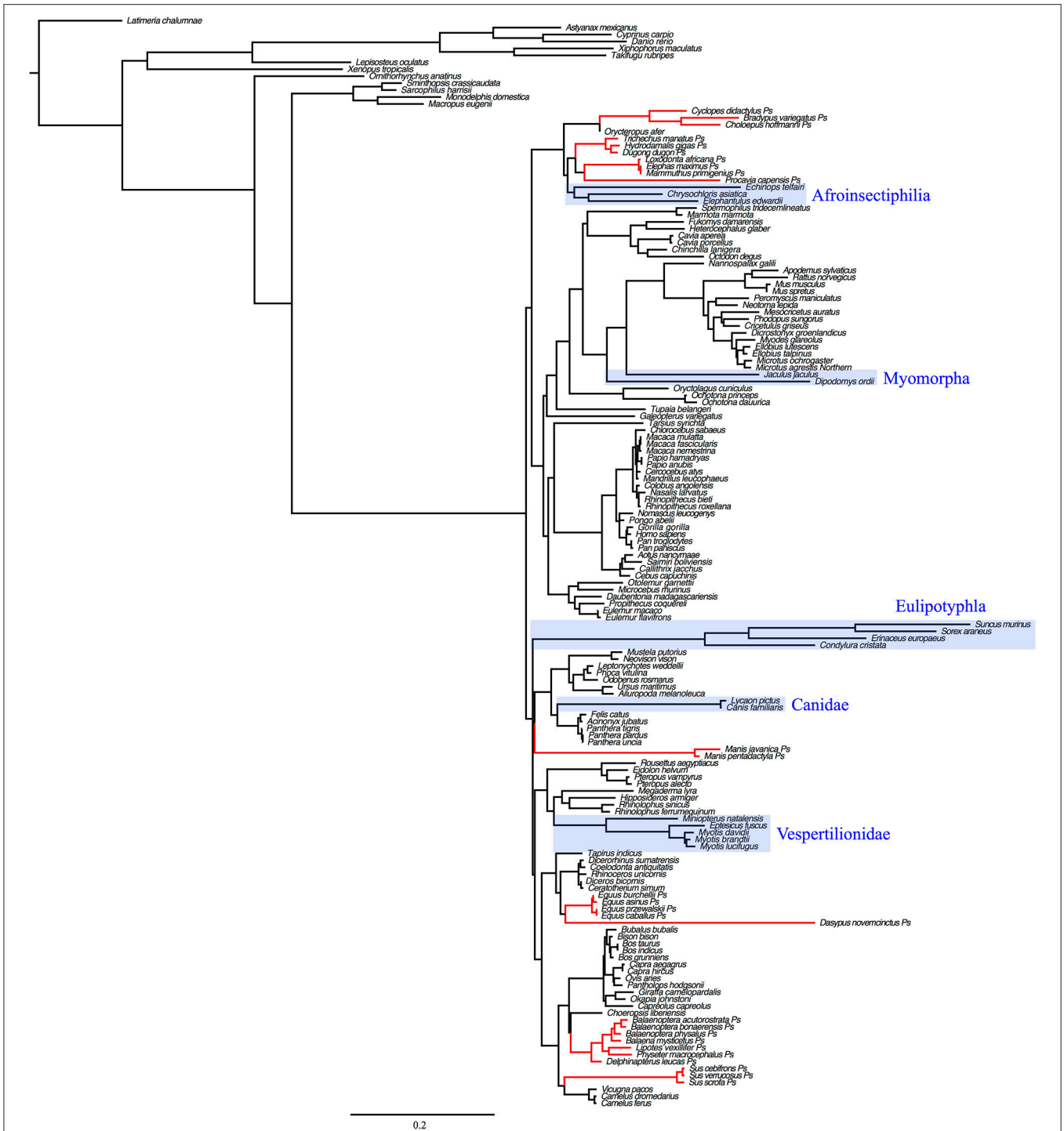

FIGURE 8 | Maximum likelihood *UCP1* coding sequence gene tree illustrating substitution rates in several eutherian lineages (eulipotyphlans, canids, afroinsectiphilians, vesper bats, myomorph rodents; boxed in blue) that are comparable or higher than lineages with *UCP1* pseudogenes (denoted in red). Branch lengths represent the number of nucleotide substitutions per site.

The CRE-2 motif is well conserved among most eutherians, however, the consensus eutherian sequence (5′-ATTCTTTA-3′; **Figure 7**) is a poor match to the mouse 5′-AGTCGTCA-3′ sequence (Kozak et al., 1994). Indeed, of seven species for which the enhancer region was screened using rVista, this site was identified as a cAMP response element only within the mouse (Table S1). Notably, several species with an intact *UCP1* display deletions within the CRE-2 motif (e.g.,

black capped squirrel monkey; *Simiri boliviensis,* thirteen-lined ground squirrel; *S. tridecemlineatus*, and natal long-fingered bat; *Miniopterus natalensis*). Similarly, the two TTCC motifs described for the mouse BRE-1 site (Kozak et al., 1994) are not found in any non-murid eutherians. This region, however, is TC-rich in nearly all species with a single convergent TTCC site found in the dog and natal long-fingered bat (**Figure 7**). In contrast, the AT-richness of the BRE-1/RARE-2 region is substantially increased in horses, whales, and pigs—all of which lack a functional UCP1—relative to species with an intact gene.

The RARE-3 site consensus sequence (5′-TGACCCTTTGGGGAT-3′; **Figure 7**) is strongly conserved among eutherians with the exception of a 2-bp deletion in the tiger (*Panthera tigris*). The PPRE motif predicted by Jastroch et al. (2008) is also a highly conserved element within the *UCP1* enhancer, with a consensus sequence of 5′-GCAAACTTTC-3′. Of note, a PPARG (or PPARγ) site with a consensus sequence of 5′-CAAACTTTCTCCTACTT-3′ was identified to overlap with this PPRE motif in six of the seven species (all except for the mouse) for which the enhancer was screened using rVista (Table S1). Conversely, the rat upTRE motif (Rabelo et al., 1995) appears to have arisen from a 14 bp deletion in this species, and is therefore not present in other lineages (**Figure 7**). Additionally, the white-headed capuchin (*Cebus capuchinis*) and polar bear (*Ursus maritimus*), both of which likely express functional BAT, have deletions within the putative upTRE region. The 5′ portion of the dnTRE motif (5′-AGGGCAGCAAGGTCA-3′) described by Rabelo et al. (1995) is also exclusive to the rat, as the consensus sequence (5′-AG**A**AGGGGTGAGGTCA-3′) has numerous differences and an insertion [bold]; deletions to this region are also found in the Damaraland mole-rat (*Fukomys damarensis*), *Myotis* spp. bats, and the lesser hedgehog tenrec (**Figure 7**). The NBRE site, which overlaps with the 3′ region of the dnTRE, is not strongly conserved in all species, with nucleotide deletions in artiodactyls, the Damaraland mole-rat, great roundleaf bat (*Hipposideros armiger*), David's myotis, and natal long-fingered bat, and insertions in both the tiger and the giant ground sloth (**Figure 7**). The most crucial nucleotides of the BRE-2 motif (5′-TTCC-3′; bases 219–222 of the enhancer alignment; **Figure 7**) described by Kozak et al. (1994) are only found in mice (the species in which it was first described) and the Chinese rufous horseshoe bat (*Rhinolophus sinicus*).

DISCUSSION

No traces of an enhancer, PRR, or CpG island were detected in the upstream region of the platypus or gray short-tailed opossum loci, though both appear to possess a TATA box within the proximal promoter. By contrast, each of these elements were observed in afrotherians, euarchontoglirans, and laurasiatherians, while a portion of the *UCP1* enhancer was also obtained in a single xenarthran, the giant ground sloth, a species that went extinct during the late Pleistocene ∼12,000 years ago (Moore, 1978). We can thus deduce that the *UCP1* gene of stem mammals contained a TATA box, while the other transcriptional regulatory elements evolved in a common ancestor of eutherians as proposed by Jastroch et al. (2008). However, despite functioning as a hypothetical methylation site (CpG island) or encompassing putative transcription factor binding sites in some species (PRR), these motifs are not required for BAT transcription, as exemplified by high *UCP1* expression within the BAT of mice and rats (Pedersen et al., 2001; Wu et al., 2012), which lack both of these elements. Indeed, these elements have repeatedly been lost in eutherian mammals (**Figure 9**). Shore et al. (2012) reached a similar conclusion as roughly half of the eutherian species they examined lacked a PRR and a CpG island. Given the proposed function of the CpG island as a regulator of UCP1 tissue-specific expression (Kiskinis et al., 2007), a lower level of methylation in BAT as opposed to other tissues would be expected, however, Shore et al. (2012) discovered that the *UCP1* CpG island remains virtually un-methylated in BAT, white adipose tissue, and liver despite greatly reduced UCP1 expression levels in the latter two tissues. Therefore, the function of this region remains unclear, however, Shore et al. (2012) did characterize a CpG island in the zebrafish suggesting its presence could be an ancestral condition of the *UCP1* gene that was lost in non-eutherian mammals, but retained (and again lost) in some eutherians (see **Figure 9**).

Alignment of the proximal promoter CRE-4 site among representative eutherians reveals that the 5′-TGACGCGC-3′ sequence proposed by Kozak et al. (1994) is conserved in the rat, but deviates considerably in the shrew, cow, and human, which are known to express functional BAT (Heaton, 1972; Alexander et al., 1975; Przełecka, 1981). Thus, while the CRE-4 site may play an important role within the murid lineage, it likely does not apply to other eutherians. Similarly, the CCAAT box proposed by Bouillaud et al. (1988) in the rat is highly variable among eutherians (and even among rodents), thus is also unlikely to be a key site for promoter activity. Of the three GCCCCT sites proposed by Yubero et al. (1994), only the two located proximal to exon 1 are conserved, however, to our knowledge transcription factors that bind to these nucleotides have not yet been identified. Overall, the TATA box of the *UCP1* promoter is highly conserved in most eutherians, but does vary in some species. For instance, the shared TACA box variant among the horse, rhino, bats, and panda is interesting given that bats and bears possess discernible BAT (Rowlatt et al., 1971; Thomas et al., 1990). While TATA box variants of the flowering plant *Arabidopsis thaliana*, including the 5′-TACAAAAG-3′ sequence, can still bind the TATA binding protein (TBP) without any structural modifications to the protein, transcription activity levels are substantially (76–85%) lower compared to the 5′-TATAAAAG-3′ sequence (Patikoglou et al., 1999). Considering the high level of TBP conservation among eukaryotes (Peterson et al., 1990), its ability to bind TATA box variants may also apply to mammals. The same T→C transition at the third nucleotide position has been described in the TATA (TACA) box of rabbit uteroglobin with respect to the rat and human, causing a 7-fold reduction in activity when binding to TBP (Klug et al., 1994). However, two other proteins (TATA core factor and TATA palindrome factor) present in uteroglobin-expressing cells bind the TACA box with high efficiency to promote cell specific-expression of the protein (Klug et al., 1994), thus the same possibility may apply to bears,

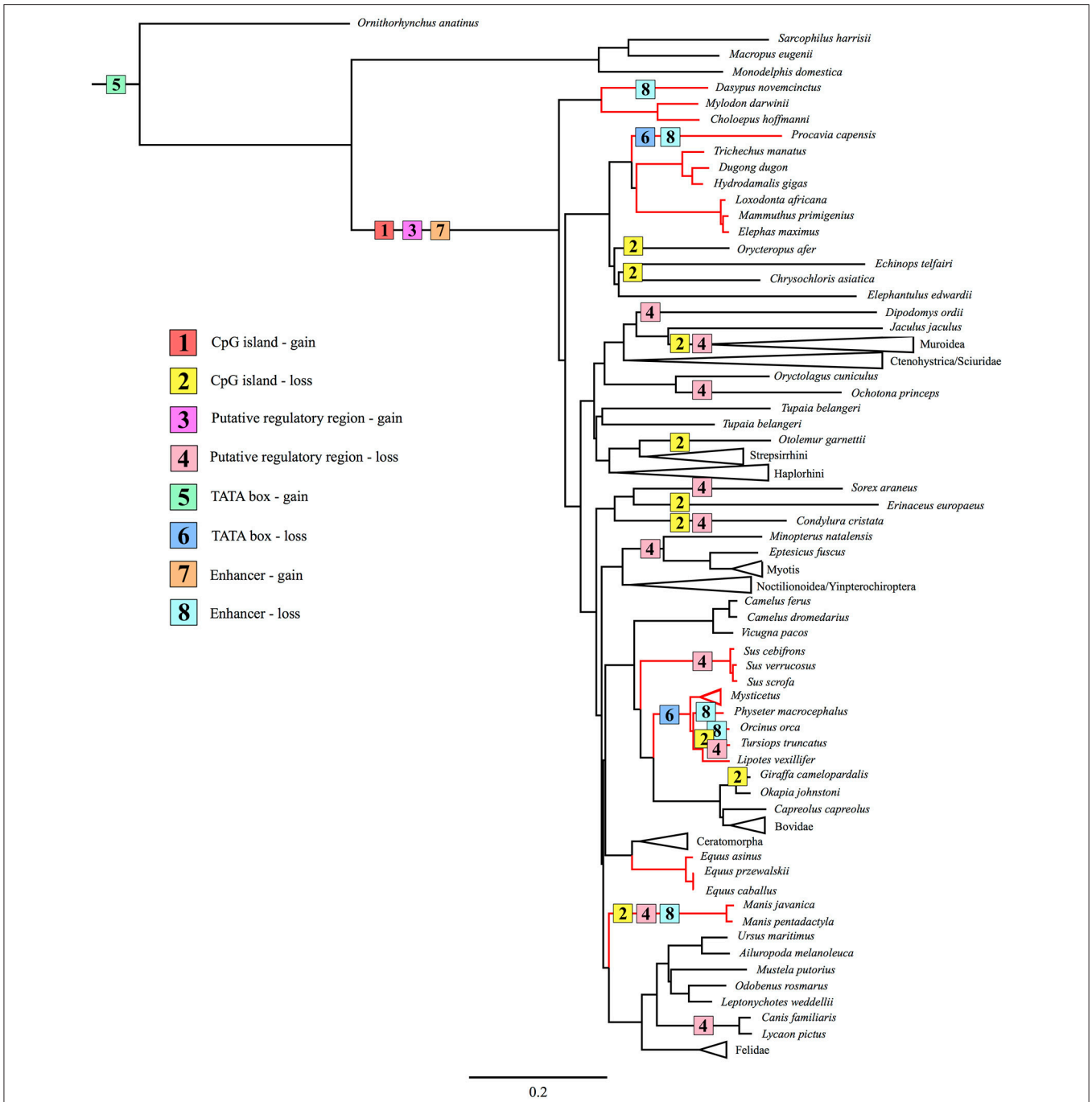

FIGURE 9 | Maximum likelihood species tree based on 41 gene segments (50,911 base pairs) composed of both coding and non-coding regions illustrating the gain and loss of known *UCP1* regulatory elements (CpG island, PRR, TATA box, enhancer) through the evolutionary history of Mammalia. Red branches indicate lineages with a non-functional *UCP1* gene (Gaudry et al., 2017).

bats, and rhinos. The mutated 5′-TAAATAA-3′ site of the walrus retains a high A/T richness and can thus likely still efficiently bind the TBP (Patikoglou et al., 1999). Notably, the TATA boxes of the hyrax and cetacean *UCP1* pseudogenes are poorly conserved, likely due to mutations accumulating under neutral evolution (**Figure 9**).

In general, the *UCP1* enhancer appears to be among the most crucial elements of transcriptional regulation as it is one of the few highly conserved regions in the upstream sequence between humans and rodents (**Figure 6**). Indeed, excluding four species with low sequence coverage (see below), the enhancer was recovered from all eutherians with an intact *UCP1* gene,

and therefore is likely essential for *UCP1* expression in BAT. This conclusion is at odds with that of Shore et al. (2012), who incorrectly deduced that this region was deleted in a number of species. While we were unable to retrieve an enhancer in four species (i.e., European hedgehog, zebu, Brazilian guinea pig, and desert woodrat), contigs of these species either do not extend ∼5 kb upstream of *UCP1* exon 1 or contain large sequencing gaps.

In concert with our prediction that large body size may be associated with relaxed selection pressures for UCP1 expression, several anomalies among putative transcription factor binding motifs exist that could be indicative of degradation of these elements were observed. For instance, rhinoceroses display a deletion within the BRE-2 site, and multiple mutations occur within the dnTRE and NBRE regions of camels and the alpaca (*Vicugna pacos*). However, deletions also occur within these regions of some small-bodied species (Damaraland mole-rat, lesser hedgehog tenrec, and *Myotis* spp. bats) that also have an intact *UCP1*, while felids display a highly divergent nucleotide sequence within this 3′ region of the enhancer box. Overall, it thus seems unlikely that these transcriptional regulatory element mutations would substantively impact *UCP1* expression in the large-bodied species. Notably, *UCP1* regulatory regions (enhancer, PRR, CpG island, promoter) are also present in all large-bodied species (e.g., rhinoceroses, pinnipeds, camel), except the giraffe where a CpG island was not detected (**Table 1**). Again, this finding suggests that the UCP1 protein may be present in BAT and/or beige tissue of these lineages, highlighting the need for future investigation of UCP1 expression in these species.

In support of our hypothesis that transcriptional regulators would be deteriorated or lost in eutherians with *UCP1* pseudogenes, at least five independent lineages (sperm whale, hyrax, pangolins, armadillo, and the family delphinidae [killer whale and bottlenose dolphin]) lack an *UCP1* enhancer (**Figure 9**); notably the TATA box is also lost/mutated in these lineages. By contrast, we identified several lineages (elephantids, sirenians, suids, equids, and some cetaceans) that retain a highly conserved enhancer despite inactivation of their *UCP1* genes >20 MYA (Gaudry et al., 2017). The presence of a conserved enhancer upstream of the pig *UCP1* pseudogene was also noted by Shore et al. (2012), who suggested that an added function might explain its high degree of sequence identity to that of humans. One such added function could be pleiotropy; the regulation multiple genes (He and Zhang, 2006). Indeed, evolutionary constraint increases (i.e., a higher degree of purifying selection) in mammalian enhancers with increasing pleiotropy (Hiller et al., 2012). Considering that pleiotropic enhancers are not uncommon among mammals (Hiller et al., 2012), this hypothesis cannot be entirely discounted. However, the loss of an *UCP1* enhancer in the sperm whale, killer whale, bottlenose dolphin, hyrax, armadillo, and pangolins implies that this enhancer is non-pleiotropic. The apparent conservation of most enhancer elements in the other species for which *UCP1* is pseudogenized (e.g., baleen whales, elephants, sirenians, horses) is presumably in part due to an inherently slow rate of molecular evolution arising from their large body size. Indeed, other pseudogenized genes (e.g., *AMBN*, *AMEL*, *ENAM*, and *MMP20*) in baleen whales and the Steller's sea cow (*H. gigas*) show exceptionally low rates of molecular decay (Meredith et al., 2011; Springer et al., 2015). Consequently the high (>80%) enhancer sequence identity shared between *UCP1*-pseudogenized species (horse, minke whale, pig, baiji, bowhead whale, African elephant, and manatee) and humans is not surprising. It thus also remains possible that slow rates of DNA evolution may explain the retention and conservation of these regulatory elements in some large-bodied species with intact *UCP1* CDS. By contrast, the higher sequence divergence in rats and mice, which share only 69 and 74% of *UCP1* enhancer similarity with humans, respectively, can likely be attributed to a relatively fast mutation rate.

Surprisingly, an elevated mutation rate is also evident in the *UCP1* coding sequence of canids as well as the small-bodied lesser hedgehog tenrec, myomorph rodents, vesper bats, and, particularly within members of the order eulipotyphla (**Figure 8**). While selection pressure analyses indicate that the *UCP1* coding sequences of these species display relatively low dN/dS ratios (<0.22; Gaudry et al., 2017), associated with functional conservation of the protein, the very high substitution rates in these groups equate to a substantively elevated number of non-synonymous amino acid substitutions relative to other eutherian lineages (Figure S1). Notably, these high substitution rates are not found for *UCP2* or *UCP3* sequences of these species (cf. **Figure 1**), suggesting that this is not solely a size-dependent phenomenon. Consequently these lineages provide intriguing comparative opportunities to study functional UCP1 attributes, as BAT-mediated NST is likely crucial for thermoregulation in these lineages.

A key finding of this study is that several transcription factor binding motifs first described in either mice or rats (BRE-1, BRE-2, upTRE, dnTRE) appear to be restricted to this clade of mammals. Other enhancer motifs (URE1, CRE-2, RARE-2, NBRE) presumed to be key for transcription factor binding in murid rodents (Kozak et al., 1994; Rabelo et al., 1996; Sears et al., 1996; Kumar et al., 2008) are also mutated in other eutherian lineages (**Figure 7**). Although both single point mutations (Bokar et al., 1988) or combination of mutations (Rabelo et al., 1996) have been shown to alter transcription factor binding to some of these motifs in murid rodents, the effect of the observed differences to these motifs in other eutherians needs to be assessed. Nonetheless, the rVista enhancer screening (Table S1) demonstrates that a number of putative transcription factor binding elements (e.g., CRE-2, PPARG) are not shared between murid rodents and the consensus sequence. This analysis also suggests that components of the transcriptional control of *UCP1* expression may be differentially regulated among eutherian mammals. For example, the CRE-3 element was identified in each species selected for screening except for the star-nosed mole (Table S1). By contrast, the high level of sequence identity of the PPRE and RARE-3 elements across Placentalia (**Figure 7**) indicates that their function has remained strongly constrained throughout eutherian evolution, and is suggestive that they are universally required for the regulation and specificity of *UCP1* transcription.

CONCLUSIONS

To our knowledge, this study represents the broadest comparative analysis of *UCP1* transcriptional regulatory elements among mammals. Our results demonstrate that the CpG island and PRR are not universally conserved among BAT-expressing eutherians and thus are likely not required for *UCP1* transcription. In contrast, the TATA box and two of the three GCCCCT sites in the promoter are highly conserved and presumably play a transcriptional role, while the CRE-4 and CCAAT sites differ substantially among eutherians and likely are unimportant. While a *UCP1* enhancer was found to be present in every eutherian superorder (Xenarthra [partial], Afrotheria, Laurasiatheria, Euarchontoglires), its absence among non-eutherian mammals supports the hypothesis that it originated with the rise of BAT in a stem placental ancestor. Within this region, however, the specificity and importance of the upTRE, dnTRE, URE1, CRE-2, RARE-2, NBRE, BRE-1, and BRE-2 enhancer elements first described from rats and mice are uncertain as these motifs differ substantially—but generally remain highly conserved—in other BAT-expressing eutherians. Conversely, the RARE-3 and PPRE motifs are among the most highly conserved putative transcription factor binding elements and are likely functional across the eutherian phylogeny. Finally, while some *UCP1*-less species still retain a *UCP1* enhancer, this sequence conservation is presumably due to a slow rate of neutral evolution. Nonetheless, lack of an enhancer in seven *UCP1*-less species strongly suggests this element is non-pleiotropic.

AUTHOR CONTRIBUTIONS

MG conceived of the project, designed research, prepared DNA libraries, performed hybridization capture experiments, conducted sequencing and genome-mining, performed comparative bioinformatic analyses, prepared the figures, interpreted the results, and drafted the manuscript. KC conceived of the project, designed research, interpreted the results, and revised the manuscript.

ACKNOWLEDGMENTS

We thank Eske Willerslev, Rasmus Havmøller, and Tom Gilbert for providing DNA/tissue samples and Mark Springer for providing DNA samples and sequence data for the 41-gene species tree. This study was funded by a National Sciences and Engineering Research Council (NSERC) Discovery Grant (238838) and an NSERC Discovery Accelerator Supplement (412336) to KC.

SUPPLEMENTARY MATERIAL

The Supplementary Material for this article can be found online at: http://journal.frontiersin.org/article/10.3389/fphys.2017.00670/full#supplementary-material

REFERENCES

Alexander, G., Bennett, J. W., and Gemmell, R. T. (1975). Brown adipose tissue in the new-born calf (*Bos taurus*). *J. Physiol.* 244, 223–234. doi: 10.1113/jphysiol.1975.sp010793

Berg, F., Gustafson, U., and Andersson, L. (2006). The uncoupling protein 1 gene (UCP1) is disrupted in the pig lineage: a genetic explanation for poor thermoregulation in piglets. *PLoS Genet.* 2:e129. doi: 10.1371/journal.pgen.0020129

Bianco, A. C., and Silva, J. E. (1987). Optimal response of key enzymes and uncoupling protein to cold inbrown adipose tissue depends on local T_3 generation. *Am. J. Physiol.* 253, E255–E263.

Bokar, J. A., Roesler, W. J., Vandenbark, G. R., Kaetzel, D. M., Hanson, R. W., and Nilson, J. H. (1988). Characterization of the cAMP responsive elements from the genes for the alpha-subunit of glycoprotein hormones and phosphoenolpyruvate carboxykinase (GTP). Conserved features of nuclear protein binding between tissues and species. *J. Biol. Chem.* 263, 19740–19747.

Bouillaud, F., Raimbault, S., and Ricquier, D. (1988). The gene for rat uncoupling protein: complete sequence, structure of primary transcript and evolutionary relationship between exons. *Biochem. Biophys. Res. Commun.* 157, 783–792. doi: 10.1016/S0006-291X(88)80318-8

Brand, M. D., and Esteves, T. C. (2005). Physiological functions of the mitochondrial uncoupling proteins UCP2 and UCP3. *Cell Metab.* 2, 85–93. doi: 10.1016/j.cmet.2005.06.002

Brent, G. A., Moore, D. D., and Larsen, R. P. (1991). Thyroid hormone regulation of gene expression. *Annu. Rev. Physiol.* 53, 17–35. doi: 10.1146/annurev.ph.53.030191.000313

Cannon, B., and Nedergaard, J. (2004). Brown adipose tissue: function and physiological significance. *Physiol. Rev.* 84, 277–359. doi: 10.1152/physrev.00015.2003

Echtay, K. (2007). Mitochondrial uncoupling proteins-What is their physiological role? *Free Radic. Biol. Med.* 43, 1351–1371. doi: 10.1016/j.freeradbiomed.2007.08.011

Edgar, R. C. (2004). MUSCLE: multiple sequence alignment with high accuracy and high throughput. *Nucleic Acids Res.* 19, 1792–1797. doi: 10.1093/nar/gkh340

Gardiner-Garden, M., and Frommer, M. (1987). CpG islands in vertebrate genomes. *J. Mol. Biol.* 196, 261–282. doi: 10.1016/0022-2836(87)90689-9

Gaudry, M. J., Jastroch, M., Treberg, J. R., Hofreiter, M., Paijmans, J. L. A., Starret, J., et al. (2017). Inactivation of thermogenic UCP1 as a historical contingency in multiple placental mammal clades. *Sci. Adv.* 3:e1602878. doi: 10.1126/sciadv.1602878

Harms, M., and Seale, P. (2013). Brown and beige fat: development, function and therapeutic potential. *Nat. Med.* 19, 1252–1263. doi: 10.1038/nm.3361

He, X., and Zhang, J. (2006). Toward a molecular understanding of pleiotropy. *Genetics* 173, 1885–1891. doi: 10.1534/genetics.106.060269

Heaton, J. M. (1972). The distribution of brown adipose tissue in the human. *J. Anat.* 112, 35–39.

Heldmaier, G. (1971). Nonshivering thermogenesis and body size in mammals. *J. Comp. Physiol.* 73, 222–248.

Herpin, P., Damon, M., and Le Dividich, J. (2002). Development of thermoregulation and neonatal survival in pigs. *Livest. Prod. Sci.* 78, 25–45. doi: 10.1016/S0301-6226(02)00183-5

Hiller, M., Schaar, B. T., and Bejerano, G. (2012). Hundreds of conserved non-coding genomic regions are independently lost in mammals. *Nucleic Acids Res.* 40, 11463–11476. doi: 10.1093/nar/gks905

Hughes, D. A., Jastroch, M., Stoneking, M., and Klingenspor, M. (2009). Molecular evolution of UCP1 and the evolutionary history of mammalian non-shivering thermogenesis. *BMC Evol. Biol.* 9:4. doi: 10.1186/1471-2148-9-4

Jastroch, M., Buckingham, J. A., Helwig, M., Klingenspor, M., and Brand, M. D. (2007). Functional characterization of UCP1 in the common carp: uncoupling activity in liver mitochondria and cold-induced expression in

the brain. *J. Comp. Physiol. B Biochem. Syst. Environ. Physiol.* 177, 743–752. doi: 10.1007/s00360-007-0171-6

Jastroch, M., Withers, K. W., Taudien, S., Frappell, P. B., Helwig, M., Fromme, T., et al. (2008). Marsupial uncoupling protein 1 sheds light on the evolution of mammalian nonshivering thermogenesis. *Physiol. Genomics* 32, 161–169. doi: 10.1152/physiolgenomics.00183.2007

Kiskinis, E., Hallberg, M., Christian, M., Olofsson, M., Dilworth, S. M., White, R., et al. (2007). RIP140 directs histone and DNA methylation to silence Ucp1 expression in white adipocytes. *EMBO J.* 26, 4831–4840. doi: 10.1038/sj.emboj.7601908

Klingenspor, M., and Fromme, T. (2012). "Brown adipose tissue," in *Adipose Tissue Biology*, ed M. E. Symonds (New York, NY: Springer), 39–79.

Klingenspor, M., Fromme, T., Hughes, D. A., Manzke, L., Polymeropoulos, E., Riemann, T., et al. (2008). An ancient look at UCP1. *Biochim. Biophys. Acta* 1777, 637–641. doi: 10.1016/j.bbabio.2008.03.006

Klug, J., Knapp, S., Castro, I., and Beato, M. (1994). Two distinct factors bind to the rabbit uteroglobin TATA-box region and are required for efficient transcription. *Mol. Cell. Biol.* 14, 6208–6218. doi: 10.1128/MCB.14.9.6208

Kozak, U. C., Kopecky, J., Teisinger, J., Enerback, S., Boyer, B., and Kozak, L. P. (1994). An upstream enhancer regulating brown-fat-specific expression of the mitochondrial uncoupling protein gene. *Mol. Cell. Biol.* 14, 59–67.

Kumar, N., Liu, D., Wang, H., Robidoux, J., and Collins, S. (2008). Orphan nuclear receptor NOR-1 enhances 3′,5′-cyclic adenosine 5′-monophosphate-dependent uncoupling protein-1 gene transcription. *Mol. Endocrinol.* 22, 1057–1064. doi: 10.1210/me.2007-0464

Lin, J., Cao, C., Tao, C., Ye, R., Dong, M., Zheng, Q., et al. (2017). Cold adaptation in pigs depends on UCP3 in beige adipocytes. *J. Mol. Cell. Biol.* doi: 10.1093/jmcb/mjx018. [Epub ahead of print].

Loots, G., and Ovcharenko, I. (2004). rVista 2.0: evolutionary analysis of transcription factor binding sites. *Nucleic Acids Res.* 32, W217–W221. doi: 10.1093/nar/gkh383

Mailloux, R. J., and Harper, M. E. (2011). Uncoupling proteins and the control of mitochondrial reactive oxygen species production. *Free Radic. Biol. Med.* 51, 1106–1115. doi: 10.1016/j.freeradbiomed.2011.06.022

Mantovani, R. (1999). The molecular biology of the CCAAT-binding factor NF-Y. *Gene* 239, 15–27. doi: 10.1016/S0378-1119(99)00368-6

McGaugh, S., and Schwartz, T. S. (2017). Here and there, but not everywhere: repeated loss of uncoupling protein 1 in amniotes. *Biol. Lett.* 13:20160749. doi: 10.1098/rsbl.2016.0749

McNab, B. K. (1983). Energetics, body size, and the limits to endothermy. *J. Zool.* 199, 1–29. doi: 10.1111/j.1469-7998.1983.tb06114.x

Meredith, R. W., Gatesy, J., Cheng, J., and Springer, M. S. (2011). Pseudogenization of the tooth gene enamelysin (*MMP20*) in the common ancestor of baleen whales. *Proc. Biol. Soc.* 278, 993–1002. doi: 10.1098/rspb.2010.1280

Meyer, M., and Kircher, M. (2010). Illumina sequencing library preparation for highly multiplexed target capture and sequencing. *Cold Spring Harb. Protoc.* 6:Pbdprot5448. doi: 10.1101/pdb.prot5448

Moore, D. I. (1978). Post-glacial vegetation in the South Patagonian territory of the giant ground sloth, Mylodon. *Bot. J. Linean. Soc.* 77, 177–202. doi: 10.1111/j.1095-8339.1978.tb01398.x

Mzilikazi, N., Jastroch, M., Meyer, C. W., and Klingenspor, M. (2007). The molecular and biochemical basis of nonshivering thermogenesis in an African endemic mammal, *Elephantulus myurus*. *Am. J. Physiol. Regul. Integr. Comp. Physiol.* 293, R2120–R2127. doi: 10.1152/ajpregu.00427.2007

Nakajima, N., Horikoshi, M., and Roeder, R. G. (1988). Factors involved in specific transcription by mammalian RNA polymerase II: purification, genetic specificity, and TATA box-promoter interactions of TFIID. *Mol. Cell. Biol.* 8, 4028–4040. doi: 10.1128/MCB.8.10.4028

Oelkrug, R., Goetze, N., Exner, C., Lee, Y., Ganjam, G. K., Kutschke, M., et al. (2013). Brown fat in a protoendothermic mammal fuels eutherian evolution. *Nat. Commun.* 4:2140. doi: 10.1038/ncomms3140

Oelkrug, R., Polymeropoulos, E. T., and Jastroch, M. (2015). Brown adipose tissue: physiological function and evolutionary significance. *J. Comp. Physiol. B Biochem. Syst. Environ. Physiol.* 185, 587–606. doi: 10.1007/s00360-015-0907-7

Patikoglou, G. A., Kim, J. L., Sun, L., Yang, S. H., Kodadek, T., and Burley, S. K. (1999). TATA element recognition by the TATA box-binding protein has been conserved throughout evolution. *Genes Dev.* 13, 3217–3230. doi: 10.1101/gad.13.24.3217

Pearson, L. E., Liwanag, H. E., Hammill, M. O., and Burns, J. M. (2014). To each its own: thermoregulatory strategy varies among neonatal polar phocids. *Comp. Biochem. Physiol. A Mol. Integr. Physiol.* 178, 59–67. doi: 10.1016/j.cbpa.2014.08.006

Pedersen, S. B., Bruun, J. M., Kristensen, K., and Richelsen, B. (2001). Regulation of UCP1, UCP2, and UCP3 mRNA expression in brown adipose tissue, white adipose tissue, and skeletal muscle in rats by estrogen. *Biochem. Biophys. Res. Commun.* 288, 191–197. doi: 10.1006/bbrc.2001.5763

Peterson, M. G., Tanese, N., Pugh, B. F., and Tjian, R. (1990). Functional domains and upstream activation properties of cloned human TATA binding protein. *Science* 248, 1625–1630. doi: 10.1126/science.249.4971.844-b

Polymeropoulos, E. T., Jastroch, M., and Frappell, P. B. (2012). Absence of adaptive nonshivering thermogenesis in a marsupial, the fat-tailed dunnart (*Sminthopsis crassicaudata*). *J. Comp. Physiol. B Biochem. Syst. Environ. Physiol.* 182, 393–401. doi: 10.1007/s00360-011-0623-x

Przełecka, A. (1981). Seasonal changes in ultrastructure of brown adipose tissue in the common shrew (*Sorex araneus L*). *Cell Tissue Res.* 214, 623–632. doi: 10.1007/BF00233501

Rabelo, R., Reyes, C., Schifman, A., and Silva, J. E. (1996). A complex retinoic acid response element in the uncoupling protein gene defines a novel role for retinoids in thermogenesis. *Endocrinology* 137, 3488–3496.

Rabelo, R., Schifman, A., Rubio, A., Sheng, X., and Silva, J. E. (1995). Delineation of thyroid hormone-responsive sequences within a critical enhancer in the rat uncoupling protein gene. *Endocrinology* 136, 1003–1013. doi: 10.1210/endo.136.3.7867554

Rowlatt, U., Mrosovsky, N., and English, A. (1971). A comparative survey of brown fat in the neck and axilla of mammals at birth. *Biol. Neonate* 17, 53–83. doi: 10.1159/000240303

Saito, S., Saito, C. T., and Shingai, R. (2008). Adaptive evolution of the uncoupling protein 1 gene contributed to the acquisition of novel nonshivering thermogenesis in ancestral eutherian mammals. *Gene* 408, 37–44. doi: 10.1016/j.gene.2007.10.018

Sears, I. B., MacGinnitie, M. A., Kovacs, L. G., and Graves, R. A. (1996). Differentiation-dependent expression of the brown adipocyte uncoupling protein gene: regulation by peroxisome proliferator-activated receptor gamma. *Mol. Cell. Biol.* 16, 3410–3419. doi: 10.1128/MCB.16.7.3410

Shore, A., Emes, R. D., Wessely, F., Kemp, P., Cillo, C., D'Armiento, M., et al. (2012). A comparative approach to understanding tissue-specific expression of uncoupling protein 1 expression in adipose tissue. *Front. Genet.* 3:304. doi: 10.3389/fgene.2012.00304

Shore, A., Karamitri, A., Kemp, P., Speakman, J. R., and Lomax, M. A. (2010). Role of UCP1 enhancer methylation and chromatin remodeling in the control of UCP1 expression in murine adipose tissue. *Diabetologia* 51, 1164–1173. doi: 10.1007/s00125-010-1701-4

Springer, M. S., Signore, A. V., Paijmans, J. L., Vélez-Juarbe, J., Domning, D. P., Bauer, C. E., et al. (2015). Interordinal gene capture, the phylogenetic position of Steller's sea cow based on molecular and morphological data, and the macroevolutionary history of Sirenia. *Mol. Phylogenet. Evol.* 91, 178–193. doi: 10.1016/j.ympev.2015.05.022

Stamatakis, A. (2006). RAxML-VI-HPC: maximum likelihood-based phylogenetic analyses with thousands of taxa and mixed models. *Bioinformatics* 22, 2688–2690. doi: 10.1093/bioinformatics/btl446

Sullivan, M. J., Petty, N. K., and Beatson, S. A. (2011). Easyfig: a genome comparison visualizer. *Bioinformatics* 27, 1009–1010. doi: 10.1093/bioinformatics/btr039

Thomas, D. W., Dorais, M., and Bergeron, J. M. (1990). Winter energy budgets and cost of arousals for hibernating little brown bats, *Myotis lucifugus*. *J. Mamm.* 71, 475–479. doi: 10.2307/1381967

Umesono, K., Murakami, K. K., Thompson, C. C., and Evans, R. M. (1991). Direct repeats as selective response elements for the thyroid hormone, retinoic acid, and vitamin D3 receptors. *Cell* 65, 1255–1266. doi: 10.1016/0092-8674(91)90020-Y

Villarroya, F., Peyrou, M., and Giralt, M. (2017). Transcriptional regulation of the uncoupling protein-1 gene. *Biochimie* 134, 86–92. doi: 10.1016/j.biochi.2016.09.017

Wu, J., Boström, P., Sparks, L. M., Ye, L., Choi, J. H., Giang, A. H., et al. (2012). Beige adipocytes are a distinct type of thermogenic fat cell in mouse and human. *Cell* 150, 366–376. doi: 10.1016/j.cell.2012.05.016

Xu, L., Thali, M., and Schaffner, W. (1991). Upstream box/TATA box order is the major determinant of the direction of transcription. *Nucleic Acids Res.* 19, 6699–6704. doi: 10.1093/nar/19.24.6699

Yubero, P., Vinas, O., Iglesias, R., Mampel, T., Villarroya, F., and Giralt, M. (1994). Identification of tissue-specific protein binding domains in the 5'-proximal regulatory region of the rat mitochondrial brown fat uncoupling protein gene. *Biochem. Biophys. Res. Commun.* 204, 867–873. doi: 10.1006/bbrc.1994.2540

Conflict of Interest Statement: The authors declare that the research was conducted in the absence of any commercial or financial relationships that could be construed as a potential conflict of interest.

frontiers in Physiology

GENERAL COMMENTARY
published: 28 November 2017
doi: 10.3389/fphys.2017.00978

Commentary: Evolution of *UCP1* Transcriptional Regulatory Elements Across the Mammalian Phylogeny

*Tobias Fromme**

Molecular Nutritional Medicine, Else Kröner-Fresenius Center for Nutritional Medicine and ZIEL Institute for Food and Health, Technical University of Munich, Freising, Germany

Keywords: uncoupling protein 1, brown adipose tissue, transcriptional regulation, enhancer, evolution, molecular

A commentary on

Evolution of *UCP1* Transcriptional Regulatory Elements Across the Mammalian Phylogeny
by Gaudry, M. J., and Campbell, K. L. (2017). Front. Physiol. 8:670. doi: 10.3389/fphys.2017.00670

Adaptive, non-shivering thermogenesis to defend a warm body temperature in a cold environment is provided by brown adipose tissue, a highly specialized organ of endothermic mammals with immense oxidative capacity. On the molecular level of heat production, all processes converge on the essential, thermogenic uncoupling protein 1 (Ucp1), located in the mitochondrial inner membrane (reviewed in Klingenspor and Fromme, 2012). This unique protein is subject to intense investigation in the fields of thermophysiology, energy metabolism and pharmacology.

The comparative study of orthologous Ucp1 gene sequences has been vital to identify the evolutionary origin as well as crucial sites for the regulation of activity and abundance (Klingenspor et al., 2008). Past hallmark findings include the presence of (non-thermogenic) Ucp1 in ectotherm fish (Jastroch et al., 2005, 2007), a rapid gene evolution on the branch leading to Eutherians (Hughes et al., 2009) and the loss of intact Ucp1 in the pig lineage (Berg et al., 2006; Hou et al., 2017). The field of comparative genetic analysis has been steadily gaining momentum with the ever-growing number of fully or partially available genome sequences. In the case of Ucp1, the development peaked this year in comprehensive analyses of more than a 100 amniote (McGaugh and Schwartz, 2017) or mammalian species (Gaudry et al., 2017) providing a framework for all previous findings. The crucial higher-level pattern appears to be a differential pace of Ucp1 evolution since the advent of eutherians: while taxa with small body size continue to race ahead in adapting their thermogenic core component to intense use, other taxa markedly slowed the rate of amino acid exchanges, probably concomitant to an increase in body mass. The reduced importance of brown adipose tissue thermogenesis in large mammals culminates in pseudogenization or complete loss of Ucp1 in pigs, whales and dolphins as well as horses, elephants and sloths. The significance of body mass and thus volume to surface ratio is illustrated by the presence of Ucp1 and brown fat in newborn large mammals and its dramatic loss during the first months of life (Giralt et al., 1989; Soppela et al., 1991). These observations certainly raise the question whether some large species with seemingly intact coding sequence in fact never express the large amounts of Ucp1 protein required for efficient heat production; essentially a pseudogenization event on the level of transcriptional regulation.

Into this context, Gaudry and Campbell place a similarly comprehensive comparison of known Ucp1 regulatory regions, most prominently the distal and complex Ucp1 enhancer (Gaudry and Campbell, 2017).

Conceptually, the validation of regulatory elements of the Ucp1—or any—gene as identified in one species by verifying conservation in orthologous promoters is not a new idea. The absence of a CpG island in the murine Ucp1 promoter and of the complete enhancer in marsupials, for instance, has been discussed before (Jastroch et al., 2008; Shore et al., 2012). The descriptive power

OPEN ACCESS

Edited by:
Elias T. Polymeropoulos, Institute for Marine and Antarctic Studies (IMAS), Australia

Reviewed by:
P. Trayhurn, University of Liverpool, United Kingdom
Michael E. Symonds, University of Nottingham, United Kingdom

***Correspondence:**
Tobias Fromme
fromme@tum.de

Specialty section:
This article was submitted to Integrative Physiology, a section of the journal Frontiers in Physiology

Received: *03 October 2017*
Accepted: *16 November 2017*
Published: *28 November 2017*

Citation:
Fromme T (2017) Commentary: Evolution of UCP1 Transcriptional Regulatory Elements Across the Mammalian Phylogeny. Front. Physiol. 8:978. doi: 10.3389/fphys.2017.00978

of the present study stems from sheer quantity and this statement should not be misunderstood as derogatory. Conversely, "just some more sequences" here turns out to be decisive to detect higher-order patterns in the first place, to then pinpoint individual aberrations worth inspecting closer. Gaudry and Campbell identify a number of regulatory regions with supposedly established function that seem non-essential for efficient Ucp1 expression in many taxa. Eventually, only the proximal TATA box and the well-known distal enhancer region seem to be universal in the control of intact Ucp1 orthologs and exclusively disrupted in pseudogenes.

The diversity of sequences, both regulatory and coding, as collected and presented by Gaudry and coworkers (Gaudry and Campbell, 2017; Gaudry et al., 2017) as well as earlier by McGaugh and Schwartz (2017) can only be described an *El Dorado* for future comparative studies of Ucp1 transcriptional and protein activity regulation. These promise vital insight into both novel options to manipulate Ucp1 expression and activity therapeutically in humans and into ecotype-specific thermoregulatory strategies. The mentioned publications inspire more questions than they answer and compel to re-think future research avenues. It is in fact even a little anticlimactic that Gaudry and Campbell, with all their expertise and amassed sequences, did not themselves choose to continue into some of the more obvious routes and use their *in silico* tools to discover new regulatory and functional elements in promoter and coding sequence instead of simply corroborating or dismissing known ones. For instance, the marsupial Ucp1 gene may be regulated by a different enhancer region than placental mammals (Li et al., 2014).

In future, the collected coding sequences ought to be functionally analyzed in comparable experimental settings (reviewed in Hirschberg et al., 2011) to discover and explore the consequences of ongoing Ucp1 evolution, e.g. the difference between Ucp1 of hibernating hedgehogs and the closely related non-hibernating moles. Functional analyses of regulatory enhancer and promoter sequences may identify taxon-specific expression strategies and their critical elements, e.g., the role of an alternative TATA box sequence in bats and bears and the consequence of an absent CRE-3 element that is extremely well conserved, except in the starmole. Ucp1 expression levels in brown adipose tissue of as many species as possible will detect possible functional pseudogenes with seemingly intact open reading frame. The restoration of Ucp1 expression in species with pseudogenes as already reported for the pig will be an interesting complementary approach to genetic knock-out strategies (Zheng et al., 2017). Furthermore, closely related species with and without expression of functional Ucp1 may prove crucial models to identify Ucp1-independent mechanisms of non-shivering thermogenesis that are suggested by accumulating evidence (Ukropec et al., 2006; Meyer et al., 2010; Bertholet et al., 2017; Keipert et al., 2017; Nyman et al., 2017).

In hindsight, past research on the Ucp1 gene and promoter serve as an apt example how the study of mice and humans may at times mislead into the interpretation of special cases as apparently general insight. It is comprehensive studies comprising many different species, genuinely and confidently descriptive, that allow for the targeted selection of diverse, specialized non-model organisms for informative comparative, physiological studies (von Praun et al., 2001; Jastroch et al., 2007, 2009; Mzilikazi et al., 2007; Trzcionka et al., 2008; Oelkrug et al., 2013; Laursen et al., 2015). It is to be hoped that the large-scale compilations published this year draw more deserved attention to the Ucp1 gene of little studied species that offer superior discovery potential as compared to popular model organisms.

AUTHOR CONTRIBUTIONS

The author confirms being the sole contributor of this work and approved it for publication.

REFERENCES

Berg, F., Gustafson, U., and Andersson, L. (2006). The uncoupling protein 1 gene (UCP1) is disrupted in the pig lineage: a genetic explanation for poor thermoregulation in piglets. *PLoS Genet.* 2:e129. doi: 10.1371/journal.pgen.0020129

Bertholet, A. M., Kazak, L., Chouchani, E. T., Bogaczynska, M. G., Paranjpe, I., Wainwright, G. L., et al. (2017). Mitochondrial patch clamp of beige adipocytes reveals UCP1-positive and UCP1-negative cells both exhibiting futile creatine cycling. *Cell Metab.* 25, 811–822e814. doi: 10.1016/j.cmet.2017.03.002

Gaudry, M. J., and Campbell, K. L. (2017). Evolution of UCP1 transcriptional regulatory elements across the mammalian phylogeny. *Front. Physiol.* 8:670. doi: 10.3389/fphys.2017.00670

Gaudry, M. J., Jastroch, M., Treberg, J. R., Hofreiter, M., Paijmans, J. L. A., Starrett, J., et al. (2017). Inactivation of thermogenic UCP1 as a historical contingency in multiple placental mammal clades. *Sci. Adv.* 3:e1602878. doi: 10.1126/sciadv.1602878

Giralt, M., Casteilla, L., Viñas, O., Mampel, T., Iglesias, R., Robelin, J., et al. (1989). Iodothyronine 5'-deiodinase activity as an early event of prenatal brown-fat differentiation in bovine development. *Biochem. J.* 259, 555–559.

Hirschberg, V., Fromme, T., and Klingenspor, M. (2011). Test systems to study the structure and function of uncoupling protein 1: a critical overview. *Front. Endocrinol.* 2:63. doi: 10.3389/fendo.2011.00063

Hou, L., Shi, J., Cao, L., Xu, G., Hu, C., and Wang, C. (2017). Pig has no uncoupling protein 1. *Biochem. Biophys. Res. Commun.* 487, 795–800. doi: 10.1016/j.bbrc.2017.04.118

Hughes, D. A., Jastroch, M., Stoneking, M., and Klingenspor, M. (2009). Molecular evolution of UCP1 and the evolutionary history of mammalian non-shivering thermogenesis. *BMC Evol. Biol.* 9:4. doi: 10.1186/1471-2148-9-4

Jastroch, M., Buckingham, J. A., Helwig, M., Klingenspor, M., and Brand, M. D. (2007). Functional characterisation of UCP1 in the common carp: uncoupling activity in liver mitochondria and cold-induced expression in the brain. *J. Comp. Physiol. B. Biochem. Syst. Environ. Physiol.* 177, 743–752. doi: 10.1007/s00360-007-0171-6

Jastroch, M., Withers, K. W., Stoehr, S., and Klingenspor, M. (2009). Mitochondrial proton conductance in skeletal muscle of a cold-exposed marsupial, Antechinus flavipes, is unlikely to be involved in adaptive nonshivering thermogenesis but displays increased sensitivity toward carbon-centered radicals. *Physiol. Biochem. Zool.* 82, 447–454. doi: 10.1086/603631

Jastroch, M., Withers, K. W., Taudien, S., Frappell, P. B., Helwig, M., Fromme, T., et al. (2008). Marsupial uncoupling protein 1 sheds light on the evolution of mammalian nonshivering thermogenesis. *Physiol. Genomics* 32, 161–169. doi: 10.1152/physiolgenomics.00183.2007

Jastroch, M., Wuertz, S., Kloas, W., and Klingenspor, M. (2005). Uncoupling protein 1 in fish uncovers an ancient evolutionary history of

mammalian nonshivering thermogenesis. *Physiol. Genomics* 22, 150–156. doi: 10.1152/physiolgenomics.00070.2005

Keipert, S., Kutschke, M., Ost, M., Schwarzmayr, T., van Schothorst, E. M., Lamp, D., et al. (2017). Long-term cold adaptation does not require FGF21 or UCP1. *Cell Metab,* 26, 437–446 e435. doi: 10.1016/j.cmet.2017.07.016

Klingenspor, M., and Fromme, T. (2012). "Brown adipose tissue," in *Adipose Tissue Biology,* ed M. E. Symonds, Vol. 414 (Heidelberg: Springer), 39–69.

Klingenspor, M., Fromme, T., Hughes, D. A. Jr., Manzke, L., Polymeropoulos, E., Riemann, T., et al. (2008). An ancient look at UCP1. *Biochim. Biophys. Acta* 1777, 637–641. doi: 10.1016/j.bbabio.2008.03.006

Laursen, W. J., Mastrotto, M., Pesta, D., Funk, O. H., Goodman, J. B., Merriman, D. K., et al. (2015). Neuronal UCP1 expression suggests a mechanism for local thermogenesis during hibernation. *Proc. Natl. Acad. Sci. U.S.A.* 112, 1607–1612. doi: 10.1073/pnas.1421419112

Li, Y. G., Lasar, D., Fromme, T., and Klingenspor, M. (2014). White, brite, and brown adipocytes: the evolution and function of a heater organ in mammals. *Can. J. Zool.* 92, 615–626. doi: 10.1139/cjz-2013-0165

McGaugh, S., and Schwartz, T. S. (2017). Here and there, but not everywhere: repeated loss of *uncoupling protein 1* in amniotes. *Biol. Lett.* 13:20160749. doi: 10.1098/rsbl.2016.0749

Meyer, C. W., Willershäuser, M., Jastroch, M., Rourke, B. C., Fromme, T., Oelkrug, R., et al. (2010). Adaptive thermogenesis and thermal conductance in wild-type and UCP1-KO mice. *Am. J. Physiol. Regul. Integr. Comp. Physiol.* 299, R1396–R1406. doi: 10.1152/ajpregu.00021.2009

Mzilikazi, N., Jastroch, M., Meyer, C. W., and Klingenspor, M. (2007). The molecular and biochemical basis of nonshivering thermogenesis in an African endemic mammal, *Elephantulus myurus*. *Am. J. Physiol. Regul. Integr. Comp. Physiol.* 293, R2120–R2127. doi: 10.1152/ajpregu.00427.2007

Nyman, E., Bartesaghi, S., Melin Rydfalk, R., Eng, S., Pollard, C., Gennemark, P., et al. (2017). Systems biology reveals uncoupling beyond UCP1 in human white fat-derived beige adipocytes. *NPJ Syst. Biol. Appl.* 3, 29. doi: 10.1038/s41540-017-0027-y

Oelkrug, R., Goetze, N., Exner, C., Lee, Y., Ganjam, G. K., Kutschke, M., et al. (2013). Brown fat in a protoendothermic mammal fuels eutherian evolution. *Nat. Commun.* 4, 2140. doi: 10.1038/ncomms3140

Shore, A., Emes, R. D., Wessely, F., Kemp, P., Cillo, C., D'Armiento, M., et al. (2012). A comparative approach to understanding tissue-specific expression of uncoupling protein 1 expression in adipose tissue. *Front. Genet.* 3:304. doi: 10.3389/fgene.2012.00304

Soppela, P., Nieminen, M., Saarela, S., Keith, J. S., Morrison, J. N., Macfarlane, F., et al. (1991). Brown fat-specific mitochondrial uncoupling protein in adipose tissues of newborn reindeer. *Am. J. Physiol.* 260(6 Pt 2), R1229–R 1234.

Trzcionka, M., Withers, K. W., Klingenspor, M., and Jastroch, M. (2008). The effects of fasting and cold exposure on metabolic rate and mitochondrial proton leak in liver and skeletal muscle of an amphibian, the cane toad *Bufo marinus*. *J. Exp. Biol.* 211(Pt 12), 1911–1918. doi: 10.1242/jeb.016519

Ukropec, J., Anunciado, R. P., Ravussin, Y., Hulver, M. W., and Kozak, L. P. (2006). UCP1-independent thermogenesis in white adipose tissue of cold-acclimated Ucp1-/- mice. *J. Biol. Chem.* 281, 31894–31908. doi: 10.1074/jbc.M606114200

von Praun, C., Burkert, M., Gessner, M., and Klingenspor, M. (2001). Tissue-specific expression and cold-induced mRNA levels of uncoupling proteins in the *Djungarian hamster*. *Physiol. Biochem. Zool.* 74, 203–211. doi: 10.1086/319665

Zheng, Q., Lin, J., Huang, J., Zhang, H., Zhang, R., Zhang, X., et al. (2017). Reconstitution of UCP1 using CRISPR/Cas9 in the white adipose tissue of pigs decreases fat deposition and improves thermogenic capacity. *Proc. Natl. Acad. Sci. U.S.A.* doi: 10.1073/pnas.1707853114

Conflict of Interest Statement: The author declares that the research was conducted in the absence of any commercial or financial relationships that could be construed as a potential conflict of interest.

frontiers in Physiology

REVIEW
published: 09 November 2017
doi: 10.3389/fphys.2017.00889

Muscle Non-shivering Thermogenesis and Its Role in the Evolution of Endothermy

Julia Nowack, Sylvain Giroud, Walter Arnold and Thomas Ruf*

Department of Integrative Biology and Evolution, Research Institute of Wildlife Ecology, University of Veterinary Medicine, Vienna, Austria

The development of sustained, long-term endothermy was one of the major transitions in the evolution of vertebrates. Thermogenesis in endotherms does not only occur via shivering or activity, but also via non-shivering thermogenesis (NST). Mammalian NST is mediated by the uncoupling protein 1 in the brown adipose tissue (BAT) and possibly involves an additional mechanism of NST in skeletal muscle. This alternative mechanism is based on Ca^{2+}-slippage by a sarcoplasmatic reticulum Ca^{2+}-ATPase (SERCA) and is controlled by the protein sarcolipin. The existence of muscle based NST has been discussed for a long time and is likely present in all mammals. However, its importance for thermoregulation was demonstrated only recently in mice. Interestingly, birds, which have evolved from a different reptilian lineage than mammals and lack UCP1-mediated NST, also exhibit muscle based NST under the involvement of SERCA, though likely without the participation of sarcolipin. In this review we summarize the current knowledge on muscle NST and discuss the efficiency of muscle NST and BAT in the context of the hypothesis that muscle NST could have been the earliest mechanism of heat generation during cold exposure in vertebrates that ultimately enabled the evolution of endothermy. We suggest that the evolution of BAT in addition to muscle NST was related to heterothermy being predominant among early endothermic mammals. Furthermore, we argue that, in contrast to small mammals, muscle NST is sufficient to maintain high body temperature in birds, which have enhanced capacities to fuel muscle NST by high rates of fatty acid import.

Keywords: brown adipose tissue, cold exposure, non-shivering thermogenesis, SERCA, sarcolipin, skeletal muscle, UCP1

OPEN ACCESS

Edited by:
Rebecca Oelkrug, University of Lübeck, Germany

Reviewed by:
Gordon Clifford Grigg, The University of Queensland, Australia
Leslie A. Rowland, Harvard Medical School, United States

****Correspondence:***
Julia Nowack
julia.nowack@vetmeduni.ac.at

Specialty section:
This article was submitted to Integrative Physiology, a section of the journal Frontiers in Physiology

Received: *29 May 2017*
Accepted: *20 October 2017*
Published: *09 November 2017*

Citation:
Nowack J, Giroud S, Arnold W and Ruf T (2017) Muscle Non-shivering Thermogenesis and Its Role in the Evolution of Endothermy. Front. Physiol. 8:889. doi: 10.3389/fphys.2017.00889

INTRODUCTION

The evolution of endothermy is of major interest in the understanding of mammalian and avian radiation. It is often debated when and how the transition from ectothermic reptiles to endothermic mammals and birds occurred. In terms of the underlying ultimate factors leading to the evolution of endothermy, there are currently two dominating hypotheses: The "increased levels of activity" or "aerobic capacity" model (Bennett and Ruben, 1979) and the "parental care" model (Koteja, 2000). In essence, the aerobic capacity model postulates that maximum metabolic rate, a proxy of aerobic capacity and sustained activity, is the target of directional selection. In this model, elevations in basal metabolic rate (BMR) are only a correlated consequence of

increased maximum metabolism. The parental care model, on the other hand, assumes that increased investment into offspring required increased rates of energy assimilation, which led to enhanced function and metabolism of visceral organs. In both models increased aerobic tissue metabolism is accompanied by increased mitochondrial density, increased mitochondrial membrane surface, and elevated enzyme activities (Hulbert and Else, 2000). It has also been proposed that BMR was elevated by increased membrane leakiness caused by the incorporation of polyunsaturated fatty acids (PUFA) (Hulbert and Else, 1999, 2000; Hulbert, 2003, 2005), a view that has been challenged by a comparative study on mammals (Valencak and Ruf, 2007). However, there still may be direct effects of certain PUFA on membrane-bound enzymes that may well affect e.g., seasonal adjustments of metabolism (reviewed in Arnold et al., 2015). While both, birds and mammals, can defend their body temperature (T_b) within the thermoneutral zone by basal metabolism based on the above described processes, the biochemical basis of heat production during cold exposure seems to differ in both groups. Hence, most researchers in the field assume that endothermy among vertebrates was developed twice: once within the bird lineage and once within mammals. A commonly accepted view is that small placental mammals were able to colonize colder habitats because they are able to maintain high T_b even in the cold by producing heat via non-shivering thermogenesis (NST) mediated by the uncoupling protein 1 (UCP1) in brown adipose tissue (BAT) (Chaffee et al., 1975; Foster and Frydman, 1978; Heaton et al., 1978). Birds, on the other hand, lack this mechanism (Emre et al., 2007) and seem to rely on shivering and non-shivering heat production in muscle during cold exposure (Dawson and Carey, 1976; Bicudo et al., 2001). However, BAT and functional UCP1 are not present in all mammalian species. Marsupials, monotremes (Jastroch et al., 2008; Polymeropoulos et al., 2012), and certain placental mammals lack functional BAT (Gaudry et al., 2016). A recent study has shown that mutations inactivating UCP1 have occurred in at least eight of the 18 placental mammal orders (Gaudry et al., 2016), questioning the importance of BAT-mediated NST as the key thermoregulatory component in all placental mammals. The existence of a mechanism of muscular NST has long been suspected, i.e., for marsupials and monotremes (e.g., Nicol et al., 1992; Grigg et al., 2004). While the principle mechanism of uncoupled NST via sarcoplasmatic reticulum Ca^{2+}-ATPase (SERCA) activity was studied and described extensively in rabbits by de Meis et al. (e.g., de Meis, 2001a; de Meis et al., 2005b), the precise mechanism, i.e., the role of sarcolipin (SLN), and its importance for thermoregulation was only recently discovered (Bal et al., 2012, 2016). Importantly, Rowland et al. (2014) suggested that NST in skeletal muscle—which can occur independently of shivering—was the earliest facultative thermogenic mechanism in vertebrates, before evolutionary pressure resulted in the development of a mechanism (UCP1 in BAT) allowing for higher rates of heat production without interference with muscle function. Muscle NST may have evolved earlier than classical UCP1-dependent BAT thermogenesis, which is not a characteristic trait of all endotherms and the transition from ectothermy to endothermy did not depend on BAT. In this review we summarize our current knowledge on muscle-based NST, from here on referred to as muscle NST to distinguish it from UCP1-mediated NST in BAT, and add more evidence to the hypothesis that muscle NST could have been the earliest mechanism of endogenous heat production in vertebrates. We also discuss hypotheses why small placental mammals, despite the existence of muscle NST, additionally evolved UCP1-mediated NST in BAT, and why birds did not.

Abbreviations: ATP, Adenosine triphosphate; BAT, Brown adipose tissue; BMR, Basal metabolic rate; NST, Non-shivering thermogenesis; PUFA, Polyunsaturated fatty acids; RyR, Ryanodine receptor; SLN, Sarcolipin; SERCA, Sarcoplasmatic reticulum Ca^{2+}-ATPase; SR, Sarcoplasmatic reticulum; T_b, Body temperature; UCP1, Uncoupling protein 1; V_{max}, Maximal Velocity.

NON-SHIVERING THERMOGENESIS IN MUSCLE: HOW DOES IT WORK?

The "classical" mechanism of NST in BAT involves the protein UCP1 that facilitates proton leakage across the inner mitochondrial membrane, leading to futile cycling of protons and to heat generation instead of adenosine triphosphate (ATP) production (Nedergaard and Cannon, 1985). Another mechanism of heat production in mammals involves Ca^{2+}-slippage in skeletal muscle cells (myocytes). A seminal study on knockout mice has shown that this form of NST is crucial in supporting the maintenance of high T_b in absence of BAT-mediated NST, and that it is controlled by the protein SLN (Bal et al., 2012). The mechanism of this muscle NST is based on activity of a Ca^{2+}-ATPase, i.e., SERCA, in the sarcoplasmatic reticulum (SR). During muscle contractions SERCA removes Ca^{2+} from the myocyte cytosol (Hasselbach and Makinose, 1961, 1963; Periasamy and Huke, 2001) back into the SR, thereby triggering muscle relaxation before the initiation of the next contraction phase. However, SERCA does not always use the entire energy derived from ATP-hydrolysis to pump Ca^{2+}-ions across the SR membrane, a variable part (between ∼10 and 25 kcal/mol ATP) is released as heat (de Meis, 2002; de Meis et al., 2005b). The partitioning is regulated by the gradient between cytosolic and SR luminal concentrations of Ca^{2+} and the protein SLN (Asahi et al., 2003; Mall et al., 2006). High luminal concentrations of Ca^{2+} uncouple ATP-hydrolysis from Ca^{2+} transport across the SR membrane by causing the release of the two Ca^{2+}-ions bound to SERCA back to the cytoplasmic side of the membrane rather than to the luminal side (reviewed in Mall et al., 2006). Such "slippage" creates an uncoupling of SERCA activity from Ca^{2+} transport into the SR, i.e., no actual transport of Ca^{2+}-ions and converts the energy from ATP-hydrolysis into heat (Asahi et al., 2003; Maurya et al., 2015). This process is fostered by SLN although it is not yet possible to explain the effect of SLN on slippage in molecular terms (Mall et al., 2006). In short, SLN allows ATP hydrolysis to occur but interferes with calcium transport, resulting in the release of calcium back into the cytosol (de Meis, 2001b). This leads to two effects: First heat is produced by SERCA and second, SLN maintains high Ca^{2+} levels in the cytosol, hence activating Ca^{2+}-dependent pathways that

regulate muscle metabolism and mitochondrial activity (Sahoo et al., 2013).

SERCA is expressed in seven different isoforms in mammalian tissues. The most likely ones involved in thermogenesis, due to their expression in skeletal muscle, are SERCA1a (mainly in fast twitch fibers) and possibly SERCA2a (in slow twitch and fast-oxidative fibers) (Periasamy and Kalyanasundaram, 2007). Muscle NST has been mainly studied in SERCA1a, but there is evidence that SERCA2a can also modulate the amount of heat produced during ATP hydrolysis (reviewed in Pant et al., 2016). Another regulator of SERCA, the protein phospholamban, is not involved in thermogenesis (Sahoo et al., 2013; Shaikh et al., 2016). Phospholamban affects the apparent affinity of SERCA for Ca^{2+} but does not affect the maximal velocity (V_{max}) of SERCA Ca^{2+} uptake into SR whereas SLN decreases the V_{max} of SERCA Ca^{2+} transport into SR but does not affect the affinity of SERCA for Ca^{2+}, i.e., can even bind to SERCA at high concentrations of Ca^{2+}. In other words, phospholamban acts as a brake on SERCA activity until it is dissociated by either phosphorylation or by high Ca^{2+} (Shaikh et al., 2016), whereas SLN facilitates heat production by SERCA. Recently, a third regulator of SERCA, myoregulin, has been identified, but to date its role is not well-understood (Anderson et al., 2015). Interestingly, SERCA can also be regulated by the concentration of certain PUFA in the surrounding SR membrane, with very large effects on SERCA activity (Swanson et al., 1989). This may explain the effects of certain dietary PUFA on hibernation (Ruf and Arnold, 2008). For instance, a study on hibernating Syrian hamsters (*Mesocricetus auratus*) has shown that cardiac SERCA activity was enhanced by high n-6 PUFA content in SR phospholipids, allowing them to reach lower T_b, but depressed by high amounts of n-3 PUFA (Giroud et al., 2013). Details on the specific effects of PUFA are reviewed elsewhere (Arnold et al., 2015).

NST via SERCA is of course only one of several different pathways of heat production in skeletal muscle cells (**Figure 1**). First, heat is generated in mitochondria during ATP synthesis since some protons always leak through the inner mitochondrial membrane, rather than through the ATP synthase (Rolfe and Brand, 1997; Clarke et al., 2013). Secondly, heat is generated during ATP hydrolysis in several enzymatic reactions, when the energy released exceeds that required to drive a reaction. This is the case for the ATP utilization by the sodium-potassium pump (Na^+-K^+-ATPase), the myosin-ATPase during muscular work or shivering, and by SERCA. SERCA activity produces up to 25% of the metabolic rate of a resting muscle (Simonides et al., 2001) and thus contributes to elevations of BMR when muscles are enlarged in response to cold (e.g., Vézina et al., 2017). Further heat will be generated by SERCA during both shivering, when Ca^{2+} pumping is coupled to myofibril contraction and when it is uncoupled, i.e., when SERCA serves as a heat generator by slippage of Ca^{2+}-ions. In this case, ATP is cleaved without apparent work and then the ADP produced is phosphorylated by the mitochondria, leading to an increase in oxygen consumption (de Meis, 2001b). Hence mitochondrial oxidative phosphorylation also contributes to muscle-NST. All of these pathways of heat generation may be increased in response to cold exposure, albeit on different time scales. For instance, in cold-adapted rats, the total volume of mitochondria was significantly increased by 37% in the musculus soleus after 3 weeks, increasing the capacity for heat production during oxidation of fuels and ATP synthesis (Buser et al., 1982). Similarly, the total activity of the Na^+-K^+-ATPase can be significantly up-regulated during cold exposure in pigs (Herpin et al., 1987). It seems, however, that this up-regulation is based on the relatively slow process of increasing the enzyme's expression level (Clarke et al., 2013), or changing the fatty acid composition or cholesterol content of the surrounding membrane (Cornelius, 2001). In contrast, the activation of heat generation upon cold exposure by SERCA via SLN should be instantaneous (Bal et al., 2012). Indeed, Suzuki et al. (2007) could demonstrate an increase of heat production in single cells within seconds after experimentally causing influx of extracellular Ca^{2+} (Suzuki et al., 2007). This increase in heat production was suppressed when SERCA activity was specifically blocked (Suzuki et al., 2007). Thus, apart from myofibril contraction, ATP hydrolysis by SERCA apparently is the only mechanism in muscle that can be immediately up-regulated in response to cold.

Heat producing mechanisms that involve SERCA are also known from birds and fishes. In birds there is a profound increase in SERCA activity during cold exposure-similar to muscle NST in mammals (Dumonteil et al., 1993, 1995). Interestingly, SERCA2a remains largely unchanged, whereas SERCA1a increases its level of expression with prolonged acclimatization (Dumonteil et al., 1995). This suggests that in birds, SERCA2a may be primarily involved in shivering thermogenesis in slow-twitch fibres, whereas SERCA1a seems responsible for ATP cleavage during muscle NST in fast-twitch fibers (Dumonteil et al., 1995). In birds, prolonged cold exposure also leads to a 30–50% increase in ryanodine receptors (RyR) (Dumonteil et al., 1995), i.e., the Ca^{2+} channels through which Ca^{2+} is normally released from the SR. Presently it is unclear whether muscle

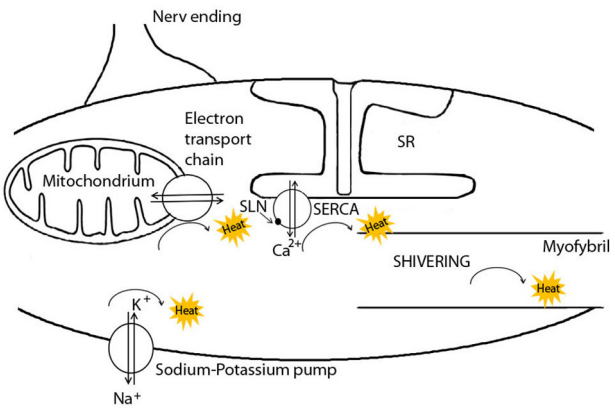

FIGURE 1 | The pathways of heat generation in muscle cells. Non-shivering thermogenesis (NST) in muscle cells is activated by the binding of the peptide sarcolipin (SLN) to the Ca^{2+} ATPase (SERCA), the transmembrane Ca^{2+} pump located in the sarcoplasmatic reticulum (SR) membrane. SLN causes Ca^{2+}-slippage with the sole purpose of heat generation. Heat is also generated by mitochondria, the sodium-potassium pump, and myofibril contraction. For more details see text. Modified after Herpin et al. (2002).

NST in birds also involves Ca^{2+} slippage controlled by SLN. However, the involvement of SLN in muscle NST in birds seem unlikely, since the C-terminus, which appears crucial for the regulation of SERCA (Barbot et al., 2016), has a differing amino acid-sequence (KSYQE/Q instead of RSYQY) (Montigny et al., 2014). Interestingly, a study on ducklings found that muscle NST was correlated to changes in avian UCP, a paralog of the mammalian UCP1, (the UCP1-locus has been lost in birds, Emre et al., 2007), which—in contrast to mammalian UCP1—is not associated with a change in mitochondrial membrane conductance, but involved in muscle thermogenesis. The exact mechanisms are still unclear (Teulier et al., 2010), however, avian UCP expression is restricted to skeletal muscle and its abundance increases under cold-acclimatization (Raimbault et al., 2001).

A form of muscle NST has also at least evolved twice in fishes, as it is found in certain fish species that show regional endothermy like billfish and butterfly mackerel (Block, 1994). The so-called "heater organ," a specialized tissue next to the eyes, derived from muscle, uses futile Ca^{2+} cycling to raise the local temperature by some degrees above that of the surrounding water (in the case of the swordfish up to 15°C), thereby enhancing temporal resolution of vision (Carey, 1982; Fritsches et al., 2005). Although derived from extraocular muscle fibers, cells of the heater organ have lost most of the contractile myofilaments that are characteristic for muscle tissue. Instead, the cells express a modified muscle phenotype with a high mitochondrial and SR content. The latter is enriched in SERCA1a pumps and RyR. These Ca^{2+} channels cause a release of sequestered Ca^{2+} from the SR, whereas SERCA1a pumps it back into the organelle, leading to futile Ca^{2+} cycling and heat production (Block et al., 1994; Morrissette et al., 2003; da Costa and Landeira-Fernandez, 2009). Taken together it seems that the mechanism of muscle NST in mammals, birds and even fish involves ATP hydrolysis by SERCA. However, although SLN is already found in fishes and reptiles (Newman et al., 2013), it is so far not known if it is involved in heat production in these taxa. If this is not the case, the SLN-induced slippage of Ca^{2+}-ions without involvement of the RyR (Mitidieri and de Meis, 1999; Mall et al., 2006) would be an alternative form of thermogenesis restricted to mammals. But at this point, this remains speculation.

Another organ that seems to benefit from local heating is the heart, for which maintaining functionality even at low T_b is most important. SERCA2a is the major isoform in the heart and is primarily involved in Ca^{2+} handling to ensure proper cardiac function. The capability of up-regulating SERCA2a activity, already present in fish, could be crucial for the maintenance of high heart rates and, as a secondary function, also for regional endothermy and therefore could have contributed to the evolution of endothermy and the colonization of cold habitats. Interestingly, gene-expression and protein levels of SERCA2a are increased in the hearts of hibernators in winter compared with those in the non-hibernating season (Yatani et al., 2004; Brauch et al., 2005): A higher density of SERCA2a in the SR membranes accelerates Ca^{2+}-uptake, an adaptation needed to counteract the temperature-dependent (Arrhenius) effect on maximum SERCA activity at low T_b during torpor. The high density of SERCA and the concomitant high amount of hydrolysis of ATP also provides the potential for muscle NST (de Meis, 2002; Andrews, 2007). More evidence for this secondary role of SERCA2a in the heart was collected by Ketzer et al. (2009), who evaluated the contribution of cardiac tissue in rabbits by measuring mitochondrial respiration in permeabilized cardiac muscle and specifically looked into heat produced by Ca^{2+} transport (Ketzer et al., 2009). They found an increase in oxygen consumption and associated heat production during Ca^{2+} transport by cardiac SR after short-term cold exposure. The extra heat produced by the heart under these conditions was mainly derived from both an increase of SERCA2a activity and an enhancement of mitochondrial oxidative phosphorylation. These data suggest that heat production through SERCA2a in cardiac muscles leads to regional endothermy, helping the heart to sustain proper contractions and work load. However, there is no evidence that this local heat production involves SLN and in fact SLN is not expressed in the ventricles of small rodents (Vangheluwe et al., 2005).

IMPORTANCE OF MUSCLE NST IN MAMMALS

Muscle NST in mammals has been known to exist for decades and the biochemical mechanisms involved in muscle NST were studied extensively in the past (e.g., Clausen et al., 1991; Mitidieri and de Meis, 1999; de Meis, 2001b). However this type of NST has been shown only recently to represent an essential source of endogenous heat production that allows mammals to remain euthermic in the cold (Bal et al., 2012), and therefore data on muscle NST in mammals are still scarce (see **Table 1**). Although only clearly confirmed in laboratory strains of mice and rats—species that usually possess functional BAT (Babu et al., 2007; Bal et al., 2012; Pant et al., 2015)—skeletal muscles meet all relevant preconditions to be the site of a ubiquitous heat production mechanism in all endotherms. Skeletal muscle represent the largest fraction of body mass in mammals and birds, and interestingly, are about 30% more massive in mammals than in similar-sized ectothermic reptiles (Ruben, 1995; Rowland et al., 2014). Even more support for the ubiquitous involvement of muscle NST in thermogenesis of mammals comes from studying hibernation. Not all mammals maintain a high T_b throughout the year. So called heterothermic mammals often reduce their energetic demands during challenging periods by using short bouts of torpor or months long hibernation, both characterized by a tremendous reduction of metabolic rate, endogenous heat production and therefore T_b, and inactivity. It has recently been shown that SERCA1a and SLN are significantly reduced during the hibernation season in skeletal muscles of thirteen-lined ground squirrels [*Ictidomys* (formely *Spermophilus) tridecemlineatus*] (Anderson, 2016; Anderson et al., 2016). While this downregulation could be due to reduced muscle function during inactivity, it is surprising that SLN, the regulator of ATP hydrolysis efficiency of SERCA, i.e., the regulator of the amount of heat produced, is also reduced. This

TABLE 1 | Evidence of muscle-based non-shivering thermogenesis in vertebrates.

Taxon	Species	Evidence for muscle NST	References
Fish	Billfish, butterfly mackerel	• No BAT, no thermogenic function of UCP1. • Heater organ- release of sequestered Ca^{2+} from the SR via ryanodine receptors. SERCA1a pumps it back into the organelle, leading to Ca^{2+} cycling and heat production.	Block, 1994; Jastroch et al., 2005
Amphibia	NA	• Not yet investigated.	
Reptilia	Potentially tegu lizards	• No BAT, no thermogenic function of UCP1. • Tegu lizards maintain a T_b of 5–6°C above ambient during the reproductive season and even during the colder night hours, when an increase of T_b via basking is not possible.	Tattersall et al., 2016
Birds	Several species	• No BAT, no UCP1. • A release of sequestered Ca^{2+} from the SR via ryanodine receptors. SERCA1a pumps it back into the organelle, leading to Ca^{2+} cycling and heat production.	Dumonteil et al., 1995
Mammals			
Monotremata	Anecdotal evidence for echidnas	• No BAT, no evidence for thermogenic UCP1; • Speculations about alternative rewarming mechanism from torpid states.	e.g., Grigg et al., 1992, 2004; Nicol et al., 1992
Marsupialia	NA	• No BAT, no thermogenic function of UCP1; speculations about alternative rewarming mechanism from torpid states.	e.g., Nicol et al., 1992; Grigg et al., 2004
Placentalia	Found in rodents, lagomorpha; strong evidence for pigs	• BAT and thermogenic function of UCP1 in most species; • Evidence of sarcolipin-regulated muscle NST in mice and rats (in addition to UCP1/BAT); • Downregulated sarcolipin gene expression in thirteen-lined ground squirrels. • Muscle NST via SERCA found in rabbits; • Likely in piglets- increasing thermogenic capacity in piglets, while at the same time shivering is decreasing.	Berthon et al., 1994, 1996; de Meis, 2001a,b; de Meis et al., 2005b; Babu et al., 2007; Bal et al., 2012, 2016; Anderson, 2016; Anderson et al., 2016; Pant et al., 2016

could suggest that the reduced expression of SLN is rather correlated to an actively down-regulation of metabolic rate to save energy, which in turn would indicate that muscle NST plays an important role in the thermogenesis and energy expenditure of ground squirrels.

Although SLN is only expressed in amounts likely to small to have a measurable effect on thermogenesis in mice with intact BAT/UCP1 (Butler et al., 2015), SLN has been proven to be important for maintenance of endothermy when NST in BAT is not possible (Bal et al., 2012). Interestingly, both mechanisms of NST—UCP1-mediated as well as muscle NST—can compensate for the loss of one system, while double-knockout mice without UCP1 and SLN are unable to survive during prolonged cold exposure, indicating that at least one of the two mechanisms is pivotal to maintain endothermy (Rowland et al., 2015). Furthermore, studies on the significance of muscle NST in UCP1-knockout mice, as well as BAT-ablated mice have shown that the efficiency of muscle NST can be increased with long-term exposure to mild cold (4°C), while shivering thermogenesis is reduced (Rowland et al., 2015; Bal et al., 2016). It is generally assumed that BAT is the principal site of NST in small cold-adapted mammals, but this notion is challenged by the finding of compensation of UCP1/BAT-dysfunction by muscle NST, although it is questionable whether UCP1-knockout mice can actually maintain their T_b at ambient temperatures below 4°C. Furthermore, a recent study has shown that UCP1-inactivating mutations have occurred in at least eight of the 18 placental mammalian orders, mainly larger-bodied species (Gaudry et al., 2016), suggesting that at least large species do not depend on UCP1-mediated NST in BAT.

A commonly shared view suggests that the thermogenic evolution of UCP1 has occurred after the divergence between placentals and marsupials (Saito et al., 2008). Interestingly, UCP1 orthologs have been identified in non-placental mammals, as well as in fish (Jastroch et al., 2005, 2008), but UCP1 has a unique function in placentals in that it is necessary for H^+-driven NST in BAT (Hughes et al., 2009). This is consistent with the fact that all studies looking into UCP1-mediated NST and the presence of BAT in marsupials and monotremes, which diverged from placental and marsupials even earlier, so far failed to find clear evidence for UCP1-mediated NST (Nicol, 1978; McNab and Wright, 1987; Hayward and Lisson, 1992; Nicol et al., 1997; Opazo et al., 1999; Rose et al., 1999; Kabat et al., 2003; but see: Polymeropoulos et al., 2012). Although the mechanism of NST in marsupials and monotremes remains elusive, it has often been speculated that an UCP1-independent mechanism of NST must exists in both groups (e.g., Nicol et al., 1992; Grigg et al., 2004). Anecdotal evidence of a hibernating echidna retrieved from its hibernaculum at a T_b of about 13°C showed that the individual rewarmed to about 18°C without any visible signs of shivering or muscular movement except for occasional very slow movements of the limbs and body, before body twitches and shivering were observed above 18°C (Grigg et al., 1992). On the first glance the idea that muscle NST might be important for rewarming from torpor contradicts the earlier finding of low SLN gene expression throughout

the hibernation season in ground squirrels (Anderson, 2016). However, ground squirrels have functional UCP1 and BAT and therefore no need to rely on muscle NST during arousals. Interestingly, monotremes and marsupials, which, although inhabiting generally warmer areas, can also be found in habitats with temperate climate and coldish winter temperatures, have lower resting T_b than placental mammals. Monotremes consist of the aquatic platypus (*Ornithorhynchus anatinus*) and terrestrial echidnas (*Tachyglossidae*). The short-beaked echidna (*Tachyglossus aculeatus*), which is the only of the echidna species we have sufficient knowledge on, has a modal T_b of about 32°C with daily amplitudes of 2–5°C and an often labile T_b that rises as a result of activity and declines during inactivity (Grigg et al., 2004). Furthermore, echidnas often enter torpid states, thereby allowing their T_b to drop to levels as low as ambient. Resting T_bs of small-sized marsupials are ranging between 32 and 35°C (Geiser, 2004) and most small-bodied marsupials are known to regularly enter torpor (Geiser and Körtner, 2010). Furthermore, some marsupials, such as antechinus (a very small, nocturnal mouse-like marsupial), are highly susceptible to develop hypothermia when cold stressed, although they are able to undergo torpor and regulate the decrease in T_b (Geiser, 1988). Thus, it seems that in the case of very small species the lack of BAT may indeed be associated with increased difficulties dealing with cold conditions.

IF MUSCLE NST WAS SUFFICIENT, WHY DID UCP1-MEDIATED THERMOGENESIS IN BAT EVOLVE?

If the anecdotal reference by Grigg et al. (1992) reported above is supported by future studies demonstrating muscle NST in monotrenes or marsupials, this would mean that NST in skeletal muscle is more ancient than NST in BAT. The existence of two mechanisms of NST, a likely more ancient mechanism in muscle and the later evolved mechanism of short-circuiting the proton gradient in BAT, leads to the question about the selective advantage associated with the latter. Speculations about the ultimate reasons for the evolution of UCP1 mediated thermogenesis in BAT include various scenarios: In addition to the hypothesis that this mechanism enabled animals to colonize colder habitats that we already mentioned above, speculations include (1) defense against the natural cold stress of birth (Cannon and Nedergaard, 2004), (2) enabling a high T_b for periods of parental care (Oelkrug et al., 2013), (3) incompatibility of locomotor performance and muscle NST (Rowland et al., 2014), and (4) rapid arousal from torpor as well as decreasing the energetic costs of rewarming from torpor (Oelkrug et al., 2011). Below, we reevaluate these hypotheses in the light of the existence of muscle NST.

It has been hypothesized that UCP1 mediated thermogenesis in BAT evolved as a defense of the cold stress of birth (Cannon and Nedergaard, 2004), when mammals leave the warm body of the mother and have to cope with considerably lower outside temperatures. Could muscle NST be not sufficient for thermoregulatory demands of neonates? Even in larger species, neonates have high demands of thermogenesis. They lose more heat than the bigger adults because of their large surface area to volume ratio and have less insulation. Interestingly, SLN expression is high in newborn mice and rats - two species that have muscle as well as UCP1-mediated NST - and is usually down-regulated during neonatal development (Babu et al., 2007; Pant et al., 2015); however, continuous cold exposure can prevent this down-regulation, leading to an increased thermogenic capacity (Pant et al., 2015). Another interesting taxon in this context are pigs. Both wild and domestic pigs lack BAT (Trayhurn et al., 1989) and the UCP1-mediated NST capacity (Berg et al., 2006), and piglets are known to have poor thermoregulatory capacities at birth (postnatal hypothermia) (Kammersgaard et al., 2011). It is assumed that pigs lost UCP1 function and the ability to use BAT for thermoregulation because of absent or only weak selection for this mechanism in a warm climate, arguably because it will be energetically costly to produce large amounts of this 32 KD protein (Berg et al., 2006). All Suidae species except the wild boar, *Sus scrofa*, live only in tropical or subtropical habitats. To cope with adverse thermal conditions in northern habitats, wild boar apparently evolved compensatory mechanisms like larger adult body size (Vetter et al., 2015), building insulating nests for offspring, and synchronizing reproduction within social groups, enabling piglets to huddle in large groups of combined litters (Graves, 1984; Berg et al., 2006). Nevertheless, piglet mortality is still high and often attributed to thermoregulatory problems (Herpin et al., 2002), which could be due to the lack of BAT. However, there is evidence that while cold-induced shivering intensity decreases, simultaneously measured metabolic rate (i.e., heat production) increases (Berthon et al., 1994). This change in the ratio between shivering and metabolic rate leads to a >five-fold apparent improvement of shivering efficiency (Berthon et al., 1994). We hypothesize that the enhancement of thermogenesis in piglets is actually due to an increasing contribution of SERCA-based Ca^{2+} slippage in skeletal muscles. Importantly, this would mean that muscle NST and shivering can occur at the same time. A recent study found that in rather cold-tolerant breeds of domestic pigs, UCP3—a paralog of UCP1 found in so called beige cells, which manifested after cold exposure and showed a similar heat production potential as BAT—has a thermoregulatory function (Lin et al., 2017). However, this mechanism is not found in all pig breeds, i.e., non-detectable in cold-sensitive pigs. Blockage of shivering did not lead to a significant drop in T_b in cold-resistant pigs, suggesting that those breeds possess a heat production mechanism other than shivering (Lin et al., 2017). Because blocking the Ca^{2+} release through the RyR-receptors also did not change T_b, the authors concluded that this mechanism cannot involve muscle NST via SERCA. However, muscle NST via SLN works independent of the activity of the RyR receptor (de Meis et al., 2005a). Furthermore, there is increasing evidence that UCP3 and UCP2 do not exhibit uncoupling function like UCP1 under physiological conditions (Trenker et al., 2007; Graier et al., 2008). The notion that muscle NST can indeed produce high amounts of heat and therefore may well play a role in piglet thermoregulation is supported by a pathological condition called malignant hyperthermia or porcine stress syndrome, as was

already pointed out earlier by Rowland et al. (2014). Porcine stress syndrome is due to a mutation in the RyR in the SR, which leads to a massive release of Ca^{2+} into the cytoplasma, causing increased SERCA activity and heat generation (MacLennan and Phillips, 1992).

The second hypothesis suggesting that UCP1-mediated thermogenesis in BAT evolved because it enabled high T_b for parental care (Oelkrug et al., 2013) is challenged by the recent finding of tegu lizards (*Salvator merianae*, formerly *Tupinambis merianae*) that maintain high T_b during the reproductive season, despite a lack of BAT. Even during the colder night hours, when an increase of T_b via basking is not possible, T_b is maintained 5–6°C above ambient (Tattersall et al., 2016). Although not fully understood yet the observed increase in T_b is correlated with an increase in heart rate and suggests that heat is produced by endogenous NST (Tattersall et al., 2016). As reptiles do not possess BAT and muscle NST has been found in mammals and birds, which have evolved from reptilian ancestors, we hypothesize that these lizards also use a similar mechanism likely involving SERCA. Similarly, short beaked-echidnas lacking BAT show more stable and high T_b throughout incubation (Beard and Grigg, 2000; Nicol and Andersen, 2006).

An obvious question to consider with respect to muscle-NST is whether this type of thermogenesis can occur simultaneously with, or only in the absence of shivering. The biochemical mechanisms of both modes of thermogenesis do not seem to exclude either possibility. Once SLN induces slippage of Ca^{2+} from SERCA, this means Ca^{2+} ions are captured by SERCA from the sarcoplasma, which is followed by ATP cleavage and heat generation, and by the release of two Ca^{2+} back to the sarcoplasma. Hence, there is thermogenesis without actual transport of Ca^{2+} into the SR, and no requirement for Ca^{2+} release by RyR following nervous system induced sarcolemmal and T-tubule depolarization, which would lead to muscle contraction (de Meis et al., 2005a). Also, it is easy to envision that a cyclic capture and release of Ca^{2+} by SERCA at the SR membrane may not cause changes in sarcoplasmatic Ca^{2+} levels that cause muscle contractions. Gaining deeper insights into this question is certainly interesting for future research, but presently it seems that both scenarios are possible. For instance, the observations of Grigg et al. (1992) on rewarming echidnas would indicate pure muscle NST at lower T_bs, while shivering is only occurring later. The data on piglets discussed above (Berthon et al., 1994), on the other hand, suggest that muscle NST, i.e., heat production that is not proportional to fiber contraction intensity, and shivering thermogenesis are not mutually exclusive. Indeed we see no mechanistic, biochemical reason why they should be. This raises the question whether muscle NST in fact is only possible during muscle activity. This seems unlikely, however, as Bal et al. (2012) found clear evidence for muscle NST in mice in which shivering was chemically blocked. Further, measurements of heat production in SR vesicles at a physiological temperature of 35°C also do not support this possibility (Mitidieri and de Meis, 1999). In these studies heat production was in fact maximal at Ca^{2+} concentrations similar to that found in the cytosol of a relaxed muscle fiber (1 μM) and decreased as the Ca^{2+} concentration was raised to a level similar to that found in the cytosol during muscle contraction (∼10 μM). Conversely Inesi and Tadini-Buoninsegni (2014) have argued that the buildup of high concentrations of Ca^{2+} in the SR lumen, a prerequisite for slippage, is too slow to occur during a muscle relaxation and that cytosolic Ca^{2+} levels during relaxation would be too low to activate SERCA1a activity. These conclusions were based, however, on the kinetics of Ca^{2+} accumulation and SERCA1a activity in vesicles studied at 25°C, a temperature that is well-known to inhibit SERCA1a activity, at least in vesicles obtained from highly homoeothermic rabbits (de Meis et al., 2005b). Thus, we conclude that the preponderance of the current evidence indicates that muscle NST may occur both during muscle contraction and muscle relaxation, but certainly, further studies on this question seem highly desirable. Even if muscle NST may occur during shivering, it seems conceivable that constant Ca^{2+} cycling at the SERCA domain during slippage might interfere with and hamper highly coordinated rapid muscle contraction and relaxation during locomotion. Thus, especially small animals with relatively high cold loads may have difficulties to reconcile muscle NST with controlled locomotor activity and foraging. Among other factors (see below) this may be one of the selective advantages of a separate thermogenic tissue, namely BAT, which does not interfere with muscle contraction; but the degree of impairment of locomotion by muscle NST remains to be investigated. In this context, Rowland et al. (2014) have suggested that the predominance of fast-type skeletal muscles in rodents, which have high amounts of BAT, may have disfavored the use of muscle NST. This is because fast-type muscles, although they contain large amounts of SERCA1a, which should facilitate muscle NST, rely on glycolytic pathways for ATP production, whereas slow or intermediate types rely predominantly on oxidative metabolism. Therefore, Rowland et al. (2014) have argued that skeletal muscles with more oxidative fibers, where muscle-based NST would probably occur, may be favored in large mammals. However, despite their large fraction of fast-twitch fibers, even small rodents make use of muscle NST. As demonstrated by Jensen et al. (2008) enhanced muscle NST in transgenic mice, which have increased capacity for muscular fatty acid uptake, was accompanied by an increase in oxidative fibers. Further, Pant et al. (2015) recently found that the down-regulation of muscle NST in fast twitch skeletal muscles of neonatal mice could be prevented by cold acclimation. Thus, the fiber type composition of skeletal muscles in small mammals is flexible and can be adjusted to thermoregulatory requirements. Currently, there are, however, insufficient studies on a large enough range of species of different size to obtain a clear picture of the impact of body mass on muscle NST capacity.

The term endothermy is often taken to imply a pattern of homeothermic endothermy, i.e., birds and mammals that maintain a less fluctuating and fairly constant T_b over various conditions. However, many endothermic mammals and birds are actually abandoning homeothermy during challenging periods and undergo heterothermic phases during which they reduce T_b and metabolic rate in a state of torpor (Ruf and Geiser, 2015). Up to date at least 214 species of heterothermic mammals and

birds have been identified (Ruf and Geiser, 2015) and it is now widely accepted that heterothermy is a plesiomorphic, ancient trait from which homeothermy has evolved (Grigg et al., 2004; Lovegrove, 2012). The mammalian ancestor was likely a small, nocturnal insectivorous animal that regularly used torpor (Luo et al., 2011; O'Leary et al., 2013). In placental heterotherms UCP1 plays an important role during rewarming from torpor (Nedergaard and Cannon, 1984). A study on UCP1-ablated mice has shown that although the lack of UCP1-mediated NST does not impair the expression of a full torpor bout (i.e., entry, maintenance, and rewarming), rewarming rates were about 50% lower and energetic costs were about 60% higher in UCP1-ablated than in wild-type individuals (Oelkrug et al., 2011). However, the mice were kept at warm conditions prior to the experiment, which prevents the cold-induced increase of muscle NST reported in later studies (Bal et al., 2016). Therefore, animals likely had to primarily rely on shivering thermogenesis and were not able to use muscle NST for rewarming. It would be interesting to see if cold acclimatization of animals prior to the experiment would lead to a differing result. Nevertheless, these data suggest that uncoupling of the proton gradient in BAT might have evolved to allow for a more rapid arousal and reduced energetic costs for rewarming, because slow rewarming increases the time spent at high metabolic rates (Oelkrug et al., 2011). If UCP1-ablated mice have lower rewarming rates this should also be the case for monotremes and marsupials. Indeed, studies report a comparatively low rewarming rate (about 50% lower than the similar sized marmot) in the monotreme echidnas (Geiser and Baudinette, 1990; Nicol et al., 2009) even though the echidnas were rewarming from about 7°C warmer minimum T_bs, and T_b (as well as T_a) is known to affect rewarming rates (Geiser et al., 1986; Geiser and Baudinette, 1987). Unfortunately, there is no comprehensive comparison between rewarming rates of marsupiala and placentalia that also take into account differences in T_a and T_b. Among known heterothermic mammals, i.e., those undergoing daily torpor or hibernation, only six species of marsupials and monotremes are hibernators (18.8%) and show minimum T_bs below 6°C (range: 1.3–5.9°C (Ruf and Geiser, 2015), whereas at least 87 (62.6%) heterothermic placental mammal species hibernate and, in contrast to marsupials and monotremes, can reduce their T_b to below zero degrees. These subzero T_bs are known from at least eight species (Ruf and Geiser, 2015), e.g., −2.9°C in the arctic ground squirrel [*Urocitellus* (formely *Spermophilus) parryii*) (Barnes, 1989)]. Low tissue temperatures pose a problem because of Arrhenius effects, i.e., the cold-induced retardation of maximum enzyme activities. These Arrhenius effects may hamper, or at least significantly slow down, rewarming to euthermia. Theoretically, this problem could be overcome by local heating of a small thermogenic tissue, i.e., the autocatalysis of heat generating processes as the tissue warms itself. This is one of the properties of BAT and therefore BAT is likely not only increasing the speed of arousals from torpor, but was also important for rewarming from torpor at low T_bs. Even if the temperatures at earth were warmer at the time of BAT evolution, animals will still have experienced daily and yearly fluctuations, similar to daily fluctuations in tropical habitats seen today. In contrast to skeletal muscle, BAT is small, mainly found between the shoulder blades and around the heart, and even in small mammals does not exceed 5% of body mass (Smith and Horwitz, 1969). Not surprisingly then, the local heating of BAT can be even detected by thermal imaging of skin (e.g., Symonds et al., 2012). In comparison, simply due to total heat capacity, using the same amount of energy for thermogenesis in skeletal muscles, which typically have a mass of 30–40% of body mass, in some species up to 50% (Hoppeler and Flück, 2002), would result in much smaller elevations of tissue temperature. Arguably then, the evolution of BAT was especially beneficial for heterothermic placental mammals, as it allowed them to tolerate lower levels of T_b as a result of the enormous reduction of metabolic rate during hibernation and torpor (Ruf and Geiser, 2015). This likely enhanced adaptive radiation of placental mammals and their ability to overwinter in the north-temperate and arctic zones. These are climates that are significantly colder than those inhabited by marsupials and monotremes, among which a preference for warm habitats (ranging from rainforests to deserts) is an ancestral trait (Mitchell et al., 2014; Oelkrug et al., 2015).

HOW CAN BIRDS BE HIGHLY ENDOTHERMIC WITHOUT BAT?

If the evolution of BAT indeed facilitated the use of hibernation, the lack of BAT in birds may help to explain why there is only a single bird species known to truly hibernate (Jaeger, 1949; Woods and Brigham, 2004), although a number of birds show shallow daily torpor (Ruf and Geiser, 2015). This suggests that the bird thermoregulatory phenotype, compared with the typical small mammal, is characterized by a high degree of homeothermy, little heterothermy, and high exercise performance. Given their lack of BAT, it seems surprising then that muscle NST, or a combination of muscle NST and shivering, is sufficient to allow many birds to maintain very high (42°C) T_b even during cold exposure. Goldfinches will become hypothermic within a few minutes after cold exposure in summer, but can withstand temperatures of −70°C for hours in winter (Dawson and Carey, 1976). In cold-acclimated ducklings skeletal-muscles were identified as the major site of NST (Duchamp and Barre, 1993). The fact that muscle NST seems more efficient in birds might be partially related to the better insulation of feathers in comparison with mammalian hair (Aschoff, 1981). While birds can decrease their conductance enormously during cold exposure due the air trapped in the rigid feather structure, mammalian hair is softer and less suitable to trap air as an insulation barrier (McNab, 1966).

However, we suggest that there is another main reason for a lack of selective advantages of a BAT-like tissue in birds, which—to our knowledge—has never been considered before: skeletal muscles in birds already reach metabolic rates that are at least twice as high as in exercising small mammals, and can be as high as 8–18 times BMR (Butler et al., 1998; Videler, 2005). The rate-limiting step causing this difference between mammals and birds is the much greater capacity of avian skeletal

muscles to take up circulating fatty acids (reviewed in Jenni-Eiermann, 2017). In contrast to mammals, endurance muscular work in birds can in fact be fueled to 95% by energy derived from lipids, and the use of this energy-dense fuel may have first evolved as an adaptation to energy-demanding flight. It seems logical then that placental mammals, possessing BAT, would much benefit from enhanced fatty acid import, compared with skeletal muscle cells. This is indeed ensured by the function of lipoprotein lipase, which, along with other enzymes, allows the massive import of fatty acids into BAT during thermogenesis at significantly higher rates than into skeletal muscle cells of placental mammals (Heldmaier et al., 1999; Townsend and Tseng, 2014). Interestingly, when the capacity of fatty acid import into muscle cells was increased by overexpression of lipoprotein lipase in transgenic mice, this improved cold resistance—independent from BAT thermogenesis—and elevated muscular fatty acid oxidation (Jensen et al., 2008). As noted by Jensen et al. (2008) this clearly reflects a shift toward "an avian phenotype". Arguably, these differences in fuel import capacity into thermogenic tissues may well-explain the absence of BAT in birds, as well as the lower thermogenic capacity of marsupials and monotremes.

CONCLUSIONS

In summary, it seems that muscle NST may have been an important step in the evolution of endothermy. Endothermy is clearly facilitated by increasing mitochondrial membrane surface (Else and Hulbert, 1981) and activity of the sodium-potassium pump, which is the greatest contributor to BMR (Clarke et al., 2013). However, apart from shivering, muscle NST via SERCA ATP hydrolysis was probably the first metabolic pathway in mammals solely used for thermogenesis. By comparison, UCP1-mediated NST in BAT seems to represent a mere "booster" of endothermy and is heavily employed only by small placental mammals, that is, by less than 20% of all endothermic mammal and bird species. A prominent role of skeletal muscle function in the evolution of endothermy, which is not only the activation of thermogenesis in response to cold load but also the static elevation of resting metabolic rates, would be expected by the above mentioned "aerobic capacity" model (Bennett and Ruben, 1979). Interestingly, after mixed support for this model from smaller studies over the last decades, strong evidence for the aerobic capacity model comes from a recent comprehensive phylogenetically informed study ranging from fish and amphibians to birds and mammals, which shows that there is in fact a positive correlation between maximum and resting metabolic rates in mammals, and that this pattern is a result of natural selection (Nespolo et al., 2017). These findings again point to an important role of enhanced muscle function and metabolism for the emergence of endothermy.

One of the reasons why the importance of muscle NST may have been underestimated in the past (but see, e.g., de Meis, 2001a; Grigg, 2004) is that it can be "masked" by shivering, which may well occur simultaneously (Berthon et al., 1994, 1996). There is no reason to assume that muscle NST and shivering are mutually exclusive as only part of the total SERCA activity may lead to Ca^{2+} cycling, and another part to the relaxation of myofibril contractions. In contrast, activation of UCP1-mediated NST occurs prior to the onset of shivering (Böckler and Heldmaier, 1983) which makes it easier to identify as a separate mechanism. However, even NST in BAT can also occur simultaneously with shivering thermogenesis (Böckler and Heldmaier, 1983). Arguably then, the evolution of endothermy was not characterized by switches from one to another, possibly improved, metabolic pathway. Instead it seems that increasing levels of endothermy were achieved by recruiting additional mechanisms of thermogenesis to muscular work during locomotion, including specialized shivering thermogenesis, increases in mitochondrial density and membrane leakage, increases in sodium-potassium pump activity, shifts in SERCA activity toward NST. Highly endothermic mammals living in cold environments apparently can use all of these mechanisms simultaneously.

There are several possible selective advantages to this last evolutionary step, the additional recruitment of UCP1-mediated NST. As already pointed out previously (Rowland et al., 2014) there may be a trade-off between fast muscle contraction and muscle NST caused by conflicting needs for fast glycolytic and slow oxidative muscle fibers, respectively. In addition, we suggest that in contrast to shivering thermogenesis, voluntary muscle contraction as needed for coordinated locomotion and foraging may be actually incompatible with Ca^{2+}slippage. Further, we suggest that the evolution of BAT in addition to muscle NST was related to heterothermy being predominant among early endothermic mammals. This is because, in comparison with large muscles, a small dedicated thermogenic tissue such as BAT is much more suited to rapidly warm up and escape limiting Arrhenius effects of low tissue temperature during hibernation and torpor in harsh habitats. Finally, we argue that additional mechanisms for NST are not required by animals that have enhanced capacities to fuel muscle NST by high rates of fatty acid import. Such a group of endotherms are birds, which probably evolved this superior fuel transport capacity as an adaptation to flight. This would explain why birds have high endothermic capacities, despite the absence of BAT.

AUTHOR CONTRIBUTIONS

JN wrote the first draft of the manuscript. All authors added text, discussed, and edited the manuscript.

FUNDING

Financial support was given from the Humboldt Foundation to JN.

REFERENCES

Anderson, D. M., Anderson, K. M., Chang, C.-L., Makarewich, C. A., Nelson, B. R., McAnally, J. R., et al. (2015). A micropeptide encoded by a putative long non-coding RNA regulates muscle performance. *Cell* 160, 595–606. doi: 10.1016/j.cell.2015.01.009

Anderson, K. J. (2016). *Multi-Omic Analysis of Hibernator Skeletal Muscle and Regulation of Calcium Handling.* Master of Science MSc thesis, University of Minnesota.

Anderson, K. J., Vermillion, K. L., Jagtap, P., Johnson, J. E., Griffin, T. J., and Andrews, M. T. (2016). Proteogenomic analysis of a hibernating mammal indicates contribution of skeletal muscle physiology to the hibernation phenotype. *J. Proteome Res.* 15, 1253–1261. doi: 10.1021/acs.jproteome.5b01138

Andrews, M. T. (2007). Advances in molecular biology of hibernation in mammals. *Bioessays* 29, 431–440. doi: 10.1002/bies.20560

Arnold, W., Giroud, S., Valencak, T. G., and Ruf, T. (2015). Ecophysiology of omega fatty acids: a lid for every jar. *Physiology* 30, 232–240. doi: 10.1152/physiol.00047.2014

Asahi, M., Sugita, Y., Kurzydlowski, K., De Leon, S., Tada, M., Toyoshima, C., et al. (2003). Sarcolipin regulates sarco(endo)plasmic reticulum Ca^{2+}-ATPase (SERCA) by binding to transmembrane helices alone or in association with phospholamban. *Proc. Natl. Acad. Sci. U.S.A.* 100, 5040–5045. doi: 10.1073/pnas.0330962100

Aschoff, J. (1981). Thermal conductance in mammals and birds: its dependence on body size and crcadian phase. *Comp. Biochem. Physiol. Part A Physiol.* 69, 611–619. doi: 10.1016/0300-9629(81)90145-6

Babu, G. J., Bhupathy, P., Carnes, C. A., Billman, G. E., and Periasamy, M. (2007). Differential expression of sarcolipin protein during muscle development and cardiac pathophysiology. *J. Mol. Cell. Cardiol.* 43, 215–222. doi: 10.1016/j.yjmcc.2007.05.009

Bal, N. C., Maurya, S. K., Singh, S., Wehrens, X. H., and Periasamy, M. (2016). Increased reliance on muscle-based thermogenesis upon acute minimization of brown adipose tissue function. *J. Biol. Chem.* 291, 17247–17257. doi: 10.1074/jbc.M116.728188

Bal, N. C., Maurya, S. K., Sopariwala, D. H., Sahoo, S. K., Gupta, S. C., Shaikh, S. A., et al. (2012). Sarcolipin is a newly identified regulator of muscle-based thermogenesis in mammals. *Nat. Med.* 18, 1575–1579. doi: 10.1038/nm.2897

Barbot, T., Montigny, C., Decottignies, P., le Maire, M., Jaxel, C., Jamin, N., et al. (2016). "Functional and structural insights into sarcolipin, a regulator of the sarcoendplasmic reticulum $Ca2^{+}$-ATPase," in *Regulation of $Ca2^{+}$-ATPases, V-ATPases and F-ATPases, Advances in Biochemestry in Health and Disease 14,* eds S. Chakraborti and N. S. Dhalla (Cham: Springer), 153–186.

Barnes, B. M. (1989). Freeze avoidance in a mammal: body temperatures below 0°C in an arctic hibernator. *Science* 244, 1593–1595. doi: 10.1126/science.2740905

Beard, L., and Grigg, G. C. (2000). Reproduction in the short-beaked echidna, *Tachyglossus aculeatus*: field observations at an elevated site in South-east Queensland. *Proc. Linn. Soc. New South Wale* 122, 89–99.

Bennett, A. F., and Ruben, J. A. (1979). Endothermy and activity in vertebrates. *Science* 206, 649–654. doi: 10.1126/science.493968

Berg, F., Gustafson, U., and Andersson, L. (2006). The uncoupling protein 1 gene (*UCP1*) is disrupted in the pig lineage: a genetic explanation for poor thermoregulation in piglets. *PLoS Genet.* 2:e129. doi: 10.1371/journal.pgen.0020129

Berthon, D., Herpin, P., Bertin, R., De Marco, F., and le Dividich, J. (1996). Metabolic changes associated with sustained 48-hr shivering thermogenesis in the newborn pig. *Comp. Biochem. Physiol. Part B Biochem. Mol. Biol.* 114, 327–335. doi: 10.1016/0305-0491(96)00044-2

Berthon, D., Herpin, P., and Le Dividich, J. (1994). Shivering thermogenesis in the neonatal pig. *J. Thermal Biol.* 19, 413–418. doi: 10.1016/0306-4565(94)90040-X

Bicudo, J. E., Vianna, C. R., and Chaui-Berlinck, J. G. (2001). Thermogenesis in birds. *Biosci. Rep.* 21, 181–188. doi: 10.1023/A:1013648208428

Block, B. A. (1994). Thermogenesis in muscle. *Annu. Rev. Physiol.* 56, 535–577. doi: 10.1146/annurev.ph.56.030194.002535

Block, B. A., O'Brien, J., and Meissner, G. (1994). Characterization of the sarcoplasmic reticulum proteins in the thermogenic muscles of fish. *J. Cell Biol.* 127, 1275–1287. doi: 10.1083/jcb.127.5.1275

Böckler, H., and Heldmaier, G. (1983). Interaction of shivering and non-shivering thermogenesis during cold exposure in seasonally-acclimatized Djungarian hamsters (*Phodopus sungorus*). *J. Thermal Biol.* 8, 97–98. doi: 10.1016/0306-4565(83)90084-0

Brauch, K. M., Dhruv, N. D., Hanse, E. A., and Andrews, M. T. (2005). Digital transcriptome analysis indicates adaptive mechanisms in the heart of a hibernating mammal. *Physiol. Genomics* 23, 227–234. doi: 10.1152/physiolgenomics.00076.2005

Buser, K. S., Kopp, B., Gehr, P., Weibel, E. R., and Hoppeler, H. (1982). Effect of cold environment on skeletal muscle mitochondria in growing rats. *Cell Tissue Res.* 225, 427–436. doi: 10.1007/BF00214693

Butler, J., Smyth, N., Broadbridge, R., Council, C. E., Lee, A. G., Stocker, C. J., et al. (2015). The effects of sarcolipin over-expression in mouse skeletal muscle on metabolic activity. *Arch. Biochem. Biophys.* 569, 26–31. doi: 10.1016/j.abb.2015.01.027

Butler, P. J., Woakes, A. J., and Bishop, C. M. (1998). Behaviour and physiology of Svalbard barnacle geese *Branta leucopsis* during their autumn migration. *J. Avian Biol.* 29, 536–545. doi: 10.2307/3677173

Cannon, B., and Nedergaard, J. (2004). Brown adipose tissue: function and physiological significance. *Physiol. Rev.* 84, 277–359. doi: 10.1152/physrev.00015.2003

Carey, F. (1982). A brain heater in the swordfish. *Science* 216, 1327–1329. doi: 10.1126/science.7079766

Chaffee, R. R., Allen, J. R., Arine, R. M., Fineg, A. J., Rochelle, R. H., and Rosander, J. (1975). Studies on thermogenesis in brown adipose tissue in temperature-acclimated *Macaca mulatta*. *Comp. Biochem. Physiol. Part A Physiol.* 50, 303–306. doi: 10.1016/0300-9629(75)90017-1

Clarke, R. J., Catauro, M., Rasmussen, H. H., and Apell, H.-J. (2013). Quantitative calculation of the role of the Na^{+},K^{+}-ATPase in thermogenesis. *Biochim. Biophys. Acta* 1827, 1205–1212. doi: 10.1016/j.bbabio.2013.06.010

Clausen, T., Van Hardeveld, C., and Everts, M. E. (1991). Significance of cation transport in control of energy metabolism and thermogenesis. *Physiol. Rev.* 71, 733–774.

Cornelius, F. (2001). Modulation of Na,K-ATPase and Na-ATPase activity by phospholipids and cholesterol. I. steady-state kinetics. *Biochemistry* 40, 8842–8851. doi: 10.1021/bi010541g

da Costa, D. C. F., and Landeira-Fernandez, A. M. (2009). Thermogenic activity of the Ca^{2+}-ATPase from blue marlin heater organ: regulation by KCl and temperature. *Am. J. Physiol. Regul. Integr. Comp. Physiol.* 297, R1460–R1468. doi: 10.1152/ajpregu.90993.2008

Dawson, W., and Carey, C. (1976). Seasonal acclimatization to temperature in cardueline finches. *J. Comp. Physiol. A* 112, 317–333. doi: 10.1007/BF00692302

de Meis, L. (2001a). Role of the sarcoplasmic reticulum Ca^{2+}-ATPase on heat production and thermogenesis. *Biosci. Rep.* 21, 113–137. doi: 10.1023/A:1013640006611

de Meis, L. (2001b). Uncoupled ATPase activity and heat production by the sarcoplasmic reticulum Ca^{2+}-ATPase. Regulation by ADP. *J. Biol. Chemi.* 276, 25078–25087. doi: 10.1074/jbc.M103318200

de Meis, L. (2002). Ca^{2+}-ATPases (SERCA): energy transduction and heat production in transport ATPases. *J. Membr. Biol.* 188, 1–9. doi: 10.1007/s00232-001-0171-5

de Meis, L., Arruda, A., and Carvalho, D. (2005a). Role of sarco/endoplasmic reticulum Ca^{2+}-ATPase in thermogenesis. *Biosci. Rep.* 25, 181–190. doi: 10.1007/s10540-005-2884-7

de Meis, L., Oliveira, G. M., Arruda, A. P., Santos, R., Madeiro Da Costa, R., and Benchimol, M. (2005b). The thermogenic activity of rat brown adipose tissue and rabbit white muscle Ca2+-ATPase. *IUBMB Life* 57, 337–345. doi: 10.1080/15216540500092534

Duchamp, C., and Barre, H. (1993). Skeletal muscle as the major site of nonshivering thermogenesis in cold-acclimated ducklings. *Am. J. Physiol.* 265, R1076–R1083.

Dumonteil, E., Barré, H., and Meissner, G. (1993). Sarcoplasmic reticulum $Ca(^{2+})$-ATPase and ryanodine receptor in cold-acclimated ducklings and thermogenesis. *Am. J. Physiol. Cell Physiol.* 265, C507–C513.

Dumonteil, E., Barre, H., and Meissner, G. (1995). Expression of sarcoplasmic reticulum Ca^{2+} transport proteins in cold-acclimating ducklings. *Am. J. Physiol. Cell Physiol.* 269, C955–C960.

Else, P. L., and Hulbert, A. J. (1981). Comparison of the "mammal machine" and the "reptile machine": energy production. *Am. J. Physiol. Regul. Integr. Comp. Physiol.* 240, R3–R9.

Emre, Y., Hurtaud, C., Ricquier, D., Bouillaud, F., Hughes, J., and Criscuolo, F. (2007). Avian UCP: the killjoy in the evolution of the mitochondrial uncoupling proteins. *J. Mol. Evol.* 65, 392–402. doi: 10.1007/s00239-007-9020-1

Foster, D. O., and Frydman, M. L. (1978). Nonshivering thermogenesis in the rat. II. Measurements of blood flow with microspheres point to brown adipose tissue as the dominant site of the calorigenesis induced by noradrenaline. *Canadian J. Physiol. Pharmacol.* 56, 110–122. doi: 10.1139/y78-015

Fritsches, K. A., Brill, R. W., and Warrant, E. J. (2005). Warm eyes provide superior vision in swordfishes. *Curr. Biol.* 15, 55–58. doi: 10.1016/j.cub.2004.12.064

Gaudry, M. J., Jastroch, M., Treberg, J. R., Hofreiter, M., Paijmans, J. L. A., Starett, J., et al. (2016). Inactivation of thermogenic UCP1 as a historical contingency in multiple placental mammal clades. *bioRxiv*. doi: 10.1101/086819

Geiser, F. (1988). Daily torpor and thermoregulation in antechinus (Marsupialia): influence of body mass, season, development, reproduction, and sex. *Oecologia* 77, 395–399. doi: 10.1007/BF00378050

Geiser, F. (2004). Metabolic rate and body temperature reduction during hibernation and daily torpor. *Annu. Rev. Physiol.* 66, 239–274. doi: 10.1146/annurev.physiol.66.032102.115105

Geiser, F., and Baudinette, R. V. (1987). Seasonality of torpor and thermoregulation in three dasyurid marsupials. *J. Comp. Physiol. B* 157, 335–344. doi: 10.1007/BF00693360

Geiser, F., and Baudinette, R. V. (1990). The relationship between body mass and rate of rewarming from hibernation and daily torpor in mammals. *J. Exp. Biol.* 151, 349–359.

Geiser, F., Baudinette, R. V., and McMurchie, E. J. (1986). Seasonal changes in the critical arousal temperature of the marsupial *Sminthopsis crassicaudata* correlate with the thermal transition in mitochondrial respiration. *Cell. Mol. Life Sci.* 42, 543–547. doi: 10.1007/BF01946695

Geiser, F., and Körtner, G. (2010). Hibernation and daily torpor in Australian mammals. *Aust. Zool.* 35, 204–215. doi: 10.7882/AZ.2010.009

Giroud, S., Frare, C., Strijkstra, A., Boerema, A., Arnold, W., and Ruf, T. (2013). Membrane phospholipid fatty acid composition regulates cardiac SERCA activity in a hibernator, the Syrian hamster (*Mesocricetus auratus*). *PLOS ONE* 8:e63111. doi: 10.1371/journal.pone.0063111

Graier, W. F., Trenker, M., and Malli, R. (2008). Mitochondrial Ca^{2+}, the secret behind the function of uncoupling proteins 2 and 3? *Cell Calcium* 44, 36–50. doi: 10.1016/j.ceca.2008.01.001

Graves, H. B. (1984). Behavior and ecology of wild and feral swine (*Sus scrofa*). *J. Anim. Sci.* 58, 482–492. doi: 10.2527/jas1984.582482x

Grigg, G. C., Beard, L. A., and Augee, M. L. (2004). The evolution of endothermy and its diversity in mammals and birds. *Physiol. Biochem. Zool.* 77, 982–997. doi: 10.1086/425188

Grigg, G. C. (2004). "An evolutionary framework for studies of hibernation and short-term torpor," in *Life in the Cold 2004: The Twelfth International Hibernation Symposium (LITC 2004)*, eds B. M. Barnes and H. V. Carey (Fairbanks, AK: Institute of Arctic Biology; University of Alaska), 131–141.

Grigg, G. C., Augee, M. L., and Beard, L. A. (1992). "Thermal relations of free-living echidnas during activity and in hibernation in a cold climate," in *Platypus and Echidnas,* ed M. Augee (Chipping Norton, NSW: Roy. Zool. Soc.), 160–173.

Hasselbach, W., and Makinose, M. (1961). Die Calciumpumpe der Erschlaffungsgrana des Muskels und ihre Abhängigkeit von der ATPSpaltung. *Biochem. Z.* 333, 518–528.

Hasselbach, W., and Makinose, M. (1963). Über den Mechanismus des Calciumtransports durch die Membranen des sarcoplasmatischen Reticulums. *Biochem. Z.* 339, 94–111.

Hayward, J. S., and Lisson, P. A. (1992). Evolution of brown fat: its absence in marsupials and monotremes. *Can. J. Zool.* 70, 171–179. doi: 10.1139/z92-025

Heaton, G. M., Wagenvoord, R. J., Kemp, A. J., and Nicholls, D. G. (1978). Brown-adipose-tissue mitochondria: photoaffinity labelling of the regulatory site of energy dissipation. *Eur. J. Biochem.* 82, 515–521. doi: 10.1111/j.1432-1033.1978.tb12045.x

Heldmaier, G., Klingenspor, M., Werneyer, M., Lampi, B. J., Brooks, S. P., and Storey, K. B. (1999). Metabolic adjustments during daily torpor in the Djungarian hamster. *Am. J. Physiol. Endocrinol. Metabol.* 276, E896–E906.

Herpin, P., Damon, M., and Le Dividich, J. (2002). Development of thermoregulation and neonatal survival in pigs. *Livestock Product. Sci.* 78, 25–45. doi: 10.1016/S0301-6226(02)00183-5

Herpin, P. R., McBride, B. W., and Bayley, H. S. (1987). Effect of cold exposure on energy metabolism in the young pig. *Can. J. Physiol. Pharmacol.* 65, 236–245. doi: 10.1139/y87-042

Hoppeler, H., and Flück, M. (2002). Normal mammalian skeletal muscle and its phenotypic plasticity. *J. Exp. Biol.* 205, 2143–2152.

Hughes, D. A., Jastroch, M., Stoneking, M., and Klingenspor, M. (2009). Molecular evolution of UCP1 and the evolutionary history of mammalian non-shivering thermogenesis. *BMC Evol. Biol.* 9:4. doi: 10.1186/1471-2148-9-4

Hulbert, A. J. (2003). Life, death and membrane bilayers. *J. Exp. Biol.* 206, 2303–2311. doi: 10.1242/jeb.00399

Hulbert, A. J. (2005). On the importance of fatty acid composition of membranes for aging. *J. Theor. Biol.* 234, 277–288. doi: 10.1016/j.jtbi.2004.11.024

Hulbert, A. J., and Else, P. L. (1999). Membranes as possible pacemakers of metabolism. *J. Theor. Biol.* 199, 257–274. doi: 10.1006/jtbi.1999.0955

Hulbert, A. J., and Else, P. L. (2000). Mechanisms underlying the cost of living in animals. *Annu. Rev. Physiol.* 62, 207–235. doi: 10.1146/annurev.physiol.62.1.207

Inesi, G., and Tadini-Buoninsegni, F. (2014). Ca^{2+}/H^{+} exchange, lumenal Ca^{2+} release and Ca^{2+}/ATP coupling ratios in the sarcoplasmic reticulum ATPase. *J. Cell Commun. Signal.* 8, 5–11. doi: 10.1007/s12079-013-0213-7

Jaeger, E. C. (1949). Further observations on the hibernation of the poor-will. *Condor* 51, 105–109. doi: 10.2307/1365104

Jastroch, M., Withers, K. W., Taudien, S., Frappell, P. B., Helwig, M., Fromme, T., et al. (2008). Marsupial uncoupling protein 1 sheds light on the evolution of mammalian nonshivering thermogenesis. *Physiol. Genomics* 32, 161–169. doi: 10.1152/physiolgenomics.00183.2007

Jastroch, M., Wuertz, S., Kloas, W., and Klingenspor, M. (2005). Uncoupling protein 1 in fish uncovers an ancient evolutionary history of mammalian nonshivering thermogenesis *Physiol. Genomics* 22, 150–156. doi: 10.1152/physiolgenomics.00070.2005

Jenni-Eiermann, S. (2017). Energy metabolism during endurance flight and the post-flight recovery phase. *J. Comp. Physiol. A* 203, 431–438. doi: 10.1007/s00359-017-1150-3

Jensen, D. R., Knaub, L. A., Konhilas, J. P., Leinwand, L. A., MacLean, P. S., and Eckel, R. H. (2008). Increased thermoregulation in cold-exposed transgenic mice overexpressing lipoprotein lipase in skeletal muscle: an avian phenotype? *J. Lipid Res.* 49, 870–879. doi: 10.1194/jlr.M700519-JLR200

Kabat, A. P., Rose, R. W., and West, A. K. (2003). Non-shivering thermogenesis in a carnivorous marsupial, *Sarcophilus harrisii*, the the absence of UCP1. *J. Thermal Biol.* 28, 413–420. doi: 10.1016/S0306-4565(03)00026-3

Kammersgaard, T. S., Pedersen, L. J., and Jørgensen, E. (2011). Hypothermia in neonatal piglets: interactions and causes of individual differences. *J. Anim. Sci.* 89, 2073–2085. doi: 10.2527/jas.2010-3022

Ketzer, L. A., Arruda, A. P., Carvalho, D. P., and de Meis, L. (2009). Cardiac sarcoplasmic reticulum Ca^{2+}-ATPase: heat production and phospholamban alterations promoted by cold exposure and thyroid hormone. *Am. J. Physiol. Heart Circul. Physiol.* 297, H556–H563. doi: 10.1152/ajpheart.00302.2009

Koteja, P. (2000). Energy assimilation, parental care and the evolution of endothermy. *Proc. R. Soc. Lond. Ser B Biol. Sci.* 267, 479–484. doi: 10.1098/rspb.2000.1025

Lin, J., Cao, C., Tao, C., Ye, R., Dong, M., Zheng, Q., et al. (2017). Cold adaptation in pigs depends on UCP3 in beige adipocytes. *J. Mol. Cell Biol.* doi: 10.1093/jmcb/mjx018. [Epub ahead of print].

Lovegrove, B. G. (2012). The evolution of endothermy in Cenozoic mammals: a plesiomorphic-apomorphic continuum. *Biol. Rev.* 87, 128–162. doi: 10.1111/j.1469-185X.2011.00188.x

Luo, Z.-X., Yuan, C.-X., Meng, Q.-J., and Ji, Q. (2011). A Jurassic eutherian mammal and divergence of marsupials and placentals. *Nature* 476, 442–445. doi: 10.1038/nature10291

MacLennan, D., and Phillips, M. (1992). Malignant hyperthermia. *Science* 256, 789–794. doi: 10.1126/science.1589759

Mall, S., Broadbridge, R., Harrison, S. L., Gore, M. G., Lee, A. G., and East, J. M. (2006). The presence of sarcolipin results in increased heat production by Ca^{2+}-ATPase. *J. Biol. Chem.* 281, 36597–36602. doi: 10.1074/jbc.M606869200

Maurya, S. K., Bal, N. C., Sopariwala, D. H., Pant, M., Rowland, L. A., Shaikh, S. A., et al. (2015). Sarcolipin is a key determinant of the basal metabolic rate, and its overexpression enhances energy expenditure and resistance against diet-induced obesity. *J. Biol. Chem.* 290, 10840–10849. doi: 10.1074/jbc.M115.636878

McNab, B. K. (1966). An analysis of the body temperatures of birds. *Condor* 68, 47–55. doi: 10.2307/1365174

McNab, B. K., and Wright, P. C. (1987). Temperature regulation and oxygen consumption in the Philippine tarsier *Tarsius syrichta*. *Physiol. Zool.* 60, 596–600. doi: 10.1086/physzool.60.5.30156133

Mitchell, K. J., Pratt, R. C., Watson, L. N., Gibb, G. C., Llamas, B., Kasper, M., et al. (2014). Molecular phylogeny, biogeography, and habitat preference evolution of marsupials. *Mol. Biol. Evol.* 31, 2322–2330. doi: 10.1093/molbev/msu176

Mitidieri, F., and de Meis, L. (1999). Ca^{2+} release and heat production by the endoplasmic reticulum Ca^{2+}-ATPase of blood platelets: effect of the platelet activating factor *J. Biol. Chem.* 274, 28344–28350. doi: 10.1074/jbc.274.40.28344

Montigny, C., Decottignies, P., Le Maréchal, P., Capy, P., Bublitz, M., Olesen, C., et al. (2014). S-Palmitoylation and S-Oleoylation of rabbit and pig sarcolipin. *J. Biol. Chem.* 289, 33850–33861. doi: 10.1074/jbc.M114.590307

Morrissette, J. M., Franck, J. P. G., and Block, B. A. (2003). Characterization of ryanodine receptor and Ca^{2+} -ATPase isoforms in the thermogenic heater organ of blue marlin (*Makaira nigricans*). *J. Exp. Biol.* 206, 805–812. doi: 10.1242/jeb.00158

Nedergaard, J., and Cannon, B. (1984). Preferential utilization of brown adipose tissue lipids during arousal from hibernation in hamsters. *Am. J. Physiol. Regul. Integr. Comp. Physiol.* 247, R506–R512.

Nedergaard, J., and Cannon, B. (1985). [^{3}H]GDP binding and thermogenin amount in brown adipose tissue mitochondria from cold-exposed rats. *Am. J. Physiol. Cell Physiol.* 248, C365–C371.

Nespolo, R. F., Solano-Iguaran, J. J., and Bozinovic, F. (2017). Phylogenetic analysis supports the aerobic-capacity model for the evolution of endothermy. *Am. Nat.* 189, 13–27. doi: 10.1086/689598

Newman, S. A., Mezentseva, N. V., and Badyaev, A. V. (2013). Gene loss, thermogenesis, and the origin of birds. *Ann. N. Y. Acad. Sci.* 1289, 36–47. doi: 10.1111/nyas.12090

Nicol, S. C. (1978). Non-shivering thermogenesis in the potoroo, *Potorous tridactylus* (Kerr). *Comp. Biochem. Physiol. Part C Comp. Pharmacol.* 59, 33–37. doi: 10.1016/0306-4492(78)90008-4

Nicol, S. C., and Andersen, N. A. (2006). Body temperature as an indicator of egg-laying in the echidna, *Tachyglossus aculeatus*. *J. Thermal Biol.* 31, 483–490. doi: 10.1016/j.jtherbio.2006.05.001

Nicol, S. C., Andersen, N. A., Arnold, W., and Ruf, T. (2009). Rewarming rates of two large hibernators: comparison of a monotreme and a eutherian. *J. Thermal Biol.* 34, 155–159. doi: 10.1016/j.jtherbio.2009.01.003

Nicol, S. C., Andersen,N. A., and Mesch, U. (1992). "Metabolic rate and ventilation pattern in the echidna during hibernation and arousal," in *Platypus and Echidnas*, ed M. L. Augee (Chipping Norton, NSW: Roy. Zool. Soc.), 150–159.

Nicol, S. C., Pavlides, D., and Andersen, N. A. (1997). Nonshivering thermogenesis in marsupials: absence of thermogenic response to β3-Adrenergic agonists. *Comp. Biochem. Physiol. Part A Physiol.* 117, 399–405. doi: 10.1016/S0300-9629(96)00357-X

O'Leary, M. A., Bloch, J. I., Flynn, J. J., Gaudin, T. J., Giallombardo, A., Giannini, N. P., et al. (2013). The placental mammal ancestor and the post–K-Pg radiation of placentals. *Science* 339, 662–667. doi: 10.1126/science.1229237

Oelkrug, R., Goetze, N., Exner, C., Lee, Y., Ganjam, G. K., Kutschke, M., et al. (2013). Brown fat in a protoendothermic mammal fuels eutherian evolution. *Nat. Commun.* 4:2140. doi: 10.1038/ncomms3140

Oelkrug, R., Heldmaier, G., and Meyer, C. W. (2011). Torpor patterns, arousal rates, and temporal organization of torpor entry in wildtype and UCP1-ablated mice. *J. Comp. Physiol. B* 181, 137–145. doi: 10.1007/s00360-010-0503-9

Oelkrug, R., Polymeropoulos, E. T., and Jastroch, M. (2015). Brown adipose tissue: physiological function and evolutionary significance. *J. Comp. Physiol. B* 185, 587–606. doi: 10.1007/s00360-015-0907-7

Opazo, J. C., Nespolo, R. F., and Bozinovic, F. (1999). Arousal from torpor in the chilean mouse-opposum (*Thylamys elegans*): does non-shivering thermogenesis play a role? *Comp. Biochem. Physiol. Part A Comp. Physiol.* 123, 393–397. doi: 10.1016/S1095-6433(99)00081-1

Pant, M., Bal, N. C., and Periasamy, M. (2015). Cold adaptation overrides developmental regulation of sarcolipin expression in mice skeletal muscle: SOS for muscle-based thermogenesis? *J. Exp. Biol.* 218, 2321–2325. doi: 10.1242/jeb.119164

Pant, M., Bal, N. C., and Periasamy, M. (2016). Sarcolipin: a key thermogenic and metabolic regulator in skeletal muscle. *Trends Endocrinol. Metabol.* 27, 881–892. doi: 10.1016/j.tem.2016.08.006

Periasamy, M., and Huke, S. (2001). SERCA pump level is a critical determinant of Ca^{2+} homeostasis and cardiac contractility. *J. Mol. Cell. Cardiol.* 33, 1053–1063. doi: 10.1006/jmcc.2001.1366

Periasamy, M., and Kalyanasundaram, A. (2007). SERCA pump isoforms: their role in calcium transport and disease. *Muscle Nerve* 35, 430–442. doi: 10.1002/mus.20745

Polymeropoulos, E. T., Jastroch, M., and Frappell, P. B. (2012). Absence of adaptive nonshivering thermogenesis in a marsupial, the fat-tailed dunnart (Sminthopsis crassicaudata). *J. Comp. Physiol. B* 182, 393–401. doi: 10.1007/s00360-011-0623-x

Raimbault, S., Dridi, S., Denjean, F., Lachuer, J., Couplan, E., Bouillaud, F., et al. (2001). An uncoupling protein homologue putatively involved in facultative muscle thermogenesis in birds. *Biochem. J.* 353, 441–444. doi: 10.1042/bj3530441

Rolfe, D. F. S., and Brand, M. D. (1997). The physiological significance of mitochondrial proton leak in animal cells and tissues. *Biosci. Rep.* 17, 9–16. doi: 10.1023/A:1027327015957

Rose, R. W., West, A. K., Ye, J.-M., McCormack, G. H., and Colquhoun, E. Q. (1999). Nonshivering thermogenesis in a marsupial (the Tasmanian bettong *Bettongia gaimardi*) is not attributable to brown adipose tissue. *Physiol. Biochem. Zool.* 72, 699–704. doi: 10.1086/316709

Rowland, L. A., Bal, N. C., Kozak, L. P., and Periasamy, M. (2015). Uncoupling protein 1 and sarcolipin are required to maintain optimal thermogenesis, and loss of both systems compromises survival of mice under cold stress. *J. Biol. Chem.* 290, 12282–12289. doi: 10.1074/jbc.M115.637603

Rowland, L. A., Bal, N. C., and Periasamy, M. (2014). The role of skeletal-muscle-based thermogenic mechanisms in vertebrate endothermy. *Biol. Rev.* 90, 1279–1297. doi: 10.1111/brv.12157

Ruben, J. (1995). The evolution of endothermy in mammals and birds: from physiology to fossils. *Annu. Rev. Physiol.* 57, 69–95. doi: 10.1146/annurev.ph.57.030195.000441

Ruf, T., and Arnold, W. (2008). Effects of polyunsaturated fatty acids on hibernation and torpor: a review and hypothesis. *Am. J. Physiol. Regul. Integr. Comp. Physiol.* 294, R1044–R1052. doi: 10.1152/ajpregu.00688.2007

Ruf, T., and Geiser, F. (2015). Daily torpor and hibernation in birds and mammals. *Biol. Rev.* 90, 891–926. doi: 10.1111/brv.12137

Sahoo, S. K., Shaikh, S. A., Sopariwala, D. H., Bal, N. C., and Periasamy, M. (2013). Sarcolipin protein interaction with sarco(endo)plasmic reticulum Ca^{2+} ATPase (SERCA) is distinct from phospholamban protein, and only sarcolipin can promote uncoupling of the SERCA pump. *J. Biol. Chem.* 288, 6881–6889. doi: 10.1074/jbc.M112.436915

Saito, S., Saito, C. T., and Shingai, R. (2008). Adaptive evolution of the uncoupling protein 1 gene contributed to the acquisition of novel nonshivering thermogenesis in ancestral eutherian mammals. *Gene* 408, 37–44. doi: 10.1016/j.gene.2007.10.018

Shaikh, S. A., Sahoo, S. K., and Periasamy, M. (2016). Phospholamban and sarcolipin: are they functionally redundant or distinct regulators of the Sarco(Endo)Plasmic Reticulum Calcium ATPase? *J. Mol. Cell. Cardiol.* 91, 81–91. doi: 10.1016/j.yjmcc.2015.12.030

Simonides, W. S., Thelen, M. H., van der Linden, C. G., Muller, A., and van Hardeveld, C. (2001). Mechanism of thyroid-hormone regulated expression of the SERCA genes in skeletal muscle: implications for thermogenesis. *Biosci. Rep.* 21, 139–154. doi: 10.1023/A:1013692023449

Smith, R. E., and Horwitz, B. A. (1969). Brown fat and thermogenesis. *Physiol. Rev.* 49, 330–425.

Suzuki, M., Tseeb, V., Oyama, K., and Ishiwata, S.,i. (2007). Microscopic detection of thermogenesis in a single HeLa cell. *Biophys. J.* 92, L46–L48. doi: 10.1529/biophysj.106.098673

Swanson, J. E., Lokesh, B. R., and Kinsella, J. E. (1989). Ca^{2+}-Mg^{2+} ATPase of mouse cardiac sarcoplasmic reticulum is affected by membrane n-6 and n-3 polyunsaturated fatty acid content. *J. Nutr.* 119, 364–372.

Symonds, M. E., Henderson, K., Elvidge, L., Bosman, C., Sharkey, D., Perkins, A. C., et al. (2012). Thermal imaging to assess age-related changes of skin temperature within the supraclavicular region co-locating with brown adipose tissue in healthy children. *J. Pediatr.* 161, 892–898. doi: 10.1016/j.jpeds.2012.04.056

Tattersall, G. J., Leite, C. A., Sanders, C. E., Cadena, V., Andrade, D. V., Abe, A. S., et al. (2016). Seasonal reproductive endothermy in tegu lizards. *Sci. Adv.* 2:e1500951. doi: 10.1126/sciadv.1500951

Teulier, L., Rouanet, J.-L., Letexier, D., Romestaing, C., Belouze, M., Rey, B., et al. (2010). Cold-acclimation-induced non-shivering thermogenesis in birds is associated with upregulation of avian UCP but not with innate uncoupling or altered ATP efficiency. *J. Exp. Biol.* 213, 2476–2482. doi: 10.1242/jeb.043489

Townsend, K. L., and Tseng, Y.-H. (2014). Brown fat fuel utilization and thermogenesis. *Trends Endocrinol. Metabol.* 25, 168–177. doi: 10.1016/j.tem.2013.12.004

Trayhurn, P., Temple, N. J., and Aerde, J. V. (1989). Evidence from immunoblotting studies on uncoupling protein that brown adipose tissue is not present in the domestic pig. *Can. J. Physiol. Pharmacol.* 67, 1480–1485. doi: 10.1139/y89-239

Trenker, M., Malli, R., Fertschai, I., Levak-Frank, S., and Graier, W. F. (2007). Uncoupling proteins 2 and 3 are fundamental for mitochondrial Ca(2+) uniport. *Nat. Cell Biol.* 9, 445–452. doi: 10.1038/ncb1556

Valencak, T. G., and Ruf, T. (2007). N−3 polyunsaturated fatty acids impair lifespan but have no role for metabolism. *Aging Cell* 6, 15–25. doi: 10.1111/j.1474-9726.2006.00257.x

Vangheluwe, P., Schuermans, M., Zádor, E., Waelkens, E., Raeymaekers, L., and Wuytack, F. (2005). Sarcolipin and phospholamban mRNA and protein expression in cardiac and skeletal muscle of different species. *Biochem. J.* 389(Pt 1), 151–159. doi: 10.1042/BJ20050068

Vetter, S. G., Ruf, T., Bieber, C., and Arnold, W. (2015). What is a mild winter? Regional differences in within-species responses to climate change. *PLoS ONE* 10:e0132178. doi: 10.1371/journal.pone.0132178

Vézina, F., Gerson, A. R., Guglielmo, C. G., and Piersma, T. (2017). The performing animal: causes and consequences of body remodeling and metabolic adjustments in red knots facing contrasting thermal environments. *Am. J. Physiol. Regul. Integr. Comp. Physiol.* 313, R120–R131. doi: 10.1152/ajpregu.00453.2016

Videler, J. J. (2005). *Avian Flight*. Oxford: Oxford University Press.

Woods, C. P., and Brigham, R. M. (2004). "The avian enigma": "hibernation" by common poorwills (*Phalaenoptilus nuttalli*)," in *Life in the Cold 2004: The Twelfth International Hibernation Symposium (LITC 2004)*, eds B. M. Barnes and H. V. Carey (Fairbanks, AK: Institute of Arctic Biology, University of Alaska), 231–240.

Yatani, A., Kim, S.-J., Kudej, R. K., Wang, Q., Depre, C., Irie, K., et al. (2004). Insights into cardioprotection obtained from study of cellular Ca^{2+} handling in myocardium of true hibernating mammals. *Am. J. Physiol. Heart Circul. Physiol.* 286, H2219–H2228. doi: 10.1152/ajpheart.01096.2003

Conflict of Interest Statement: The authors declare that the research was conducted in the absence of any commercial or financial relationships that could be construed as a potential conflict of interest.

frontiers in Physiology

OPINION
published: 14 June 2018
doi: 10.3389/fphys.2018.00714

Sarcolipin Makes Heat, but Is It Adaptive Thermogenesis?

Kevin L. Campbell[1]* *and Alysha A. Dicke*[2]

[1] Department of Biological Sciences, University of Manitoba, Winnipeg, MB, Canada, [2] Technology Specialist, Fish and Richardson P.C., Minneapolis, MN, United States

Keywords: sarcolipin, thermogenesis, evolution, muscle, calcium, SERCA

A regulatory protein (sarcolipin or SLN) bound to SERCA pumps in the sarcoplasmic reticulum (SR) of cardiac and skeletal muscle has been shown to increase heat production *in vitro*. Here, we review recent work in this area, assess the potential of *in vivo* heat generation by this mechanism, and advocate that a comparative approach is the best path toward resolving many outstanding questions on the physiological function, regulation, and evolution of SLN.

INTRODUCTION

Precise control of cytosolic Ca^{2+} levels underlies the modulation of optimal contraction strengths, frequencies, and relaxation rates by cardiac and skeletal muscle over a wide range of activities. This regulation is largely achieved by metering the release of SR Ca^{2+} stores into the cytosol via ryanodine receptor channels and the subsequent uptake of Ca^{2+} by sarco/endoplasmic reticulum Ca^{2+}-ATPase (SERCA) pumps. Briefly, SERCA harnesses the phosphate bond energy of one ATP molecule to translocate two Ca^{2+} ions into the SR lumen, thereby generating a ∼15,000-fold (1.5 mM vs. 0.1 μM) lumen-to-cytosol Ca^{2+} concentration gradient in resting muscle (Toyoshima and Inesi, 2004). Several single-pass transmembrane peptides—including phospholamban, myoregulin, and sarcolipin (SLN)—interact with SERCA isoforms to modify Ca^{2+} uptake in a tissue specific manner. SLN, for example, is a relatively short (31 amino acid) helical peptide that was initially shown to alter Ca^{2+} uptake kinetics by inhibiting SERCA1a and SERCA2a activity in the atria and skeletal muscles of mammals (Odermatt et al., 1998; MacLennan et al., 2003). Subsequent *in vitro* evidence that SLN increases the heat generated by SERCA by partially uncoupling Ca^{2+} re-sequestration from ATP hydrolysis in rabbit and mouse skeletal muscle (Smith et al., 2002; Mall et al., 2006) has led to the hypothesis that SLN contributes to non-shivering thermogenesis (NST) *in vivo* (Bal et al., 2012). It should be noted that this proposed heat generating process is mechanistically distinct from, and hence unrelated to, known Ca^{2+}-linked thermogenic processes in skeletal muscle, which will not be further discussed here, such as futile Ca^{2+} cycling in the non-contractile extraocular muscles of regionally endothermic billfishes and ryanodine receptor mutations associated with malignant hyperthermia. While there remains a lack of consensus regarding adaptive muscle NST in mammals by any mechanism, the proposal that SLN increases energy turnover in the skeletal muscles where it is expressed has generated substantial interest in the biomedical research community as a potential target for obesity and other metabolic syndromes. To date, however, studies on the structure, function, and regulation of SLN, its interaction with SERCA, and its potential role in facultative muscle NST predominantly remain limited to a few model systems that reside within the same mammalian clade (Glires; rodents and rabbits). While this work is tantalizing, several key mechanistic aspects remain unanswered such as (1) whether uncoupling of Ca^{2+} transport from ATP hydrolysis in SERCA primarily arises from slippage of the SERCA-bound Ca^{2+} ions into the cytosol after ATP hydrolysis or

OPEN ACCESS

Edited by:
Elias T. Polymeropoulos, Institute for Marine and Antarctic Studies (IMAS), Australia

Reviewed by:
Barbara Cannon, Stockholm University, Sweden

***Correspondence:**
Kevin L. Campbell
kevin.campbell@umanitoba.ca

Specialty section:
This article was submitted to Integrative Physiology, a section of the journal Frontiers in Physiology

Received: *27 February 2018*
Accepted: *24 May 2018*
Published: *14 June 2018*

Citation:
Campbell KL and Dicke AA (2018) Sarcolipin Makes Heat, but Is It Adaptive Thermogenesis? Front. Physiol. 9:714. doi: 10.3389/fphys.2018.00714

from passive leak of luminal Ca^{2+} back into the cytosol through SERCA (**Figure 1A**), (2) what region(s) and/or residue(s) of SLN and SERCA are involved in this uncoupling, and (3) whether SLN-mediated Ca^{2+} uncoupling occurs in resting muscle when SR luminal Ca^{2+} concentration is high and cytosolic [Ca^{2+}] is low, or in actively-contracting and/or shivering muscle when cytosolic Ca^{2+} is elevated (de Meis, 2001; Smith et al., 2002; Inesi and Tadini-Buoninsegni, 2014). Also unclear are broader questions pertaining to how SLN-mediated Ca^{2+} uncoupling evolved, and its occurrence and potential thermogenic importance—i.e., how much heat is produced relative to shivering—across the mammalian phylogeny (and beyond).

HEAT YES, BUT HOW MUCH?

It is imperative to delineate the potential amount of heat generated via SLN-mediated NST from that of other ATP consuming processes coupled to Ca^{2+} turnover during a muscle contraction-relaxation cycle. These include activation of sarcolemma Na^+-K^+-ATPases for membrane repolarization, myosin-ATPases for cross-bridge relaxation, and SERCA Ca^{2+}-ATPases for Ca^{2+} sequestration (**Figure 1B**). As SLN is not associated with the former two ATPases, back of the napkin calculations suggest its thermogenic contribution is limited to a small fraction of that liberated by shivering. For simplicity, if we arbitrarily assume that 1,000 Ca^{2+} ions are released into the cytosol following nervous activation, then transporting these Ca^{2+} ions back into the SR will hydrolyze 500 ATP (assuming no Ca^{2+} backflux or leak), with an additional 750–1,167 ATP hydrolyzed by the Na^+-K^+ and myosin ATPases (these two ATPases are estimated to contribute ∼60–70% of the energetic cost of an isometric muscle contraction; Barclay et al., 2007). For SLN to not interfere with muscle relaxation speeds, and hence maximal contraction frequencies—an especially important consideration for small mammals—SLN uncoupling is likely to predominantly operate when SR luminal concentrations are elevated (Inesi and Tadini-Buoninsegni, 2014). Thus, assuming Ca^{2+} slippage/leak occurs at a cytosolic [Ca^{2+}] low enough to preclude cross-bridge formation—say below 100 Ca^{2+} ions in our example—and that the Ca^{2+}/ATP coupling ratio is lowered by 35% (Bombardier et al., 2013), then this mechanism would only hydrolyze an additional ∼25 ATP, or ∼2% of the heat produced by a single contraction-relaxation cycle. Results of *in vitro* biochemical assays demonstrate that SERCA activity is almost undetectable at Ca^{2+} levels found in resting muscle (Gorski et al., 2013; Sahoo et al., 2013). Nonetheless, even if we assume that SLN lowers net Ca^{2+} pumping efficiency to zero in this state, then >3-fold more Ca^{2+} ions than are released during a single muscle contraction would need to "slip" for SLN to generate an equivalent amount of heat within the same timeframe. Of course, this latter scenario also requires that cytosolic Ca^{2+} levels remain below the contraction threshold, whereby few SERCA Ca^{2+} binding sites would be populated relative to that following muscle contraction (Barclay et al., 2007). Taken together, these calculations question whether SLN-NST can contribute meaningfully to thermogenesis relative to shivering and other non-shivering processes (e.g., brown adipose tissue).

EVIDENCE FOR SLN-MEDIATED NON-SHIVERING THERMOGENESIS IS INCONCLUSIVE

Crucially, heat released via the SLN and SERCA complex has been shown to increase linearly with SLN concentration *in vitro* (Mall et al., 2006), which current data suggests varies markedly among skeletal muscles in rodents. Briefly, moderate concentrations of SLN are present in small muscles of mice such as the soleus and diaphragm that are predominantly composed of slow-twitch oxidative fibers, though (nearly) undetectable in fast-twitch glycolytic fibers that form the bulk of the limb musculature (e.g., quadriceps; Vangheluwe et al., 2005; Babu et al., 2007; Bombardier et al., 2013). Consequently, any NST linked to SLN may be expected to be imperceptible in these small mammals. This conclusion is in line with recent work on SLN knock-out mice that revealed no differences in body mass, food intake, or resting whole body and isolated soleus muscle O_2 consumption rates relative to wild-type littermates, despite indications that SLN reduced the apparent Ca^{2+}/ATP coupling ratio within the soleus (but not fast-twitch extensor digitorum longus muscles) by up to 35% (Bombardier et al., 2013). Similarly, SLN overexpressing mice exhibited no differences in body mass or energy expenditure, even on high fat diets, relative to wild-type individuals whose muscles contained ∼25-fold lower SLN concentrations (Butler et al., 2015). It should be noted, however, that these findings are not universal, as pair-fed SLN knock-out mice gained weight relative to wild-type mice, while SLN overexpression resulted in weight loss and an increased rate of O_2 consumption (Maurya et al., 2015). The basis for these contradictory findings remains unclear, though differences in O_2 consumption may have arisen in part due to values being presented in a mass-specific basis for the latter study. Nonetheless, results of the Maurya study are ostensibly bolstered by several mouse studies that contend that loss of SLN hinders muscle-based NST (Bal et al., 2012, 2017; Rowland et al., 2015), although it is also conceivable that the observed effects of SLN ablation arise from an impaired shivering response, altered Ca^{2+} signaling pathways, and/or compromised Ca^{2+} handling.

Unfortunately, *in vivo* experiments in support of muscle NST that involved curare (e.g., Bal et al., 2012) are inconclusive as none of the animals required artificial respiration, thus indicating that shivering may not have been completely blocked. Additional support for a thermogenic role for SLN is that cold acclimation mitigates the natural developmental reduction in SLN levels in neonatal mice and results in elevated SLN transcription in slow-twitch adult skeletal muscle (Pant et al., 2015). However, this interpretation is complicated by studies conducted on non-cold stressed wheel running mice whose soleus SLN mRNA expression profiles show a distinct exercise effect, being 2- to 3-fold higher than found in sedentary mouse muscle (de Snoo, 2009). Consequently, the observed elevations in muscle SLN levels in cold challenged mice may simply reflect a shivering induced "training effect." While additional research in this area is

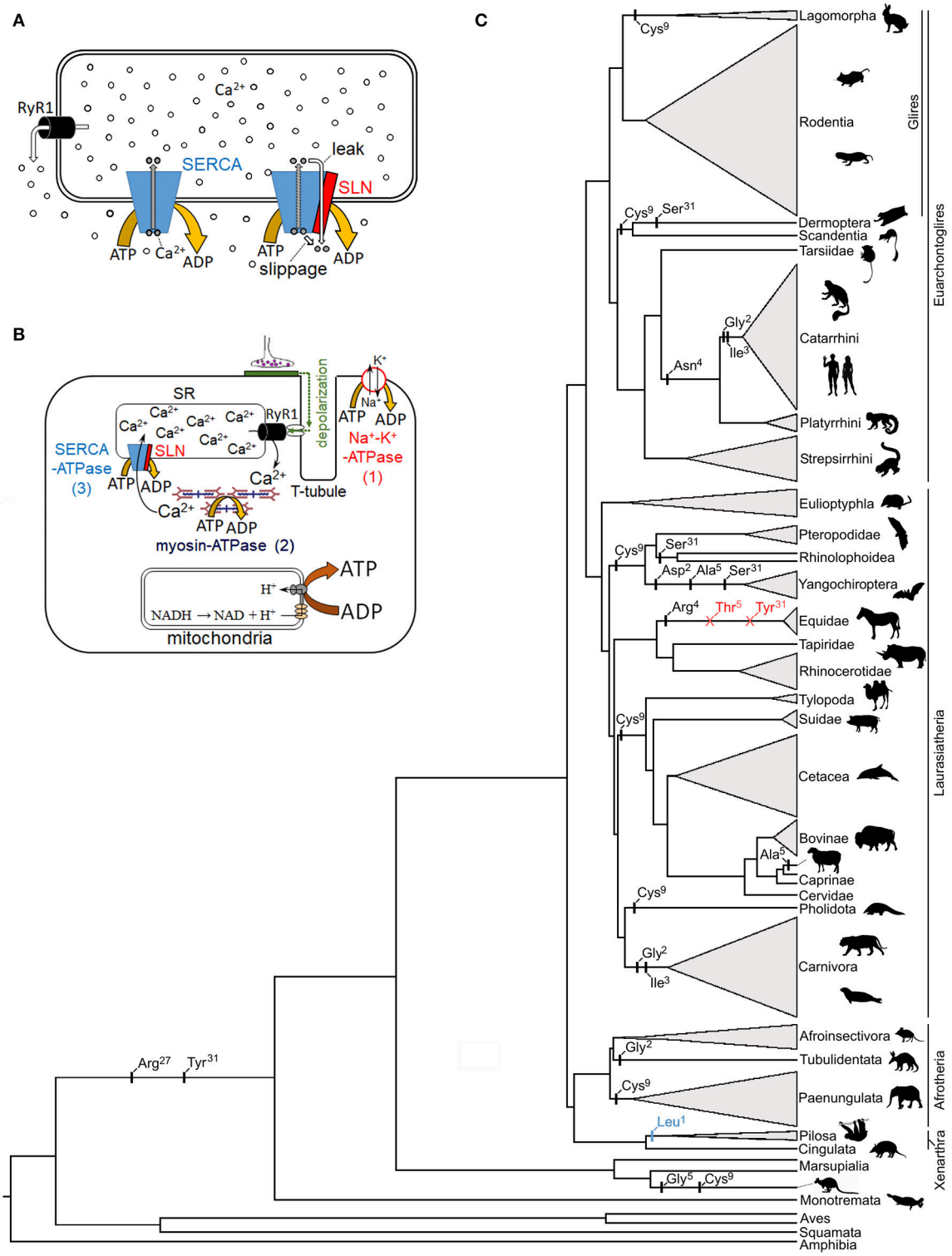

FIGURE 1 | Proposed mechanism of sarcolipin in skeletal muscle non-shivering thermogenesis, and its genetic evolution. **(A)** The two functional mechanisms by which SLN is postulated to return SERCA-bound Ca^{2+} to the cytosol following ATP hydrolysis: enzyme slippage and passive leak (*right complex*). **(B)** Primary mechanisms of ATP hydrolysis in a typical skeletal muscle fiber following a nervous stimulation: (1) Na^{+}-K^{+}-ATPase, (2) myosin-ATPase, and (3) SERCA Ca^{2+}-ATPase. Note that while some heat is liberated by these ATPases, most muscle thermogenesis is via mitochondrial catabolic processes which generate the proton motive force required for ATP synthesis. **(C)** Mammalian phylogenetic tree denoting potentially relevant SLN residue substitutions (black), start codon mutations (blue), and deletions (red)

(Continued)

FIGURE 1 | based on data in Gaudry et al. (2017). SLN residue replacement and deletion events are not dated and are placed on the phylogenetic branches in sequential order. The height of collapsed branches (gray triangles) is proportional to the number of SLN sequences available for each clade. Note that published functional studies pertaining to SLN-NST have been restricted to a few model species in the Glires clade (predominantly mice). Silhouettes are taken from phylopic.org (image credits: megabat, Oren Peles/vectorized by Yan Wong; rabbit and sloth, Sarah Werning; https://creativecommons.org/licenses/by/3.0/).

required, the findings of the wheel running mice studies are not consistent with an adaptive thermogenic role for SLN, as elevated ATP hydrolysis due to futile Ca^{2+} pumping would be expected to impair exercise performance (see below).

SLN EXPRESSION AND EVOLUTIONARY ANALYSES

Previous work has shown SLN mRNA and/or protein levels to be several magnitudes higher in both slow and fast twitch skeletal muscles of rabbits, pigs, dogs, and humans than lab rodents, leading to suggestions that SLN-NST may be of greater thermogenic importance in larger mammals (Barbot et al., 2016). However, given that larger mammals also possess lower surface-area-to-volume ratios, thicker insulation, and the ability to further minimize heat loss via countercurrent heat exchangers, this contention is puzzling. Similarly, implications that larger mammals may exhibit a stronger reliance on SLN-NST due to small (or even absent) depots of thermogenic brown adipose tissue (BAT) are unsatisfactory, as it is precisely for the reasons outlined above that these species have a reduced reliance on BAT thermogenesis (i.e., a reduction in BAT mass does not need to be counterbalanced by other heat generating mechanisms). Indeed, recent work has illustrated that ancient magnitude increases in body mass in five mammalian lineages [cetaceans (whales and dolphins), elephantids, sirenians (sea cows), hyracoids (hyraxes), and equids (horses and kin)] were temporally coupled with inactivation of thermogenic *UCP1* (Gaudry et al., 2017), suggesting that costs of maintaining an elevated thermogenic capacity outweighed its benefits.

If SLN plays a prominent thermoregulatory role in mammals, then this locus may be expected to have evolved under relaxed selection or potentially even be pseudogenized in large or tropically distributed species and/or mammalian lineages lacking a functional UCP1 protein. The latter assemblage offers particularly good model systems as members of some UCP1 lacking lineages (cetaceans, woolly mammoths, Steller's sea cows, and horses) have nonetheless evolved extreme cold tolerance while others (pangolins, xenarthrans, hyraxes, pigs, and extant sea cows) are notoriously cold intolerant (even often as adults). In contrast to such expectations, not only is the SLN locus functionally intact in each of these cases (i.e., able to encode a ∼31 unit peptide), but its primary structure has remained exceptionally well conserved despite highly divergent body sizes and thermoregulatory capacities among species. For example, UCP1-lacking elephants, whales, pigs, and hyraxes all possess *identical* SLN peptides to those of rabbits, while SLN sequences of "proto-endothermic" tenrecs and golden moles precisely match those of cold tolerant deer mice and meadow voles (*cf.* Figure S4 of Gaudry et al., 2017). This remarkable degree of sequence conservation—over evolutionary timescales exceeding 65 million years, and in large bodied and tropical species for which NST should have no apparent adaptive benefit—is not readily compatible with a thermogenic function. Intriguingly, the start codon of SLN is mutated in weakly endothermic sloths (**Figure 1C**), which moreover have nonfunctional UCP1 (Gaudry et al., 2017), though its primary structure remains highly conserved; whether the start codon mutation inhibits protein translation or is rescued by alternative splicing remains unknown and should be examined.

While there is evidence that SLN interaction with SERCA results in an elevated rate of ATP hydrolysis *in vitro*, taken together, the above findings argue that the primary role of SLN in skeletal muscle of mammals is not thermoregulatory in nature. Nonetheless, SLN expression and *in vitro* studies on a range of large-bodied mammals, including species lacking functional UCP1, are required to confirm or refute the above contentions. An examination of representative marsupials and monotremes are also required to assess the thermogenic potential of SLN across Mammalia and better pinpoint if and when the proposed thermogenic function arose in evolutionary time. Finally, it is worth noting that the high expression level of SLN in mammalian atria—the concentration of which is 10-to 1,000-fold higher than in the soleus of rodents (Babu et al., 2007; Bombardier et al., 2013)—is also difficult to envision within a thermogenic framework, though in line with a role in modulating intracellular Ca^{2+} homeostasis by modulating the (apparent) Ca^{2+} affinity of SERCA. Indeed, both elevated and lowered atrial SLN concentrations are linked to cardiac pathologies (Babu et al., 2007).

HOW IS SLN REGULATED?

Surprisingly, the mechanism underling SERCA inhibition by SLN is also equivocal. For example, some labs report a decrease in SERCA's apparent Ca^{2+} affinity in the presence of SLN (Hellstern et al., 2001; Buck et al., 2003; Buffy et al., 2006; Gorski et al., 2013) whereas others do not observe a change in Ca^{2+} affinity and only observe a decrease in Ca^{2+} uptake (Smith et al., 2002; Sahoo et al., 2013). There are several potential reasons for these discordant observations including the use of different assays to measure ATP hydrolysis as well as the use of different test species employed (with different SLN and SERCA sequences). It is essential to both understand and reconcile these inconsistencies to determine the mechanism of inhibition, and whether or not this process is linked to thermogenic Ca^{2+} uncoupling/leak. Similarly, comparative (and, potentially, site-directed mutagenesis) studies are also required to elucidate what component of the SLN peptide is involved in thermogenesis. Two recent studies have implicated the cytosol-oriented N-terminus to underlie Ca^{2+} uncoupling (Sahoo et al., 2015; Autry et al., 2016). Specifically, rabbit SLN residues Glu^2 and Glu^7 are predicted to form salt-bridges with Arg^{324} and Lys^{328} of rabbit

SERCA1a, thereby perturbing one of the SERCA Ca^{2+} binding sites (E^{309} on helix M4), although only Glu^7 was predicted as necessary to induce the uncoupling structural change (Autry et al., 2016). Dicke (2017) has questioned the role of this region in uncoupling due to a substantial degree of sequence variability among mammals (e.g., MGINTRE^7 in catarrhine primates vs. MERSTQE^7 in most rodents; Gaudry et al., 2017), and it remains unknown whether *in vitro* SLN Ca^{2+}/ATP uncoupling is compromised by the $Glu^2 \rightarrow Gly^2$ replacement in human, carnivore, and aardvark SLN, the $Glu^2 \rightarrow Asp^2$ replacement in vesper bats, or the $Glu^7 \rightarrow Asp^7$ replacement in sloths, dugonid sea cows, and false vampire bats (**Figure 1C**). It should be further noted that *Xenopus* and zebrafish—for which a non-shivering thermogenic mechanism would be most unexpected—possess the identical SLN N-terminal MERSTQE motif found in rodents (their SERCA proteins also contain Arg^{324} and Lys^{328}). By contrast, the luminal C-terminal sequence (^{27}RSYQY^{31})—which underlies both the proper SR/ER cellular localization of SLN and its apparent inhibition of SERCA (Gramolini et al., 2004; Gorski et al., 2013)—is nearly 100% conserved among mammals, and thus may be a better candidate for an uncoupling function (Dicke, 2017). Importantly, two C-terminal residues (Arg^{27} and Tyr^{31}) that are proposed to be essential for SLN inhibition (Gorski et al., 2013) are only found in mammals, with other vertebrates having Lys^{27} and Glu/Asp^{31} at these sites, except falcons which have Gln^{31} (Montigny et al., 2014; Gaudry et al., 2017). Interestingly, $Tyr^{31} \rightarrow Ser^{31}$ substitutions appear to have evolved independently at least three times in mammals (twice in bats and again in flying lemurs), while this C-terminal residue is deleted in equids (**Figure 1C**). These species accordingly provide natural model systems to help evaluate the potential role of the cytosolic (N-terminus) and luminal (C-terminus) regions of SLN in both decreasing SERCA's apparent Ca^{2+} affinity and uncoupling of Ca^{2+} transport.

In addition to supplying sufficient heat to help maintain thermal balance in sub-thermoneutral temperatures, a key feature for any adaptive, facultative thermogenic process is the ability to rapidly activate it once the need arises and inactivate it once additional thermogenesis is no longer required. If, for example, SLN-NST is simply an unregulated by-product associated with Ca^{2+} pumping during muscle contraction, then this mechanism would become maladaptive in many circumstances such as during exercise in temperatures near or above the lower limit of the thermoneutral zone, as this supplemental heat production would tax heat-dissipating processes thereby promoting hyperthermia-induced muscle fatigue and impaired motor performance (Silva, 2011; Nybo et al., 2014). To our knowledge, no studies have yet demonstrated that SLN-NST can be activated/inactivated independently from muscle contraction, let alone have identified the molecular mechanism by which this process can be mediated. While phosphorylation of one or more residues (Ser^4 and/or Thr^5) within the cytosolic domain have been shown to relieve the inhibitory effect of SLN on cardiac SERCA pumps (Gramolini et al., 2004; Bhupathy et al., 2009), likely via structural changes to the SLN-SERCA complex, it remains unknown whether this mechanism alters uncoupling activity (Autry et al., 2016; Barbot et al., 2016). However, primary sequence analysis of available data reveal that either one or both of Ser^4 and Thr^5 are—with one exception (equids)—universally present from fish to mammals (Barbot et al., 2016; Gaudry et al., 2017), indicating that this inhibitory mechanism of control is likely both ancient and highly conserved. Key insights into this regulation may thus be provided by studies on horses/donkeys whose SLN peptides (in addition to lacking the C-terminal Tyr^{31} residue; see above) also lack the potential for reversible phosphorylation (one of the two residues at positions 4–5 is deleted, while the other exhibits a dephospho-mimetic Thr→Arg substitution; **Figure 1C**).

In addition to phosphorylation as a post-translational modification, it was recently shown that Cys^9 of native SLN from rabbits and pigs was S-palmitoylated and S-oleylated (Montigny et al., 2014), and that depalmitoylation treatment increased Ca^{2+}-ATPase activity of rabbit SR by 30%. Rodents, by contrast, possess Phe^9 and show a smaller increase in Ca^{2+}-ATPase activity following depalmitoylation (20%; Montigny et al., 2014), suggesting a potential (albeit limited) role for this residue position in the regulation of SLN activity. However, the presence of Cys^9—found in mammals ranging from rabbits, bats, kangaroos, and pangolins to elephants and whales (**Figure 1C**)—does not appear to be linked with either body mass or metabolic intensity. While this phylogenetic distribution is consistent with a pattern of both repeated (convergent) evolution of Cys^9 and its reversion back to the ancestral Phe^9 found in the majority of vertebrate species, the potential physiological and thermogenic effects of this residue replacement are yet to be assessed.

CONCLUSIONS

While there can be little doubt that the interaction of SLN with SERCA lowers the metabolic efficiency of Ca^{2+} transport *in vitro*, unequivocal support for an adaptive thermogenic role *in vivo* is lacking. Suggestions that SLN plays any meaningful thermogenic role in larger bodied mammals (including humans) or non-mammalian vertebrates (e.g., birds) is also without empirical evidence and remains purely speculative. Comparative studies taking advantage of naturally occurring variability in SLN concentrations and primary sequence among vertebrates provide ideal avenues to explore the function of this regulatory peptide, and its evolution.

AUTHOR CONTRIBUTIONS

KC drafted the manuscript, prepared the figures, and approved the final version. AD contributed to manuscript writing, provided important interpretations, critically revised the work, and provided final approval of the opinion content.

ACKNOWLEDGMENTS

KC is funded by the Natural Sciences and Engineering Research Council (NSERC) of Canada (RGPIN/6562-2016). We thank Mike Autry, Jay Treberg, Vitaly Vostrikov, Todd Duhamel, and Jens Franck for constructive comments on an earlier version of this paper.

REFERENCES

Autry, J. M., Thomas, D. D., and Espinoza-Fonseca, L. M. (2016). Sarcolipin promotes uncoupling of the SERCA Ca^{2+} pump by inducing a structural rearrangement in the energy-transduction domain. *Biochemistry* 55, 6083–6086. doi: 10.1021/acs.biochem.6b00728

Babu, G. J., Bhupathy, P., Carnes, C. A., Billman, G. E., and Periasamy, M. (2007). Differential expression of sarcolipin protein during muscle development and cardiac pathophysiology. *J. Mol. Cell. Cardiol.* 42, 215–222. doi: 10.1016/j.yjmcc.2007.05.009

Bal, N. C., Maurya, S. K., Sopariwala, D. H., Sahoo, S. K., Gupta, S. C., Shaikh, S. A., et al. (2012). Sarcolipin is a newly identified regulator of muscle-based thermogenesis in mammals. *Nat. Med.* 18, 1575–1579. doi: 10.1038/nm.2897

Bal, N. C., Singh, S., Reis, F. C. G., Maurya, S. K., Pani, S., Rowland, L. A., et al. (2017). Both brown adipose tissue and skeletal muscle thermogenesis processes are activated during mild to severe cold adaptation in mice. *J. Biol. Chem.* 292, 16616–16625. doi: 10.1074/jbc.M117.790451

Barbot, T., Montigny, C., Decottignies, P., le Maire, M., Jaxel, C., Jamin, N., et al. (2016). "Functional and structural insights into sarcolipin, a regulator of the sarco-endoplasmic reticulum Ca^{2+}-ATPases," in *Regulation of Ca^{2+}-ATPases, V-ATPases and F-ATPases,* eds S. Chakraborti and N.S. Dhalla (Cham: Springer International Publishing), 153–186.

Barclay, C. J., Woledge, R. C., and Curtin, N. A. (2007). Energy turnover for Ca^{2+} cycling in skeletal muscle. *J. Muscle Res. Cell Motil.* 28, 259–274. doi: 10.1007/s10974-007-9116-7

Bhupathy, P., Babu, G. J., Ito, M., and Periasamy, M. (2009). Threonine-5 at the N-terminus can modulate sarcolipin function in cardiac myocytes. *J. Mol. Cell. Cardiol.* 47, 723–729. doi: 10.1016/j.yjmcc.2009.07.014

Bombardier, E., Smith, I. C., Vigna, C., Fajardo, V. A., and Tupling, A. R. (2013). Ablation of sarcolipin decreases the energy requirements for Ca^{2+} transport by sarco (endo) plasmic reticulum Ca^{2+}-ATPases in resting skeletal muscle. *FEBS Lett.* 587, 1687–1692. doi: 10.1016/j.febslet.2013.04.019

Buck, B., Zamoon, J., Kirby, T. L., DeSilva, T. M., Karim, C., Thomas, D., et al. (2003). Overexpression, purification, and characterization of recombinant Ca-ATPase regulators for high-resolution solution and solid-state NMR studies. *Protein Expr. Purif.* 30, 253–261. doi: 10.1016/S1046-5928(03)00127-X

Buffy, J. J., Buck-Koehntop, B. A., Porcelli, F., Traaseth, N. J., Thomas, D. D., and Veglia, G. (2006). Defining the intramembrane binding mechanism of sarcolipin to calcium ATPase using solution NMR spectroscopy. *J. Mol. Biol.* 358, 420–429. doi: 10.1016/j.jmb.2006.02.005

Butler, J., Smyth, N., Broadbridge, R., Council, C. E., Lee, A. G., Stocker, C. J., et al. (2015). The effects of sarcolipin over-expression in mouse skeletal muscle on metabolic activity. *Arch. Biochem. Biophys.* 569, 26–31. doi: 10.1016/j.abb.2015.01.027

de Meis, L. (2001). Uncoupled ATPase activity and heat production by the sarcoplasmic reticulum Ca^{2+}-ATPase. Regulation by ADP. *J. Biol. Chem.* 276, 25078–25087. doi: 10.1074/jbc.M103318200

de Snoo, M. (2009). *Responses of Mouse Skeletal Muscle to Endurance Exercise: Functional, Metabolic, and Genomic Adaptations*. Ph.D. thesis, Utrecht University, Utrecht.

Dicke, A. (2017). *Biophysical Characterization of Interactions Between Two Membrane Proteins: SERCA and Sarcolipin*. Ph.D. thesis, University of Minnesota, Minneapolis, MN.

Gaudry, M. J., Jastroch, M., Treberg, J. R., Hofreiter, M., Paijmans, J. L. A., Starrett, J., et al. (2017). Inactivation of thermogenic UCP1 as a historical contingency in multiple placental mammal clades. *Sci. Adv.* 3:E1602878. doi: 10.1126/sciadv.1602878

Gorski, P. A., Glaves, J. P., Vangheluwe, P., and Young, H. S. (2013). Sarco (endo) plasmic reticulum calcium ATPase (SERCA) inhibition by sarcolipin is encoded in its luminal tail. *J. Biol. Chem.* 288, 8456–8467. doi: 10.1074/jbc.M112.446161

Gramolini, A. O., Kislinger, T., Asahi, M., Li, W., Emili, A., and MacLennan, D. H. (2004). Sarcolipin retention in the endoplasmic reticulum depends on its C-terminal RSYQY sequence and its interaction with sarco (endo) plasmic Ca^{2+}-ATPases. *Proc. Natl. Acad. Sci. U.S.A.* 101, 16807–16812. doi: 10.1073/pnas.0407815101

Hellstern, S., Pegoraro, S., Karim, C. B., Lustig, A., Thomas, D. D., Moroder, L., et al. (2001). Sarcolipin, the shorter homologue of phospholamban, forms oligomeric structures in detergent micelles and in liposomes. *J. Biol. Chem.* 276, 30845–30852. doi: 10.1074/jbc.M102495200

Inesi, G., and Tadini-Buoninsegni, F. (2014). Ca^{2+}/H^{+} exchange, lumenal Ca^{2+} release and Ca^{2+}/ATP coupling ratios in the sarcoplasmic reticulum ATPase. *J. Cell Commun. Signal.* 8, 5–11. doi: 10.1007/s12079-013-0213-7

MacLennan, D. H., Asahi, M., and Tupling, A. R. (2003). The regulation of SERCA-type pumps by phospholamban and sarcolipin. *Ann. N.Y. Acad. Sci.* 986, 472–480. doi: 10.1111/j.1749-6632.2003.tb07231.x

Mall, S., Broadbridge, R., Harrison, S. L., Gore, M. G., Lee, A. G., and East, J. M. (2006). The presence of sarcolipin results in increased heat production by Ca^{2+}-ATPase. *J. Biol. Chem.* 281, 36597–36602. doi: 10.1074/jbc.M606869200

Maurya, S. K., Bal, N. C., Sopariwala, D. H., Pant, M., Rowland, L. A., Shaikh, S. A., et al. (2015). Sarcolipin is a key determinant of the basal metabolic rate, and its overexpression enhances energy expenditure and resistance against diet-induced obesity. *J. Biol. Chem.* 290, 10840–10849. doi: 10.1074/jbc.M115.636878

Montigny, C., Decottignies, P., Le Maréchal, P., Capy, P., Bublitz, M., Olesen, C., et al. (2014). S-palmitoylation and s-oleoylation of rabbit and pig sarcolipin. *J. Biol. Chem.* 289, 33850–33861. doi: 10.1074/jbc.M114.590307

Nybo, L., Rasmussen, P., and Sawka, M. N. (2014). Performance in the heat—physiological factors of importance for hyperthermia-induced fatigue. *Compr. Physiol.* 4, 657–689. doi: 10.1002/cphy.c130012

Odermatt, A., Becker, S., Khanna, V. K., Kurzydlowski, K., Leisner, E., Pette, D., et al. (1998). Sarcolipin regulates the activity of SERCA1, the fast-twitch skeletal muscle sarcoplasmic reticulum Ca^{2+}-ATPase. *J. Biol. Chem.* 273, 12360–12369. doi: 10.1074/jbc.273.20.12360

Pant, M., Bal, N. C., and Periasamy, M. (2015). Cold adaptation overrides developmental regulation of sarcolipin expression in mice skeletal muscle: SOS for muscle-based thermogenesis? *J. Exp. Biol.* 218, 2321–2325. doi: 10.1242/jeb.119164

Rowland, L. A., Bal, N. C., Kozak, L. P., and Periasamy, M. (2015). Uncoupling protein 1 and sarcolipin are required to maintain optimal thermogenesis, and loss of both systems compromises survival of mice under cold stress. *J. Biol. Chem.* 290, 12282–12289. doi: 10.1074/jbc.M115.637603

Sahoo, S. K., Shaikh, S. A., Sopariwala, D. H., Bal, N. C., Bruhn, D. S., Kopec, W., et al. (2015). The N terminus of sarcolipin plays an important role in uncoupling sarco-endoplasmic reticulum Ca^{2+}-ATPase (SERCA) ATP hydrolysis from Ca^{2+} transport. *J. Biol. Chem.* 290, 14057–14067. doi: 10.1074/jbc.M115.636738

Sahoo, S. K., Shaikh, S. A., Sopariwala, D. H., Bal, N. C., and Periasamy, M. (2013). Sarcolipin protein interaction with sarco (endo) plasmic reticulum Ca^{2+} ATPase (SERCA) is distinct from phospholamban protein, and only sarcolipin can promote uncoupling of the SERCA pump. *J. Biol. Chem.* 288, 6881–6889. doi: 10.1074/jbc.M112.436915

Silva, J. E. (2011). Physiological importance and control of non-shivering facultative thermogenesis. *Front. Biosci.* 3, 352–371. doi: 10.2741/s156

Smith, W. S., Broadbridge, R., and East, J. M. (2002). Sarcolipin uncouples hydrolysis of ATP from accumulation of Ca^{2+} by the Ca^{2+}-ATPase of skeletal-muscle sarcoplasmic reticulum. *Biochem. J.* 361, 277–286. doi: 10.1042/bj3610277

Toyoshima, C., and Inesi, G. (2004). Structural basis of ion pumping by Ca^{2+}-ATPase of the sarcoplasmic reticulum. *Annu. Rev. Biochem.* 73, 269–292. doi: 10.1146/annurev.biochem.73.011303.073700

Vangheluwe, P., Schuermans, M., Zádor, E., Waelkens, E., Raeymaekers, L., and Wuytack, F. (2005). Sarcolipin and phospholamban mRNA and protein expression in cardiac and skeletal muscle of different species. *Biochem. J.* 389, 151–159. doi: 10.1042/BJ20050068

Conflict of Interest Statement: AD was employed by Fish & Richardson P.C. at the time of writing. The ideas and opinions in the article are her own, and predominantly arose from biophysical research on SLN interactions with SERCA at the University of Minnesota during the course of her Ph.D. These viewpoints have not been vetted with the law firm where she works or its clients, and do not represent the positions of the firm, its lawyers, or any of its clients. None of this writing is intended as legal advice and it should not be taken as such.

The remaining author declares that the research was conducted in the absence of any commercial or financial relationships that could be construed as a potential conflict of interest.

frontiers in Physiology

ORIGINAL RESEARCH
published: 15 September 2017
doi: 10.3389/fphys.2017.00704

Comparison of Mitochondrial Reactive Oxygen Species Production of Ectothermic and Endothermic Fish Muscle

*Lilian Wiens[1], Sheena Banh[1], Emianka Sotiri[1], Martin Jastroch[2], Barbara A. Block[3], Martin D. Brand[4] and Jason R. Treberg[1,5]**

[1] Department of Biological Sciences, University of Manitoba, Winnipeg, MB, Canada, [2] Helmholtz Diabetes Center at Helmholtz Zentrum München, Institute for Diabetes and Obesity, Munich, Germany, [3] Tuna Research and Conservation Center, Hopkins Marine Station, Stanford University, Stanford, CA, United States, [4] Buck Institute for Research on Aging, Novato, CA, United States, [5] Department of Human Nutritional Sciences, University of Manitoba, Winnipeg, MB, Canada

OPEN ACCESS

Edited by:
Giovanni Li Volti, University of Catania, Italy

Reviewed by:
Susanna Iossa, University of Naples Federico II, Italy
Gautham Yepuri, University of Fribourg, Switzerland

***Correspondence:**
Jason R. Treberg
jason.treberg@umanitoba.ca

Specialty section:
This article was submitted to Integrative Physiology, a section of the journal Frontiers in Physiology

Received: *31 May 2017*
Accepted: *31 August 2017*
Published: *15 September 2017*

Citation:
Wiens L, Banh S, Sotiri E, Jastroch M, Block BA, Brand MD and Treberg JR (2017) Comparison of Mitochondrial Reactive Oxygen Species Production of Ectothermic and Endothermic Fish Muscle. Front. Physiol. 8:704. doi: 10.3389/fphys.2017.00704

Recently we demonstrated that the capacity of isolated muscle mitochondria to produce reactive oxygen species, measured as H_2O_2 efflux, is temperature-sensitive in isolated muscle mitochondria of ectothermic fish and the rat, a representative endothermic mammal. However, at physiological temperatures (15° and 37°C for the fish and rat, respectively), the fraction of total mitochondrial electron flux that generated H_2O_2, the fractional electron leak (FEL), was far lower in the rat than in fish. Those results suggested that the elevated body temperatures associated with endothermy may lead to a compensatory decrease in mitochondrial ROS production relative to respiratory capacity. To test this hypothesis we compare slow twitch (red) muscle mitochondria from the endothermic Pacific bluefin tuna (*Thunnus orientalis*) with mitochondria from three ectothermic fishes [rainbow trout (*Oncorhynchus mykiss*), common carp (*Cyprinus carpio*), and the lake sturgeon (*Acipenser fulvescens*)] and the rat. At a common assay temperature (25°C) rates of mitochondrial respiration and H_2O_2 efflux were similar in tuna and the other fishes. The thermal sensitivity of fish mitochondria was similar irrespective of ectothermy or endothermy. Comparing tuna to the rat at a common temperature, respiration rates were similar, or lower depending on mitochondrial substrates. FEL was not different across fish species at a common assay temperature (25°C) but was markedly higher in fishes than in rat. Overall, endothermy and warming of Pacific Bluefin tuna red muscle may increase the potential for ROS production by muscle mitochondria but the evolution of endothermy in this species is not necessarily associated with a compensatory reduction of ROS production relative to the respiratory capacity of mitochondria.

Keywords: endothermy, ectothermy, tuna, mitochondrial energetics, superoxide, hydrogen peroxide, fractional electron leak

INTRODUCTION

Fishes of the family Scombridae (the mackerels, bonitos, and tunas) are highly active marine predators. Within this clade, endothermy has evolved and is most expressed in the three species of bluefin tunas that occupy cooler temperate waters and, as adults, subpolar seas (Block et al., 2005; Boustany et al., 2007; Whitlock et al., 2015). Endothermy is also found in members of the tribe Thunnini (the tunas), and other fishes including cranial endothermy in billfishes and butterfly mackerel, endothermy in lamnid sharks, and systemic endothermy in the Opah (Wegner et al., 2015). Since temperature can affect the rate of biological processes, including enzymatic reaction rates, such endothermy has been a particular focus for comparative physiologists. The research on heat production, evolutionary convergence, and potential selective advantages of endothermy in fishes have been discussed and reviewed elsewhere (for examples see Block, 1994; Block and Finnerty, 1994; Bernal et al., 2001; Dickson and Graham, 2004; Graham and Dickson, 2004).

Bluefin tunas maintain elevated slow-twitch red muscle temperatures in the core of the body, up to 21°C above surrounding ambient water temperatures (Stevens et al., 2000; Marcinek et al., 2001; Blank et al., 2007), and swim constantly to respire. Mitochondria must play a key role in resupplying the ATP that is constantly being consumed by muscle contraction. Although, mitochondria are the primary consumers of oxygen during aerobic metabolism they can also produce reactive oxygen species (ROS), primarily as superoxide and H_2O_2. ROS production is generally measured as H_2O_2 efflux, which combines the net production of superoxide and H_2O_2. Excessive production of ROS may lead to macromolecular damage (Murphy, 2009; Jastroch et al., 2010). Studies on mitochondria isolated from ectotherms indicate that the rate of ROS production increases with temperature (Abele et al., 2002; Heise et al., 2003; Chung and Schulte, 2015; Banh et al., 2016); raising the possibility that the warming of specific regions in endothermic fish may also result in increased potential for mitochondrial H_2O_2 efflux. If higher physiological temperatures could lead to elevated potential for ROS production then compensatory mechanisms to minimize mitochondrial H_2O_2 production may co-evolve with endothermy.

We recently demonstrated that H_2O_2 efflux from muscle mitochondria isolated from three ectothermic fishes was much lower than rates for rat muscle mitochondria when assayed at physiological temperatures of 15° and 37°C for the ectothermic fish and rat respectively (Banh et al., 2016). However, the fractional electron leak (FEL), a value that normalizes ROS production relative to total mitochondrial electron flux, was markedly higher for fish mitochondria compared to the rat at physiological temperatures (Banh et al., 2016). The high FEL in the fish suggests that relative to the overall metabolic capacity of the mitochondria (including the electron transport chain and Krebs cycle where the majority of superoxide/H_2O_2 producing complexes are found) ectothermic fish mitochondria have intrinsically higher potential for H_2O_2 production compared to the rat. For all species examined the rate of mitochondrial H_2O_2 production was greater at higher temperatures. Indeed, in some cases, mitochondria from trout and carp produced as much or more H_2O_2 at 25°C than rat mitochondria did at 37°C (Banh et al., 2016). Taken together these findings suggest that muscle mitochondria from ectotherms may have a greater propensity for H_2O_2 production compared to a representative endotherm.

Our recent work proposed that mitochondrial H_2O_2 producing and consuming pathways have differing temperature sensitivities (Banh et al., 2016). This thermal mismatch hypothesis of mitochondrial H_2O_2 metabolism (Banh et al., 2016) predicts that compensatory mechanisms may have been crucial in the evolution of endothermy because excess ROS production would be associated with oxidative stress and disruption of redox homeostasis. Thus, one can hypothesize that some compensatory response to mitigate the influence of elevated body temperatures could be concomitant with the evolution of endothermy. The current study tests this hypothesis by comparing mitochondria isolated from red muscle of the endothermic Pacific Bluefin tuna (*Thunnus orientalis*), maintained at an elevated 25°C, with three ectothermic fishes at 15°C. For reference we also evaluate the well-studied rat as a representative endothermic mammal. For all species the respiratory capacity and rate of H_2O_2 formation was measured at the respective physiological temperatures and a common temperature of 25°C to test if tuna had reduced potential for ROS formation relative to their mitochondrial metabolic capacity (estimated by respiration rate). Overall, we find that tuna red muscle mitochondria are similar to those of ectothermic fish species in both the capacity and thermal sensitivity of ROS formation. Thus, enhanced mitochondrial superoxide/H_2O_2 production may be an underappreciated consequence of the tissue warming found in the muscle of endothermic fishes.

MATERIALS AND METHODS

Animals and Sampling

All animal use procedures were based on the policies from the Canadian Council on Animal Care and approved by the University of Manitoba Fort Garry Campus Animal Care Committee (for ectothermic fish and rat) or the Stanford Administrative Panel on Laboratory Animal Care Committee in accordance to all policies of Stanford University (tuna).

Pacific Bluefin Tuna

Pacific bluefin tuna (*T. orientalis*) were housed at the Tuna Research and Conservation Center at Stanford University's Hopkins Marine Station, Pacific Grove, CA. Animal collection, transport and husbandry were the same as previously reported (Galli et al., 2009; Clark et al., 2010) and all animals in this study were acclimated to 20°C prior to experimental initiation for at least 30 days. Fish were of both sexes and ∼13–15 kg and 80–90 cm in fork length. For sampling, fish were killed by pithing, followed by spinal severance at the junction between the spine and skull. Tissues were immediately removed and placed in ice-cold isolation medium for preparation of mitochondria.

Ectothermic Fish

The ectothermic fishes in this study include two other teleosts, the relatively high aerobic capacity rainbow trout (*Oncorhynchus mykiss*) and the low activity benthic-dwelling common carp (*Cyprinus carpio*) as well as the lake sturgeon (*Acipenser fulvescens*), a relatively inactive Acipenseriform species. Rainbow trout and carp were obtained from commercial suppliers. Lake sturgeon were reared from eggs fertilized at the University of Manitoba. All ectothermic fish were maintained at 15°C, for at least 8 weeks, on a 12:12 photoperiod in flow-through tanks and fed commercial pelleted food to satiation at least every other day. Fish were of both sexes and were ∼1.5–4.5 kg. For sampling, fish were killed by a blow to the head, followed by severing of the gill arches, and tissues were immediately dissected out and placed in ice-cold isolation medium.

Rats

Male Sprague–Dawley rats, ∼250–400 g, were from the University of Manitoba and housed at the Duff–Roblin Animal Holding facility in standard cages with wood shaving or cardboard bedding along with shelters, washers and other plastic environmental enrichment. Rats had *ad libitum* access to chow and water. Rats were killed by asphyxiation with CO_2 followed by pneumothorax and hindlimb muscle was dissected off and put in ice-cold isolation medium prior to processing for isolation of mitochondria.

Mitochondrial Isolation

Tissues were rinsed in ice-cold isolation medium and diced to facilitate homogenization. Two isolation media were used in this study. For tuna, we used 140 mM KCl, 20 mM HEPES, 2 mM EGTA, pH 7.0 at 20°C whereas 120 mM KCl, 20 mM HEPES, 1 mM EGTA, pH 7.1 at 20°C was used for the rats and carp. For rainbow trout and sturgeon we tested both isolation media and found no difference in results. All steps were maintained at 0–4°C. The procedure for rats (Affourtit et al., 2012) and the ectothermic fishes (Banh et al., 2016) are described in detail elsewhere but, briefly, involved incubating diced tissue with a protease followed by disruption by homogenization and isolation of mitochondria by differential centrifugation. The final pellet was resuspended in a small volume of isolation medium at ∼20–45 mg mitochondrial protein · ml^{-1} (determined by biuret assay with BSA as standard).

For tuna, diced tissue was mixed with ice-cold homogenization medium (isolation medium plus 0.5% w/v BSA) and homogenized with a motor-driven Teflon (Polytetrafluoroethylene) to glass homogenizer. The homogenate was centrifuged for 5 min at 900 × *g*. The supernatant was collected and filtered through a fine plastic mesh to aid in lipid and particulate removal. Following filtration, the supernatant was centrifuged at 9,000 × *g* for 10 min. The resulting pellet was washed by resuspending in isolation medium followed by centrifugation 9,000 × *g* for 10 min. Care was taken to not transfer any of the lipid in the supernatant or resuspend any material that was clearly not mitochondria (for example red blood cells and particulate matter). The resulting pellet was washed a second time (as described above) and the final pellet was resuspended in a small volume of isolation medium at ∼30–60 mg mitochondrial protein · ml^{-1} (determined by biuret assay with BSA as standard).

Mitochondrial H_2O_2 Production

Combined superoxide and hydrogen peroxide production by mitochondria was measured spectrofluorometrically as H_2O_2 efflux in the same medium as used for respiration. In some cases phosphate was omitted or 1 μg · ml^{-1} oligomycin was added, we found these had relatively little (c. 10% or less) influence on the observed rates and thus pooled all data. The assay medium also contained an H_2O_2 detection system consisting of 5 IU · ml^{-1} of horseradish peroxidase, 25 IU · ml^{-1} superoxide dismutase, and 50 μM Amplex UltraRed in a total volume of 2 ml using either an Agilent Eclipse or a Shimadzu RF-5301PC. Fluorescence was monitored, with constant stirring, at 560 nm excitation and 590 nm emission wavelengths, respectively. Raw fluorescence values were transformed to moles of H_2O_2 based on calibration with known amounts of H_2O_2. Background rates of product formation prior to the addition of substrate were low (typically <10% of rate with substrate) and were subtracted from rates in the presence of substrate.

Mitochondrial Respiration

Mitochondrial substrate oxidation was measured in a water-jacketed chamber with a Rank Brothers Clark-type oxygen electrode (Cambridge, U.K) or using the Oroboros O2K (Innsbruck, Austria). Tuna mitochondria used the following respiration medium: 140 mM KCl, 20 mM Hepes, 1 mM EGTA, 5 mM K_2HPO_4, and 0.5% (w/v) BSA, pH 7.3 at 20°C. For ectotherm fish and rats the standard medium was 120 mM KCl, 20 mM Hepes, 1 mM EGTA, 5 mM K_2HPO_4, and 0.3% (w/v) BSA, pH 7.4 at 20°C. Note, we found comparable (within 10%) results between the two respiration media with the ectothermic fish mitochondria.

Following addition of mitochondria to the chamber the rates of oxygen consumption were measured under the following respiratory conditions: (i) non-phosphorylating, in the presence of exogenous substrate (state 2); (ii) phosphorylating, the rate with exogenous substrate plus 500 or 800 μM ADP (state 3); (iii) a pharmacologically induced non-phosphorylating state, with 1 μg · ml^{-1} oligomycin (which blocks ATP synthesis) (state 4o). These conditions were measured in sequence and the respiratory control ratios (RCR) were calculated as the rate of oxygen consumption of mitochondria in state 3/state 4o.

Data Analysis

All data are shown as mean ± SEM. Values were compared either by ANOVA (with Student-Newman–Keuls *post-hoc* test) or *t*-test (Welch's) with $p < 0.05$ being considered significant.

To determine the FEL we calculated values based on:

$$\text{FEL} = 100\times\Big[(\text{rate of } H_2O_2 \text{ efflux})\times\big(\text{rate of } H_2O_2 \text{ efflux} + \text{rate of } O_2 \text{ consumption}\big)^{-1}\Big]$$

Where H_2O_2 efflux rate is in nmol min^{-1} mg $protein^{-1}$ and O_2 consumption rate is in nmol O min^{-1} mg $protein^{-1}$. In some cases rates of H_2O_2 efflux and O_2 consumption could

not be measured at all assay temperatures for mitochondria isolated from the same individual animal therefore values are expressed as mean ± SEM where the SEM was derived by standard error propagation procedures. Differences among these mean values were compared by 2-tailed Welch's *t*-test ($p < 0.05$ being considered significant).

RESULTS

Interspecific Patterns in Rates of H_2O_2 Production

Aerobic locomotion in both fish and mammals is largely fuelled by carbohydrate and lipid oxidation (Lauff and Wood, 1996, 1997; McClelland, 2004), as such, we evaluated the potential for mitochondrial ROS formation during the oxidation of either pyruvate or palmitoylcarnitine to reflect these respective fuels. In both cases saturating malate was also included to alleviate the trapping of intramitochondrial coenzyme-A as acetyl-CoA by the provisioning of oxaloacetate and to supply NADH for complex I via malate dehydrogenase. When compared at physiological temperatures, 15°, 25°, and 37°C for ectothermic fish, Bluefin tuna and rat respectively, there was a pattern of increasing capacity for ROS production as physiological temperature increased but the tuna mitochondrial ROS production at 25°C was comparable to the rat mitochondria at 37°C (**Figure 1**).

In all species the mitochondrial H_2O_2 production was sensitive to temperature (**Figure 1**) with similar sensitivity across species. At higher temperatures the rate of H_2O_2 production was increased. Overall the rates of H_2O_2 production by isolated Pacific bluefin tuna mitochondria were comparable to other fishes. When measured at a common assay temperature of 25°C, the physiological temperature for the bluefin tuna red muscle, rates of H_2O_2 production by tuna mitochondria were not different from mitochondria isolated from the other fishes (**Figure 1**). In all cases the rates at 25°C in fish mitochondria were markedly higher than the rate seen with rat muscle mitochondria with both carbohydrate and lipid based oxidative substrates (**Figure 1**). Within species we found no pattern of difference in rates of H_2O_2 formation between oxidation of pyruvate or palmitoylcarnitine (**Figures 1A,B**).

Comparisons of Respiratory Rates

To evaluate if the differences seen in H_2O_2 production rates might be linked to mitochondrial respiratory capacity we measured the rates of respiration at physiological temperatures as well as at a common temperature of 25°C. Under conditions of phosphorylating respiration (presence of ADP) and non-phosphorylating respiration (absence of ADP phosphorylation) there was an overall tendency for increasing rates with increasing physiological temperature (**Figure 2**). At the common temperature of 25°C the rates of respiration with either pyruvate or palmitoylcarnitine (both supplemented with malate) were not different across fish mitochondria, with the exception of sturgeon being higher than trout with pyruvate and malate under phosphorylating conditions (**Figure 2**). Rates of respiration were generally higher for rat mitochondria. The respiratory control ratio (RCR) was not affected by assay temperature except for trout (**Figure 2C**) and at 25°C the RCR for Pacific bluefin tuna was not different from the other fishes. The stability of RCR values across temperatures suggests collapsing mitochondrial coupling efficiency with changing temperature is an unlikely explanation for differences in H_2O_2 production with assay temperature.

Fractional Electron Leak

At a common assay temperature of 25°C the FEL for all fish species was markedly greater than for rat, with Pacific

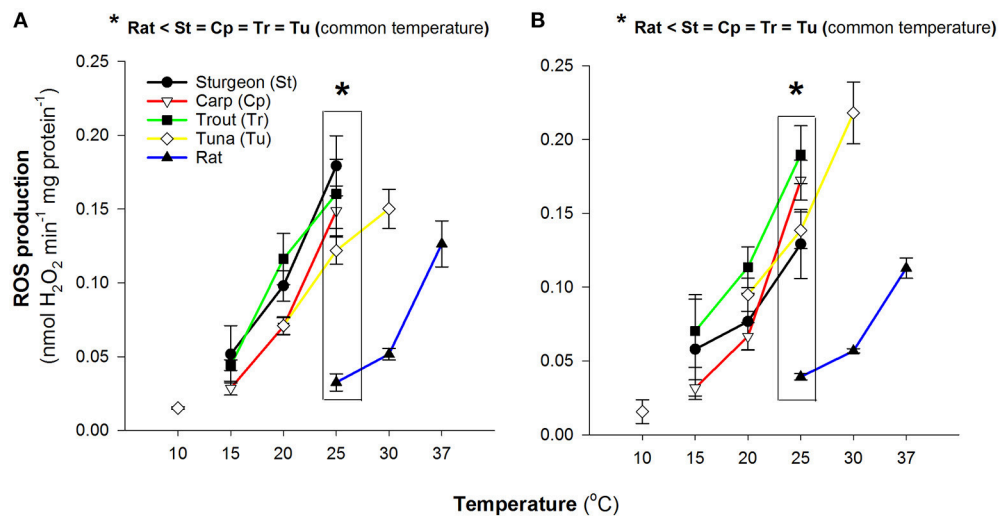

FIGURE 1 | Comparison of reactive oxygen species production by isolated muscle mitochondria. Data are mean ± SEM (n = 3–5 depending on species) and substrates were 5 mM pyruvate and malate **(A)** or 0.05 mM D/L-palmitoylcarnitine and 5 mM malate **(B)**. Assay temperature is indicated and rates were determined as H_2O_2 efflux normalized to mitochondrial protein. Physiologically relevant temperatures are 15°C for sturgeon, carp and trout; 25°C for Bluefin tuna; 37°C for rat.

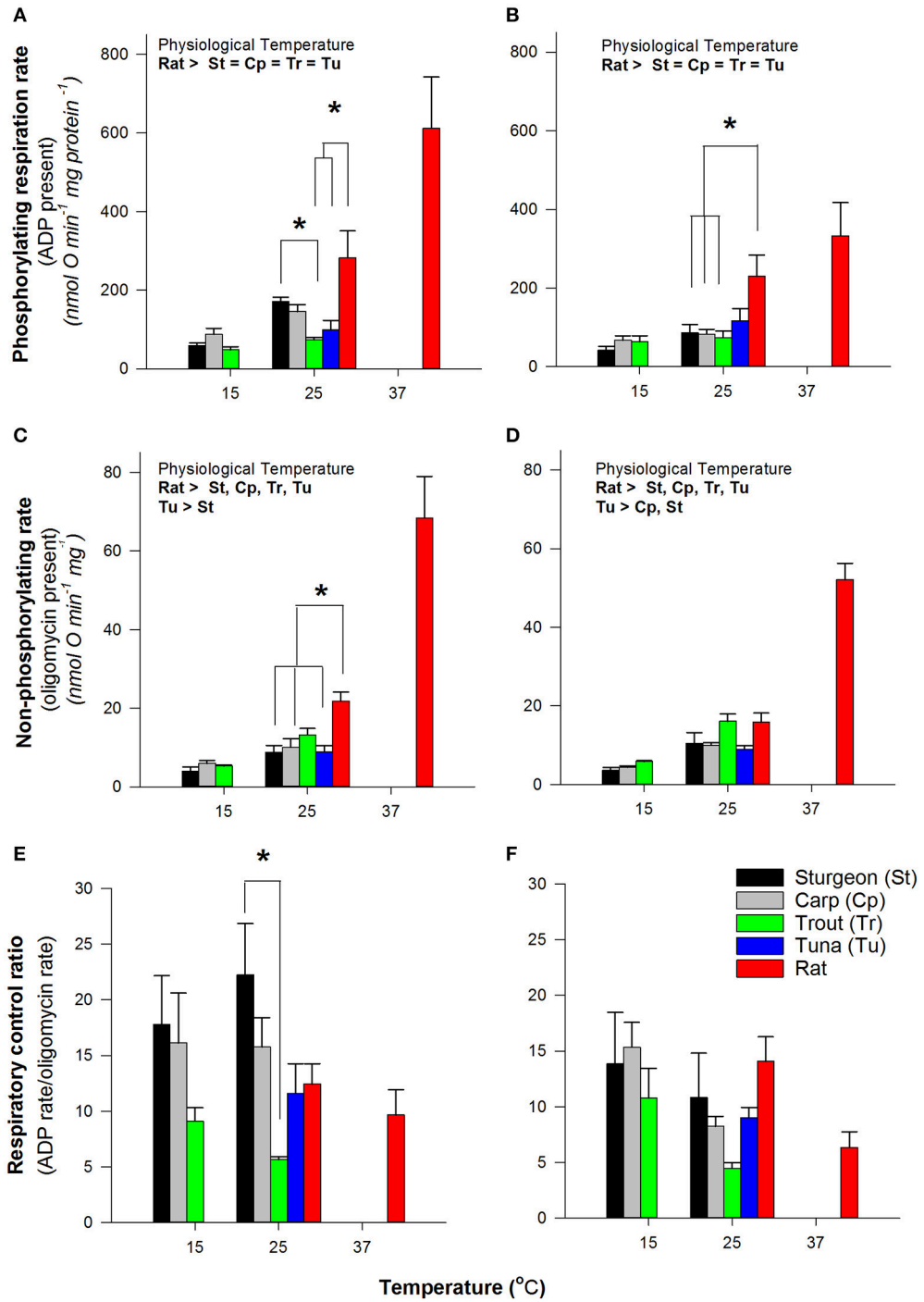

FIGURE 2 | Comparison of respiration rates by isolated muscle mitochondria. Data are mean ± SEM (n = 3–5 depending on species) and substrates were 5 mM pyruvate and malate **(A,C,E)** or 0.05 mM D/L-palmitoylcarnitine and 5 mM malate **(B,D,F)**. Assay temperature is indicated and contrasts were made at a common temperature (indicated by * and brackets) or physiological temperatures as indicated within figures. Physiologically relevent temperatures are 15°C for sturgeon, carp and trout; 25°C for Bluefin tuna; 37°C for rat.

bluefin tuna being unexceptional in comparison to the other fish (**Figure 3**). For species where two test temperatures were used (all species but the tuna) there was a tendency for increasing FEL with higher assay temperature. This thermal sensitivity led to some ectothermic fishes having values for FEL that were not different from the rat at physiological temperatures (**Figure 3**), but the high levels of variation warrant some caution with interpretation of this result.

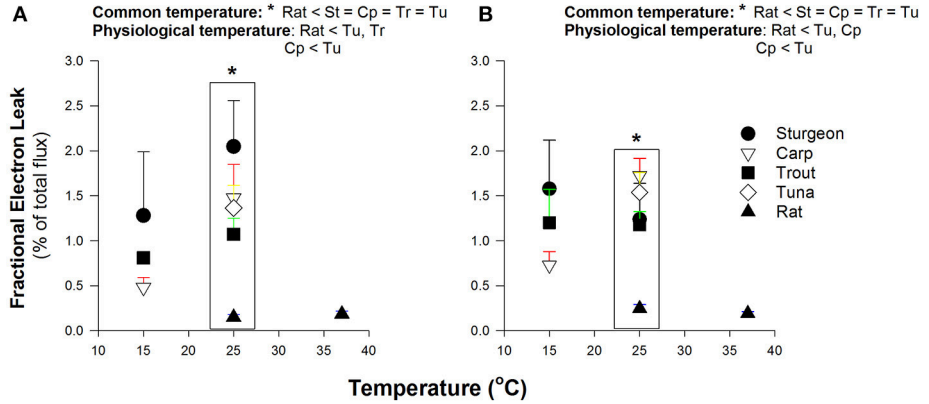

FIGURE 3 | Fractional electron leak by isolated muscle mitochondria. Data are mean ± SEM (n = 3–5 depending on species) and substrates were 5 mM pyruvate and malate **(A)** or 0.05 mM D/L-palmitoylcarnitine and 5 mM malate **(B)**. Assay temperature is indicated and contrasts were made at a common temperature (indicated by * and brackets) or physiological temperatures as indicated within figures. Physiologically relevent temperatures are 15°C for sturgeon, carp and trout; 25°C for Pacific bluefin tuna; 37°C for rat. Species abbreviations are as indicated in **Figures 1**, **2**.

DISCUSSION

Comparisons among Fishes

For all species examined the production of H_2O_2 by isolated muscle mitochondria was a function of assay temperature. Higher assay temperatures led to higher rates of production (**Figure 1**). However, across assay temperatures and using all substrate mixes tested, the rates of H_2O_2 production by isolated Pacific bluefin tuna mitochondria compared favorably with other fish mitochondria. Similarly, Pacific bluefin tuna mitochondria had similar respiration rates to most other fish red muscle mitochondria when measured at a common assay temperature irrespective of the physiological body temperature for the mitochondria (**Figure 2**). Our respiration rates with pyruvate also compare well with those for other teleosts over a range of both *in vitro* assay and physiological temperatures (Johnston et al., 1994, 1998) suggesting our mitochondrial preparations are reasonably consistent with those used in other studies on temperature effects on fish mitochondria.

A potential way to separate mitochondrial H_2O_2 production from the mitochondrial roles in oxygen consumption is to express the electron leakage to H_2O_2 as a fraction of the overall electron flux (FEL). Using the FEL we find no evidence for reduced potential for H_2O_2 formation relative to substrate oxidation rates; tuna mitochondria were similar to mitochondria from ectothermic fishes (**Figure 3**). The respiratory capacity, measured as ADP-stimulated respiration rate, was similar in Pacific bluefin tuna mitochondria to most other fish red muscle mitochondria. This similarity in respiration rate is consistent with no compensatory change in the endothermic tuna red muscle in the overall metabolic systems responsible for electron flux to oxygen either as respiration or leaking as mitochondrial H_2O_2 production. Of note, one could argue that the ADP-stimulated rate of oxygen consumption better reflects the overall amount of biochemical "machinery" in the mitochondrion, and thus the phosphorylating rate of respiration (state 3) is a better denominator to normalize H_2O_2 production; however, we find the same overall pattern is seen as that for FEL indicating that regardless of the respiration rate used to normalize H_2O_2 production all fish muscle mitochondria appear comparable at the same assay temperature (data not shown).

Comparison of Muscle Mitochondria from Fish and the Rat

We included one representative mammal, the rat. Overall, mitochondria from all fish assayed appear to have greater potential for electron leak relative to their respiratory capacity (FEL) compared to the rat. The similarity of FEL across fishes in this study suggests fishes, and possibly other ectotherms, may have a propensity toward increased electron leakage compared to more derived endothermic species. This may represent an adaption to minimize the ROS induced damage that could occur at higher endogenous temperatures common in mammals and birds. This pattern warrants further investigation to determine if it holds more broadly across taxa. Contrasting endothermic and ectothermic representative birds and reptiles would be a particularly interesting comparison along these lines.

Fuel Selection: Is There a Trade-Off between H_2O_2 Production and Specific Carbon Source?

During aerobic locomotion both lipid and carbohydrate are important carbon sources for oxidation in teleost fishes (Lauff and Wood, 1996, 1997) and mammals (McClelland, 2004). This is consistent with relatively similar rates of pyruvate and fatty acid oxidation by isolated muscle mitochondria from teleosts as seen by us and others (Moyes et al., 1989, 1992; Chamberlin et al., 1991). Thus, pyruvate and palmitoylcarnitine were used as representative carbohydrate- and lipid-based oxidative substrates in the present study.

These physiologically important substrates were also chosen because they are known to produce H_2O_2 in isolated mitochondria (reviewed in Brand, 2010). Pyruvate and

palmitoylcarnitine may contribute directly to mitochondrial ROS production via the matrix enzymes involved with their metabolism, as well as indirectly by producing NADH and QH_2 which reduce electron transport chain complexes I and III respectively. It has been reported that palmitoylcarnitine driven respiration in rodent mitochondria may have high capacity for H_2O_2 production compared to other NADH-generating substrates (St Pierre et al., 2002; Seifert et al., 2010); although more recent work found the rates comparable to that found with other NADH-generating substrates (Perevoshchikova et al., 2013). If lipid fuelled respiration was to lead to greater potential for H_2O_2 production then there is a possibility that the enhanced lipid oxidation proposed for high-performance fishes (Weber and Haman, 1996) may have consequences on mitochondrial H_2O_2 production. However, we broadly find comparable rates of H_2O_2 production, FEL, and ADP-stimulated respiration rates with isolated muscle mitochondria from several fishes and one mammal. As such, our evidence does not support a trade-off between selection for lipid or carbohydrate oxidation in muscle and potential for H_2O_2 production.

Limitations of the Study

ADP Availability in Fish Red Muscle

The rate of H_2O_2 production from mitochondria isolated from several tissues, including brain, liver and muscle, typically declines in the presence of ADP (Starkov and Fiskum, 2003; Starkov et al., 2004; Santiago et al., 2008; Quinlan et al., 2012; Goncalves et al., 2015). This decline appears to be primarily due to decreased protonmotive force and the consequent decreased reduction state of electron carriers and the enzyme complexes involved with electron transport and substrate oxidation. Although, some ADP is always being produced in skeletal muscle due to ATP hydrolysis, we are unaware of precise data to estimate the exact ADP availability typical in the red muscle of the various fish species we examined here. For this reason we use the rate of H_2O_2 production in the absence of ADP as a worst case scenario of ROS production under conditions of saturating substrate and oxygen availability. Even though the ADP availability in red muscle of constantly swimming fish should alleviate some ROS formation, our results suggest that mitochondria in a teleost with elevated muscle temperature should be exposed to a greater H_2O_2 production rate than if the same mitochondria were respiring at a lower temperature.

Underestimations of H_2O_2 Production Due to Matrix Consumers

Using H_2O_2 efflux as a measure of H_2O_2 production by isolated mitochondria underestimates the actual production and with rat muscle mitochondria this underestimate is a function of the production rate, with high rates leading to lower underestimates (Munro et al., 2016). It was not possible to undertake the complex procedure to compromise the matrix H_2O_2 consuming pathways (see Munro et al., 2016 for full details) and thus we cannot exclude the possibility that patterns seen here may not fully reflect the actual rates of production for each species. As such, it is possible a compensatory increase in antioxidant capacity is found in Bluefin tuna that our dataset may not capture. Alternatively, the increased antioxidant capacity with increasing temperature, even if incomplete as proposed elsewhere (Banh et al., 2016), may be sufficient to compensate for increase H_2O_2 production capacity.

Size Scaling Effects

The production of H_2O_2 by isolated mitochondria may scale with body size with larger animals having lower rates of H_2O_2 production than smaller species (Lambert et al., 2007). We have not tried to account for mass-scaling effects but in the case of the rat, the smallest species used, it would be expected this pattern would disproportionately elevate H_2O_2 production. Conversely, rat has the lowest rate of H_2O_2 formation at a common assay temperature. For the fishes, the Pacific bluefin tuna was the largest of the species and thus may have somewhat lower rates of H_2O_2 production due to scaling effects. Even if the bluefin tuna H_2O_2 values are low due to their larger size this would not change our primary thesis in this study: there is no support for reduced H_2O_2 production by isolated muscle mitochondria from this endothermic fish species since correcting for mass would be expected to increase the rates in tuna relative to smaller fish species.

Muscle Fiber Type

Finally, all fish muscle mitochondrial preparations were from red muscle, which is almost exclusively slow-twitch muscle because of the anatomical separation of slow and fast twitch fibers in most fishes making fish excellent models for studying muscle mitochondrial function from specific fiber types (Leary et al., 2003). However, the rat muscle preparation will be a mix of fiber types and it has been reported that the H_2O_2 formation varies by fiber type in rodent muscle (Anderson and Neufer, 2006). But again the pattern found should have biased the rat mitochondrial preparation toward elevated H_2O_2 production because fast-twitch muscle appears to produce more H_2O_2 than slow-twitch fibers (Anderson and Neufer, 2006). Therefore, we conclude that our finding of markedly lower H_2O_2 formation in the representative mammal should not be compromised but the use of a mixed muscle type for this species alone.

Summary

The elevated red muscle temperature in endothermic fishes should increase the potential for H_2O_2 formation but we see no evidence for compensatory decrease in H_2O_2 production in the Pacific Bluefin tuna, whereas we do see this in a representative endothermic mammal. Slow-twitch red muscle has a primary function in locomotion in these fish. This suggests that there is a trade-off in red, slow-twitch muscle between thermal effects that are selected for to improve muscle performance at elevated temperature (Altringham and Block, 1997), and the propensity toward mitochondrial H_2O_2 formation in the evolution of endothermy in fishes.

AUTHOR CONTRIBUTIONS

LW: Helped write initial manuscript draft, contributed original data and data analysis; SB: Contributed original data, analysis and

editorial contribution to manuscript; ES: Contributed original data and editorial contribution to manuscript; MJ: Contributed to study design, provided original data, and assisted in writing manuscript; BB: Contributed to study design and with writing of manuscript; MB: Contributed to study design and with writing of manuscript; JT contributed to study design, provided original data, and assisted in writing manuscript.

FUNDING

Funding was provided by a NSERC Discovery Grant (#418503 to JT) and the Canada Research Chairs Program (#223744 to JT), Funds from Stanford and the Monterey Bay Aquarium in support of the Tuna Research and Conservation Center (BB), NIH (R01-AG033542 to MB), and DFG grant JA 1884/2-1 (MJ).

ACKNOWLEDGMENTS

The authors thank Dr. George Somero and his lab for accommodating spectrophotometer use at Hopkins Marine Station, as well as, to the staff of the Tuna Research and Conservation Centre and the Duff Roblin Animal Holding Facility staff (University of Manitoba) for their exceptional assistance with sampling and logistics.

REFERENCES

Abele, D., Heise, K., Portner, H. O., and Puntarulo, S. (2002). Temperature-dependence of mitochondrial function and production of reactive oxygen species in the intertidal mud clam *Mya arenaria*. *J. Exp. Biol.* 205, 1831–1841.

Affourtit, C., Quinlan, C. L., and Brand, M. D. (2012). Measurement of proton leak and electron leak in isolated mitochondria. *Methods Mol. Biol.* 810, 165–182. doi: 10.1007/978-1-61779-382-0_11

Altringham, J. D., and Block, B. A. (1997). Why do tuna maintain elevated slow muscle temperatures? Power output of muscle isolated from endothermic and ectothermic fish. *J. Exp. Biol.* 200, 2617–2627.

Anderson, E. J., and Neufer, P. D. (2006). Type II skeletal myofibers possess unique properties that potentiate mitochondrial H_2O_2 generation. *Am. J. Physiol. Cell Physiol.* 290, C844–C851. doi: 10.1152/ajpcell.00402.2005

Banh, S., Wiens, L., Sotiri, E., and Treberg, J. R. (2016). Mitochondrial reactive oxygen species production by fish muscle mitochondria: potential role in acute heat-induced oxidative stress. *Comp. Biochem. Physiol. B* 191, 99–107. doi: 10.1016/j.cbpb.2015.10.001

Bernal, D., Dickson, K. A., Shadwick, R. E., and Graham, J. B. (2001). Review: analysis of the evolutionary convergence for high performance swimming in lamnid sharks and tunas. *Comp. Biochem. Physiol. A* 129, 695–726. doi: 10.1016/S1095-6433(01)00333-6

Blank, J. M., Morrissette, J. M., Farwell, C. J., Price, M., Schallert, R. J., and Block, B. A. (2007). Temperature effects on metabolic rate of juvenile Pacific bluefin tuna *Thunnus orientalis*. *J. Exp. Biol.* 210, 4254–4261. doi: 10.1242/jeb.005835

Block, B. A. (1994). Thermogenesis in muscle. *Annu. Rev. Physiol.* 56, 535–577. doi: 10.1146/annurev.ph.56.030194.002535

Block, B. A., and Finnerty, J. R. (1994). Endothermy in fishes: a phylogenetic analysis of constraints, predispositions, and selection pressures. *Environ. Biol. Fishes* 40, 283–302. doi: 10.1007/BF00002518

Block, B. A., Teo, S. L. H., Walli, A., Boustany, A., Stokesbury, M. J. W., Farwell, C. J., et al. (2005). Electronic tagging and population structure of Atlantic bluefin tuna. *Nature* 434, 1121–1127. doi: 10.1038/nature03463

Boustany, A. M., Matteson, R., Castleton, M., Farwell, C., and Block, B. A. (2007). Movements of Pacific bluefin tuna (*Thunnus orientalis*) in the Eastern North Pacific revealed with archival tags. *Prog. Oceanogr.* 86, 94–104. doi: 10.1016/j.pocean.2010.04.015

Brand, M. D. (2010). The sites and topology of mitochondrial superoxide production. *Exp. Geront.* 45, 466–472. doi: 10.1016/j.exger.2010.01.003

Chamberlin, M. E., Glemet, H. C., and Ballantyne, J. S. (1991). Glutamine metabolism in a holostean (*Amia calva*) and teleost fish (*Salvelinus namaycush*). *Am. J. Physiol.* 260, R159–R166.

Chung, D. J., and Schulte, P. M. (2015). Mechanisms and costs of mitochondrial thermal acclimation in a eurythermal killifish (*Fundulus heteroclitus*). *J. Exp. Biol.* 218, 1621–1631. doi: 10.1242/jeb.120444

Clark, T. D., Brandt, W. T., Nogueira, J., Rodriguez, L. E., Price, M., Farwell, C. J., et al. (2010). Postprandial metabolism of Pacific bluefin tuna (*Thunnus orientalis*). *J. Exp. Biol.* 213, 2379–2385. doi: 10.1242/jeb.043455

Dickson, K. A., and Graham, J. B. (2004). Evolution and consequences of endothermy in fishes. *Physiol. Biochem. Zool.* 77, 998–1018. doi: 10.1086/423743

Galli, G. L., Lipnick, M. S., and Block, B. A. (2009). Effect of thermal acclimation on action potentials and sarcolemmal K^+ channels from Pacific bluefin tuna cardiomyocytes. *Am. J. Physiol.* 297, R502–R509. doi: 10.1152/ajpregu.90810.2008

Goncalves, R. L., Quinlan, C. L., Perevoshchikova, I. V., Hey-Mogensen, M., and Brand, M. D. (2015). Sites of superoxide and hydrogen peroxide production by muscle mitochondria assessed *ex vivo* under conditions mimicking rest and exercise. *J. Biol. Chem.* 290, 209–227. doi: 10.1074/jbc.M114.619072

Graham, J. B., and Dickson, K. A. (2004). Tuna comparative physiology. *J. Exp. Biol.* 207, 4015–4024. doi: 10.1242/jeb.01267

Heise, K., Puntarulo, S., Pörtner, H. O., and Abele, D. (2003). Production of reactive oxygen species by isolated mitochondria of the Antarctic bivalve *Laternula elliptica* (King and Broderip) under heat stress. *Comp. Biochem. Physiol. C* 134, 79–90. doi: 10.1016/S1532-0456(02)00212-0

Jastroch, M., Divakaruni, A. S., Mookerjee, S., Treberg, J. R., and Brand, M. D. (2010). Mitochondrial proton and electron leaks. *Essays Biochem.* 47, 53–67. doi: 10.1042/bse0470053

Johnston, I. A., Calvo, J., Guderley, H., Fernandez, D., and Palmer, L. (1998). Latitudinal variation in the abundance and oxidative capacities of muscle mitochondria in perciform fishes. *J. Exp. Biol.* 201, 1–12.

Johnston, I. A., Guderley, H., Franklin, C., Crockford, T., and Kamunde, C. N. (1994). Are mitochondria subject to evolutionary temperature adaptation? *J. Exp. Biol.* 195, 293–306.

Lambert, A. J., Boysen, H. M., Buckingham, J. A., Yang, T., Podlutsky, A., Austad, S. N., et al. (2007). Low rates of hydrogen peroxide production by isolated heart mitochondria associate with long maximum lifespan in vertebrate homeotherms. *Aging Cell* 6, 607–618. doi: 10.1111/j.1474-9726.2007.00312.x

Lauff, R. F., and Wood, C. M. (1997). Effects of training on respiratory gas exchange, nitrogenous waste excretion, and fuel usage during aerobic swimming in juvenile rainbow trout (*Oncorhynchus mykiss*). *Can. J. Fish. Aquat. Sci.* 54, 566–571. doi: 10.1139/f96-315

Lauff, R., and Wood, C. (1996). Respiratory gas exchange, nitrogenous waste excretion, and fuel usage during aerobic swimming in juvenile rainbow trout. *J. Comp. Physiol. B* 166, 501–509. doi: 10.1007/BF02338293

Leary, S. C., Lyons, C. N., Rosenberger, A. G., Ballantyne, J. S., Stillman, J., and Moyes, C. D. (2003). Fiber-type differences in muscle mitochondrial profiles. *Am. J. Physiol.* 285, R817–R826. doi: 10.1152/ajpregu.00058.2003

Marcinek, D. J., Blackwell, S. B., Dewar, H., Freund, E. V., Farwell, C., Dau, D., et al. (2001). Depth and muscle temperature of Pacific bluefin tuna examined with acoustic and pop-up satellite archival tags. *Mar. Biol.* 138, 869–885. doi: 10.1007/s002270000492

McClelland, G. B. (2004). Fat to the fire: the regulation of lipid oxidation with exercise and environmental stress. *Comp. Biochem. Physiol. B* 139, 443–460. doi: 10.1016/j.cbpc.2004.07.003

Moyes, C. D., Buck, L. T., Hochachka, P. W., and Suarez, R. K. (1989). Oxidative properties of carp red and white muscle. *J. Exp. Biol.* 143, 321–331.

Moyes, C. D., Mathieucostello, O. A., Brill, R. W., and Hochachka, P. W. (1992). Mitochondrial metabolism of cardiac and skeletal muscles from a fast (*Katsuwonus pelamis*) and a slow (*Cyprinus carpio*) fish. *Can. J. Zool.* 70, 1246–1253. doi: 10.1139/z92-172

Munro, D., Banh, S., Sotiri, E., Tamanna, N., and Treberg, J. R. (2016). The thioredoxin and glutathione-dependent H_2O_2 consumption pathways in muscle mitochondria: Involvement in H_2O_2 metabolism and consequence to H_2O_2 efflux assays. *Free Radic. Biol. Med.* 96, 334–346. doi: 10.1016/j.freeradbiomed.2016.04.014

Murphy, M. P. (2009). How mitochondria produce reactive oxygen species. *Biochem. J.* 417, 1–13. doi: 10.1042/BJ20081386

Perevoshchikova, I. V., Quinlan, C. L., Orr, A. L., Gerencser, A. A., and Brand, M. D. (2013). Sites of superoxide and hydrogen peroxide production during fatty acid oxidation in rat skeletal muscle mitochondria. *Free Radic. Biol. Med.* 61, 298–309. doi: 10.1016/j.freeradbiomed.2013.04.006

Quinlan, C. L., Treberg, J. R., Perevoshchikova, I. V., Orr, A. L., and Brand, M. D. (2012). Native rates of superoxide production from multiple sites in isolated mitochondria measured using endogenous reporters. *Free Radic. Biol. Med.* 53, 1807–1817. doi: 10.1016/j.freeradbiomed.2012.08.015

Santiago, A. P. S., Chaves, E. A., Oliveira, M. F., and Galina, A. (2008). Reactive oxygen species generation is modulated by mitochondrial kinases: correlation with mitochondrial antioxidant peroxidases in rat tissues. *Biochimie* 90, 1566–1577. doi: 10.1016/j.biochi.2008.06.013

Seifert, E. L., Estey, C., Xuan, J. Y., and Harper, M. E. (2010). Electron transport chain-dependent and -independent mechanisms of mitochondrial H_2O_2 emission during long-chain fatty acid oxidation. *J. Biol. Chem.* 285, 5748–5758. doi: 10.1074/jbc.M109.026203

St Pierre, J., Buckingham, J. A., Roebuck, S. J., and Brand, M. D. (2002). Topology of superoxide production from different sites in the mitochondrial electron transport chain. *J. Biol. Chem.* 277, 44784–44790. doi: 10.1074/jbc.M207217200

Starkov, A. A., and Fiskum, G. (2003). Regulation of brain mitochondrial H_2O_2 production by membrane potential and NAD(P)H redox state. *J. Neurochem.* 86, 1101–1107. doi: 10.1046/j.1471-4159.2003.01908.x

Starkov, A. A., Fiskum, G., Chinopoulos, C., Lorenzo, B. J., Browne, S. E., Patel, M. S., et al. (2004). Mitochondrial α-ketoglutarate dehydrogenase complex generates reactive oxygen species. *J. Neurosci.* 24, 7779–7788. doi: 10.1523/JNEUROSCI.1899-04.2004

Stevens, E. D., Kanwisher, J. W., and Carey, F. G. (2000). Muscle temperature in free-swimming giant Atlantic bluefin tuna (*Thunnus thynnus* L.). *J. Therm. Biol.* 25, 419–423. doi: 10.1016/S0306-4565(00)00004-8

Weber, J. M., and Haman, F. (1996). Pathways for metabolic fuels and oxygen in high performance fish. *Comp. Biochem. Physiol. A* 113, 33–38 doi: 10.1016/0300-9629(95)02063-2

Wegner, N. C., Snodgrass, O. E., Dewar, H., and Hyde, J. R. (2015). Whole-body endothermy in a mesopelagic fish, the opah, *Lampris guttatus*. *Science* 348, 786–789. doi: 10.1126/science.aaa8902

Whitlock, R. E., Hazen, E. L., Walli, A., Farwell, C., Bograd, S. J., Foley, D. G., et al. (2015). Direct quantification of energy intake in an apex marine predator suggests physiology is a key driver of migrations. *Sci. Adv.* 1:e1400270. doi: 10.1126/sciadv.1400270

Conflict of Interest Statement: The authors declare that the research was conducted in the absence of any commercial or financial relationships that could be construed as a potential conflict of interest.

frontiers in Physiology

HYPOTHESIS AND THEORY
published: 11 December 2017
doi: 10.3389/fphys.2017.01005

Quantitative Genetic Modeling of the Parental Care Hypothesis for the Evolution of Endothermy

Leonardo D. Bacigalupe[1], Allen J. Moore[2], Roberto F. Nespolo[1], Enrico L. Rezende[3,4] and Francisco Bozinovic[3]*

[1] Instituto de Ciencias Ambientales y Evolutivas, Facultad de Ciencias, Universidad Austral de Chile, Valdivia, Chile, [2] Department of Genetics, University of Georgia, Athens, GA, United States, [3] Departamento de Ecología, Facultad de Ciencias Biológicas, Center of Applied Ecology and Sustainability, Pontificia Universidad Católica de Chile, Santiago, Chile, [4] Facultad de Ecología y Recursos Naturales, Universidad Andres Bello, Santiago, Chile

There are two heuristic explanations proposed for the evolution of endothermy in vertebrates: a correlated response to selection for stable body temperatures, or as a correlated response to increased activity. Parental care has been suggested as a major driving force in this context given its impact on the parents' activity levels and energy budgets, and in the offspring's growth rates due to food provisioning and controlled incubation temperature. This results in a complex scenario involving multiple traits and transgenerational fitness benefits that can be hard to disentangle, quantify and ultimately test. Here we demonstrate how standard quantitative genetic models of maternal effects can be applied to study the evolution of endothermy, focusing on the interplay between daily energy expenditure (DEE) of the mother and growth rates of the offspring. Our model shows that maternal effects can dramatically exacerbate evolutionary responses to selection in comparison to regular univariate models (breeder's equation). This effect would emerge from indirect selection mediated by maternal effects concomitantly with a positive genetic covariance between DEE and growth rates. The multivariate nature of selection, which could favor a higher DEE, higher growth rates or both, might partly explain how high turnover rates were continuously favored in a self-reinforcing process. Overall, our quantitative genetic analysis provides support for the parental care hypothesis for the evolution of endothermy. We contend that much has to be gained from quantifying maternal and developmental effects on metabolic and thermoregulatory variation during adulthood.

Keywords: endothermy, parental care, quantitative genetics, daily energy expenditure, maternal effects

OPEN ACCESS

Edited by:
Rebecca Oelkrug, University of Lübeck, Germany

Reviewed by:
Paweł Koteja, Jagiellonian University, Poland
Piter Bijma, Wageningen University & Research, Netherlands

****Correspondence:***
Leonardo D. Bacigalupe
lbacigal@gmail.com

Specialty section:
This article was submitted to Integrative Physiology, a section of the journal Frontiers in Physiology

Received: *28 April 2017*
Accepted: *21 November 2017*
Published: *11 December 2017*

Citation:
Bacigalupe LD, Moore AJ, Nespolo RF, Rezende EL and Bozinovic F (2017) Quantitative Genetic Modeling of the Parental Care Hypothesis for the Evolution of Endothermy. Front. Physiol. 8:1005. doi: 10.3389/fphys.2017.01005

INTRODUCTION

The evolution of endothermy in birds and mammals is one of the most puzzling topics in evolutionary physiology (Ruben, 1995; see reviews in Hayes and Garland, 1995; Koteja, 2004; Kemp, 2006; Nespolo et al., 2011). Although endothermy has evolved in many taxonomic groups from plants to insects, birds and mammals are unique because they are able to maintain elevated body temperatures at rest employing the heat produced mainly in the visceral organs (heart, kidneys, liver, intestines) instead of muscle contraction (Ruben, 1995). Those organs have high metabolism per unit of tissue and thus contribute disproportionately to the maintenance metabolism, or basal

metabolic rate (BMR), which ultimately determines endothermy (Konarzewski and Diamond, 1995). Despite its multiple benefits, however, organisms are not able to switch-off these expensive organs when they do not need them (e.g., elevated temperatures), and consequently their constant maintenance seems a wasteful strategy from an energetic point of view (Koteja, 2004). Given the elevated energy costs associated with endothermy, the selective pressures that have favored the emergence of high-energy turnover rates remain highly controversial (Nespolo et al., 2011).

Several hypotheses have been advanced to explain the evolution of elevated BMR in mammals and birds. Most of the debate revolves around two main hypotheses, namely that endothermy evolved as a correlated response to selection for higher and stable body temperatures on the one hand, or for higher levels of aerobic metabolism for sustained activity on the other hand (Hayes and Garland, 1995; Ruben, 1995; Koteja, 2004; Kemp, 2006). Importantly, a shared characteristic of both hypotheses is that they focus solely on selection of adult organisms and subsequent evolutionary responses. Alternatively, parental care was recently proposed as a major target of selection during the evolution of endothermy (Farmer, 2000; Koteja, 2000, 2004; Clavijo-Baquet et al., 2016), which is not mutually exclusive with the previous scenarios but highlights potential fitness benefits to the offspring that have been previously ignored. Specifically, the selective advantages of decreased mortality of the offspring by means of a faster growth rate, either due to the ability of the parents to control incubation temperature (Farmer, 2000) and/or to provide food (Farmer, 2000; Koteja, 2000), could potentially offset the energy costs associated with a highly active endothermic lifestyle. Therefore, even though different hypotheses do not agree on the proximate mechanism by which a higher metabolic levels evolved, they do agree that to understand the evolution of endothermy we should look at the complete life history of organisms (Koteja, 2000; Clavijo-Baquet and Bozinovic, 2012).

Our aim here is to present a theoretical framework for testing the parental care hypothesis (Farmer, 2000; Koteja, 2000) based on adapting a simple quantitative genetic model of maternal effects develop by Cheverud (1984) and Cheverud and Moore (1994). We work with the premise that parental care is energetically costly fundamentally because providing food to the offspring requires high and sustained locomotor activity fueled by assimilated food (Koteja, 2000, 2004). High energy turnover rates involve processing greater amounts of food and therefore require high capacities in the visceral organs associated with these processes, namely the organs that contribute disproportionately to BMR (Bacigalupe and Bozinovic, 2002; Bacigalupe et al., 2004) and, eventually, to elevated body temperature as heat dissipation decreases with better thermal insulation. This suggests that both the energy costs and the putative benefits of parental care, which involve primarily food provisioning and the ability to control incubation temperatures, can be captured by daily energy expenditure (DEE) of the parents. Therefore, following the approach that is outlined in detail by Cheverud and Moore (1994), we model the phenotypic evolution of offspring growth rate as a partial consequence of mother parental care, expressed as DEE (Koteja, 2000).

This approach follows the theoretical modeling of maternal effects (Kirkpatrick and Lande, 1989; Cheverud and Moore, 1994) or more generally interacting phenotypes (Moore et al., 1997), treating the offspring and maternal traits as different and separate. Thus, traits expressed by the mother provide an environmental influence on offspring but the maternal trait itself can vary due to genetic variation amongst mothers, and is heritable. Thus, there are two important aspects of maternal interacting phenotypes. First, a trait in one individual influences the phenotype of the other. Here, we assume that maternal DEE affects the expression of the offspring trait, but the offspring trait does not influence the maternal DEE. This results in genetic contributions to offspring traits such as growth rate that reflect both direct genetic effects expressed in the offspring and indirect genetic effects arising from DEE expressed in the mother that is acting as an environment on the offspring. Second, selection acts on *both* traits, so that genetic variation in one trait can influence the evolution in a second trait. This can enhance or retard evolution, and the focal trait can evolve even if there are no direct genetic effects for that trait (Moore et al., 1997; Bijma, 2014). The effect discussed here is that the evolution of the offspring trait is influenced by the evolution of maternal DEE as well. Thus, our model is not simply a mathematical treatment of the parental care hypothesis but goes one step further. That is, apart from understanding the consequences of selection acting on parental care only, as proposed by Koteja (2000) and Farmer (2000), we also model the evolutionary consequences of selection acting on offspring growth rates for both offspring and mothers.

For details of the derivations of models of maternal effects and associated selection, the primary literature should be consulted (e.g., Cheverud, 1984; Riska et al., 1985; Kirkpatrick and Lande, 1989; Cheverud and Moore, 1994 and references therein). As detailed in Cheverud (1984) and Cheverud and Moore (1994), the model presented here has the usual assumptions of quantitative genetics (Lynch and Walsh, 1998), including the phenotype is affected by many genes of small additive effect, there is no dominance or epistasis, and selection is weak. We also assume maternal effects are unidirectional (i.e., there are no maternal effects on offspring DEE and there is no feedback from the offspring growth rate to the maternal DEE; see Moore et al., 1997; McGlothlin and Brodie, 2009; Bijma, 2014 for more detailed discussions of other assumptions). These assumptions can be relaxed; particularly the feedback assumption (Riska et al., 1985), but the main message and parameters to measure remain unchanged.

MATERNAL EFFECTS AND ENDOTHERMY: THE MODEL

Here we present a variance component model for the evolution of offspring performance affected by maternal endothermy. This model incorporates social effects; that is, the influence of traits expressed in others that also influence the traits of a focal

individual. Such traits, or interacting phenotypes (Moore et al., 1997), are likely common (Bijma, 2014) and have consequences for both selection and inheritance, due to "indirect genetic effects" (Moore et al., 1997; Bijma, 2014). Because there are often prolonged associations between mothers and offspring, as well as prenatal provisioning of the egg by the mother, the most common form of indirect genetic effect are maternal genetic effects arising from maternal effects. It is this form of interacting phenotype model and indirect genetic effect that we consider here. Although we have focused on care by a single sex and interchangeably describe maternal or parental effects, this model can easily be extended to include effects from the father as well as the mother (Cheverud and Moore, 1994).

Because offspring performance and endothermy are both influenced by many different traits within an individual, here we employ the more general variance component model. We believe that this model is heuristically the most easily understood. Importantly, the parameters that our model suggests should be measured are the same regardless of the specific maternal effect model used (McGlothlin and Brodie, 2009). For example, Kirkpatrick and Lande (1989) developed a general model that considers maternal effects and specific traits, and their multivariate model is most appropriate when all traits are known and measured, which is not the case here (see McGlothlin and Brodie, 2009; Bijma, 2014 for a discussion of the difference). Aside from being somewhat more tractable empirically, without knowledge of all the maternal traits that contribute to the offspring phenotype, the most reliable empirical approach is to estimate offspring performance as a way of estimating maternal effects.

Inheritance When Phenotypes Interact–Indirect Genetic Effects

Consider a trait that contributes to performance and survival, such as body weight or growth rate. In quantitative genetic terms, such trait can be described in terms of the additive genetic and environmental components that make up that trait:

$$z = a + e \tag{1}$$

Where z is any phenotype (measured trait), a is the additive genetic effect, and e is the environmental contribution, or all non-additive genetic effects plus all environmental effects.

Although this is the standard linear model for any trait (Lynch and Walsh, 1998), many focal phenotypes of an individual are influenced by the phenotypes of other individuals in the environment, especially relatives such as mothers. Body weight and growth rate are offspring performance traits, which are often influenced by both the genes expressed in the individual and the environment provided by the mother (or any parental effect). We therefore add subscripts to indicate which trait, maternal or offspring, is being considered where traits expressed in the offspring are given the subscript O and traits expressed in the mother are given the subscript DEE as we are assuming here that DEE is the trait in the mother that influences offspring performance. For example, z_{DEE} in our model is the maternal DEE influenced by additive genetic effects and non-additive and environmental effects:

$$z_{DEE} = a_{DEE} + e_{DEE} \tag{2a}$$

Equation 2a is a standard quantitative genetic description for any phenotypic trait. However, here we are considering offspring traits such as growth rate that may be influenced by the parent in contributions that go beyond genetics; i.e., maternal effects arising from parental care (here, maternal DEE). Thus, the description for the offspring growth rate (z_O) includes the contribution of the mother's phenotype:

$$z_O = a_O + e_O + z_{DEE(t-1)} \tag{2b}$$

The new term that is added is z_{DEE}, which reflects that the offspring trait is influenced by additive genetic effects, non-additive and environmental effects, and—subdividing the environmental effect into another specific component—the maternal environment created by DEE of the mother.

$$z_O = a_O + e_O + a_{DEE(t-1)} + e_{DEE(t-1)} \tag{2c}$$

In Equation 2c, we have further divided the environment provided by the mother [maternal DEE, $z_{DEE(t-1)}$] which itself reflects genetic influences on the mother as well as the environment influenced by the mother. The $t-1$ subscript indicates that these effects were expressed in the previous generation of the mother but are having an influence on the current offspring generation.

Equation 2c is a standard and general quantitative genetic model of maternal effects. This phenotypic model can then be used further to consider how traits evolve; i.e., respond to selection and change across generations. For this it is useful to define the total breeding value, A, which is calculated from the sum of the individual trait breeding values reflecting the average effect of an individual on the population. In the case of a trait that is influenced by maternal effects:

$$A = A_O + \frac{1}{2}A_{DEE} \tag{3}$$

where ½ reflects the fact that in diploid organisms only ½ of the genes are contributed by each parent. Because we are modeling a maternal trait, we have to account for the fact that only ½ of the genetic influence arises from the mother. We illustrate these influences on phenotypes and inheritance in **Figure 1**.

Evolution of Interacting Phenotypes–Direct and Correlated Responses

Evolutionary change in a trait (symbolized $\Delta\bar{z}$ for change over a single generation) is reflected by two components, inheritance and selection. Using the terminology and equations provided by Lande and Arnold (1983):

$$\Delta\bar{z} = V_A\beta = h^2S \tag{4a}$$

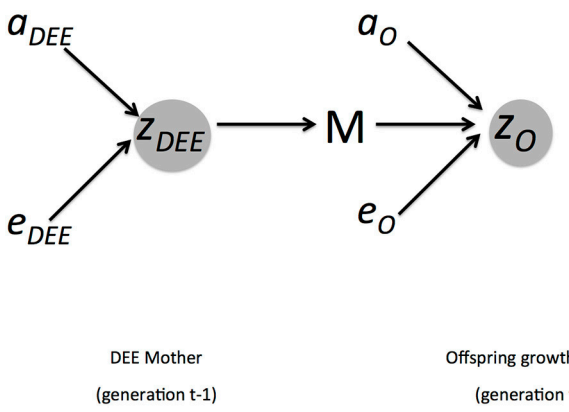

FIGURE 1 | Summary of genetic and environmental influences of mothers DEE (z_{DEE}) on offspring growth rate (z_O). Arrows indicate direction of causality. The offspring phenotype is influenced by direct additive genetic effects (a_O), non-additive and environmental effects (e_O), and the maternal environment M. This is part of the environment of the offspring, but as a maternal trait it is also influenced by direct additive genetic effects (a_{DEE}) and non-additive and environmental ones (e_{DEE}). The covariance (Cov(A_O, A_{DEE}), not shown here) between growth rate and DEE arises because the offspring also inherits the DEE genes from the mother.

where $\Delta\bar{z}$ is the mean change in a single given phenotype from one generation to the next, V_A is the additive genetic variance (i.e., variance in breeding values, A; Lynch and Walsh, 1998), and β is the selection gradient. This is equivalent to the familiar "breeder's equation," where the mean change reflects the heritability (h^2) and the selection differential, S. Selection gradients and differentials are defined by Lande and Arnold (1983) and a practical description on their measurement and applications is provided in Brodie et al. (1995). Quantitative genetic modeling is facilitated by focusing on selection gradients, which measure the strength of the association between any phenotypic trait and fitness (i.e., the covariance between a trait and fitness) independent of other traits. Alternatively, in terms of evolution of breeding values, this can be expressed as a change in the total breeding value after selection.

$$\Delta\bar{z} = \Delta\overline{A} \tag{4b}$$

We can thus substitute Equations 2a–c for z, or Equation 3 for A, to calculate potential evolution.

The Lande and Arnold (1983) equation is easily generalizable to multiple genetic influences; i.e., we can generalize the genetic contributions beyond simple direct genetic effects and additive genetic variance. Any given trait may share genetic influences with other traits through pleiotropy or linkage disequilibrium, and therefore the evolution of that trait is influenced by changes in genetically correlated traits. Under these conditions, we should consider all the combined genetic contributions; i.e., both genetic variances and covariances. Thus, we must consider genetics of multiple traits even when examining the evolution of a single trait. Furthermore, the traits should be measured on a common scale, typically where the mean = 0 and variance = 1, after first being transformed (when necessary) to meet the assumption of normality. Such standardization of phenotypic traits also results in standardized regression coefficients (Lande and Arnold, 1983), which also allows us to compare evolutionary change in phenotypic standard deviation and facilitates comparisons.

When maternal effects are present, we must consider the effects of genes that influence both the maternal trait and the offspring trait, because any given individual will carry genes for both (Equation 3; **Figure 1**). We can still consider single trait evolution, but now we can include correlated responses to selection due to genetic covariances arising from linkage disequilibrium or pleiotropy. Thus, considering Equation 2b or 3, we can now consider how maternal traits that influence offspring might change alongside the focal trait of interest in offspring because mothers and offspring share genetic influences.

As a first step, we can consider the evolution of each trait separately, reflecting just direct selection on that trait. Beginning with the offspring trait z_O, corresponding to growth rate, its selection gradient β_O and substituting from the equations for the phenotypes (Equation 2c) we obtain:

$$\Delta\bar{z}_O = \left[V_{AO} + \frac{3}{2}Cov\left(A_O, A_{DEE}\right) + \frac{1}{2}V_{A(DEE)}\right]\beta_O \tag{5}$$

Equation 5 illustrates how direct selection on the offspring growth rate z_O can result in complex evolutionary responses due to maternal effects (Equation 4). The coefficients 3/2 and 1/2 arise from the relatedness of mothers and offspring ($r = 0.5$), thus only ½ of the genes in the offspring were derived from the mother.

This equation reflects several aspects of maternal effects. In particular, genetic variation in the focal individual (here, the offspring) reflects traits that have influences in two generations.

Moreover, this equation describes the change in growth rates of the offspring arising from direct selection on this trait. There are two important outcomes illustrated by this model. First, the evolutionary response of offspring growth rate $\Delta\bar{z}_O$ does not depend only on the presence of additive genetic effects on this trait, as would be expected under the standard quantitative genetic model that assumes that $h^2 = V_{AO}/V_{ZO}$ (or $h^2 = V_A$ if the phenotypic variance is scaled to 1). Interestingly, this equation also shows that heritable variation in the maternal trait [i.e., $V_{A(DEE)}$] can lead to evolutionary change $\Delta\bar{z}_O = \frac{1}{2}V_{A(DEE)}\beta_O$ even in the absence of genetic variation in growth rates! In eco-physiological terms, the effect occurs because growth rates are partly mediated by DEE and the amount of parental investment (Equations 2b,c), hence selection for faster growth rates can elicit an evolutionary response by favoring higher levels of parental investment. Second, selection on offspring β_O is filtered through the genetic covariance Cov(A_O, A_{DEE}), and consequently the response to selection on offspring growth rate will be affected by the sign and magnitude of this correlation. The result of any non-zero covariance is, therefore, that selection on the offspring will produce a correlated response on mother's DEE (i.e., when female offspring become mothers in the future generation $t + 1$)

and selection on DEE in the maternal generation will produce an evolutionary response in offspring growth rate.

We next consider how selection would influence DEE in the mothers. We are assuming there is no feedback between offspring and the mother, in such a way that the mother's DEE affects offspring growth rate, but the offspring growth rate does not affect mother's DEE. Although we realize this might not always be the case (i.e., a demanding offspring might induce higher levels of activity on mothers and thus on her DEE) including these reciprocal effects tend to accelerate the rate of evolution even further (Moore et al., 1997). In this context, the evolution of DEE is described by the standard model:

$$\Delta\bar{z}_{DEE} = V_{A(DEE)}\beta_{DEE} \quad (6)$$

where $V_{A(DEE)}$ is the additive genetic variance of maternal DEE and β_{DEE} the selection gradient acting on DEE.

Having analyzed how growth rates and DEE should respond to, respectively, directional selection β_O in the offspring (generation t) and β_{DEE} in the parents (generation t–1), we can now assess how these traits respond in tandem to both selective pressures. In this case, the total response depends on the selection gradients and both direct and correlated responses, or:

$$\Delta\bar{z}_O = \left[V_{AO} + \frac{3}{2}Cov\left(A_O, A_{DEE}\right) + \frac{1}{2}V_{A(DEE)}\right]\beta_O + \left[V_{A(DEE)} + Cov(A_O, A_{DEE})\right]\frac{1}{2}\beta_{DEE} \quad (7a)$$

$$\Delta\bar{z}_{DEE} = \left[\frac{1}{2}V_{A(DEE)} + Cov(A_O, A_{DEE})\right]\beta_O + \left[V_{A(DEE)}\right]\frac{1}{2}\beta_{DEE} \quad (7b)$$

These equations highlight the importance of maternal effects in the context of the evolution of endothermy, showing that selection on growth rates (β_O) and maternal DEE (β_{DEE}) should generally result in a correlated response in the other trait for two reasons. First, a correlated response is expected if there is a non-zero genetic covariance Cov(A_O, A_{DEE}), which is by no means surprising. Second, correlated responses could occur even in the absence of genetic covariance due to maternal effects *sensu stricto* (i.e., environmental effects). In this scenario, for instance, selection β_{DEE} for elevated maternal DEE should elicit an evolutionary response in $\Delta\bar{z}_O$ (**Figure 2**) because parental investment is expected to increase at a rate proportional to ½ $V_{A(DEE)}$(Equation 7a). Alternatively, selection for higher offspring growth rates β_O should affect maternal DEE (Equation 7b) because, as one selects for offspring that grow faster at generation t, one is indirectly favoring increased parental investment at generation t–1 and genes associated with DEE (**Figure 3**). However, because selection occurs in different generations, there will be time-lags and evolution may not be direct (see Kirkpatrick and Lande, 1989 for a description of the effects of time-lags, which tend to be short term). Long-term evolution is not affected (i.e., evolution continues toward an optimum) but the path is not as direct when there are maternal effects, depending on the nature of the genetic covariance between the maternal and offspring trait. If it is positive, evolution will be enhanced. If it is negative, evolution will be slowed and may, temporarily, occur in a direction away from an optimum.

Overall, these equations suggest that, depending on their sign and magnitude, selection gradients β_O and β_{DEE} and the genetic covariance Cov(A_O, A_{DEE}) between maternal and offspring traits can have synergistic effects (**Figures 2**, **3**). During the evolution of endothermy, higher growth rates and DEE should be favored by selection, resulting in positive β_O and β_{DEE}, and we would also expect Cov(A_O, A_{DEE}) to be positive because elevated assimilation rates should increase both growth rates and DEE. Under these circumstances, synergistic effects

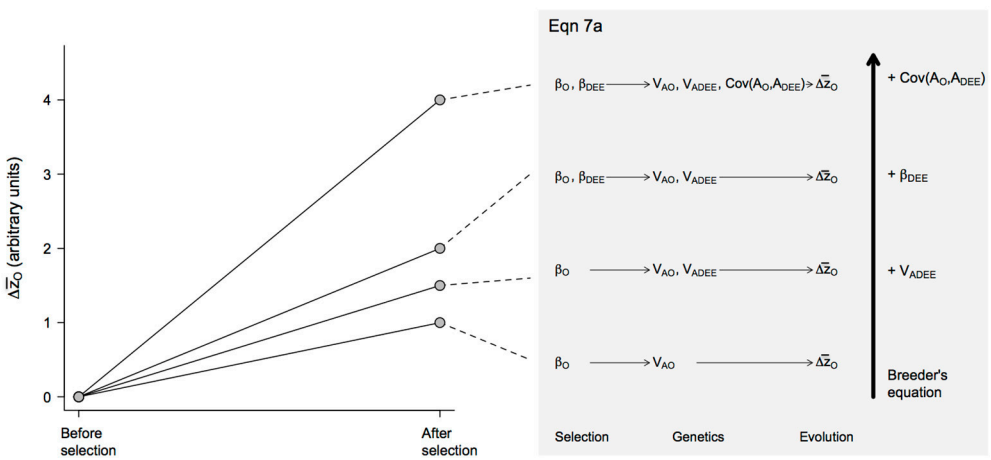

FIGURE 2 | Predicted evolutionary responses of offspring growth rates ($\Delta\bar{z}_O$) in different evolutionary scenarios. The magnitude of the response was estimated from Equation 7a, with the presence or absence of different effects—$V_{A(DEE)}$, β_{DEE} and Cov(A_O, A_{DEE})—included by setting these coefficients to 1 or 0, respectively. Similarly, the coefficients V_{AO} and β_O that were always present in the model were set to 1. The resulting evolutionary scenarios are illustrated with the diagrams on the right size, which increase in complexity from bottom to top as an increasing number of effects are incorporated in the model.

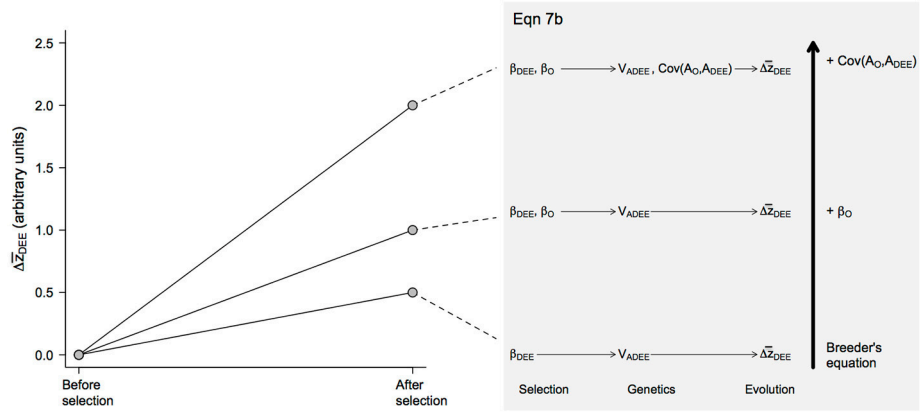

FIGURE 3 | Predicted evolutionary responses of maternal DEE ($\Delta\bar{z}_{DEE}$) in different evolutionary scenarios. The magnitude of the response was calculated from Equation 7b following the same procedure detailed for offspring growth rates (**Figure 2**). Note that the magnitude of the response is smaller than in offspring growth rates because selection is assumed to impact only mothers, not fathers, resulting in some terms being multiplied by ½ as is the case with breeder's equation when β_O is set to 0 (see Equation 7b).

should exacerbate evolutionary responses of both parental and offspring phenotypes (**Figure 4**). This self-reinforcement process could be sustained until one of three things happen. First, there are no longer fitness benefits for faster growth rate ($\beta_O = 0$) or increased DEE levels ($\beta_{DEE} = 0$). Second, these traits reach a physiological limit (Bacigalupe and Bozinovic, 2002) so that V_{AO} and $V_{A(DEE)} = 0$. Third, the covariance Cov(A_O, A_{DEE}) between maternal and offspring phenotypes becomes negative due, for instance, to constraints in time and energy allocation (e.g., a trade-off between looking for food vs. taking care of the offspring).

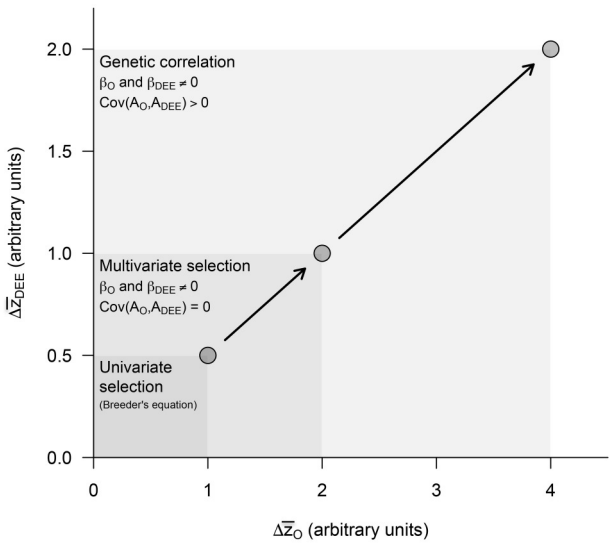

FIGURE 4 | Predicted evolutionary responses in offspring growth rates ($\Delta\bar{z}_O$) and maternal DEE ($\Delta\bar{z}_{DEE}$) in increasingly complex evolutionary scenarios. The presence or absence of an effect was simulated by setting the different parameters to 0 or 1 (see **Figures 2**, **3**). We start estimating evolutionary responses to univariate selection exerted separately in each of these traits (i.e., $\beta_{DEE} = 0$ in Equation 7a and $\beta_O = 0$ in Equation 7b) in the absence of genetic covariance [i.e., Cov(A_O, A_{DEE}) = 0], and then quantify the impact of multivariate selection and of a positive genetic covariance between traits. These two synergistic effects, which emerge from the standard quantitative genetic model including maternal effects, are expected to exacerbate evolutionary responses to selection in both traits and provide strong support to the parental care hypothesis for the evolution of endothermy.

DISCUSSION

In this article, we present a theoretical analysis for the evolution of endothermy by parental care by adapting a simple quantitative genetic model of maternal effects. The equations we present are discussed in detail in Cheverud and Moore (1994), see also Moore et al. (1998). Our model shows that maternal effects may have had an important contribution to the evolution of increased metabolic levels, due to a positive covariance between growth rates and DEE and synergistic effects of selection acting on these traits (**Figures 2**, **3**). These would translate into greater evolutionary change per generation in both offspring and maternal traits (**Figure 4**) and are expected to result in elevated BMR—and eventually body temperature—as visceral organs increase in size and activity to maintain elevated assimilation rates (Koteja, 2000, 2004).

The evolutionary consequences of maternal effects have long been known in animal breeding (e.g., Falconer, 1965; Willham, 1972) and have been increasingly incorporated into an evolutionary framework (e.g., Cheverud, 1984; Kirkpatrick and Lande, 1989; Cheverud and Moore, 1994; Mousseau and Fox, 1998; Wilson and Réale, 2005; Räsänen and Kruuk, 2007). Unlike other abiotic environmental influences, the environmental influence exerted by mothers or close relatives is unique: if there is variation on the environment provided and if that variation results from genetic differences between individuals, the environment can have a heritable basis and evolve (Moore et al., 1997; Wolf et al., 1998). Three important evolutionary

consequences arise from the environment having a genetic basis, as evidenced in our results. First, the rate and/or direction of phenotypic change in response to selection in the focal trait can be quite different from what would be predicted by standard quantitative genetics. Second, phenotypic evolution might not be constrained by the absence of heritability in the focal trait (Cheverud and Moore, 1994; Moore et al., 1997). And third, the synergistic effects of more than a single selective pressure on DEE and growth rates (Equations 7a,b) would not only drive faster rates of evolution of these traits, but might have also contributed to the continued directional sustained selection over longer periods of time required for the emergence of endothermy as we know it (Clarke and Pörtner, 2010).

Much of the mechanistic basis underlying the parental care hypothesis for the evolution of endothermy has been discussed previously, as well as the evidence available supporting this proposition (Farmer, 2000; Koteja, 2000). The main contribution of our model is to provide a formal assessment of the impact of parental care on the evolution of increased metabolic levels on the one hand and growth rates on the other. In this context, results indeed support the contention that parental care may have been a crucial factor behind the emergence of highly aerobic endothermic birds and mammals. According to our model, the presence of maternal effects may exacerbate the response to selection due to two independent effects that could act synergistically (**Figure 4**): a positive genetic covariance between maternal and offspring phenotypes, embedded in component $\mathrm{Cov}(A_O, A_{DEE})$ (Equations 7a,b), and an environmentally-mediated component driving the correlated evolution of growth rates to selection on maternal DEE (β_{DEE} on Equation 7a) and vice-versa (β_O on Equation 7b). This result also leads to the counterintuitive possibility that growth rates and DEE could respond in tandem even when their genetic covariances were negative, as reported for maternal performance at weaning and offspring weight (Cheverud and Moore, 1994), although in this case evolutionary change may be seriously reduced (Kirkpatrick and Lande, 1989).

For tractability, our model treats DEE as a single trait. In reality, it is likely a composite trait. DEE is typically linked with multiple traits that influence parental care, such as BMR and assimilation rates (Koteja, 2000), as well as maternal body temperature and, indirectly, with incubation temperature (Farmer, 2000). While the association between DEE and BMR finds strong support in the literature (reviewed in Auer et al., 2017), how DEE is related to assimilation rates, body temperature and parental investment remains contentious (but see Sadowska et al., 2013, 2015). Confounding effects such as for instance, contrasting environmental temperatures, food availability, clutch size and the existence of multiple forms of parental care, preclude the establishment of general associations between these traits in extant lineages, let alone in transitional forms during the evolution of endothermy. Thus, while it might be argued that our model overestimates the importance of parental care, the main take-home message that synergistic evolutionary responses due to maternal effects may be substantially larger than predictions in the absence of these effects remains largely unchanged (see also Wolf and Wade, 2001).

Importantly, our model also highlights that selection on life-history traits that are mediated by maternal effects, such as growth rates and survival, can have important carryover effects in other aspects of the phenotype such as metabolic levels. While an increasing number of studies describe, for instance, the metabolic impact of changes in incubation temperatures in the offspring metabolic rates (e.g., Nord and Nilsson, 2011; DuRant et al., 2012; Sun et al., 2015), we contend that these effects may transcend early stages of ontogeny and have an impact on adult phenotypes and on evolutionary trajectories in the long term (Equations 7a,b). In this context, the role of maternal and developmental effects on metabolic and thermoregulatory performance during adulthood remains, we believe, virtually unexplored (but see Russel et al., 2008). In light of the comparative, mechanistic and theoretical evidence that support a key role of parental care during the evolution of endothermy, studying how maternal and developmental effects contributes to physiological variation during adulthood constitutes a promising venue for future research.

AUTHOR CONTRIBUTIONS

Conception and design: LB and AM. All authors collaborated with the draft of the work and approved the final version of the manuscript.

ACKNOWLEDGMENTS

Funded by FONDECYT grants 1150029 and 1170017 to LB and ER, respectively, NSF IOS-1354358 to AM, and CAPES FB0002-2014 line 3 to FB. The comments of several reviewers, especially Piter Bijma and Pawel Koteja helped us to clarify many points and avoid several mistakes.

REFERENCES

Auer, S. K., Killen, S. S., and Rezende, E. L. (2017). Resting vs. active: a meta-analysis of the intra- and inter-specific associations between minimum, sustained, and maximum metabolic rates in vertebrates. *Funct. Ecol.* 31, 1728–1738. doi: 10.1111/1365-2435.12879

Bacigalupe, L. D., and Bozinovic, F. (2002). Design, limitations and sustained metabolic rate: lessons from small mammals. *J. Exp. Biol.* 205, 2963–2970.

Bacigalupe, L. D., Nespolo, R. F., Bustamante, D. M., and Bozinovic, F. (2004). The quantitative genetics of sustained energy budget in a wild mouse. *Evolution* 58, 421–429. doi: 10.1111/j.0014-3820.2004.tb01657.x

Bijma, P. (2014). The quantitative genetics of indirect genetic effects: a selective review of modelling issues. *Heredity (Edinb)* 112, 61–69. doi: 10.1038/hdy.2013.15

Brodie, E. D. III, Moore, A. J., and Janzen, F. J. (1995). Visualizing and quantifying natural selection. *Trends Ecol. Evol.* 10, 313–318. doi: 10.1016/S0169-5347(00)89117-X

Cheverud, J. M. (1984). Evolution by kin selection: a quantitative genetic model illustrated by maternal performance in mice. *Evolution* 38, 766–777. doi: 10.1111/j.1558-5646.1984.tb00349.x

Cheverud, J. M., and Moore, A. J. (1994). "Quantitative genetics and the role of the environment provided by relatives in behavioral evolution," in *Quantitative*

Genetic Studies of Behavioral Evolution, ed C. R. B. Boake (Chicago, IL: University of Chicago Press), 67–100.

Clarke, A., and Pörtner, H. O. (2010). Temperature, metabolic power and the evolution of endothermy. *Biol. Rev. Camb. Philos. Soc.* 85, 703–727. doi: 10.1111/j.1469-185X.2010.00122.x

Clavijo-Baquet, S., and Bozinovic, F. (2012). Testing the fitness consequences of the thermoregulatory and parental care models for the origin of endothermy. *PLoS ONE* 7:e37069. doi: 10.1371/journal.pone.0037069

Clavijo-Baquet, S., Cumplido, N., and Bozinovic, F. (2016). Resting metabolic rate is positively correlated with parental care behavior in dwarf hamster. *J. Exp. Zool. Physiol.* 325A, 274–282. doi: 10.1002/jez.2014

DuRant, S. E., Hopkins, W. A., Wilson, A. F., and Hepp, G. R. (2012). Incubation temperature affects the metabolic cost of thermoregulation in a young precocial bird. *Funct. Ecol.* 26, 416–422. doi: 10.1111/j.1365-2435.2011.01945.x

Falconer, D. S. (1965). "Maternal effects and selection response," in *Genetics Today, Proceedings of the XI International Congress on Genetics*, Vol. 3, ed S. J. Geerts (Pergamon: Oxford), 763–774.

Farmer, C. G. (2000). Parental care: the key to understanding endothermy and other convergent features in birds and mammals. *Am. Nat.* 155, 326–334. doi: 10.1086/303323

Hayes, J. P., and Garland, T. Jr. (1995). The evolution of endothermy: testing the aerobic capacity model. *Evolution* 49, 836–847. doi: 10.1111/j.1558-5646.1995.tb02320.x

Kemp, T. S. (2006). The origins of mammalian endothermy: a paradigm for the evolution of complex biological structure. *Zool. J. Linn. Soc.* 147, 473–488. doi: 10.1111/j.1096-3642.2006.00226.x

Kirkpatrick, M., and Lande, R. (1989). The evolution of maternal characters. *Evolution* 43, 485–503. doi: 10.1111/j.1558-5646.1989.tb04247.x

Konarzewski, M., and Diamond, J. (1995). Evolution of basal metabolic rate and organ masses in laboratory mice. *Evolution* 49, 1239–1248. doi: 10.1111/j.1558-5646.1995.tb04450.x

Koteja, P. (2000). Energy assimilation, parental care and the evolution of endothermy. *Proc. R. Soc. Lond. B* 267, 479–484. doi: 10.1098/rspb.2000.1025

Koteja, P. (2004). The evolution of concepts on the evolution of endothermy in birds and mammals. *Physiol. Biochem. Zool.* 77, 1043–1050. doi: 10.1086/423741

Lande, R., and Arnold, S. J. (1983). The measurement of selection on correlated characters. *Evolution* 37, 1210–1226. doi: 10.1111/j.1558-5646.1983.tb00236.x

Lynch, M., and Walsh, B. (1998). *Genetics and Analysis of Quantitative Traits*. Sunderland, MA: Sinauer Press.

McGlothlin**,** J. W., and Brodie, E. D. III. (2009). How to measure indirect genetic effects: the congruence of trait-based and variance-partitioning approaches. *Evolution* 63, 1785–1795. doi: 10.1111/j.1558-5646.2009.00676.x

Moore, A. J., Brodie, E. D. III, and Wolf, J. B. (1997). Interacting phenotypes and the evolutionary process: I. Direct and indirect genetics effects of social interactions. *Evolution* 51, 1352–1362. doi: 10.1111/j.1558-5646.1997.tb01458.x

Moore, A. J., Wolf, J. B., and Brodie, I. I. I., E. D. (1998). "The influence of direct and indirect genetic effects on the evolution of behavior: social and sexual selection meet maternal effects," in *Maternal Effects As Adaptations,* eds T. A. Mousseau and C. W. Fox (Oxford: Oxford University Press), 22–41.

Mousseau, T. A., and Fox, C. W. (1998). *Maternal Effects as Adaptations*. Oxford: Oxford University Press.

Nespolo, R. F., Bacigalupe, L. D., Figueroa, C. C., and Opazo, J. C. (2011). Using new tools to solve an old problem: the evolution of endothermy in vertebrates. *Trends Ecol. Evol.* 26, 414–423. doi: 10.1016/j.tree.2011.04.004

Nord, A., and Nilsson, J. Å. (2011). Incubation temperature affects growth and energy metabolism in blue tit nestlings. *Am. Nat.* 178, 639–651. doi: 10.1086/662172

Räsänen, K., and Kruuk, L. E. B. (2007). Maternal effects and evolution at ecological time scales. *Funct. Ecol.* 21, 408–421. doi: 10.1111/j.1365-2435.2007.01246.x

Riska, B., Rutledge, J. J., and Atchley, W. R. (1985). Genetic-analysis of crossfostering data with sire and dam records. *J. Hered.* 76, 247–250. doi: 10.1093/oxfordjournals.jhered.a110086

Ruben, J. (1995). The evolution of endothermy in mammals and birds: from physiology to fossils. *Ann. Rev. Physiol.* 57, 69–95. doi: 10.1146/annurev.ph.57.030195.000441

Russel, G. A., Rezende, E. L., and Hammond, K. A. (2008). Development partly determines the aerobic performance of adult deer mice, *Peromyscus maniculatus*. *J. Exp. Biol.* 211, 35–41. doi: 10.1242/jeb.012658

Sadowska, J., Gebczynski, A. K., and Konarzewski, M. (2013). Basal metabolic rate is positively correlated with parental investment in laboratory mice. *Proc. R. Soc. London B* 280:20122576. doi: 10.1098/rspb.2012.2576

Sadowska, J., Gebczynski, A. K., Paszko, K., and Konarzewski, M. (2015). Milk output and composition in mice divergently selected for basal metabolic rate. *J. Exp. Biol.* 218, 249–254. doi: 10.1242/jeb.111245

Sun, B. J., Li, T., Gao, J., Ma, L., and Du, W. G. (2015). High incubation temperatures enhance mitochondrial energy metabolism in reptile embryos. *Sci. Rep.* 5:8861. doi: 10.1038/srep08861

Willham, R. L. (1972). The role of maternal effects in animal breeding: III. Biometrical aspects of maternal effects in animals. *J. Anim. Sci.* 35, 1288–1293. doi: 10.2527/jas1972.3561288x

Wilson, A. J., and Réale, D. (2005). Ontogeny of additive and maternal genetic effects: lessons from domestic mammals. *Am. Nat.* 167, E23–E38. doi: 10.1086/498138

Wolf, J. B., Brodie, E. D. III, Cheverud, J. M., Moore, A. J., and Wade, M. J. (1998). Evolutionary consequences of indirect genetic effects. *Trends Ecol. Evol.* 13, 64–69. doi: 10.1016/S0169-5347(97)01233-0

Wolf, J. B., and Wade, M. J. (2001). On the assignment of fitness to parents and offspring: whose fitness is it and when does it matter? *J. Evol. Biol.* 14, 347–356. doi: 10.1046/j.1420-9101.2001.00277.x

Conflict of Interest Statement: The authors declare that the research was conducted in the absence of any commercial or financial relationships that could be construed as a potential conflict of interest.

frontiers in Physiology

ORIGINAL RESEARCH
published: 18 December 2017
doi: 10.3389/fphys.2017.01070

A Shift in the Thermoregulatory Curve as a Result of Selection for High Activity-Related Aerobic Metabolism

Clare Stawski[1,2]*, *Paweł Koteja*[1] and *Edyta T. Sadowska*[1]

[1] Faculty of Biology and Earth Sciences, Institute of Environmental Sciences, Jagiellonian University, Kraków, Poland,
[2] Department of Biology, Norwegian University of Science and Technology, Trondheim, Norway

According to the "aerobic capacity model," endothermy in birds and mammals evolved as a result of natural selection favoring increased persistent locomotor activity, fuelled by aerobic metabolism. However, this also increased energy expenditure even during rest, with the lowest metabolic rates occurring in the thermoneutral zone (TNZ) and increasing at ambient temperatures (T_a) below and above this range, depicted by the thermoregulatory curve. In our experimental evolution system, four lines of bank voles (*Myodes glareolus*) have been selected for high swim-induced aerobic metabolism and four unselected lines have been maintained as a control. In addition to a 50% higher rate of oxygen consumption during swimming, the selected lines have also evolved a 7.3% higher mass-adjusted basal metabolic rate. Therefore, we asked whether voles from selected lines would also display a shift in the thermoregulatory curve and an increased body temperature (T_b) during exposure to high T_a. To test these hypotheses we measured the RMR and T_b of selected and control voles at T_a from 10 to 34°C. As expected, RMR within and around the TNZ was higher in selected lines. Further, the T_b of selected lines within the TNZ was greater than the T_b of control lines, particularly at the maximum measured T_a of 34°C, suggesting that selected voles are more prone to hyperthermia. Interestingly, our results revealed that while the slope of the thermoregulatory curve below the lower critical temperature (LCT) is significantly lower in the selected lines, the LCT (26.1°C) does not differ. Importantly, selected voles also evolved a higher maximum thermogenesis, but thermal conductance did not increase. As a consequence, the minimum tolerated temperature, calculated from an extrapolation of the thermoregulatory curve, is 8.4°C lower in selected (−28.6°C) than in control lines (−20.2°C). Thus, selection for high aerobic exercise performance, even though operating under thermally neutral conditions, has resulted in the evolution of increased cold tolerance, which, under natural conditions, could allow voles to inhabit colder environments. Further, the results of the current experiment support the assumptions of the aerobic capacity model of the evolution of endothermy.

Keywords: bank vole, body temperature, endothermy, evolution, mammals, metabolic rate, thermal conductance, thermoneutral zone

OPEN ACCESS

Edited by:
Elias T. Polymeropoulos, Institute for Marine and Antarctic Studies (IMAS), Australia

Reviewed by:
Steve Portugal, Royal Holloway, University of London, United Kingdom
Stewart C. Nicol, University of Tasmania, Australia

***Correspondence:**
Clare Stawski
clare.stawski@ntnu.no

Specialty section:
This article was submitted to Integrative Physiology, a section of the journal Frontiers in Physiology

Received: *01 July 2017*
Accepted: *05 December 2017*
Published: *18 December 2017*

Citation:
Stawski C, Koteja P and Sadowska ET (2017) A Shift in the Thermoregulatory Curve as a Result of Selection for High Activity-Related Aerobic Metabolism. Front. Physiol. 8:1070. doi: 10.3389/fphys.2017.01070

INTRODUCTION

One of the central issues in evolutionary physiology is the question of what mechanisms led to the evolution of complex adaptations. The evolution of endothermy, the internal production of heat, has been of particular interest as this mode of living not only provides benefits, but also harbors many costs (Bartholomew, 1982; Withers et al., 2016). Endothermy allowed birds and mammals to uncouple their lives from external sources of heat to become nocturnal and also to be active in cold habitats. However, to fuel such an existence endotherms must consume large amounts of food to provide enough energy to maintain a high and stable body temperature (T_b). Therefore, the question of what selection forces have led to such an energetically wasteful strategy has been subject to vivid discussion for already several decades (e.g., Bennett and Ruben, 1979; Hayes and Garland, 1995; Farmer, 2000, 2003; Koteja, 2000, 2004; Angilletta and Sears, 2003; Grigg et al., 2004; Kemp, 2006; Geiser, 2008; Clarke and Pörtner, 2010; Lovegrove, 2012, 2016). According to one of the hypotheses, the aerobic capacity model, high basal metabolic rates (BMR), i.e., a key feature of mammalian and avian endothermy, evolved as a correlated response to selection for high perpetual locomotion fueled by aerobic metabolism (Bennett and Ruben, 1979). The assumption of a positive correlation between aerobic capacity and BMR has been subject to numerous comparative, individual-level phenotypic and quantitative genetic analyses, which have generally provided convincing support (e.g., Hayes and Garland, 1995; Sadowska et al., 2005; Auer et al., 2017). However, to our knowledge, the question of how selection for high aerobic exercise performance affects other thermoregulatory traits has not been intensively studied. Therefore, the present study is based on a unique experimental evolution model system, with lines of the bank vole (*Myodes glareolus*) selected for several generations toward an increased exercise-induced aerobic metabolism (Sadowska et al., 2008; Konczal et al., 2015). In our previous reports, we showed that the selection indeed resulted in an increased BMR (Sadowska et al., 2015) and increased thermogenic capacity (the maximum cold-induced rate of oxygen consumption; Dheyongera et al., 2016). Here we ask, how the selection affected the "thermoregulatory curve" and other thermoregulatory traits.

The thermoregulatory curve (**Figure 1**), also known as the Scholander-Irving model, depicts the pattern of changes of resting metabolic rate (RMR) of an endothermic homeotherm over a range of ambient temperatures (T_a) (Scholander et al., 1950; McNab, 2002; Riek and Geiser, 2013; Levesque et al., 2016). In a range of T_a termed the thermoneutral zone (TNZ), heat balance can be maintained without producing extra heat above the level of BMR. At T_a below the lower boundary of TNZ (i.e., the lower critical temperature; LCT), RMR increases to compensate for greater heat loss. According to a simplified linear model, the heat loss, and hence RMR, is proportional to a total thermal conductance coefficient (c), which incorporates both the properties of thermal insulation of the animal's body and characteristics of evaporative heat loss: $RMR = c(T_b - T_a)$ (McNab, 2002). If heat loss exceeds the thermogenic capacity of the animal, hypothermia occurs. On the other hand, at T_a above the upper boundary of the TNZ (i.e., the upper critical temperature; UCT), costly mechanisms of dissipating excess heat must be engaged to avoid overheating, such as increased evaporative cooling and increased blood circulation to distal body parts (these are depicted by the entire thermoregulatory curve model and cannot be explained by the Scholander-Irving model itself). Such processes, as well as passive thermodynamic effects due to an increased T_b, result in an elevated RMR, and consequently an enhanced thermoregulatory burden. Therefore, the increase of RMR above the TNZ is typically more rapid than that below the TNZ, and animals may become severely hyperthermic at T_a's just above the TNZ.

In the current study we aimed to quantify how the above-described thermoregulatory characteristics changed in lines of bank voles subject to selection for high rates of oxygen consumption achieved during swimming ($\dot{V}O_2$swim; Sadowska et al., 2008, 2015, 2016). In generations 11–14 of the selection experiment, voles from the selected "Aerobic" (A) lines achieved about a 50% higher $\dot{V}O_2$swim than those from unselected, control (C) lines. Not surprisingly, both the spontaneous locomotor activity in cages and the maximum forced-running oxygen consumption (the aerobic capacity *per se*) were also increased in the A lines (Jaromin et al., 2016a), as well as some other morphological and biochemical traits related to exercise metabolism (Stawski et al., 2015b; Jaromin et al., 2016b). Importantly, the swimming trials are performed at 38°C, therefore the direct selection is imposed on locomotor performance only, and not on thermoregulatory capability. According to the aerobic capacity model, however, we predicted that the evolution of aerobic exercise performance should also drive the evolution of thermoregulatory properties. Indeed, voles from the A lines evolved also a 7.3% higher mass-adjusted BMR, increased rate of food consumption (and hence presumably an increased average daily heat production), and increased thermogenic capacity (Sadowska et al., 2008, 2015; Dheyongera et al., 2016). Thus, a few traits crucial in shaping the thermoregulatory curve have changed in response to selection for aerobic exercise performance (although others, namely the capacity for nonshivering thermogenesis, NST, remained unaffected; Stawski et al., 2015a). Therefore, we hypothesize that other characteristics, especially the boundaries of the TNZ, thermal conductance, and T_b at high T_a have also changed.

As we already know that BMR (i.e., RMR measured in the TNZ in fasted animals; McNab, 2002), measured at a T_a of 28°C chosen to be plausibly within the TNZ of voles based on published data (Górecki, 1968), increased in the A lines (Sadowska et al., 2015), a straightforward expectation is that RMR measured at T_a around 28°C should be also higher in the A than in the C lines. However, further predictions can be only conditional, depending on how thermal conductance and T_b have changed (**Figure 1**). Under the laboratory conditions of our selection experiment, the voles are housed at 20°C, i.e., at a temperature below the TNZ. Thus, there is no strong argument to expect that increased BMR should result in a change of thermal insulation in the A lines. If this is the case we should expect

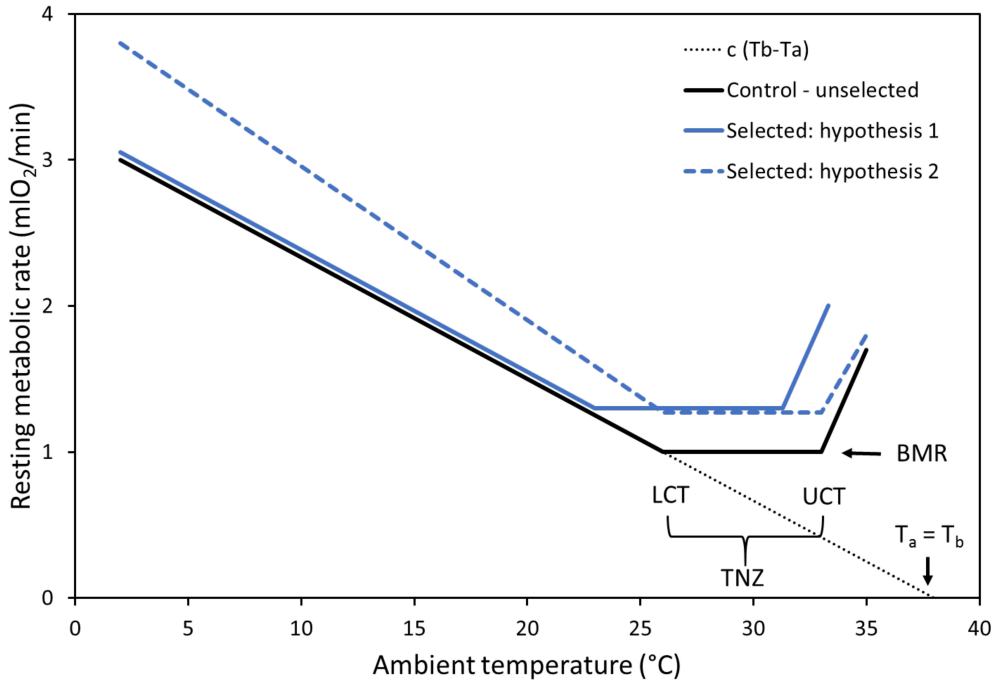

FIGURE 1 | Graphical representation of the thermoregulatory curve and hypotheses concerning changes in response to selection for high activity-related metabolism. Control (C) lines are represented by the solid black line, with the thermoneutral zone (TNZ) depicted and encompassed by the lower critical temperature (LCT) and upper critical temperature (UCT). As we already know that BMR is increased in selected (A) lines, RMR in the TNZ should also be increased (blue lines). The solid blue line represents hypothesis 1, according to which in the A lines: (1a) both the LCT and the UCT are markedly shifted downwards, (1b) above the UCT the increase of RMR is higher, and (1c) below the LCT the thermoregulatory curve overlaps with that of the C lines. The dashed blue line represents hypothesis 2, according to which in the A lines: (2a) the position of the TNZ remains unaffected, (2b) above the UCT the increase of RMR is less steep, and (2c) below the LCT the thermoregulatory curve is steeper than in the control lines. See Introduction for justification of the hypothetical patterns. The dotted line represents heat balance = 0, condition extended to body temperature (T_b) equal to ambient temperature (T_a).

that in the A lines: (1a) both the LCT and the UCT will be markedly shifted downwards (although not necessarily by the same amount, as the values are determined by distinct physical and physiological process), (1b) as a consequence of a lower UCT, at a particular T_b above the UCT the increase of RMR will be higher and a more profound hyperthermia will occur, and (1c) below the LCT the thermoregulatory curve will overlap with that of the C lines. However, if the thermal insulation of the selected voles has decreased proportionally to the increase of BMR, and they evolved a more efficient mechanism for dissipating excess heat by evaporative cooling or transferring excess heat to distal body parts, we can expect that in the A lines: (2a) the position of the TNZ will remain unaffected, (2b) above the UCT the increase of RMR will be less steep, and (2c) below the LCT the thermoregulatory curve will be steeper than in the C lines as a result of higher heat loss. If, on the other hand, voles from the A lines have an increased T_b yet their thermal insulation properties have not changed, then we might expect that: (3) the entire thermoregulatory curve will be shifted upwards, but the lines will remain parallel. Still more scenarios can be envisioned if we consider the possibility that both thermal insulation and T_b have evolved. Thus, even though the physical process we consider is relatively simple and technically "hard" predictions can be formulated, the experiment has, inevitably, an exploratory nature.

MATERIALS AND METHODS

This study was undertaken on bank voles (*M. glareolus*) from the 13th and 14th generations of the artificial selection experiment. Information about the base population, the rationale of the ongoing experiment, selection protocol, and direct response to the selection has been presented in our earlier work (Sadowska et al., 2008, 2015; Konczal et al., 2015). To summarize, the base colony was founded using ∼320 voles captured in the Niepołomice Forest in southern Poland in 2000 and 2001. The animals were bred randomly for 6–7 generations, and the colony was used for quantitative genetic analyses of metabolic rates (Sadowska et al., 2005). In 2004, the multidirectional selection experiment was established (Sadowska et al., 2008). In the selected "Aerobic" (A) lines used in this current work, the selection criterion was the maximum mass-independent (residual from regression) 1-min rate of oxygen consumption achieved during an 18-min swimming trial, performed at the age of 75–85 days. The swim test was conducted at 38°C, at a temperature close to T_b of the voles, so that no thermoregulatory burden was imposed (neither excessive heat loss nor overheating load; see Supplementary Material 1). The test was terminated earlier than the maximum 18-min if an animal was struggling to swim, irrespective of the selection direction of the individual. Four replicate A-selected lines and four unselected Control (C) lines

are maintained (to allow valid tests of the effects of selection; Henderson, 1997), with 15–20 reproducing families in each of the eight lines (which prevents excess inbreeding). The selection was applied mostly within families, but if more than 16 families were available, families in which all individuals scored below the adjusted line mean were excluded. The animals were kept in standard plastic mouse cages with sawdust bedding at a constant temperature (20 ± 2°C) and photoperiod (16:8 L:D) and supplied with food (a standard rodent chow: 24% protein, 3% fat, 4% fiber; Labofeed H, Kcynia, Poland) and water *ad libitum*. All of the procedures associated with the breeding scheme and the selection protocol were approved by the Local Bioethical Committee in Kraków, Poland (No. 99/2006, 21/2010, and 22/2010).

One week before measurements of RMR all individuals were implanted with miniature data loggers to measure T_b (resolution 0.125°C, iButton thermochron DS1921H, Maxim Integrated Products, Inc., Sunnyvale, California, USA). These data loggers were programmed to record T_b every 5-min yielding ∼2,144 data points per animal (3 iButtons malfunctioned and no data were retrieved). Data loggers were coated in wax (mean total mass: 2.43 g) and calibrated over a temperature range of 15–43°C against an Albhorn precision thermometer (Albhorn Therm 2244-1, probe: NTC type C 856-1). The procedure was performed as described in Jefimow and Wojciechowski (2014). The surgery was performed under Nembutal (95 mg kg^{-1}; Morbital, Biowet, ZAP, Poland) anesthesia in voles from generation 13 or under ketamine (40 mg kg^{-1}; Ketamine 10%, Biowet, Puławy, Poland) followed by xylazine (8 mg kg^{-1}; Sedazin 2%, Biowet, Puławy, Poland) in voles from generation 14. A 1 to 1.5-cm incision was made to the skin and muscle layers and a sterilized (95% alcohol) logger was inserted into the abdominal cavity. The muscle and skin were sutured using absorbable suture (Safil 5/0, AesculapAG, Tuttlingen, Germany) and voles were provided water containing the antibiotic enrofloxacin (50 mg L^{-1}) *ad libitum*. Post-surgical care was continued for the next 3 days.

RMRs of voles were measured as rates of O_2 consumption (mLO_2 min^{-1}) at T_a ranging from 10 to 34°C (10°C: selected $n = 61$, control $n = 61$; 20°C: selected $n = 71$, control $n = 71$; 25–34°C: selected $n = 32$, control $n = 32$). Throughout all experiments T_a was measured once every 10-min with data loggers (the same type as used for T_b) placed in the experimental chambers.

Four hours before measurements the voles were weighed and placed in plastic respirometric chambers (850 mL), without access to food or water, at the required T_a to allow animals to acclimatize to the chambers. The chambers were fitted with wire tops suspended 3 cm below the ceiling of the chamber. With the air inlet near the bottom and the outlet at the top of the chamber. This was to ensure that the voles could not exhale air directly into the outgoing air and the incoming air was mixed with the air in the chamber.

The measurements were performed at two time intervals (the actual timing varied ±0:30 h from the following values): the "Morning" group of voles were placed in the chambers at 06:00, the chambers were connected to the system only at 10:00 and the recordings continued until 13:00. The "Afternoon" group was placed in the respirometric chambers at 09:00, the chambers were connected to the system only at 13:00 and the recordings continued until 16:00. The "Timing" group was included as a cofactor in all statistical analyses.

Rates of oxygen consumption ($\dot{V}O_2$) were measured using an open-flow positive-pressure respirometric system. Fresh air was dried (silica gel) and pumped into the chambers containing the animals. The rate of air flowing into the chambers was stabilized at either 350 mL min^{-1} (for T_a of 20–34°C) or 450 mL min^{-1} (for T_a of 10°C) (STPD) with thermal mass-flow controllers (Alborg, Orangeburg, NY, USA). The actual flow was corrected after calibrating the mass-flow controllers against a precise LO 63/33 rotameter (Rota, Germany). Samples of air flowing out of the animal chamber were pre-dried with ND2 non-chemical drier (Sable Systems Inc.), dried with a small volume of chemical absorbent (magnesium perchlorate) and passed through the O_2 analyzers. Mean values of analog outputs from the O_2 analyzer were recorded once per second with Lab Jack UE-9 AD interface and a custom-made protocol using DAQ Factory acquisition system (Azotech, Ashlans, OR, USA). $\dot{V}O_2$ was calculated according to equation 1b in Koteja (1996). We assumed RQ equals 0.85, which was confirmed by measurements performed together with a CO_2 analyzer in a subset of the animals.

Two experimental setups were used, one for stable temperatures of 10 and 20°C and another for increasing T_a from 25 to 34°C.

The rates of oxygen consumption for T_a of 10 and 20°C were measured with a five-channel respirometric system with a FOX O_2 analyzer (Sable Systems Inc. Las Vegas, NV, USA). Samples of air flowing out of a reference (empty) and four measurement chambers (with animals) were analyzed sequentially, in a 13-min cycle. In each cycle, the reference channel and the first measurement channel were active for 165-s, and the remaining three measurement channels were active for 150-s, which ensured a complete washout of the system after switching channels (the time was longer for the reference and the first measurement channels because the change of air composition after switching to those channels is larger than in the case of the other channels). The last 20-s before switching channels was used to calculate the rate of O_2 uptake. Importantly, as the air flow/chamber volume ratio was low (0.44), the last 20-s effectively represented a signal integrated from a longer period.

For the second protocol only two animals were measured simultaneously during each trial during which T_a was increased from 25 to 34°C in 3°C increments. Throughout the measurements animals were kept at 25 and 28°C for 1 h and at 31 and 34°C for 30-min. The shorter time periods at high T_a were to prevent hyperthermia, particularly in individuals from the A lines. The rates of oxygen consumption for T_a 25 to 34°C were measured continuously with either a FOX O_2 analyzer or FC-10a analyzer (Sable Systems Inc. Las Vegas, NV, USA). The rate of O_2 uptake was obtained for the lowest 1-min reading for each experimental T_a.

Maximum thermogenic capacity ($\dot{V}O_2$cold) was measured as the rate of oxygen consumption (ml min^{-1}) in completely soaked individuals placed in a wet chamber for up to 18-min at +23°C (procedure similar to Sadowska et al., 2005 and

Dheyongera et al., 2016). The voles were weighed, soaked in warm (+38°C) water containing a drop of dog shampoo to ensure complete saturation and then placed in wet respirometric chambers (500 mL) maintained at +23°C in a temperature-controlled cabinet (PTC-1 Peltier; Sable Systems, Las Vegas, NV, USA). The respirometric chambers were connected to one of two separate open-flow, positive pressure respirometric systems. The airflow rate through the chambers (about 2,000 mL min^{-1} at standard temperature and pressure), was controlled to ±1% with mass flow controllers (either Model ERG3000, Beta-Erg, Warsaw, Poland: or Model GFC-171S, Aalborg Instruments, Orangeburg, NY, USA). Excurrent air was pre-dried with ND2 non-chemical drier (Sable Systems, Las Vegas, NV, USA) or DG-1 Dewpoint Generator with Pelt-4 Condenser PC-2 (Sable Systems, Las Vegas, NV, USA) and dried with a small volume of chemical absorbent (magnesium perchlorate) and passed through the O_2 analyzers. (FC-10A or FC2 Oxzilla: Sable Systems, Las Vegas, NV, USA). In both systems, the concentration of gases was recorded every second with UI2 (Sable Systems, Las Vegas, NV, USA) interface and protocol using Expedata acquisition system. Thermogenic capacity was defined as the highest 1-min instantaneous rates of oxygen consumption (Bartholomew et al., 1981; effective volume of the chambers was 650 and 700 mL, respectively). At the end of each trial we measured rectal temperature ($T_b$cold) using an Albhorn thermometer (Albhorn Therm 2244-1, probe: NTC type C 856-1).

Two values of T_b were calculated from the data: (1) $T_b$mean is the mean T_b from 30-min of data that were recorded 4.5–5-h after putting the animal in the chamber and (2) $T_b$rmr is the T_b recorded at the time of the lowest RMR measurement. From measurements of $T_b$rmr and RMR we also calculated the thermal conductance [CT, $mLO_2/(min \times °C)$] of the voles at each of the measurement T_as:

$$CT = RMR/(T_b rmr - T_a) \quad (1)$$

For statistical analyses we used SAS (v. 9.4, SAS Institute, Inc., Cary, NC, USA). To compare $T_b$mean, $T_b$rmr, RMR and CT of voles from A and C lines at each of the measurement T_as and also for $T_b$cold and $\dot{V}O_2$cold from the maximum thermogenic capacity trials we applied a cross-nested Mixed ANCOVA model implemented with the Mixed Procedure (with REML method) with Selection (A vs. C) as the main, top-level fixed factor, and replicated Lines as a random effect nested within Selection. Further, we also included fixed cofactors and covariates: Sex, Generation (13 or 14), Timing (Morning or Afternoon), Age, and Body Mass. The model included also a fixed interaction of Selection × Sex and the random interaction of Sex × Line. Values that were obtained from active individuals were omitted from the analyses. Additionally, studentized residuals were analyzed and observations with residuals below −3 or above 3 were considered outliers and removed from the final analyses.

Next, we used a repeated-measures extension of the above model to perform analyses for combined results from the trial performed at temperatures around the TNZ (25, 28, 31, and 34°C). In addition to the factors described above, the model included a fixed repeated-measures factor for T_a (treated as a grouping factor), interactions of T_a with Selection, Sex and Line, and the random effect of Individual ("subject"). As the analyses performed separately for each T_a revealed large differences of residual variance, in the repeated measures model an "unstructured" type of residual (co)variance matrix was assumed. To compare the four T_a groups, Tukey-Kramer post-hoc tests were performed. A similar but simpler model (with no interactions between T_a and other factors and compound symmetry variance structure) was used to analyze initial body mass measured before the three trials (at 10, 20, and 25–34°C). In all of the above analyses, variance was constrained to non-negative values (default approach in SAS), and Satterthwaite approximation for non-orthogonal models was applied to calculate the denominator degrees of freedom.

Finally, to analyze the main characteristics of the thermoregulatory curve we applied a stage-regression model, implemented in SAS mixed nonlinear procedure (NLMIXED). The data available could not allow a reliable estimate of the UCT and therefore the analyses were performed only for the temperature range of 10–31°C, and was focused on the question of whether selection affected LCT, the level of RMR above LCT (RMR_{TNZ}; conceptually equivalent to BMR), and the slope of the relationship between RMR and T_a below LCT (C_t; i.e., another measure of thermal conductance). The model includes also random effects of individuals (ID) and residual error e, each assumed to have a normal distribution. The logic of the model was as follows:

$$RMR = \begin{cases} \text{for } T_a >= \text{LCT: } RMR_{TNZ} + ID + e \\ \text{for } T_a < \text{LCT: } RMR_{TNZ} + CT \times (LCT - T_a) \\ +ID + e \end{cases} \quad (2)$$

However, all of the three parameters of the model are known to depend on body mass (e.g., McNab, 2002). Therefore, they were introduced to the model as linear functions of body mass (M_b), each with an intercept and a mass-slope coefficient:

$$LCT = t_0 + t_m \times M_b \quad (3a)$$

$$RMR_{TNZ} = b_0 + b_m \times M_b \quad (3b)$$

$$C_t = c_0 + c_m \times M_b \quad (3c)$$

Finally, each of the six parameters were introduced to the model as either a value common for both of the selection directions or specific for the A and C lines. Thus, the initial "full" model had a total of 12 fixed parameters (in addition to two random effects), i.e., allowed not only difference in intercepts between the selection directions, but also heterogeneous mass-slopes. The model was then stepwise reduced, first by removing the coefficients responsible for differences in mass-slope coefficients (which resulted in a model with homogeneous mass-slopes), and then by removing other components. We first compared the models using AIC criterion, and then to formally test significance of difference in a particular parameter between the A and C lines a likelihood ratio test (LRT) was applied.

Here we present adjusted least square means (with standard error) for the main factor only (Selection). In the supplementary files we also provide the complete tables with descriptive statistics

and results of the mixed ANCOVA models and NLMIXED (Supplementary Material 2) and also raw data (Supplementary Material 3).

RESULTS

Body mass (M_b) measured before the three respirometric trials (at 10, 20, and 25–34°C) increased with age [$F_{(1, 148)} = 4.91$, $p = 0.028$] and was on average 0.32 ± 0.15 g lower in the afternoon than in the morning trials [$F_{(1, 215)} = 4.19$, $p = 0.042$], but did not differ between generations [$F_{(1, 135)} = 0.94$, $p = 0.33$] or the three trials [$F_{(2, 198)} = 0.96$, $p = 0.39$]. The M_b adjusted for these cofactors was higher in the selected (A) than in control (C) lines, and higher in males than in females [LSM ± SE for the age of 140 days; A line females: 24.6 ± 0.9 g, males: 28.0 ± 0.9 g, C line females: 21.6 ± 0.9 g, males 25.3 ± 0.9 g; effect of selection: $F_{(1, 6.1)} = 6.55$, $p = 0.042$; effect of sex: $F_{(1, 5.6)} = 39.8$, $p = 0.001$].

The results for $T_b$mean and $T_b$rmr were similar and here we only present the results for $T_b$rmr (see **Table 1** for values of both variables). $T_b$rmr was elevated in the A lines at higher T_a but not at lower T_a, in comparison to the C lines. Specifically, at 10°C $T_b$rmr was virtually identical in the lines, and at 20°C it was only 0.08°C higher in the A lines ($p > 0.71$; **Table 1**, **Figure 2A**). At T_as around the TNZ, $T_b$rmr tended to be higher in the A than in the C lines (at 25°C: 0.38°C difference, at 28°C: 0.23°C, at 31°C: 0.25°C), but the difference was nearly significant only at 25°C ($p = 0.07$; otherwise $p > 0.44$; **Table 1**, **Figure 2A**). The difference in $T_b$rmr between the A and C lines was greatest at the T_a of 34°C (1.01°C), but because individual variance dramatically increased the difference was still not significant ($p = 0.15$; **Table 1**, **Figure 2A**). However, the repeated measures analysis performed for combined T_as around TNZ (25, 28, 31, and 34°C) showed that $T_b$rmr, averaged across the four temperatures, was clearly significantly higher in the A than in the C lines [A lines = 38.72 ± 0.13°C; C lines = 38.12 ± 0.12; effect of Selection: $F_{(1, 8.7)} = 10.8$, $p = 0.009$]. The analysis showed also that $T_b$rmr averaged across the A and C lines was similar at 25°C (38.03°C) and 28°C (38.01°C), slightly increased at 31°C (38.13°C), and increased significantly at 34°C [39.51°C; effect of T_a: $F_{(3, 55.9)} = 24.0$, $p < 0.0001$]. Further, the analysis also revealed a significant interaction between the effects of T_a and Selection [$F_{(3, 55.8)} = 5.12$, $p = 0.003$]; while the differences in $T_b$rmr between the lines at T_a ranging from 25 to 31°C were similar (∼0.3°C), at 34°C $T_b$rmr in the A lines was more than 1.5°C higher than that in the C lines.

At all measurement T_as, RMR increased with increasing body mass ($p < 0.0001$; **Table 1**). At T_as below the LCT (10 and 20°C), RMR did not differ between the A and C lines ($p > 0.19$; **Table 1**). Specifically, RMR for A lines was only 2.6% higher at 10°C and 2.1% higher at 20°C (**Table 1**, **Figure 2B**). In contrast, at measurement T_as between 25 and 31°C RMR was ∼9% higher in the A than in the C lines, however, these differences were not significant ($p > 0.15$; **Table 1**, **Figure 2B**). At 34°C RMR in the A lines was 4.2% higher than in the C lines (**Table 1**, **Figure 2B**), but this difference was also not significant ($p = 0.53$). Yet, similarly to $T_b$rmr, the repeated measures analysis performed for combined T_as around TNZ (25, 28, 31, and 34°C) revealed that RMR, averaged across the four temperatures, was significantly higher in the A than in the C lines [A lines = 1.24 ± 0.03 mLO_2min^{-1}; C lines = 1.12 ± 0.03 mLO_2min^{-1}; effect of Selection: $F_{(1, 19.4)} = 7.65$, $p = 0.01$]. Additionally, the RMR of the lines combined was significantly affected by T_a [$F_{(3, 8.5)} = 12.08$, $p = 0.002$]: it was higher at 25°C (1.21 ± 0.02 mLO_2min^{-1}) and 34°C (1.24 ± 0.03 mLO_2min^{-1}) in comparison to 28°C (1.14 ± 0.02 mLO_2min^{-1}) and 31°C (1.13 ±0.03 mLO_2min^{-1}). However, unlike for $T_b$rmr, the interaction between Selection and T_a was not significant for RMR [$F_{(3, 8.5)} = 0.32$, $p = 0.81$], i.e., the differences between the A and C lines were consistent across the T_as (and *vice versa*).

Similarly to RMR, thermal conductance (CT) increased significantly with increasing body mass at all measurement T_as ($p < 0.0001$; **Table 1**). Further, CT followed a similar trend to $T_b$rmr and RMR, such that at the lower T_as of 10 and 20°C the CT values were nearly identical in the A and C lines ($p > 0.28$; **Table 1**). At measurement T_as between 25 and 31°C the CT of the A lines was ≈6% higher than that measured in the C lines. However, this was reversed at 34°C, such that the CT of control voles was 3% higher than that of the selected voles. While these results were not significant, the repeated measures analysis performed for combined T_as (25, 28, 31, and 34°C) revealed that CT, averaged across the four temperatures, was nearly significantly higher in the A than in the C lines [A lines = 0.15 ± 0.003 $mLO_2/(min \times °C)$; C lines = 0.14 ± 0.002 $mLO_2/(min \times °C)$; $p = 0.07$]. As expected, the CT of the lines combined increased significantly with increasing T_a (25°C = 0.09±0.001 $mLO_2/(min \times °C)$; 28°C = 0.11±0.002 $mLO_2/(min \times °C)$; 31°C = 0.16±0.003 $mLO_2/(min \times °C)$; 34°C = 0.24±0.005 $mLO_2/(min \times °C)$; $p = 0.04$). Further, similarly to RMR, the interaction between the effect of Selection and T_a was not significant for CT ($p = 0.19$).

The analysis of the stage-regression model applied to characterize the thermoregulatory curve showed that the best fit model according to the AIC Fit statistic (**Table 2**, model 8) had a common LCT (26.1 ± 0.3°C), which did not depend significantly on either body mass or selection direction. The rate of metabolism above LCT (RMR_{TNZ}), adjusted for the effect of body mass, was 0.11 ± 0.03 mlO_2/min higher in the A than in the C lines ($\chi^2 = 13.2$, $p < 0.001$). The slope of the increase of RMR below LCT (C_t), which can be treated as another characteristic of thermal conductance, increased with body mass ($\chi^2 = 4.8$, $p = 0.028$), and was significantly lower in the A than in the C lines [for a vole with a mean mass of 25 g: A lines: 0.078 $mLO_2/(min \times °C)$, C lines: 0.081 $mLO_2/(min \times °C)$, difference: 0.006 ± 0.003 $mLO_2/(min \times °C)$; $\chi^2 = 5.0$, $p = 0.025$]. Thus, the thermoregulatory curve lines for the A and C voles meet at 7.5°C (**Figure 2B**). However, as RMR was not measured at even lower temperatures, the results do not allow us to resolve whether the lines intersect or converge. Below the LCT, RMR increased so that for the A lines at 20°C it was about 1.4-fold higher, and at 10°C was 2-fold higher, than RMR in the TNZ. As RMR in the TNZ was lower for the C lines, these differences were greater, such that RMR at 20°C was 1.5-fold higher, and at 10°C was 2.2-fold higher, than RMR in the TNZ.

TABLE 1 | Summary statistics showing values (adjusted least square means ± standard error, LSM ± SE) for control (C) and selected (A) lines for each measured variable for each experimental procedure.

Trial	Variable	LSM ± SE		Significance of effects						
		Control (C)	Selected (A)	Selection	Sex	Selection * sex	Generation	Timing	Body mass	Age
10°C	$T_b$mean	38.51 ± 0.13	38.35 ± 0.13	0.12	0.57	0.16	0.79	0.87	0.75	0.34
	$T_b$rmr	38.32 ± 0.14	38.27 ± 0.14	0.74	0.93	0.82	0.87	0.38	0.85	0.76
	RMR	2.36 ± 0.03	2.42 ± 0.03	0.19	0.07	0.74	0.95	0.13	**<0.0001**	0.74
	CT	0.08 ± 0.001	0.09 ± 0.001	0.44	0.31	0.63	0.76	0.35	**<0.0001**	0.44
20°C	$T_b$mean	38.11 ± 0.08	38.11 ± 0.08	0.54	0.11	0.09	**0.02**	0.11	**0.02**	**0.01**
	$T_b$rmr	37.94 ± 0.11	38.02 ± 0.11	0.72	0.35	0.16	**0.05**	0.80	**0.03**	**0.04**
	RMR	1.61 ± 0.02	1.64 ± 0.02	0.53	0.64	0.77	**0.001**	0.11	**<0.0001**	**0.02**
	CT	0.09 ± 0.001	0.09 ± 0.001	0.28	0.94	0.84	**0.002**	0.17	**<0.0001**	0.10
25°C	$T_b$mean	38.07 ± 0.11	38.17 ± 0.11	0.61	0.18	0.96	0.43	0.99	0.28	0.18
	$T_b$rmr	37.83 ± 0.12	38.22 ± 0.12	0.07	0.94	0.81	0.54	0.24	0.26	0.72
	RMR	1.15 ± 0.02	1.26 ± 0.02	0.19	0.44	0.09	0.96	0.57	**<0.0001**	0.42
	CT	0.09 ± 0.002	0.10 ± 0.002	0.56	0.69	0.08	0.77	0.92	**<0.0001**	0.37
28°C	$T_b$mean	37.95 ± 0.12	38.26 ± 0.12	0.23	0.86	0.79	0.36	0.53	0.97	0.29
	$T_b$rmr	37.887 ± 0.123	38.116 ± 0.124	0.447	0.69	0.732	0.461	0.306	0.975	0.32
	RMR	1.08 ± 0.04	1.19 ± 0.04	0.18	0.84	0.59	0.36	0.93	**<0.0001**	0.29
	CT	0.11 ± 0.002	0.12 ± 0.002	0.19	0.91	0.73	0.22	0.11	**<0.0001**	0.20
31°C	$T_b$mean	38.18 ± 0.18	38.66 ± 0.18	0.27	0.45	0.75	0.88	0.59	0.29	0.99
	$T_b$rmr	38.00 ± 0.13	38.25 ± 0.14	0.57	0.52	0.64	0.64	0.13	0.93	0.88
	RMR	1.09 ± 0.05	1.19 ± 0.05	0.15	0.10	0.69	0.36	0.28	**<0.0001**	0.57
	CT	0.15 ± 0.004	0.16 ± 0.005	0.15	0.23	0.58	0.43	**0.05**	**<0.0001**	0.67
34°C	$T_b$mean	39.46 ± 0.40	40.08 ± 0.39	0.29	0.76	0.69	0.76	0.38	0.15	0.24
	$T_b$rmr	39.05 ± 0.40	40.05 ± 0.39	0.15	0.66	0.78	0.42	0.97	**0.04**	0.57
	RMR	1.19 ± 0.06	1.25 ± 0.07	0.53	0.89	0.74	0.31	0.89	**<0.0001**	0.39
	CT	0.25 ± 0.007	0.24 ± 0.008	0.45	0.83	0.80	0.12	0.06	**<0.0001**	0.07
$\dot{V}O_2$cold	$T_b$cold	28.48 ± 0.20	28.60 ± 0.22	0.36	0.06	0.34	**0.03**	NA	**0.01**	0.59
	$\dot{V}O_2$cold	4.20 ± 0.07	4.69 ± 0.07	**0.0003**	0.06	0.90	0.06	NA	**<0.0001**	0.25

LSM are calculated for a fixed body mass (25 g) and age (140 days). Shown also are the significance of each of the effects, significant effects are shown in bold.
$T_b$mean (°C) = mean body temperature of 30-min of data (data from 4.5 to 5-h after putting animal in the chamber); $T_b$rmr (°C) = body temperature at time of lowest RMR; RMR (mLO_2min^{-1}) = lowest resting metabolic rate; CT [mLO_2/(min × °C)] = thermal conductance; $T_b$cold (°C) = T_b after maximum thermogenesis experiment; $\dot{V}O_2$cold (mLO_2min^{-1}) = maximal MR during thermogenesis experiment; NA = not applicable to these measurements.

The maximum thermogenesis ($\dot{V}O_2$cold) of voles from the A lines was 10% higher than that measured in voles from the C lines ($p < 0.0001$; **Table 1**). However, the $\dot{V}O_2$cold measured during the maximum thermogenesis trials did not differ between the A and C lines ($p = 0.70$; **Table 1**). An extrapolation of the thermoregulatory curve toward low temperatures and $\dot{V}O_2$cold values allows an estimation of the lower lethal temperature (LLT), at which the thermoregulatory demand meets the ceiling of maximum thermogenesis. Although the slope of the curve was lower for the A lines, the difference may not hold at lower temperatures. Therefore, for the extrapolation below 7.5°C (where the lines meet) we used a common slope of 0.058 mLO_2/(min ×°C). The LLT calculated in this way for a 25 g vole was 8.4°C lower in the A (−28.6°C) than in the C lines (−20.2°C).

DISCUSSION

Our study provides data that fill in the gaps in our knowledge on how selecting for high-activity related aerobic metabolism can also result in correlated changes in thermal physiological traits. Specifically, as predicted by our previous studies on BMR (Sadowska et al., 2015), RMR within the TNZ was higher in selected (A) lines in comparison to control (C) lines. Resting metabolism is correlated with many life history traits, such as growth, survival, or reproductive output, which suggests that the fitness of an individual can be associated with RMR (Boratynski and Koteja, 2009, 2010; Burton et al., 2011). Thus, the increase in RMR in the TNZ in the voles from the A lines suggests that the evolution of increased aerobic exercise capacity leads to many other correlated changes. In addition, the T_b of selected voles

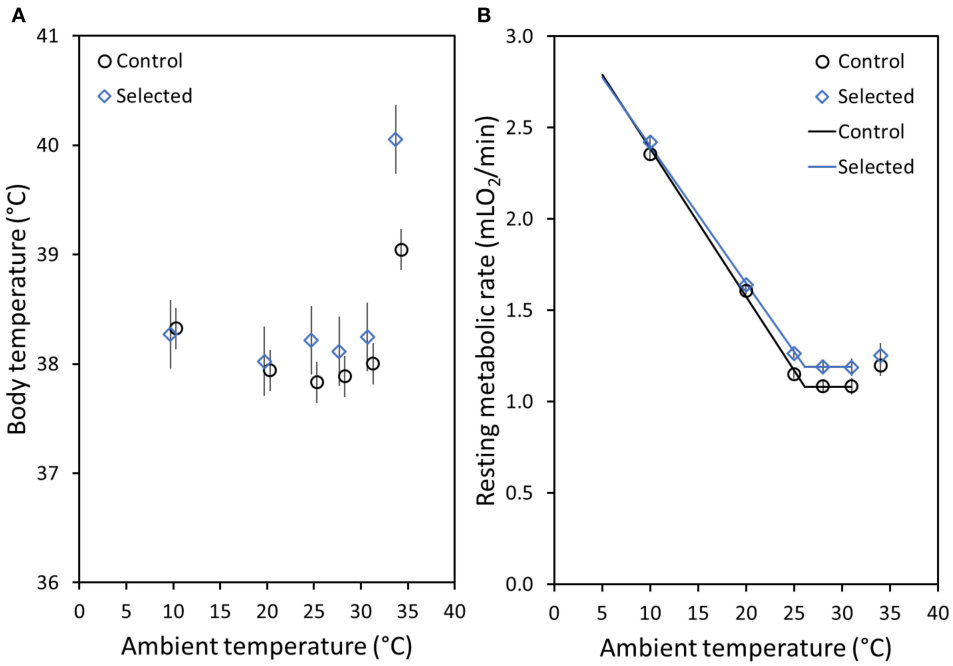

FIGURE 2 | (A) Mean body temperatures ($T_b$rmr) of bank voles at the time of the lowest measured resting metabolic rate (RMR) at each measurement temperature (T_a) for control (C: black dots) and selected (**A**: blue diamonds) lines. **(B)** Mean RMR of bank voles at each measurement T_a for the C (black dots) and the A (blue diamonds) lines. For both figures means are the adjusted least square means (LSM calculated for a fixed body mass, 25 g, and age, 140 days) and the whiskers above and below each mean value represent the standard error (note: for most RMR results the SE range is not visible, because it is smaller than the size of the symbols). The lines on **(B)** represent the best-fit model, with a common lower critical temperature (LCT = 26.1 ± 0.27°C), but different levels of RMR above LCT (RMR_{TNZ}, for a 25 g vole; A lines: 1.19 mLO_2/min, C lines: 1.08 mLO_2/min), and different slopes [C_t, for a 25 g vole; A lines: 0.055 mLO_2/(min ×°C), C lines: 0.061 mLO_2/(min ×°C)].

in the TNZ was ≈0.3°C higher in comparison to control voles, and the difference increased to ≈1.5°C at a T_a of 34°C, revealing that the increased heat production resulting from higher RMR was not completely balanced by increased heat dissipation. While there are advantages for animals to have a high BMR or RMR, such as increased maximal MR for longer activity periods, there are also advantages to having a low BMR or RMR (Larivée et al., 2010). For example, individuals with a low BMR or RMR do not have to eat as much (Dheyongera et al., 2016); therefore their foraging requirements are reduced along with exposure to predators (Larivée et al., 2010). Importantly, while endotherms can maintain high metabolism and a stable T_b to remain active over a range of T_a, this comes at a cost.

Selection for high-activity related metabolism could influence RMR at T_a below the LCT in several ways (**Figure 1**). The results of the stage-regression analysis supported a model in which the LCT does not differ between the A and C lines, and the slope of the thermoregulatory curve is lower in A lines, so that the lines meet at T_a = 7.5°C (**Table 2**, **Figure 2B**). Because we do not have results for T_as below 10°C or between 10 and 20°C, we could not attempt to fit a more complex model, which would allow to determine whether the thermoregulatory curves for the A and C lines converge at low T_a, or if indeed they intersect, so that below ≈ 7°C RMR would become lower in the A than in the C lines. However, as the thermal conductance (CT), calculated from individual values of RMR and T_b measured at T_a = 10°C, does not differ significantly between the lines, and the CT value is actually even slightly higher in the A than in the C lines (**Table 1**), we can predict that the lines actually converge, rather than intersect. In addition to the similar RMR in the A and C lines measured at the moderately low temperatures, there were also no significant differences in T_b. This result suggests that RMR and T_b at cold T_a are conserved regardless of selection for higher MR during activity, possibly to reduce the amount of energy needed to maintain normothermia below the LCT.

Importantly, while many endotherms employ physiological mechanisms to deal with cold temperatures, such as non-shivering thermogenesis (NST) and torpor, such tools are not employed by all species (Jackson et al., 2001; Ruf and Geiser, 2015; Stawski et al., 2015a). Interestingly, NST capacity measured in bank voles from the same generations as those in the current study did not differ between the A and C lines (Stawski et al., 2015a). Therefore, in bank voles NST capacity does not appear to be genetically correlated to activity-related metabolism and is likely a plastic trait, which would be advantageous in predictable environments such as those that bank voles occupy (Stawski et al., 2015a). By conserving RMR and NST capacity at low T_a regardless of selection pressures acting on activity-related aerobic metabolism, bank voles with high BMR can also survive these cold temperatures by not increasing the amount of energy used to remain normothermic (however, their overall energy needs may be increased if they maintain a higher locomotor activity). Importantly, as RMR in the TNZ is higher for the A lines in comparison to the C lines, the

TABLE 2 | Summary of Fit statistics for nonlinear, stage-regression models (implemented in SAS NLMIXED procedure), applied to determine how selection affected the main characteristics of the thermoregulatory curve in bank voles.

	Model specification (parameters included)				Fit statistics and criteria			
	Model number	**N fixed parameters**	**Mass-slope coefficients**	**Different intercepts**	**−2 Log Likelihood**	**AIC**	**AICC**	**BIC**
Heterogeneous mass-slopes	1	12	b_m, c_m, t_m different (selection-specific)	b_0, ct_0, lc_0	−338.8	−310.8	−309.8	−269.6
Homogeneous mass-slopes (b_m, c_m, t_m common in all further models)								
All mass-slope coefficients included	2	9	b_m, c_m, t_m	b_0, c_0, t_0	−331.2	−309.2	−308.6	−276.9
	3	8	b_m, c_m, t_m	c_0, t_0	−321.0	−301.0	−300.5	−271.6
	4	8	b_m, c_m, t_m	b_0, t_0	−328.8	−308.8	−308.3	−279.4
	5	8	b_m, c_m, t_m	b_0, c_0,	−331.1	−311.1	−310.6	−281.7
Homogeneous slopes, but CT or LCT mass-slope coefficients excluded (mass-independence of the trait assumed)	6	8	b_m, t_m	b_0, c_0, t_0	−328.7	−308.7	−308.2	−279.3
	7	8	b_m, c_m	b_0, c_0, t_0	−331.3	−311.3	−310.8	−281.9
	8	**7**	***b*$_m$, *c*$_m$**	***b*$_0$, *c*$_0$,**	**−331.1**	**−313.1**	**−312.7**	**−286.7**
	9	6	b_m, c_m	b_0	−326.1	−310.1	−309.8	−286.6
	10	6	b_m, c_m	c_0	−317.9	−301.9	−301.6	−278.4
	11	6	b_m,	b_0, c_0	−326.3	−310.3	−309.9	−286.7

The three main parameters were entered in the model as linear functions of body mass (M_b), with an intercept and mass-slope coefficients ("0" and "m" subscripts, respectively): the lower critical temperature ($LCT = t_0 + t_m \times M_b$), resting metabolic rate above LCT ($RMR_{TNZ} = b_0 + b_m \times M_b$), and thermal conductance ($C_t = c_0 + c_m \times M_b$). The intercepts and mass-slope parameters were specified either as common or different for the A and C lines. Thus, the full model had 12 fixed parameters (plus two random effects, not shown), which were then step-wise reduced. The common intercept coefficients were always retained in the model, and therefore are not shown in the table. A lower value of the Fit criteria indicates a better fit of the model, and the best-fit model is highlighted in bold.

selected voles do not need to increase their RMR as much at T_a below the LCT. This smaller increase in energy expenditure as the temperature drops was likely important during the evolution of endothermy and also currently in terms of adapting rapidly to colder weather. Additionally, our data also revealed that voles from the A lines have a 10% higher thermogenic capacity (**Table 1**). Consequently, as RMR and CT below the LCT practically do not differ between the selection directions, the selected voles presumably have a 7°C lower LLT than voles from the C lines, i.e., have a higher capacity to withstand very cold T_a.

Hotter temperatures can be more difficult for endotherms to cope with than cold. Endotherms in particular can overheat rapidly and this can lead to organ failure and death. Therefore, for T_a above the UCT endotherms need to dissipate heat and often do so by increasing evaporative water loss and MR (Pis, 2010; Rezende and Bacigalupe, 2015). Due to the higher RMR and T_b of the selected voles in the TNZ, we predicted that the slope of the line would be steeper above the UCT in comparison to control lines. While we were unable to estimate the UCT based on our data, the RMR and T_b of some voles already showed an increase at the measurement T_a of 31°C, and an even greater increase at 34°C. Therefore, while there appears to be considerable individual variation, we hypothesize that the UCT of voles is around 31°C. Importantly, the T_b of voles from the A lines at 34°C was much higher in comparison to the C lines. This result suggests that selection for high activity-related metabolism can reduce the capacity of effective thermoregulation at high T_a, and therefore decrease the upper lethal temperature.

The results of our current and previous studies show that selection for increased aerobic capacity during activity leads to many other correlated changes, such as a shift in the thermoregulatory curve as shown here. Specifically, the selection for high aerobic exercise performance, even though operating under thermally neutral conditions, has resulted in the evolution of increased cold tolerance, which, under natural conditions, could allow voles to inhabit colder environments. Conversely, this selection has also resulted in voles overheating at high T_a, which may lead to difficulties in a warming climate. Bank voles offer an ideal model to analyse metabolic adjustments to differing climates as they have a wide distribution throughout Europe, extending in the North all the way into the Arctic Circle and down to the Mediterranean in the South (Raczyński, 1983). In the West they are found in Ireland and in the East they inhabit a large portion of Russia (Raczyński, 1983). Throughout this large range bank voles experience a variety of climates, suggesting they may display physiological flexibility to enable adaptation to differing weather patterns. Yet, surprisingly, the possibility of geographical variation of their metabolic traits has not been explored extensively and we are only aware of one study (Aalto et al., 1993). This research revealed that bank voles do not appear to display evident variation in BMR across a wide geographical range, from Northern Finland to the Balkan Peninsulas. The authors suggested that throughout this wide climatic range voles can select similar microclimates (Aalto et al., 1993). However, the methodology of this study was not perfect, because the measurements were conducted neither on voles' immediately after capture nor on ones maintained under common-garden conditions. Thus, the data do not

represent effects of current local conditions, and do not represent genetically-based differences, either. Therefore, it would be beneficial to repeat such an experiment with a more robust experimental design, and compare the outcome with that of our selection experiment. To conclude, the results of the current thermoregulatory curve experiment and the results from the whole experimental evolutionary model research support the assumptions of the aerobic capacity model of the evolution of endothermy.

AUTHOR CONTRIBUTIONS

All authors designed the study, analyzed the results, worked on the manuscript and gave approval for publication. CS and ES performed the experiments.

FUNDING

This research was funded by the Jagiellonian University and the European Union under the European Social Fund (POKL.04.01.01-053/09) to CS, a grant for the development of young scientists and doctoral students from Jagiellonian University (DS/MND/WBiNoZ/INoS/2/2011) to CS and ES, Jagiellonian University (DS/WBINOZ/INOS/757) to PK, the Polish Ministry of Science and Higher Education (8167/B/P01/2011/40 to PK and 0595/B/P01/2011/40 to ES), and the National Science Centre Poland (2016/22/E/NZ8/00416) to ES.

ACKNOWLEDGMENTS

For their help with this research we would like to thank Katarzyna Baliga-Klimczyk, Katarzyna M. Chrzaścik, Agata Rudolf, and Paulina Szymanska. We are grateful to Michał S. Wojciechowski for lending us his data loggers and teaching us the implantation surgery.

SUPPLEMENTARY MATERIAL

The Supplementary Material for this article can be found online at: https://www.frontiersin.org/articles/10.3389/fphys.2017.01070/full#supplementary-material

REFERENCES

Aalto, M., Górecki, A., Meczeva, R., Wallgren, H., and Weiner, J. (1993). Metabolic rates of the bank voles (*Clethrionomys glareolus*) in Europe along a latitudinal gradient from Lapland to Bulgaria. *Ann. Zool. Fennici* 30, 233–238.

Angilletta, M. J., and Sears, M. W. (2003). Is parental care the key to understanding endothermy in birds and mammals? *Am. Nat.* 162, 821–825. doi: 10.1086/380921

Auer, S. K., Killen, S. S., and Rezende, E. L. (2017). Resting vs. active: a meta-analysis of the intra-and inter-specific associations between minimum, sustained, and maximum metabolic rates in vertebrates. *Funct. Ecol.* 31, 1728–1738. doi: 10.1111/1365-2435.12879

Bartholomew, G. A. (1982). "Energy metabolism," in *Animal Physiology: Principles and Adaptations*, ed M. S. Gordon (New York, NY: MacMillian Publishing Co., Inc.), 46–93.

Bartholomew, G. A., Vleck, D., and Vleck, C. M. (1981). Instantaneous measurements of oxygen consumption during pre-flight warm-up and post-flight cooling in sphingid and saturnid moths. *J. Exp. Biol.* 90, 17–32.

Bennett, A. F., and Ruben, J. A. (1979). Endothermy and activity in vertebrates. *Science* 206, 649–654. doi: 10.1126/science.493968

Boratynski, Z., and Koteja, P. (2009). The association between body mass, metabolic rates, and survival of bank voles. *Funct. Ecol.* 23, 330–339. doi: 10.1111/j.1365-2435.2008.01505.x

Boratynski, Z., and Koteja, P. (2010). Sexual and natural selection on body mass and metabolic rates in free-living bank voles. *Funct. Ecol.* 24, 1252–1261. doi: 10.1111/j.1365-2435.2010.01764.x

Burton, T., Killen, S. S., Armstrong, J. D., and Metcalfe, N. B. (2011). What causes intraspecific variation in resting metabolic rate and what are its ecological consequences? *Proc. R. Soc. B* 278, 3465–3473. doi: 10.1098/rspb.2011.1778

Clarke, A., and Pörtner, H.-O. (2010). Temperature, metabolic power and the evolution of endothermy. *Biol. Rev.* 85, 703–727. doi: 10.1111/j.1469-185X.2010.00122.x

Dheyongera, G., Grzebyk, K., Rudolf, A. M., Sadowska, E. T., and Koteja, P. (2016). The effect of chlorpyrifos on thermogenic capacity of bank voles selected for increased aerobic exercise metabolism. *Chemosphere* 149, 383–390. doi: 10.1016/j.chemosphere.2015.12.120

Farmer, C. G. (2000). Parental care: the key to understanding endothermy and other convergent features in birds and mammals. *Am. Nat.* 155, 326–334. doi: 10.1086/303323

Farmer, C. G. (2003). Reproduction: the adaptive significance of endothermy. *Am. Nat.* 162, 826–840. doi: 10.1086/380922

Geiser, F. (2008). Ontogeny and phylogeny of endothermy and torpor in mammals and birds. *Comp. Biochem. Physiol. A* 150, 176–180. doi: 10.1016/j.cbpa.2007.02.041

Górecki, A. (1968). Metabolic rate and energy budget in the bank vole. *Acta Theriol.* 13, 341–365. doi: 10.4098/AT.arch.68-20

Grigg, G. C., Beard, L. A., and Augee, M. L. (2004). The evolution of endothermy and its diversity in mammals and birds. *Physiol. Biochem. Zool.* 88, 982–997. doi: 10.1086/425188

Hayes, J. P., and Garland, T. (1995). The evolution of endothermy: testing the aerobic capacity model. *Evolution* 49, 836–847. doi: 10.1111/j.1558-5646.1995.tb02320.x

Henderson, N. D. (1997). Spurious associations in unreplicated selected lines. *Behav. Genet.* 27, 145–154.

Jackson, D. M., Trayhurn, P., and Speakman, J. R. (2001). Associations between energetics and over-winter survival in the short-tailed field vole *Microtus agrestis*. *J. Anim. Ecol.* 70, 633–640. doi: 10.1046/j.1365-2656.2001.00518.x

Jaromin, E., Sadowska, E. T., and Koteja, P. (2016a). A dopamine and noradrenaline reuptake inhibitor (bupropion) does not alter exercise performance of bank voles. *Curr. Zool.* 62, 307–315. doi: 10.1093/cz/zow026

Jaromin, E., Wyszkowska, J., Labecka, A. M., Sadowska, E. T., and Koteja, P. (2016b). Hindlimb muscle fibre size and glycogen stores in bank voles with increased aerobic exercise metabolism. *J. Exp. Biol.* 219, 470–473. doi: 10.1242/jeb.130476

Jefimow, M., and Wojciechowski, M. S. (2014). Effect of dietary fatty acids on metabolic rate and nonshivering thermogenesis in golden hamsters. *J. Exp. Zool. A* 321, 98–107. doi: 10.1002/jez.1840

Kemp, T. S. (2006). The origin of mammalian endothermy: a paradigm for the evolution of complex biological structure. *Zool. J. Linn. Soc.* 147, 473–488. doi: 10.1111/j.1096-3642.2006.00226.x

Konczal, M., Babik, W., Radwan, J., Sadowska, E. T., and Koteja, P. (2015). Initial molecular-level response to artificial selection for increased aerobic metabolism occurs primarily through changes in gene expression. *Mol. Biol. Evol.* 32, 1461–1473. doi: 10.1093/molbev/msv038

Koteja, P. (1996). Measuring energy metabolism with open-flow respirometric systems: which design to choose. *Funct. Ecol.* 10, 675–677. doi: 10.2307/2390179

Koteja, P. (2000). Energy assimilation, parental care and the evolution of endothermy. *Proc. R. Soc. Lond. B* 267, 479–484. doi: 10.1098/rspb.2000.1025

Koteja, P. (2004). The evolution of concepts on the evolution of endothermy in birds and mammals. *Physiol. Biochem. Zool.* 77, 1043–1050. doi: 10.1086/423741

Larivée, M. L., Boutin, S., Speakmean, J. R., McAdam, A. G., and Humphries, M. M. (2010). Associations between over-winter survival and resting metabolic rate in juvenile North American red squirrels. *Funct. Ecol.* 24, 597–607. doi: 10.1111/j.1365-2435.2009.01680.x

Levesque, D. L., Nowack, J., and Stawski, C. (2016). Modelling mammalian energetics: the heterothermy problem. *Clim. Change Responses* 3:7. doi: 10.1186/s40665-016-0022-3

Lovegrove, B. G. (2012). The evolution of endothermy in the Cenozoic mammals: a plesiomorphic-apomorphic continuum. *Biol. Rev.* 87, 128–162. doi: 10.1111/j.1469-185X.2011.00188.x

Lovegrove, B. G. (2016). A phenology of the evolution of endothermy in birds and mammals. *Biol. Rev.* 92, 1213–1240. doi: 10.1111/brv.12280

McNab, B. K. (2002). *The Physiological Ecology of Vertebrates*. Ithaca, NY: Cornell University Press.

Pis, T. (2010). The link between metabolic rate and body temperature in galliform birds in thermoneutral and heat exposure conditions: the classical and phylogenetically corrected approach. *J. Therm. Biol.* 35, 309–316. doi: 10.1016/j.jtherbio.2010.06.010

Raczyński, J. (1983). Taxonomic position, geographical range and the ecology of distribution. *Acta Theriol.* 28(Suppl. 1), 3–30.

Rezende, E. L., and Bacigalupe, L. D. (2015). Thermoregulation in endotherms: physiological principles and ecological consequences. *J. Comp. Physiol. B* 185, 709–727. doi: 10.1007/s00360-015-0909-5

Riek, A., and Geiser, F. (2013). Allometry of thermal variables in mammals: consequences of body size and phylogeny. *Biol. Rev.* 88, 564–572. doi: 10.1111/brv.12016

Ruf, T., and Geiser, F. (2015). Daily torpor and hibernation in birds and mammals. *Biol. Rev.* 90, 891–926. doi: 10.1111/brv.12137

Sadowska, E. T., Baliga-Klimczyk, K., Chrzaśik, K. M., and Koteja, P. (2008). Laboratory model of adaptive radiation: a selection experiment in the bank vole. *Physiol. Biochem. Zool.* 81, 627–640. doi: 10.1086/590164

Sadowska, E. T., Król, E., Chrzaścik, K. M., Rudolf, A. M., Speakmam, J. R., and Koteja, P. (2016). Limits to sustained energy intake. XXIII. Does heat dissipation capacity limit the energy budget of lactating bank voles? *J. Exp. Biol.* 219, 805–815. doi: 10.1242/jeb.134437

Sadowska, E. T., Labocha, M. K., Baliga, K., Stanisz, A., Wróblewska, A. K., Jagusiak, W., et al. (2005). Genetic correlations between basal and maximum metabolic rates in a wild rodent: consequences for evolution of endothermy. *Evolution* 59, 672–681. doi: 10.1111/j.0014-3820.2005.tb01025.x

Sadowska, E. T., Stawski, C., Rudolf, A., Dheyongera, G., Chrzaścik, K. M., Baliga-Klimczyk, K., et al. (2015). Evolution of basal metabolic rate in bank voles from a multidirectional selection experiment. *Proc. R. Soc. B.* 282:20150025. doi: 10.1098/rspb.2015.0025

Scholander, P. F., Hock, R., Walters, V., and Irving, L. (1950). Adaptation to cold in arctic and tropical mammals in relation to body temperature, insulation, and basal metabolic rate. *Biol. Bull.* 99, 259–271. doi: 10.2307/1538742

Stawski, C., Koteja, P., Sadowska, E. T., Jefimow, M., and Wojciechowski, M. S. (2015a). Selection for high activity-related aerobic metabolism does not alter the capacity of non-shivering thermogenesis in bank voles. *Comp. Biochem. Physiol. A* 180, 51–56. doi: 10.1016/j.cbpa.2014.11.003

Stawski, C., Valencak, T. G., Ruf, T., Sadowska, E. T., Dheyongera, G., Rudolf, A., et al. (2015b). Effect of selection for high activity-related metabolism on membrane phospholipid fatty acid composition in bank voles. *Physiol. Biochem. Zool.* 88, 668–679. doi: 10.1086/683039

Withers, P. C., Cooper, C. E., Maloney, S. K., Bozinovic, F., and Cruz-Neto, A. P. (2016). *Ecological and Environmental Physiology of Mammals*. Oxford: Oxford University Press.

Conflict of Interest Statement: The authors declare that the research was conducted in the absence of any commercial or financial relationships that could be construed as a potential conflict of interest.

frontiers in Physiology

ORIGINAL RESEARCH
published: 25 July 2017
doi: 10.3389/fphys.2017.00532

It Takes Time to Be Cool: On the Relationship between Hyperthermia and Body Cooling in a Migrating Seaduck

Magella Guillemette[1], Elias T. Polymeropoulos[2], Steven J. Portugal[3] and David Pelletier[4]*

[1] Departement de Biologie, Universite du Quebec a Rimouski, Rimouski, QC, Canada, [2] Institute for Marine and Antarctic Studies, University of Tasmania, Hobart, TAS, Australia, [3] School of Biological Sciences, Royal Holloway University of London, Egham, United Kingdom, [4] Departement de Biologie, Cegep de Rimouski, Rimouski, QC, Canada

The large amount of energy expended during flapping flight is associated with heat generated through the increased work of the flight muscles. This increased muscle work rate can manifest itself in core body temperature (T_b) increase of 1–2°C in birds during flight. Therefore, episodic body cooling may be mandatory in migratory birds. To elucidate the thermoregulatory strategy of a short-distance migrant, common eiders (*Somateria mollissima*), we implanted data loggers in the body cavity of wild birds for 1 year, and report information on T_b during their entire migration for 19 individuals. We show that the mean body temperature during flight (T_{bMean}) in the eiders was associated with rises in T_b ranging from 0.2 to 1.5°C, largely depending on flight duration. To understand how eiders are dealing with hyperthermia during migration, we first compare, at a daily scale, how T_b differs during migration using a before-after approach. Only a slight difference was found (0.05°C) between the after (40.30°C), the before (40.41°C) and the migration (40.36°C) periods, indicating that hyperthermia during flight had minimal impact at this time scale. Analyses at the scale of a flight cycle (flight plus stops on the water), however, clearly shows that eiders were closely regulating T_b during migration, as the relationship between the storage of heat during flight was highly correlated (slope = 1) with the level of heat dumping during stops, at both inter-individual and intra-individual levels. Because T_b at the start of a flight (T_{bStart}) was significantly and positively related to T_b at the end of a flight (T_{bEnd}), and the maximal attained T_b during a flight (T_{bMax}), we conclude that in absence of sufficient body cooling during stopovers, eiders are likely to become increasingly hyperthermic during migration. Finally, we quantified the time spent cooling down during migration to be 36% of their daily (24 h) time budget, and conclude that behavioral body cooling in relation to hyperthermia represents an important time cost.

Keywords: body cooling, common eiders, endothermy, hyperthermia, migration, thermoregulation

OPEN ACCESS

Edited by:
Leonardo Alexandre Peyré-Tartaruga, Universidade Federal do Rio Grande do Sul, Brazil

Reviewed by:
Carlos Gabriel Fàbrica, University of the Republic, Uruguay
James Todd Pearson, National Cerebral and Cardiovascular Center, Japan

****Correspondence:***
Magella Guillemette
Magella_Guillemette@uqar.ca

Specialty section:
This article was submitted to Integrative Physiology, a section of the journal Frontiers in Physiology

Received: *11 May 2017*
Accepted: *10 July 2017*
Published: *25 July 2017*

Citation:
Guillemette M, Polymeropoulos ET, Portugal SJ and Pelletier D (2017) It Takes Time to Be Cool: On the Relationship between Hyperthermia and Body Cooling in a Migrating Seaduck. Front. Physiol. 8:532. doi: 10.3389/fphys.2017.00532

INTRODUCTION

Homeothermic endotherms—animals that maintain a constant, regulated, body temperature—have the unique ability to maintain a high core body temperature (T_b) across a wide range of ambient temperatures (T_a; Crompton et al., 1978). Birds display the highest T_b of all endothermic animals, exceeding that of mammals, for example, on average by up to ≈2.5°C (Prinzinger et al.,

1991). It has been proposed that such a high T_b in birds is prevalent to enhance the performance of powered flight through Q_{10}—the factor by which the rate of a reaction increases for every 10 degree rise in temperature—driven effects on muscle contractile activity (Torre-Bueno, 1976). Although, birds are known to regulate body temperature to a high degree and within very narrow margins, there is building evidence that substantial deviations from normothermia naturally occur (Guillemette et al., 2016). Indeed, hypothermic events such as torpor is evident in many families of afrotropical birds while there are numerous studies reporting cases of controlled hypothermia as a strategy to conserve energy in temperate and arctic environments as well (McKechnie and Mzilikazi, 2011; Lewden et al., 2014). While T_b may be lowered as an energy-saving mechanism in many bird species, the result of the high-energy demands imposed by flight, with flapping flight often being described as the costliest locomotion mode among vertebrates (Butler and Woakes, 1990; Butler, 2016), is associated with the highest levels of known heat production among endotherms (Clarke and Rothery, 2008). It is estimated that 80–96% of the metabolic energy used during flapping flight in birds and bats is dissipated as heat, while only 4–20% is converted into mechanical power (Carpenter, 1986; Speakman and Thomas, 2003). Such dramatic increases in T_b during flight (Platania et al., 1986) require accurate regulation to avoid critical levels of hyperthermia being reached, and the associated deleterious physiological consequences such as excessive evaporative water loss (Boyles et al., 2011). Long-distance avian migrations can include non-stop flights of over 10,000 km, involving millions of wingbeats (Gill et al., 2005). Therefore, in flying birds, mechanisms for body cooling are likely to be an important feature of migration strategies, when flight time is considerably increased and the risk of hyperthermia may be highest.

To cope with the increases in T_b during long-duration flights, a diverse range of behavioral and physiological strategies have evolved in birds as a means to maintain a constant T_b, and thus retain cellular homeostasis. Unlike endothermic mammals, however, birds lack sweat glands and thus rely on other mechanisms of effective heat loss. The respiratory tract, through panting or gular fluttering, plays an important role in evaporative heat loss in some species, while the plumage, skin, bill as well as the legs and feet are known important sites of heat exchange that may assist in alleviating the large water loss through the respiratory tract (Steen and Steen, 1965; Dawson, 1982; Giladi and Pinshow, 1999; Tattersall et al., 2016). Evaporative heat loss through the limbs has been well documented, notably in seabirds (Steen and Steen, 1965; Baudinette et al., 1976). The arteries and veins in the legs of many birds lie in close contact with each other, forming a rete mirabile (a net-like-complex of arteries and veins), and function as a countercurrent heat exchange system (Midtgård, 2008). In addition, many birds can adjust the blood flow through the legs by muscular contraction, and can thus regulate heat loss to some degree depending on environmental conditions (Kilgore and Schmidt-Nielsen, 1975).

The behavioral and physiological mechanisms employed by many birds to regulate body temperature are most pertinent during long-duration flights, chiefly those associated with migration when heat loss becomes a particularly challenging problem. Some species may increase their flight altitude to reach cooler temperatures or wind conditions (Torre-Bueno, 1976; Bäckman and Alerstam, 2001) whereas other species are known to fly predominantly at night-time in cooler temperatures which may be related to thermoregulation (Kerlinger and Moore, 1989). For many migratory birds, stopovers are a crucial component of migration and serve to replenish and restore energy reserves (Moore and Kerlinger, 1987), but such breaks from flight may also play a role in avoiding hyperthermic conditions and maintaining homeostasis.

Recently, Guillemette et al. (2016) demonstrated that common eiders (*Somateria mollissima*) experience large departures from normothermia during migratory flights. These increases in T_b ranged on average between 0.2 and 2.4°C during migratory flights, and were likely due to the high wing-loading found in eiders (a large body to small wings ratio), the morphology of which is linked to their diving lifestyle. Indirect evidence that eiders proactively avoid deleterious levels of hyperthermia during flight is given by their migratory style, whereby they use a stop-and-go strategy where they perform many flights of short duration (15 min) during which T_b increased by 1°C on average (Guillemette et al., 2016). In addition, about 60% of the migratory flights were stopped while T_b was still increasing (Guillemette et al., 2016). Therefore, it appears that behaviorally mediated body cooling, might be an important component of the thermoregulatory strategy during migration for eiders.

In this paper, we evaluate the role of body cooling during migration stop-overs of common eiders while they migrate from breeding grounds to their late-summer molting sites. More specifically, we (1) compare daily T_b during migration to T_b prior to the migratory flights, and predict that daily T_b during migration is higher overall than daily T_b during the pre-migratory phase when flight time is significantly lower. We (2) predict that hyperthermia is a constraint to flight duration in migrating eiders, and therefore they should decrease their T_b to within a normothermic range before engaging in any further flight activity. We thus tested, at both the inter- and intra-individual level, that the duration between flights is governed by the time it takes to become normothermic. Finally, we (3) quantified the rate of body cooling and the time to reach a minimum T_b, during stops between flights, in order to evaluate if it could influence migration speed.

MATERIALS AND METHODS

Model Species and Population Studied

Common eiders are large (2 kg) sea ducks that dive for food living in the benthos. They are characterized by short-pointed wings resulting in high wing-loadings and high flight speed (Day et al., 2004; Guillemette and Ouellet, 2005). The population studied is breeding in Baltic and molting in the Wadden Sea (Rigou and Guillemette, 2010). During migration, eider ducks usually follow the coast and rarely fly over areas of unsuitable feeding habitats (Guillemette, 2001; Guillemette et al., 2016). As with many other species of waterfowl, common eiders undergo a molt migration in late summer. They move from breeding habitats to

their molting areas where they lose their wing feathers all at once leading to a period of flightlessness that last 36 days on average (Guillemette et al., 2007). The molt migration of this population in summer, involves movement from the breeding grounds in the central Baltic to the molting quarters located in the Wadden sea, covering a distance of 714 km (±286) on average.

The study was performed on Christiansø Island (55°19′N, 15°12′E), an old Danish fortress located in the southern Baltic Sea, 18 km from the Danish island of Bornholm. The general approach of our work involved the monitoring and deployment of data loggers on breeding females, using heart rate data to determine the start and the end of each flight, and computing variation of body temperature during and between flights. Using the mean eider groundspeed velocities estimated at 83.5 ± 0.3 km h^{-1} by Day et al. (2004) and the total time spent flying (see below) during each migration day of each individual, we calculated the migration distance of each instrumented female. Using that information together with the molting movements of this Danish population, as described previously (Lyngs, 2000), we estimated the location and used the date of migration for all individuals to estimate air [15.5 ± (*SD*) 1.8] and (surface) water temperature [15.5 ± (*SD*) 1.9].

Deployment of Data Loggers

On Christiansø island, 45 common eiders were captured in 2003, 2004, and 2005 and implanted with custom made data loggers (DLs, Biometistics, A. J. Woakes) under license from Dyreforsøgtilsynet (Danish Royal Veterinarian Corporation) and approved by the Canadian Council of Animal Care (# CPA 16-03-07-01). Only females were caught as males leave the colony when incubation starts. All surgical procedures were conducted indoors according to the procedure described by Guillemette et al. (2002). The 45 DLs were 36 mm long (±*SD* = 0.5) × 28 mm (0.2) wide × 11 mm thick (0.3) and weighed 21 g (0.3), that is 1.2% of body mass at implantation (Guillemette et al., 2007). Thirty nine (87%) experimental females returned to the study area 1 year later, which is similar to previously reported survival rate in that species (Coulson, 2008). The last result being most likely related to the fact that implanted DLs do not alter aerodynamic and hydrodynamic properties of experimental individuals (Guillemette et al., 2002; White et al., 2013). One year after the implantation, 36 females were re-captured of which 17, 7, and 12 (respectively for 2003, 2004, and 2005) had their data logger removed. For all studied years, data loggers recorded pressure and heart rate every 2 s and body temperature every 16 s, except for 2003 females as the temperature sensor was not operational for that deployment. We thus analyzed for this paper data from 19 females (2004 and 2005 deployment only).

Time Spent Flying

Flight schedules (number and duration of flights) were compiled for each bird following the method described by Pelletier et al. (2007). This method is based on the dramatic increases and decreases of heart rate upon take-offs and landings respectively, where heart rate is typically three to four times the resting level. For every female, the daily time spent flying (TSF) was obtained by summing the duration of all flights that occurred during 1 day.

Body Temperature during a Flight Cycle

A flight cycle is composed of flight followed by a period of time spent on the water before the next flight (stop). Body temperature (T_b) was recorded at the start (T_{bStart}) and at the end (T_{bEnd}) of each flight together with maximum T_b (T_{bMax}), whenever it occurred during each flight (**Figure 1**). The T_b sensor time inertia was evaluated to be 3 min as we observed changes in T_b only after 3 min of flight. Thus, all flights <3 min were excluded from our analysis (n = 412). In addition, the minimum T_b (T_{bMin}) occurring during each stop interval was recorded. We define the heat storage index (HSI) as T_b in relation to elapsed time (°C. h^{-1}). Here, we calculate the heat stored during flight for each time interval and hence report the interval specific HSI for each flight segment (0–5, 5–10 min). Similarly, we computed a body cooling index (BCI) by calculating the difference of T_b between the end of flight and T_b at 5 min increment after the end of each flight.

Data Analysis

First, we were interested to know how and if eiders ducks were able to regulate T_b during migration at a daily scale compared to periods before and after migration. Daily body temperature (T_{bDaily}) during migration was calculated as the average of all T_b datum (5,400 per day) recorded during migration days of each individual. This average value was subtracted in a before-after fashion using a similar time interval (3 days), giving two individual deltas per individual. These deltas were averaged over the 19 females for which confidence intervals were computed using the bootstrap method (see main text for results).

Second, we were interested to know if body cooling between flights was sufficient to dump all the heat gained during flight. We started our analysis by relating the heat gain during flight with heat loss during stops at the intra-individual level. We

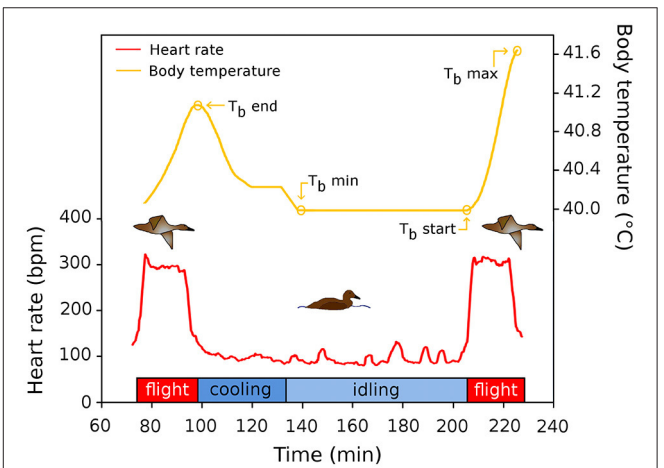

FIGURE 1 | Schematic representation of a flight cycle during migration of common eiders. The red line depicts the heart rate of two flights, and the time interval between flights, used to quantify flight occurrence and flight duration of this study. The yellow line shows the (smoothed) variation of T_b in relation to time in the flight cycle. See text for definitions of acronyms.

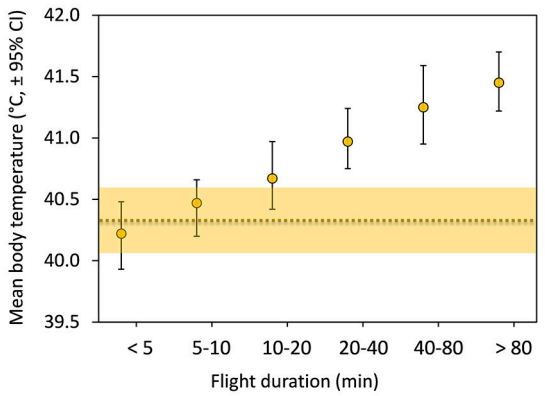

FIGURE 2 | Mean body temperature (T_{bMean}) in relation to flight duration with error bars depicting (95%) bootstrap confidence intervals ($N = 19$ females, $n = 412$ flights). The horizontal dotted line represents the daily (24 h) body temperature (T_{bDaily}) of the 19 females during a total of 49 days of migration together with (shaded area) 95% bootstrap confidence intervals.

calculated an intra-individual reduced-major axis (RMA) slope between the temperature gained during all flights performed in relation to the temperature lost between flights (stops) for each individual taken separately and then tested if the intra-individual slope averaged over all individuals differs from the theoretical value of one (i.e., complete T_b regulation). The average slope and its associated confidence intervals (CI) was computed using a bootstrap and 10,000 re-samplings (Lunneborg, 2000). In a further step, we tested the complete regulation hypothesis at the inter-individual level by summing all gains and losses in T_b (in relation to T_{bStart}) occurring during an average migration day for each individual in turn. From these data, a RMA equation was computed where the correlation coefficient was tested for significance using a permutation test.

Finally, we calculated the intra-individual correlation level between T_{bStart}, T_{bEnd}, T_{bMax} for all flights performed, which was averaged over all individuals with CIs computed from a bootstrap and ten thousand re-samplings.

RESULTS

Mean T_b during flight increased positively with flight duration during the molt migration of the common eiders, from about 40.2°C for short flights to 41.5°C for longer flights (**Figure 2**). Mean T_b of short flights (3–10 min) were within the mean daily variation of T_b (T_{bDaily}) during migration days and only longer flights (>10 min) were outside the confidence intervals (**Figure 2**). Given that migration effort of these 19 females is slightly more than 200 min spent flying on average per day (Guillemette et al., 2016), we tested if average T_b at a daily scale would be influenced by flight time.

This was achieved by comparing T_{bDaily} during migration with periods before and after migration (**Figure 3**). We found that T_{bDaily} before migration [40.41 ± (*SD*) 0.58°C] was slightly higher, on average, than during migration [40.36 ± (*SD*) 0.54°C], as the mean difference between the two temperatures (before and during migration) exclude zero [average difference = 0.05°C ± (bootstrap CI) 0.04]. In contrast, T_{bDaily} after migration [40.30 ± (*SD*) 0.54°C] was lower on average than during migration [average difference = 0.06°C ± (bootstrap CI) 0.06]. Although, T_{bDaily} varied little but significantly, on average, the shape of the frequency distribution was influenced by flight and migration. Unsurprisingly, during migration eiders experienced more T_b between 41.4 and 42.2°C when compared to the before and after migration periods (**Figures 3B,C**).

We then tested the idea that body cooling between flights was a determining factor in the migration strategy of eiders, by relating the body heat gain during flight with body heat loss during stops, at the intra-individual level. We calculated an intra-individual RMA slope between the temperature increases during flights in relation to the temperature decreases between flights for each flight cycle taken separately, and then tested if the average intra-individual slope differs from the theoretical value of one (i.e., complete T_b regulation). The RMA slope ranged between 0.75 and 1.35 among individuals, with a mean of 1.04 ± 0.06 (bootstrap CI) when averaged over all individuals (mean Pearson $r = 0.737$, **Figure 4A**). We further tested this hypothesis at the inter-individual level by summing all increases and decreases in T_b occurring during an average migration day for each individual in turn; we also found a strong and linear relationship ($y = 0.985x–0.11$, $r = 0.976$, permutation test, $p < 0.0001$; **Figure 4B**). Notably, cumulative daily individual variation of T_b related to flight activity during migration was high (3–15°C).

The close regulation of T_b observed (**Figure 4**) at the scale of a flight cycle led us to postulate that reduction of T_b to a minimum level is likely to be mandatory, as it would reduce the likelihood of an occurrence of reaching an unacceptable level of hyperthermia for the subsequent flight. Despite the seemingly large variation between individuals, body temperature at the start of a flight (T_{bStart}) was positively related to body temperature at the end (T_{bEnd}) of a flight at the intra-individual level [average correlation = 0.263 ± (bootstrap CI) 0.095, **Figure 5A**]. A similar observation was made for T_{bMax} [average correlation = 0.325 ± (bootstrap CI) 0.101] which supports our hypothesis (**Figure 5B**). In addition, at the inter-individual level (results not shown), a similar relationship with T_{bStart} reveals a significant coefficient of correlation for both T_{bEnd} (0.664, $p < 0.05$) and T_{bMax} ($r = 0.685$, $p < 0.05$).

During temporary migratory stop-overs, the body temperature of the eiders decreased at an exponential rate, which stabilized at about 45–50 min, on average, from the end of the preceding flight (**Figure 6A**). Indeed, the highest average cooling rate was during the first 10 min after landing, which itself was substantially higher following longer flights, reaching 6–7°C. h^{-1} (**Figures 6B,C**). Nevertheless, the average time required to cool down to T_{bMin} [40.10 ± (*SD*) 0.56], the minimum level between flights [47.14 ± (*SD*) 21.73 min], is substantially shorter than the average duration of each stop between flights [72.1 ± (*SD*) 21.6 min], which raises the question of why birds are taking extra time during stops before resuming flight.

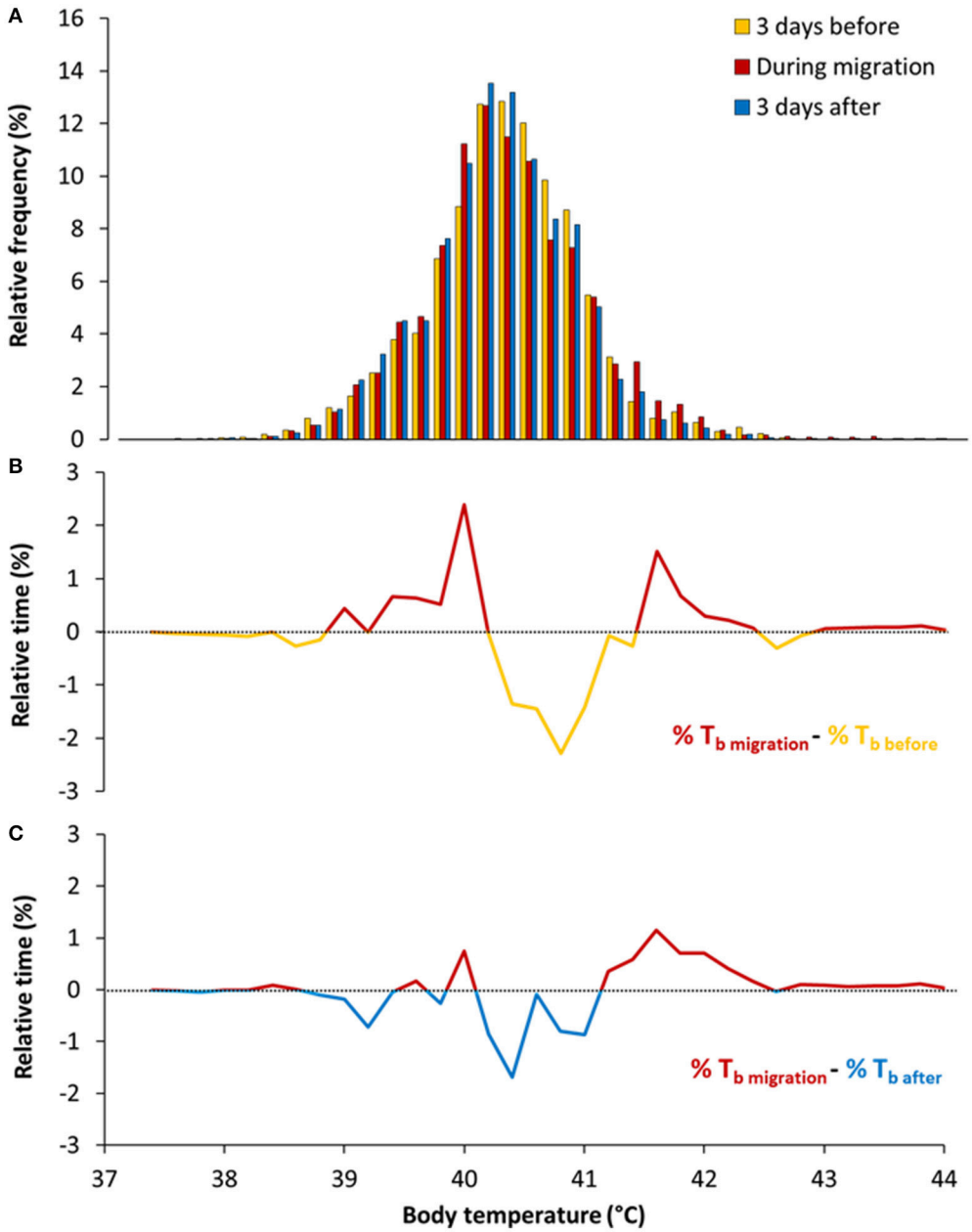

FIGURE 3 | (A) Frequency distribution of daily T_b during, before and after migration. Given that implanted loggers sampled regularly T_b (every 16 s) during each day of migration, the frequency distribution is giving the relative (%) time spent in each T_b classes (0.2°C). **(B)** Differences in relative time in T_b between migration and 3 days before migration (delta migration-before). **(C)** Differences in relative time in T_b between migration and 3 days after migration (delta migration-after).

DISCUSSION

In a former paper, we have presented evidence that hyperthermia might dictate flight duration in a migrating bird (Guillemette et al., 2016). Here, we present evidence that body cooling is an integral part of the migration of common eiders by showing that daily fluctuations in T_{bs} caused by flight were precisely regulated at the scale of a flight cycle, despite large cumulative deviations in T_b caused by the migration and associated flights. We thus suggest below that such a level of regulation results from behavioral thermoregulation together with the intrinsic physiological flexibility of birds.

T_{bDaily} and Heat Dumping during Stop-Overs

It is apparent that birds have higher body temperature tolerance in comparison to mammals (Prinzinger et al., 1991; McNab,

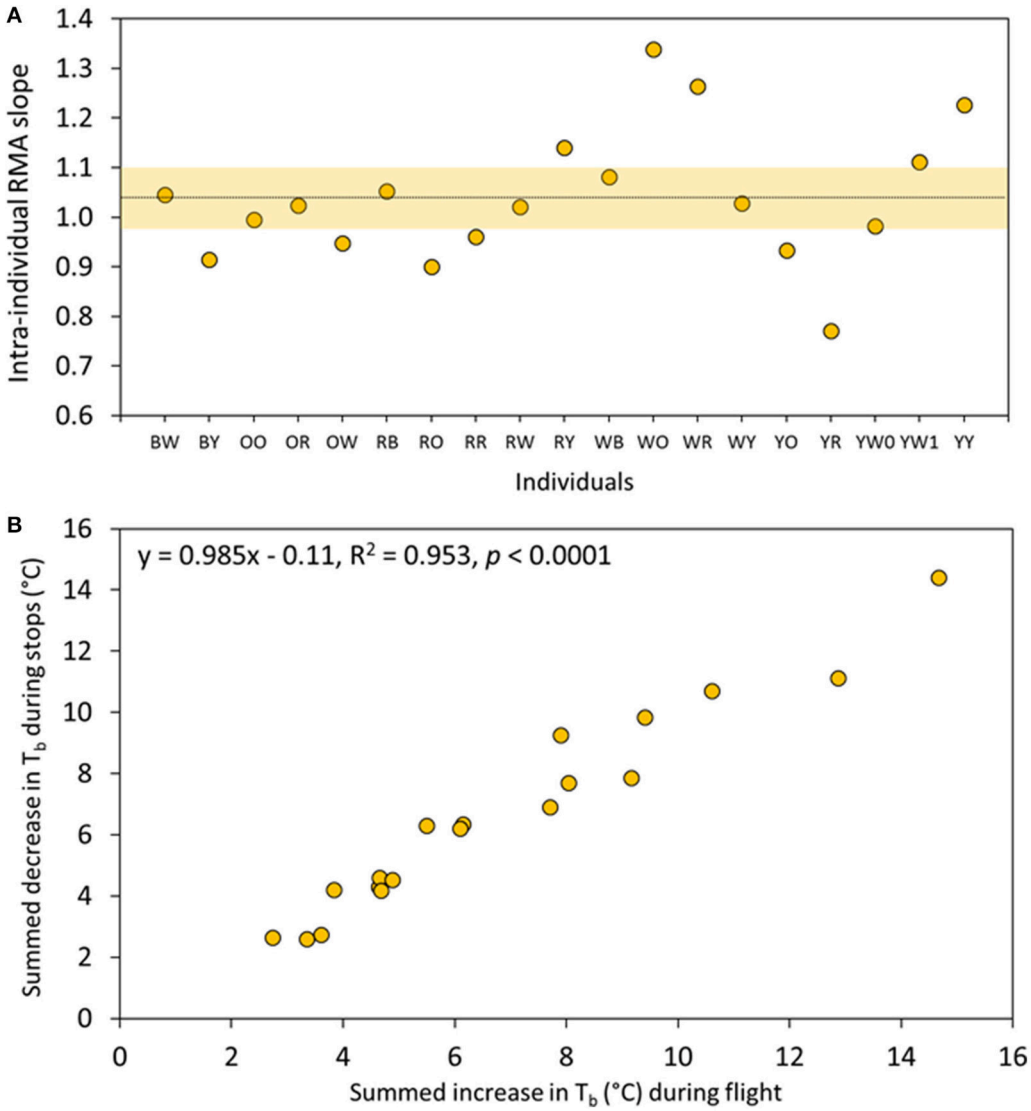

FIGURE 4 | Linear relationships between the numbers of °C gained during flight and the number of °C lost during stops between flights. **(A)** Intra-individual relationships where each point represents a RMA slope for each female eider duck of this study. The dotted line depicts the average slope (1.04) for all individuals while the shaded area shows the (bootstrap) confidence intervals (see Section Materials and Methods). **(B)** Inter-individual relationships where each point is an individual for which the number of °C gained or lost during a flight cycle were summed during an average migration day.

2002). During molt migration, Baltic common eiders fly 205 min per day, on average (Guillemette et al., 2016), and individuals experience daily cumulative variations in T_b ranging between 3 and 15°C (**Figure 3B**). Despite this large variation in T_b associated with flight activity, T_{bDaily} during migration days (40.36 ± 0.54°C) was only slightly different, by 0.05 degrees on average, when compared to before (40.41 ± 0.58°C) and after (40.30 ± 0.54°C) periods. The most distinctive features of migration were the time spent at T_b values in the range of 41.4–42.4 and 40.0–40.2°C (**Figures 2B,C**), which correspond respectively to T_b encountered during long flights (see Guillemette et al., 2016, **Figure 1**) and T_b while idling during stops. The observation that eiders regulate T_b around T_{bMin} at 40.1°C during stops, idling between flights, suggests a selected body temperature target while waiting to perform the next flight. It is also interesting to note this temperature range to be at the low range of T_{bDaily} confidence intervals (**Figure 2**) together with the fact that average T_b during flights of 0–10 min are within the confidence intervals of T_{bDaily}. Altogether, it thus appears that migrating common eiders defend T_{bDaily} with success and we suggest that a part of the absolute level of hyperthermia reached by an exercising animal, the time spent at a high level of T_b is also an important point to consider when evaluating the potential and deleterious effects of hyperthermia.

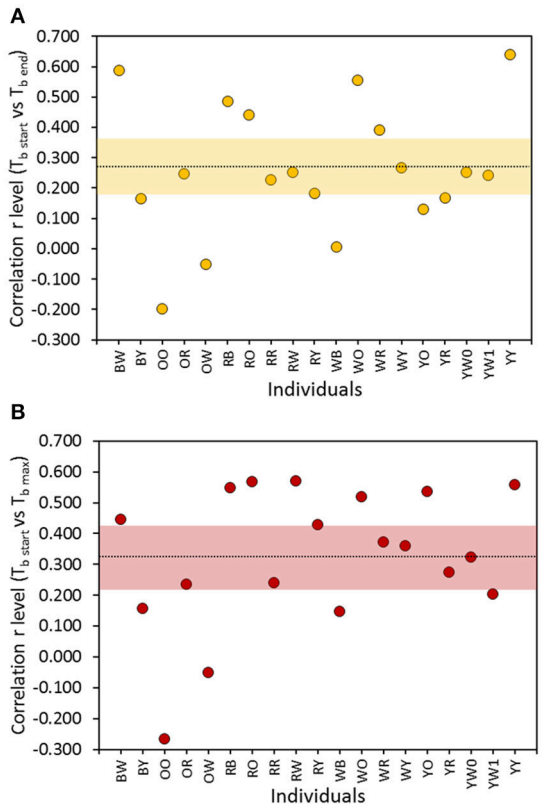

FIGURE 5 | Correlation level between Tb at the start of a flight (T_{bStart}) and **(A)** T_b at the end (T_{bEnd}) of a flight (yellow circles) and **(B)** maximum T_b (T_{bMax}) occurring while aloft (red circles) at the intra-individual level. The overall average ($n = 19$) correlation level is shown with 95% (bootstrap) confidence intervals (shaded area).

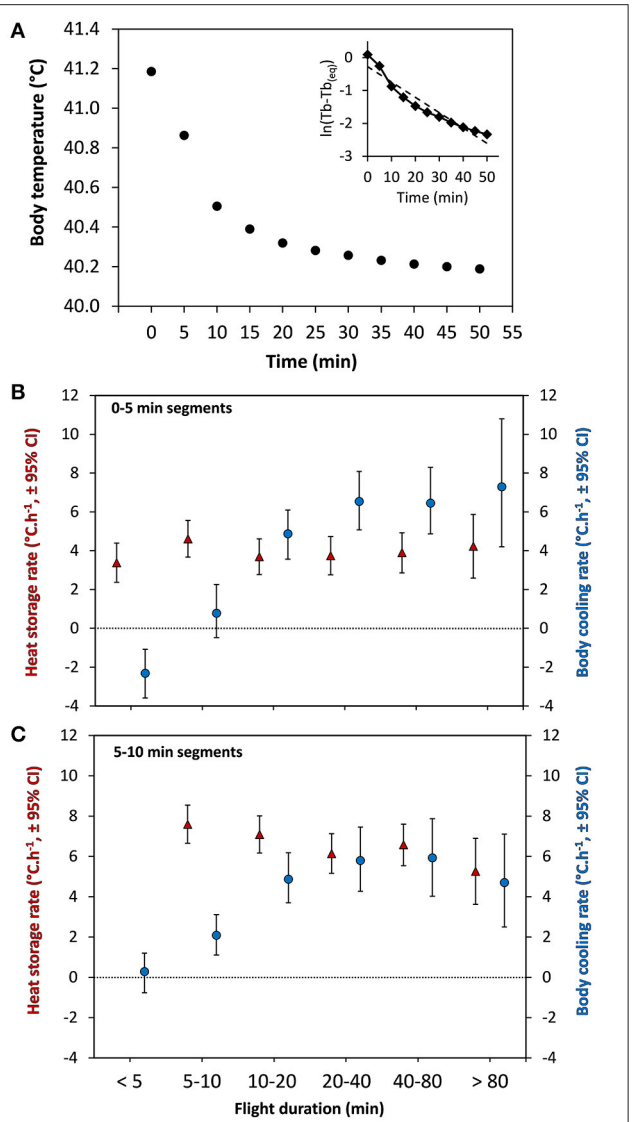

FIGURE 6 | Body temperature and cooling rates in relation to time from the end of a migratory flight. **(A)** Average body temperature (T_b) in relation to time for all flights performed by the 19 females. The curve follows an exponential decrease with highest body cooling rates for 0–5 (representative of flights <5 min) and 5–10 min cooling segments. (**A**, insert) Natural logarithm of the adjusted T_b values (T_b minus the equilibrium T_b) plotted against time (min). The dashed line is the linear regression through these data representative of the relationship expected from a Newtonian cooling curve **(B)** Rate of 0–5 min cooling segments during stops (blue circles) in relation to flight duration compared to heat storage rate during flights (red triangles) for similar independent segments (0–5 min) as computed by Guillemette et al. (2016). **(C)** Rate of 5–10 min cooling segments during stops (blue circles) in relation to flight duration compared to heat storage rate during flights (red triangles) computed by Guillemette et al. (2016). Note that heat storage rate for 5–10 min segments cannot be presented for flight duration of 0–5 min.

Indeed, the return to normothermia was relatively rapid in migrating eiders (**Figure 6A**). Support for this interpretation is given by various cancer treatment therapies using hyperthermia in humans (Wang et al., 2013), which induces intracellular reactive oxygen species (ROS) production and mitochondrial ROS generation in a time-dependent manner. One advantage of maintaining T_b at a low level before the next flight is to eventually reduce the level of hyperthermia reached during that subsequent flight. This hypothesis was supported by the data as we found a positive correlation between T_{bStart} and T_{bEnd} and T_{bStart} and T_{bMax} (see Section Results).

Body Cooling Rate and Idling Time

It is expected that marine birds potentially dissipate heat at a high rate following landing, due to being on water. Indeed, the rate of cooling of migrating common eiders is high for the first 10 min after landing, particularly after longer flights (**Figures 6B,C**), with average rates of cooling ranging from 6 to 7°C. h^{-1}. These estimates of body cooling are difficult to compare with any other species, given the paucity of data. From birds shot while flying, Platania et al. (1986) observed a decrease of T_b varying between 1.2 and 3.6°C h^{-1} for three species (222–449 g), 9.0°C h^{-1} for the smallest species (40 g) and 1.7°C h^{-1} for the largest species (765 g). Unfortunately, Platania et al. (1986) do not give any details about the medium (air vs. water) where these shot birds were cooling down when taking the measurements. One further complication is that we expect dead birds to cool down more

slowly than live birds given they cannot divert blood flow to the periphery or legs to cool down more rapidly (see below).

Interestingly, the cooling rates observed during stop-overs of eiders are similar to the highest heat storage rates occurring at the beginning of a flights (**Figures 6B,C**), indicating that body cooling and heat storage reach equivalent maximum values. In his review, McNab (2002) also reports similar values for ectotherms for both cooling and heat storage rates in air. However, it could be expected that body cooling in aquatic birds would occur at faster rates than heat storage, given the heat dissipation potential of sea water is much higher than air. In humans, cooling rates have been measured in circulated water baths (14 and 20°C water) after exercise in air (65% VO_{2Max} at 38°C) and reaching a rectal temperature of 40.0°C (Proulx et al., 2003). They observed an exponential decrease of T_b with the largest decrease occurring in the first 10 min after immersion, similar to eiders during stop-overs (**Figure 6A**), with the difference that maximum (11.4–15.6°C h^{-1}) and average (9–11.4°C h^{-1}) cooling rates were much higher than average heat storage rates (3–4°C h^{-1}) in the seven human subjects. Unfortunately, Proulx et al. (2003) did not report the maximum rate of heat storage though a maximum rate of 6°C h^{-1} was reported in a very similar experimental setting (González-Alonso et al., 1999). Thus, although humans are much larger animals, maximum body cooling in water seems to be much more rapid than maximum body cooling of migrating eiders, the other main difference being, of course, that humans are naked and deprived of fur or body feathers.

The naked legs of many bird species (Steen and Steen, 1965; Kilgore and Schmidt-Nielsen, 1975; Midtgård, 2008) have been shown to serve as controlled heat conduits, being of paramount importance for thermoregulation in both water (Steen and Steen, 1965; Kilgore and Schmidt-Nielsen, 1975; Midtgård, 2008) and air (Baudinette et al., 1976; Martineau and Larochelle, 1988). The evidence for this is stemming from calorific studies and blood flow measurements. For example, blood flow to the legs of mallards (*Anas platyrhynchos)* and fulmars (*Macronectes giganteus)* is reduced and heat conservation occurs (Johansen and Wesley Millard, 1973; Kilgore and Schmidt-Nielsen, 1975), when water temperature is reduced experimentally during rest. In contrast, heat dissipation can increase considerably where legs are serving as heat dumping organs during both flying and swimming, although the rate of heat loss can vary considerably given the varying experimental conditions used by the different studies. From a behavioral point of view, trailing or retracting the legs and feet in the plumage while flying (Udvardy, 1983; Neumann and Neumann, 2016) or swimming (Harris et al., 2010) is further modulating heat dissipation of birds.

Time as the Cost of Behavioral Thermoregulation

The fact that eiders stop flying when overheating can be seen as another example of behavioral thermoregulation. In his thorough review, McNab (2002) concluded that time is the major cost associated with behavioral thermoregulation of ectotherms although his book almost eludes the subject in relation to endotherms, most probably because examples were few (Smit et al., 2016). Here, we propose that cooling time is a major cost of the migration strategy of common eiders. As such, eiders take about 47 min on average to cool down by 1.1°C and reach T_{bMin}, corresponding to an overall cooling rate of 1.4°C h^{-1}, which is much lower than the max rate observed at the beginning of the cooling period (6–7°C h^{-1}, **Figure 6**). This is readily explained by the (exponential) nature of the cooling curve and the fact that most flights of eiders during molt migration are short (16 min average, Guillemette et al., 2016) when the level of heat stored in the body is still relatively low (**Figure 2**). Interestingly, body cooling in eiders does not appear to be a passive cooling process as predicted by Newton's law of cooling because the relationship between $\ln(T_b\text{-}T_{b(eq)})$ and time (see **Figure 6A** insert), does not fit a linear relationship. In fact, it appears that cooling is initially enhanced and slows down progressively just before reaching the level of equilibrium. Although speculative, the initially increased rate of cooling may be indicative of an active processes of heat dissipation related to e.g., an increased blood flow through the legs of the birds in cooler water.

However, it remains that the 47 min to cool down is still lower than the average duration of stops between flights observed in our sample (72.1 ± 21, 6 min). This indicates that the time spent between flights is not entirely devoted to body cooling (**Figure 1**) and we hypothesized that such an extra time taken between flights is caused by unfavorable wind conditions. Nevertheless, assuming that cooling down to T_{bMin} is a prerequisite to perform the next flight, the daily time spent cooling down on a typical migration day (with about 14 flights per day, Guillemette et al., 2016) would represent 523 min or 36% of the 24 h of the daily time budget. If we add the idling time (about 300 min or 20%) we obtain that eiders are spending altogether 56% of the time spent cooling and idling, between flights, during a typical migration day. This indicates that behavioral thermoregulation of common eiders during migration represents a major component of their time budget.

In conclusion, it is likely that the occurrence of hyperthermia in common eiders is due to their high wing loading and costs of flight, which in turn is a consequence of their morphology being adapted for diving. A fruitful future research direction would be to establish the prevalence of hyperthermia in other diving bird species during migratory flights, and whether some species show flight altitudinal changes in direct response to increases in T_b. It is likely hyperthermia is a hitherto underestimated contributing factor to migration strategies, and the possible daily distances that can be traveled. Moreover, hyperthermia may be one of major contributing factors of why other diving species with high loading (e.g., alcids) undertake a significant portion of their migrations swimming as opposed to flying (Olsson et al., 1999), with the constant contact of their feet with the water, coupled with the lower work-rate of the leg muscles compared to flight, ameliorating the effects of hyperthermia.

AUTHOR CONTRIBUTION

MG, DP conceived the ideas, conducted the experiments, prepared the manuscript and figures, and approved the manuscript. EP and SP prepared manuscript, assisted in analysis and approved the manuscript.

FUNDING

This study was undertaken in collaboration with the National Environmental Research Institute of Denmark and was funded through the Canadian Natural Sciences and Engineering Research Council (NSERC) discovery and equipment grants to MG.

REFERENCES

Bäckman, J., and Alerstam, T. (2001). Confronting the winds: orientation and flight behaviour of roosting swifts, *Apus apus*. *Proc. R. Soc. Lond. B Biol. Sci.* 268, 1081–1087. doi: 10.1098/rspb.2001.1622

Baudinette, R. V., Loveridge, J. P., Wilson, K. J., Mills, C. D., and Schmidt-Nielsen, K. (1976). Heat loss from feet of herring gulls at rest and during flight. *Am. J. Physiol. Leg. Content* 230, 920–924.

Boyles, J. G., Seebacher, F., Smit, B., and McKechnie, A. E. (2011). Adaptive thermoregulation in endotherms may alter responses to climate change. *Integr. Comp. Biol.* 51, 676–690. doi: 10.1093/icb/icr053

Butler, P. J. (2016). The physiological basis of bird flight. *Philos. Trans. R. Soc. B Biol. Sci.* 371:20150384. doi: 10.1098/rstb.2015.0384

Butler, P. J., and Woakes, A. J. (1990). "The physiology of bird flight," in *Bird Migration: Physiology and Ecophysiology*, ed E. Gwinner (Berlin; Heidelberg: Springer), 300–318.

Carpenter, R. E. (1986). Flight physiology of intermediate-sized fruit bats (Pteropodidae). *J. Exp. Biol.* 120, 79–103.

Clarke, A., and Rothery, P. (2008). Scaling of body temperature in mammals and birds. *Funct. Ecol.* 22, 58–67. doi: 10.1111/j.1365-2435.2007.01341.x

Coulson, J. C. (2008). The population dynamics of the Eider Duck *Somateria mollissima* and evidence of extensive non-breeding by adult ducks. *IBIS* 126, 525–543. doi: 10.1111/j.1474-919X.1984.tb02078.x

Crompton, A. W., Taylor, C. R., and Jagger, J. A. (1978). Evolution of homeothermy in mammals. *Nature* 272, 333–336. doi: 10.1038/272333a0

Dawson, W. R. (1982). Evaporative losses of water by birds. *Comp. Biochem. Physiol. Part A Physiol.* 71, 495–509. doi: 10.1016/0300-9629(82)90198-0

Day, R. H., Rose, J. R., Prichard, A. K., Blaha, R. J., and Cooper, B. A. (2004). Environmental effects on the fall migration of eiders at Barrow, Alaska. *Mar. Ornithol.* 32, 13–24.

Giladi, I., and Pinshow, B. (1999). Evaporative and excretory water loss during free flight in pigeons. *J. Comp. Physiol. B* 169, 311–318. doi: 10.1007/s003600050226

Gill, R. E., Piersma, T., Hufford, G., Servranckx, R., and Riegen, A. (2005). Crossing the ultimate ecological barrier: evidence for an 11 000-km-long nonstop flight from Alaska to New Zealand and Eastern Australia by bar-tailed godwits. *Condor* 107, 1–20. doi: 10.1650/7613

González-Alonso, J., Teller, C., Andersen, S. L., Jensen, F. B., Hyldig, T., and Nielsen, B. (1999). Influence of body temperature on the development of fatigue during prolonged exercise in the heat. *J. Appl. Physiol.* 86, 1032–1039.

Guillemette, M. (2001). Foraging before spring migration and before breeding in common eiders: does hyperphagia occur? *Condor* 103, 633–638. doi: 10.1650/0010-5422(2001)103[0633:FBSMAB]2.0.CO;2

Guillemette, M., and Ouellet, J.-F. (2005). Temporary flightlessness in pre-laying common eiders *Somateria mollissima*: are females constrained by excessive wing-loading or by minimal flight muscle ratio? *IBIS* 147, 293–300. doi: 10.1111/j.1474-919x.2005.00401.x

Guillemette, M., Pelletier, D., Grandbois, J.-M., and Butler, P. J. (2007). Flightlessnessand the energetic cost of wing molt in a large sea duck. *Ecology* 88, 2936–2945. doi: 10.1890/06-1751.1

Guillemette, M., Woakes, A. J., Flagstad, A., and Butler, P. J. (2002). Effects of data-loggers implanted for a full year in female common eiders. *Condor* 104, 448–452. doi: 10.1650/0010-5422(2002)104[0448:EODLIF]2.0.CO;2

Guillemette, M., Woakes, A. J., Larochelle, J., Polymeropoulos, E. T., Granbois, J., Butler, P. J., et al. (2016). Does hyperthermia constrain flight duration in a short-distance migrant? *Philos. Trans. R. Soc. B.* 371:20150386. doi: 10.1098/rstb.2015.0386

Harris, M. P., Daunt, F., Newell, M., Phillips, R. A., and Wanless, S. (2010). Wintering areas of adult Atlantic puffins *Fratercula arctica* from a North Sea colony as revealed by geolocation technology. *Mar. Biol.* 157, 827–836. doi: 10.1007/s00227-009-1365-0

Johansen, K., and Wesley Millard, R. (1973). Vascular responses to temperature in the foot of the giant fulmar, *Macronectes giganteus*. *J. Comp. Physiol.* 85, 47–64. doi: 10.1007/BF00694140

Kerlinger, P., and Moore, R. F. (1989). "Atmospheric structure and avian migration," in *Current Ornithology*, ed D. M. Power (New York, NY: Plenum Press), 109–141.

Kilgore, D. L., and Schmidt-Nielsen, K. (1975). Heat loss from ducks' feet immersed in cold water. *Condor* 77:475. doi: 10.2307/1366094

Lewden, A., Petit, M., Milbergue, M., Orio, S., and Vézina, F. (2014). Evidence of facultative daytime hypothermia in a small passerine wintering at northern latitudes. *IBIS* 156, 321–329. doi: 10.1111/ibi.12142

Lunneborg, C. E. (2000). *Data Analysis by Resampling: Concepts and Applications.* Pacific Grove, CA: Brooks/Cole.

Lyngs, P. (2000). Status of the Danish Breeding population of Eiders *Somateria mollissima* 1988–93. *Dansk. Ornitol. Foren. Tidsskr.* 94, 12–18.

Martineau, L., and Larochelle, J. (1988). The cooling power of pigeon legs. *J. Exp. Biol.* 136, 193–208.

McKechnie, A. E., and Mzilikazi, N. (2011). Heterothermy in afrotropical mammals and birds: a review. *Integr. Comp. Biol.* 51, 349–363. doi: 10.1093/icb/icr035

McNab, B. K. (2002). *The Physiolgical Ecology of Vertebrates.* Ithaca, NY; London: Cornell University Press.

Midtgård, U. (2008). Heat loss from the feet of mallards *Anas platyrhynchos* and arterio-venous heat exchange in the rete tibiotarsale. *IBIS* 122, 354–359. doi: 10.1111/j.1474-919X.1980.tb00889.x

Moore, F., and Kerlinger, P. (1987). Stopover and fat deposition by North American wood-warblers (Parulinae) following spring migration over the Gulf of Mexico. *Oecologia* 74, 47–54. doi: 10.1007/BF00377344

Neumann, C., and Neumann, C. (2016). Behavioural thermoregulation in the Common Swift during flight. *Br. Birds* 109, 10–13.

Olsson, O., Fransson, T., and Larsson, K. (1999). Post-fledging migration of common murres *Uria aalge* in the Baltic Sea: management implications. *Ecography* 22, 233–239. doi: 10.1111/j.1600-0587.1999.tb00497.x

Pelletier, D., Guillemette, M., Grandbois, J.-M., and Butler, P. J. (2007). It is time to move: linking flight and foraging behaviour in a diving bird. *Biol. Lett.* 3, 357–359. doi: 10.1098/rsbl.2007.0088

Platania, S. P., Grant, G. S., and Lee, D. S. (1986). Core temperatures of non-nesting Western Atlantic Seabirds. *Brimleyana* 12, 13–18.

Prinzinger, R., Preßmar, A., and Schleucher, E. (1991). Body temperature in birds. *Comp. Biochem. Physiol. Part A Physiol.* 99, 499–506. doi: 10.1016/0300-9629(91)90122-S

Proulx, C. I., Ducharme, M. B., and Kenny, G. P. (2003). Effect of water temperature on cooling efficiency during hyperthermia in humans. *J. Appl. Physiol.* 94, 1317–1323. doi: 10.1152/japplphysiol.00541.2002

Rigou, Y., and Guillemette, M. (2010). Foraging effort and pre-laying strategy in breeding common eiders. *Waterbirds Int. J. Waterbird Biol.* 33, 314–322. doi: 10.1675/063.033.0307

Smit, B., Zietsman, G., Martin, R. O., Cunningham, S. J., McKechnie, A. E., and Hockey, P. A. R. (2016). Behavioural responses to heat in desert birds: implications for predicting vulnerability to climate warming. *Clim. Chang. Respons.* 3, 9. doi: 10.1186/s40665-016-0023-2

Speakman, J. R., and Thomas, D. W. (2003). "Physiological ecology and energetics of bats," in *Physiological Ecology and Energetics of Bats*, eds T. H. Kunz and M. B. Fenton (Chicago, IL: The University of Chicago Press), 430–490.

Steen, I., and Steen, J. B. (1965). The importance of the legs in the thermoregulation of birds. *Acta Physiol. Scand.* 63, 285–291. doi: 10.1111/j.1748-1716.1965.tb04067.x

Tattersall, G. J., Arnaout, B., and Symonds, M. R. E. (2016). The evolution of the avian bill as a thermoregulatory organ. *Biol. Rev.* 92, 1630–1656. doi: 10.1111/brv.12299

Torre-Bueno, J. R. (1976). Temperature regulation and heat dissipation during flight in birds. *J. Exp. Biol.* 65, 471–482.

Udvardy, M. D. F. (1983). The role of the feet in behavioral thermoregulation of hummingbirds. *Condor* 85, 281. doi: 10.2307/1367060

Wang, Z., Cai, F., Chen, X., Luo, M., Hu, L., and Lu, Y. (2013). The role of mitochondria-derived reactive oxygen species in hyperthermia-induced platelet apoptosis. *PLoS ONE* 8:e75044. doi: 10.1371/journal.pone.0075044

White, C. R., Green, J. A., Martin, G. R., Butler, P. J., and Grémillet, D. (2013). Energetic constraints may limit the capacity of visually guided predators to respond to Arctic warming. *J. Zool.* 289, 119–126. doi: 10.1111/j.1469-7998.2012.00968.x

Conflict of Interest Statement: The authors declare that the research was conducted in the absence of any commercial or financial relationships that could be construed as a potential conflict of interest.

frontiers in Physiology

MINI REVIEW
published: 24 August 2017
doi: 10.3389/fphys.2017.00624

REM Sleep and Endothermy: Potential Sites and Mechanism of a Reciprocal Interference

*Matteo Cerri *, Marco Luppi, Domenico Tupone, Giovanni Zamboni and Roberto Amici*

Department of Biomedical and NeuroMotor Sciences, University of Bologna, Bologna, Italy

Numerous data show a reciprocal interaction between REM sleep and thermoregulation. During REM sleep, the function of thermoregulation appears to be impaired; from the other hand, the tonic activation of thermogenesis, such as during cold exposure, suppresses REM sleep occurrence. Recently, both the central neural network controlling REM sleep and the central neural network controlling thermoregulation have been progressively unraveled. Thermoregulation was shown to be controlled by a central "core" circuit, responsible for the maintenance of body temperature, modulated by a set of accessory areas. REM sleep was suggested to be controlled by a group of hypothalamic neurons overlooking at the REM sleep generating circuits within the brainstem. The two networks overlap in a few areas, and in this review, we will suggest that in such overlap may reside the explanation of the reciprocal interaction between REM sleep and thermoregulation. Considering the peculiar modulation of thermoregulation by REM sleep the result of their coincidental evolution, REM sleep may therefore be seen as a period of transient heterothermy.

Keywords: REM sleep, thermoregulation, heterothermy, median preoptic nucleus, periaqueductal gray, lateral parabrachial nucleus, orexin, melanin concentrating hormone

OPEN ACCESS

Edited by:
Rebecca Oelkrug,
University of Lübeck, Germany

Reviewed by:
Carola Waltraud Meyer,
Max Planck Institute for Heart and Lung Research (MPG), Germany
Pablo Torterolo,
University of the Republic, Uruguay

****Correspondence:***
Matteo Cerri
matteo.cerri@unibo.it

Specialty section:
This article was submitted to Integrative Physiology, a section of the journal Frontiers in Physiology

Received: *08 June 2017*
Accepted: *11 August 2017*
Published: *24 August 2017*

Citation:
Cerri M, Luppi M, Tupone D, Zamboni G and Amici R (2017) REM Sleep and Endothermy: Potential Sites and Mechanism of a Reciprocal Interference. Front. Physiol. 8:624. doi: 10.3389/fphys.2017.00624

The primary function of rapid-eye movement sleep (REMS) is still unknown, but the finding that the daily amount of REMS is "homeostatically" regulated (Cerri et al., 2005; Amici et al., 2008) suggests that it may satisfy some primary physiological needs. Pioneering studies showed that REMS occurrence is depressed at an ambient temperature (Ta) outside the thermoneutral range of the species (Parmeggiani and Rabini, 1967a), and thermoregulatory responses, such as shivering and panting, are suppressed during REMS (Parmeggiani and Rabini, 1967b). This thermoregulatory impairment has been confirmed by different studies (Parmeggiani, 2003; Heller, 2005). Also, since the direct warming and cooling of the preoptic area (POA) was shown to be inefficient in eliciting appropriate thermoregulatory responses during REMS, such an impairment was ascribed to a suspension in the central control of body temperature (Tb) (Parmeggiani et al., 1973, 1977; Glotzbach and Heller, 1976; Martelli et al., 2014).

However, the few studies on changes in POA neuronal thermosensitivity during sleep (Parmeggiani et al., 1983, 1986, 1987; Glotzbach and Heller, 1984; Alam et al., 1995) have not clarified the mechanisms of POA unresponsiveness during REMS. Consequently, investigations into the relationship between REMS and thermoregulation have been mostly phenomenal. A more mechanistic milieu has arisen from recent studies on thermoregulatory circuits (Morrison and Nakamura, 2011), and the critical role of the hypothalamus in sleep has been recognized (Saper et al., 2005). In this mini-review we will: (i) provide a brief data overview describing the interaction

between REMS and thermoregulation; (ii) summarize the central networks regulating REMS and Tb and the areas in which they overlap and, (iii) suggest possible mechanisms of the reciprocal interaction between REMS and thermoregulation.

REM SLEEP AND THERMOREGULATION

Initial studies on the interaction between sleep and thermoregulation were carried out, in different species, at both low and high Tas (Parmeggiani and Rabini, 1970; Schmidek et al., 1972; Haskell et al., 1981; Sichieri and Schmidek, 1984). They showed that REMS amount plotted against Ta values took the shape of an inverted U curve, with a maximum value moving in accordance with acclimation to Ta. In rats, the peak of REMS occurrence defined a thermoneutral zone (TNZ) that was narrower than that delimited by the minimal O_2 consumption (Szymusiak and Satinoff, 1981). Thus, REMS occurrence is influenced by thermoregulation and declines at Tas beyond the TNZ limits. In accordance with this, not only REMS expression is higher at the circadian nadir of Tb, but also the two rhythms are phase-locked in free-running conditions (Lee et al., 2009).

It is worth noting that, in the latter condition, REMS occurrence is preceded, during Wake and NREM sleep (NREMS), by postural adjustments that optimize thermal exchanges (Parmeggiani, 1980); the potential inhibition of REMS occurrence according to Ta belongs to the same repertoire of behavioral thermoregulation. In the rat, the efficacy of this mechanism is revealed by the observation that, during the acclimation to Tas close to the TNZ boundaries, REMS occurrence is initially reduced and then restored to control levels in about 1 week (Mahapatra et al., 2005; Kaushik et al., 2012).

Since endothermic homeotherms evolved with a Tb that was much closer to the upper than to the lower limit of their lethal core temperature, the interaction between REMS and thermoregulation has mostly been addressed within the wider span of cold defense mechanisms. In the rat, this approach showed that REMS is reduced proportionally to Ta and that the REMS debt is fully recovered, following the return to TNZ, through a mechanism based on the frequency rather than the duration of episodes (Cerri et al., 2005; Amici et al., 2008). This pattern, qualitatively described in early reports (Schmidek et al., 1972; Sichieri and Schmidek, 1984), appears to conform to the energetic constrains of polyphasic sleep in small mammals (Capellini et al., 2008).

Long-term selective REMS deprivation studies have been performed in the rat (Rechtschaffen et al., 1983). The results showed that animals progressively developed a severe hypothermia, caused by an increase in heat loss (Bergmann et al., 1989). This appeared to be counteracted by behavioral thermoregulation, since deprived animals were able to select progressively higher Tas in a thermal gradient (Prete et al., 1991), but not by an increase in metabolic rate, which was concomitant with an incremental hyperphagia. These results were further clarified by the finding, in REMS-deprived rats, of an increased expression of the uncoupling protein-1 in the brown adipose tissue (BAT) and a decrease in leptin secretion (Koban and Swinson, 2005). Thus, it appears that a long-lasting deficiency of periods of central thermoregulatory unresponsiveness, represented by REMS, will progress to a malfunctioning of the different thermoeffector loops balancing Tb (Romanovsky, 2007).

The onset of REMS is characterized by an increase in hypothalamic temperature (Thy) (Kawamura and Sawyer, 1965), which is usually in the range of decimals of a degree and evident even outside the TNZ (Parmeggiani, 2003). This change was conditionally coupled to the increase in cerebral blood flow characterizing REMS (Franzini, 1992) until it was shown that it mainly depends on an larger increase in the flow from vertebral arteries compared to that from carotid arteries, the former circle supplying the brain with warmer blood than the latter (Azzaroni and Parmeggiani, 1993).

The thermal irrelevance of the Thy increase during REMS episodes contrasts with its strictly controlled decrease, during NREMS episodes leading to REMS occurrence (Parmeggiani et al., 1975). With respect to this, a quantitative study on the slope of that decrease showed the possibility to predict the onset of REMS within a 1 min interval (Capitani et al., 2005).

The thermal irresponsiveness of POA, decrease in the overall O_2 consumption and increase in the overall heat loss (Roussel and Bittel, 1979; Schmidek et al., 1983), probably due to changes in peripheral vasomotion in opposition to a homeothermic control of Tb (Parmeggiani et al., 1977; Franzini et al., 1982; Alfoldi et al., 1990), support the view that REMS is a poikilothermic state, while Wake and NREMS remain homeothermic (Parmeggiani, 2003).

By taking into account the autonomic irregularities associated with REMS (Parmeggiani, 1980; Amici et al., 2014) this dichotomy may be extended to systemic physiological regulations, indicating a poikilostatic control for REMS and the permanence of a homeostatic control for Wake and NREMS (Parmeggiani, 2003). According to this view, POA thermal irresponsiveness depends on an impairment of diencephalic integrative activity. Thus, physiological regulation during REMS should mainly operate through a brainstem reflex activity, destitute of the hypothalamic control (Parmeggiani, 2003). However, hypothalamic osmoregulation, which is phylogenetically older than thermoregulation, is not impaired during REMS (Luppi et al., 2010), and REMS occurrence is hardly affected by a long-lasting water deprivation (Martelli et al., 2012). These results raise the possibility that the distinctive trait of REMS is the development of a poikilothermic condition, and this may be the reason why REMS occurrence is so intensely influenced by thermoregulation.

THE CENTRAL CIRCUITS CONTROLLING REM SLEEP AND THERMOREGULATION

The Central Network Controlling REM Sleep

The neural network controlling REMS onset was initially outlined in the cat (Jouvet, 1962) and, later, in the rat (Luppi et al., 2014, 2017). In the cat, a central role in REMS generation has

been attributed to pontine cholinoceptive/cholinergic neurons (Vanni-Mercier et al., 1989; Sakai and Koyama, 1996). In the rat, the crucial role of pontine structures in REMS generation has been confirmed, and general agreement has been reached regarding the prominent role of REMS-on glutamatergic neurons of the sublaterodorsal tegmental nucleus (SLD) (Luppi et al., 2014, 2017). Projections from SLD have been shown to activate neural networks underlying both brain cortical and somatic hallmarks of REMS (Luppi et al., 2014, 2017).

SLD neurons receive a tonic excitatory glutamatergic input from different brain areas and are kept inhibited during Wake and NREMS by projections from REMS-off neurons of the ventrolateral periaqueductal gray (VlPAG) and the dorsal deep mesencephalic reticular nuclei (dDPMe) (Luppi et al., 2014, 2017). VlPAG/dDPMe REMS-off neurons are excited by both orexin neurons in the lateral hypothalamus (LH) and monoaminergic neurons in the brainstem and tuberomammillary wake-promoting areas.

The inhibition of these VlPAG/dDPMe REMS-off neurons is apparently crucial for REMS onset. Active inhibition is promoted by a sub-population of VlPAG GABAergic REMS-on neurons, while disfacilitation is due to the suppression of firing, during REMS, of monoaminergic wake-promoting neurons, to which GABAergic REMS-on VlPAG neurons also send their terminals. It has been proposed that further inhibitory inputs arise from ascending GABAergic projections from the medulla in both rats (Luppi et al., 2014, 2017) and mice (Weber et al., 2015).

A crucial role in the inhibition of VlPAG/dDPMe REMS-off neurons is played by REMS-on neurons of the posterior hypothalamus, including LH, zona incerta, and perifornical hypothalamus, many of which release GABAand/or the peptide melanin-concentrating hormone (MCH) (Luppi et al., 2014, 2017). In fact, this group of neurons is considered the "master generator" of REMS (Luppi et al., 2014). The central role of the hypothalamic MCH/GABAergic neurons in REMS occurrence has been underlined by optogenetic and chemogenetic studies in rats (Jego et al., 2013) and mice (Vetrivelan et al., 2016), respectively. MCH neurons, inhibited by monoaminergic wake-promoting neurons, may also contribute to the active inhibition of orexin neurons in the LH during REMS.

At a preoptic-hypothalamic level, the median preoptic nucleus (MnPO) and the ventrolateral preoptic nucleus (VLPO) play a role in REMS regulation (Gvilia et al., 2006; Dentico et al., 2009). In both structures, the degree of cellular activity appears to be related to the homeostatic need for REMS, which, increases during REMS deprivation and decreases during the following REMS rebound. It has been suggested that both structures are part of the network for the switching-off of the brainstem and hypothalamic wake-promoting centers when sleep need is increased, but the MnPO has been shown to have a closer link with REMS regulation (Szymusiak and McGinty, 2008; McKinley et al., 2015). A similar REMS-related pattern has been found at the pontine level in the Lateral Parabrachial Nucleus (lPBN), largely active during both REMS deprivation and the following REMS rebound (Verret et al., 2005).

The Central Network Controlling Thermoregulation

Research in thermoregulation has led to a better definition of the neural pathways through which cutaneous thermal receptors activate BAT thermogenesis, as well as shivering thermogenesis, and cutaneous vasoconstriction (CVC) for heat retention, necessary for cold defense (Cano et al., 2003; Nakamura and Morrison, 2007, 2008, 2010, 2011; Morrison and Nakamura, 2011; Morrison et al., 2012).

Cold and warm signals from the skin are transmitted, through glutamatergic second order ascending neurons from the dorsal horn to the externolateral- (el) and dorsolateral- (dl) PBN neurons, respectively. From here, elPBN glutamatergic neurons convey the cold thermal signal to the GABAergic Median preoptic (MnPO) neurons (Tan et al., 2016), which in turn inhibit the warm-sensitive GABAergic neurons within the medial preoptic (MPO) projecting to the dorso-medial hypothalamus (DMH) and raphe pallidus (RPa). This leads to an increased activity of thermogenesis-promoting neurons in the DMH, which provide the main excitatory drive for the rostral RPa (rRPa) premotor neurons with consequent activation of thermogenesis (Morrison et al., 1999; Cerri et al., 2010). Alternatively, warm thermal signals retransmitted by dlPBN glutamatergic neurons activate the MnPO glutamatergic neurons, which in turn activate MPO GABAergic neurons projecting to the DMH and rRPa. This leads to an inhibition of thermogenesis-promoting neurons in the DMH, reducing the excitatory drive to the rRPa premotor neurons. The inhibition of RPa neurons increases thermal dissipation and leads to a reduction in body temperature (Cerri et al., 2010, 2013).

The thermoregulatory network sends its branches to several brain areas that control metabolic, cardiovascular, osmolar and respiratory functions and, conversely, receives feedback from these areas, thus modulating thermoregulatory responses (Morrison et al., 2014). Among these areas, the role of the LH and the PAG is of particular interest in the context of this review.

Two relevant populations of neurons that modulate thermoregulation are located within the LH: orexin neurons and MCH neurons. Orexin neurons send direct projections to the rRPa (Oldfield et al., 2002; Berthoud et al., 2005; Tupone et al., 2011), are directly involved in the modulation of BAT thermogenesis (Tupone et al., 2011; Luong and Carrive, 2012), are indispensable to mediate the prostaglandin E2-induced fever, and are necessary for the defense against environmental cooling in mice (Takahashi et al., 2013). MCH signal deficiency has been shown to increase Tb (Ahnaou et al., 2011; Takase et al., 2014).

PAG neurons receive projections from the main thermoregulatory hypothalamic nuclei (Rizvi et al., 1992; Yoshida et al., 2005) and project directly to the rRPa (Hermann et al., 1997) and, multi-synaptically, to BAT (Cano et al., 2003), mostly from the ventromedial and the ventrolateral regions, respectively. The caudal portion of the lateral PAG contains BAT sympatho-excitatory neurons (Chen et al., 2002; Nakamura and Morrison, 2007), whereas the rostral PAG contains BAT sympatho-inhibitory neurons (Rathner and Morrison, 2006).

POTENTIAL SITES AND MECHANISMS AT THE BASE OF THE INTERACTION BETWEEN REM SLEEP AND THERMOREGULATION

The tight reciprocal link between REMS and thermoregulation suggests the existence of mechanisms underlying this interaction at the level of the brain areas shared by the two regulatory networks. In fact, it is noteworthy that the sleep network and the thermoregulation network overlap in some brain areas (**Figure 1**). This overlap is particularly evident in the case of the LH, where two populations of wake-promoting neurons, expressing orexin (Adamantidis et al., 2007) or GABA (Venner et al., 2016), are intermingled with a population of REMS-promoting neurons expressing GABA and MCH (Hanriot et al., 2007). MCH neurons are also segregated from the orexin neurons (Kerman et al., 2007), and send reciprocal connections to each other (Guan et al., 2002). The entire area also has relevant effects on thermoregulation and behavioral state regulation when activated (Cerri and Morrison, 2005; Di Cristoforo et al., 2015), or inhibited (Cerri et al., 2014). In particular, the LH inhibition by the local delivery of the GABA-A agonist muscimol led to REMS suppression in rats (Clement et al., 2012; Cerri et al., 2014).

Another overlap between the two networks occurs at the POA level, in particular, the MnPO. The MnPO is a very important integrative site for homeostatic function, since it receives inputs from different sensory pathways and contains osmoresponsive, thermoresponsive, and sleep-related neurons, which, to some extent, reciprocally interact (McKinley et al., 2015). Intrinsic MnPO GABAergic neurons, which are activated by projections from the elPBN might directly or indirectly inhibit the REMS-related neurons in the MnPO, contributing to Wake enhancement and REMS suppression at a low Ta.

A further possible site of overlap between REMS regulation and thermoregulation is the VlPAG. On one hand, a consistent number of either REMS-off or REMS-on neurons have been found in VlPAG (Sapin et al., 2009). On the other hand, neurons from this region directly project to the RPa (Hermann et al., 1997; Cano et al., 2003), some of which are able to indirectly promote BAT activity (Chen et al., 2002; Nakamura and Morrison, 2007). However, these neurons appear to be differently controlled. In fact, while REMS-off neurons are apparently kept active by orexinergic and monoaminergic afferents (Luppi et al., 2014, 2017), thermoregulatory neurons apparently receive inputs from the DMH/dorsal hypothalamic area (Yoshida et al., 2005) and the MPO (Rizvi et al., 1992). As discussed by others (Martelli et al., 2013), a further possible site of overlap can be found at the level of the lPBN, since lPBN neurons may influence REMS occurrence via direct projections to the SLD (Boissard et al., 2003).

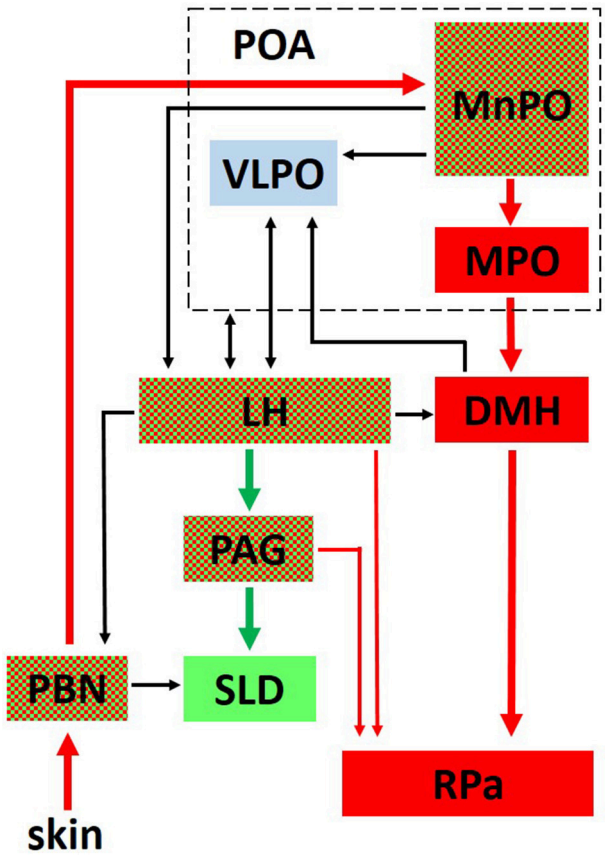

FIGURE 1 | This figure outlines the interaction between the central network controlling thermoregulation (in red) and the central network controlling REM sleep (in green). Areas belonging to both networks are red and green checked. Interactions of both networks with the ventrolateral preoptic nucleus (VLPO, in light blue), a critical part of the network controlling non-REM sleep onset, are also shown. PBN, Parabrachial Nucleus; MPO, Medial Preoptic; MnPO, Median Preoptic; DMH, Dorsomedial Hypothalamus; RPa, Raphe Pallidus; LH, Lateral Hypothalamus, PAG, Periaqueductal Gray; SLD, sublaterodorsal tegmental nucleus; Thin lines represent a modulatory influence.

CONCLUSIONS

A way to consider changes in the activity of MnPO in REMS deprivation and recovery (Gvilia et al., 2006; Dentico et al., 2009) is that this nucleus belongs to a preoptic set which is thought to form, with the DMH, a visceromotor pattern generator (HVPG) (Thompson and Swanson, 2003). As suggested by the normality of fluid regulation (Luppi et al., 2010; Martelli et al., 2012), the thermal irresponsiveness of POA may change the visceromotor response patterns of HPVG.

The clamping of Thy, during REMS, by a diathermic warming of the thermally irresponsive POA, doubled episode duration even at a Ta well below the lower limit of TNZ (Parmeggiani et al., 1974), and this extra REMS was fully accounted for within deprivation-recovery processes (Parmeggiani et al., 1980). This increase in REMS duration may be interpreted as a direct thermal effect on sleep-regulating circuits, whereas hypothermia has the opposite effect (Jones et al., 2008; Del Vecchio et al., 2014). However, its striking efficacy may, alternatively, be viewed as a sign that Thy is monitored by POA before REMS onset, and by the DMH subdivision of HPVG during its occurrence. Along these lines, the diathermic warming of POA did not change c-FOS expression in that area, but suppressed a c-FOS increase induced in DMH by previous cold exposure (Yoshida

et al., 2002). The potential role for DMH in the peculiar thermoregulatory set of REMS is further supported by the finding that a transection separating POA from DMH transforms the input of peripheral thermoreceptors into a response, by thermal effectors, that is directly proportional to Ta (inverted thermoregulation) (Tupone et al., 2017).

Thus, taken together, these results suggest that REMS may be considered as a transient heterothermic state fulfilling, within the far-reaching protection of a rest period, specific needs of endotherms brain activity, rather than energy saving. This view appears in line with the hypothesis of a coevolution of REMS and thermoregulation (Lee Kavanau, 2002) and the observation of an occurrence of REMS-like episodes in hibernating lemurs only at the highest Ta still compatible with torpor (Krystal et al., 2013; Blanco et al., 2016).

On these bases, the interplay between REMS and thermoregulation may be linked to the simultaneous evolution of the two functions, and the sharing of regulatory areas may be the results of some evolutionary constraint in terms of developmental physiology. Thus, the study of the interaction between REMS and thermoregulation may open new perspectives on how the two functions developed and shed light on the yet unknown purpose of REMS.

AUTHOR CONTRIBUTIONS

This manuscript is the result of the common effert of MC, ML, DT, GZ, and RA. All the authors contributed to the development of the manuscript.

FUNDING

Funding for this paper came from the University of Bologna (RFO).

ACKNOWLEDGMENTS

The authors thank Mrs. Melissa Stott for reviewing the English.

REFERENCES

Adamantidis, A. R., Zhang, F., Aravanis, A. M., Deisseroth, K., and de Lecea, L. (2007). Neural substrates of awakening probed with optogenetic control of hypocretin neurons. *Nature* 450, 420–424. doi: 10.1038/nature06310

Ahnaou, A., Dautzenberg, F. M., Huysmans, H., Steckler, T., and Drinkenburg, W. H. (2011). Contribution of melanin-concentrating hormone (MCH1) receptor to thermoregulation and sleep stabilization: evidence from MCH1 (-/-) mice. *Behav. Brain Res.* 218, 42–50. doi: 10.1016/j.bbr.2010.11.019

Alam, M. N., McGinty, D., and Szymusiak, R. (1995). Preoptic/anterior hypothalamic neurons: thermosensitivity in rapid eye movement sleep. *Am. J. Physiol.* 269(5 Pt 2), R1250–R1257.

Alfoldi, P., Rubicsek, G., Cserni, G., and Obal, F. Jr. (1990). Brain and core temperatures and peripheral vasomotion during sleep and wakefulness at various ambient temperatures in the rat. *Pflugers Arch.* 417, 336–341. doi: 10.1007/BF00371001

Amici, R., Bastianini, S., Berteotti, C., Cerri, M., Del Vecchio, F., Lo Martire, V., et al. (2014). Sleep and bodily functions: the physiological interplay between body homeostasis and sleep homeostasis. *Arch. Ital. Biol.* 152, 66–78. doi: 10.12871/000298292014232

Amici, R., Cerri, M., Ocampo-Garces, A., Baracchi, F., Dentico, D., Jones, C. A., et al. (2008). Cold exposure and sleep in the rat: REM sleep homeostasis and body size. *Sleep* 31, 708–715. doi: 10.1093/sleep/31.5.708

Azzaroni, A., and Parmeggiani, P. L. (1993). Mechanisms underlying hypothalamic temperature changes during sleep in mammals. *Brain Res.* 632, 136–142. doi: 10.1016/0006-8993(93)91148-L

Bergmann, B. M., Everson, C. A., Kushida, C. A., Fang, V. S., Leitch, C. A., Schoeller, D. A., et al. (1989). Sleep deprivation in the rat: V. Energy use and mediation. *Sleep* 12, 31–41. doi: 10.1093/sleep/12.1.31

Berthoud, H. R., Patterson, L. M., Sutton, G. M., Morrison, C., and Zheng, H. (2005). Orexin inputs to caudal raphe neurons involved in thermal, cardiovascular, and gastrointestinal regulation. *Histochem. Cell Biol.* 123, 147–156. doi: 10.1007/s00418-005-0761-x

Blanco, M. B., Dausmann, K. H., Faherty, S. L., Klopfer, P., Krystal, A. D., Schopler, R., et al. (2016). Hibernation in a primate: does sleep occur? *R. Soc. Open Sci.* 3:160282. doi: 10.1098/rsos.160282

Boissard, R., Fort, P., Gervasoni, D., Barbagli, B., and Luppi, P.H. (2003). Localization of the GABAergic and non-GABAergic neurons projecting to the sublaterodorsal nucleus and potentially gating paradoxical sleep onset. *Eur. J. Neurosci.* 18, 1627–1639. doi: 10.1046/j.1460-9568.2003.02861.x

Cano, G., Passerin, A. M., Schiltz, J. C., Card, J. P., Morrison, S. F., and Sved, A. F. (2003). Anatomical substrates for the central control of sympathetic outflow to interscapular adipose tissue during cold exposure. *J. Comp. Neurol.* 460, 303–326. doi: 10.1002/cne.10643

Capellini, I., Nunn, C. L., McNamara, P., Preston, B. T., and Barton, R. A. (2008). Energetic constraints, not predation, influence the evolution of sleep patterning in mammals. *Funct. Ecol.* 22, 847–853. doi: 10.1111/j.1365-2435.2008.01449.x

Capitani, P., Cerri, M., Amici, R., Baracchi, F., Jones, C. A., Luppi, M., et al. (2005). Changes in EEG activity and hypothalamic temperature as indices for non-REM sleep to REM sleep transitions. *Neurosci. Lett.* 383, 182–187. doi: 10.1016/j.neulet.2005.04.009

Cerri, M., and Morrison, S. F. (2005). Activation of lateral hypothalamic neurons stimulates brown adipose tissue thermogenesis. *Neuroscience* 135, 627–638. doi: 10.1016/j.neuroscience.2005.06.039

Cerri, M., Del Vecchio, F., Mastrotto, M., Luppi, M., Martelli, D., Perez, E., et al. (2014). Enhanced slow-wave EEG activity and thermoregulatory impairment following the inhibition of the lateral hypothalamus in the rat. *PLoS ONE* 9:e112849. doi: 10.1371/journal.pone.0112849

Cerri, M., Mastrotto, M., Tupone, D., Martelli, D., Luppi, M., Perez, E., et al. (2013). The inhibition of neurons in the central nervous pathways for thermoregulatory cold defense induces a suspended animation state in the rat. *J. Neurosci.* 33, 2984–2993. doi: 10.1523/JNEUROSCI.3596-12.2013

Cerri, M., Ocampo-Garces, A., Amici, R., Baracchi, F., Capitani, P., Jones, C. A., et al. (2005). Cold exposure and sleep in the rat: effects on sleep architecture and the electroencephalogram. *Sleep* 28, 694–705. doi: 10.1093/sleep/28.6.694

Cerri, M., Zamboni, G., Tupone, D., Dentico, D., Luppi, M., Martelli, D., et al. (2010). Cutaneous vasodilation elicited by disinhibition of the caudal portion of the rostral ventromedial medulla of the free-behaving rat. *Neuroscience* 165, 984–995. doi: 10.1016/j.neuroscience.2009.10.068

Chen, X. M., Nishi, M., Taniguchi, A., Nagashima, K., Shibata, M., and Kanosue, K. (2002). The caudal periaqueductal gray participates in the activation of brown adipose tissue in rats. *Neurosci. Lett.* 331, 17–20. doi: 10.1016/S0304-3940(02)00757-7

Clement, O., Sapin, E., Libourel, P. A., Arthaud, S., Brischoux, F., Fort, P., et al. (2012). The lateral hypothalamic area controls paradoxical (REM) sleep by means of descending projections to brainstem GABAergic neurons. *J. Neurosci.* 32, 16763–16774. doi: 10.1523/JNEUROSCI.1885-12.2012

Del Vecchio, F., Nalivaiko, E., Cerri, M., Luppi, M., and Amici, R. (2014). Provocative motion causes fall in brain temperature and affects sleep in rats. *Exp. Brain Res.* 232, 2591–2599. doi: 10.1007/s00221-014-3899-8

Dentico, D., Amici, R., Baracchi, F., Cerri, M., Del Sindaco, E., Luppi, M., et al. (2009). c-Fos expression in preoptic nuclei as a marker of sleep rebound in the rat. *Eur. J. Neurosci.* 30, 651–661. doi: 10.1111/j.1460-9568.2009.06848.x

Di Cristoforo, A., Cerri, M., Del Vecchio, F., Hitrec, T., Luppi, M., Perez, E., et al. (2015). Wake-sleep, thermoregulatory, and autonomic effects of cholinergic activation of the lateral hypothalamus in the rat: a pilot study. *Arch. Ital. Biol.* 153, 67–76. doi: 10.12871/000398292015232

Franzini, C. (1992). Brain metabolism and blood flow during sleep. *J. Sleep Res.*. 1, 3–16. doi: 10.1111/j.1365-2869.1992.tb00002.x

Franzini, C., Cianci, T., Lenzi, P., and Guidalotti, P. L. (1982). Neural control of vasomotion in rabbit ear is impaired during desynchronized sleep. *Am. J. Physiol.* 243, R142–146.

Glotzbach, S. F., and Heller, H. C. (1976). Central nervous regulation of body temperature during sleep. *Science* 194, 537–539. doi: 10.1126/science.973138

Glotzbach, S. F., and Heller, H. C. (1984). Changes in the thermal characteristics of hypothalamic neurons during sleep and wakefulness. *Brain Res.* 309, 17–26. doi: 10.1016/0006-8993(84)91006-0

Guan, J. L., Uehara, K., Lu, S., Wang, Q. P., Funahashi, H., Sakurai, T., et al. (2002). Reciprocal synaptic relationships between orexin- and melanin-concentrating hormone-containing neurons in the rat lateral hypothalamus: a novel circuit implicated in feeding regulation. *Int. J. Obes. Relat. Metab. Disord.* 26, 1523–1532. doi: 10.1038/sj.ijo.0802155

Gvilia, I., Xu, F., McGinty, D., and Szymusiak, R. (2006). Homeostatic regulation of sleep: a role for preoptic area neurons. *J. Neurosci.* 26, 9426–9433. doi: 10.1523/JNEUROSCI.2012-06.2006

Hanriot, L., Camargo, N., Courau, A. C., Leger, L., Luppi, P. H., and Peyron, C. (2007). Characterization of the melanin-concentrating hormone neurons activated during paradoxical sleep hypersomnia in rats. *J. Comp. Neurol.* 505, 147–157. doi: 10.1002/cne.21482

Haskell, E. H., Palca, J. W., Walker, J. M., Berger, R. J., and Heller, H. C. (1981). The effects of high and low ambient temperatures on human sleep stages. *Electroencephalogr. Clin. Neurophysiol.* 51, 494–501. doi: 10.1016/0013-4694(81)90226-1

Heller, H. C. (2005). "Temperature, Thermoregulation, and Sleep," in *Principle and Practice of Sleep Medicine*, eds. M. H. Kryger, T. Roth, and W. E. Dement (Philadelphia, PA: W*b Saunders)*, 292–304.

Hermann, D. M., Luppi, P. H., Peyron, C., Hinckel, P., and Jouvet, M. (1997). Afferent projections to the rat nuclei raphe magnus, raphe pallidus and reticularis gigantocellularis pars alpha demonstrated by iontophoretic application of choleratoxin (subunit b). *J. Chem. Neuroanat.* 13, 1–21. doi: 10.1016/S0891-0618(97)00019-7

Jego, S., Glasgow, S. D., Herrera, C. G., Ekstrand, M., Reed, S. J., Boyce, R., et al. (2013). Optogenetic identification of a rapid eye movement sleep modulatory circuit in the hypothalamus. *Nat. Neurosci.* 16, 1637–1643. doi: 10.1038/nn.3522

Jones, C. A., Perez, E., Amici, R., Luppi, M., Baracchi, F., Cerri, M., et al. (2008). Lithium affects REM sleep occurrence, autonomic activity and brain second messengers in the rat. *Behav. Brain Res.* 187, 254–261. doi: 10.1016/j.bbr.2007.09.017

Jouvet, M. (1962). Research on the neural structures and responsible mechanisms in different phases of physiological sleep. *Arch. Ital. Biol.* 100, 125–206.

Kaushik, M. K., Kumar, V. M., and Mallick, H. N. (2012). Hypothalamic temperature: a key regulator in homeostatic restoration of sleep during chronic cold exposure in rats. *Indian J. Physiol. Pharmacol.* 56, 301–313.

Kawamura, H., and Sawyer, C. H. (1965). Elevation in brain temperature during paradoxical sleep. *Science* 150, 912–913. doi: 10.1126/science.150.3698.912

Kerman, I. A., Bernard, R., Rosenthal, D., Beals, J., Akil, H., and Watson, S. J. (2007). Distinct populations of presympathetic-premotor neurons express orexin or melanin-concentrating hormone in the rat lateral hypothalamus. *J. Comp. Neurol.* 505, 586–601. doi: 10.1002/cne.21511

Koban, M., and Swinson, K. L. (2005). Chronic REM-sleep deprivation of rats elevates metabolic rate and increases UCP1 gene expression in brown adipose tissue. *Am. J. Physiol. Endocrinol. Metab.* 289, E68–E74. doi: 10.1152/ajpendo.00543.2004

Krystal, A. D., Schopler, B., Kobbe, S., Williams, C., Rakatondrainibe, H., Yoder, A. D., et al. (2013). The relationship of sleep with temperature and metabolic rate in a hibernating primate. *PLoS ONE* 8:e69914. doi: 10.1371/journal.pone.0069914

Lee Kavanau, J. (2002). REM and NREM sleep as natural accompaniments of the evolution of warm-bloodedness. *Neurosci. Biobehav. Rev.* 26, 889–906. doi: 10.1016/S0149-7634(02)00088-X

Lee, M. L., Swanson, B. E., and de la Iglesia, H. O. (2009). Circadian timing of REM sleep is coupled to an oscillator within the dorsomedial suprachiasmatic nucleus. *Curr. Biol.* 19, 848–852. doi: 10.1016/j.cub.2009.03.051

Luong, L. N., and Carrive, P. (2012). Orexin microinjection in the medullary raphe increases heart rate and arterial pressure but does not reduce tail skin blood flow in the awake rat. *Neuroscience* 202, 209–217. doi: 10.1016/j.neuroscience.2011.11.073

Luppi, M., Martelli, D., Amici, R., Baracchi, F., Cerri, M., Dentico, D., et al. (2010). Hypothalamic osmoregulation is maintained across the wake-sleep cycle in the rat. *J. Sleep Res.* 19, 394–399. doi: 10.1111/j.1365-2869.2009.00810.x

Luppi, P. H., Adamantidis, A. R., and Fort, P. (2014). "The neurophysiology and neurobiology of sleep," in *Sleep Medicine Textbook*, eds C. Basssetti, P. Dogasz, and P. Peigneux (Regensburg: European Sleep Research Society), 3–11.

Luppi, P. H., Peyron, C., and Fort, P. (2017). Not a single but multiple populations of GABAergic neurons control sleep. *Sleep Med. Rev.* 32, 85–94. doi: 10.1016/j.smrv.2016.03.002

Mahapatra, A. P., Mallick, H. N., and Kumar, V. M. (2005). Changes in sleep on chronic exposure to warm and cold ambient temperatures. *Physiol. Behav.* 84, 287–294. doi: 10.1016/j.physbeh.2004.12.003

Martelli, D., Luppi, M., Cerri, M., Tupone, D., Mastrotto, M., Perez, E., et al. (2014). The direct cooling of the preoptic-hypothalamic area elicits the release of thyroid stimulating hormone during wakefulness but not during REM sleep. *PLoS ONE* 9:e87793. doi: 10.1371/journal.pone.0087793

Martelli, D., Luppi, M., Cerri, M., Tupone, D., Perez, E., Zamboni, G., et al. (2012). Waking and sleeping following water deprivation in the rat. *PLoS ONE* 7:e46116. doi: 10.1371/journal.pone.0046116

Martelli, D., Stanic, D., and Dutschmann, M. (2013). The emerging role of the parabrachial complex in the generation of wakefulness drive and its implication for respiratory control. *Respir. Physiol. Neurobiol.* 188, 318–323. doi: 10.1016/j.resp.2013.06.019

McKinley, M. J., Yao, S. T., Uschakov, A., McAllen, R. M., Rundgren, M., and Martelli, D. (2015). The median preoptic nucleus: front and centre for the regulation of body fluid, sodium, temperature, sleep and cardiovascular homeostasis. *Acta Physiol.* 214, 8–32. doi: 10.1111/apha.12487

Morrison, S. F., Madden, C. J., and Tupone, D. (2012). Central control of brown adipose tissue thermogenesis. *Front. Endocrinol.* 3:5. doi: 10.3389/fendo.2012.00005

Morrison, S. F., Madden, C. J., and Tupone, D. (2014). Central neural regulation of brown adipose tissue thermogenesis and energy expenditure. *Cell Metab.* 19, 741–756. doi: 10.1016/j.cmet.2014.02.007

Morrison, S. F., and Nakamura, K. (2011). Central neural pathways for thermoregulation. *Front. Biosci.* 16, 74–104. doi: 10.2741/3677

Morrison, S. F., Sved, A. F., and Passerin, A. M. (1999). GABA-mediated inhibition of raphe pallidus neurons regulates sympathetic outflow to brown adipose tissue. *Am. J. Physiol.* 276(2 Pt 2), R290–R297.

Nakamura, K., and Morrison, S. F. (2007). Central efferent pathways mediating skin cooling-evoked sympathetic thermogenesis in brown adipose tissue. *Am. J. Physiol. Regul. Integr. Comp. Physiol.* 292, R127–136. doi: 10.1152/ajpregu.00427.2006

Nakamura, K., and Morrison, S. F. (2008). A thermosensory pathway that controls body temperature. *Nat. Neurosci.* 11, 62–71. doi: 10.1038/nn2027

Nakamura, K., and Morrison, S. F. (2010). A thermosensory pathway mediating heat-defense responses. *Proc. Natl. Acad. Sci. U.S.A.* 107, 8848–8853. doi: 10.1073/pnas.0913358107

Nakamura, K., and Morrison, S. F. (2011). Central efferent pathways for cold-defensive and febrile shivering. *J. Physiol.* 589(Pt 14), 3641–3658. doi: 10.1113/jphysiol.2011.210047

Oldfield, B. J., Giles, M. E., Watson, A., Anderson, C., Colvill, L. M., and McKinley, M. J. (2002). The neurochemical characterisation of hypothalamic pathways projecting polysynaptically to brown adipose tissue in the rat. *Neuroscience* 110, 515–526. doi: 10.1016/S0306-4522(01)00555-3

Parmeggiani, P. L. (1980). Behavioral phenomenology of sleep (somatic and vegetative). *Experientia* 36, 6–11. doi: 10.1007/BF020 03941

Parmeggiani, P. L. (2003). Thermoregulation and sleep. *Front. Biosci.* 8, s557–s567. doi: 10.2741/1054

Parmeggiani, P. L., Agnati, L. F., Zamboni, G., and Cianci, T. (1975). Hypothalamic temperature during the sleep cycle at different ambient

temperatures. *Electroencephalogr. Clin. Neurophysiol.* 38, 589–596. doi: 10.1016/0013-4694(75)90159-5

Parmeggiani, P. L., and Rabini, C. (1967a). Phases of sleep and environmental temperature. *Helv. Physiol. Pharmacol. Acta* 25, CR214-216. doi: 10.1016/0006-8993(67)90139-4

Parmeggiani, P. L., and Rabini, C. (1967b). Shivering and panting during sleep. *Brain Res.* 6, 789–791.

Parmeggiani, P. L., and Rabini, C. (1970). Sleep and environmental temperature. *Arch. Ital. Biol.* 108, 369–387.

Parmeggiani, P. L., Azzaroni, A., Cevolani, D., and Ferrari, G. (1983). Responses of anterior hypothalamic-preoptic neurons to direct thermal stimulation during wakefulness and sleep. *Brain Res.* 269, 382–385. doi: 10.1016/0006-8993(83)90152-X

Parmeggiani, P. L., Azzaroni, A., Cevolani, D., and Ferrari, G. (1986). Polygraphic study of anterior hypothalamic-preoptic neuron thermosensitivity during sleep. *Electroencephalogr. Clin. Neurophysiol.* 63, 289–295. doi: 10.1016/0013-4694(86)90096-9

Parmeggiani, P. L., Cevolani, D., Azzaroni, A., and Ferrari, G. (1987). Thermosensitivity of anterior hypothalamic-preoptic neurons during the waking-sleeping cycle: a study in brain functional states. *Brain Res.* 415, 79–89. doi: 10.1016/0006-8993(87)90270-8

Parmeggiani, P. L., Cianci, T., Calasso, M., Zamboni, G., and Perez, E. (1980). Quantitative analysis of short term deprivation and recovery of desynchronized sleep in cats. *Electroencephalogr. Clin. Neurophysiol.* 50, 293–302. doi: 10.1016/0013-4694(80)90157-1

Parmeggiani, P. L., Franzini, C., Lenzi, P., and Zamboni, G. (1973). Threshold of respiratory responses to preoptic heating during sleep in freely moving cats. *Brain Res.* 52, 189–201. doi: 10.1016/0006-8993(73)90658-6

Parmeggiani, P. L., Zamboni, G., Cianci, T., Agnati, L. F., and Ricci, C. (1974). Influence of anterior hypothalamic heating on the duration of fast wave sleep episodes. *Electroencephalogr. Clin. Neurophysiol.* 36, 465–470. doi: 10.1016/0013-4694(74)90203-X

Parmeggiani, P. L., Zamboni, G., Cianci, T., and Calasso, M. (1977). Absence of thermoregulatory vasomotor responses during fast wave sleep in cats. *Electroencephalogr. Clin. Neurophysiol.* 42, 372–380. doi: 10.1016/0013-4694(77)90173-0

Prete, F. R., Bergmann, B. M., Holtzman, P., Obermeyer, W., and Rechtschaffen, A. (1991). Sleep deprivation in the rat: XII. Effect on ambient temperature choice. *Sleep* 14, 109–115. doi: 10.1093/sleep/14.2.109

Rathner, J. A., and Morrison, S. F. (2006). Rostral ventromedial periaqueductal gray: a source of inhibition of the sympathetic outflow to brown adipose tissue. *Brain Res.* 1077, 99–107. doi: 10.1016/j.brainres.2006.01.035

Rechtschaffen, A., Gilliland, M. A., Bergmann, B. M., and Winter, J. B. (1983). Physiological correlates of prolonged sleep deprivation in rats. *Science* 221, 182–184. doi: 10.1126/science.6857280

Rizvi, T. A., Ennis, M., and Shipley, M. T. (1992). Reciprocal connections between the medial preoptic area and the midbrain periaqueductal gray in rat: a WGA-HRP and PHA-L study. *J. Comp. Neurol.* 315, 1–15. doi: 10.1002/cne.903150102

Romanovsky, A. A. (2007). Thermoregulation: some concepts have changed. Functional architecture of the thermoregulatory system. *Am. J. Physiol. Regul. Integr. Comp. Physiol.* 292, R37–R46. doi: 10.1152/ajpregu.00668.2006

Roussel, B., and Bittel, J. (1979). Thermogenesis and thermolysis during sleeping and waking in the rat. *Pflugers Arch.* 382, 225–231. doi: 10.1007/BF00583706

Sakai, K., and Koyama, Y. (1996). Are there cholinergic and non-cholinergic paradoxical sleep-on neurones in the pons? *Neuroreport* 7, 2449–2453. doi: 10.1097/00001756-199611040-00009

Saper, C. B., Scammell, T. E., and Lu, J. (2005). Hypothalamic regulation of sleep and circadian rhythms. *Nature* 437, 1257–1263. doi: 10.1038/nature04284

Sapin, E., Lapray, D., Berod, A., Goutagny, R., Leger, L., Ravassard, P., et al. (2009). Localization of the brainstem GABAergic neurons controlling paradoxical (REM) sleep. *PLoS ONE* 4:e4272. doi: 10.1371/journal.pone.0004272

Schmidek, W. R., Hoshino, K., Schmidek, M., and Timo-Iaria, C. (1972). Influence of environmental temperature on the sleep-wakefulness cycle in the rat. *Physiol. Behav.* 8, 363–371. doi: 10.1016/0031-9384(72)90384-8

Schmidek, W. R., Zachariassen, K. E., and Hammel, H. T. (1983). Total calorimetric measurements in the rat: influences of the sleep-wakefulness cycle and of the environmental temperature. *Brain Res.* 288, 261–271. doi: 10.1016/0006-8993(83)90102-6

Sichieri, R., and Schmidek, W. R. (1984). Influence of ambient temperature on the sleep-wakefulness cycle in the golden hamster. *Physiol. Behav.* 33, 871–877. doi: 10.1016/0031-9384(84)90221-X

Szymusiak, R., and McGinty, D. (2008). Hypothalamic regulation of sleep and arousal. *Ann. N. Y. Acad. Sci.* 1129, 275–286. doi: 10.1196/annals.1417.027

Szymusiak, R., and Satinoff, E. (1981). Maximal REM sleep time defines a narrower thermoneutral zone than does minimal metabolic rate. *Physiol. Behav.* 26, 687–690. doi: 10.1016/0031-9384(81)90145-1

Takahashi, Y., Zhang, W., Sameshima, K., Kuroki, C., Matsumoto, A., Sunanaga, J., et al. (2013). Orexin neurons are indispensable for prostaglandin E2-induced fever and defence against environmental cooling in mice. *J. Physiol.* 591, 5623–5643. doi: 10.1113/jphysiol.2013.261271

Takase, K., Kikuchi, K., Tsuneoka, Y., Oda, S., Kuroda, M., and Funato, H. (2014). Meta-analysis of melanin-concentrating hormone signaling-deficient mice on behavioral and metabolic phenotypes. *PLoS ONE* 9:e99961. doi: 10.1371/journal.pone.0099961

Tan, C. L., Cooke, E. K., Leib, D. E., Lin, Y. C., Daly, G. E., Zimmerman, C. A., et al. (2016). Warm-sensitive neurons that control body temperature. *Cell* 167, 47 e15–59 e15. doi: 10.1016/j.cell.2016.08.028

Thompson, R. H., and Swanson, L. W. (2003). Structural characterization of a hypothalamic visceromotor pattern generator network. *Brain Res. Brain Res. Rev.* 41, 153–202. doi: 10.1016/S0165-0173(02)00232-1

Tupone, D., Cano, G., and Morrison, S. F. (2017). Thermoregulatory inversion - a novel thermoregulatory paradigm. *Am. J. Physiol. Regul. Integr. Comp. Physiol.* 312, R779–R786. doi: 10.1152/ajpregu.00022.2017

Tupone, D., Madden, C. J., Cano, G., and Morrison, S. F. (2011). An orexinergic projection from perifornical hypothalamus to raphe pallidus increases rat brown adipose tissue thermogenesis. *J. Neurosci.* 31, 15944–15955. doi: 10.1523/JNEUROSCI.3909-11.2011

Vanni-Mercier, G., Sakai, K., Lin, J. S., and Jouvet, M. (1989). Mapping of cholinoceptive brainstem structures responsible for the generation of paradoxical sleep in the cat. *Arch. Ital. Biol.* 127, 133–164.

Venner, A., Anaclet, C., Broadhurst, R. Y., Saper, C. B., and Fuller, P. M. (2016). A novel population of wake-promoting GABAergic Neurons in the ventral lateral hypothalamus. *Curr. Biol.* 26, 2137–2143. doi: 10.1016/j.cub.2016.05.078

Verret, L., Leger, L., Fort, P., and Luppi, P. H. (2005). Cholinergic and noncholinergic brainstem neurons expressing Fos after paradoxical (REM) sleep deprivation and recovery. *Eur. J. Neurosci.* 21, 2488–2504. doi: 10.1111/j.1460-9568.2005.04060.x

Vetrivelan, R., Kong, D., Ferrari, L. L., Arrigoni, E., Madara, J. C., Bandaru, S. S., et al. (2016). Melanin-concentrating hormone neurons specifically promote rapid eye movement sleep in mice. *Neuroscience* 336, 102–113. doi: 10.1016/j.neuroscience.2016.08.046

Weber, F., Chung, S., Beier, K. T., Xu, M., Luo, L., and Dan, Y. (2015). Control of REM sleep by ventral medulla GABAergic neurons. *Nature* 526, 435–438. doi: 10.1038/nature14979

Yoshida, K., Konishi, M., Nagashima, K., Saper, C. B., and Kanosue, K. (2005). Fos activation in hypothalamic neurons during cold or warm exposure: projections to periaqueductal gray matter. *Neuroscience* 133, 1039–1046. doi: 10.1016/j.neuroscience.2005.03.044

Yoshida, K., Maruyama, M., Hosono, T., Nagashima, K., Fukuda, Y., Gerstberger, R., et al. (2002). Fos expression induced by warming the preoptic area in rats. *Brain Res.* 933, 109–117. doi: 10.1016/S0006-8993(02)02287-4

Conflict of Interest Statement: The authors declare that the research was conducted in the absence of any commercial or financial relationships that could be construed as a potential conflict of interest.

Advantages of publishing in Frontiers

OPEN ACCESS
Articles are free to read for greatest visibility and readership

FAST PUBLICATION
Around 90 days from submission to decision

HIGH QUALITY PEER-REVIEW
Rigorous, collaborative, and constructive peer-review

TRANSPARENT PEER-REVIEW
Editors and reviewers acknowledged by name on published articles

Frontiers
Avenue du Tribunal-Fédéral 34
1005 Lausanne | Switzerland

Visit us: www.frontiersin.org
Contact us: info@frontiersin.org | +41 21 510 17 00

REPRODUCIBILITY OF RESEARCH
Support open data and methods to enhance research reproducibility

DIGITAL PUBLISHING
Articles designed for optimal readership across devices

FOLLOW US
@frontiersin

IMPACT METRICS
Advanced article metrics track visibility across digital media

EXTENSIVE PROMOTION
Marketing and promotion of impactful research

LOOP RESEARCH NETWORK
Our network increases your article's readership